

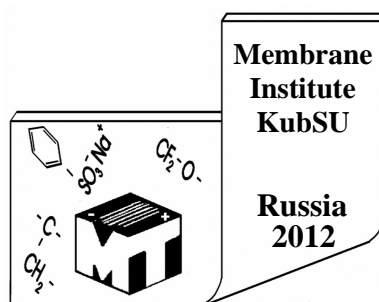
RUSSIAN ACADEMY OF SCIENCES  
RUSSIAN MEMBRANE SOCIETY  
RUSSIAN FOUNDATION FOR BASIC RESEARCH  
KUBAN STATE UNIVERSITY  
KURNAKOV INSTITUTE OF GENERAL AND INORGANIC CHEMISTRY, RAS  
'MEMBRANE TECHNOLOGY' INNOVATION ENTERPRISE

INTERNATIONAL CONFERENCE

*Ion transport in organic  
and inorganic membranes*

**Conference Proceedings**

**28 May – 2 June 2012**



**Krasnodar 2012**

## SCIENTIFIC/ORGANIZING COMMITTEE

<b>YAROSLAVTSEV A.B.</b>	<b>Chairman</b> , Corresponding Member RAS, Prof., Kurnakov Institute of General and Inorganic Chemistry, RAS, Moscow, Russia
<b>ZABOLOTSKY V.I.</b>	<b>Co-chairman</b> , Academician Int. Hi. Ed. Acad., Prof., Head of the Membrane institute, Kuban State University, Krasnodar, Russia
<b>POURCELLY G.</b>	<b>Co-chairman</b> , Prof., Institut Européen des Membranes, Université de Montpellier II, Montpellier, France
<b>AGEEV E.P.</b>	Prof., Moscow State University, Moscow, Russia
<b>BEREZINA N.P.,</b>	Prof., Kuban State University, Krasnodar, Russia
<b>BILDYUKEVICH A.V.</b>	Prof., Institute of Physico-Organic Chemistry NAS, Minsk, Belarus
<b>DAMMAK L.</b>	Prof., Institut de Chimie et des Matériaux – Université Paris-Est, Paris, France
<b>FILIPPOV A.N.</b>	Prof., Gubkin Russian State University of Oil and Gas, Moscow, Russia
<b>GNUSIN N.P.</b>	Prof., Kuban State University, Krasnodar, Russia
<b>GRAFOV B.M.</b>	Prof., Frumkin Institute of Physical Chemistry and Electrochemistry RAS, Moscow, Russia
<b>KHOHLOV A.R.</b>	Academician RAS, Prof., Moscow State University, Moscow, Russia
<b>KONONENKO N.A.</b>	<b>Scientific secretary</b> , Prof., Kuban State University, Krasnodar, Russia
<b>LARCHET C.</b>	Prof., Institut de Chimie et des Matériaux – Université Paris-Est, Paris, France
<b>NIKONENKO V.V.</b>	<b>Scientific secretary</b> , Prof., Kuban State University, Krasnodar, Russia
<b>NOVAK L.</b>	President, MEGA, Strazh pod Ralskem, Czech Republic
<b>OZERIN A.N.</b>	Corresponding Member RAS, Prof., Karpov Physical Chemistry Institute, Moscow, Russia
<b>PISMENSKAYA N.D.</b>	Prof., Kuban State University, Krasnodar, Russia
<b>RUBINSTEIN I.</b>	Prof., The Jakob Blaustein Institutes for Desert Research, Sede Boker Campus, Israel
<b>SHAPOSHNIK V.A.</b>	Prof., Voronezh State University, Voronezh, Russia
<b>SHUDRENKO A.A.</b>	General director., Noncommercial Partnership Innovation-Technology Centre "Kuban-Yug", Russia
<b>SISTAT P.</b>	Prof., Institut Européen des Membranes, Université de Montpellier II, Montpellier, France
<b>STAROV V.M.</b>	Prof., Loughborough University, Leicestershire, UK
<b>TSKHAY A.A.</b>	President, JSC Membrane Technologies, Alma Ata, Kazakhstan
<b>VOLFKOVICH Yu.M.</b>	Prof., Frumkin Institute of Physical Chemistry and Electrochemistry RAS, Moscow, Russia
<b>VOLKOV V.V.</b>	Prof., Topchiev Institute of Petrochemical Synthesis RAS, Moscow, Russia

## *PREFACE*

### **Membrane electrochemistry and Black Sea Conferences**

We do not realize that our every movement from the flick of the wrist to the spiritual impulse is a membrane process. Maybe we are not even aware that the faces of the conference participants are the most beautiful of the membranes, and that all functions determining our life are the membranes' functions.

The first person who took this idea from nature in the simplest form and used it for the human's good was French scientist and abbé Jean-Antoine Nollet. In 1748 he used a pig bladder as a membrane and separated the most exciting substances for man, water and alcohol. From the rich history of membrane science, we choose another event that has occurred just one hundred years ago. In 1912, Loeb and Beutner have established the phenomenon of selective permeability of cations across an apple skin as a membrane.

Apples have always been a reliable object of knowledge, ranging from the apple, which Eve plucked from the tree of knowledge, and including the apple whose falling led Newton to the discovery of the law of universal gravitation. In our time, the company Apple is trying to continue this tradition.

Let us return from the trip through time to the beginning of our conferences on membrane electrochemistry. From 1975 to 1993 they were annually held in the village of Dzhubga on the Black Sea. Their organizer was Nikolai Petrovich Gnusin, Titan in life and work. The conferences he held allowed the scientists of the Soviet Union working in the field of membrane electrochemistry to form a united scientific community. Its distinction was a combination of friendly relations between colleagues with a productive criticism and mutual aid. We did not meet other communities in which friendship and adherence to principles were combined so lucky. A feature of the Dzhubga conferences was inobservance of time limits, as questions and discussions were not limited, and there was a case of their continuation during a whole night until morning.

Since 1994, the organizer of the conference was Victor Ivanovich Zabolotsky. The peculiarity of the Conference 1994 was holding it completely in English. There was extensive involvement of European scientists, which became possible due to research activity by Victor Vasilievich Nikonenko at the Paris 12 University and his scientific contacts with scientists from France. Millennium 2000 was held in Sochi, and then the annual conferences began to be held in this blessed

place, near Tuapse. By this time, the ranks of professionals in electro dialysis were cut so that the conference had to expand its scope. However, the community maintained a high scientific potential through the participation of the outstanding scientists of the institutes of the Russian Academy of Sciences and Moscow University, who reported on a variety of issues of inorganic chemistry, physical chemistry and electrochemistry, coupled with the problems of membrane electrochemistry. Now the number of participants increases from year to year, and the English language becomes more and more fluent in communications and discussions.



Andrey Borisovich Yaroslavtsev participates actively in the Conference since 2000. Now he is the Chairman of Organizing Committee.

The Young Competitions have the increasing popularity. They are organized annually within the framework of Conference as tradition.



There are still a lot of unsolved problems challenging activities within our scientific community. Let us mention some of them:

1. There are no mathematical models of real electrolysers, such as EDI with ion exchange bed filling the intermembrane space.
2. We can not measure concentration fields in the membranes.
3. The problems of membrane scaling and fouling during electro dialysis are not fully resolved, which prevents the wide use of electro dialysis for demineralization and purification of waste waters from of heavy metals and in other application.
4. There are no ion exchange membranes with an active layer on the substrate like membranes for reverse osmosis.
5. Despite the fairly large number of ion exchange membranes produced in different countries, there are no membranes, which fully meet the specificity of particular electromembrane processes. There are no satisfactory membranes for fuel cells, no stable anion exchange membranes for the separation of solutions containing large organic anions (dairy industry, separation of amino acids, etc.), no low-cost and quality bipolar membranes, no membranes for high-temperature electro dialysis.
6. There is no microscopic theory of membrane transport on the basis of quantum chemical and molecular dynamic methods.

To the problems listed above, I would add the problem of visualization of solution electroconvection in electro dialyzer compartments, although it can be solved by laser Doppler anemometry with the same success with which the problem of visualization of concentration fields was solved by the method of laser interferometry. John Bernal believed that it is much more difficult to see a problem than to find a solution for it. But in this case, the vision of problems so far not led to their solution. Richard Bowen said: "If you are tired of membranes, you are tired of life." We are not tired of membranes, or of life, because there are a lot of unresolved problems stimulating our activity, and we wish to the participants of the Conference success in their solution.

*Vladimir Alexeevich Shaposhnik,  
Professor at Voronezh State University*

# Contents

1. **Olga Amosova, Vladimir Teplyakov** Membrane-adsorption systems for hydrogen recovery: potential and prospects (*Moscow, Russia*) 13
2. **Lidiya Annikova, Jan Křivčík, David Neděla** Investigation of bipolar membranes properties by electro dialysis method (*Straz pod Ralskem, Czech Republic*) 14
3. **Pavel Apel, Irina Blonskaya, Alexandr Fedotov, Oleg Orelovich, Vladimir Skuratov, Jiri Vacik, Kay-Obbe Voss, Sergey Dmitriev** Engineered ion-track membranes for micro- and nanofluidics (*Dubna – Minsk – Řež – Darmstadt, Russia – Belarus – Czech Republic – Germany*) 16
4. **Saloua Ayadi, Matthieu Rivallin, Frédéric Gillot, Sophie Cerneaux, Raja Ben Amar, Marc Cretin** Carbon membranes for the treatment of effluents by advanced oxidation process (*Montpellier – Sfax, France – Tunisia*) 19
5. **Ninel Berezina, Sergey Timofeev, Natalya Kononenko, Olga Dyomina, Anna Sytcheva, Svetlana Shkirskaya, Irina Falina, Mariya Kolechko, Mariya Chernyaeva, Natalya Loza, Sergey Dolgopолоv** Fluoran-type composite materials on the base of perfluorinated polymers and polyaniline. From synthesis to application (*Krasnodar – St. Petersburg – Miskolc, Russia – Hungary*) 22
6. **Vladimir Berezkin, Alexander Vasiliev, Vladimir Artiomov, Nickolas Kiseliy, Boris Mchedlishvili** Microcrystalline structures formation under supersaturated  $\text{HIO}_3$  solution flow through track membrane pores (*Moscow, Russia*) 24
7. **Olga Bessmertnaya, Nikolai Shel'deshov, Viktor Zabolotsky** Investigation of dimethylacetamide and isobutyl alcohol influence on the obtaining lithium hydroxide by electro dialysis with bipolar membranes from technological solutions (*Krasnodar, Russia*) 27
8. **David Bilenko, Victor Galushka, Inna Mysenko, Konstantin Razumov, Denis Uchaikin, Aleksandr Smirnov, Denis Terin** Membranes in memristor's structures (*Saratov – Engels, Russia*) 30
9. **Olga Bobreshova, Anna Parshina, Ekaterina Safronova, Sergey Timofeev, Andrey Yaroslavtsev** Electrode activity of perfluorinated sulfocation-exchange membranes (*Voronezh – Moscow – St. Petersburg, Russia*) 32
10. **Irina Bodyakina, Vasiliy Bagryantsev, Vladimir Kotov, Alexey Loukine** Electromembrane regeneration of saline acid from acidulous pectin extracts (*Voronezh, Russia*) 34
11. **Alina Chanaewa, Beatriz Juarez, Horst Weller** Composites on the base of metaloxides ( $\text{TiO}_2$ ,  $\text{ZnO}$ ) and carbon nanotubes for electrical devices (*Hamburg, Germany*) 36
12. **Ai-Fu Che, Vincent Germain, Marc Cretin, David Cornu, Christophe Innocent, Sophie Tingry** Free-standing electrospun carbon nanofibers mat as efficient electrode materials for bioelectrocatalysis of  $\text{O}_2$ . (*Montpellier, France*) 37
13. **Ruslan Chermit, Mikhail Sharafan, Viktor Zabolotsky** Influence of modification strong basic anionexchange membrane MA-41 at Chemical stability under overlimiting current mode (*Krasnodar, Russia*) 39
14. **Mariya Chernyaeva, Natalia Kononenko, Yurii Volkovich, Marina Kardash, Georgii Aleksandrov** Correlation between structural and selective properties OF ion-exchange membranes (*Krasnodar – Moscow – Engels, Russia*) 42
15. **Sunil Datta, Manju Agarwal, Anatoly Filippov** Cell model for a membrane consisting of parallel cylinders under hydromagnetic axial flow (*Lucknow – Moscow, India – Russia*) 44

16. **George Dibrov, Eduard Novitsky, Rostislav Trifonov, Vladimir Ostrovsky, Alexey Volkov** Permeance and diffusion of gases in Poly(2-methyl-5-vinyl tetrazole) (*Moscow – St. Petersburg, Russia*) 47
17. **George Dibrov, Eduard Novitsky, Vladimir Volkov** Elaboration of high flux composite PTMSP membranes (*Moscow, Russia*) 48
18. **Alexander Dyukov, Svetlana Shishkina** Influence of mercury (II) on properties of anion-exchange membranes MA-40 and MA-41 and electro dialysis process (*Kirovo-Chepetsk – Kirov, Russia*) 50
19. **Yuliya Dzyazko, Ludmila Ponomarova, Yurii Volfkovich, Valentin Sosenkin, Vladimir Belyakov** Ion-exchange resin doped with zirconium hydrophosphate: selective sorption (*Kiev – Moscow, Russia – Ukraine*) 52
20. **Ekaterina Efimova, Darya Syrtsova, Olga Shornikova, Aleksandr Kharitonov, Vladimir Teplyakov** Transport of lower hydrocarbons through graphite foil modified by direct gas-phase fluorination (*Moscow, Russia*) 55
21. **Ivan Evdokimov, Dmitry Volodin, Irina Kulikova, Alexander Donskih, Maria Greshnyakova** A comparative study of technological properties of demineralized milk permeate (*Stavropol, Russia*) 57
22. **Evgenie Egorov, Alexey Svitsov** Utilization of industrial wastes by electro dialysis (*Moscow, Russia*) 58
23. **Edil Ergozhin, Tulegen Chalov, Tatyana Kovrigina** Synthesis of nanostructured ion exchange membranes for electrochemical processes of water purification (*Almaty, Republic of Kazakhstan*) 59
24. **Irina Falina, Ninel Berezina, Marya Chernyaeva, Vyacheslav Roldugin, Ivan Senchychin** Comparizon of properties of MF-4SC/polyaniline composites prepared in concentration and electric fields (*Krasnodar – Moscow, Russia*) 61
25. **Alexander Fedotov, Julia Fedotova, Pavel Apel, Dmitry Ivanou, Yulia Ivanova, Ivan Svito, Eugen Streltsov** A huge magnetoresistivity in n-Si/SiO<sub>2</sub>/Ni nanostructures fabricated in track-etched pores (*Minsk – Dubna, Belarus – Russia*) 64
26. **Anatoly Filippov** Mathematical modeling of the membrane processes (*Moscow, Russia*) 67
27. **Anatoly Filippov, Sergey Dolgopolov, Natalia Kononenko** Mathematical model of anisotropic nanocomposite membrane for estimation of asymmetry of current-voltage curve parameters (*Moscow – Krasnodar, Russia*) 68
28. **Anatoly Filippov, Vladimir Ivanov, Alexey Volkov, Alexey Yushkin, Yulia Bogdanova, Valentina Dolzhikova** Influence of hydrophobicity of PMP and PTMSP nanoporous membranes on a flow rate of aqueous alcohol mixtures under applying of external pressure drop (*Moscow, Russia*) 71
29. **Wendy Garcia-Vasquez, Lassâad Dammak, Christian Larchet, Victor Nikonenko, Daniel Grande** Degradation of ion-exchange membranes used in electro dialysis for whey desalination (*Paris – Krasnodar, France – Russia*) 75
30. **Elena Goleva, Vera Vasil'eva, Kristina Chegereva** Stationary dialysis of the mixture of phenylalanine and sodium chloride with profiled sulphocation-exchange membrane (*Voronezh, Russia*) 77
31. **Daniil Golubenko, Yuliya Karavanova, Andrei Yaroslavtsev** Synthesis and Study the diffusion properties of membranes AMEX, modified by cerium oxide (*Moscow, Russia*) 80
32. **Vladislav Gorshkov, Lev Polyanskii, Tamara Kravchenko** Redox sorption of oxygen by cathodic polarized metal-ion exchanger nanocomposite (*Voronezh, Russia*) 82

33. **Daniel Grande, Ahlem Raies, Lassâad Dammak, Alexander Fainleib, Olga Grigoryeva, Kristina Gusakova** Investigation of structure-permeability relationships in nanoporous polycyanurate-based membranes (*Thiais – Kyiv, France – Ukraine*) 85
34. **Vladimir Guterman, Tatiana Lastovina, Helena Pahomova, Natalia Tabachkova, Andrey Paharev** PEMFC electrocatalyst based on M-core – Pt-shell nanoparticles (*Rostov-on-Don – Moscow, Russia*) 86
35. **Yuliya Karavanova, Vitaly Volkov, Andrei Yaroslavtsev** Ion mobility in surface-modified MC-40 membranes in mixed alkali forms (*Chernogolovka – Moscow, Russia*) 88
36. **Marina Kardash, George Aleksandrov, Denis Aynetdinov** Cation-exchange membranes“policoni”. structure, properties, application (*Engels, Russia*) 90
37. **Marina Kardash, Denis Terin, Ivan Tyurin, Margarita Batura** Implementation of Fe nanopowder into chemisorbtion polimeric materials - «POLYCON K» (*Engels, Russia*) 92
38. **Marina Kardash, Denis Terin, Ivan Tyurin, Margarita Batura** Modification and implementation of ni nanopowder into «POLYCON K». structure characteristics, morphology and electrodynamic properties of chemisorbtion polimeric materials (*Engels, Russia*) 93
39. **Larisa Karpenko-Jereb, Anne-Marie Kelterer** Study of sulfonic acid group dissociation and water connectivity in polystyrene and perfluorinated membranes (*Graz, Austria*) 94
40. **Victor Kasperchik, Alla Yaskevich, GeorgePoleshko** Transport of salt mixtures through polylayered composite ultrafiltration membrane (*Minsk, Belarus*) 97
41. **Yury Kochnev, Alexandr Vilensky, Boris Mchedlishvili** Polyethyleneterephthalate track etched membranes with Asymmetrical shape pores (*Moscow, Russia*) 99
42. **Natalia Kononenko, Ninel Berezina, Sergey Dolgopolov, Irina Falina** Preparation of composites based on MF-4SC membrane and polyaniline in external electrical field (*Krasnodar, Russia*) 101
43. **Anna Kovalenko, Mahamet Urtenov, Aminat Uzdenova** Analytical solutions boundary problems models electroconvection in membrane systems (MS) (*Krasnodar – Karachaevsk, Russia*) 104
44. **Anna Kovalenko, Andriy Yaroshchuk, Victor Nikonenko, Mahamet Urtenov** Estimation of influence of water transfer through a membrane on the transfer of binary electrolyte in electrodialysis (*Krasnodar – Barcelona, Russia – Spain*) 107
45. **Tamara Kravchenko** Chemical and ion-exchange reactions in metal – ion exchanger nanocomposites (*Voronezh, Russia*) 109
46. **Elena Krisilova, Tatyana Eliseeva** Atomic force microscopy for the study of ion-exchange membrane FBM surface morphology (*Voronezh, Russia*) 112
47. **Ekaterina Kuznetsova, Ekaterina Safronova, Andrei Yaroslavtsev** Hybrid materials based on MF-4SC membrane and ceria synthesized by the casting method (*Moscow, Russia*) 114
48. **Darya Leontieva, Alexey Rychagov, Nina Smirnova, Yury Volfkovich** Elecctochemical synthesis of NiO/C composition material (*Novocherkassk – Moscow, Russia*) 117
49. **Natalia Loza, Sergey Dolgopolov, Natalia Kononenko, Ninel Berezina, Sergey Lakeev** Effects of Ph change in electromembrane system with MF-4SC surface modified by polyaniline (*Krasnodar – Moscow, Russia*) 119

50. **Sergey Loza, Victor Zabolotsky** Development and research of electro dialyzer for demineralization of electrolyte solutions based on profiled membranes (*Krasnodar, Russia*) 121
51. **Semyon Mareev, Victor Nikonenko, Natalia Pismenskaya** Determination of the diffusion layer thickness of the warburg impedance spectra, taking into account the concentration dependence of the diffusion coefficient (*Krasnodar, Russia*) 123
52. **Natalia Matushkina, Alla Dolgova, Evgeny Ageev** Influence of crazing on pervaporation properties of PA-6 (*Moscow, Russia*) 125
53. **Nina Maygurova, Elena Krisilova, Tatiana Eliseeva, Anastasiya Sholokhova** The kinetics of arginine and histidine sorption by cation-exchange membranes (*Voronezh, Russia*) 128
54. **Nadezhda Melnik, Natalia Pismenskaya, Victor Nikonenko** Study of mass transfer characteristics of the modified membranes in electro dialysers simulating large-scale apparatus (*Krasnodar, Russia*) 130
55. **Alexandr Mikheev, Ekaterina Safronova** Transport properties of hybrid MF-4SC membranes doped by silica and silica with surface modified by amino-groups (*Moscow, Russia*) 133
56. **Natalya Morozova, Alexandr Vvedenskii, Alexandr Maximenko, Irina Beredina** Hydrogen permeability of metal films of Cu,Pd-alloys by the data of potentiostatic double-step measurements (*Voronezh, Russia*) 136
57. **Kseniya Nebavskaya, Andrey Nebavsky, Victor Nikonenko, Natalia Pismenskaya** Effect of thermal treatment on hydrophobicity of Nafion surface (*Krasnodar, Russia*) 139
58. **Andrey Nebavsky, Veronica Sarapulova** Determination of hydrotartrate diffusion coefficient in infinitely dilute solution (*Krasnodar, Russia*) 142
59. **Ekaterina Nevakshenova, Victor Nikonenko, Natalia Pismenskaya** Electrical conductivity of gel phase of some commercial membranes in ampholyte solutions (*Krasnodar, Russia*) 145
60. **Victor Nikonenko, Mahamet Urtenov, Aminat Uzdenova, Natalia Pismenskaya, Vera Vasil'eva** Theoretical and experimental study of overlimiting mass transfer in electro dialysis (*Krasnodar – Voronezh, Russia*) 147
61. **Viktoriya Novikova, Mikhail Chayka, Tamara Kravchenko** Silver-ion-exchange nanocomposite electrode material based on homogeneous perfluorinated membrane and carbon support (*Voronezh, Russia*) 150
62. **Yoram Oren, Evgenia Gulaev, Meital Assraf-Snir, Nofar Asa-Wolfson, Jack Gilron** Membrane scaling issues in electro dialysis of brackish water reverse osmosis brines (*Beer-Sheva, Israel*) 153
63. **Helena Pakhomova, Aleksey Mar'janov, Aleksey Mikheykin, Vasily Pryadchenko, Aleksey Kozakov, Maria Evstegneeva, Vladimir Guterman** Microstructural characteristics of carbon supported Ag<sub>x</sub>@Pt electrocatalysts for low temperature fuel cells (*Rostov-on-Don, Russia*) 155
64. **Ivan Pantyukhin, Darya Medyantseva, Svetlana Shishkina** Behaviour features of ion-exchange membranes in the ammonium salt solutions (*Kirov – Kirovo-Chepetsk, Russia*) 158
65. **Anna Parshina, Olga Bobreshova, Sergey Timofeev** Influence of ion-molecular composition of the MF-4SC membrane on the characteristics of Pd-sensors in multiionic aqueous solutions (*Voronezh – St. Petersburg, Russia*) 160
66. **Tamara Philippova, Anatoly Filippov, Vasily Kalinin** Interaction of a charged particle and a pore in an ionexchange membrane: case of known surface charge densities (*Moscow, Russia*) 162

67. **Natalia Pismenskaya, Nadezhda Melnik, Victor Nikonenko, Gerald Pourcelly** What membrane properties have impact on the electroconvection in electrodialysis of dilute solutions? (*Krasnodar – Montpellier, Russia – France*) 165
68. **Sergey Podojnitsyn, Tatyana Tsyganova, Sergey Shatov, Boris Mchedlishvili** Current-voltage characteristics and electric breakdown of the metal-coated track-etched membranes (*Moscow, Russia*) 169
69. **Lev Polyanskiy, Svetlana Khorolskaya, Dmitriy Konev, Tamara Kravchenko** Dynamics of oxygen redox sorption by metal (Ag, Cu, Bi)–ion exchanger nanocomposites (*Voronezh, Russia*) 172
70. **Ardalion Ponomarev, Emil Abdrashitov, Veslav Bokun, Dina Kritskaya, Evgeny Sanginov, Yury Dobrovolsky** Synthesis and properties of the proton exchanging polyvinylidene fluoride-sulfonated polystyrene membranes and testing them in the hydrogen and methanol fuel cells (*Chernogolovka, Russia*) 175
71. **Mikhail Porozhnyi, Semen Mareev, Natalia Pismenskaya, Victor Nikonenko, Veronica Sarapulova** Comparative study of electrodialysis desalination of a wine model solution with commercial and experimental ion exchange membranes (*Krasnodar, Russia*) 178
72. **Larisa Potehina, Valentiny Sedelkin, Antonina Surkova, Olga Chirkova** Modifying of polymeric raw materials for the purpose of regulation of structure and properties of selectively nontight membranes (*Saratov, Russia*) 181
73. **Gérald Pourcelly, Laurent Bazinet** A review of electro-dialytic phenomena and applications in the food, beverage and nutraceutical industries (*Montpellier – Québec, France – Canada*) 183
74. **Marina Pozdeeva, Valentine Sedelkin, Olga Chirkova** Adsorption characteristics of cellulose acetate semipermeable membranes (*Engels – Saratov, Russia*) 184
75. **Vjacheslav Roldughin** Non-equilibrium thermodynamics of colloidal systems (*Moscow, Russia*) 185
76. **Vjacheslav Roldughin, Elena Sherysheva, Vladimir Zhdanov** Effect of surface diffusion on the binary gas mixture separation (*Moscow, Russia*) 188
77. **Elena Ryzhkova, Anna Parshina, Olga Bobreshova** Potentiometric multisensory systems with pd-sensors for quantitative determination of lysine and thiamine in aqueous organics medium (*Voronezh, Russia*) 190
78. **Konstantin Sabbatovsky, Aleksandr Vilensky, Vladimir Sobolev, Boris Mchedlishvili** Electro-surface and structural properties of polymer matrix based on PET (*Moscow, Russia*) 191
79. **Ekaterina Safronova, Philippe Sizat, Andrey Yaroslavtsev** MF-4SC based hybrid membranes with incorporated nanoparticles of silica and zirconia with functionalized surface (*Moscow – Montpellier, Russia – France*) 193
80. **Ekaterina Sakardina, Ekaterina Zolotukhina, Tamara Kravchenko, Svetlana Nikitina** Applications of ion exchangers with silver nanoparticles for oxidation of methanal in water and ethanal in ethanol: effect of molecular oxygen (*Voronezh – Chernogolovka, Russia*) 195
81. **Mykola Sakhnenko, Marina Ved, Marina Mayba, Marina Glushkova, Svetlana Zjubanova** D-metals based materials for hydrogen energetics (*Kharkov, Ukraine*) 197
82. **Veronica Sarapulova, Natalia Pismenskaya, Victor Nikonenko, Tatyana Garshina, Piotr Kulintsov** Electrical conductivity of anion exchange materials in sodium chloride and potassium hydrotartrate solutions (*Krasnodar – Shchekino, Russia*) 198

83. **Olga Shapovalova, Nicolai Sheldeshov, Victor Zabolotsky** Study of electrochemical characteristics of modified bipolar membranes (*Krasnodar, Russia*) 201
84. **Svetlana Shkirskaya, Ninel Berezina, Mariya Kolechko** Electrokinetic properties of composite membranes MF-4SC/polyaniline in dependence on the counter-ions type *Krasnodar, Russia*) 204
85. **Liudmila Shmukler, Nguyen Van Thuc, Liubov Safonova** Single-walled carbon nanotube-pmma composites for polymer gel electrolytes: influence on proton conductivity (*Ivanovo, Russia*) 206
86. **Philippe Sizat, Stella Lacour, Gérald Pourcelly, Ekaterina Belashova** Transient electrochemical methods for the transport study through ion-exchange membranes—review and new trends (*Montpellier – Krasnodar, France – Russia*) 208
87. **Nina Smirnova, Alexandra Kuriganova, Daria Leontyeva** Alternating current synthesis of nanomaterials the based on metals and metal oxides (*Novochercassk, Russia*) 210
88. **Antonina Surkova, Valentine Sedelkin, Olga Chirkova, Olga Pachina, Larisa Potekhina, Sergey Apostolov** Rheological, optical and structural properties solutions of cellulose diacetate to mold semipermeable membranes (*Engels, Russia*) 211
89. **Nguyen Van Thuc, Liudmila Shmukler, Yulia Fadeeva, Liubov Safonova** Polymer gel electrolytes: influence of composition on proton conductivity (*Ivanovo, Russia*) 214
90. **Sergey Timofeev, Lyubov' Bobrova, Elena Lyutikova, Lyubov' Fedotova, Valery Dyakov, Sergey Grigoryev** Novel MF-4SK membranes for hydrogen-air fuel cells (*Sankt Petersburg, Russia*) 217
91. **Ashish Tiwari, Satya Deo, Anatoly Filippov** Influence of Magnetic Field on Hydrodynamic Permeability of a Membrane (*Pilani – Allahabad – Moscow, India – Russia*) 219
92. **Valery Ugrozov, Anatoly Filippov** Mechanism of asymmetric transmembrane transfer through the modified membrane (*Moscow, Russia*) 222
93. **Raushan Usenkyzy, Kuanyshbek Musabekov, Nurlan Musabekov** Diffusion of anti-cancer drug molecules in membrane-modified hydrogel (*Almaty, Republic of Kazakhstan*) 225
94. **Stanislav Utin, Victor Zabolotsky, Konstantin Lebedev, Nikolay Sheldeshov, Polina Vasilenko** Regularities of electrolyte dilute solutions pH correction by electrodialysis with bipolar membranes (*Krasnodar, Russia*) 227
95. **Vera Vasil'eva, Ekaterina Sirota, Elmara Akberova, Mikhail Malykhin, Natalya Kranina, Larisa Krasnorutskaya** Development and experimental testing of software package for determining the share of ion-conductive surface of heterogeneous membranes by data of scanning electron microscopy (*Voronezh, Russia*) 230
96. **Vera Vasil'eva, Anna Zhiltsova, Vladimir Shaposhnik, Victor Zabolotsky, Konstantin Lebedev, Mikhail Malykhin** Direct observation of convective instability in electromembrane systems by laser interferometry (*Voronezh – Krasnodar, Russia*) 233
97. **Sergey Vasin, Anatoly Filippov, Tatiana Kharitonova** Composite microcapsule in a viscous liquid (*Moscow, Russia*) 236
98. **Yurii Volfkovich, Daniil Bograchev, Alexey Mikhalin, Alexey Rychagov, Daewook Park** Capacitive deionisation of water solutions (*Moscow – Gyeonggi-do, Russia – Korea*) 239
99. **Mikhail Vorotyntsev, Dmitriy Konev, Ekaterina Zolotukhina, Charles** 243

- Devillers, Igor Bezverkhy, Olivier Heintz** A new family of electroactive polymer materials on the basis of porphyrin units, with unusual electronic and optical properties (*Moscow – Chernogolovka – Dijon, Russia – France*)
100. **Mikhail Vorotyntsev, Veronika Zinovyeva, Ekaterina Zolotukhina, Jean-Cyrille Hierso, Igor Bezverkhy, Olivier Heintz, Tatiana Magdesieva, Oleg Nikitin, Oleg Levitsky** One-step chemical synthesis of pd-polypyrrole nanocomposites and their applications in organic catalysis (*Moscow – Chernogolovka – Dijon, Russia – France*) 245
101. **Kristina Yankina, Olga Bobreshova, Anna Parshina, Ekaterina Safronova, Andrey Yaroslavtsev** Potentiometric determination of anions by using of the perfluorinated sulfocation-exchange membranes modified with zirconia (*Voronezh – Moscow, Russia*) 248
102. **Andrei Yaroslavtsev** Hybrid membrane materials: properties and perspectives of application (*Moscow, Russia*) 250
103. **Polina Yurova, Yuliya Karavanova, Andrei Yaroslavtsev** Synthesis and diffusion properties of cation-exchange membrane based on MC-40, MF-4SC and polyaniline (*Moscow, Russia*) 253
104. **Victor Zabolotsky, Aslan Achoh, Stanislav Melnikov** Study of diary whey model solution electro dialysis demineralization (*Krasnodar, Russia*) 255
105. **Victor Zabolotsky, Olga Dyomina, Svetlana Eterevska, Kirill Protasov** Transport characteristics of hybrid cation-exchange membranes in electro dialysis concentration process of electrolytes from nonaqueous solvents (*Krasnodar, Russia*) 258
106. **Victor Zabolotsky, Konstantin Lebedev, Polina Vasilenko** Mathematical model of electroconvection in systems with ion-exchange membranes (*Krasnodar, Russia*) 260
107. **Victor Zabolotsky, Konstantin Lebedev, Polina Vasilenko, Stanislav Utin** Mathematical model of natural water pH correction by electro dialysis with bipolar membrane in long membrane channels (*Krasnodar, Russia*) 262
108. **Victor Zabolotsky, Stanislav Melnikov, Olga Dyomina, Svetlana Eterevska, Lubosh Novak, Filipp Auinger, Lubomir Machuca** Forecasting of mass exchange characteristics of concentrator electro dialyzers by compartmentation method (*Krasnodar – Straz pod Ralskem, Russia – Czech Republic*) 264
109. **Evgenija Zhelonkina, Tatyana Kononova, Vladimir Mamaev, Svetlana Shishkina** Transport properties of anion exchange membranes in chrome-containing solutions (*Kirov, Russia*) 266
110. **Anna Zhiltsova, Vera Vasil'eva, Mikhail Malykhin, Natalia Pismenskaya, Mahamet Urtenov, Aminat Uzdenova, Victor Nikonenko** The nature influence membranes on the formation and development of convective instability in electromembrane systems (*Voronezh – Krasnodar, Russia*) 268
111. **Yuriy Zmievskiy, Valeriy Myronchuk, Dmitriy Kucheruk, Inna Gudzovska** Whey separation by means of electro dialyser with non circulating concentration cells (*Kyiv, Ukraine*) 271

---

# MEMBRANE-ADSORPTION SYSTEMS FOR HYDROGEN RECOVERY: POTENTIAL AND PROSPECTS

<sup>1,2</sup>Olga Amosova, <sup>1,2</sup>Vladimir Teplyakov

<sup>1</sup>Topchiev Institute of Petrochemical Synthesis of RAS, Moscow, Russia

<sup>2</sup>Lomonosov Moscow State University, Moscow, Russia, *E-mail: o.amosova@gmail.com*

## Introduction

Nowadays, the study of hydrogen-containing multicomponent gas mixtures separation is of great importance because the demand of hydrogen is increasing. Hydrogen is used in many important chemical process industries, such as hydro-cracking, methanol production, manufacture of silicon, fuel cells, etc. Due to the environmental concern, clean-burning characteristics of H<sub>2</sub> make it attractive as vehicular fuel, especially for urban areas. There are a lot of available gas mixtures seems to be promising sources for hydrogen production for example bio-sources (bio-hydrogen obtained by means of bacteria [1,2] and bio-syngas produced as a result of solid organic waste or wood pyrolysis [1,3]). The problems of hydrogen recovery from multicomponent gas mixtures assume the development of safe technologies with low power consumption. Membrane and adsorption methods are examples of such processes, since they do not require energy for phase transition.

## Experiments

This study is focused on the recovery of hydrogen from multicomponent gas mixtures by integrated membrane/PSA system. The paper presents the following results: computational estimation of the six-component mixture (H<sub>2</sub>/CO/CO<sub>2</sub>/N<sub>2</sub>/CH<sub>4</sub>/H<sub>2</sub>S) separation by means of membrane modules; estimation of the integrated membrane/PSA system efficiency; experimental results of gas mixtures separation by integrated membrane/PSA system with commercially available membranes (GENERON<sup>®</sup> hollow fiber membrane module and PVTMS flat sheet membrane module). The experiments were carried out using model gas mixtures (He/CO<sub>2</sub>/O<sub>2</sub> which imitates H<sub>2</sub>/CO<sub>2</sub>/CO mixture and He/H<sub>2</sub>/CO<sub>2</sub>/N<sub>2</sub>).

## Results and Discussion

It is shown that hydrogen recovery degree may achieve 90-97% for bio-synthesis gas and petrochemical gas in case of 70% hydrogen pre-concentration at the membrane stage. As a result, the hydrogen of 99.9 % purity may be obtained at the PSA stage. Obtained results could be considerably improved by application of new membrane materials and new adsorbents. The H<sub>2</sub>S, CO and H<sub>2</sub>O permeability through the membranes was estimated by means of the correlation analysis. Prospects of suggested hybrid technology are considered as well.

*Acknowledgements: This work is partially supported by GK № 16.516.11.6139*

## References

1. *Ruggeri B., Tommasi T.* Efficiency and efficacy of pre-treatment and bioreaction for bio-H<sub>2</sub> energy production from organic waste // *Int. J. Hydrogen Energy*, 2012. V.37. P. 6491-6502.
2. *Gasanova L.G., Satraddinova E.R., Netrusov A.I., Teplyakov V.V., Zinkevich V.B., Modigell M.* Membrane bio-reactor for combustible gas obtaining // *Membranes*, 2007. №1. V.33. P. 32-42 (in Russian).
3. *Levin D.B., Pitt L., Love M.* Biohydrogen production prospects and limitations to practical application // *Int. J. Hydrogen Energy*, 2004. V.9. P.173-185.

# INVESTIGATION OF BIPOLAR MEMBRANES PROPERTIES BY ELECTRODIALYSIS METHOD

Lidia Annikova, Jan Křivčík, David Neděla

"MemBrain s.r.o.", Straz pod Ralskem, Czech Republic, E-mail: lidia.annikova@membrain.cz, david.nedela@membrain.cz

## Introduction

This study shows the properties of experimental heterogeneous bipolar membrane samples [1] which were analyzed by the electro dialysis apparatus with industrial solutions.

## Experiments

Three compartment electro dialysis stack was assembled to study properties of bipolar membranes. This stack is shown in Fig.1 and it consists of three compartments: diluate compartment (2, 5, 8) concentrate (acid and base) compartment and electrode compartment (1, 11). The cell in the electro dialysis stack consists of cation-exchange, anion-exchange and bipolar membranes.

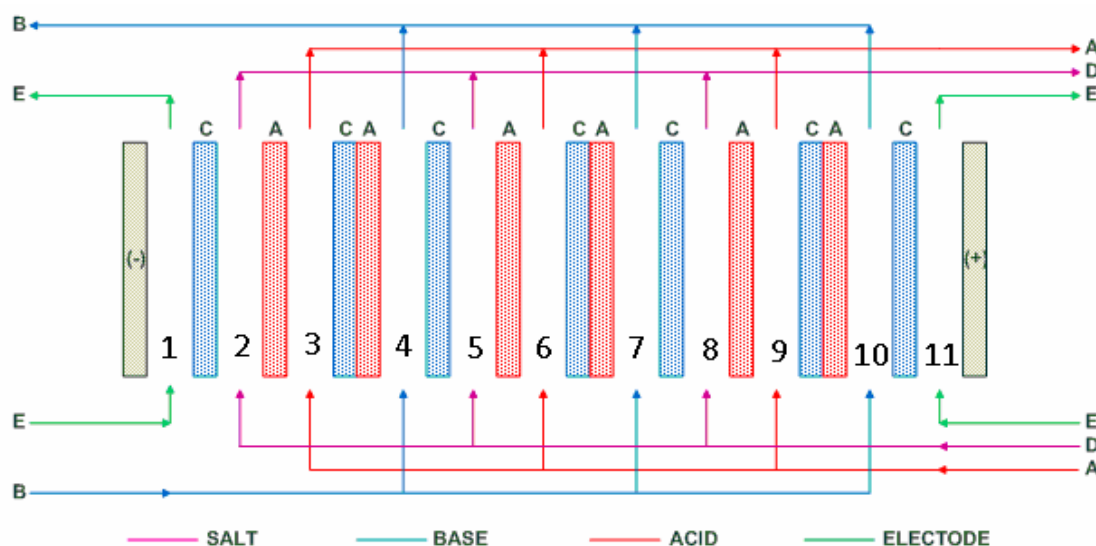


Figure 1. Scheme of the stack configurations by electrolytic dialysis with bipolar membranes

It is a standard three-compartment stack in conjunction with the electrodes [2]. All membranes in cell were heterogeneous type. In table 1 you can see quantities analysis of initial industrial solutions.

Table 1: Composition of salt solution

Parameters	Unit	industrial solution
pH		3-4
conductivity	mS/cm	60 – 65
Na <sub>2</sub> SO <sub>4</sub>	g/l	65 – 85
Cl	mg/l	800 – 1000
Ca <sup>2+</sup> ,	mg/l	< 30
Mg	mg/l	< 30
U	mg/l	< 0,05

Table 2 presents test conditions of electro dialysis apparatus with model solution (A) and real solution (B).

**Table 2: Conditions of electro dialysis apparatus**

Condition	B
type of apparatus	EDR-Z
active area of the membrane in the cell S, cm <sup>2</sup>	64
type of assembly (three-compartment)	AM BM CM
compartments number	6
membranes numbers	
bipolar (BM)	6
anion-exchange (AM)	6
cation-exchange (CM)	7
solution Na <sub>2</sub> SO <sub>4</sub>	real
salt volume V(Na <sub>2</sub> SO <sub>4</sub> ), L	50
volume of chamber in the stacks for generations acid and base V(H <sub>2</sub> O), L	0,5
unit voltage U (V/cell)	1,5-5,0
solutions circulation rate, v l/h	25
work apparatus regime	batch

### Results and Discussion

In the Table 3 there are process parameters at tested conditions. There are also final acid and alkali concentrations including current efficiency, production rate and specific energy consumption. The optimum process voltage is between 3–4 V per cell. Increasing voltage above 4 V doesn't have effect on acid and alkali production and only lead to increase energy consumption.

**Table 3: Electro dialysis Process Parameters**

No.	U, (V/cell)	I, A/m <sup>2</sup>	time t, min	Concentration C, g/l		Current efficiency η, %		production rate, eq/(h m <sup>2</sup> )		specific energy consumption W, Wh/g	
				H <sub>2</sub> SO <sub>4</sub>	NaOH	H <sub>2</sub> SO <sub>4</sub>	NaOH	H <sub>2</sub> SO <sub>4</sub>	NaOH	H <sub>2</sub> SO <sub>4</sub>	NaOH
1	1,5	68,75	1100	49,8	53,3	52,10	68,17	1,42	1,13	3,22	2,48
2	2,0	71,88	1100	62,4	71,1	55,83	59,00	1,95	1,93	2,62	2,22
3	3,0	228,12	1100	94,3	102,5	64,43	42,90	3,03	3,01	9,26	5,72
4	4,0	342,19	1100	117,5	117,1	65,70	42,65	3,79	3,98	12,85	7,97
5	5,0	376,56	1100	132	118,1	54,60	30,31	4,47	3,82	17,14	12,29

### References

1. *Wilhelm F.G.* Bipolar membrane electro dialysis, Twente University Press, Enschede. 2001.
2. *Xu T., Yang Weihu Y.* Effect of cell configurations on the performance of citric acid production by a bipolar membrane electro dialysis // J. Membr. Sci. 2002. V. 203. P. 145-153.

---

# ENGINEERED ION-TRACK MEMBRANES FOR MICRO- AND NANOFUIDICS

<sup>1,2</sup>Pavel Apel, <sup>1</sup>Irina Blonskaya, <sup>3</sup>Alexandr Fedotov, <sup>1</sup>Oleg Orelovich, <sup>1</sup>Vladimir Skuratov, <sup>4</sup>Jiri Vacik, <sup>5</sup>Kay-Obbe Voss, <sup>1</sup>Sergey Dmitriev

<sup>1</sup>Flerov Laboratory of Nuclear Reactions, JINR, Dubna, Russia; *E-mail: apel@nrmmail.jinr.ru*

<sup>2</sup>The International University "Dubna", Dubna, Russia

<sup>3</sup>Belarusian State University, Minsk, Belarus

<sup>4</sup>Institute of Nuclear Physics, Řež, Czech Republic

<sup>5</sup>GSI Helmholtzzentrum für Schwerionenforschung GmbH, Darmstadt, Germany

## Introduction

Narrow pores, produced by the track-etching process in dielectric foils, have been successfully used as model cylindrical channels with electrically charged walls since the 1970's [1, 2]. The uniqueness of the track-etching technology arises from the possibility to independently vary the pore number and the pore size. Moreover, the pore geometry can also be varied at will. Recently, several etching methods were developed which allow for the formation of pores of pre-determined configuration. Sophisticated irradiation equipment makes it possible to produce single tracks, or regular arrays of tracks, in polymer foils. Therefore, the ion track technology is a good platform for developing engineered micro- and nanoporous membranes, the transport properties of which can be finely tuned. In the present report, different irradiation and etching procedures that allow for the fabrication of nanoporous membranes, with pre-set pore geometry and pore number, are presented. Such membranes can be used for nano- and ultrafiltration, for the development of sensors, ion pumps and other nanofluidic devices.

## Experiments

The membranes were produced from polymer foils and inorganic thin films. Polyethylene terephthalate (PET) and polycarbonate (PC) foils were 10-23  $\mu\text{m}$  thick. Silicon oxide and silicon nitride films were 300-500 nm in thickness. Irradiation with heavy ions was performed on the U-400 and IC-100 cyclotrons of the Flerov Laboratory (JINR, Dubna), the linear accelerator UNILAC (the GSI Helmholtzzentrum fuer Schwerionenforschung GmbH, Darmstadt) and the Tandatron tandem accelerator (INP, Řež). These accelerators provide ion beams with energies from 0.1 to 11 MeV/u. Further chemical etching was performed using appropriate reagents, depending on the particular material.

### Asymmetric diode-like nanopores

One-sided etching with electro-stopping provides conical nanopores [3]. Asymmetric etching using a surfactant-doped etchant opens up the possibility of creating longitudinal profiles other than conical, i.e., with a degree of taper that varies along the pore [4]. One-sided pre-treatment with ultra-violet radiation and subsequent two-sided etching in the surfactant-doped alkaline solution makes it possible to fabricate pores with a highly-tapered ('bullet-like') pore tip (Figure 1A). In electrolyte solutions, the asymmetric pores with a highly-tapered tip exhibit substantially non-linear current-voltage characteristics (Figure 1C). The formation of nanopores with different tip shapes is based on the interplay between chemical attack by alkali and the protective effect of surfactant. These two components of etching solution diffuse into the pore at different rates. Varying the etchant component concentrations makes it possible to tune the degree of taper and, thus, the ion current rectification properties of the nanopore. Among all of the structures fabricated and tested, the asymmetric bullet-like pores, with a tip radius of 13 to 20 nm and a base radius of 100 to 150 nm, showed the highest rectification. In contrast, the relatively short conical pores that widen too much (see Figure 1B) showed almost symmetric current-voltage characteristics. Therefore, we have found an optimum shape of pores to be used as nanofluidic diodes.

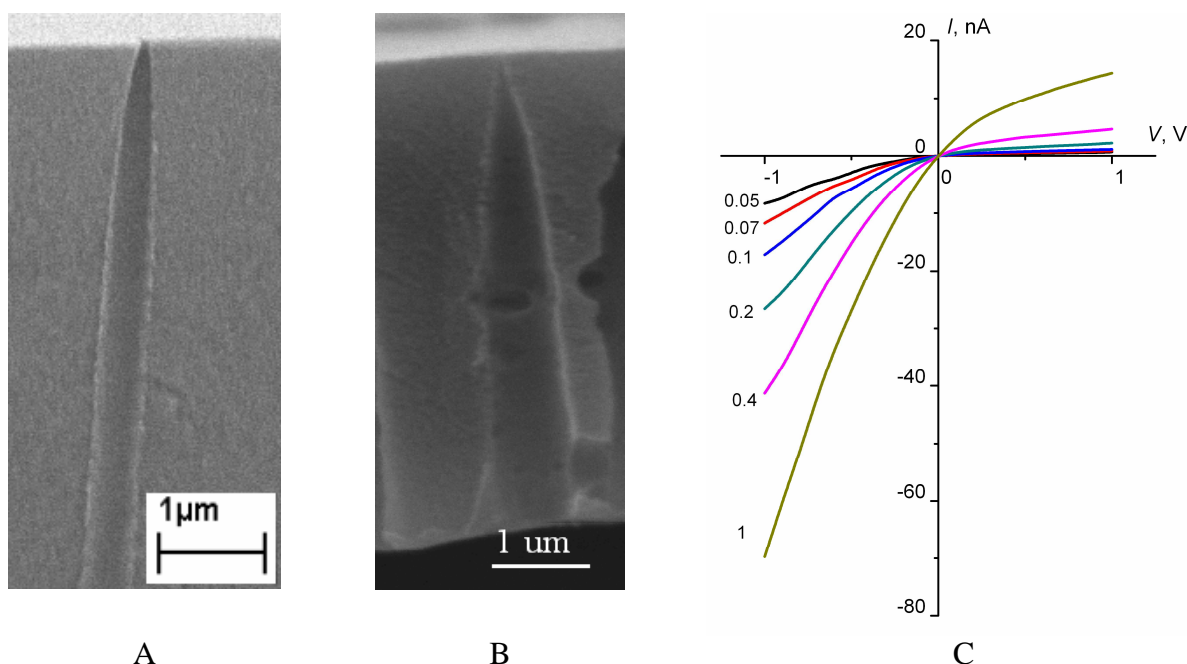


Figure 1. A, B – FESEM images of asymmetric pores in PET foils with a highly-tapered tip and a wide cone angle; C – the I-V characteristics of the pores with the bullet-like tip. The numbers at curves denote KCl concentration. The pore diameter on the upper side of both membranes is 50 nm

### Nanopores in thin inorganic matrices

To provide improved membrane robustness, allow for miniaturisation and integration with other ionic and electronic devices, silicon-based platforms are the perfect choice. Attempts have been made to develop nanopore membranes of silicon oxide and silicon nitride. Silicon nitride is extremely radiation-resistant. We succeeded in getting a satisfactory nanopore structure by irradiating SiN films with particles as heavy as Bi ions at an energy of 710 MeV. The obtained ultrathin freestanding membranes (with a thickness of 200-300 nm, and a pore diameter of 3-100 nm) feature excellent selectivity based on the permeate charge and size [5]. Due to their small thickness, membranes with extremely low diffusion resistance can be fabricated.

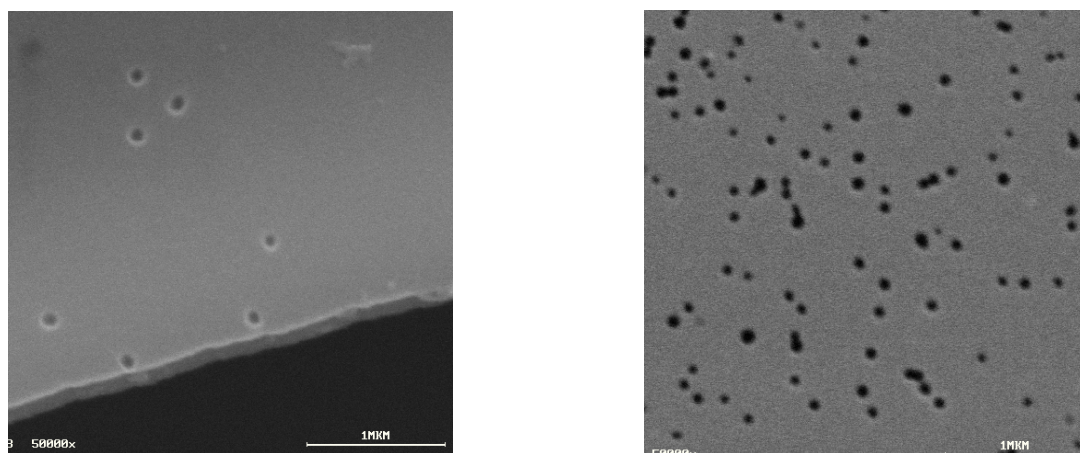


Figure 2. Nanopores in freestanding thin film, with an average diameter of 70 nm. left: SiO<sub>2</sub> irradiated with 1 MeV/u Xe ions and etched in 4% HF at 22°C; right: SiN irradiated by Bi ions and etched in H<sub>3</sub>PO<sub>4</sub> at 143°C

### Regular nanopore arrays

For nanotechnological applications, an array of nano-apertures with a regular spatial distribution is favored, whereas the normal ion irradiation technique distributes ion tracks at random. The microbeam facility at GSI (Darmstadt, Germany) allows a „deterministic“ irradiation

so that a regular pattern of a pre-set number of single tracks, placed at certain distances, is produced [6]. SEM images in Fig. 3 show the appearance of the membranes having conical pores spaced at a 5  $\mu\text{m}$  interval. Due to the highly asymmetrical shape, the narrow pore tips can be considered as pinholes in a thin partition to be used in atomic beam optics and in sensor applications. All the transport characteristics of the membrane can be precisely adjusted either by pore geometry and number of pores.

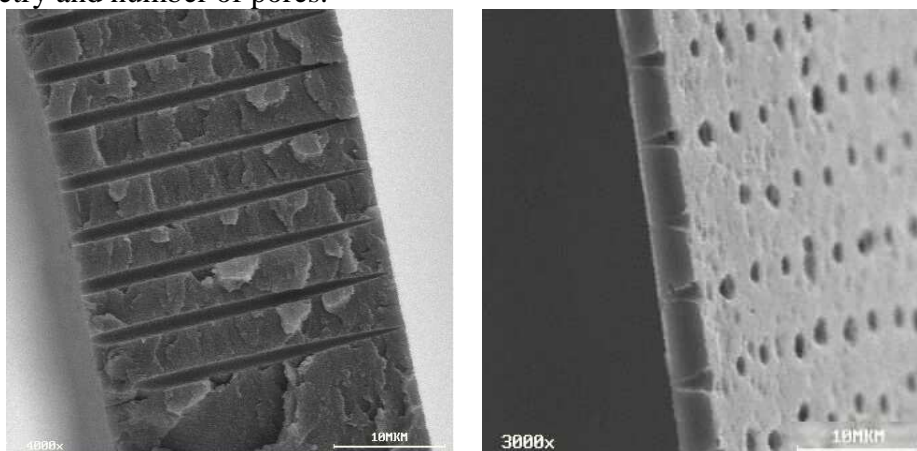


Figure 3. Arrays of regularly distributed conical pores produced using the microbeam irradiation [6] and the asymmetrical etching [4]. Left: polycarbonate foil 28  $\mu\text{m}$  thick; right: PET foil 4  $\mu\text{m}$  thick. The larger pore diameter is about 2  $\mu\text{m}$ , and the smaller pore diameter is about 50 nm in both membranes. The smaller pore diameter is below the observation limit at the magnification used. Scale bars: 10  $\mu\text{m}$

The same principles allow control over the hydraulic resistance of the membrane. The diameter of a wide part of the pores provides for a relatively high flow rate through the membrane, whereas the small diameter of pore necks governs the retention properties. Our study shows that the degree of tapering and, thus, the viscous flow rate can be varied at will [7]. A wide variety of engineered porous membranes, with specific architecture, can be fabricated and used in micro- and nanofluidics.

### References

1. Meares P., Page K.R. Rapid force-flux transitions in highly porous membranes // Philos. Trans. Ser. 1972. V. A272, P. 1-47.
2. Ibanez J.A., Tejerina A.F. Surface Charge Density in Passive Membranes from Membrane Potential, Diffusion Potential and Ionic Permeabilities of the Permeating Species // J. Non-Equilib. Thermodyn. 1982. V. 7. P. 83-94.
3. Apel P.Yu., Y.E. Korchev, Z. Siwy, R. Spohr, M. Yoshida. Diode-like single-ion track membrane produced by electro-stopping // Nucl. Instrum. Meth. Phys. Res. 2001. V. B 184. P. 337-346.
4. Apel P.Yu., I.V. Blonskaya, O.L. Orelovitch, S.N. Dmitriev. Nucl. Instrum. Meth. in Phys. Res. B267, 1023-7 (2009); Apel P.Yu. , Blonskaya I.V., Orelovitch O.L., Ramirez P., Sartowska B.A. Effect of nanopore geometry on ion current rectification // Nanotechnology. 2011. V. 22, 175302 (13 pp).
5. Vlasiouk I., Apel P.Yu., Dmitriev S.N., Healy K., Siwy Z.S. Versatile Ultrathin Nanoporous Silicon Nitride Membranes // Proc. Nat. Acad. Sci. USA. 2009. V.106 P. 21039-44.
6. Fischer B.E., Heiß M. A facility to mass-produce ordered single-hit patterns in continuous 35 mm films // Nucl. Instrum. Meth. in Phys. Res. 2007. V. B 260. P. 442; Voss K.O., Fournier C., Taucher-Scholz G. Heavy ion microprobes: a unique tool for bystander research and other radiobiological applications // New Journal of Physics. 2008. V. 10 075011.
7. Apel P.Yu., Dmitriev S.N. Optimization of pore shape in track membranes. Membrany, 2004. V. 3(23). P. 32-37 (in Russian).

# CARBON MEMBRANES FOR THE TREATMENT OF EFFLUENTS BY ADVANCED OXIDATION PROCESS

<sup>2</sup>Saloua Ayadi, <sup>1</sup>Matthieu Rivallin, <sup>1</sup>Frédéric Gillot, <sup>1</sup>Sophie Cerneaux, <sup>2</sup>Raja Ben Amar, <sup>1</sup>Marc Cretin

<sup>1</sup>IEM (Institut Européen des Membranes), UMR 5635 (CNRS-ENSCM-UM2), Université Montpellier 2, Place E. Bataillon, F- 34095, Montpellier, France. Marc.Cretin@iemm.univ-montp2.fr

<sup>2</sup>Laboratory of Materials Science and Environment, Faculty of Science of Sfax, Sfax, Tunisia

## Introduction

Numerous biological, physical, chemical, photochemical or electrochemical processes were developed for water treatment. Electrochemical processes are particularly interesting because of their relative simplicity and the possibility to generate in situ oxidizing species. Electrochemical techniques are for example used to eliminate organic compounds such as pesticides or dyes via the electro-Fenton reaction in which hydroxyl radicals with a strong oxidizing ability are electro-generated [1]. Two main routes are used to in situ synthesize hydroxyl radicals. The first one is the dioxygen reduction on carbon electrodes to produce hydrogen peroxide which is chemically reduced to hydroxyl radicals by  $\text{Fe}^{2+}$  used as catalysis, according to equation (1).



The second route is water oxidation on boron doped diamond which directly electro-generates radicals because of the high overpotential of oxygen production on this materials. The main drawback of the use of boron doped diamond is the high equipment cost.

For this purpose, we focused our attention on the elaboration of electronic conductive carbon materials to produce porous membranes that will be used as electrodes for the electro-Fenton reaction. Carbon membrane materials are becoming more important in the area of membrane technology due to their high selectivity, permeability and stability in corrosive and high temperature operations [2, 3]. With the aim to develop graphitic porous membranes, we describe here the synthesis and characterization of carbon based tubular supports and their use as contactors for the electro-Fenton reaction.

## Experiments

Different graphite carbon powders (Timcal Corporation, Switzerland) with various particles sizes (25, 44 and 150  $\mu\text{m}$  average particle size) are mixed with a phenol-formaldehyde resin solution and organic additives. The formulation was extruded and treated at different temperatures under nitrogen atmosphere to get first a porous tubular support with a highly uniform porous structure. The composite membrane was analyzed by scanning electron microscopy, X-ray diffraction, Raman spectroscopy, and mercury porosimetry. Conductivity and mechanical resistance were also determined.

First results showed the porosity and the conductivity of the tube which constitutes the support can be sharply controlled depending on the organic additives nature, carbon particles size and carbonization temperature. The optimal carbonization temperature is 1000°C leading to average conductivity values of 10  $\text{ohm}^{-1}.\text{cm}^{-1}$  (Fig. 1).

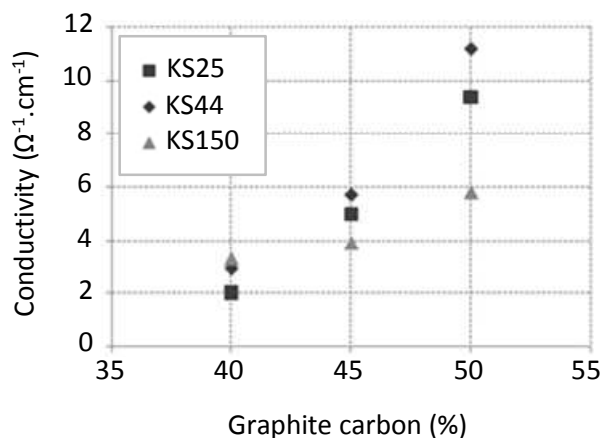


Figure 1. Evolution of the conductivity with the proportion of graphite carbon in membrane material. Three different sizes of carbon powders were used: 25 (KS25), 44 (KS44) and 150  $\mu\text{m}$  (KS150)

This porous carbon tube was then used as support to prepare micro-filtration active layer. The mineral charge used in the formulation developed for the slip casting process is a graphite powder of 4  $\mu\text{m}$  average particle size. Layers of 20  $\mu\text{m}$  thickness with a mean pore size of 0.8  $\mu\text{m}$  were obtained (Fig. 2).

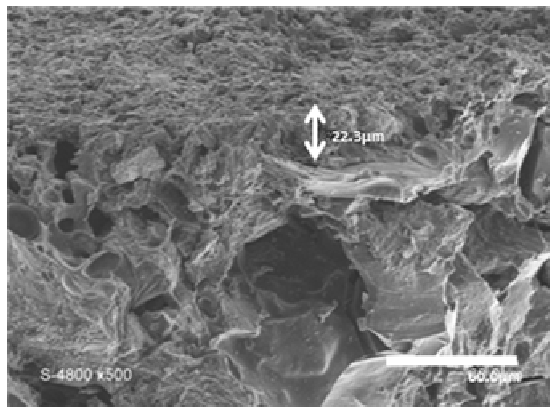


Figure 2. SEM micrograph of porous carbon tube with filtration layer

Performances of the as-prepared porous graphite membranes were determined toward the electro-Fenton reaction. Best chemical and electrochemical conditions to produce hydrogen peroxide were determined.

The Acid Orange 7 (AO7), a common dye, was then used as a model molecule to determine the ability of the membranes to mineralize this pollutant. Spectrophotometric measurements were conducted on the treated solutions as a function of chemical and electrochemical conditions to determine the degradation kinetic of AO7.

Mineralization rate (i.e. the turn of organic carbon to inorganic carbon) was also measured as a function of time (Fig. 3).

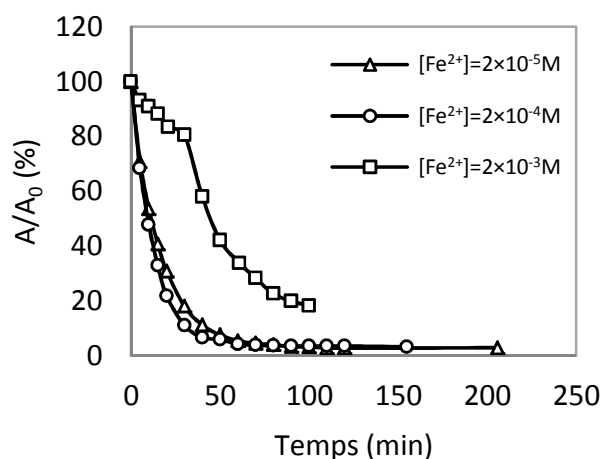
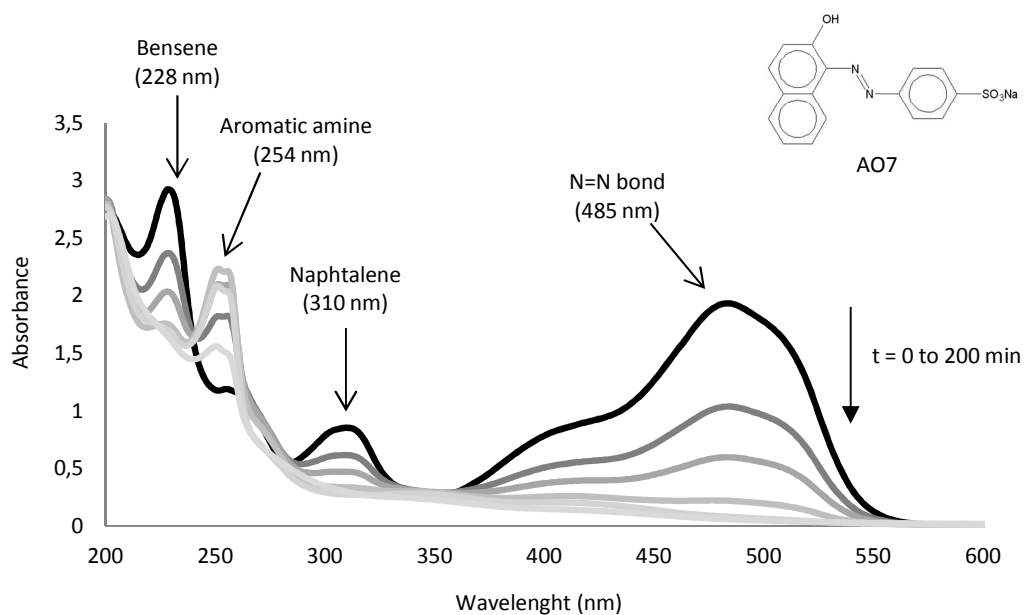


Figure 3. Decolorization of AO7 solution during electro-Fenton process with porous graphite membrane

A total decolorization of AO7 solution at 10<sup>-5</sup> M was recorded after 40 minutes in the best conditions. Nevertheless the total mineralization of the dye was not effective after several hours.

Figure 4 presents the evolution of the UV/Vis spectrum of AO7 solution during the electro-Fenton process with carbon membrane. All the peaks can be attributed to different molecule groups. The TOC (total organic carbon) is due to the slow degradation of aromatic rings (228, 254 and 310 nm).



*Figure 4. Evolution of AO7 solution during electro-Fenton process with porous graphite membrane*

This study shows that porous graphite membranes can easily be used as electrode in an advanced oxidation process, the electro-Fenton process. Work in progress consists in the optimization of this process via (i) the optimization of the electrochemical and chemical conditions, (ii) the study of the relation between structure and properties of the membrane material and (iii) the optimization of the membrane material elaboration.

#### References

1. Chemical Reviews. 109 (2009) 6570-6631.
2. Ceramics International 35 (2009) 2747-2753.
3. Journal of Hazardous Materials 172 (2009) 152-158.

# FLUORAN-TYPE COMPOSITE MATERIALS ON THE BASE OF PERFLUORINATED POLIMERS AND POLYANILINE. FROM SYNTHESIS TO APPLICATION

<sup>1</sup>Ninel Berezina, <sup>2</sup>Sergey Timofeev, <sup>1</sup>Natalya Kononenko, <sup>1</sup>Olga Dyomina,  
<sup>3</sup>Anna Sytcheva, <sup>1</sup>Svetlana Shkirskaya, <sup>1</sup>Irina Falina, <sup>1</sup>Mariya Kolechko,  
<sup>1</sup>Mariya Chernyaeva, <sup>1</sup>Natalya Loza, <sup>1</sup>Sergey Dolgoplov

<sup>1</sup>Kuban State University, Krasnodar, Russia, E-mail: ninel\_berezina@mail.ru

<sup>2</sup>JSC "Plastpolymer", St. Petersburg, Russia

<sup>3</sup>Institute of Materials Science, University of Miskolc, Miskolc, Hungary, E-mail: kubaisy@mail.ru

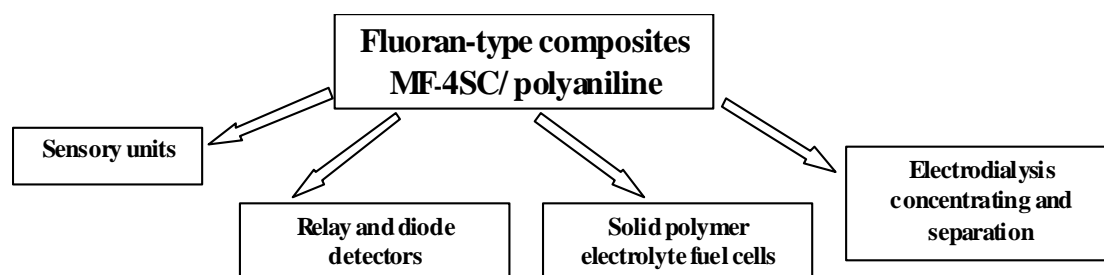
The investigations of synthesis and properties of composite membranes MF-4SC/polyaniline (Flourans) are carrying out in Membrane Materials Laboratory study of Physical Chemistry Department, Kuban State University. Variety of the synthesis conditions permits to elaborate a number of preparation methods, which allow to obtain 8 different type of surface and bulk-modified by polyaniline MF-4SC composite membranes. Physico-chemical properties and electrochemical behavior have been studied with help of up-to-date experimental techniques such as Atomic Force Microscopy, Electron Scanning Microscopy, Differential Scanning Calorimetry, membrane conductometry, voltammetry and electroosmosis. New effects of PAN influence on the nanostructure of flouropolymer membranes are:

- evolution of morphological and transport properties in relation with PAn localization in fluorocarbon matrix nanostructure;
- the peculiarities of transport properties in dependence on membrane orientation by polyaniline layer to ions and water fluxes;
- the varying of parameters of current-voltage curves and etc.

The scale of ratio between diffusion and conductive properties and structure of composites is represented.

The description of conductivity, diffusion, electroosmotic properties of composites are performed with help of micro-heterogeneous and three conductive model approaches, percolation theory and others. The set of parameters that reveal interaction between structure and transport properties is offered.

The effects of PAn influence on composite characteristics are used to evaluate application fields for composites family obtained. The barrier properties of surface-modified membranes towards water transference are employed to increase electro dialysis concentrating efficiency. Composites with asymmetric diffusion permeability in which PAn intercalation leads to hydrophility and proton conductivity stabilization and thermostability increase can be used for application in membrane-electrode assemblies of polymer electrolyte fuel cells. There is the ability to select fluoran-type composites conductivity in range from 0.15 to 5 S/m by means of synthesis conditions fitting. The bipolar function of surface modified membrane in polarization conditions due to the presence of interpolymer complex between  $\text{SO}_3^-$ -groups and nitrogen-containing aromatic chains of PAn was discovered. Pan intercalation causes 'locking' effect to proton flux and could be applied for membrane switches and diode devices. Anion-exchange function of PAn layer on the surface of non-charged perfluorinated matrix can be used as pH-sensor.



*The authors are thankful to the Russian Foundation for Basic Research for financial support (project No 10-08-00758)*

## References

1. *Berezina N.P., Kubaisy A.A.-R., Alpatova N.M., Andreev V.N., Griga E.I.* // *Electrochimiya*. 2004. V. 40. №3. P. 333-341.
2. *Loza N.V., Kononenko N.A., Shkirskaya S.A., Berezina N.P.* // *Electrochimiya*. 2006. V.42. №8. P. 907-915.
3. *Berezina N.P., Kubaisy A.A.-R.* // *Electrochimiya*. 2006. V. 42. №1. P. 91-99.
4. *Berezina N.P., Kubaisy A.A.-R., Timofeev S.V., Karpenko L.V.* // *Journal of Solid State Electrochemistry*. 2006. DOI 10.1007/s10008-006-0159-2. P.1-12.
5. *Kubaisy A., Smolka R., Sukhatskiy A.* // *Desalination*. 2006. Vol. 200. P. 443-445.
6. *Loza N.V., Berezina N.P., Kononenko N.A., Shkirskaya S.A.* // *Izvestiya Vuzov. Northern Caucasus region. Natural Science. Application*. 2006. № 2. P. 51-58.
7. *Berezina N.P., Schirskaya S.A., Sytcheva A.A.-R., Krishtopa M.V., Timofeev S.V.* // *Sorbition and chromatographic processes*. 2007. V.7. №.4 P. 544-547.
8. *Compan V., Riande E., Fernandez-Carretero F.J., Berezina N.P., Sytcheva A.A.-R.* // *Journal of Membrane Science* 2008, V. 318, P. 255-263.
9. *Berezina N.P., Schirskaya S.A., Sytcheva A.A.-R., Krishtopa M.V.* // *Kolloidny jurnal*. 2008. V.70. №4. P.437-446
10. *Berezina N.P., Gnusin N.P., Dyomina O.A., Annikova L.A.* // *Electrochimiya*. 2009. V.45, № 11. P. 1325-1332.
11. *Berezina N.P., Kononenko N.A., Sytcheva A.A.-R., Loza N.V., Shkirskaya S.A., Hegman N., Pungor A.* // *Electrochimica Acta*. 2009. V.54. P. 2342-2352.
12. *Compan V., Molla S., Sytcheva A.A.-R., N.P. Berezina, Suarez K., Solorza O, Riande E.* // *The Electrochemical Society*. 2009. V.25. P.645-658.
13. *Sytcheva A.A.-R., Falina I.V., Berezina N.P.* // *Electrochimiya*. 2009. V.45. № 1. P. 114-121.
14. *Filippov A.N., Iksanov R.H., Kononenko N.A., Berezina N.A., Falina I.V.* // *Kolloidny jurnal*. 2009. V. 72. № 2. P. 238-250.
15. *Berezina N.P., Kononenko N.A., Filippov A.N., Shkirskaya S.A., Falina I.V., Sytcheva A.A.-R.* // *Electrochimiya*. 2010. V. 46, №5. P. 515-524
16. *Protasov K.V., Shkirskaya S.A., Berezina N.P., Zabolotsky V.I.* // *Electrochimiya*. 2010. V. 46, № 10. P. 1209-1218.
17. *Falina I.V., Berezina N.P.* // *Polymer Science. Series B*. 2010, V. 52, No 34, P. 244-251.
18. *Berezina N., Falina I., Sytcheva A., Shkirskaya S., Timofeyev S.* // *Desalination and Water Treatment*. 2010. V.14. P. 246-251.
19. *Munar A., Suarez K.; Solorza O; Berezina, N.P., Compan V.* // *J Electrochemical society* 2010. V. 4.
20. *Berezina N.P., Schirskaya S.A., Kolechko M.V., Popova O.V., Sentchichin I.N., Roldugin V.I.* // *Electrochimiya*, 2011, V.47, № 9. P. 1066-1077.
21. *Kolechko M.V., Schirskaya S.A., Berezina N.P., Timofeev S.V.* // *Sorbition and chromatographic processes*. 2011, V. 11, № 5, P. 663-672.
22. *Kolechko M.V., Schirskaya S.A., Berezina N.P.* // *Kuban Science*. 2012. №3. P. 11-16.
23. *Falina I.V., Berezina N.P., Sytcheva A.A.-R., Pisarenko E.V.* // *Journal of Solid State Electrochemistry*. 2012. V. 16, №5. P. 1983-1991.

## Patents

1. *Schirskaya S.A., Sytcheva A.A.-R., Berezina N.P., Timofeev S.V., Krishtopa M.V.* Patent RF №2411070 Composite ionexchange membrane Published 10.02.2011. Priority 18.08.2009r.
2. *Berezina N.P., Schirskaya S.A., Kolechko M.V., Timofeev S.V.* Patent RF №111775 Multilayered composite membrane Published 27.12.2011. Priority 03.05.2011r.
3. *Berezina N.P., Schirskaya S.A., Kolechko M.V., Timofeev S.V.* Invitation application № 2011117676 Method of multilayered composite membrane preparation. From 03.05.2011.
4. *Berezina N.P., Schirskaya S.A., Kolechko M.V., Timofeev S.V.* Invitation application № 2012113799 Method of preparation of composite membrane with fixed polyaniline layer thickness. From 06.04.2012.

# MICROCRYSTALLINE STRUCTURES FORMATION UNDER SUPERSATURATED $\text{HIO}_3$ SOLUTION FLOW THROUGH TRACK MEMBRANE PORES

Vladimir Berezkin, Alexander Vasiliev, Vladimir Artiomov, Nickolas Kiseliy, Boris Mchedlishvili

Shubnikov Institute of Crystallography RAS. Moscow, Russia, E-mail: [berezkin38@mail.ru](mailto:berezkin38@mail.ru)

## Introduction

The track membranes (TM) was shown to be effective in the some processes of the liquid and gas mixtures separation [1-3]. The results of investigations devoted to TM application in template nanostructures formation are published permanently in last decade [4]. Particularly, it was shown the metallic nanostructures of extended surface formation possibility with metal plating in TM pores [5-6]. On our opinion, it is very interesting to investigate the water-soluble crystal nanostructures formation with TM ability as these structures can possess with special properties as compared with macrocrystalline ones.

## Experiments

The goal of investigation was the process of the acid  $\text{HIO}_3$  microchips formation in the TM pores. The  $\text{HIO}_3$  crystals are optically active and the ones can be used in the light high harmonics generation. The acid  $\text{HIO}_3$  is applied in acoustic line of optoacoustical equipment generation, in medicine, in definition of carbon monoxide microquantities, in gas mask as absorber.

The SEM microscope JSM-740 1F was applied to get microphotographics of the TM surface and cleavage. Prior investigations have shown that ordinary membrane staying in supersaturated solution (supersaturation was around 20 %) didn't result in crystals formation in TM pores. Apparently, it was stipulated with depletion of crystallization solution in boundary layer. The flow of supersaturated  $\text{HIO}_3$  solution through TM pores in the dead-end filtration cell (Fig. 1) was used to realize the supersaturated solution supply to crystallization centers at TM pores surface.

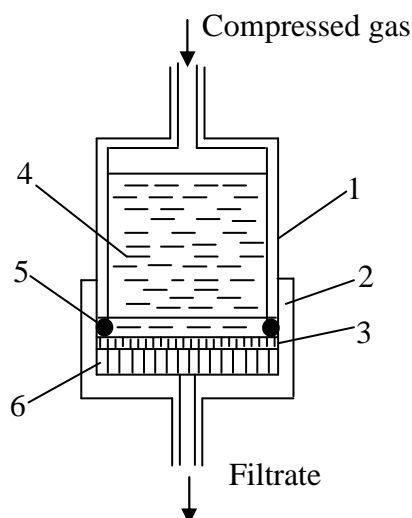


Figure 1. Filtration cell scheme: 1 – cell body; 2 – cell base; 3 – track membrane; 4 –  $\text{HIO}_3$  supersaturated solution; 5 – silicone gasket; 6 – macroporous substrate

TM with pore diameter of 110 nm and surface pore density  $10^8 \text{ cm}^{-2}$  were used in experiments.

The membrane was putted on macroporous substrate and pressurized with silicone gasket. The  $\text{HIO}_3$  supersaturated solution was embedded in the cell and forced through TM with compressed nitrogen under transmembrane pressure of  $0.4 \text{ kgf/cm}^2$ . Te experiments are executed under room temperature. The supersaturation varied from 10 % up to 22 %.

## Results and Discussion

Crystallization process qualitatively different stages was shown to be registered under solution concentration increase with step of 1.5–2 %. Transition from lack of microchips falling-out in TM pores to partial covering of pore walls with microchips was observed at first (Fig. 2). The microchips overlapped the pores considerably and solution flow through membrane decreased under solution supersaturation increase up to 16 % (Fig. 3).

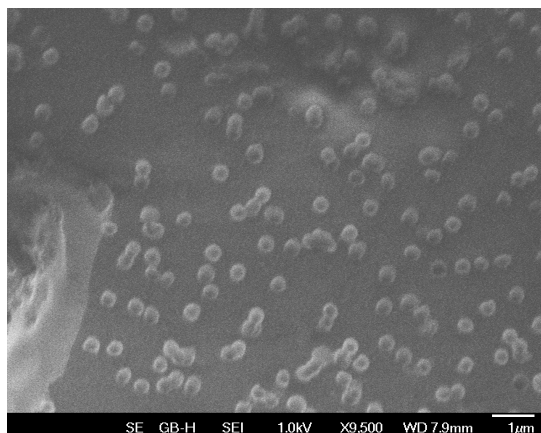


*Figure 2. First stage– microchips cover the TM pore walls*

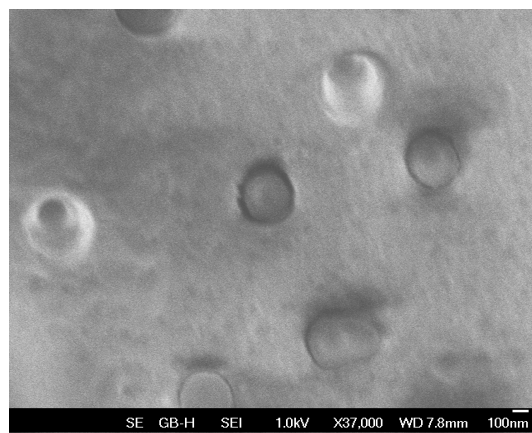


*Figure 3. Second stage – TM pores overlapped with microchips*

Greater supersaturation (up to 20 %) resulted in long microchips formation on both sides of membrane. It must be noted that formed microchips were longer at the membrane side faced to solution flow. Effect of microchips growth was weaker at the membrane opposite side. Apparently it was result of the solution depletion in growth zone stipulated with pore overlapping and solution flow decrease. Cross sizes and direction of microchips corresponded to the ones of membrane pores (Fig.4). The formed microchips cutting correspond to  $\text{HfO}_3$  crystallographic one. The founded crystallization process was shown to be mass one. It covered considerable membrane surface (Fig.5).

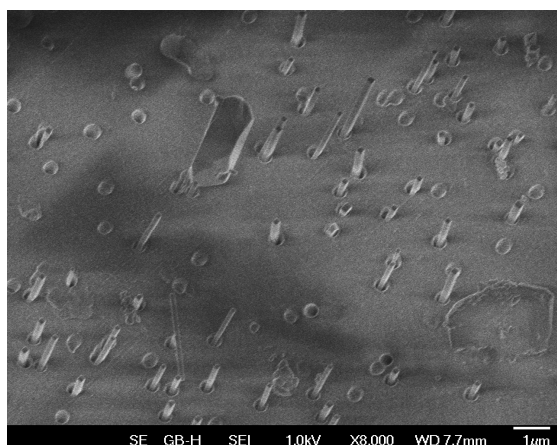


*Figure 4. Third stage – the microchips formed in the pores arise above TM surface*

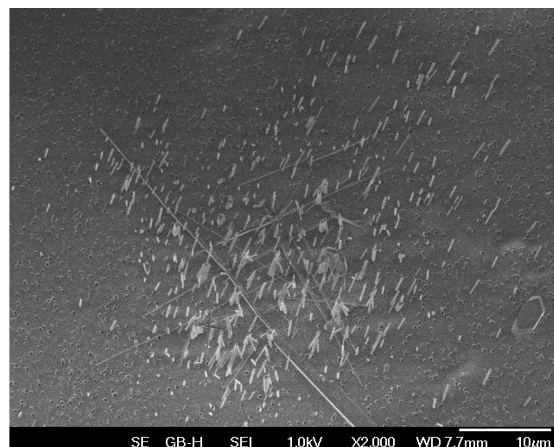


*Figure 5. The evidence of the microchips formation mass character*

Microphotography of track membrane cleavage prove the pores role in observed mass crystallization phenomena (Fig.6). This photo was performed with element composition attachment. Iodine content is highlighted with white colour.

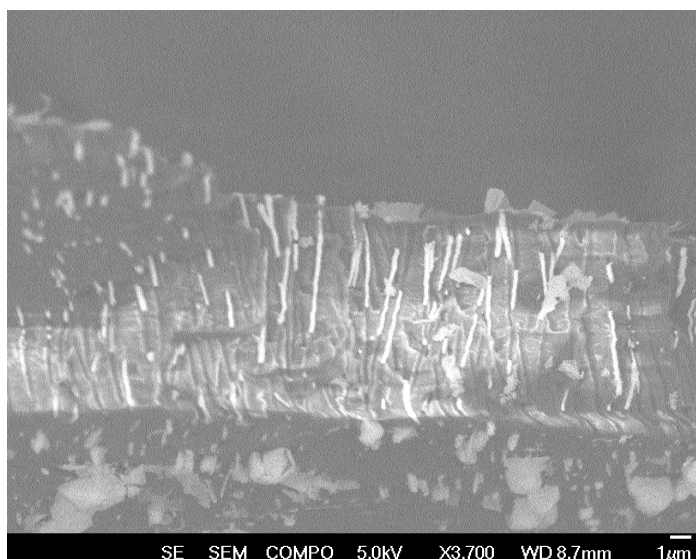


Figure 6. The TM cleavage reveals the pore function in microchips formation

Presented investigation results have proved that supersaturated crystallization solution filtration through track membrane pores results in formation of monocrystalline structures with cross sizes and direction corresponding to the pore ones.

#### References

1. *Mchedlishvili B.V., Beriozkin V.V., Oleinikov V.A., Vilensky A.I., Vasilyev A.B.* Structure, physical and chemical properties and applications of nuclear filters as a new class of membranes // *J. Memb. Sci.*, 1993, V.79, P.285
2. *Berezkin V.V., Nechaev A.N., Mchedlishvili B.V.* The track membranes as a model porous system for the investigation of the polyvalent electrolyte solutions separation. // *Radiation Measurements*, 1995, Vol. 25, N 1-4, P. 703-707.
3. *Mchedlishvili B.V., Berezkin V.V., Vasiliev A.B. et al.* Problems and prospects of nanomembrane technology development. // *Crystallography*. 2006. V.51. No 5, P. 906-919 (in Russian).
4. *Ferain E., Legras R.* Track-etch templates designed for micro- and nanofabrication // *Nucl. Instr. Meth.Phys.Res.* 2003. V. B 208. P. 115-122.
5. *Baranova L.A., Baryshev S.V., Gusinskii G.M., Konnikov S.G., Nashchekin A.V.* Nickel field-field emission microcathode: art of fabrication, properties and application // *Nucl. Instr. Meth. Phys. Res.* 2010. V. B 268. P. 1686-1688.
6. *Mitrofanov A.V., Tokarchuk D.N., Gromova T.I., Apel P.Yu., Didyk A.Yu.* Fabrication of metal micritubes using particle track membranes processing // *Rad.Meas.* 1995. Vol.25. No 1-4, P. 733-734.

# INVESTIGATION OF DIMETHYLACETAMIDE AND ISOBUTYL ALCOHOL INFLUENCE ON THE OBTAINING LITHIUM HYDROXIDE BY ELECTRODIALYSIS WITH BIPOLAR MEMBRANES FROM TECHNOLOGICAL SOLUTIONS

Olga Bessmertnaya, Nikolai Shel'deshov, Viktor Zabolotsky

Kuban State University, Krasnodar, Russia, E-mail: kirpichenko@inbox.ru

## Introduction

The necessity of technological solutions' neutralization containing dimethylacetamide, isobutyl alcohol, lithium chloride, hydrochloric acid and water for producing paraaramide fibers appears in industry. Electrodialysis with bipolar membranes allows reagent-free producing hydrochloric acid and alkali from solution containing lithium chloride instead of consumption of lithium hydroxide. As a result the cost of paraaramid fibers is reduced. Information about the characteristics of electro dialyzer-synthesizer (EDS) in the processing of aqueous-organic solutions is required for determination of the optimum operating conditions of industrial electromembrane device. The purpose of this work was the determination of the basic electrochemical characteristics of the laboratory EDS designed to obtain the lithium hydroxide from solution of lithium chloride and comparison of the process characteristics depending on the composition of technological solution.

## Experiments

In this work the electrodialysis process of lithium hydroxide and hydrochloric acid obtaining from the aqueous-organic solutions was studied. Compositions of these solutions are given in the Table 1.

**Table 1: The chemical composition of the initial of technological solutions**

Technological solution	Concentration of components			
	DMAA, %	IBA, %	H <sub>2</sub> O, %	LiCl, M
1	0	0	98,7	0,3
2	24.9	24.1	49.8	0.3
3	40.6	38.10	20.0	0.3

Effective area of each membrane in electro dialyzer-synthesizer was 1 dm<sup>2</sup>, the intermembrane distance was 0.9 mm, the width of the working membrane area was 5 cm, length–20 cm. Chambers were filled with net-shaped separator for prevention of membranes bending due to pressure difference between chambers and in order to increase the limiting electrodiffusion current at the membranes as a result of the decrease of the thickness of diffusion layers near the membranes. Free volume of each chamber filled with separator was 80% of the chamber volume. Industrial heterogeneous MB-3 bipolar membranes, MC-40 cation-exchange membrane and MA-40 anion-exchange membranes were used in the membrane stack of electro dialyzer-synthesizer (Fig. 1). During investigation of the process the density of supplied electric current was 1 A/dm<sup>2</sup>.

In order to investigate the main electrochemical characteristics of EDS the device (Fig. 1), that allows to determine current efficiency of lithium hydroxide and hydrochloric acid, specific productivity and specific power consumption of EDS on lithium hydroxide and hydrochloric acid was used. Investigation of electro dialyzer-synthesizer electrochemical characteristics was made in a circulation mode.

Current density, which was used in the experiments (1 A/dm<sup>2</sup>, galvanostatic regime), was less than the maximum electrodiffusion current density at the membranes, which constrain the chamber 4. The difference of potentials across the membrane MC-40 and MA-40 was measured out using capillaries Luggin – Haber, which were filled with solutions, the composition and concentration which coincided with the composition and concentrations of solutions in contact with the membrane. The capillaries were connected to silver chloride electrodes.

Differential current efficiency  $\eta$  (Fig. 3a), specific power consumption  $W_{sp}$  (Fig. 3b) and specific productivity  $P_{sp}$  (Fig. 3c) of EDS on lithium hydroxide and hydrochloric acid were calculated from the formulas:

$$\eta = \frac{FV}{nI} \frac{dn}{d\tau}, W_{sp} = \frac{FU_{un.cell}}{\eta}, P_{sp} = \frac{V}{nS} \frac{dn}{d\tau},$$

where  $F$ –Faraday number, C/mole;  $n$ –number of unit cell, pcs,  $V$ –volume of treated solution, L;  $I$  –EDS supplied current, A;  $U_{un.cell}$ –unit cell voltage, V;  $S$ –effective area of membrane, m<sup>2</sup>. The dependence of amount of lithium hydroxide and hydrochloric acid (Fig. 2) in the contours of chambers 2 and 3 on the time  $\tau$  was approximated by second-degree polynomial.

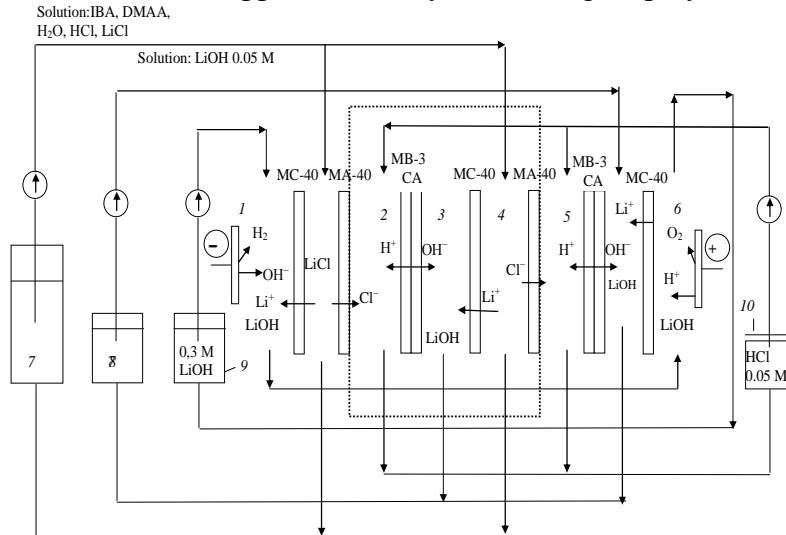


Figure 1. Scheme of electromembrane device for testing of EDS, intended for reagent-free producing from lithium chloride, contained in the solution, lithium hydroxide, used for neutralizing the technological solution. 1 – cathodic chamber; 2 – acidic chamber; 3 – alkaline chamber; 4 – salt chamber; 5 – acidic chamber; 6 – anodic chamber; 7 – volume with spent neutralized technological solution, which passed micro-filtration; 8 – reservoir with solution, in which lithium hydroxide is accumulated; 9 – reservoir with lithium hydroxide solution, which circulates through the electrode chambers; 10 – reservoir with solution, in which hydrochloric acid is accumulated

### Results and Discussion

Fig. 2 and 3 shows that the rate of accumulation and differential current efficiency of lithium hydroxide and hydrochloric acid in alkaline 3 and acid 2 circuits are close. The differential current efficiency of alkali and acid reduces when its concentrations increase due to increasing of co-ions transport numbers through the bipolar, cation-exchange and anion-exchange membranes. Current efficiency of acid is always lower than alkali regardless of technological solution composition. It may be related with acid consumption on protonation of secondary and tertiary groups of MA-40 anion-exchange membrane while acid's accumulation in the solution, circulating through chamber 2. The decrease of differential current efficiency of acid and alkali results in reduce of EDS productivity and increase of power consumption.

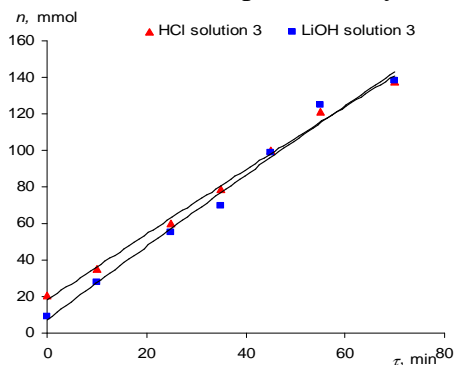


Figure 2. Dependence of amount of lithium hydroxide and hydrochloric acid, produced in the electro-dialyzer-synthesizer from solution 3 on time

The table 2 shows that current efficiency of acid and alkali and specific productivity of EDS is greater but specific energy consumption is smaller if initial solution is 1. Increase of specific energy consumption in salt solution with increasing concentration of organic compounds

(solutions 2 and 3) is explained by reduction of electrical conductivity of solution, thereby increasing the voltage at the unit cell.

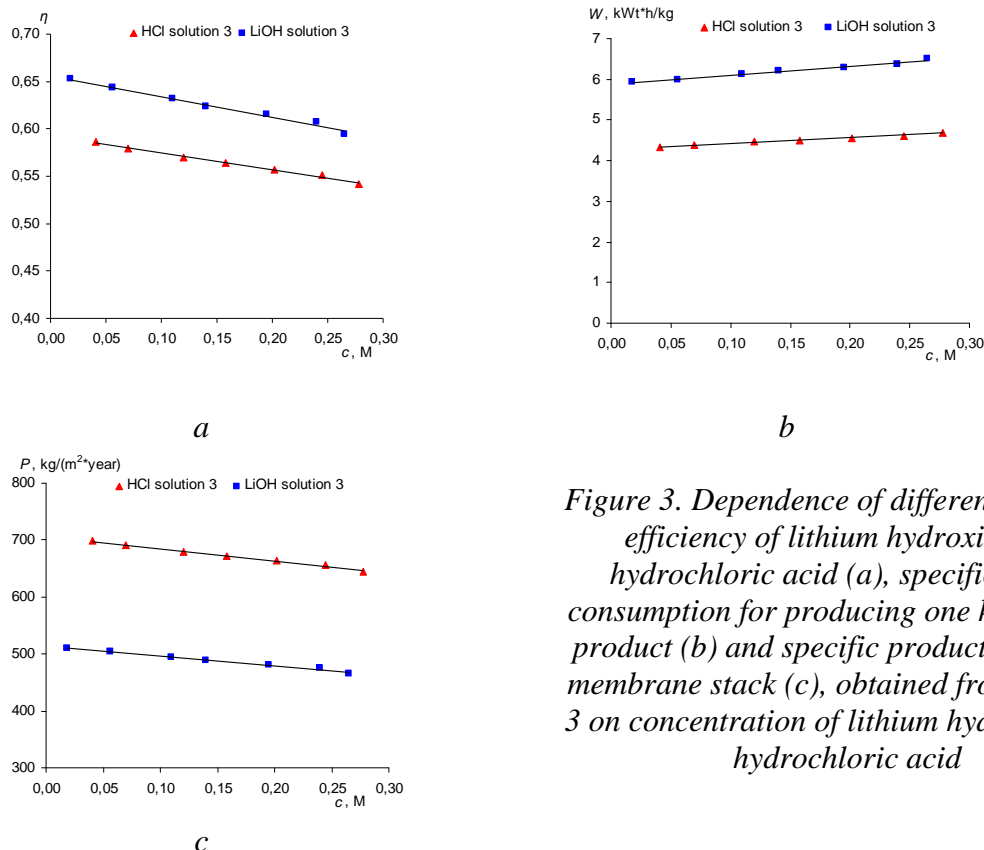


Figure 3. Dependence of differential current efficiency of lithium hydroxide and hydrochloric acid (a), specific power consumption for producing one kilogram of product (b) and specific productivity of the membrane stack (c), obtained from solution 3 on concentration of lithium hydroxide and hydrochloric acid

Reduction of the current efficiency of acid and alkali and specific productivity of EDS is due to both a decrease in the transport numbers of counter-ions through the cation-exchange and anion-exchange membranes in consequence of an increase the rate of dissociation of water molecules at the membrane–solution boundary and the influence of organic components on the structure of the cation- and anion-exchange membranes. As a result transport numbers of co-ions across membranes are increasing and current efficiency is reducing.

**Table 2: The average values of the electrochemical characteristics of the EDS measured using 1 – 3 solutions**

Technological solution	$\eta$ (HCl)	$\eta$ (LiOH)	$P_{acid}$ , kg/(m <sup>2</sup> *year)	$P_{alc}$ , kg/(m <sup>2</sup> *year)	$W_{acid}$ , kWt*h/kg	$W_{alc}$ , kWt*h/kg
1	0,620	0,640	742	520	1,34	1,54
2	0,589	0,630	702	500	1,57	2,30
3	0,564	0,623	672	489	4,50	6,20

### Conclusions

The use of electrodialysis with bipolar membranes allows obtain lithium hydroxide and hydrochloric acid from the aqueous-organic solutions of lithium chloride with different content of organic components with comparable current efficiency. Specific power consumption of electrodialysis process increases when content of organic compounds in solution increasing. Investigated electrodialysis process of obtaining lithium hydroxide from lithium chloride using a bipolar membrane is a basis for the complex industrial electromembrane technology for reagent-free neutralization of spent technological solution with further removing of lithium chloride by electrodialysis and its concentration. Basic electrochemical characteristics of EDS allows to evaluate the cost-effectiveness of implementing the method of reagent-free neutralization

*This work was supported by Foundation for Assistance to Small Innovative Enterprises in Science and Technology, State Contract № 8665p/13954 and grant of RFBR № 09-03-96527 r\_yug\_a.*

## MEMBRANES IN MEMRISTOR'S STRUCTURES

<sup>1</sup>David Bilenko, <sup>1</sup>Victor Galushka, <sup>1</sup>Inna Mysenko, <sup>1</sup>Konstantin Razumov,  
<sup>1</sup>Denis Uchaikin, <sup>1</sup>Aleksandr Smirnov, <sup>1,2</sup>Denis Terin

<sup>1</sup>Saratov State University, Saratov, Russia, *E-mail: bil@sgu.ru*

<sup>2</sup>Engels Technological Institute of Saratov State Technical University, Engels, Russia,  
*E-mail: terinden@mail.ru*

### Introduction

Increasing information content stimulates the search of new principles of information storage and transformation. Structures with memristor effect [1] are of great interest. Works [2, 3] show the possibility of creation of switching devices with memory and logic elements using solid-state electrolyte on the argentum halogenide basis. The principle of these structures operation is based on changing conductance of tunnel gap by mass transfer and oxidized/reduction reaction on the borders of ionic conduction layers

### Experiments

We have seen the opportunity of application vacuum tunnel-thin barrier instead of membrane from organic dielectric (polystyrene) layers and porous silicon (PS). Porous silicon layers were produced both by an electrochemical etching and by aqueous non electrolytic etching method. We observed Ag mass transfer through layers with ionic conduction directly under the electronic beam in SEM effect.

### Results and Discussion

We used as nanometer ionic conduction layers, the layers created by direct iodine vapor interaction with metallic argentum film and nanoparticles AgI coated with PVP shell on metallic argentum film. Figure 1 presents Ag clusters produced under the influence of AgI layers exposure by electronic beam on Ag wafer in SEM.

It has been found experimentally that interaction of iodine vapor with Ag surface leads to creation of non solid films (at starting stage). Mass transfer through discontinuous film is not observed. AgI Nanoparticles consists of AgI core and PVP shell. Nanoparticles interacting with electronic beam produce more solid production of Ag clusters on the surface as compared to AgI films. Thus, Ag transfer through PVP shell is stated.

In our work we have shown the opportunity of creation a switching device with memristors effect on the basis of Ag-AgI-IK-nSi structure. Silicon wafer КЭС – 0.01 (111) and Cr film evaporated on Ag layer function as ohmic contact. Ohmic contacts (square 1 mm<sup>2</sup>) were produced by resistance evaporation method in vacuum.

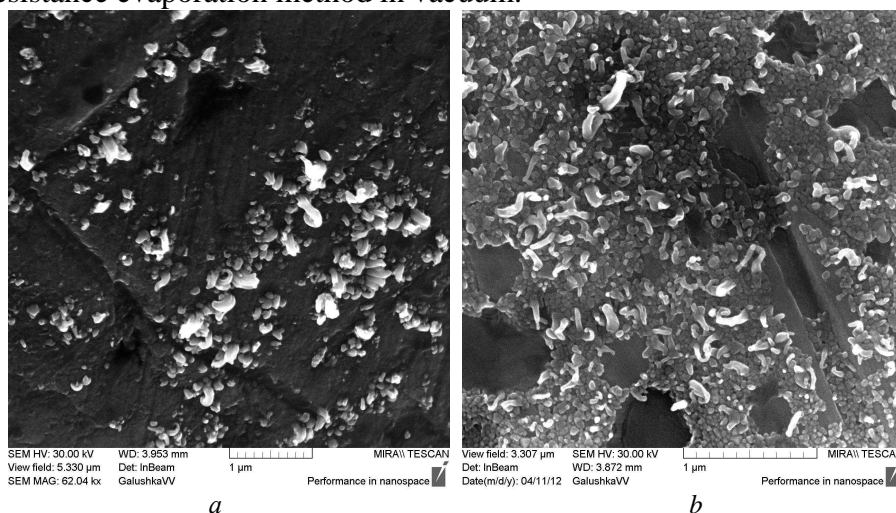


Figure 1. Ag mass transfer in Ag – Ag structures under the effect of electric beam in SEM  
a - AgI nanolayer produced by iodination of Ag, b - AgI nanoparticles in PVP on Ag wafer

Volt-ampere characteristic structure show that resistance is changing from 12 to 1.5 K $\Omega$  under operating voltage less then 1.5V. Voltage is shown concerning Si wafer. Resistance changing are shown with arrows. Threshold voltage switching is less than 1.5V. Current linear dependences from voltage let us not to take into consideration barrier effects rectification on the borders of layers.

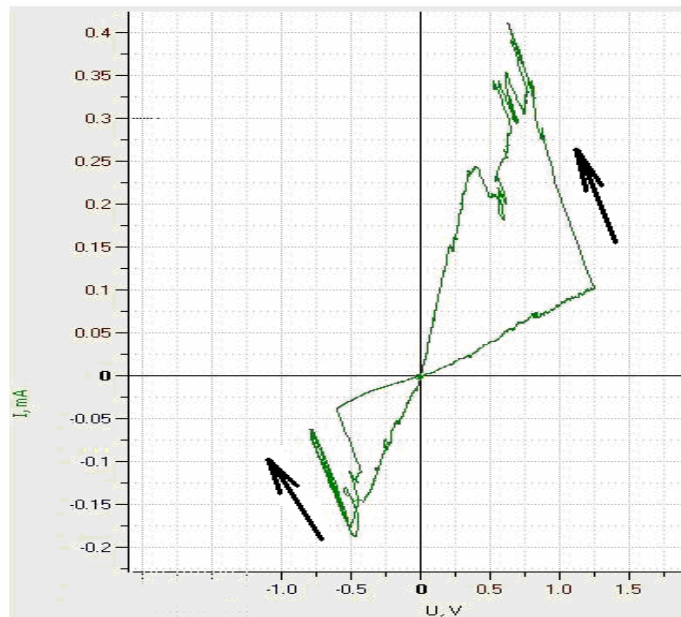


Figure 2. Volt-ampere characteristic structure Ag-AgI-IJK-nSi

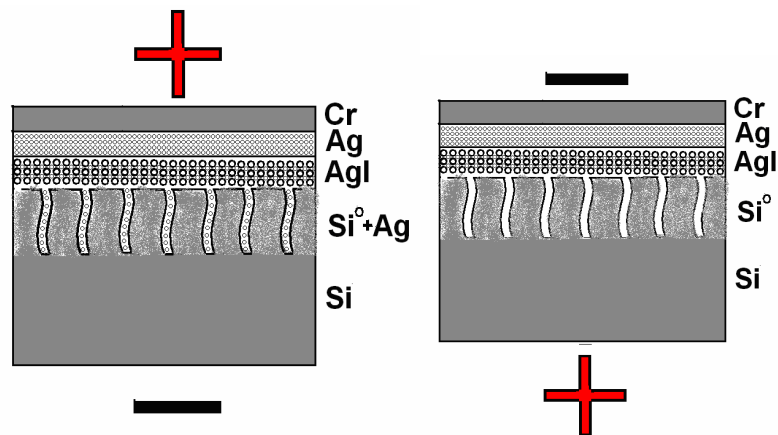


Figure 3. Structures scheme consists of PS layer and Ag-AgI

The produced memristor structure is schematically shown on fig. 3. Reversible resistance change of structure is determined by Ag transfer through ionic conductor and filling or releasing of pore PS layer. Thus, it is shown that porous silicon layers and PVP possess with membrane effect and could be used in structures with reversible ionic mass transfer.

### References

1. Tamura T., Hasegawa T., Terabe K. Switching Property of Atomic Switch Controlled by Solid Electrochemical Reaction, Received January 13, 2006
2. Symanczyk R., Balakrishnan M., Gopalan C., Happ T., Kozicki M., Kund M., Mikolajick T., Mitkova M., Park M., Pinnow C.U., Robertson J., Ufert K.D. Electrical Characterization of Solid State Ionic Memory Elements, <http://enpub.fulton.asu.edu/mitkova/Infineon%20and%20we%20NVMTS03.pdf>
3. Strukov D.B., Snider G.S., Stewart D.R., Williams R.S. The missing memristor found, Nature 453, 80-83 (1 May 2008) |doi:10.1038/nature06932; Received 6 December 2007; Accepted 17 March 2008

# ELECTRODE ACTIVITY OF PERFLUORINATED SULFOCATION-EXCHANGE MEMBRANES

<sup>1</sup>Olga Bobreshova, <sup>1</sup>Anna Parshina, <sup>2</sup>Ekaterina Safronova, <sup>3</sup>Sergey Timofeev,

<sup>2</sup>Andrey Yaroslavtsev

<sup>1</sup> Voronezh State University, Voronezh, Russia, *E-mail: olga1@box.vsi.ru*

<sup>2</sup> Kurnakov Institute of General and Inorganic Chemistry RAS, Moscow, Russia

<sup>3</sup> Plastpolimer, St. Petersburg, Russia

## Introduction

Homogeneous perfluorinated sulfonated cation-exchange polymeric membranes and tubes MF-4SC, which are Russian analogues of Nafion<sup>®</sup>, were used as an electrodoactive material in PD-sensors for the quantitative determination of vitamins and pharmaceuticals in polyionic aqueous solutions and dosage forms [1-4]. The presence of hydrophobic (i.e., polytetrafluoroethylene chains) and hydrophilic (i.e., sulphonate ionic groups) regions in such membranes provides the matrix with labile structural components, which allows for the electrochemical properties of MF-4SC membranes to be controlled by changing the ion-molecular composition of the membranes.

The protolytic and ion-exchange reactions at the interfaces of ion-exchangers and test solutions are potential determining for the PD-sensors. As a consequence, hydrophobicity of the MF-4SC membranes matrix and complete absence of macropores together provides the increasing of analytical signal, sensitivity and accuracy of PD-sensors in comparison with hydrocarbonic membranes. The treatment of MF-4SC membranes with polar organic electrolytes (alcohols, glycols, amides, etc.) leads to inversion of sulphonate ionic groups to the surface, expansion of pores and channels, and an increase in hydration number of ion-exchange groups both in the phase and on the surface of the polymer.

The possibility of use perfluorinated sulfocation-exchange membranes, doped with zirconia, as electrodoactive material of potentiometric sensors, which are sensitive to organic anions in multiionic aqueous solutions was investigated.

## Experiments

Initial and modified membranes MF-4SC were used as an active material in electrode. PSP membranes doped with zirconia were obtained via two methods described in [5].

The individual aqueous solutions of HCl, HNO<sub>3</sub>, KCl and KGly (equimolar solutions of KOH and amino acid glycine with pH ranged from 6.54±0.05 to 11.61±0.05) were investigated for estimation of influence counter- and co-ion nature on the response of PD-sensors.

The aqueous solutions of amino acid cysteine (Cys) and potassium hydroxide (KOH) were investigated for estimation of the possibility of organic and sulfurous anions determination in multiionic aqueous solutions by MF-4SC -based PD-sensors. Such solutions contain excess of KOH (pH ranged from 9.71±0.05 to 13.55±0.05). The ionic composition of such solutions is presented by anions CH<sub>3</sub>COCOO<sup>-</sup>, HS<sup>-</sup>, OH<sup>-</sup> and cations K<sup>+</sup>, NH<sub>4</sub><sup>+</sup>. Analytical concentrations of the various solution components in individual and multiionic solutions ranged from 1.0·10<sup>-4</sup> to 5.0·10<sup>-2</sup> M.

## Results and Discussion

ZrO<sub>2</sub> incorporation into MF-4SC results in the increase of ion conductivity in comparison with unmodified membranes. The highest value of ion conductivity is observed for the MF-4SC modified with 5 wt.% of ZrO<sub>2</sub>. Conductivity value amounts to 6.5·10<sup>-2</sup> Ohm<sup>-1</sup>sm<sup>-1</sup> at 25°C that is 0.5 order of magnitude higher than conductivity of initial membranes. Moreover MF-4SC modification results in the decrease in the value of the conductivity activation energy from 13.7±0.2 kJ/mol for unmodified membranes to 10-12 kJ/mol for modified membranes.

Diffusion coefficients of MF-4SC membranes doped with 5 and 7 wt.% ZrO<sub>2</sub> in 0.1 M NaCl solution amount to (7.00±0.05)·10<sup>-8</sup> cm<sup>2</sup>/s, (9.41±0.05)·10<sup>-9</sup> cm<sup>2</sup>/s, accordingly that is lower for the initial membrane ((7.00±0.05)·10<sup>-8</sup> cm<sup>2</sup>/s) correspondingly. Cations diffusion rate is greatly

higher than anions diffusion rate in the membranes. Thus diffusion permeability is limited by the anion diffusion rate. Thus zirconia incorporation results in the considerable selectivity increase.

It was shown, that sensitivity of PD-sensor based on MF-4SC with gradient zirconia distribution to counter-ions decreases insignificantly in comparison with unmodified MF-4SC - based PD-sensor. The use of membrane with gradient  $ZrO_2$  distribution for PD-sensor organization leads to significant contribution of anions into analytical signal of sensor in contrast to unmodified samples. It is important to note, that coefficients of calibration equations, which define sensitivity of sensor calibration to cations and anions, have opposite sign.

The difference in electrochemical behaviour of unmodified and modified with  $ZrO_2$  MF-4SC, samples depends on next factors. Firstly, concentration of available cation-exchange fixed groups of membrane ( $-SO_3H$ ) decreases after  $ZrO_2$  incorporation due to reduce of free volume of pores and channels. Secondly,  $ZrO_2$  particles in modified membranes display both cation- and anion-exchange properties [5]. So co-ions concentration near modified MF-4SC/ test solution of electrolyte interface increases in comparison with initial membranes. This allows to increase sensitivity of gradient modified MF-4SC -based PD-sensors to co-ions in aqueous solutions. The influence of co-ions nature on the response of uniform distribution modified MF-4SC - based PD-sensors is insignificant. The reason of this is that co-ions concentration gradients on the MF-4SC/ test solution and MF-4SC/reference solution interfaces are oppositely directed and compensate each other.

Obtained results evidences of the possibility of use modified  $K^+$ -type MF-4SC samples with gradient on the length  $ZrO_2$  distribution as electrodoactive material in PD-sensors, which are sensitive to organic anions in aqueous solutions. Such PD-sensors with set of ion-selective electrodes can be used for determination of organic and sulfurous anions in multiionic aqueous solutions.

#### Acknowledgements

*This work was financially supported by the RFBR (projects 12-08-00743-a and 11-08-93105).*

#### References

1. Bobreshova O.V., Parshina A.V., Agupova M.V., Timofeev S.V. RF Patent 2376591, 2009, Byull. izobret., 2009, no. 35, 6 p.
2. Bobreshova O.V., Parshina A.V., Ryzhkova E.A. // Russian J. of Anal. Chem. 2010. V.65. P. 866-872.
3. Bobreshova O.V., Agupova M.V., Parshina A.V., Polumestnaya K.A. // Russian J. of Electrochem. 2010. V.46. P. 1252-1262.
4. Bobreshova O.V., Parshina A.V., Polumestnaya K.A., Timofeev S.V. // Petroleum Chemistry. 2011. V. 51 P. 496-505.
5. Voropaeva E.Yu., Stenina I.A., Yaroslavtsev A.B. // Zhurnal neorganicheskoi khimii. 2008. V.53 P. 1677. (Russ. J. Inorg. Chem. 2008. V. 53. P.1797).

# ELECTROMEMBRANE REGENERATION OF SALINE ACID FROM ACIDULOUS PECTIN EXTRACTS

Irina Bodyakina, Vasiliy Bagryantsev, Vladimir Kotov, Alexey Loukine

Voronezh State Agricultural University, Voronezh, Russia E-mail: [irina.bodyakina@inbox.ru](mailto:irina.bodyakina@inbox.ru)

## Introduction

Pectin is a polyelectrolyte of plant origin, which makes physiological processes in our body work without a failure. It is used in food technology as a structure building element. Also, it is a detoxicant of the human body. The pectin molecule consists of a series of chains of polygalacturonic acid. Some of its carboxy groups are methoxylated. Pectin is extracted from horticulture products with help of acids, mainly saline acid. This is followed by neutralization and ethanol precipitation [1]. Such a method, however, leads to a waste of saline acid. In our experiment we used electro dialysis with ion exchange membranes in order to extract saline acid from pectin extracts for reusing it. In this way it is possible to reduce the amount of alkali reagents as well as pollution level of the precipitator and the environment.

## Experiments

We analysed pectin extracts made from sugar beetroot and apple press with help of saline acid. The original amount of HCl was 0.05 moles per litre for each one. The extracts underwent electro dialysis in a 4-section machine consisting of anode-anode section (1)–a membrane MK-40–the concentration section (2) - a membrane MA-40–a deionization section (3) - a membrane MA-40 –cathode section (4)–cathode. The size of the sections was 100 cm<sup>3</sup> and the working area of the membranes was 30.8 cm<sup>2</sup>. The experiment was repeated 5 times and the current density was 5mA/cm<sup>2</sup> within an hour. The extracts were put into the deionization section (3), from which chloride-ions were transferred through the membrane separating sections 2 and 3. Chloride-ions together with the hydrogen ions, generated on the anode and transferred through membrane MK-40, formed saline acid. Hydroxyl ions, generated on the cathode, were transferred through the membrane MA-40 into the deionization section (3), where the saline acid was neutralized. After the experiments, the solutions in sections 2 and 3 were analyzed argentometrically in order to identify chloride-ions. The results then were used to identify the degree of acid regeneration, namely: the number of chloride-ions concentration was compared with that in the deionization section. The demineralization degree was established through identifying the difference between the initial and final number of chloride-ions in the deionization section and the initial number as well as that of transferred in the membrane MA-40. Using ethanol, we then extracted pectin from the extracts and solutions, which underwent electro dialysis. The pectin was analysed potentiometrically in order to identify free and esterified carboxy groups [1].

## Results and Discussion

Table 1 illustrates the results of the research.

**Table 1: Concentration of HCl after electro dialysis in the concentration section (C<sub>2</sub>) and the ionization section (C<sub>3</sub>), mmoles per litre; concentration of transference number of chloride-ions in the membrane MA-40 (t<sub>Cl</sub>), the degree of the acid regeneration (P, %) and the demineralization of the extract (R, %)**

Pectin	C <sub>2</sub>	C <sub>3</sub>	t <sub>Cl</sub>	P, %	R, %
from apples	0,0485±0,0035	0,0059±0,0016	0,826±0,052	97,0±7,0	88,2±3,2
from beetroot	0,0492±0,0038	0,0068±0,0003	0,831±0,064	98,4±7,6	86,4±0,6

The figures show that a final amount of the saline acid becomes close to its concentration necessary for extracting pectin (0.05 moles/l, pH 1.30). As for the number of transportations of chloride-ions in the membrane MA-40, it is lower than usual (0.94) [2]. It is due to the fact that pectin molecules in the deionization section, sorbed on the membrane MA-40 which separates

sections 2 and 3, form some potential barrier for chloride-ions. It is also the reason for a lower degree of demineralization of the extract as compared with the degree of the acid regeneration.

Table 2 illustrates how electromembrane processing of pectin extracts influences the functional composition of pectin molecules.

**Table 2: The number of free ( $C_{\text{free}}$ ), esterified ( $C_{\text{esterified}}$ ) carboxy groups and their total number ( $C_{\text{total}}$ ) (mmoles/l) in pectin**

<b>Pectin</b>	<b><math>C_{\text{free}}</math></b>	<b><math>C_{\text{esterified}}</math></b>	<b><math>C_{\text{total}}</math></b>
<b>Extracted from beetroot</b>			
<i>before electro dialysis</i>	1,95	1,56	3,51
<i>after electro dialysis</i>	1,46	2,42	3,38
<b>Extracted from apples</b>			
<i>before electro dialysis</i>	1,66	2,49	4,15
<i>after electro dialysis</i>	1,52	2,72	4,24

After the electro dialysis the molecules of both apple and beetroot pectin show the decrease in the number of free carboxy groups and the increase in the number of esterified groups. This change is more vivid with the beetroot pectin, though. It is apparently due to the fact that the beetroot pectin has lower molecular weight than the apple pectin [3]. It seems that during the electro dialysis the most low-molecular fractions of beetroot pectin with a higher containment of free carboxy groups are transferred through the membrane MA-40 and, as a result, the pectin is enriched with molecules with higher ester groups.

### Conclusions

Electro dialysis with ion-exchange membranes of acidulous pectin extracts makes it possible to fully regenerate saline acid necessary for reusing. Electro dialysis of the pectin extracts results in the decrease of free carboxy groups and the increase of esterified groups.

### References

1. *Donchenko L.V.* Technology of producing pectin and pectin products. M.:DeLi, 2000. 256p.
2. Ionite membranes. Granulates. Bulk solids. Catalogue. M.: Mir, 1977. 16p.
3. *Kuznetsova E.A., Grebenkin A.D., Lukin A.L., Kotov V.V.* Russian pectin. Materials of the scientific conference. Voronezh, 2006. p.8.

---

## COMPOSITES ON THE BASE OF METALOXIDES (TiO<sub>2</sub>, ZnO) AND CARBON NANOTUBES FOR ELECTRICAL DEVICES

Alina Chanaewa, Beatriz Juarez, Horst Weller

Hamburg University, Hamburg, Germany

In this thesis carbon nanotubes were combined with metal oxides such as zinc oxide and titanium dioxide. They were tested in several electrical devices. Therefore, CNTs were coated with ZnO nanoparticles as well as a few nanometer thin TiO<sub>2</sub> film, representing two very different morphologies. To achieve a high degree of coverage wet chemistry methods were applied to pristine CNTs. CNTs were not covalently functionalized preserving their electronic structure, which ensures the outstanding transport properties of the CNTs. ZnO-CNT composites were investigated particularly in regard to the nature of binding between nanoparticles and the graphitic surface of CNTs. Raman spectroscopy and transmission electron spectroscopy along with computer simulations indicate electrostatic interactions being the reason for nanoparticle attachment to CNTs. Furthermore, the influence of CNTs on ZnO-NP synthesis was studied in oriented attachment and Ostwald ripening regimes. It was found that CNTs can efficiently prevent the formation of elongated structures (vis. oriented attachment). In contrast, they do not show any impact on the Ostwald ripening.

By using a ZnO-DWCNT composite as a field-effect transistor channel, oxygen and light sensitivity of the formed device was ascertained by transfer characteristics. Comparable behaviour of blank devices with untreated DWCNTs was not observed.

In addition to commercial CNTs, which were used in suspensions, three dimensional CNT arrays were integrated into the coating procedure. The CNT arrays were produced via chemical vapor deposition using two different ovens. Both ovens represent novel steady-state setups which were developed and built up in the course of this thesis. CNT growth was performed on transparent ITO substrates using iron as the catalyst. Changes in the synthetic procedure yielded nanotubes with an average length of 200 nm or with a length of 3-6 μm. It is worth to emphasize that CNT growth on ITO substrates is not trivial due to its chemical and thermal instability.

Electrocatalytical activity of the CNT-ITO electrode was monitored using the Fe[(CN)<sub>6</sub>]<sup>4-</sup>/Fe[(CN)<sub>6</sub>]<sup>3-</sup> redox pair. Cyclic voltammetry analysis showed doubled increase in activity compared to a simple ITO electrode.

Finally, suitability of metal oxide CNT-ITO electrodes for the use in photovoltaic devices was studied. ZnO coated CNT-ITO substrate was integrated into a P3HT/PCBM-based solar cell, which showed rather low efficiency of 0.07%. Nevertheless, the efficiency is expected to be improved in future by optimizing the manufacturing technique.

The coating of CNTs with nanometer thick metal oxide films was performed successfully using a low-cost wet chemical procedures. The following integration of composite materials into electrical devices demonstrated several examples for application-oriented material design on the nanometer scale.

# FREE-STANDING ELECTROSPUN CARBON NANOFIBERS MAT AS EFFICIENT ELECTRODE MATERIALS FOR BIOELECTROCATALYSIS OF O<sub>2</sub>.

Ai-Fu Che, Vincent Germain, Marc Cretin, David Cornu, Christophe Innocent, Sophie Tingry

Institut Européen des Membranes (IEM) UMR 5635, ENSCM / CNRS / UM2, Place E. Bataillon, CC 047, Montpellier, France, E-mail: [sophie.tingry@univ-montp2.fr](mailto:sophie.tingry@univ-montp2.fr)

## Introduction

Electrospinning is a simple and versatile technique for preparing nanofibrous materials from a variety of precursors including organics and inorganics [1]. The resulting electrospun membrane, with high specific surface area, is a weblike structure composed of continuous fibers with diameters ranging from tens of nanometers to several micrometers. In order to produce conductive nanofibers, an efficient method consists on subsequent carbonization at high temperature of the electrospun nanofibers prepared from polymer precursors with high carbon yield [2]. Investigation of these materials to fabricate electrodes with good conductivity and high specific surface has been carried out to evaluate their performance as suitable supports for redox enzyme immobilization applied to oxygen reduction.

## Experiments

In this research, carbon nanofibers electrodes have been synthesized by electrospinning. During this process, the nanoscale fibers are generated by the application of a strong electric field of a polyacrylonitrile (PAN) solution, followed by convenient stabilization treatment at 250°C and carbonization between 700 and 1400°C. The resulting mat consists of a carbon residue with high mechanical properties and conductivity [3]. The appropriate conditions of electrospinning and thermal treatment have been determined. The morphology of the nanofibers was characterized by IR, Raman and XRD techniques.

Two nanofibrous mats, with electrical conductivity of 30 S cm<sup>-1</sup> and different thickness (50 and 90 μm) were prepared by varying the deposition time (5 h and 10 h, respectively) during the electrospinning process. For the thicker nanofibrous mat, we demonstrated the potentiality of the CNFs mat as efficient electrode material for laccase immobilization, known to catalyze the four-electron reduction of O<sub>2</sub> completely to H<sub>2</sub>O [4]. The enzyme was co-immobilized with the 2,2'-azinobis (3-ethylbenzothiazoline-6-sulfonate) (ABTS) as redox mediator within a polypyrrole matrix adsorbed on the CNF electrode (fig. 1).

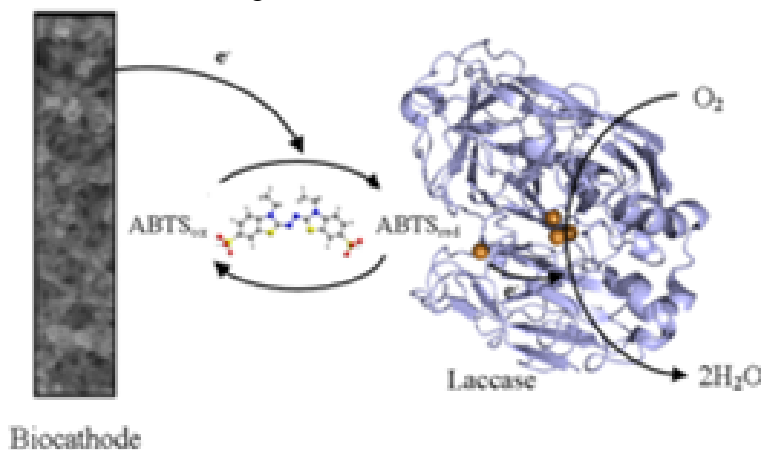


Figure 1. Electron transfer processes at the electrode

## Results and Discussion

The fibrous morphology of the electrospun nanofibers was observed by SEM (Fig. 2). During the chemical conversion of PAN nanofibers to carbon nanofibers, structural changes were induced and the diameters of the nanofibers decreased from ~ 250 nm to ~ 180 nm, due to the weight loss resulting. When used as an electrode, the resulting electrospun mat did not need adding any polymer binder or conductive material and the structure affords an easy handling.

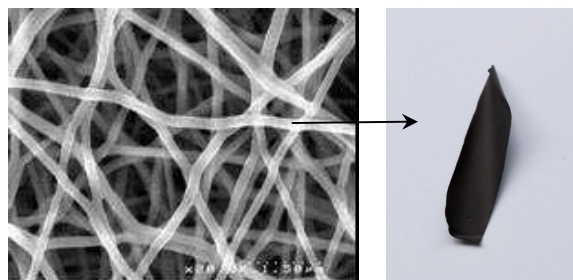


Figure 2. SEM image of carbon nanofibers after heating treatment, and image of the carbon nanofibrous mat

By varying the temperature of the heating-treatment (from 700 to 1400 °C), the carbon nanofibers present higher electrical conductivity induced to more ordered carbon microstructures, observed by Raman spectroscopy. The influence of the nanofibrous mats thickness on the electrochemical properties of the electrodes was evaluated from characteristics of the voltammograms of a redox probe in solution. The results suggested the benefit effect of thicker electrospun nanofibers mat (90  $\mu\text{m}$ ) that may enhance electron transfer kinetics.

Finally, the benefit effect of the electrospun CNFs as efficient conductive support for the immobilization of laccase enzyme was evaluated from the electrocatalytic reduction current of  $\text{O}_2$  to water observed on the current density vs. voltage curves (Fig. 3). In the absence of the redox mediator ABTS (square curve), the current densities are  $\sim 0.5 \text{ mA cm}^{-2}$  and the oxygen reduction current on the biocathode begins at 0.42 V vs Ag/AgCl, indicating that the CNFs are sufficient to promote the adsorbed enzyme orientation for direct electron transfer between the electrode, the copper centers of laccase and the oxygen. In the presence of immobilized ABTS (circle curve), the bioelectroreduction of  $\text{O}_2$  is enhanced, as reflected by a more positive reduction potential (0.58 V) and intensified cathodic current densities ( $\sim 1 \text{ mA cm}^{-2}$ ), two to six times higher than results previously reported. The contribution of the CNFs results in higher performance by inducing higher loading of active species and faster kinetics at the electrode surface.

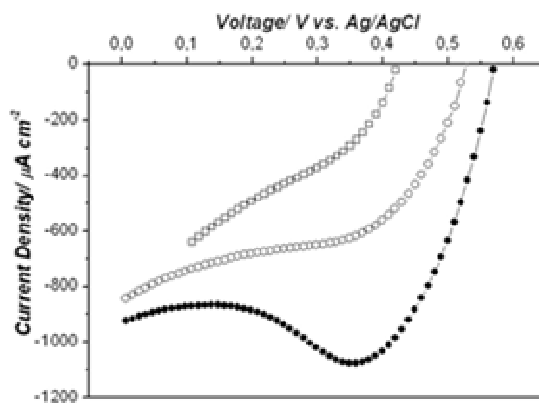


Figure 3. Polarization curves of laccase/ABTS modified CNFs in  $\text{O}_2$ -saturated CPB solution (pH 3, 0.1 M) obtained initially ( $\bullet$ ) and after 3 ( $\circ$ ) days, respectively. Comparison with the polarization curve of laccase modified CNFs ( $\square$ ).  $v = 10 \text{ mV}\cdot\text{s}^{-1}$

The specific interactions between laccase-ABTS-CNFs lead to efficient electrode materials for mediated bioelectrocatalysis. The simple and facile procedure makes the CNFs electrode promising prospect in developing bioelectrochemical devices.

### References

1. Li D., Xia Y. N. // *Adv. Mater.* 2004. V.16. P. 1151.
2. Liu J., Yue Z. R., Fong H. // *Small.* 2009. V. 5. P. 536.
3. Che A.-F., Germain V., Cretin M., Cornu D., Innocent C., Tingry S. // *New J. Chem.* 2011. V. 35. P. 2848.
4. Bilewicz R., Opallo M. *Fuel Cell Science: Theory, Fundamentals and Biocatalysis*, (ch. 5), John Wiley & Sons, Inc., 2010.

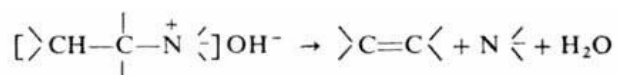
# INFLUENCE OF MODIFICATION STRONG BASIC ANIONEXCHANGE MEMBRANE MA-41 AT CHEMICAL STABILITY UNDER OVERLIMITING CURRENT MODE

Ruslan Chermit, Mikhail Sharafan, Victor Zabolotsky  
Kuban State University, Krasnodar, Russia

## Introduction

Until now, detailed studies of ion-exchange membranes with a wide variety of theoretical and experimental approaches were mainly carried out for cation-exchange membranes. So far, the study electric transport properties of anion-exchange membranes has been paid less attention. However, the actual process of electro dialysis separation efficiency of various ions determined by the properties of membrane pairs. Since the functional groups in the anion-exchange membranes are less stable than the cation-exchange samples, and more susceptible to poisoning in the process of electro dialysis, the transport and chemical properties of these membranes are essential in membrane processes. Also important is the fact that the hydroxyl ions forming during reaction of water dissociation can significantly modify the structure and chemical composition of the surface layer of anion exchange membranes.

It was shown earlier [1] that the OH<sup>-</sup> ions provoke termohydrolysis quaternary ammonium groups, which takes place on the border of anion-exchange membrane / solution from the reaction of Hoffmann, by changing the composition of the surface layer of anion-exchange membrane. During the Hoffmann's cleavage of quaternary ammonium bases are formed tertiary ammonium base, olefin and water [2].



This approach explains the high intensity of the dissociation of water molecules in the strongly basic anion exchange membranes AMH and MA-41, containing mainly quaternary amine groups, which according to the series (1) [3] is not active in the dissociation of water. Thus, it remains an open question about the search for ways to improve the chemical stability is strongly basic anion-exchange membranes at high densities of electric current in membrane systems, as well as finding new ways to improve the mass transport and the operational characteristics of these membranes.

The purpose of this paper is to study the regularities of the processes mass transfer and dissociation of water and study of chemical stability of the original MA-41 and modified anion-exchange membrane MA-41M in condition of overlimiting current mode, using the installation with a rotating membrane disk (RMD). The investigation methodology of EMS by RMD method was described in detail in [4].

## Results and discussion

Current-voltage characteristics electromembrane system containing the initial membrane under study are shown in (Fig. 1). It is seen that for a membrane MA-41 form CVC differs from the classical form due to conjugate effects of concentration polarization.

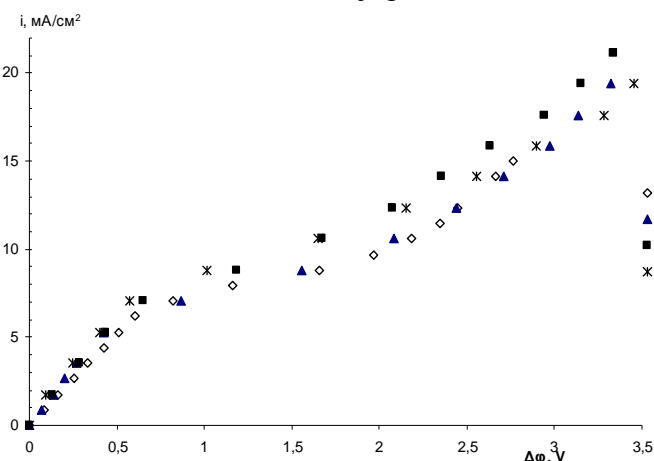


Figure 1. Total current-voltage characteristics electromembrane system containing the membrane MA-41 in 0.01 M NaCl solution at different rotation speeds of the membrane disc (rev/min): 1 - 100 2 - 200 3 - 300 4 - 500

Despite the fact that the original strongly basic anion-exchange membrane MA-41 initially contains mostly quaternary ammonium bases and according to the catalytic activity of ionic groups in relation to the dissociation of water on the border of the membrane / solution should not initiate it [3], in reality there is quite a different picture. At the beginning of the experiment the dissociation of water is about 25% of the total mass transfer on the initial anion-exchange membrane MA-41, (Fig. 2a, points 1), whereas after 10 hours (Fig. 2a points 3) the part of a current transported by hydroxyl ions through the membrane is about 40%.

Maximum diffusion current of salt ions are practically unchanged, and the transport of salt ions decreases in condition of overlimiting current due to decrease the amount of space charge in the surface layer of the membrane and reduce the electroconvection and mass transfer of salt ions, as evidenced by Fig.2b

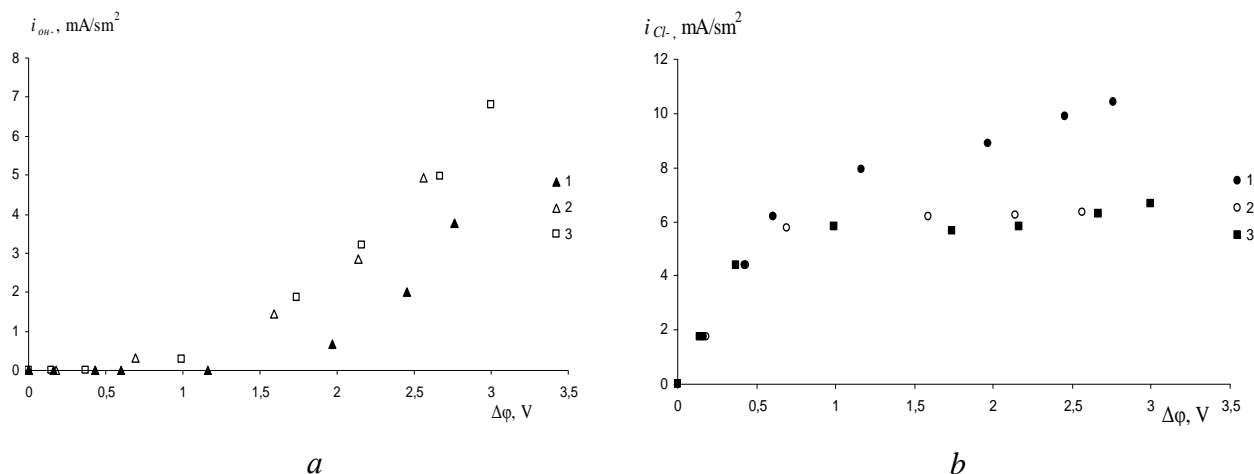


Figure 2. The partial current-voltage characteristics of hydroxyl ions (a) and chlorine (b) EMC containing membrane MA-41 in 0.01 M NaCl solution at a rate of rotation of the disk membrane 100 r / min: where 1 - the original membrane, 2 - after 6 hours of work, 3 - after 10 hours of work

Analysis of the partial current-voltage characteristics of chlorine and hydroxyl ions for the original MA-41 and modified MA-41M is shown in (Fig. 3a, b).

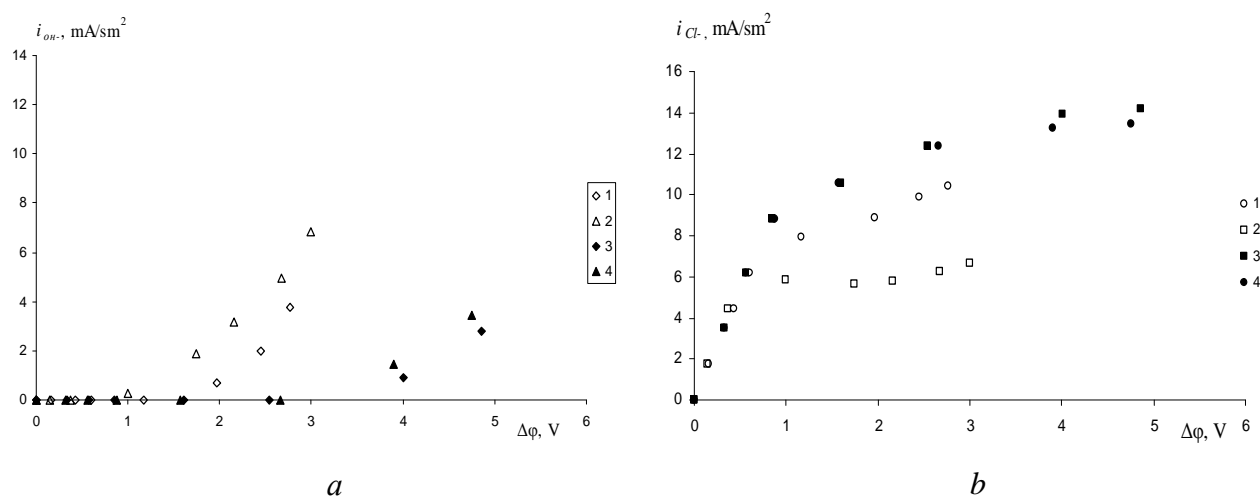


Figure 3. The partial current-voltage characteristics of hydroxyl ions (a) and chlorine (b) EMC-containing membranes MA-41, and MA-41M in 0.01 M NaCl solution at a rotation speed 100 rev / min with 1-MA-41 after 2 hours, 2 - MA-41 after 8 hours of work, 3-MA-41M after 2 hours, 4 - MA-41M after 8 hours

As seen from (Fig. 3 a) dissociation of water molecules is much lower on the modified membrane than on the original and only begins when the potential jump  $\Delta\phi = 4V$ , while in the original membrane this process begins already at  $\Delta\phi = 2V$ . At the same time on the modified

membrane MA-41M observed a significant increase in mass transfer of salt ions (35%), as evidenced by the partial current-voltage characteristics of the ions Cl-(Fig. 3. b, points 3 and 4)

In Fig. 4 shows the dependence of the limiting current (found by the method of tangents) of the square root of angular velocity ( $\omega$ ) for all investigated systems. The dotted line in this figure shows the calculation of the dependence of the limiting current of the  $\sqrt{\omega}$  in conformity with the theory of Levich.

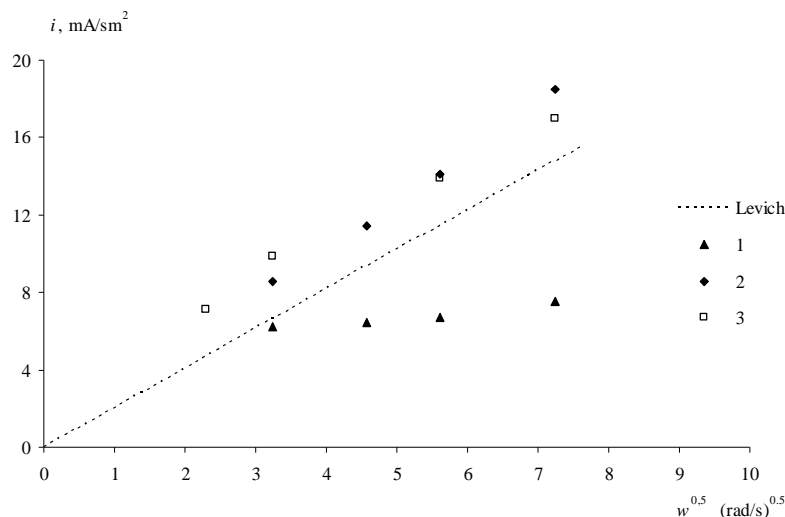


Figure 4. The dependence of the limiting current density on the square root of the angular velocity of the membrane disk: dashed line - calculation by the theory of Levich; points - experimental limiting currents for membranes: 1 - MA-41, 2 - MA-41M, 3 - AMX

The figure shows that the values of the limiting diffusion current in all speed range of the rotating membrane disk for the modified MA-41M and homogeneous AMX membrane is almost identical and slightly higher than the values of limiting currents, calculated by the formula Levich. Thus, developed heterogeneous anion-exchange membrane MA-41 allows to completely suppress the reaction of dissociation of water molecules at the boundary of the membrane / solution (in operating voltage range), while significantly increasing a mass transfer in the system (+35%), and by modifying the initial heterogeneous membrane impart this membrane (MA-41M) the properties of homogeneous membranes AMX.

This work was supported by RFBR grant № 11-03-96504-p\_юг\_у and RFTP №02.740.11.0861.

#### References

1. Zabolotskii V.I., Bugakov V.V., Sharafan M.V., Chermit R.H. Transfer electrolyte ions and water dissociation in the anion-exchange membrane at intensive current modes // Russ. J. Electrochem. 2012. V. 48. № 6. P. 721-731.
2. Ui-Son Hwang, Jae-Hwan Choi Changes in the electrochemical characteristics of a bipolar membrane immersed in high concentration of alkaline solutions. // Separation and Purification Technology 2006 V. 48. P. 16-23.
3. V.I. Zabolotsky, N.V. Sheldeshov, N.P. Gnusin. // Uspehi khimii. 1988. V. 57. P. 1403.
4. Pat. №78577 RU. 27.11.2008.

# CORRELATION BETWEEN STRUCTURAL AND SELECTIVE PROPERTIES OF ION-EXCHANGE MEMBRANES

<sup>1</sup>Mariya Chernyaeva, <sup>1</sup>Natalia Kononenko, <sup>2</sup>Yurii Volkovich, <sup>3</sup>Marina Kardash,  
<sup>3</sup>Georgii Aleksandrov

<sup>1</sup>Kuban State University, Krasnodar, Russia

<sup>2</sup>Frumkin Institute of Physical Chemistry and Electrochemistry of RAS, Moscow, Russia

<sup>3</sup>Engels Technological Institute (branch) of Saratov State Technical University, Engels, Russia

The aim of this work is the estimation of membrane selectivity from the structural characteristics. The porous structure of ion-exchange membranes was studied with method of standard contact porosimetry. The maximal value of water content ( $V_0$ ), the specific internal surface area ( $S$ ) and the distance between the fixed groups ( $L$ ) were calculated from the porosimetry curves of the relative water content ( $V$ ) as a function of the effective radii of pores  $r$  (nm) in the membrane:

$$S = 2 \int_0^{\infty} \frac{1}{r^2} \left( \frac{dV}{d \ln r} \right) dr = 2 \int_0^{\infty} \frac{dV}{r}, \quad L = \sqrt{\frac{S}{QN_A}},$$

where  $dV$  is the differential of water content,  $Q$  is the ion-exchange capacity,  $N_A$  is the Avogadro's number.

Selectivity is provided by only micro- and mesopores in gel with effective radius no more than 100 nm. The fraction of these pores in the total pores volume ( $V_{gel}/V_0$ ) is parameter for characterization of membrane selectivity. Membrane selective properties were investigated also experimentally with help of membrane potential measurement in 0.1/0.2 M NaCl solutions. The transport numbers of counter-ions ( $t_{app}$ ) were calculated using equation:

$$t_{+(app)} = \frac{1}{2} \left( 1 + \frac{E}{E_{ideal}} \right)$$

where  $E$  is the membrane potential,  $E_{ideal}$  is the concentration potential.

The porosimetry curves of the ion-exchange membranes are shown in Figure 1. Table 1 presents structural characteristics and the transport numbers of these membranes. As can be seen from the table, the parameter  $V_{gel}/V_0$  has greater value in the case of MF-4SC membranes. It correlates with measurements of transport numbers by membrane potential method.

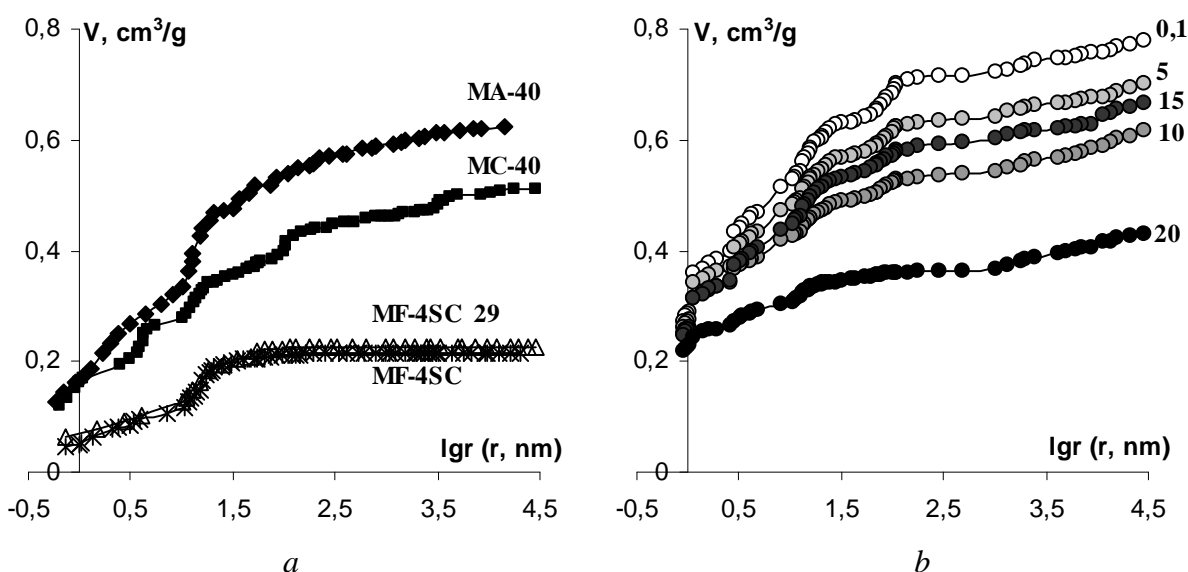


Figure 1. Integral curves of water distribution on the effective pore radii ( $r$ , nm) for ion-exchange membranes (The curve number (b) corresponds to the pressure of Polycon pressing  $P$ , MPa)

**Table 1: The structural and selectivity characteristics of ion-exchange membranes**

	$V_0, \text{cm}^3/\text{H}_2\text{O/g}$	$Q, \text{mmol/g}$	$S, \text{m}^2/\text{g}$	$L, \text{nm}$	$V_{gel}/V_0$	$t_{app}$
<b>MK-40</b>	0,54	1,67	421	0,52	0,78	0,97
<b>MA-40</b>	0,62	2,30	514	0,60	0,87	0,92
<b>MF-4SC 29</b>	0,23	0,93	207	0,51	0,98	0,97
<b>MF-4SC</b>	0,21	0,70	167	0,57	0,95	0,96

It was revealed the correlation between structural and selective properties of new membrane materials Polycon, which contains phenolsulfocationic matrix and fibrous component. The compacting pressure of samples ( $P$ ) varied from 5 MPa up to 20 MPa. Figure 1b shows the curves of water distribution in these samples. The structural characteristics and the transport numbers of Polycon membranes are summarized in the Table 2. As indicated in Figure, the  $V_0$  value of Polycon samples is higher than for membranes base on perfluorinated and polystyrene matrix. The presence of macropores in region  $10^4$  nm in Polycon samples are caused by formation of structural defects at the interface between the resin and polyacrylonitrile fibers. It results in lower value of  $V_{gel}/V_0$  parameter. According to Table 2,  $V_{gel}/V_0$  parameter varies from 0.82 to 0.89. Thus the selectivity of these samples is lower in comparative with heterogeneous ion-exchange membranes; however it is sufficiently high for fibrous materials. The value of  $V_{gel}/V_0$  parameter correlates with the value of the transport numbers of Polycon membranes.

**Table 2: The structural and selectivity characteristics of fibrous composite membranes Polycon**

Number of sample	Compacting pressure	$V_0, \text{cm}^3/\text{g}$	$S, \text{m}^2/\text{g}$	$V_{gel}, \text{cm}^3/\text{g}$	$V_{gel}/V_0$	$t_{app}$
<b>1</b>	-	0,71	751	0,63	0,89	0,80
<b>2</b>	5 MPa	0,61	655	0,53	0,87	0,89
<b>3</b>	10 MPa	0,52	596	0,43	0,83	0,80
<b>4</b>	15 MPa	0,61	646	0,52	0,85	0,79
<b>5</b>	20 MPa	0,34	407	0,28	0,82	0,90

The fraction of gel pores volume ( $V_{gel}/V_0$  parameter) can be applied to characterize the membrane selectivity, but this estimation has approximate character.

*The present work is supported by the Russian Foundation for Basic Research (project № 10-08-00074-a).*

### References

1. Volkovich Yu.M., Bagotzky V.S., Sosenkin V.E., Blinov I.A. // Colloids and Surfaces A: Physicochemical and Engineering Aspects. 2001. V. 187-188. P. 349-365.
2. Berezina N.P., Kononenko N.A., Dyomina O.A., Gnusin N.P. // Advances Colloid Interface Sci., V. 139. 2008. P.3-28.
3. Volkovich Yu.M., Kononenko N.A., Chernyaeva M.A., Kardash M.M., Shkabara A.I., Pavlov A.V. // Membranes. 2008. N 3. P. 35-40.

# CELL MODEL FOR A MEMBRANE CONSISTING OF PARALLEL CYLINDERS UNDER HYDROMAGNETIC AXIAL FLOW

<sup>1</sup>Sunil Datta, <sup>1</sup>Manju Agarwal, <sup>2</sup>Anatoly Filippov

<sup>1</sup>Lucknow University, Lucknow-226007, India

<sup>2</sup>Gubkin Russian State University of Oil and Gas, Moscow, Russia, E-mail: a.filippov@mtu-net.ru

## Introduction

In this work we propose to study the flow of an electrically conducting fluid through a membrane composed of an array of parallel circular non conducting cylinders using cell model initiated by Happel. The flow is taken along the axes of the cylinders and the magnetic field in a fixed direction transverse to the flow. It may be remarked here that we have not taken the induced electric/magnetic field to be zero as is done by many authors; non-vanishing of the induced electric field is exhibited in the sequel. In Hartman's paper too this induced field is present. In Gold's [1] study of magnetohydrodynamic pipe flow, which has motivated us to take up this MHD problem, induced electromagnetic fields appear and are significant. Also, it is seen that the problem is not axial symmetric and quantities are functions of both radial distance  $r$  and polar angle. It should also be noted that in this problem there is only one component of velocity along the axes of the cylinders and then as in the concerned references [2] and [3] mentioned earlier the four cell flow boundary conditions are all identical. Electromagnetic boundary conditions are also needed. The system is simulated by a single cylinder enveloped by a concentric cylindrical enveloping surface with axial flow. The analysis leads to the evaluation of the permeability parameter. The results are then graphically presented and discussed. The effect of magnetic field is seen to increase the permeability. The similar problem neglecting induced electric field for a swarm of partially porous parallel cylinders was investigated in [4].

## Theory

We have seen that in the cell method, the problem gets reduced to the investigation of a single particle enveloped in a cell. Here the single particle is an impenetrable cylinder of radius 1 with axis along the  $z$  axis and the cell is a concentric cylinder of radius  $c$ . The external flow, induced by constant axial pressure gradient is  $e_z$  along the axis of the cylinder. The applied magnetic field is uniform field  $e_x$  along the transverse  $x$ -direction (Fig. 1).

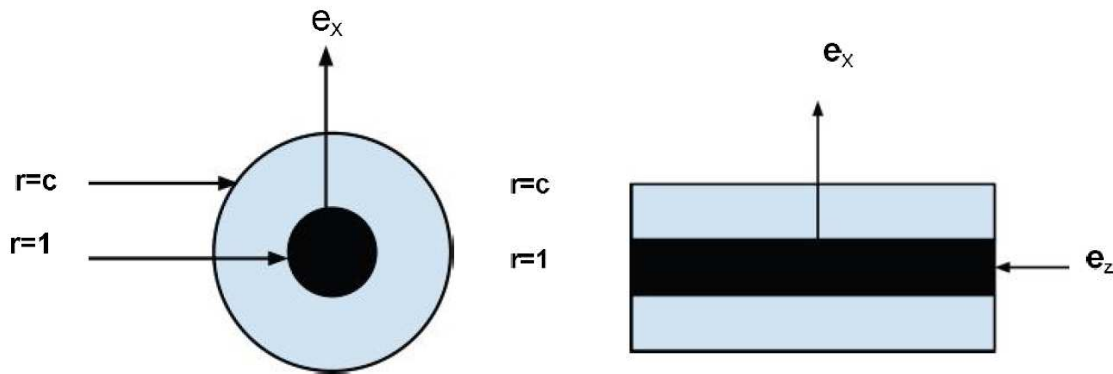


Figure 1. Transverse (left side) and longitudinal (right side) view of the cell in non-dimensional form

As observed earlier the problem is not axial symmetric, hence we cannot take quantities to be function of  $r$  alone. These will be functions of both  $x$  and  $y$  in Cartesian coordinates or both  $r$  and  $\theta$  in polar coordinates. Thus, we take for vectors of velocity and magnetic field

$$\mathbf{u} = u(x; y)\mathbf{e}_z = u(r; \theta)\mathbf{e}_z \quad (1)$$

$$\mathbf{B} = \mathbf{e}_x + b(x; y)\mathbf{e}_z = \mathbf{e}_x + b(r; \theta)\mathbf{e}_z \quad (2)$$

Here, since all conditions are satisfied, we may assume that the induced magnetic field  $b$  is only in the  $z$ -direction and then find that

$$\mathbf{u} \times \mathbf{B} = u(x; y)\mathbf{e}_y \quad (3)$$

Thus, providing non-zero

$$\nabla \cdot (\mathbf{u} \times \mathbf{B}) = \frac{\partial u}{\partial y} \quad (4)$$

Therefore, we have induced electric field

$$\mathbf{E} = E_x \mathbf{e}_x + E_y \mathbf{e}_y \quad (5)$$

where in terms of electric potential  $\varphi$

$$\mathbf{E} = -\nabla \varphi \quad (6)$$

Using (1)-(6) the system of dimensionless MHD equations (not presented here) can be reduced to the following three equations:

$$p(x, y, z) = -\frac{M^2}{2R_m} b^2 - Pz, \quad (7)$$

$$\nabla^2 u - \frac{M^2}{R_m} \frac{\partial b}{\partial x} = 0, \quad (8)$$

$$-\nabla^2 b = R_m \frac{\partial u}{\partial x}, \quad (9)$$

where  $p$  is a pressure,  $u$  is an axial velocity,  $R_m$  is a magnetic Reynolds number,  $M$  is a Hartman number,  $P = -\frac{\partial p}{\partial z}$  is a constant pressure drop applied along  $z$ -axis. The above MHD equations (8), (9) are in terms of flow field  $u$  and induced magnetic field  $b$  corresponding to Gold's paper [1] but for our purpose it will be more convenient to use the flow field  $u$  and the electric potential  $\varphi$ ; the equations then are expressible as

$$\nabla^2 u + M^2 \left( \frac{\partial \varphi}{\partial y} - u \right) = -P \quad (10)$$

$$\nabla^2 \varphi = \frac{\partial u}{\partial y} \quad (11)$$

Since the boundary conditions are conveniently expressible in terms of the radial distance  $r$ , we shall render the equations (10) and (11) in cylindrical polar coordinates ( $r; \theta; z$ ):

$$\nabla^2 u + M^2 \left( \frac{1}{r} \frac{\partial \varphi}{\partial \theta} \cos \theta + \frac{\partial \varphi}{\partial r} \sin \theta - u \right) = -P, \quad (12)$$

$$\nabla^2 \varphi = \frac{1}{r} \frac{\partial u}{\partial \theta} \cos \theta + \frac{\partial u}{\partial r} \sin \theta \quad (13)$$

These equation are to be solved under the boundary conditions, no-slip and no normal current at the non conducting cylinder boundary  $r = l$ :

$$u(1) = 0, \quad \frac{\partial \varphi}{\partial r}(1) = 0; \quad (14)$$

no stress and no surface current at the cell boundary  $r = c$ :

$$\frac{\partial u}{\partial r}(c) = 0, \quad \frac{\partial \varphi}{\partial \theta}(c) = cu(c) \cos \theta. \quad (15)$$

## Results and Discussion

As it is a stupendous task to analyze the system for general value of Hartman number  $M$ , we applied the perturbation method to obtain the solution for small values of  $M^2$ ; hence we substitute

$$u = u_0 + M^2 u_1, \quad \varphi = \varphi_0 + M^2 \varphi_1 . \quad (16)$$

in equations (12) and (13) to obtain the zero and first order solution.

Using obtained analytical solution in the form of (16) (not presented here), the dependence of hydrodynamic permeability on magnetic field is depicted in Fig. 2.

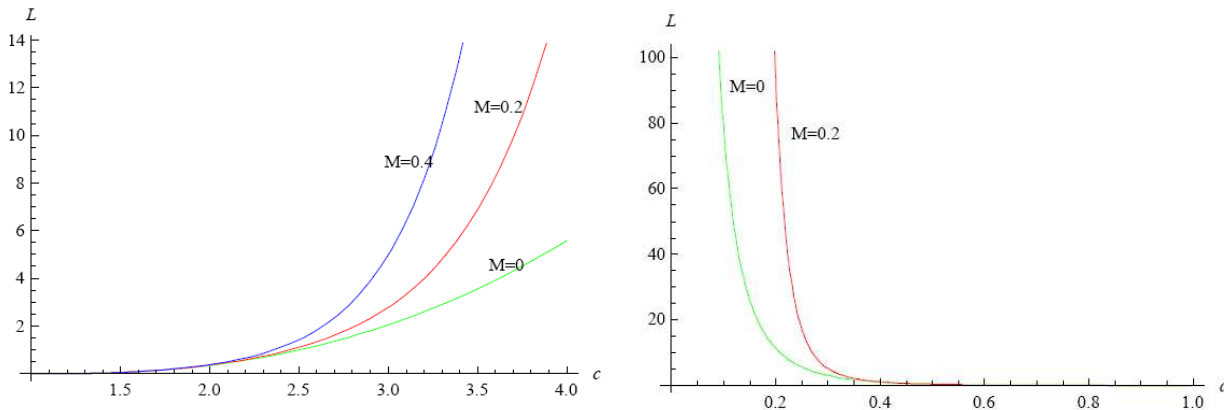


Figure 2. Variation of permeability  $L$  with  $c$  (left side) and  $d=1/c$  (right side) for different values of Hartman number  $M$

From the left figure 3 we conclude that the effect of magnetic field is to increase the permeability but this increase gets smaller/negligible when  $c < 1:5$  implying that greater the gap, greater is the effect of magnetic field. Also it is seen that the effect of increasing the gap is to increase the permeability, and takes place for all the values of  $M$ . From the right figure 3 we again conclude that the effect of magnetic field is to increase the permeability. But this increase gets smaller/negligible when  $d > 0.6$  implying that smaller the gap, greater is the effect of magnetic field. Again it is seen that the effect of increasing the gap is to increase the permeability.

We believe that taking into account external magnetic field allows us to describe more accurately the influence of magnetic stirrers on flows of conducting liquid through porous membranes.

*The present work is supported by the Russian Foundation for Basic Research (projects nos 10-08-92652\_IND and 12-08-92690\_IND).*

## References

1. Gold R.R. Magnetohydrodynamic pipe flow. Part1 // J. Fluid Mech. 1962. V. 13. P. 505-512.
2. Vasin S.I., Filippov A.N. Hydrodynamic permeability of the membrane as a system of rigid particles covered with porous layer (cell model) // Colloid J. 2004. V. 66. No. 3. P. 266-270.
3. Vasin S.I., Filippov A.N. Cell models for flows in concentrated media composed of rigid impenetrable cylinders covered with a porous layer // Colloid J. 2009. V. 71. No. 2. P. 141-155.
4. Tiwari A., Deo S., Filippov A. Effect of the Magnetic Field on the Hydrodynamic Permeability of a Membrane // Colloid J. 2012. V.74. No. 4 (in press).

# PERMEANCE AND DIFFUSION OF GASES IN POLY(2-METHYL-5-VINYL TETRAZOLE)

<sup>1</sup>George Dibrov, <sup>1</sup>Eduard Novitsky, <sup>2</sup>Rostislav Trifonov, <sup>2</sup>Vladimir Ostrovsky, <sup>1</sup>Alexey Volkov

<sup>1</sup>Topchiev Institute of Petrochemical Synthesis RAS, Moscow, Russia, E-mail: george.dibrov@ips.ac.ru

<sup>2</sup>State Institute of Technology, St. Petersburg, Russia

## Introduction

A search in new barrier materials with unusual properties is in progress due to the increasing importance of gaseous feed streams for industry and energy generation. Poly(2-methyl-5-vinyl tetrazole) (PMVT) is distinguished from other polymers by its unique chemical composition –  $[C_4N_4H_6]_n$ . The backbone of its macromolecule is decorated with side groups which are heterocycles primarily composed of nitrogen atoms. This chemical composition has triggered interest for studying sorption and permeability of PMVT with respect to gases ( $N_2$ ,  $O_2$ , etc.).

## Experiments

PMVT with  $M_w=68400$  was synthesized by method described elsewhere [1]. Permeability and diffusion coefficients of nitrogen, oxygen and carbon dioxide for the PMVT film with a thickness of 50  $\mu m$  were measured at a feed pressure of 0.6 - 0.8 bar and at temperatures of 25-45°C using a constant volume/variable pressure experimental setup (GKSS Time-Lag Machine) [2].

## Results and Discussion

PMVT gas permeability was studied for the first time. The Arrhenius plots were built (Fig. 1) from which is seen that permeability coefficient decreases in an order:  $P(CO_2) > P(O_2) > P(N_2)$ . The diffusion coefficient decreases with increasing the molecular diameter of penetrant (Table 1) and with decreasing temperature. High permeability coefficient for  $CO_2$  is attributed to its high solubility coefficient. Such gas transport characteristics make PMVT an attractive material for further studies in gas separation.

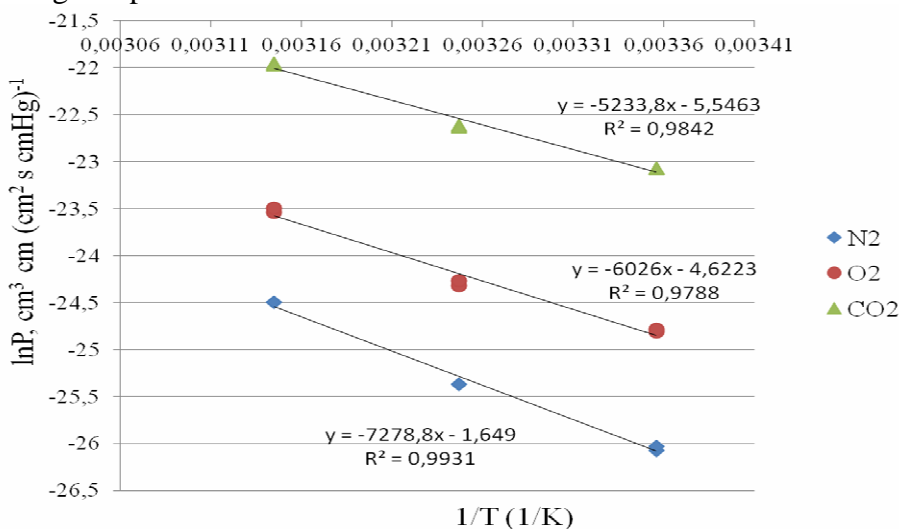


Figure 1. Temperature dependences of gas permeability coefficients for PMVT

Table 1: Diffusion coefficient of  $N_2$ ,  $O_2$  and  $CO_2$  at different temperatures in PMVT

Temperature, °C	25	35	45	Kinetic molecular diameter, nm [3]
$D(CO_2)$ , $10^{-8} \text{ cm}^2/\text{s}$	0,4	0,9	1,9	0,407
$D(N_2)$ , $10^{-8} \text{ cm}^2/\text{s}$	2,3	6,8	11,1	0,370
$D(O_2)$ , $10^{-8} \text{ cm}^2/\text{s}$	3,6	7,2	15,8	0,358

This work was partially supported by RFBR

## References

1. M. Uspenskaya, Tetrazole containing polymers, St. Petersburg. 2008.
2. Shishatskiy S.M., Yampolskii Yu.P., Peinemann K.V. // J. Membr. Sci. 1996. V.112. P.275-285
3. Hirschfelder, Curtiss, Bird, Molecular Theory of Gases and Liquids, Wiley, New York 1954

# ELABORATION OF HIGH FLUX COMPOSITE PTMSP MEMBRANES

George Dibrov, Eduard Novitsky, Vladimir Volkov

Topchiev Institute of Petrochemical Synthesis RAS, Moscow, Russia, *E-mail: george.dibrov@ips.ac.ru*

## Introduction

Membrane technologies are an attractive alternative to the existing conventional technologies of separation and purification. To be useful in an industrial separation process, a membrane must exhibit the following characteristics: high flux and selectivity, tolerance to the process conditions, manufacturing reproducibility [1]. In this case composite membranes, consisting of thin selective polymer layer atop a porous support appear to be attractive. The following techniques of composite membrane fabrication were explored over the last decades: solution coating, interfacial polymerization, plasma polymerization and dynamical coating [2]. The first two methods are commonly used in large scale industrial processes.

This work is focused on the elaboration of composite membranes based on high-permeable glassy polymer poly[1-(trimethylsilyl)-1-propyne] (PTMSP) for application in organic solvent nanofiltration (OSN), membrane gas desorption (MGD) and termopervaporation (TPV) processes.

## Experiments

Thin film composite (TFC) membranes are usually fabricated using ultrafiltration level porous supports such as polyacrylonitrile [3, 4] with N<sub>2</sub> permeance typically below 200 m<sup>3</sup>(STP)\* (m<sup>2</sup>\*h\*bar)<sup>-1</sup>. Unfortunately it eventually results in insufficiently high flux of composite membrane due to the resistance of porous support to gas transport. In this work commercially available high-flux microfiltration membranes with specific for each application features were carefully selected, pretreated and used as supports (table 1).

**Table 1: Support material features.**

Membrane application	Industrial material	Required properties	N <sub>2</sub> permeance, m <sup>3</sup> (STP)* (m <sup>2</sup> *h*bar) <sup>-1</sup>	pore size, μm	
				max	mean
MGD	metal-ceramic (MC)	Stability at 100°C, 40 bar, pH ≥12	638	0,50	0,15
OSN	Polypropylene (PP)	Chemical stability in organic solvents	707	0,57	0,30
TPV	PVDF-PTFE (copolymer)	Hydrophobicity	756	0,48	0,31

Solution coating for lab and pilot scale fabrication of composite membranes was employed. Standard test method, namely gas-liquid displacement was applied for determination of pore size characteristics of porous supports [5]. Pure nitrogen and carbon dioxide permeance of porous supports and composite membranes was measured using volumetric method at pressures up to 40 bar and temperature 25°C. The PTMSP/PVDF composite membrane was applied in the process of butanol recovery from model fermentation broths using the TPV method described previously [6]. The PTMSP/PP composite membrane was applied for removal of dyes from ethanol solutions using the OSN method described elsewhere [7].

## Results and Discussion

Gas transport characteristics of elaborated membranes are presented in table 2. The PTMSP/MC membrane was annealed at 100°C and its permeance decreased by a factor of 20 after 150 hours of exposure to high temperature. However the same membrane showed stable performance for the next 200 hours of annealing at 100°C keeping nearly the same CO<sub>2</sub>/N<sub>2</sub> selectivity. Upon desorption of CO<sub>2</sub> from the saturated 50% aqueous solution of N-methyl-diethanolamine at 40 bar and 100°C, no liquid phase flow through the aged membranes annealing at 150°C) takes place. Therefore, the as-prepared composite membranes can be used

for the regeneration of chemical absorbents of CO<sub>2</sub> at elevated temperatures and pressures and this approach makes it possible to solve two following problems: (i) to provide high CO<sub>2</sub> flux and (ii) to ensure high barrier characteristics with respect to a liquid absorbent (the absence of hydrodynamic flow of an absorbent through the membrane). The PTMSP/PVDF composite membrane exhibited a flux of 0,43 kg (m<sup>2</sup> h)<sup>-1</sup>. The PTMSP/PP composite membrane exhibited ethanol flux of 5,5 kg (m<sup>2</sup> h)<sup>-1</sup> at 5 bar.

**Table 2: Gas transport characteristics of elaborated composite membranes at 25°C**

Membrane application		MGD	OSN	TPV
Gas permeance, m <sup>3</sup> (STP)* (m <sup>2</sup> *h*bar) <sup>-1</sup>	N <sub>2</sub>	7,7	3,5	3,5
	CO <sub>2</sub>	36,3	16,7	16,6
Selectivity, α(CO <sub>2</sub> /N <sub>2</sub> )		4,7	4,7	4,7

The membranes for TPV and OSN can be optimized further in terms of layer thickness to provide optimum flux/selectivity combination. Therefore they represent a perspective alternative to commercial PDMS membranes. To the best of our knowledge the membrane developed for MGD has the highest CO<sub>2</sub> permeance at the given conditions in combination with barrier properties to liquid absorbent.

*This work was partially supported by Presidium of RAS (PRAS-3)*

#### References

1. *Pinnau I., Freeman B.D.* Formation and Modification of Polymeric Membranes Overview, In Membrane Formation and Modification; ACS Symposium Series; American Chemical Society: Washington, DC (1999).
2. *Kopeć K.K., Dutczak S.M., Wessling M., Stamatialis D.F.* Chemistry in a spinneret—On the interplay of crosslinking and phase inversion during spinning of novel hollow fiber membranes // Journal of Membrane Science. 2011. V. 369. P. 308-318.
3. *Peter J., Peinemann K.-V.* Multilayer composite membranes for gas separation based on crosslinked PTMSP gutter layer and partially crosslinked Matrimid® 5218 selective layer // Journal of Membrane Science. 2009. V.340. P. 6272
4. *Henis J.M.S., Tripodi M.K.* Composite hollow fiber membranes for gas separation: the resistance model approach // Journal of Membrane Science. 1981. V. 8. P. 233-246
5. ASTM Designation: F 316–03, Standard Test Methods for Pore Size Characteristics of Membrane Filters by Bubble Point and Mean Flow Pore Test (2003).
6. Patent RF 2408416, 11.11.2008.

# INFLUENCE OF MERCURY (II) ON PROPERTIES OF ANION-EXCHANGE MEMBRANES MA-40 AND MA-41 AND ELECTRODIALYSIS PROCESS

<sup>1</sup>Alexander Dyukov, <sup>2</sup>Swetlana Shishkina

<sup>1</sup>“KCKK Mineral Fertilizer Plant” OJSC, Kirovo-Chepetsk, Russia, E-mail: Aleksandr.Dyukov@kckk.ru

<sup>2</sup>Vyatka State University, Kirov, Russia, E-mail: vgu\_tep@mail.ru

## Introduction

Despite worldwide reduction of usage of highly toxic mercury its application in chlorine industry, measuring and lighting device productions is still in use. So to decrease ecological danger of such productions it is necessary to find effective methods of treatment of mercury containing wastes which allow both to protect the environment and to return precious mercury back to the process. From this point of view the application of electrodialysis (ED) has many advantages in comparison with conventional techniques but requires detailed study of membrane properties in contacting solutions.

## Experiments

In this research the influence of mercury (II) on electrochemical properties such as electrical conductivity (EC) and total water content (WC) of anion-exchange membranes MA-40 and MA-41 in mercury (II) chloride and nitrate solutions and their behavior during the process of ED was studied. Some characteristic of the membranes are shown in Table 1. Calculations made with the use of equilibrium and material balances according to [1] show that in chloride solutions mercury exists mostly in neutral and negatively charged chloride particles.

**Table 1: Characteristics of the Membranes under Study**

Membrane Type	Type of Matrix	Functional Group	Exchange Capacity, mg-eq/g <sub>dry</sub> [2]
MA-40	Copolymer of ethylene diamine and epichlorohydrin	$\begin{aligned} & \equiv \overset{+}{N}- \\ & \equiv N : \\ & \dots \\ & = N H \end{aligned}$	2,19
MA-41	Styrene divinylbenzene	$N(CH_3)_3^+$	1,44

## Results and Discussion

It was obtained that electrical conductivity of both membranes in mercury (II) nitrate solutions is much higher than that in mercury (II) chlorides (Table 2). It is explained by low mobility of negatively charged complicated mercury (II) chloride ions.

**Table 2: EC of the membranes in 0,02 eq mercury containing solutions**

Membrane Type	EC of the membranes, mS/cm	
	HgCl <sub>2</sub>	Hg(NO <sub>3</sub> ) <sub>2</sub>
MA-40	0,019	2,0
MA-41	0,012	2,6

The presence of mercury (II) in sodium chloride solutions changes significantly as total WC so as free and fixed water fraction which was measured by means of gravimetric method and differential scanning calorimeter DSC respectively. The WC of the cation-exchange membrane MK-40, for example, remains nearly the same (Table 3). This phenomenon can be caused by specific interaction between functional amino-groups of anion-exchange membranes with mercury ions which was also proved by changes in IR-spectra and X-ray diagrams [3].

**Table 3: Hydration characteristics of the membranes**

Membrane	Solution (0,02 eq)	Water Content,%	Free water fraction,%	Fixed water fraction,%	n
MK-40	NaCl	61,82	19,52	42,30	7,23
	HgCl <sub>2</sub> +NaCl	53,37	21,43	31,94	7,51
MA-40	NaCl	59,02	30,60	28,42	4,52
	HgCl <sub>2</sub> +NaCl	15,20	6,22	8,98	1,98
MA-41	NaCl	41,22	25,89	15,32	4,20
	HgCl <sub>2</sub> +NaCl	17,10	7,71	9,39	3,09

n—the number of water molecules per a functional group

The (ED) of sodium chloride solutions containing mercury ions with "hollow" cells formed by membrane pairs of MC-40 and MA-40 under current densities below limiting ones has shown presence of material balance, absence of hydroxides formation and decrease of mercury concentration in desalination cells by 70-76 %. Filling the desalination cells with granules of ion-exchange resin of AV-17-8 type increases the degree of mercury desalination up to 95-97% (Figure 1).

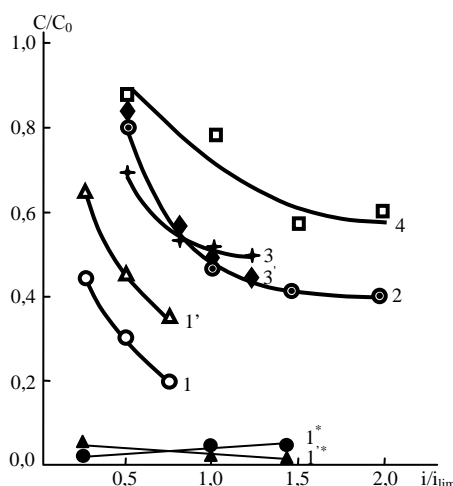


Figure 1. Efficiency of ED of Sodium Chloride Solution Containing Mercury Ions in Desalination Cells: 1, 1' – concentration changes of NaCl and HgCl<sub>2</sub> respectively 1\*, 1'\* – the same in packing ED

Thus, the presence of mercury in the contacting solution slightly decreases the transport properties of anion-exchange membranes. It is shown that ED may be used as an effective method of non-detergent waste water treatment from mercury compounds.

### References

1. Butler J. Ionic Equilibrium, Reading, Massachusetts, 1964.
2. Zabolotskiy V.I., Nikonenko V.V. Ion Transport in Membranes.-M.: Nauka, 1996.-392 p
3. Dyukov A.V, Shishkina S.V., Zheludkov A.N. Electrochemical Properties of Ion-Exchange Membranes in Chloride Solutions Containing Ions Hg(II). Ion Transport in Membranes, abstracts book, Tuapse, 2006. P. 178.

# ION-EXCHANGE RESIN DOPED WITH ZIRCONIUM HYDROPHOSPHATE: SELECTIVE SORPTION

<sup>1</sup>Yuliya Dzyazko, <sup>1</sup>Ludmila Ponomarova, <sup>2</sup>Yurii Volkovich, <sup>2</sup>Valentin Sosenkin, <sup>1</sup>Vladimir Belyakov

<sup>1</sup>Vernadskii Institute of General & Inorganic Chemistry of the NAS of Ukraine, Ukraine  
E-mail: dzyazko@ionc.kiev.ua

<sup>2</sup>Frumkin Institute of Physical Chemistry & Electrochemistry of RAS, Moscow, Russia,  
E-mail: yuvolf40@mail.ru

## Introduction

Composites based on ion-exchange resins are used in catalytic and electrocatalytic processes particularly for oxygen removal from water and liquid hydrocarbons as well as for ion exchange processes [1]. The ion-exchangers, which are selective to As(III) и As(V) anions, were obtained by modification of anion-exchange resins with Fe(III) oxide [2]. Regarding to heavy metal cations, zirconium hydrophosphate (ZHP) can be considered as a prospective dopant due to selectivity towards these species [3]. Moreover organic-inorganic materials demonstrate high rate of ion exchange [4]. Polymer ion-exchange resins are characterized by complex porous structure, which involves micro- and mesopores containing functional groups (gel phase), spaces between gel fields (mesopores) and structure defects (macropores) [5]. The dopant can occupy both gel fields and spaces between them. Location of particles of the inorganic constituent undoubtedly determines functional properties of the composite material.

## Experiments

Strongly acidic gel-like cation-exchange resin Dowex HCR-S has been chosen as a model matrix. The resin was immersed with a sol of hydrated zirconium dioxide followed by treatment with H<sub>3</sub>PO<sub>4</sub>. The synthesis procedure was repeated 1 (sample 1), 3 (sample 2), 5 (sample 3) and 7 (sample 4) times. Porous structure of the samples was investigated with a method of standard contact porometry, which can be applied to polymers [5, 6]. The method allows us to investigate only polymeric constituent since the pretreatment conditions (heating at 353 K) cannot provide water removal from HZP surface. Also Cd<sup>2+</sup>→H<sup>+</sup> exchange from individual and combined solutions was investigated both under static and dynamic conditions. Morphology of the samples was researched using transmission electron microscopy.

## Results and Discussion

The composite ion-exchangers contained 31-52 mass % ZHP. TEM and SEM images show large ZHP aggregates, which consist of brick-like ribbed fragments (Fig. 1). The fragments are formed due to aggregation of the nanoparticles (≈10 nm). The aggregates of micron size are evidently located in structure defects. Smaller aggregates (from ≈50 nm) have been also found. They can be placed both in spaces between gel fields and also in mesopores containing functional groups.

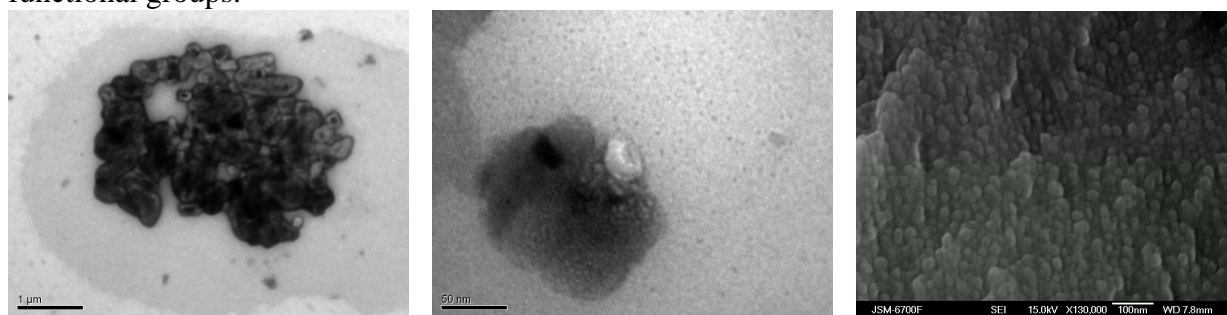


Figure 1. ZHP aggregates

Differential pore distributions demonstrate several maxima (Fig. 2). Regarding to the initial resin, the maximum I ( $\log r \approx 1$ (nm)) and probably maximum II ( $\log r \approx 1.4$ (nm)) can be related to pores, which contain functional groups [5, 6]. The maxima III ( $\log r \approx 3.2$  (nm)) and IV ( $\log r \approx 4$

(nm)) are attributed to cracks on the particle surface. Spaces between the particles give the largest pores. It is possible to observe a shift of the maxima I and II towards lower  $r$  values (modified samples). The maxima II are seen as shoulders of the maxima I. Three constituents are visible instead of the maxima III (sample 1). The peaks at  $\log r \approx 3.3$  and  $3.4$  (nm) correspond to pores, when the dopant is located. The sharp peak ( $\log r \approx 3.7$  (nm)) is related to pores, which are free from ZHP. These pores become regular due to polymer stretching.

Decrease of size of pores I and II can be caused by a decrease of swelling pressure and also by squeezing of these pores under the influence of the aggregates. Ribbed fragments can provide a small contact surface between the particles and pore walls. As a result, the pressure due to inorganic constituent can be comparable with swelling pressure ( $\approx 1.5 \times 10^7$  Pa). This causes incomplete filling of pores with water and decrease of total ion-exchange capacity. For instance, the total capacity of the initial resin is  $4.2 \text{ mmol g}^{-1}$ . The content of polymer in the sample 4 is 48 mass %, thus the contribution of the polymer into total capacity is  $2 \text{ mmol g}^{-1}$ . However the total capacity of this sample is only  $1.8 \text{ mmol g}^{-1}$  in spite of ZHP.

Intensity of the maxima I as well as microporosity increase within the order: sample 4 > sample 3 > sample 1 > sample 2. A change of porosity is probably due to competition of several factors: decrease of the polymer content, incomplete filling of pores with water and stretching of pore walls caused by squeezing. Stretching of the polymer leads to increase of distance between functional groups and more complete hydration of counter-ions of functional groups.

Intensity of the maxima at  $\log r \approx 3.7$  (nm) decreases within the order: sample 2 > sample 1 > sample 3 > sample 4 probably due to competition between stretching of the polymer and filling of the macropores with ZHP.

Isotherms of  $\text{Ca}^{2+} \rightarrow \text{H}^+$  and  $\text{Cd}^{2+} \rightarrow \text{H}^+$  exchange are described by the Langmuir equation (Fig. 3, here  $n$  is the number of modification cycle):

$$\frac{C}{A} = \frac{1}{A_{\infty}k} + \frac{C}{A_{\infty}},$$

where  $C$  is the concentration of equilibrium solution,  $A$  is the exchange capacity,  $A_{\infty}$  is the capacity of monolayer,  $k$  is the constant, which corresponds to energy of interaction of sorbed ions with a surface.

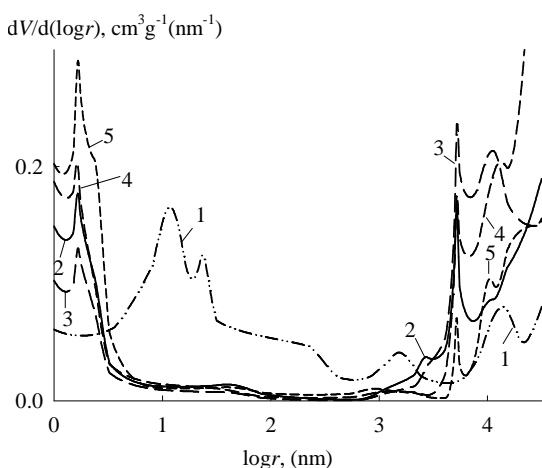


Figure 2. Differential distributions of pore volume for initial resin (1) and samples 1 (2), 2 (3), 3 (4), 4 (5)

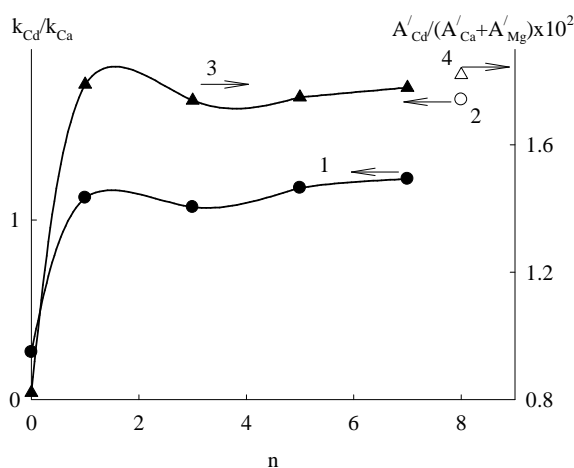


Figure 3. Relations of  $k_{Cd}/k_{Ca}$  (1, 2) and  $A'_{Cd}/(A'_{Ca} + A'_{Mg}) \times 10^2$  (3, 4) as functions of a number of modification cycle. Initial resin and samples 1-4 (1, 2), individual ZHP (3, 4)

The  $k$  values for the modified samples and individual ZHP are close to each other, thus ion-exchange properties of the composites are determined by the dopant. It was found that the relation of  $k_{Cd}/k_{Ca}$ , is larger than 1 both for inorganic and organic-inorganic ion-exchangers

(Fig. 3). A minimum of the  $k_{Cd}/k_{Ca} - n$  curve at  $n=3$  can be caused by a competition of two factors. The first one is a decrease of microporosity of the polymeric constituent, the second one is an increase of ZHP amount in the composites.

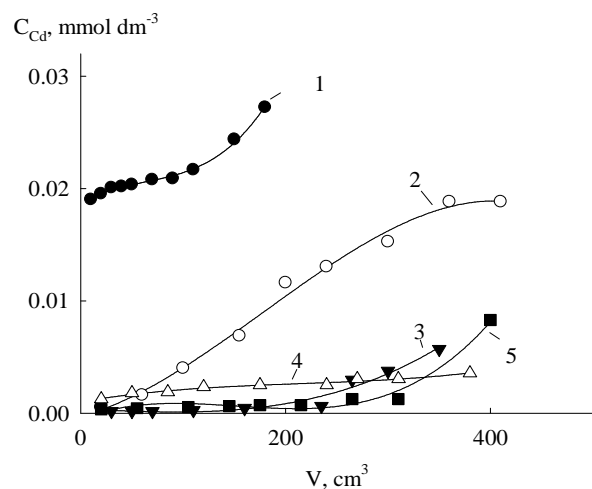


Figure 4.  $Cd^{2+}$  concentration at the column outlet as a function of volume of passed solution, which contained initially ( $mg\ dm^{-3}$ ):  $Cd^{2+} - 4$ ,  $Ca^{2+} - 57$ ,  $Mg^{2+} - 12$ . Samples: initial resin (1), individual ZHP (2), sample 1 (3), sample 2 (4), sample 3 (5)

As found, all the modified samples demonstrate better selectivity towards  $Cd^{2+}$  during deionization of combining solution, which contains also  $Ca^{2+}$  and  $Mg^{2+}$  (Fig. 4). The lowest  $Cd^{2+}$  concentration at the column outlet has been found in the case of composite ion-exchangers, at the same time the worst results have been obtained for the non-modified resin. The largest relations of  $A'_{Cd}/(A'_{Ca} + A'_{Mg})$  (here  $A'$  is the breakthrough capacity) have been found both for composite materials and individual ZHP (see Fig. 3). A shape of the curves of  $k_{Cd}/k_{Ca} - n$  and  $A'_{Cd}/(A'_{Ca} + A'_{Mg}) - n$  is similar. This indicates correlation of data obtained under dynamic and static conditions.

Thus ion-exchange properties of the composite ion-exchangers are determined by inorganic constituent.

## Conclusions

Modification of cation-exchange resin with inorganic dopant causes transformation of porous structure of the polymer influenced by aggregates of ZHP nanoparticles. The method of standard contact porometry, which allows us to investigate only polymeric constituent, was applied. Analysis of differential pore distribution shows, that this transformation is due to squeezing of pores, which contain  $-SO_3H$  groups, and stretching of the polymer. Moreover these pores are evidently free from water. Thus the inorganic constituent determines ion-exchange properties of the composites. They are remove preferably  $Cd^{2+}$  ions from combining solution, which contains also  $Ca^{2+}$  and  $Mg^{2+}$ .

## References

1. Kravchenko T.A., Kalinichev A.I., Polyanskii L.N., Konev D.V. Nanocomposites of metal-ion-exchanger. M.: Nauka, 2009.
2. Sarkar S., Chatterjee P.K., Cumbal L.H., SenGupta A.K. Hybrid ion exchanger supported nanocomposites: Sorption and sensing for environmental applications // Chem. Eng. J. 2011. V. 166. P. 923 - 931.
3. Yaroslavtsev A. B. Ion exchange on inorganic sorbents // Russ. Chem. Rev. 1997. V. 66. P. 579-596.
4. Dzyazko Yu.C., Ponomarouva L.N., Volfkovich Yu.M., Sosenkin V.E. Effect of the porous structure of polymer on the kinetics of  $Ni^{2+}$  exchange on hybrid inorganic-organic ionites // Russ. J. Phys. Chem. A. 2011. V. 85. P. 913-919.
5. Berezina N. P., Kononenko N. A., Dyomina O.A., Gnusin N. P. Characterization of ion-exchange membrane materials: properties vs structure // Adv. Colloid Interface Sci. 2008. V. 139, P. 3-28.
6. Volfkovich Yu.M., Sosenkin V.E., Bagotzky V.S. Structural and wetting properties of fuel cell components // J. Power Sources. 2010. V. 195. P. 5429--5441.

---

# TRANSPORT OF LOWER HYDROCARBONS THROUGH GRAPHITE FOIL MODIFIED BY DIRECT GAS-PHASE FLUORINATION

<sup>1</sup>Ekaterina Efimova, <sup>1</sup>Darya Syrtsova, <sup>2</sup>Olga Shornikova, <sup>3</sup>Aleksandr Kharitonov, <sup>1</sup>Vladimir Teplyakov

<sup>1</sup>Topchiev Institute of Petrochemical Synthesis RAS, Moscow, Russia

<sup>2</sup>Lomonosov Moscow State University, INUMIT Company, Moscow, Russia

<sup>3</sup>Institute of Energy Problems for Chemical Physics (Branch), RAS, Russia

## Introduction

One of the membrane technology and particularly gas separation processes keynote goals is research and development of new membrane materials with high separation and transport properties at thermal and chemical stability [1]. Alternative way for solving of this challenge task is modification of already existing materials and membranes. Nowadays a lot of different methods for membrane post treatment are known: chemical, electrochemical, plasma chemical, surface modification, including gas-phase fluorination and etc. One of the most effective methods is a direct gas-phase fluorination method which is traditionally used for polymeric membrane [2-3]. However, inorganic nanoporous materials which demonstrate very perspective gas separation properties, for example, zeolites and carbon based matrix also could be modified by this method. Particularly this modification method can seriously influent on surface gas flow and as result on separation properties of nanoporous materials. One of interesting materials for fluorination is the nanoporous graphite foils (GF) based on pressed intercalated graphite compounds which provides high H<sub>2</sub>/CO<sub>2</sub> and C<sub>4</sub>H<sub>10</sub>/CO<sub>2</sub> separation [4]. In the present work the influence of the direct gas-phase fluorination treatment on GF gas transport and separation properties was investigated.

## Studied objects

In the present work gas separation properties of the membranes base of exfoliated graphite foils produced by Inumit Co (Russian Federation) with range of density 0,98-1,50 g/cm<sup>3</sup> and thickness 0,3–0,6 mm were studied.

GF based on exfoliated graphite was obtained by following technique provided required thickness and density of foil samples: the intercalated graphite was prepared from graphite nitrate of II stage by following method [5]: natural graphite had been treated by 98 % nitric acid at mass relation 1:0.8. Then intercalated graphite had been treated by hydrolysis, and then it was termo-expanded at 900 °C to obtain exfoliated graphite. Then pressing procedure was used to obtain GF with high mechanical properties.

## Fluorination technique

The modification of GF by gas-phase fluorination was carried out by following technique: the samples were placed in a closed reactor, after that the reactor was degassed till vacuum (10<sup>-1</sup>-10<sup>-2</sup> Torr), than the reactor was heated up in oven. In 3 hour (under continuous de-gassing) temperature reached the steady-state values that were varied from 195 to 350 °C and pure fluorine was pumped in the reactor till pressure equal 1 bar is reached. Pressure in the reactor was kept constant (1.00±0.02 bar) and time of treatment was varied from 1.5 to 2.5 hours. Samples weight was measured before and after fluorination.

## Gas permeance experiment

The permeance of He, N<sub>2</sub>, H<sub>2</sub>, CO<sub>2</sub>, CH<sub>4</sub>, C<sub>3</sub>H<sub>8</sub> and n-C<sub>4</sub>H<sub>10</sub> was measured by differential method with chromatography analysis using two techniques:

- sweeping of permeate by carrier gas (He, Ar) in temperature range 296-373 K;
- evacuation of permeate (p<sub>perm</sub> ~ 10<sup>-2</sup> atm).

## Results and Discussion

It was found that GF gas-phase fluorination leads to increasing of samples weight by 2-3 % depending on modification conditions. No variation of samples weight was mentioned after permeability experiments.

Gas-phase fluorination of GF resulted in decreasing of the permeance of He, N<sub>2</sub>, H<sub>2</sub> and especially CO<sub>2</sub> (CO<sub>2</sub> permeance decreased almost in 2 times). However, the modification didn't seriously influence on the n-C<sub>4</sub>H<sub>10</sub> permeability. It should be mentioned that fluorination provides enough high level of gas permeance in comparison with initial samples to use modified membranes in separation processes. Thus the difference of CO<sub>2</sub> and hydrocarbons achieved permeability difference C<sub>4</sub>H<sub>10</sub>/CO<sub>2</sub> selectivity increased approximately in 1.5 times.

Temperature dependencies of H<sub>2</sub>, CO<sub>2</sub>, N<sub>2</sub> permeance were studied for initial and fluorinated GF with different density. It was shown that the gas permeance decreasing of fluorinated GF is less significant and has monotonous form in comparison with initial ones with temperature growing. It can be result of the significant decreasing of surface flow contribution in overall flow through the membrane, especially in the case of CO<sub>2</sub>. Analysis of obtained experimental data shows that molecular diffusion became more important in comparison with initial samples at not so significant decrease of gas flux. In this case the flux decrease can be connected with changing of the least pore diameters as result of fluorine molecules influence.

### Conclusion

In the present work it was demonstrated that long-time direct gas-phase fluorination of GF significantly affects on gas transport properties of studied membranes, especially on temperature dependences of gas permeability.

Thus the results demonstrate the possibility of application of the direct gas-phase fluorination modification method for improving of gas transport properties not only of polymeric but also of inorganic carbon-based membranes.

### Acknowledgements

Authors thank:

- Dr. D.V.Dmitriev, Association «ASPECT» (Moscow, Russia) for permoporometry analysis.
- Group ENSIC (Nancy, France) for help with SEM analysis of samples.
- Grants RFBR № 11-03-00793 and № 12-03-00901 for financial support.

### References

1. *Yampolskii Yu. , Pinnau I., Freeman B.* Material Science of Membranes for Gas and Vapor Separation.- John Wiley and Sons, Ltd, England. 2006. P. 435.
2. *Syrtsova, D.A., Kharitonov A.P., Teplyakov V.V., Koops G.-H.* Improving gas separation properties of polymeric membranes based on glass polymer by gas phase fluorination // Desalination. 2004. V. 163. P. 273-279.
3. *Kharitonov A.P., Moskvina Yu.L., Syrtsova, D.A., Starov V.M., Teplyakov V.V.* Direct Fluorination of the Polyimide Matrimid 5218: The Formation Kinetics and Physicochemical Properties of the Fluorinated Layers // Journal of Applied Polymer Science. 2004. V. 92. P. 6-17.
4. *Teplyakov V.V., Syrtsova, D.A., Efimova, E.A., Sorokina, N.E., Ionov S.G., Avdeev V.V.* 2009. Composite material for gas separation, membrane and membrane module from this material. RU patent 2347604 C1.

# A COMPARATIVE STUDY OF TECHNOLOGICAL PROPERTIES OF DEMINERALIZED MILK PERMEATE

<sup>1</sup>Ivan Evdokimov, <sup>2</sup>Dmitry Volodin, <sup>1</sup>Irina Kulikova, <sup>1</sup>Alexander Donskih, <sup>1</sup>Maria Greshnyakova

<sup>1</sup>North Caucasias State Technical University, Stavropol, Russia; E-mail: eia@ncstu.ru

<sup>2</sup>Ltd "MEGA. Profiline", Stavropol, Russia, E-mail: vdn@mpline.ru

## Introduction

Milk permeate is the by-product of milk processing by ultrafiltration to produce protein concentrates. Permeate contains the soluble parts of the milk or whey; dairy salts and lactose. Permeate has many different applications. For example spray dried permeate is used in confectionary products or as a filler for food products or a carrier for seasonings. In addition whey and milk ultrafiltration permeate are base for various beverages [1]. In our studies nanofiltration (NF) and electro dialysis (ED) were used to compare the influence of these processes on technological properties of permeate [2].

## Experiments

Skim milk permeate (Table 1) was processed on nanofiltration pilot plant (Test Unit M20 (Alfa Laval)) with polymeric roll membranes. The process temperature was 12°C, the process pressure was 20 bar, the concentration factor was 3–4. Then part of concentrated permeate was demineralized on ED-Y pilot plant. The process temperature was 15°C, heterogeneous ion-exchange membranes Ralex were used and the demineralization level was more than 90%.

## Results and Discussion

The composition various types of permeate shown in Table 1, sensory characteristics shown in figure 1.

**Table 1: The composition of permeate after nanofiltration and electro dialysis**

Parameter	Permeate		
	native	NF treatment	NF and ED treatment
Total dry extract, %	5,1±0,1	17,5±0,1	15,2±0,2
Lactose %	4,6±0,2	12,7±0,2	13,0±0,3
Total protein, %	0,19±0,12	0,60±0,13	0,65±0,15
Conductivity (mS)	5,6±0,1	15,6±0,3	0,9±0,1
pH	6,06±0,01	4,56±0,03	3,32±0,01

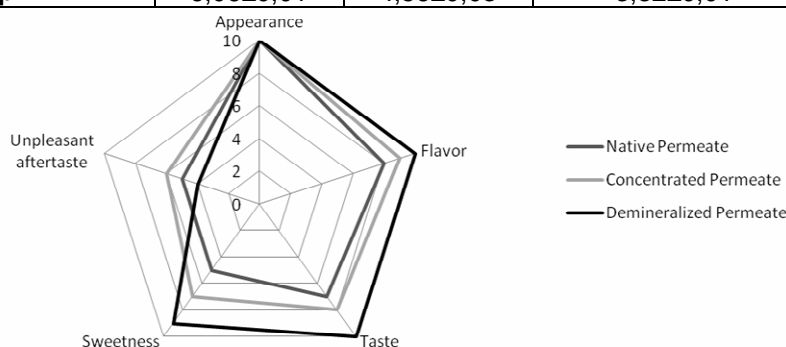


*Figure 1. Sensory characteristics of permeate*

According to the results demineralized permeate consists less amount of mineral substances; its taste is sweeter and cleaner. Therefore, demineralized permeate is the preferred raw material in the manufacture of beverages.

## References

1. Hattem H.E., Elham H. Abouel-Einin, Mehanna N.M. // J. Brewing and Distilling. 2011. V.2. P.24-27.
2. Suarez E. et al. // Desalination. 2009. V. 241. P.272–280.

# UTILIZATION OF INDUSTRIAL WASTES BY ELECTRODIALYSIS

<sup>1</sup>Evgenie Egorov, <sup>2</sup>Alexey Svitsov

<sup>1</sup>Mendeleev's university of chemical technology of Russia, Moscow, Russia,

<sup>2</sup>"Hydrotech" LLC, Moscow, Russia, *E-mail: enegorov@gmail.com*

## Introduction

Although pressure driven membrane methods for water solutions separation are applying widely, the electrodialysis (ED) process for a number of practical applications has no alternative. The theoretical and practical investigations of some ED applications are carrying out in the membrane technology department of the MUCTR.

## Experiments

The technology of vat residue deactivation after the liquid radioactive wastes treatment was introduced in the last decade. This technology allows to obtain the non-radioactive brines with total salinity ca. 100-150 g/l. The brines are considered as the source of chemicals (alkali and acids solutions primarily) for nuclear power plants operation. In this case the problem of brines disposal from overloaded storages will also solve. One of the most demanded product of the brines utilization is boron acid. The two-chamber ED with cation-exchange and bipolar membranes proposed as a stage of boron acid recovery process chain. The laboratory experiments with model solutions ( $\text{NaNO}_3 + \text{Na}_2\text{B}_4\text{O}_7$ ) as the previous before real solutions were carried out.

The modern apatite (calcium halogen phosphate) and nepheline (sodium and potassium aluminosilicate) processing technology related to large amount of mineral acids using and mineralized waste water generation. These wastes may be utilized with acid, alkali and demineralized silica solutions obtaining. The acid and alkali solutions may be recycled, and silica solutions may be used in construction materials manufacturing. For this process investigation the ordinary three-chamber ED with bipolar membranes is proposed. The laboratory experiments with model solutions (potassium alum and aluminum sulfate) and solution after the opening of the nepheline were carried out.

## Results and discussion

In the experiments with the two-chamber ED solutions of sodium hydroxide with  $\text{pH} \approx 12.5$  and nitric and boron acids blend with  $\text{pH} \approx 1.5$  were observed. The sharp change of pH in the acid chamber were detected (fig.1).

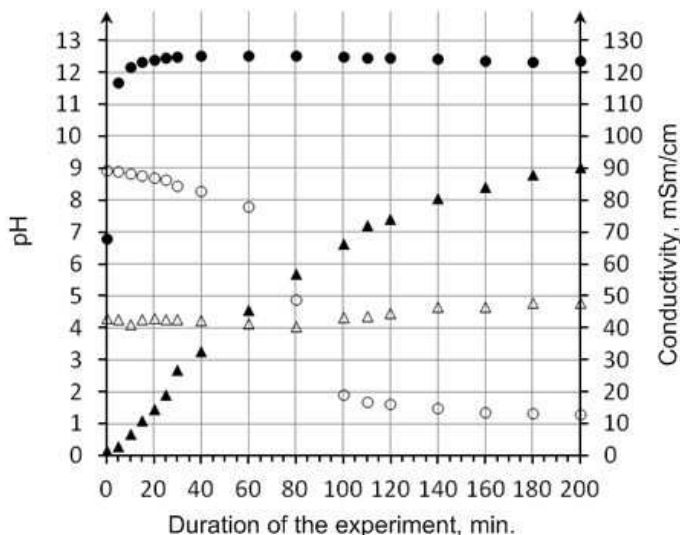


Figure 1. The changes in the properties of initial (50 g/l of  $\text{NaNO}_3$  and 10 g/l of  $\text{Na}_2\text{B}_4\text{O}_7$ ) and alkali solutions during the experiment.  $\circ$  - pH of initial solution;  $\bullet$  - pH of alkali solution;  $\triangle$  - conductivity of initial solution;  $\blacktriangle$  - conductivity of alkali solution

In the experiments with aluminum containing solutions the typical picture of acid and alkali generation while initial solution desalination. A high concentration of aluminum in initial solution does not lead to membrane fouling.

## References

1. Dudnik S.N., Svitsov A.A., Demkin V.I. // Memb. Critical techn. series. 2008. №4 V.40. P.9.
2. Vedernikov A.A., Hubetsov, Svitsov A.A., Bondarenko A.M. // Atomeco. Collection of art. 2009. P. 25.
3. Panteleev V.I., Demkin V.I., Amelin V.S. // Report on the researchwork implementation. 2011. P.38.

# SYNTHESIS OF NANOSTRUCTURED ION EXCHANGE MEMBRANES FOR ELECTROCHEMICAL PROCESSES OF WATER PURIFICATION

Edil Ergozhin, Tulegen Chalov, Tatyana Kovrigina

JSC "Institute of chemical sciences named after A.B. Bekturov", Almaty, Republic of Kazakhstan,  
E-mail: chalov.45@mail.ru

## Introduction

Methods of membrane technology are increasingly used in various fields of industrial production, and therefore physical-chemical and electrochemical property demands to the ion-exchange membranes are raised. Currently directed search for the source of reactive compounds and synthesis based on these different types of membranes for electro dialysis processes is carried out.

## Experimental

The synthesis of interpolymer membranes was performed in a three-necked reactor with a polymeric binder - polyvinyl chloride (PVC) in the total solvent. Next, into the reactor was placed an ether (diglycidyl ether of resorcinol (DGER) and vinyl ether of monoethanolamine (VEMEA)), allyl bromide (AB) and amine (polyethylene polyamine (PEPA), hexamethylenediamine (HMDA), polyethyleneimine (PEI)) pre-dissolving in cyclohexanone (CH). The reaction temperature was maintained at 70°C for two hours stirring. Then the reaction mixture was cast onto a smooth surface and dried under UV light [1-4].

## Results and Discussion

In order to find optimal process conditions the effect of the ratio of initial components and their nature on the electrochemical and physico-mechanical properties of indicators of the formed membranes is investigated. Definition of basic electrochemical characteristics was carried out on laboratory electro dialysis cell. We found that most static exchange (SEC–4.2 mg-equiv./g) have ion-exchange membranes at a weight ratio DGER+VEMEA+AB+amine+PVC = 70 : 30 wt.%. The samples have a low electrical resistivity and sufficiently high to unreinforced membrane mechanical strength. Further increase in the concentration of the amine has little effect on changes in SEC membranes (Table 1).

**Table 1: Electrochemical properties of interpolymer membranes on the basis of VEMEA, DGER, AB and binding PVC received in the presence of different polyamines**

Membranes on the basis of VEMEA:DGER:AB in the presence of	SEC of 0,1 n HCl solution, mg-equiv./g	The resistivity, Ohm·cm	Transfer number, %	Specific water permeability, $K \cdot 10^{-14}, \text{cm}^3 \cdot \text{sec/g}$
PEPA	2,9	90	0,98	1,3
HMDA	3,2	65	0,97	1,8
PEI	4,2	54	0,98	1,9
MA-40	3,4	240	0,94	—

Note: MA-40 – industrial membrane brand.

The structure of obtained ion-exchange membranes containing in its composition the different functional groups was examined by standard and mercury porometry (Figures 1, 2).

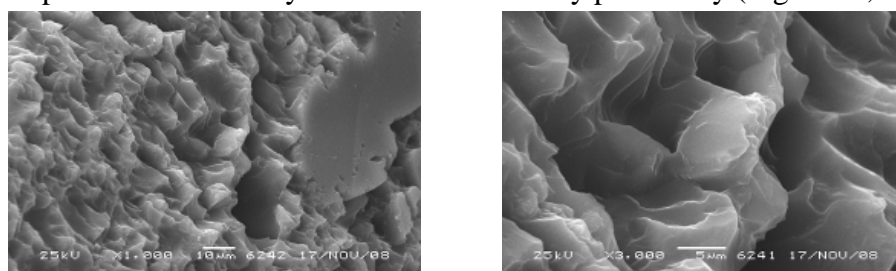


Figure 1. Microphotography of samples of synthesized ion exchange membranes

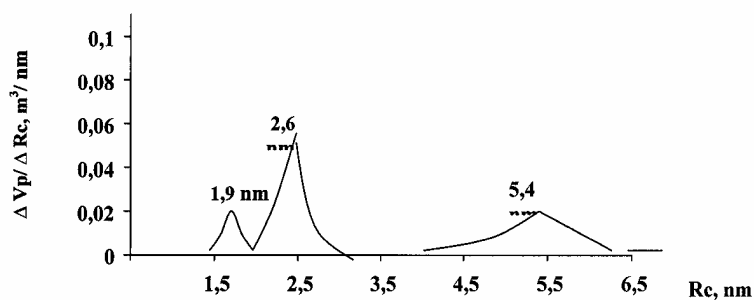


Figure 2. Pore distribution with radius in synthesized ion exchange membranes on the basis of VEMEA, DGER, AB and PEPA

The study of the relative and volume porosity of membranes is of some theoretical and practical interest, since their number and relative position in the ion exchanger has a significant influence on the sorption and electrochemical properties of the final products. The structure of the dry samples is significantly different from their structure in the working swollen state, as the swelling leads to a multiple increase in pore volume due to hydration of functional groups [5].

The porosity ion exchange membranes of interpolymer type based on DGER, VEMEA, AB and PEPA depends on the duration of curing and nature of the starting monomers. It was found that they are characterized by the specific porosity of 0.2 to 2.0 mg/g, which decreases with increasing length of curing.

It is shown that the samples synthesized at 60°C have the most homogeneous pore structure in all the film thickness. Raising the temperature to 80°C and increasing the duration of curing to 24 h leads to an increase in SEC and a decrease in the relative volume porosity of the membranes from 12.9 to 0.8 cm<sup>3</sup>/g, depending on the nature of the starting monomers. It follows that the increase in temperature leads to a decrease in pore size and thus reduce permeability.

The study of the porous structure of synthesized interpolymer membranes by the method of mercury porosimetry showed that the samples generally contain pores of radius 1.9-2.6 nm and a slightly smaller number of pores of radius 5.4 nm. The relative specific porosity of the membranes is 6.8-1.0 cm<sup>3</sup>/g [6].

Thus, on the basis of the available reactive monomers and oligomers the ion-exchange resins and membranes with a high sorption, physical, mechanical and electrochemical properties are synthesized. By standard and mercury porosimetry methods the sizes of pores of the received membranes are determined. Sizes and most narrow distribution of pores with radius of the synthesized membranes indicate that they are identical in structure with homogeneous, which opens up broad prospects for their practical application [7].

## References

1. Ergozhin E.E., Chalov T.K., Tskhay A.A., Kovrigina T.V., Khakimbatova K.Kh. // The III Intern. Scientific Conf. «Modern Tendencies of Development of Science in Central Asia» To the 70<sup>th</sup> Anniversary of Korean Diaspora's Residing in Central Asia. Almaty, 2007. P.129, 130.
2. Ergozhin E.E., Chalov T.K., Kovrigina T.V., Izatbekov E.U. // V Russian Kargyn's conf. «Polymers-2010». M.: 2010. P. 107.
3. Ergozhin E.E., Chalov T.K., Kovrigina T.V., Khakimbatova K.Kh. // Conf. «Plastics with special properties» Book of abstracts. St. Petersburg: 2011. P. 215-218.
4. Innovational patent Kazakhstan № 23162. / Ergozhin E.E., Chalov T.K., Kovrigina T.V., Бегенова Б.Е., Khakimbatova K.Kh., Izatbekov E.U.; publ. 15.11.2010, № 11.
5. Zabolotsky V.I., Nikonenko V.V. Ion transfer in membranes. M: Nauka, 1996. 392 p.
6. Volkovitch Yu.M. // Abstracts of Russian sci. conf. «Membranes-2007». M.: 2007. P. 93.
7. Ergozhin E.E., Chalov T.K., Tskhay A.A., Kovrigina T.V., Khakimbatova K.Kh. // Journal: Water, chemistry and ecology. 2011. № 7. P. 25-32.

# COMPARISON OF PROPERTIES OF MF-4SC/POLYANILINE COMPOSITES PREPARED IN CONCENTRATION AND ELECTRIC FIELDS

<sup>1</sup>Irina Falina, <sup>1</sup>Ninel Berezina, <sup>1</sup>Marya Chernyaeva, <sup>2</sup>Vyacheslav Roldugin, <sup>2</sup>Ivan Senchychin

<sup>1</sup>Kuban State University, Krasnodar, Russia, E-mail: Irina\_falina@mail.ru

<sup>2</sup>Frumkin Institute of Physical Chemistry & Electrochemistry of RAS, Moscow, Russia

## Introduction

The main problem in perfluorinated membranes application in polymer electrolyte fuel cell (PEFC) is retention of high humidity and proton conductance at working temperatures [1]. Nowadays the composites based on Nafion type membranes and electron conducting polymer polyaniline (PAn) are widely explored to resolve this problem [1,2]. The aim of this work is to reveal the influence of membrane modification method by PAn on the water management and thermal characteristics of basic matrix. For this aim the differential scanning calorimetry (DSC), thermogravimetry (TGA), FTIR-spectroscopy, membrane conductometry and diffusion permeability methods were used.

## Experiments

We explored composites MF-4SC/PAn prepared by two different methods: under concentration gradient (successive diffusion method) with surface PAn layer placed afterwards (fig. 1a) and under simultaneous action of concentration and electric fields (fig. 1b). As the polymerization initiator FeCl<sub>3</sub> solution was used. These samples possess balanced electro-transport properties: reduced anisotropic diffusion permeability and conductivity close to initial MF-4SC membrane (fig. 2, where  $\kappa$  is conductivity of membrane, P is diffusion permeability coefficient of unmodified sample, P<sub>s</sub> and P<sub>w</sub> are diffusion permeability coefficients in cases when composite membrane is faced by modified and unmodified surfaces towards electrolyte flow correspondingly).

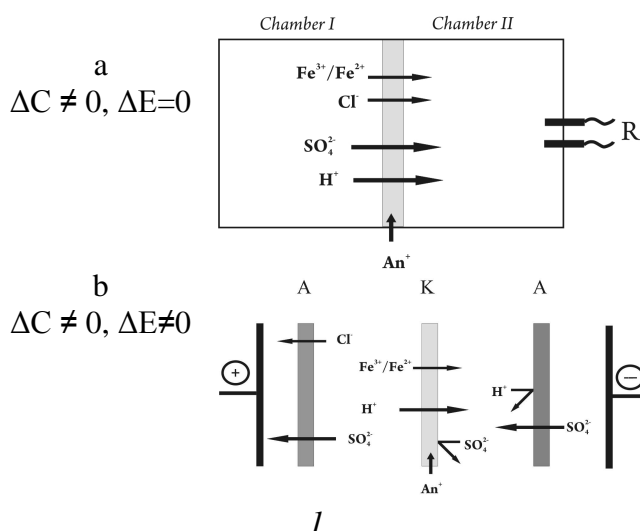


Figure 1. Schematic presentation of cells for chemical template synthesis of composites MF-4SC/PAn: (a) successive diffusion method and (b) synthesis in external electric field

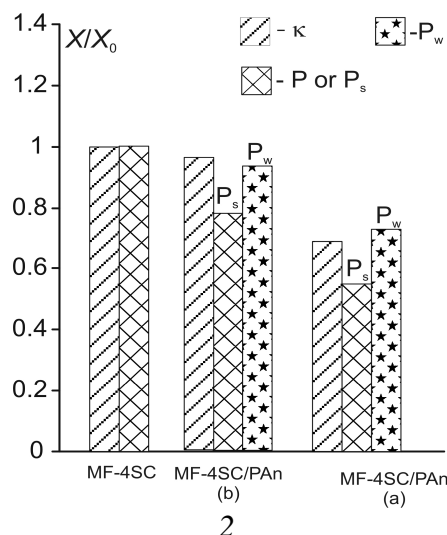


Figure 2. Relative presentation of conductivity and diffusion permeability data of initial MF-4SC and composite MF-4SC/PAn membranes

## Results and discussion

The FTIR-analysis of membrane detected peaks at 1493 and 1620 cm<sup>-1</sup> corresponding to benzoid and quinoid rings vibration with equal intensity. This indicates the presence of PAn in middle oxidation and most conductive state - emeraldine.

TGA-analysis showed that for composites desulfonation process begins at higher temperature by 3-5°C than for initial membrane. It's caused by interaction between PAn chains and fixed sulfur-groups of template matrix. The magnitude of solid residue for MF-4SC/PAn (b) is higher than for MF-4SC/PAn (a), that points to a greater quantity of PAn introduced in electric field synthesis conditions.

On fig. 3a the DSC-profiles for composite and basic membranes are presented. For MF-4SC/PAn (b) sample the temperatures of II, III, IV transitions are higher than for the basic membrane. Analysis of areas under II and III peaks shown, that PAn intercalation causes water reorganization between intermediate (II transition) and cluster zones (III transition). Comparison of DSC-data with porosimetric curves obtained by standard contact porosimetry method (fig. 3b) showed that main water displacement occurs in pores with effective radii 1-100 nm (nanosize level). This area corresponds to II transition on the DSC-profiles. For MF-4SC/PAn (a) sample significant changes in water organization do not happen, except slight increase of II transition temperature.

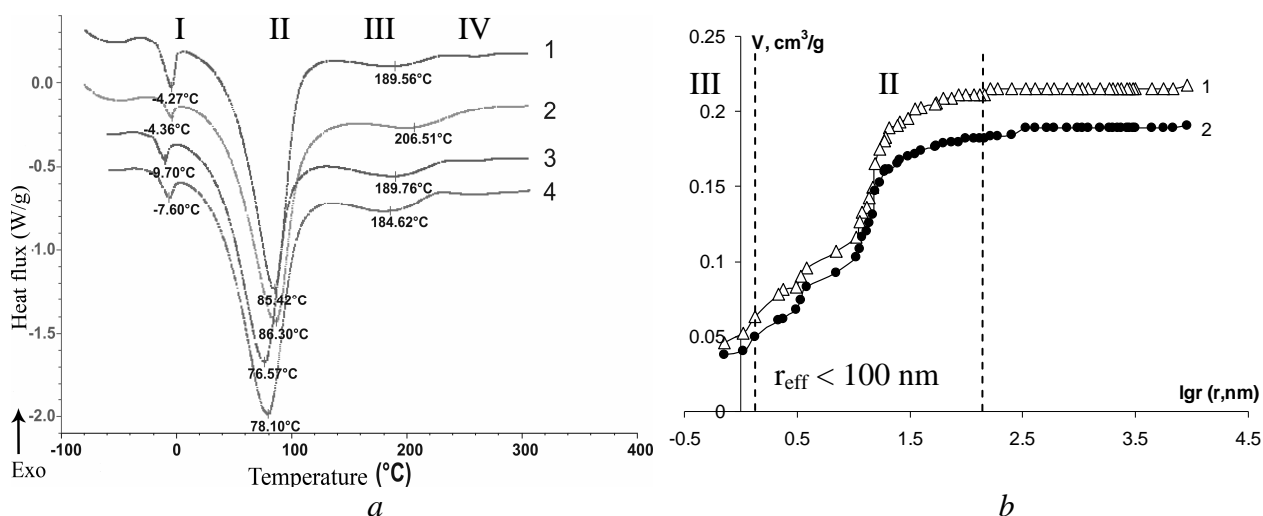


Figure 3. DSC profiles (a) and porosimetry curves (b) for bare MF-4SC membranes (1,3) and for composites MF-4SC/PAn (2,4). 2 – MF-4SC/PAn (B), 4 – MF-4SC/PAn (A)

Presented results show that PAn chains and fixed ions form in membrane phase interpolymer complex, which contains water molecules. The aromatic chains of PAn localize both in the intermediate area and in the cluster zone and change nanosystem of the basic matrix. As a result, the composite purchases greater thermal stability than the initial MF-4SC membrane. The formation of interpolymer complex MF-4SC/PAn promotes retention of water quantity enough to provide high protonic conductance at operating temperatures of PEFC. The influence of electric field on the PAn synthesis process consists in following: anilinium and Fe<sup>3+</sup> ions (counter-ions relative to basic matrix) hastened by electric field, easily enters into the membrane bulk. As a result the PAn chains form across the transport channels of the template matrix.

On the base of performed research the influence of simultaneous action of concentration and electric fields (under the rest equal conditions) on the Pan distribution in the basic matrix is revealed and corresponding structural model is suggested. When the composite membrane was modified under concentration gradient the PAn distributes in matrix volume in a random way mainly in the intermediate area (fig. 4a). This leads to reduction of conducting and diffusion characteristics.

In the case of PAn synthesis under simultaneous action of concentration and electric fields the pore walls are 'laminated' with PAn chains (fig. 4b). Hence the modifier localizes in cluster zone near the fixed ions, it does not make the steric hindrance for the diffusion transfer (with the exception of the PAn compact layer on the surface).

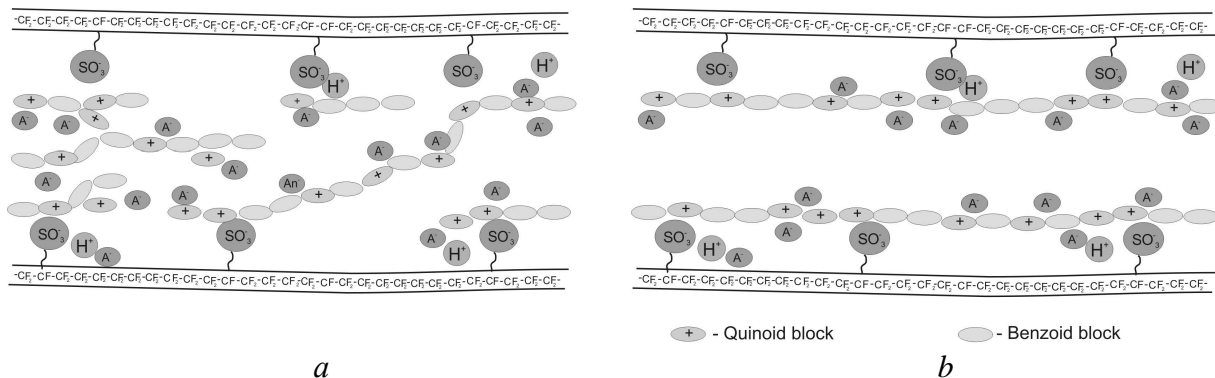


Figure 4. The character of Pan distribution in cluster-channel structure of basic matrix.  
*a* – random distribution, *b* – “lamination” of transport channels

The conductivity of lengthy PAn chains contributes into the total conductivity of the material and permits to possess the high conductivity level of the composite MF-4SC/PAn (*b*) comparable with the initial membrane. When the synthesis is carried out in the external electric field the PAn distribution could be regulated and the material created possesses by the optimized complex of physico-chemical properties.

*The work was supported by Russian Foundation for Basic Research (Project No 12-08-01092).*

### References

1. Peighambaroust S.J., Rowshanzamir S., Amjadi M. Review of the proton exchange membranes for fuel cell applications // *Int Journal of Hydrogen Energy*. 2010. V.35. P. 9349-9384.
2. Munar A., Suarez K., Solorza O., Berezina N.P., Compañ V. Performance of Hydrogen Fuel Cell MEAs Based on Perfluorinated Nanocomposite Membranes Modified by Polyaniline // *Journal of Electrochemical Society*. 2010. V. 4, №1. P. B1186-B1194.
3. Molla S., Falina I.V., Berezina N.P., Suarez K., Solorza O., Riande E., Compañ V. PEMFC performance of MEAs based on Perfluorinated nanocomposite membranes modified by polyaniline // *11<sup>th</sup> Grove Fuel Cell Symp.* London. 2009.

# A HUGE MAGNETORESISTIVITY IN N-Si/SiO<sub>2</sub>/Ni NANOSTRUCTURES FABRICATED IN TRACK-ETCHED PORES

<sup>1</sup>Alexander Fedotov, <sup>2</sup>Julia Fedotova, <sup>3,4</sup>Pavel Apel, <sup>1</sup>Dmitry Ivanou, <sup>1</sup>Yulia Ivanova, <sup>1</sup>Ivan Svito, <sup>1</sup>Eugen Streltsov

<sup>1</sup>Belarusian State University, Minsk, Belarus

<sup>2</sup>National Center of Particles and High Energy Physics of BSU, Minsk, Belarus

<sup>3</sup>Flerov Laboratory of Nuclear Reactions, JINR, Dubna, Russia; *E-mail: apel@nrmil.jinr.ru*

<sup>4</sup>The International University "Dubna", Dubna, Russia

## Introduction

Synthesis of nanorod arrays, containing nanogranular materials on Si substrate and utilizing the enhanced magnetoresistive (MR) effect, shows much promise for the design of Si-compatible magnetoelectronic devices [1, 2]. In this work we study the carrier transport and magneto-transport properties in the bundles of Ni nanorods (or NanoRods-In-Pores – NRIPs) embedded into the n-Si/SiO<sub>2</sub> porous template created by selective etching of swift heavy ion tracks in a SiO<sub>2</sub> layer when the pores are filled with nickel nanoparticles.

## Experiments

We used underpotential electrodeposition of Ni nanoparticles into the nanopores in a SiO<sub>2</sub> layer as a template created on the phosphorous-doped n-Si(100) substrate with 4.5 Ω·cm resistivity to produce magnetosensitive nanostructures n-Si/SiO<sub>2</sub>/Ni. A SiO<sub>2</sub> layer with the thickness 700 nm was thermally grown on the Si(100) substrate by the standard procedure (1100°C, 10 hours, pure oxygen). To produce a nanoporous SiO<sub>2</sub> layer, scanned beams of 350 MeV <sup>197</sup>Au<sup>26+</sup> ions were employed for the bombardment of the oxidized Si wafers with fluences of about 5·10<sup>8</sup> cm<sup>-2</sup>. The pores were formed by chemical etching of latent tracks in a dilute HF acid for a whole depth of the SiO<sub>2</sub> layer down to the Si substrate. The regimes and electrochemical properties of the samples studied were described in [3]. Etching resulted in the formation of the nanopores randomly distributed over the sample surface and shaped like truncated cones with heights about 400–500 nm and down/upper diameters of 100/250 nm. The nanopores filled with Ni nanoparticles enable one to form a system of NRIPs randomly distributed within the SiO<sub>2</sub> layer.

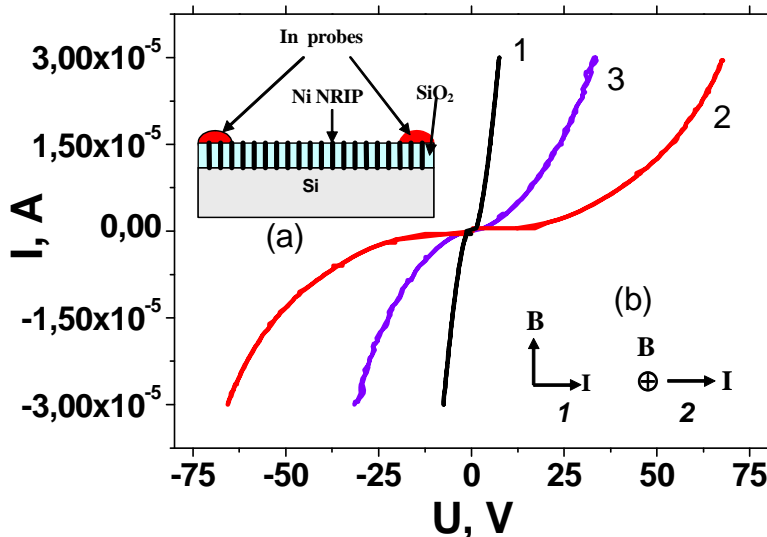


Figure 1. *I-V characteristics at 25 K for the magnetic field inductions  $B = 0$  (1) and  $B = 8$  T with  $B$ - $I$  configurations  $i = 1$  (2) or  $i = 2$  (3) shown in insert (b). Inserts show a schematic view Ni-NRIPs and In probes in n-Si/SiO<sub>2</sub>/Ni nanostructures (a) and a scheme of mutual alignments of magnetic induction vector  $B$ , current vector  $I$  and Si substrate plane at MR measurements (configurations  $i = 1, 2$ )*

Electrodeposited Ni-NRIPs had granular structure with the Ni particles having the face-centered cubic structure and dimensions of about 30–70 nm. The I-V characteristics and DC resistance of n-Si/SiO<sub>2</sub>/Ni nanostructures were measured at temperatures  $T = 2 \div 300$  K and magnetic fields  $B$  up to 8 T between two electric In probes shown in the sketch of the sample in insert (a) in Fig. 1. As is seen from insert (b) in Fig. 1, measurements were performed for two different mutual alignments  $i$  of vectors  $B$  and  $I$  and the substrate plane in n-Si/SiO<sub>2</sub>/Ni nanostructures. For  $i = 1$  vector  $B$  is parallel to NRIPs axis and normal to vector  $I$  in them and to Si substrate plane. For  $i = 2$  vector  $B$  is parallel to NRIPs axis and vector  $I$  in them but parallel to vector  $I$  in Si substrate plane.

## Results and Discussion

Fig. 1 shows that the I-V characteristics of n-Si/SiO<sub>2</sub>/Ni nanostructures exhibit non-linear behavior and strong dependence on mutual alignments of magnetic induction vector  $B$ , current vector  $I$  and Si substrate plane (NRIPs axis). The symmetry of I-V branches and the behavior of I-Vs at different temperatures shows that two nanorod bundles (contacting the Si substrate) under the electric probes electrically resemble two Si/Ni Schottky diodes serially joined and switched-on opposite to each other.

The typical temperature dependences of the resistance  $R = V/I$  for n-Si/SiO<sub>2</sub>/Ni nanostructures measured at  $B = 0$  and plotted in logarithmic scale are shown in Fig. 2a.

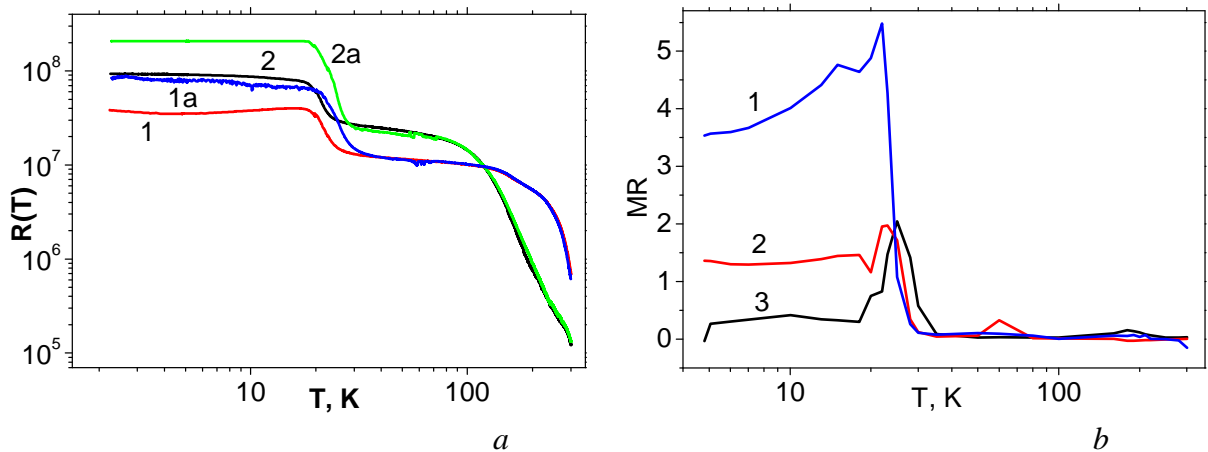


Figure 2. a - Temperature dependencies of resistance at  $B = 0$  (curves 1 and 2) and at  $B = 8$  T (curves 1a and 2a) for different measuring currents: 1, 1a – 1000 nA; 2, 2a – 100 nA. Mutual alignments of vectors  $B$ ,  $I$  and Si substrate plane corresponded to configuration  $i = 1$ . b – Temperature dependence of  $MR(B = 8$  T) for  $I = 10$  nA (1), 100 nA (2) and 10 nA (3)

We would note the following main features of these curves. Firstly, position of  $R(T)$  curves on ordinate scale in Fig. 2a is strongly dependent on the measuring current  $I$  although their shape is similar for different  $I$  values in the region 10–1000 nA.

The second feature is that the shape of  $R(T)$  curves for n-Si/SiO<sub>2</sub>/Ni nanostructures are principally different from behavior of metallic granular Ni films [4] which displayed metallic progress of  $R(T)$  with positive sign of  $dR/dT$ . As is seen, for n-Si/SiO<sub>2</sub>/Ni nanostructures  $dR/dT < 0$  that is characteristic for semiconductors or some of granular or disorderd systems. The analysis of the observed behavior of  $R(T)$  suggests that in the studied nanostructures at temperatures ranging 15–300 K the activation (exponential) carrier transport by the Si substrate dominates—intrinsic carrier transport at  $T > 100$  K and impurity transport in the region lower than 100 K.

As is seen from Figs. 1 and 2, the application of a magnetic field to the n-Si/SiO<sub>2</sub>/Ni nanostructure for both measurement configurations  $i = 1, 2$  caused strong increase of resistance ( $MR > 0$ ) approaching a huge values at around 25 K. Note also, that at temperatures higher than 180 K, when measuring currents  $I$  decrease, magnetoresistance become negative. This effect is

more pronounced on MR(B) curves shown in Fig. 2b which was calculated by point-to-point subtracting of the curves in Fig. 2a measured at different currents in  $B = 8$  T and  $B = 0$  correspondingly. The MR(B) curves behavior presented in Fig. 2b show that at low temperatures MR strongly increases with measuring current decrease approaching 200-600 % at temperatures of about 20-27 K for  $10 < I < 1000$  nA.

As we observed, at  $T > 180$  K, where conductance by Si substrate is predominant, the values of MR effects in n-Si/SiO<sub>2</sub>/Ni nanostructures for configurations  $i = 1, 2$  were negative as for the samples of Ni films studied. This probably means that magnetoresistance in this temperature region is similar to the anisotropic magnetoresistive effect [5] observed in Ni nanogranular films.

At temperatures lower than 100 K, where impurity conductance is realized, MR values for n-Si/SiO<sub>2</sub>/Ni nanostructures were always positive approaching maximum at approximately 23-25 K. These results enable one to assume that a huge positive magnetoresistive effect at these temperatures in n-Si/SiO<sub>2</sub>/Ni nanostructures can be associated with two possible contributions - the influence of Si/Ni Schottky barriers and/or movement of electrons along the electron-enriched Si/SiO<sub>2</sub> interfacial channel. To separate these two mechanisms we need to make additional experiments.

### Acknowledgement

The work was partially supported by VISBY Program of the Swedish Institute, the Joint Institute for Nuclear Research (Dubna, Russia), the Belarusian State Scientific Program 'NANOTECH' and Belarusian Fundamental Research Foundation by Contracts № Ф11D-005.

### References

1. *Imry Y.* Nanostructures and Mesoscopic Systems, ed. by W. P. Kirk and M. A. Reed, Academic, New York, 1992, P. 11.
2. Template-based synthesis of nanorod or nanowire arrays. In: Springer Handbook of nanotechnology. Bharat Brushan (Ed.). Springer. 2007, P. 161-178.
3. *Ivanova Yu. A., Ivanou D. K., Fedotov A. K., Streltsov E. A., Demyanov S. E., Petrov A. V., Kaniukov E. Yu., Fink D.* Electrochemical deposition of Ni and Cu onto monocrystalline n-Si(100) wafers and into nanopores in Si/SiO<sub>2</sub> template. // J. Mater. Sci. 2007. Vol. 42. P. 9163-9169.
4. *Fedotova Ju., Saad A., Ivanou D., Ivanova Yu., Fedotov A., Mazanik A., Svito I., Streltsov E., Tyutyunnikov S., Koltunowich T.* Magnetotransport in nanostructured Ni films electrodeposited on Si substrate. // Electrical Review. 2012. Vol. 88. P. 90-92.
5. *Toth B.G., Peter L., Revesz A., Padar J., Bakonyi I.* Eur. Phys. J. 2010. Vol. 75. P. 167-177.

---

## MATHEMATICAL MODELING OF THE MEMBRANE PROCESSES

Anatoly Filippov

Gubkin Russian State University of Oil and Gas, Moscow, Russia, E-mail: a.filippov@mtu-net.ru

Mathematical modeling is a powerful instrument to describe quantitatively the variety of membrane processes like as reverse osmosis, nano-, ultra-, microfiltration, electro dialysis and etc. The *goal* of mathematical modeling is to provide *simple but effective model* of the process under consideration. When an investigator desires to formulate *mathematical model for a new process* he usually selects *one, two or maximum three main features* of the new phenomenon. Then he tries to set up the *physicochemical model* of the chosen features of the process. And only afterwards the investigator turns to write the governing equations and boundary conditions i.e. he formulates the *boundary value problem* (BVP). As a first stage of modeling the new phenomenon only very *simplified* set of quasi-state ordinary or partial differential equations can be written. Practically in all cases of the first modeling stage, *exact analytical solution* of the BVP can be obtained. Such solution presents the measured quantity as a known function of coordinates and/or running time in dependence on *system parameters* which were chosen at the stage of preliminary physicochemical modeling. If this stage was successful in the sense of *adequate description* of experimental data connected to the phenomenon then the same or other investigator starts to create *extended mathematical model* in order to take into account other peculiarities of the phenomenon. Usually the extended model is *multi-dimensional and nonstationary* one and requires only *numerical solution*. So, the importance of exact solution for the simplified model is growing up because it is a simplest way to check obtained numerical results. As examples of simplified and extended models in the membrane electrochemistry we can bring the models for well-known electroconvection phenomena in electro dialysis under overlimiting regime. It is interesting to mention that sometimes even well-known scholars confuse the term "mathematical model" with the formulas for engineering calculations, which are obtained by approximating the experimental curves by means of analytical expressions.

During the lecture several examples of mathematical models developed for different phenomena in membrane systems will be considered: an asymmetry of the diffusion permeability [1-2], rejection coefficient [3-4] and current-voltage curves of ion-exchange membranes; increasing of the flow rate through thin capillary with internal porous layer [5]; an influence of a slipping of tangential stresses at porous-liquid interfaces and external magnetic field on the hydrodynamic permeability of a membrane [6, 7]; interactions between a charged particle and a charged surface of a membrane pore [8]; an appearance of flow of aqueous alcohol mixtures through nanoporous membranes under applying of trans-membrane pressure drop and etc. A very important question concerning boundary conditions for concentrations of ions and electric potential at membrane-liquid interfaces will be discussed also.

*The present work is supported by the Russian Foundation for Basic Research (projects nos 11-08-01043 and 11-08-96518).*

### References

1. Filippov A.N., Starov V.M., Kononenko N.A., Berezina N.P. // Adv. Colloid Interface Sci. 2008. V. 139. No. 1-2. P. 29-44.
2. Filippov A.N., Kononenko N.A., Vasin S.I., Kasperchik V.P., Yaskevich A.L., Chernyaeva M.A. // Colloid J. 2010. V. 72. No. 6. P. 846-856.
3. Vasin S.I., Filippov A.N. // Colloid J. 2012. V. 74. No. 1. P. 12-21.
4. Filippov A.N., Iksanov R.Kh. // Russ. J. of Electrochemistry. 2012. V. 47. No. 2. P. 181-188.
5. Filippov A.N., Khanukaeva D.Yu., Vasin S.I., Sobolev V.D., Starov V.M. // Colloid J. 2012. V. 74 (submitted).
6. Tiwari A., Deo S., Filippov A. // Colloid J. 2012. V.74. No. 4 (in press).
7. Deo S., Filippov A., Tiwari A., Vasiv S.I., Starov V.M. // Adv. Colloid Interface Sci. 2011. V. 164. No. 1-2. P. 21-37.
8. Filippov A.N., Iksanov R.Kh., Volkov A.V. // Petroleum Chemistry. 2011. V.51. No.7. P. 536-541.

# MATHEMATICAL MODEL OF ANISOTROPIC NANOCOMPOSITE MEMBRANE FOR ESTIMATION OF ASYMMETRY OF CURRENT-VOLTAGE CURVE PARAMETERS

<sup>1</sup>Anatoly Filippov, <sup>2</sup>Sergey Dolgoplov, <sup>2</sup>Natalia Kononenko

<sup>1</sup>Gubkin Russian State University of Oil and Gas, Moscow, Russia, *E-mail: a.filippov@mtu-net.ru*

<sup>2</sup>Kuban State University, Krasnodar, Russia

New mathematical model allowing description of complex electro-mass transfer processes through modified ion-exchange membranes possessing anisotropic structure and asymmetric transport characteristics is developed [1]. The model is based on the one-dimensional Nernst-Planck equations for steady state ion fluxes through heterogeneous membrane system with two diffusion layers under applied external electric field. (Fig.1).

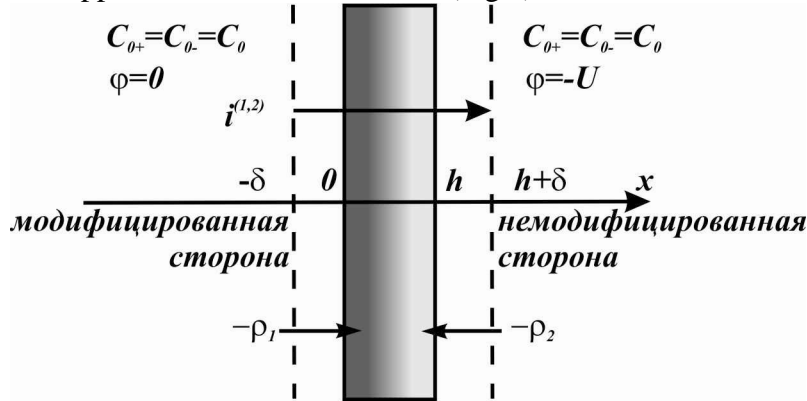


Figure 1. The scheme of the electrodiffusion in the MF-4-SC membrane with neighboring diffusive layers

Structural peculiarities and functional properties of the membrane are taking into account by the set of physicochemical parameters of the membrane system like as the distribution coefficients ( $\gamma$ ), the diffusivities ( $D$ ,  $D_m$ ) of electrolyte molecules in a bulk solution and in the membrane, values of the fixed charge densities on modified ( $\rho_1$ ) and opposite ( $\rho_2$ ) side of the membrane.

Equations for the ion fluxes have the following form, in diffusive layers:

$$J_{\pm} = -D(c_{\pm}' \pm c_{\pm}\phi'), \quad (1)$$

in the membrane:

$$J_{\pm} = -D_m(c_{\pm}' \pm c_{\pm}\phi'), \quad (2)$$

where  $\phi$ —dimensionless electric potential in  $F/RT$  units,  $c_{\pm}$ —ion concentrations.

Electroneutrality conditions are complimentary ones in the diffusive layers:

$$c_+(x) - c_-(x) = 0 \quad (3)$$

and inside the membrane:

$$c_+(x) - c_-(x) - \left[ \rho_2 - \frac{x}{h}(\rho_2 - \rho_1) \right] = 0. \quad (4)$$

The equalities of electrochemical potentials at interfaces  $x = 0$  и  $x = h$  lead to:

$$\begin{aligned} c_+(-0) &= c_+(+0)\gamma_+ \exp(\Delta\phi_0), \\ c_-(-0) &= c_-(+0)\gamma_- \exp(-\Delta\phi_0), \\ c_+(h-0)\gamma_+ \exp(-\Delta\phi_h) &= c_+(h+0), \\ c_-(h-0)\gamma_- \exp(\Delta\phi_h) &= c_-(h+0), \end{aligned} \quad (5)$$

and continuity of concentrations and electric potential on boundaries of diffusive layers provide:

$$c_{0\pm} = c_{\pm}(-\delta), \quad c_{\pm}(h+\delta) = c_{0\pm}, \quad \phi(-\delta) = 0, \quad \phi(h+\delta) = -U \quad (6)$$

Additionally we should take into account the electroneutrality beyond external boundaries of diffusive layers:

$$c_0 = c_{0+} = c_{0-} . \quad (7)$$

The electric current density is determined by the following formula:

$$i = F (J_+ - J_-) . \quad (8)$$

We introduced the following notations in the abovementioned formulas:  $\Delta\varphi_0, \Delta\varphi_h$  - jumps of electric potential through the membrane surfaces,  $U$  - the system voltage.

The model was successfully applied [2, 3] for evaluation of the asymmetry effect for the diffusion permeability of several modified ion-exchange membranes. The model was expanded [4] for description of current-voltage curves (CVC) of bi-layer membranes accounting for both diffusive layers ( $\delta$ ). Further development of the model led to supposition about linear distribution of the fixed charge density along the thickness of the modified membrane [5]. The supposition was based on the analysis of literature sources considering the structure of composites [6] when penetration of polyaniline chains takes place through the membrane under polymerization inside MF-4SC. It is seen from Table 1 [2] that charge densities on both sides are equal ( $\rho_1 = \rho_2$ ) only for initial unmodified membrane. After modification both values  $\rho_1$  and  $\rho_2$  were changed.

**Table 1: Physicochemical parameters of the initial MF-4SC and composite membranes MF-4SC/PAn [2] in dependence on the polymerization time**

Membrane	Membrane thickness, m	$-\rho_2, \text{mol/m}^3$	$-\rho_1, \text{mol/m}^3$	$C_0, \text{mol/m}^3$	$D, \text{m}^2/\text{s}$	$D_m, \text{m}^2/\text{s}$	$\gamma$
Initial	0,00019	-860	-860	50	$2,8 \cdot 10^{-9}$	$5,1 \cdot 10^{-11}$	0,26
1 h	0,00021	-360	-200	50	$2,8 \cdot 10^{-9}$	$1,4 \cdot 10^{-10}$	1,1
2 h	0,00022	-300	-120	50	$2,8 \cdot 10^{-9}$	$1,6 \cdot 10^{-10}$	1,38
3 h	0,00023	-290	-120	50	$2,8 \cdot 10^{-9}$	$2,2 \cdot 10^{-10}$	1,33

We assume that electric potential is monotonic function inside the membrane under given voltage  $U$  or electric current density  $i$  in the case of linear law for modulus of the fixed charge density  $\rho$  across the modified membrane:

$$\rho = \rho_2 - \frac{x}{h}(\rho_2 - \rho_1), \quad \rho > 0, \quad \rho_2 > 0, \quad \rho_1 > 0. \quad (9)$$

We found exact analytical expressions for the limiting current densities under different orientations of anisotropic membrane in a cell:

$$i_{\text{lim}}^{(\text{unmod})} = \frac{2C_0FD}{\delta} \cdot \sqrt{1 + \frac{16C_0^2}{\rho_1^2\gamma^2}} - \frac{16C_0^2FD_m}{h|\rho_1|\gamma^2} \cdot \left(\frac{\rho_2}{\rho_1} - 1\right) \quad (10)$$

$$i_{\text{lim}}^{(\text{mod})} = \frac{2C_0FD}{\delta} \cdot \sqrt{1 + \frac{16C_0^2}{\rho_2^2\gamma^2}} + \frac{16C_0^2FD_m}{h|\rho_2|\gamma^2} \cdot \left(1 - \frac{\rho_1}{\rho_2}\right) \quad (11)$$

where  $C_0$  - bulk electrolyte concentration;  $h$  - membrane thickness;  $F$  - Faraday number. The first term in (10)-(11) is the main one and the second term determines the asymmetry of the limiting current. So, the asymmetry is larger when the difference between  $\rho_1$  and  $\rho_2$  is stronger.

Theoretical calculations showed that CVC of modified membrane is asymmetric one [4]. Experimental investigations of CVC for templates made by method of matrix synthesis of polyaniline inside surfacial layer of MF-4SC membrane were performed to check the adequacy of the model. (Fig.2).

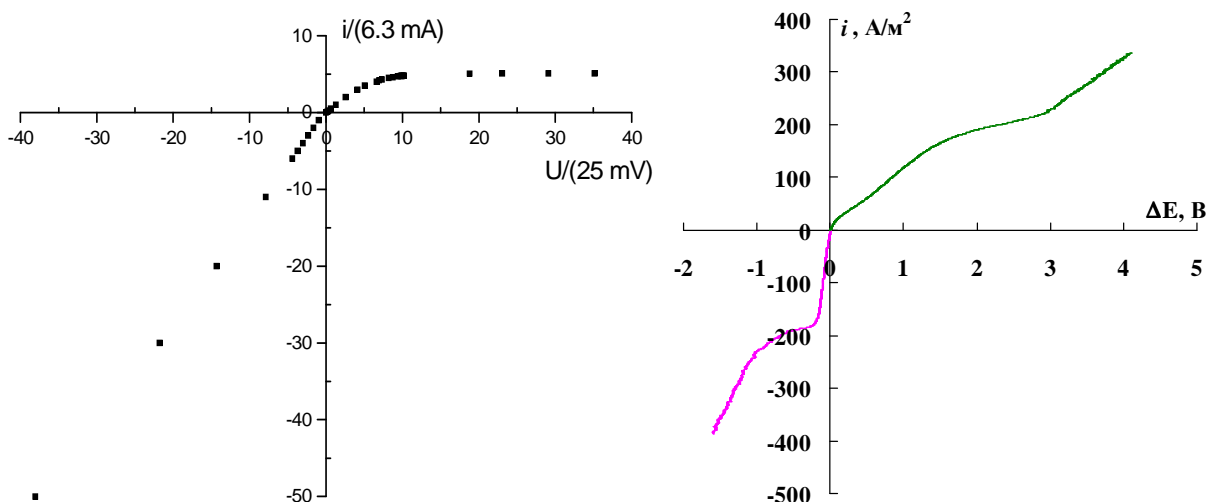


Figure 2. Theoretical CVC in dimensionless coordinates [4] for  $\frac{\delta}{h} = 0,2$ ,  $\frac{\rho_1}{C_0} = 1$ ,  $\frac{\rho_2}{C_0} = 17$ ,

$\frac{D}{D_m} = 10$ ,  $\gamma = 0,9$  and experimental CVC for MF-4SC/Pan in 0,05 M solution of HCl

Calculation of the magnitude of  $i_{lim}$  under different orientation of the membrane towards the counter-ion flux was performed using formulas (10) и (11). Necessary physicochemical parameters were taken from Table 1 for the sample modified by PAn during 1 h. The thickness of diffusive layers  $\delta$  was supposed to be constant for given hydrodynamical regime and has been evaluated by means of (10) or (11) under  $\rho = \rho_1 = \rho_2$  using experimentally found magnitude of  $i_{lim}$  for the initial MF-4SC membrane. We found therefore that  $\delta$  equals to  $1,85 \cdot 10^{-4}$  m and so  $i_{lim} = 167$  A/m<sup>2</sup> when modified side of the membrane is turned to anode while  $i_{lim} = 189$  A/m<sup>2</sup> for opposite orientation. The comparison between calculated and experimental values of the limiting current densities under current reversing revealed their satisfactory agreement within error of 10-15%. The last fact approves the adequacy of the model suggested to evaluation of the limiting current for electromembrane systems with surfacially modified membranes.

The present work is supported by the Russian Foundation for Basic Research (project № 11-08-96518).

### References

1. *Filippov A.N., Starov V.M., Kononenko N.A., Berezina N.P.* // Advances in Colloid and Interface Science. 2008. V. 139, № 1-2. P. 29-44.
2. *Berezina N.P., Kononenko N.A., Filippov A.N., Shkirskaya S.A., Falina I.V., Sytcheva A.A.-R.* // Russ. J. Electrochemistry. 2010. V. 46, N 5. P. 515-524.
3. *Filippov A.N., Iksanov R.Kh., Kononenko N.A., Berezina N.P., Falina I.V.* // Colloid J. 2010. V. 72, N 2. P. 238-250.
4. *Filippov A.N.* Asymmetric current-voltage curves of nanocomposites membranes // Abstracts of 25-th Conference of European Colloid and Interface Society. Berlin, Germany. P. T198.
5. *Filippov A.N., Iksanov R.Kh.* // Russ. J. Electrochemistry. 2012. V. 48, N 2. P. 200-207.
6. *Berezina N.P., Kononenko N.A., Sytcheva A.A.-R., Loza N.V., Shkirskaya S.A., Hegman N., Pungor A.* // Electrochimica Acta. 2009. V.54. P. 2342-2352.

# INFLUENCE OF HYDROPHOBICITY OF PMP AND PTMSP NANOPOROUS MEMBRANES ON A FLOW RATE OF AQUEOUS ALCOHOL MIXTURES UNDER APPLYING OF EXTERNAL PRESSURE DROP

<sup>1</sup>Anatoly Filippov, <sup>1</sup>Vladimir Ivanov, <sup>2</sup>Alexey Volkov, <sup>2</sup>Alexey Yushkin,  
<sup>3</sup>Yulia Bogdanova, <sup>3</sup>Valentina Dolzhikova

<sup>1</sup>Gubkin Russian State University of Oil and Gas, Moscow, Russia, E-mail: [a.filippov@mtu-net.ru](mailto:a.filippov@mtu-net.ru)

<sup>2</sup>Topchiev Institute of Petrochemical Synthesis of RAS, Moscow, Russia, E-mail: [halex@ips.ac.ru](mailto:halex@ips.ac.ru)

<sup>3</sup>Lomonosov Moscow State University, Moscow, Russia, E-mail: [yuliabogd@yandex.ru](mailto:yuliabogd@yandex.ru)

## Introduction

During nanofiltration of water-organic mixtures through hydrophobic membranes based on poly (trimethylsilyl propyne) - PTMSP [1] and poly (4-methyl-2-pentyne)–PMP [2] there is a lack of fluid flow through the membrane under considerable pressure drops depending on concentration of organic matter (Fig. 1b). The effect is explained by the fact that the surface of the membrane is hydrophobic, and to start the filtering process is necessary to overcome the capillary pressure that occurs in the pores of the membrane, which have a characteristic distribution along the radius (Fig. 1a) [3]. The resulting liquid percolation threshold is an important characteristic of the effectiveness of nanofiltration of water-organic mixtures through polymer membranes. Weighing and volumetric methods which are used to determine this quantity are very time consuming. Therefore, the development of express methods for assessing the threshold of the liquid flow and optimize the precision experiments is an urgent task. In developing such procedures, dependence of capillary pressure or flow rate of liquid through the pores of the membrane on the wettability of the membrane material by this liquid can be used [4].

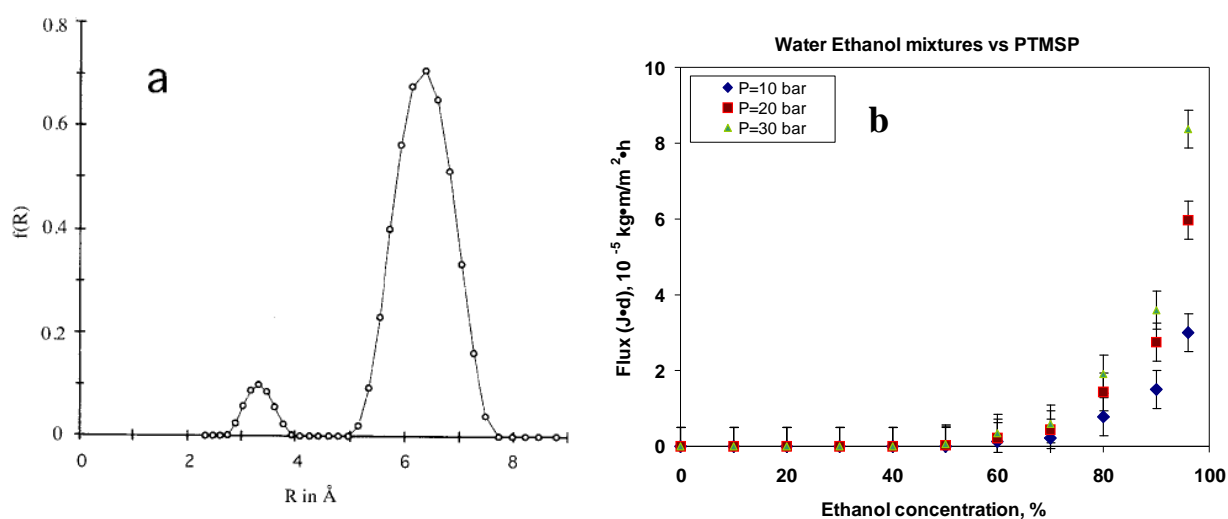


Figure 1. (a) Free volume element (FVE) size distributions for PTMSP [3]; (b) Flux through PTMSP membrane versus ethanol concentration for different values of the membrane pressure drop

## Theoretical Background

Upon application of the pressure difference  $P = P_{cr}$  across the membrane, pores with radius  $a_{cr}$  are opening and the filtration of water-alcohol mixture in all the pores whose radius is not less than  $a_{cr}$  [4] is going on. In order to find the lowest dimensionless radius  $r_{cr}$  of the pores which are opened under pressure  $P = P_{cr}$ , we need to solve the implicit equation of the form:

$$\left(\frac{P}{P_0}\right) \cdot r_{cr} + \alpha_1 \cdot \ln \left( 1 + k_0 \exp \left( \frac{\alpha_2}{r_{cr}^3} \right) \right) = 1, \quad (1)$$

where  $P_0 = \frac{2\sigma^0 \cos \theta_A^0}{a_0}$  is the characteristic of capillary pressure, which depends on the distribution of membrane pore size, composition of the mixture filtered, and pore surface

wettability,  $A$ –Hamaker constant,  $A_0$  - area occupied by the alcohol molecule on the surface of the membrane,  $N_A$  - Avogadro's number,  $K$  - equilibrium constant of adsorption process,  $a_0$  - scale of the pore radii (for example average radius),  $\theta_A^0$  - advancing angle of wetting, and notations are used:  $a = a_0 \cdot r$ ,  $a_{cr} = a_0 \cdot r_{cr}$ ,  $\alpha_1 = \frac{RT}{\sigma^0 \cos \theta_A^0 A_0 N_A}$ ,  $\alpha_2 = \frac{16A}{kT a_0^3}$ ,  $k_0 = K \cdot C_\infty$ . To

find the flow rate of water-organic mixture through the membrane at the chosen trans-membrane pressure drop, it is necessary to integrate the local flows in all opened pores, the fluid motion in which obeys the Hagen-Poiseuille law:

$$Q = \frac{1}{8} \pi a_0^2 N_m \frac{a_0^2 P}{\mu h} \int_{r_{cr}}^{r_{max}} r^4 f(r) dr = \frac{1}{8} \pi a_0^2 N_m \frac{a_0^2 P_0}{\mu h} \frac{1}{r_{cr}} \left( 1 - \alpha_1 \ln \left( 1 + k_0 \exp \left( \frac{\alpha_2}{r_{cr}^3} \right) \right) \right) \int_{r_{cr}}^{r_{max}} r^4 f(r) dr \quad (2)$$

where  $N_m$  - number of pores per unit area of the membrane,  $\mu$  - viscosity of the mixture, which extremely depends on the bulk concentration of alcohol  $C_\infty$ ,  $h$  - membrane thickness, and instead of  $r_{cr}$  we must substitute the solution of equation (1), which can be written as  $r_{cr} = \varphi(P/P_0, \alpha_1, \alpha_2)$ . Comparing the expression (2) with Darcy's law

$$Q = \frac{L_{11}}{\mu} \cdot \frac{P}{h}, \quad (3)$$

we obtain that

$$L_{11} = \frac{1}{8} \pi a_0^4 N_m \int_{\varphi(P/P_0, \alpha_1, \alpha_2)}^{r_{max}} r^4 f(r) dr \quad (4)$$

is the specific hydrodynamic permeability of the membrane ( $m^2$ ) with a partially opened pores at a given pressure  $P$ , and

$$L_{11}^\infty = \frac{1}{8} \pi a_0^4 N_m \int_{r_{min}}^{r_{max}} r^4 f(r) dr \quad (5)$$

is the specific hydrodynamic permeability of the membrane with all opened pores. Here  $r_{min} = a_{min}/a_0$ ,  $r_{max} = a_{max}/a_0$  - dimensionless radii of the smallest and largest pores, respectively and  $f(r)$  - dimensionless function of the distribution of radii of membrane pores.

Fig. 2 and 3 show AFM images of surfaces of PMP and PTMSP membranes, respectively. We see a large number of pores ranging in size from several nanometers to 20 (dark areas). And the number of pores per unit membrane surface of PMP is higher than that PTMSP, and their size is smaller. If we focus on the form of the distribution curve for the membrane pores of PTMSP shown in Fig. 1a and close to a bi-logarithmically normal distribution, we can neglect the little amount of small pores ranging in size from 0.3 to 0.4 nm. For the remaining pores ranging in size from 0.5 to 0.8 nm with a high degree of accuracy sufficient for practical applications, we can choose the density distribution  $f(r)$  of the pores in the form of an isosceles triangle base from  $a_{min} = 0.5$  nm to  $a_{max} = 0.8$  nm and height of  $2/(a_{max} - a_{min})$ . At the same time as the scale length, we can choose the average pore radius  $a_0 = (a_{max} + a_{min})/2$ , which accounts for the maximum density. In this case, an analytical expression for the function  $f(r)$  is as follows:

$$f(r) = \left\{ \begin{array}{l} 0, \text{ if } r < \frac{2}{\alpha+1} \\ \frac{\alpha+1}{\alpha-1} \left( \frac{\alpha+1}{\alpha-1} (r-1) + 1 \right), \text{ if } \frac{2}{\alpha+1} \leq r < 1 \\ \frac{\alpha+1}{\alpha-1} \left( -\frac{\alpha+1}{\alpha-1} (r-1) + 1 \right), \text{ if } 1 \leq r < \frac{2\alpha}{\alpha+1} \\ 0, \text{ if } r \geq \frac{2\alpha}{\alpha+1} \end{array} \right\}, \quad (6)$$

where  $\alpha = \frac{a_{\max}}{a_{\min}} \geq 1$ .

### Experimental Part

In this work we studied the wetting and the modifying effect of aqueous solutions of butanol in the concentration range  $C = (0,15 \div 1,0)$  M with respect to poly (4-methyl-2-pentene) (PMP). It is shown that the wetting tension isotherm has a maximum at  $C = 0.125$ M, which appears to be associated with a decrease in the concentration of butanol in the solution which is in contact with the surface of PMP, compared with the initial solution concentrations  $C \geq 0.125$ M. Using method of Owens-Wendt-Kabli, we defined the polar  $\gamma_{SV}^p$  and dispersion  $\gamma_{SV}^d$  components of the specific surface free energy for the initial PMP membrane and studied their variation for the adsorption modification of the polymer by aqueous solutions of butanol. It is found that with increasing concentration of the modifying solution,  $\gamma_{SV}^d$  decreases and  $\gamma_{SV}^p$  increases to the constant values for  $C \geq 0.125$ M. This result may be related to decompression of the surface layer of PMP, due to the inclusion of a polar liquid in the polymer. A comparison of the limiting adsorption of butanol on the boundaries of "solution-air" and "solution-polymer", as well as the calculation of the degree of hydrophilization of the surface of the PMP, which is modified by butanol solutions, show that a saturated monolayer of butanol is not formed on the surface of the polymer, which is probably due to the depletion butanol solutions in contact with the PMP.

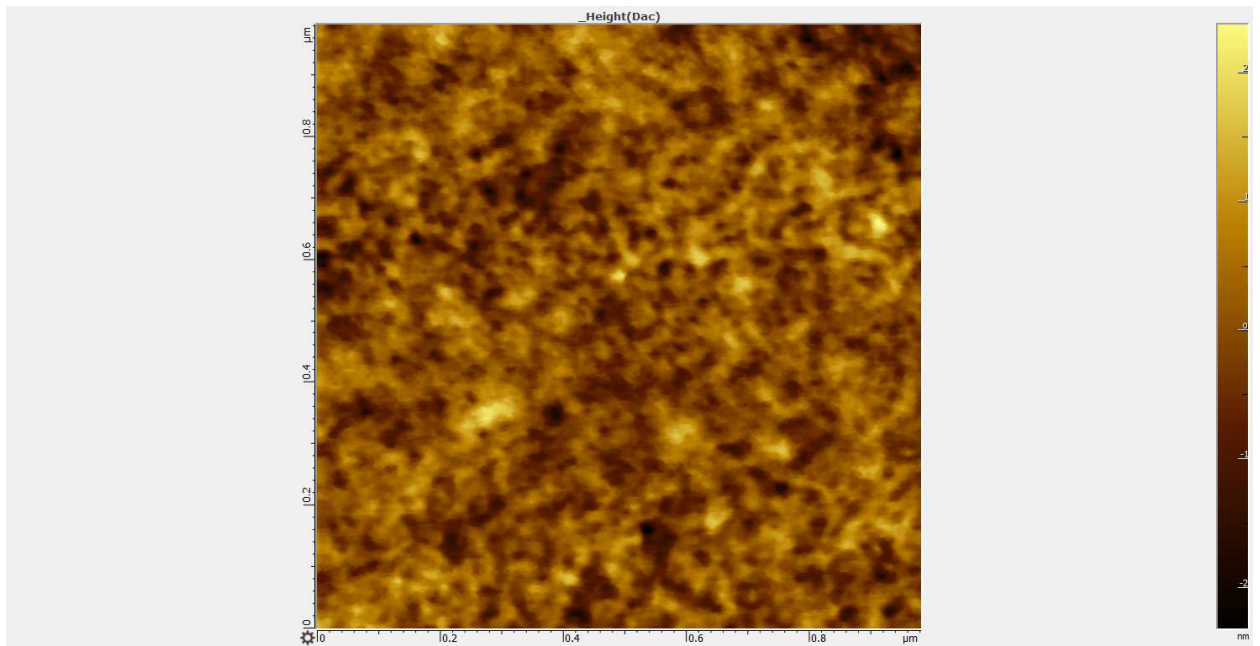


Figure 2. The atomic force microscopy image of the membrane on the base of poly (4-methyl-2-pentene) – PMP (1000x1000 nm)

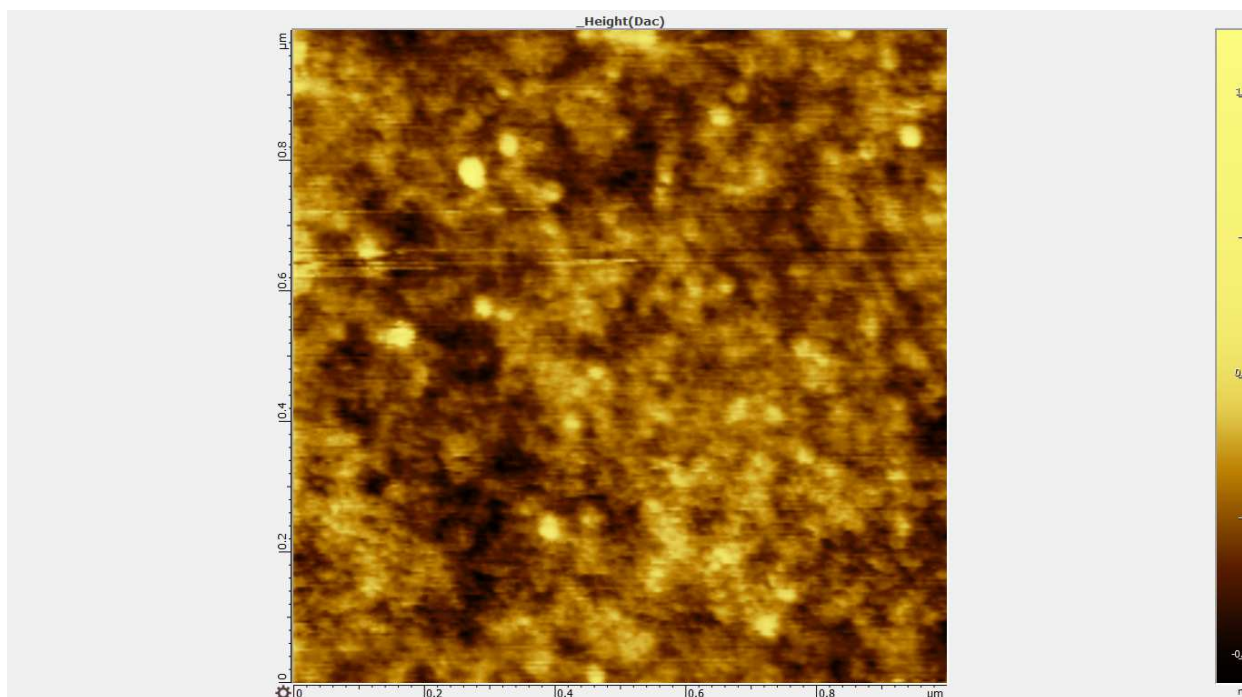


Figure 3. The atomic force microscopy image of the membrane on the base of poly(trimethylsilyl propyne) - PTMSP (1000x1000 nm)

### Conclusions

The results show that the method of wetting can be used for rapid determination of the percolation threshold, i.e. threshold concentration  $C_{\infty}$  of oil and water sensitive organic compounds in aqueous solutions, providing a maximum flow rate during nanofiltration through polymeric membranes. Besides, the formulas (1) - (6) presented for a fixed composition of aqueous-organic mixture is allowed to determine the critical pressure of the start of filtering through the membrane and the pressure that yields a maximum flow rate of the mixture.

*The present work is supported by the Russian Foundation for Basic Research (projects № 11-08-01043).*

### References

1. Volkov A.V. Transport of wetting/non-wetting mixtures through hydrophobic high permeability glassy polymers. Third International Conference on Organic Solvent Nanofiltration. 2010. Imperial College London. UK.
2. Khotimskii V.S., Matson S.M., Litvinova E.G., Bondarenko G.N., Rebrov A.I. Synthesis of Poly(4-methyl-2-pentyne) with Various Configurational Composition // *Vysokomolekulyarnye Soedineniya. A.* 2003. V. 45. No. 8. P. 1259-1267.
3. Hofmann D., Heuchel M., Yampolskii Yu., Khotimskii V., Shantarovich V. Free Volume Distributions in Ultrahigh and Lower Free Volume Polymers: Comparison between Molecular Modeling and Positron Lifetime Studies // *Macromolecules.* 2004. V. 35. P. 2129-2140.
4. Ivanov. V.I. Investigation of the Process of Disclosing of the Pores of Hydrophobic Nanoporous Membranes at the Filtration of Water-Organic Mixtures // *Vestnik Nizhegorodskogo Universiteta.* 2011. No. 4(2). P. 438-439.

# DEGRADATION OF ION-EXCHANGE MEMBRANES USED IN ELECTRODIALYSIS FOR WHEY DESALINATION

<sup>1</sup>Wendy Garcia-Vasquez, <sup>1</sup>Lassâad Dammak, <sup>1</sup>Christian Larchet, <sup>2</sup>Victor Nikonenko, <sup>1</sup>Daniel Grande

<sup>1</sup>Institut de Chimie et des Matériaux Paris-Est, ICMPE, UMR 7182 CNRS – Université Paris-Est, E-mail: grande@icmpe.cnrs.fr

<sup>2</sup>Membrane Institute, Kuban State University, Krasnodar, Russia, E-mail: v\_nikonenko@mail.ru

## Introduction

For many years electrodialysis (ED) has been successfully used on the dairy industry to reduce the salt content in whey without changing the proteins or vitamins of the feed solution. However, the long-term behaviour and degradation mechanisms of ion-exchange membranes (IEMs) still need to be understood in order to overcome many technical hurdles, as the decline of IEM properties is accompanied by a decrease in ED performance and a cost augmentation due to membrane replacement.

In this investigation, we profoundly inquire about physicochemical, structural and mechanical properties of a cation-exchange membrane (CMX-SB) and an anion-exchange membrane (AMX-SB) associated with their utilization in ED for whey desalination. We have taken samples from an industrial ED stack at 2000, 3122 and 4537 h, and have compared the results with a fresh new sample. The case studied was chosen as the membrane durability is several times lower than the standard durability of the same membranes in this application.

## Experiments

These membranes are based on a paste of styrene and DVB mixed with finely powdered PVC; the paste is coated onto a polymer cloth, and the monomers copolymerize at a certain temperature in the PVC gel phase to be then functionalized.

Exchange capacity measurements demonstrate that the functional sites decreased by no more than 20% even if membranes were used for more than 4500 h. Nevertheless, Fig. 1 shows that some physicochemical characteristics of membranes have dramatically changed. Up to 2000 h of functioning, changes linked to an overall hydrophilicity reduction occurred for both CMX-SB and AMX-SB. There is a decrease in conductivity, water content and thickness, accompanied with an increase in membrane density which is consistent with the diminution of membrane volume.

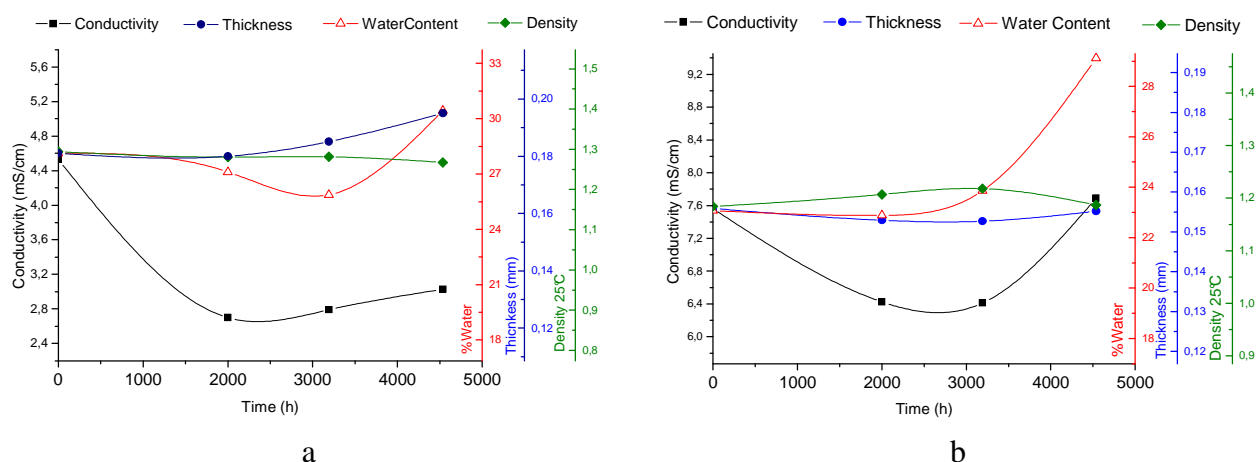


Figure 1. Conductivity, water content, thickness and density of CMX-SB (a) and AMX-SB (b) in 0.1 M NaCl

From 2000 h, all those properties remain practically stable until 3000 h of utilization. After 3000 h, the conductivity increases as well as the water content in more than 25%.—The latter modifications indicate that significant changes occur in membrane structure. Moreover, it is

seen that electrolyte permeability increases as well, especially for the AMX-SB as solution leaks through the membrane decreasing then its selectivity.

Thanks to an energy-dispersive X-ray (EDX) analysis, a progressive augmentation of calcium and appearance of magnesium is observed in CMX-SB samples, even if they go through cleaning several times. These results are consistent with those obtained from ICP-MS analyses realized dissolving membranes in H<sub>2</sub>SO<sub>4</sub>.

For used AMX-SB, there is an absorbance increase observed by transmission FTIR at 1730 cm<sup>-1</sup>, due to new components coming from the feeding ED solution which is observable also with an EDX analysis. It shows an augmentation in sulphur, oxygen and carbon on membrane surface.

Calcium and magnesium are progressively present in CMX-SB as they precipitate in the membrane interstices. This causes a decrease in membrane conductivity and water content without important decrease in the exchange capacity. At 3000 h of utilization, the structure variation leads to a slight increase in the water content.

A Soxhlet extraction of organic matter in used AMX-SB membranes with ethanol allows us to identify the fouling by FTIR with the presence of C=O bonding in the extractables which are not present in the original membranes but are coming indeed from whey or from oxidation products caused by cleaning agents in ED.

SEM images show that new samples are flat and smooth. However, there is a progressive degradation in the surface throughout the process; at 4537 h there is a formation of roughness and irregularities of 100-200 nm in CMX-SB surface and formation of nanocavities of 50-100 nm on AMX-SB surface. This phenomenon is not observed on the cross-section SEM images. Accordingly, the specific surface area values -as determined by BET porosimetry- increases from 0 to 22 m<sup>2</sup>/g for CMX-SB and from 0 to 212 m<sup>2</sup>/g for AEM.

A Soxhlet extraction during 48 h with THF allows us to isolate the soluble parts of the membrane. It is seen that the percentage of extractable, which is identified by NMR spectroscopy as PVC, decreases from 45 to 12% for the new AMX-SB sample and the used one at 4537 h respectively. The residue is identified by FTIR as the functional crosslinked polymer. Therefore, the loss of PVC in the membrane causes a loss of membrane rigidity, and a decrease in breaking strength is confirmed by tensile strength tests.

The loss of PVC might weaken the mechanical strength of membranes. The AMX-SB samples become brittle and fragile, and tear up causing leakages through the ED stack compartments. Moreover, it is observed a persisting fouling of organic molecules; this is the reason why membrane density does not decrease dramatically in spite of the significant augmentation of water content and PVC loss.

Further research is needed to determine the causes of membrane ageing; the development of ex-situ tests to identify the consequences of temperature, cleaning agents, and stack design on IEM structures is crucial, and is currently in progress.

### **Acknowledgments**

*Part of the work was carried out in accordance with the cooperation programme of International Associated French-Russian Laboratory "Ion-Exchange Membranes and Related Processes" The authors are grateful to the CNRS, RFBR (Grant Nos. 11-08-96511, and 12-08-00188) and FP7 Marie Curie Actions "CoTraPhen" Project PIRSES-GA-2010-269135*

---

# STATIONARY DIALYSIS OF THE MIXTURE OF PHENYLALANINE AND SODIUM CHLORIDE WITH PROFILED SULPHOCATION-EXCHANGE MEMBRANE

Elena Goleva, Vera Vasil'eva, Kristina Chegereva

Voronezh State University, Voronezh, Russia, *E-mail: vorobjeva\_ea@mail.ru*

## Introduction

Possibility of carrying out process in soft conditions, without expenses of chemical reagents and an electricity allows to apply a dialysis (diffusive process of separation of the dissolved substances with different molecular weights through semipermeable membranes under the influence of a gradient of chemical potential [1]) in biotechnology when receiving and cleaning a number of biologically active substances and expensive medicines. Low velocity and selectivity of diffusion transport of compound through membrane is essential obstacle for implementing of dialysis as a method. For it's increasing it is necessary to uncover the supplementary effect, which can intensify mass transfer.

## Experiments

Dialysis of solutions was carried out using two-compartment flowing dialyzer of continuous action. The height and width of the working area of the membrane were 4.2 and 1.7 cm., respectively. Examined solution was passed in section 1 with velocity  $V_1=4.5 \cdot 10^{-4}$  m/s, and water was passed through section 2 with velocity  $V_2=5.8 \cdot 10^{-4}$  m/s. All the experiments were done at stationary conditions.

The individual and mixed solutions of non-polar alkylaromatic amino acid–phenylalanine and mineral salt–sodium chloride were objects of research. The acidity of the amino acid solutions were pH 5.20-5.60 for phenylalanine, value close to the isoelectric point ( $pJ=5.91$ ). As a result, the amino acid existed in the form of bipolar ions.

At a dialysis used a heterogeneous sulphocation-exchange membrane MK-40P with geometrical-nonuniform (profiled) surface. Zabolotsky V. I. et al. developed the technique of ion-exchange membranes profiling by wet hot pressing, which is patented in RF [2], and defined conditions which are not degrading physical, chemical, transporting and structure characteristics of membranes.

## Results and Discussion

The possibility of hydrodynamic intensification of the process of dialysis amino acid and mineral salt through the sulphocation-exchange membrane in the hydrogen form is studied. It is established that the use of a profiled membrane increases velocity of mass transfer components in 6-8 times as compared to having a smooth surface. The effectiveness of mass transfer intensification is accomplished by increasing the area of mass transfer and flow's turbulization at protrusions on surface of modified membrane.

The concentration dependence of the diffusion fluxes through the membrane (fig. 1) showed that in dilute solutions of phenylalanine flux is much higher than the flow of the electrolyte, due to the conjugation transfer amino acid from the chemical reaction in the membrane phase, the so-called "facilitated transport" and Donnan exclusion of electrolyte.

For diffusive transport of phenylalanine and sodium chloride from mixed solution through a cation-exchange membrane revealed the competitive nature of conjugation flows. Comparative analysis of the diffusion of phenylalanine and sodium chloride solutions from the individual and equimolar mixtures showed that the presence of the mineral component slightly reduces the flow of amino acids. In turn, the presence of phenylalanine in solution significantly reduces the mass transfer of sodium chloride through the membrane. A possible explanation for this phenomenon is to reduce the moisture content of the membrane during the transition in the amino acid form and the steric hindrance of transport of sodium chloride due to the fact that some of the counterions of hydrogen in the membrane phase is replaced by cations an amino acid formed of large size.

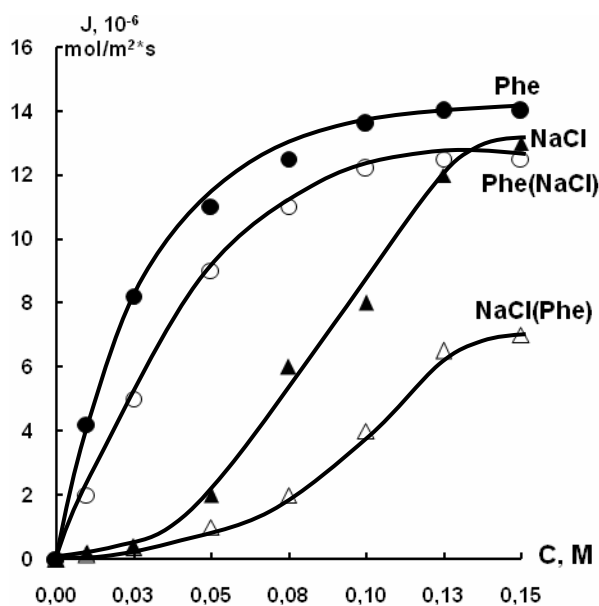


Figure 1. Concentration dependences of the phenylalanine and sodium chloride diffusion fluxes in dialysis of individual Phe, NaCl and equimolar solutions Phe(NaCl), NaCl(Phe) through profiled membrane MK-40P in hydrogen form

Depending on the separation factor  $S_F$  of the concentration in dialysis mixed equimolar solutions (a) and the relative concentrations of components in a solution of a mixture of phenylalanine and sodium chloride (b) through profiled membrane MK-40P in the hydrogen form shown in fig. 2. When equimolar mixtures of dialysis, the maximum separation efficiency was observed for solutions with concentrations of  $C < 3,0 \cdot 10^{-2}$  M. In this concentration range the acceleration of transport phenylalanine with hydrogen counterions had highest values and the flow of the mineral component, which prevents the "facilitated diffusion", was still small. A further increase in concentration of the components resulted in a reduction factor of separation, due to the fact that the Donnan exclusion effect is reduced and was observed a competitive mass transport amino acid and mineral component. It should be noted that for all the investigated concentration range is characterized by the selective transport of amino acid and the separation factor values remained greater than unity. Conjugation of phenylalanine fluxes and sodium chloride in sulphocation-exchange membrane results in less efficient separation of substances.

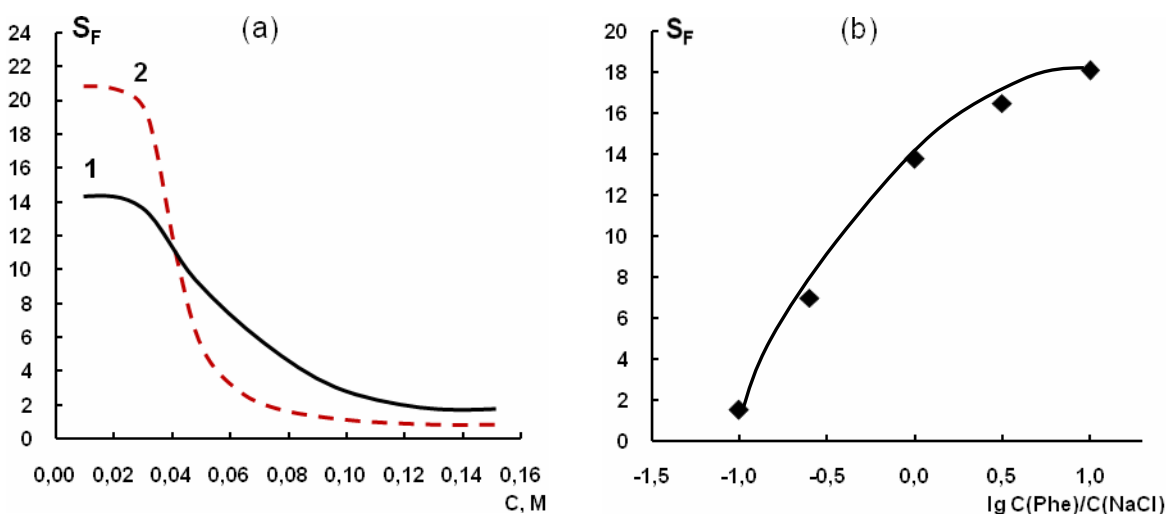


Figure 2. Concentration dependences of phenylalanine and sodium chloride separation factors in dialysis of equimolar solutions (a) and the relative concentrations of components in a solution of a mixture  $C_0(\text{Phe})=0,025$  M (b) through profiled membrane MK-40P in hydrogen form: 1- without of conjugation flows, 2- with the account of conjugation flows

Dependence of separation factor in dialysis mixture of phenylalanine and sodium chloride concentration on the ratio of the components in the initial solution has shown that a decrease in the proportion of the electrolyte in a mixed solution of the separation factor increased.

The experimental results suggest the possibility of development of environmentally sound methods of dialysis separation of amino acids from a mixture of products of microbiological synthesis.

#### **Acknowledgments**

*We are grateful prof. V.I. Zabolotsky (Kuban State University) for the provided samples of a profiled cation-exchange membranes.*

#### **References**

1. *Mulder M.* Basic principles of membrane technology. M.: World, 1999. 513 p.
2. *Zabolotskii V.I., Loza C.A., Sharafan M.V.* Method of profiling of ion-exchange membrane. Pat. RF 2284851, BO1D 61/52, 10.10.2006.

# SYNTHESIS AND STUDY THE DIFFUSION PROPERTIES OF MEMBRANES AMEX, MODIFIED BY CERIUM OXIDE.

Daniil Golubenko, Yuliya Karavanova, Andrei Yaroslavtsev

Kurnakov Institute of General and Inorganic Chemistry RAS, Moscow, Russia,

E-mail: yuka@igic.ras.ru

Water waste treatment is in the focus of government programs in different countries. The main unsolved problem in this area is nitrates removing. There is no economical technology abled to output nitrate anion nowadays. Solution of this and similar problems associated with the use of membrane technology, which does not always satisfy the needs of production, so work on modification of membrane materials, and especially preparation of membranes containing inorganic and macromolecular components extensively develop. There are two approaches to the modification. First, in situ is synthesis of nanoparticles of the dopant in the pores of the finished membrane. Second, the method of casting is to add precursor or the dopant in the solution for the manufacture of membranes. Among the inorganic oxides, ability of cerium oxide to selective chemisorptions of nitrate ions is a unique property. The purpose of this work is the synthesis of an inorganic oxide in the pores and channels by in situ method, and the study of diffusion properties of resulting membrane.

## Experiments

For the synthesis of modified samples anion-exchange membrane AMEX (MEGA) were doped by ceria. To determine the transport properties of the obtained membranes ionic conductivity and diffusion of membrane in different ionic forms (hydroxyl, nitrate and chloride) were investigated. Determination of the ionic conductivity was measured by impedance spectroscopy.

## Results and Discussion

The study of ionic conductivity of membranes in the hydroxyl form (Fig. 1) shows that the introduction of large amounts of dopant decreases ion mobility. With high probability it is due to steric hindrances emerging.

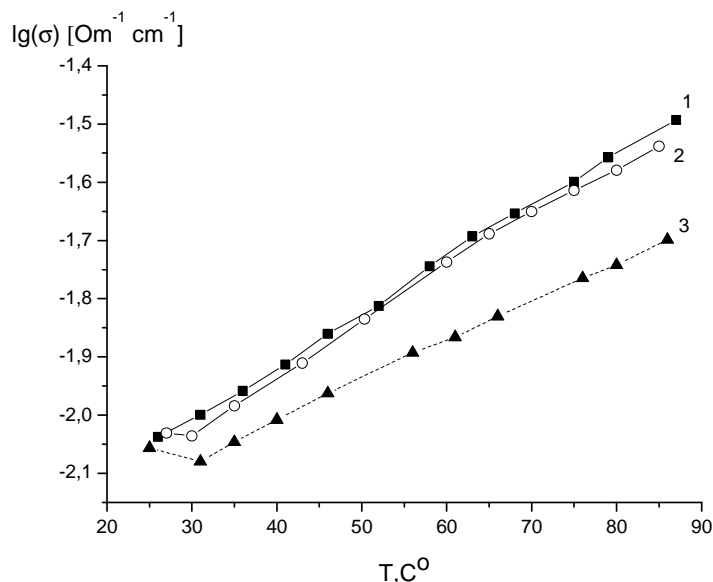


Figure 1. The temperature dependences of conductivity for initial AMEX and membranes in the hydroxyl form doped with ceria obtained from the solution of  $Ce(NO_3)_3$ . (1)-AMEX, (2)-AMEX+Ce(III)<sub>0.1M</sub>, (3)-AMEX+Ce(III)<sub>0.2M</sub>

Conductivity activation energy decrease was observed (Table1), which agrees well with the semi-stretched pore model: the introduction of the dopant leads to a broadening of the pores, and

to the broadening of the channels, reducing the activation barrier. An additional reduction of the activation energy can also be linked with the dopant surface involvement in the transport.

**Table 1: The activation energy for membranes in the hydroxyl form**

Membranes	$E_a$ (kJ/mol)
AMEX	$19.0 \pm 0.3$
AMEX+Ce(III)_0.1M	$19.0 \pm 0.1$
AMEX+Ce(III)_0.2M	$14.2 \pm 0.1$

The conductivity of the modified membrane increases in the nitrate form, and the hydroxyl and chloride form decreases, as a result of largest ionic conductivity is achieved for the modified membranes in the nitrate form.

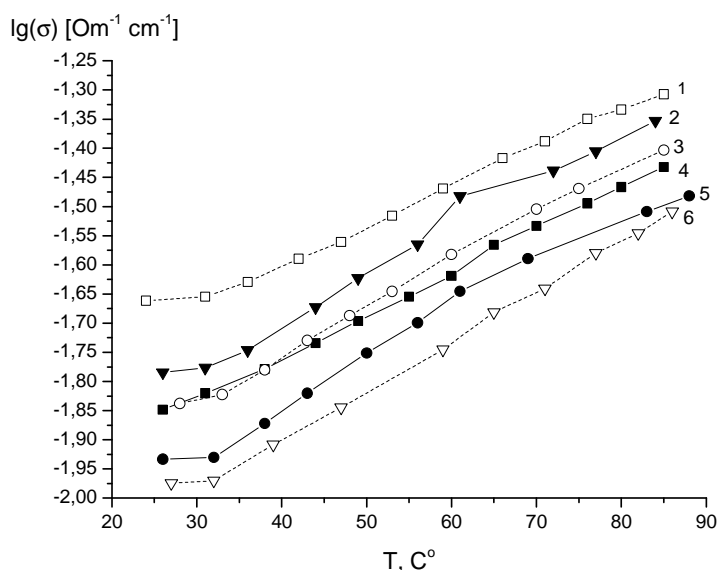


Figure 2. The temperature dependences of conductivity for initial AMEX(1,3,6) and membranes(2,4,5) doped with ceria obtained from the solution of  $Ce(NO_3)_3$ , in different salt forms (1,4)-  $OH^-$ , (2,6)-  $NO_3^-$ , (3,5)-  $Cl^-$

Also, for the modified membrane reduced the activation energy of transport of nitrate anion is observed. These facts can be explained by the appearance in the pores of membrane cerium oxide, surface which reacts with nitrate anion.

**Table 2: The activation energy for membranes in the different salt forms, (kJ/mol)**

Ion	Initial membranes	Modified (Ce(III)_0.1M)
$OH^-$	$14,0 \pm 0,3$	$14,1 \pm 0,4$
$Cl^-$	$17,1 \pm 0,1$	$17,1 \pm 0,5$
$NO_3^-$	$18,0 \pm 0,4$	$16,5 \pm 0,6$

In this study industrial membrane AMEX modified by cerium oxide was received. The ionic conductivity in different ionic forms was investigated. It is shown that the modification leads to a significant increase in the mobility of the nitrate anion.

## REDOX SORPTION OF OXYGEN BY CATHODIC POLARIZED METAL-ION EXCHANGER NANOCOMPOSITE

Vladislav Gorshkov, Lev Polyanskii, Tamara Kravchenko

Voronezh State University, Voronezh, Russia, E-mail: krav@chem.vsu.ru

The redox sorption of molecular oxygen from the flow of deionized water with cathodic polarized copper-ion exchanger nanocomposite layer is investigated. Mathematical description is given under the external diffusion transport model. Unlike the known approaches the conditions that are closed to the limiting diffusion current are realized. The conditions can be achieved by separation of the granular layer into thin layers and with the help of polarization of each layer a current that is closed to the limit.

The study of electroreduction of oxygen was carried out on copper-ion exchanger nanocomposite Cu<sup>0</sup>·KU-23 in H<sup>+</sup>-form to keep the invariance of the internal environment pH. The quantity of copper is 10±1 mmol·ekv/cm<sup>3</sup>. The size of copper particles is 5-10 nm (transmission microscopy). Studies were carried out in oxygenated deionized water. Deoxygenation is carried out in the sorption-membrane electrolysis cell with special design [1]. The cell was made of a polymeric material and separated by cation-exchange membrane to anode and cathode sections. The space between the cation exchange membrane and the anode in the anode section was filled by layer of sulpho cation exchanger KU-23. Cathode section includes seven cameras, hydraulically connected in series, each having its own system of the cathodes polarization. The space between the cathode and the cation exchange membrane is filled by a layer of nanocomposite.

The polarization was performed in galvanostatic mode. The initial value of the polarizing current was selected that the process of electroreduction of oxygen was not followed to the decomposition of water.

Previously the output curve of redox sorption of oxygen was taken without passing an electric current ( $I = 0$ ). In the absence of polarization the oxygen concentration at the outlet of granular layer increases steadily. At the same time with cathodic polarization over a long period of time (400 hours), the concentration of oxygen at the outlet of granular layer was relatively low and stayed even several lower in comparison to the theoretically calculated. The total height of the layer  $L$  is 10.5 cm, height of a single step  $l$  is 1.5 cm.

Current which is required for oxygen reduction on the layer height  $y$ , is

$$I(y) = I_{com} [1 - \exp(-Ay)], \quad (1)$$

where  $I_{com}$ —common (total) current required for restore whole the oxidizer, wick coming into the column ( $y \rightarrow \infty$ ),

$$I_{com} = zFSuc_0. \quad (2)$$

There  $S$ —cross-sectional area of the granular layer,  $z$ —number of electrons,  $F$ —Faraday constant,  $u$ —linear flow rate,  $c_0$ —oxygen concentration in the inlet of the column.

In a galvanostatic polarization maximum permitted a stationary current density  $i_{st}$  can not exceed the density of the limiting diffusion current  $i_{lim}$  at the end of the granular layer height  $\ell$ , i.e. at the output of oxygen from the layer. In this case, the relative concentration of oxygen at the outlet of the granular layer and the a stationary current density can be expressed by the equation

$$\frac{c(\ell)}{c_0} = \frac{i_{st}(\ell)}{i_{lim}(0)} = \frac{1}{1 + A\ell}, \quad (3)$$

and the power of a stationary current

$$\frac{I_{st}(\ell)}{I_{com}} = \frac{A\ell}{1 + A\ell}. \quad (4)$$

The density of the limiting diffusion current  $i_{lim}(0)$  of oxygen at the inlet of the layer is calculated by the equation

$$i_{\text{lim}}(0) = \frac{zFDc_0}{\delta} \left( 1 + \frac{\delta}{R_0} \right), \quad (5)$$

where  $D$ –the diffusion coefficient,  $R_0$ –radius of the grain of nanocomposite,  $\delta$ –thickness of the diffusion layer.

The constant  $A$  is given by

$$A = \frac{3\alpha i_{\text{lim}}(0)}{zFuR_0c_0}, \quad (6)$$

there  $\square$  - the coefficient of filling the column by grains of nanocomposite.

We have worked out the patterns of redox sorption of oxygen on the granular layer of the nanocomposite that is divided on individual steps in height  $\ell$ . Suppose that the total height of the granular layer  $L$ , height of of each step  $\ell = \frac{L}{n}$ , where  $n$ –number of steps, current density at the  $j$ -th step  $i_j$ .

Density of the limiting current can be expressed

$$i_{j,\text{lim}}(y) = \frac{zFDc_{j-1}}{\delta} \left( 1 + \frac{\delta}{R_0} \right) - Ai_j [y - (j-1)\ell], \quad (7)$$

and the maximum current density on the site  $\ell$  is

$$i_j = \frac{zFDc_{j-1}}{\delta} \left( 1 + \frac{\delta}{R_0} \right) \frac{1}{1 + A\ell}. \quad (8)$$

At the exit of a granular layer

$$\frac{c(L)}{c_0} = \left( 1 + A \frac{L}{n} \right)^{-n}. \quad (9)$$

The power of a stationary current on the  $n$ -stepped granular layer with cross-section  $S$  is

$$I_{st}(L) = \frac{3\alpha S}{R_0} \sum_{j=1}^n i(j\ell)\ell. \quad (10)$$

$$\frac{I_{st}(L)}{I_{com}} = 1 - \left( 1 + A \frac{L}{n} \right)^{-n}. \quad (11)$$

Power of a stationary current which given by each  $j$ -step can be found by the equation

$$I_j = I_{com} A \frac{L}{n} \left( 1 + A \frac{L}{n} \right)^{-j}. \quad (12)$$

Assigning a specific oxygen concentration at the outlet  $c(L)/c_0$ , we can choose the optimal size of the granular layer from the ratio between the total height  $L$  and the number of steps  $n$ :

$$L = \frac{n}{A} \left( \left[ \frac{c_0}{c(L)} \right]^{1/n} - 1 \right). \quad (13)$$

A theoretical calculation parameters of the redox-sorption of oxygen process was carried out for given experimental conditions. Calculation with the help of equation (2) gives the total current  $I_{com}$ , which is required for complete reduction of oxygen at a given flow rate. For a given values: flow rate of water  $u = 0.23$  cm/sec,  $z = 4$ ,  $F = 96500$  A·sec/mol, cross-sectional area of the granular layer  $S = 3$  cm<sup>2</sup>,  $c_0 = 2.5 \cdot 10^{-7}$  mol/cm<sup>3</sup>,  $I_{com} = 63$  mA.

The calculation of a stationary current at the granular layer was carried out by the equation (12). In selected for the experiment parameters of the layer height  $L = 10.5$  cm and the number of stages  $n = 1$  the current does not exceed 12 mA. The release of hydrogen is happen at higher current. Increase the value of a stationary current is possible if the whole granular layer divided into thin by layers (steps). In this case, each step can be polarized by different currents in

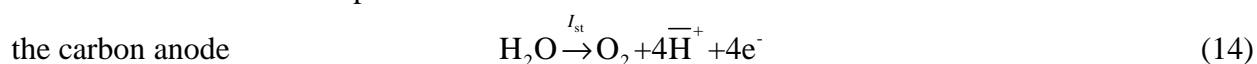
according to various concentrations of oxygen, coming out of the layer. In this way we can organized the process in the layered polarizable nanocomposite. Calculated values of stationary currents for each  $j$ -step was performed with the help of equation (11).

The results of layered polarization are shown in table 1. As can be seen from the table, there is a good agreement between theoretical and experimental values  $c(L)/c_0$ . Some experimental value indicates the further process in addition to the electroreduction of oxygen.

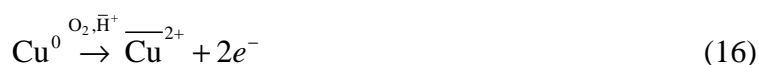
**Table 1: Process parameters of redox-sorption of oxygen on stepped polarized nanocomposite**

The height of layer $L$ , cm	Number of steps of the electrolyzer $n$	The height of each step $\ell$ , cm	The total current $I_{com}$ , mA	The relative concentration of oxygen in the water at the outlet of the granulated layer $c(L)/c_0$	
				The calculation by the equation (9)	Experiment
10.5	7	1.5	63	0.24	0.10±0.03

Under the conditions of stabilization process at the cathodic polarization of granular layer of a nanocomposite the oxygen is mainly electrochemically reduced. The system processes that occur under the current can be represented:



on a copper cathode with the filling up of a nanocomposite



The bar over a symbol means that the ion in the nanocomposite is in the form of a counterion near the fixed groups of the opposite sign of charge.

Formed at the anode according to reaction (14) the counter-ions of hydrogen pass through the cation exchange membrane and are involved in the electroreduction of oxygen on metal nanocomposite according to reaction (15). Step (16) is the spontaneous ionization of copper nanoparticles under the influence of oxygen and the hydrogen counterions with the localization of the copper ions formed near the fixed groups  $-\text{SO}_3^-$ . It provides the additional absorption of oxygen.

The possibility of continuous maintenance of the oxygen level at the output of the stepwise polarizable granular layer nanocomposite were established after long tests. Stability is provided by the simultaneous reduction of oxygen by an electric current as well as by chemical activity of nanodispersed copper particles.

Improve the depth of water deoxygenation is possible by increasing the overall height of the granular layer. The calculation showed that the oxygen content in the water after passing through a 40-step granular layer of the overall height of 60 cm is less than 2 ppb.

*This work was supported by the RFBR (project № 11-08-00174\_a).*

### References

1. Polyanskiy L.N., Gorshkov V.S., Chayka M.Yu. and other. A device for deep water deoxygenation. Pat. № 105284 Russia. Claim. 19.11.2010. Pub. 10.06.2011. Bull. № 16.

---

## INVESTIGATION OF STRUCTURE-PERMEABILITY RELATIONSHIPS IN NANOPOROUS POLYCYANURATE-BASED MEMBRANES

<sup>1</sup>Daniel Grande, <sup>1</sup>Ahlem Raies, <sup>1</sup>Lassâad Dammak, <sup>2</sup>Alexander Fainleib,

<sup>2</sup>Olga Grigoryeva, <sup>2</sup>Kristina Gusakova

<sup>1</sup>Institut de Chimie et des Matériaux Paris-Est, UMR 7182 CNRS – Université Paris-Est-Créteil Val-de-Marne, 2, rue Henri Dunant, Thiais, France, E-mail: grande@icmpe.cnrs.fr

<sup>2</sup>Institute of Macromolecular Chemistry, National Academy of Sciences of Ukraine (NASU), Kyiv, Ukraine

Over the last decades, membrane processes have significantly expanded, as they constitute simple, cost-effective and low-consuming energy separation techniques. They quite often operate continuously at room temperature and low pressure. These techniques are increasingly diversified. In particular, ultrafiltration relies on porous membranes which pore diameters are about 10 to 100 nanometers and which play the role of selective barriers to compounds and molecules depending on their sizes and charges.

In this work, we have characterized two membranes recently synthesized by our groups based on polycyanurates (PCNs) as well as a commercial membrane as a reference. First, we have performed a morphological analysis of the membranes using Scanning Electron Microscopy (average pore diameter) and Differential Scanning Calorimetry (DSC)-based thermoporometry (pore size distribution). Second, we have focused on a dynamic characterization via the determination of the streaming potential (electrokinetic properties of the membrane pores), the hydraulic permeability (water flow) and ion permeability (ion selectivity).

The results of the morphological analysis show that the pore diameters of the three membranes under investigation are about 10-45 nm. Concerning the dynamic characterization, the synthetic membrane is more efficient than the commercial one from the viewpoint of ion selectivity. We have correlated the dynamic parameters to the porosity characteristics of the membranes. The potential application of such synthetic ultrafiltration membranes are expected in water treatment for example.

**Keywords:** polycyanurates, nanoporosity, Scanning Electron Microscopy, DSC-based thermoporometry, streaming potential, hydraulic permeability, ionic permeability.

# PEMFC ELECTROCATALYST BASED ON M-CORE – PT-SHELL NANOPARTICLES

<sup>1</sup>Vladimir Guterman, <sup>1</sup>Tatiana Lastovina, <sup>1</sup>Helena Pahomova, <sup>2</sup>Natalia Tabachkova, <sup>1</sup>Andrey Paharev

<sup>1</sup>Southern Federal University, Rostov-on-Don, Russia, E-mail: [gut57@mail.ru](mailto:gut57@mail.ru)

<sup>2</sup>National University of Science and Technology «MISIS», Moscow, Russia

## Introduction

The development of composition and synthesis method to prepare stable nanoparticles with metal or hollow core and Pt shell is one of the perspective ways for electrocatalyst improvement. Consecutive deposition of core metal and Pt shell could have some positive effects: essential reduce of Pt loading accompanied by mass activity increase, more strong nanoparticles anchoring to the carbon surface, increasing of M/C boundary stability to the oxidation during Fuel Cell operation. The aims of our investigation were to find the alloying component and develop a synthesis method for the preparation of M@Pt/C electrocatalysts describable by high mass activity and improved stability.

## Experiments

$\text{Cu}_x\text{Pt}/\text{C}$  and  $\text{Ag}_x\text{Pt}/\text{C}$  catalysts were prepared by successive reduction of  $\text{Cu}^{2+}$  ( $\text{Ag}^+$ ) and Pt (IV) from water-organic solutions of their precursors at room temperature. Influence of catalyst composition and post-treatment conditions on the microstructure, electrochemical active surface area (ECSA) and oxygen reduction reaction (ORR) specific activity of the electrocatalysts was investigated. XRD, TEM, XPS, cyclic voltammetry and some other methods were used for the characterization of prepared catalysts. The corrosion stability of PtM/C was investigated too.

## Results and Discussion

Prepared  $\text{Cu}_x\text{Pt}/\text{C}$  and  $\text{Ag}_x\text{Pt}/\text{C}$  ( $1 \leq x \leq 3$ ) materials contained from 20 to 53% wt. of metals. An average crystallites size  $D_{av}$  calculated by XRD data was from 3 to 15 nm, depending on composition and synthesis conditions. As opposed to  $\text{PtM}_x/\text{C}$  alloy catalysts some X-ray diffractograms of prepared core-shell materials demonstrated peaks overlapping (superposition) for two phases—solid solutions based on M and on Pt (Fig. 1).

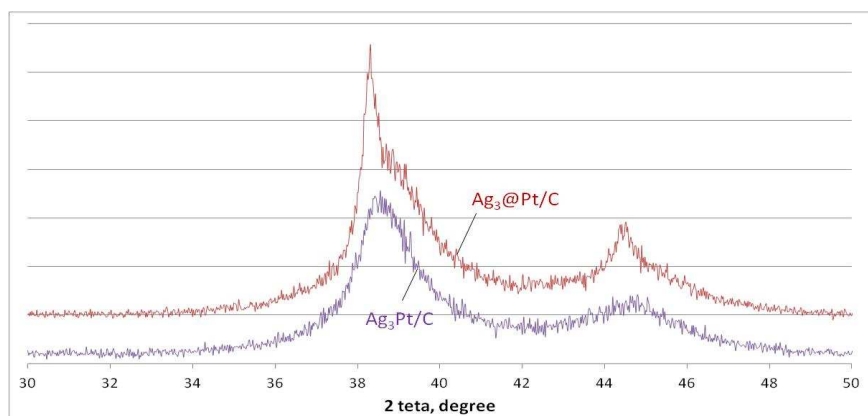


Figure 1. X-ray diffractograms of “alloy”  $\text{Ag}_3\text{Pt}/\text{C}$  and “core-shell”  $\text{Ag}_3\text{Pt}/\text{C}$  electrocatalysts

The formation of nanoparticles with core–shell structure was confirmed by TEM data (Fig. 2). It is important that a great number of nanoparticles with core–shell structure were detected at the carrier surface (Fig. 2a). Core – shell structure of nanoparticles didn't fail after the 1 hour treatment in the hot ( $\sim 100^\circ\text{C}$ ) 1M  $\text{H}_2\text{SO}_4$  or  $\text{HClO}_4$  acids (Fig. 2a, Table 1). XPS data confirmed increased surface concentration of Pt in the surface layer of  $\text{Ag}@\text{Pt}$  nanoparticles in comparing with “alloy” nanoparticles with similar composition (Table 1). Cyclic voltammograms of “alloy” and “core-shell” electrocatalysts essentially differed from each other (Fig. 3).

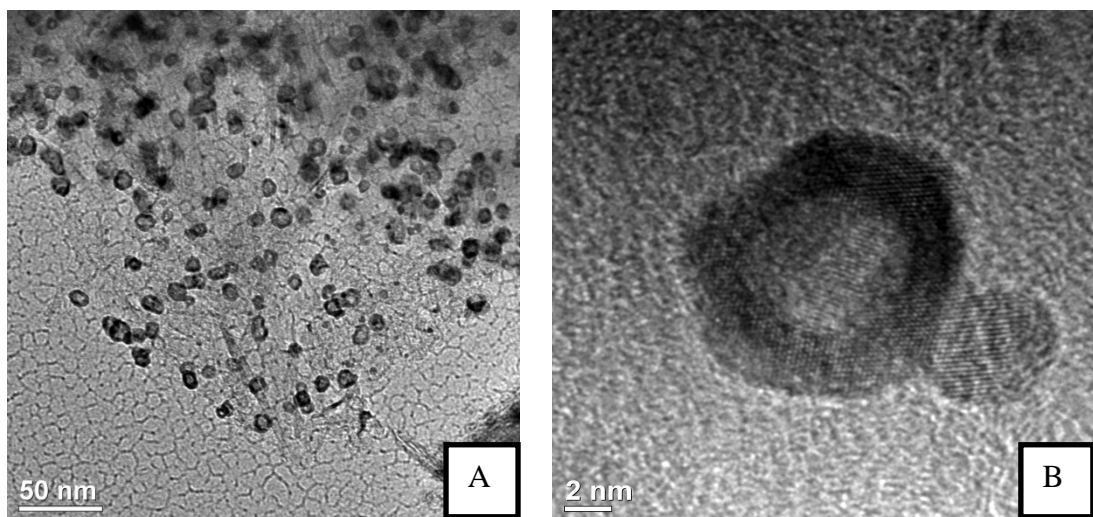


Figure 2. TEM of  $\text{Cu}_2\text{@Pt/C}$  electrocatalyst after 1 h treatment in 1 M  $\text{H}_2\text{SO}_4$  at  $100^\circ\text{C}$

**Table 1: Characteristics of PtAg/C and Ag@Pt/C materials before and after treatment in hot (90 – 100 °C) 1M  $\text{HClO}_4$**

Composition (Calculated by precursors loading)	Metals atomic ratio (X ray photoelectron spectroscopy data)	Metals loading, %wt.	Cell parameter, nm (XRD data)	Average diameter of crystallites, nm (XRD data)
<b>PtAg/C</b>	$\text{Pt}_{1,2}\text{Ag}_1$	34,6	0,4025	3,8
<b>PtAg/C 1 hour posttreatment</b>	$\text{Pt}_{1,4}\text{Ag}_1$	22,7	0,4011	4,1
<b>Ag@Pt/C</b>	$\text{Pt}_{2,54}\text{Ag}_1$	21,4	0,4030	3,4
<b>Ag@Pt/C 1 hour posttreatment</b>	$\text{Pt}_{2,17}\text{Ag}_1$	15,8	0,3986	3,4

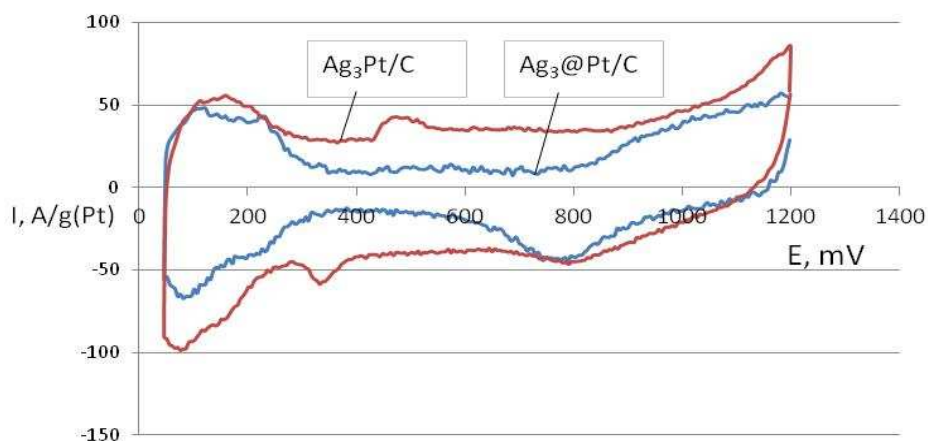


Figure 3. Cyclic voltammograms of  $\text{Ag}_3\text{Pt/C}$  and  $\text{Ag}_3\text{@Pt/C}$  electrocatalysts in 1M  $\text{H}_2\text{SO}_4$ . Potential rate 100 mV/s. Ar atmosphere

This work was supported by Russian Foundation for Basic Research, projects nos. 10-03-00474a and 11-08-00499a.

## References

1. Lastovina T.A., Guterman V.E., Manokhin S.S. Influence Of Different Types of  $(\text{CuPt}_{0,1})_2\text{@Pt/C}$  Posttreatment on Their Composition, Microstructure and Electrochemical Active Surface Area // Int. Scientific J. for Alternative Energy and Ecology. 2011. i.9. P. 111–115.

# ION MOBILITY IN SURFACE-MODIFIED MC-40 MEMBRANES IN MIXED ALKALI FORMS

<sup>1</sup>Yuliya Karavanova, <sup>2</sup>Vitaly Volkov, <sup>1</sup>Andrei Yaroslavtsev

<sup>1</sup>Kurnakov Institute of General and Inorganic Chemistry RAS, Moscow, Russia,

E-mail: yuka@igic.ras.ru

<sup>2</sup>Institute of Chemical Physics RAS, Chernogolovka, Russia

## Introduction

Membrane materials have found an application in such global areas like water purification and alternative energetic. But quantity of different commercial membranes can't satisfy the increasing needs of today world. So, modification of existing membrane materials and studying of their diffusion characteristics have both fundamental and practical importance. Ion transport investigation in membrane materials permits to study diffusion processes passing on phase boundary. And investigation of mixed alkali forms gives opportunity to evaluate the influence of phase boundary on the transport of individual cation.

## Experiments

Membranes MC-40 with surface modified by MF-4SC with implanted inorganic particles were obtained. Their diffusion characteristics and ionic conductivity in different ionic forms were studied. Diffusion properties were examined for solutions listed below:

0.1M HCl + (x - 0.1) M NaCl / xM NaCl (x=0.1, 0.2, 0.4, 0.6, 0.8, 1).

Ionic conductivity was studied for membranes equilibrated with next solutions:

0.1M MCl and 0.1M HCl + xM MCl (x=0-0.9, M=Li, Na, K, Rb).

## Results and Discussion

The ionic conductivity of membranes in mixed H<sup>+</sup>/M<sup>+</sup> forms can be expressed as:

$$\sigma = \frac{q^2 E}{kT} \left( \frac{D_M K_{ex} x}{K_{ex} x + 1} + \frac{D_H (1-x)}{K_{ex} x + 1} \right), \quad (1)$$

where  $x = c(\text{Na})/(c(\text{H})+c(\text{Na}))$  in solution. And from experimental dependence of ionic conductivity on concentrations in solution diffusion coefficients and ionic exchange constant can be obtained. So, if we know ionic exchange constant, we can characterize mixed alkali effect (fig. 1).

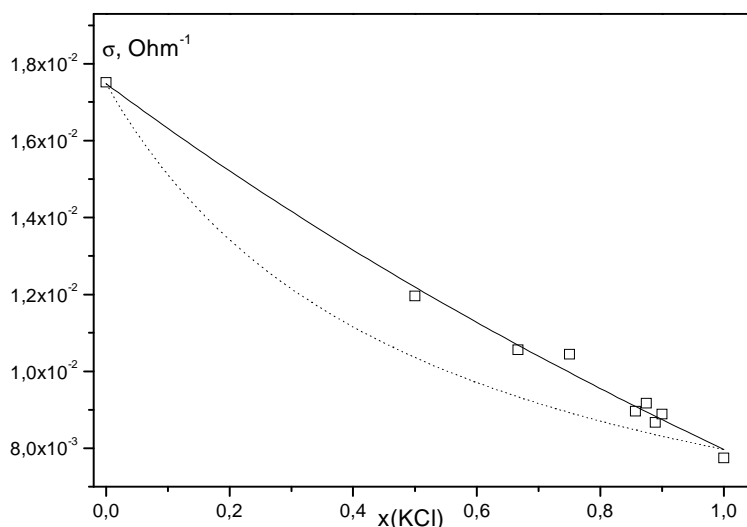


Figure 1. The dependence of ionic conductivity of the membrane MK 40 from the mole fraction of KCl in the solution. The dotted line is the theoretical curve for  $K_{ex} = 2,27$

The experimental data are well described by theoretical curves. The data obtained (table 1) shows that surface modification increases proton diffusion coefficients. For MF-4SC modified samples diffusion coefficients of lithium cation also increases. But the incorporation of oxide

particles decreases the mobility of lithium cations and increases the mobility of sodium and potassium cations.

**Table 1: Diffusion coefficients of cations**

M <sup>+</sup>	D (M <sup>+</sup> ), cm <sup>2</sup> /s	D (H <sup>+</sup> ), cm <sup>2</sup> /s	K <sub>ex</sub> H <sup>+</sup> /M <sup>+</sup>	K <sub>eff</sub>
<b>MC-40</b>				
Li <sup>+</sup>	(0,75±0,08)·10 <sup>-6</sup>	(2,8±0,1)·10 <sup>-6</sup>	0,84±0,01	0,5±0,1
Na <sup>+</sup>	(1,39±0,05)·10 <sup>-6</sup>	(2,78±0,06)·10 <sup>-6</sup>	1,40±0,03	1,4±0,3
K <sup>+</sup>	(1,20±0,03)·10 <sup>-6</sup>	(2,63±0,04)·10 <sup>-6</sup>	2,27±0,07	1,2±0,2
<b>MC-40/MF-4SC</b>				
Li <sup>+</sup>	(1,7±0,2)·10 <sup>-6</sup>	(7,7±0,3)·10 <sup>-6</sup>	0,44±0,05	1,3±0,2
Na <sup>+</sup>	(1,2±0,3)·10 <sup>-6</sup>	(6,8±0,3)·10 <sup>-6</sup>	1,5±0,1	1,1±0,2
K <sup>+</sup>	(1,6±0,2)·10 <sup>-6</sup>	(6,6±0,2)·10 <sup>-6</sup>	1,8±0,1	1,1±0,1
<b>MC-40/MF-4SC+SiO<sub>2</sub></b>				
Li <sup>+</sup>	(1,2±0,1)·10 <sup>-6</sup>	(6,9±0,1)·10 <sup>-6</sup>	0,40±0,05	1,1±0,1
Na <sup>+</sup>	(1,6±0,2)·10 <sup>-6</sup>	(6,8±0,3)·10 <sup>-6</sup>	1,65±0,1	1,3±0,3
K <sup>+</sup>	(2,2±0,1)·10 <sup>-6</sup>	(6,7±0,2)·10 <sup>-6</sup>	1,8±0,1	2,3±0,3
<b>MC-40/MF-4SC+ZrO<sub>2</sub></b>				
Li <sup>+</sup>	(1,2±0,4)·10 <sup>-6</sup>	(8,0±0,5)·10 <sup>-6</sup>	0,50±0,05	1,0±0,3
Na <sup>+</sup>	(1,5±0,3)·10 <sup>-6</sup>	(6,4±0,3)·10 <sup>-6</sup>	1,5±0,1	1,2±0,2
K <sup>+</sup>	(1,9±0,2)·10 <sup>-6</sup>	(6,8±0,3)·10 <sup>-6</sup>	1,7±0,1	1,0±0,2

NMR studying of different ionic forms confirms obtained results. For example, in table 3 there is NMR line widths for one of membranes. Protonic mobility decrease for Na<sup>+</sup> form and increases for K<sup>+</sup> form.

**Table 2: NMR line widths and chemical shifts for MC-40/MF-4SC+ZrO<sub>2</sub> membrane in different ionic forms**

form	<sup>1</sup> H spectra		M spectra	
	w	δ	w	δ
H <sup>+</sup>	413	6,54	-	-
Li <sup>+</sup>	370	4,73	138	0,87
Na <sup>+</sup>	340	4,29	258	0,89
K <sup>+</sup>	354	4,09	-	-

Similar plots can be obtained from the study of interdiffusion in various mixed alkali forms. Evaluated changes in diffusion coefficients of cations close to those obtained from data on the ionic conductivity (table 3). But also this method allows to study the asymmetry of ion transport.

**Table 3: Assymetry of diffusion coefficients of cations**

	D(Na <sup>+</sup> )·10 <sup>7</sup> , sm <sup>2</sup> /s, modified surf.	D (Na <sup>+</sup> )·10 <sup>7</sup> , sm <sup>2</sup> /s, nonmodified surf.	D (H <sup>+</sup> ) ·10 <sup>6</sup> , sm <sup>2</sup> /s, modified surf.	D (H <sup>+</sup> ) ·10 <sup>6</sup> , sm <sup>2</sup> /s, nonmodified surf.
<b>MC-40</b>	9,1 ± 0,6		2,1 ± 0,4	
<b>MC-40/MF-4SC</b>	4,1 ± 0,5	3,4 ± 0,2	4,1 ± 0,5	1,5 ± 0,5
<b>MC-40/MF-4SC +SiO<sub>2</sub></b>	2,7 ± 0,3	1,9 ± 0,3	6,2 ± 0,7	1,8 ± 0,4
<b>MC-40/MF-4SC +ZrO<sub>2</sub></b>	5,0 ± 0,5	3,9 ± 0,3	4,4 ± 0,5	1,4 ± 0,5

The main result of modification is the increase of proton mobility. For all samples transport from modified layer is faster than from unmodified. The incorporation of silica particles results in increase of proton diffusion coefficient, and incorporation of zirconia particles results in increase of sodium diffusion coefficient, similar to impedance spectroscopy data. Consistency of all obtained data shows the probability of using this complex of methods to membranes characterizing.

*This work was supported by the Program №7 of RAS Presidium "The development of the methods of the synthesis of chemical substances and the creation of new materials".*

# CATION-EXCHANGE MEMBRANES “POLICON”. STRUCTURE, PROPERTIES, APPLICATION

Marina Kardash, George Aleksandrov, Denis Aynetdinov

Engels Technological Institute, Saratov State Technical University, Engels, Russia;

E-mail: kardash@techn.sstu.ru

## Introduction

Native and foreign industrial heterogeneous cation-exchange membranes, used as semipermeable partitions in electroalytic devices, have similar structure and composition containing an active component – ion-exchange resin, and inactive components – inert filler and reinforcing fibers.

The modern tendencies in development of membrane technologies put forward new requirements to the properties of the membranes as well as to the reinforcing systems. Lately, special attention of scientists of Engels Technological Institute was paid to investigation of influence of manufacturing technological parameters on their structure, electrotransport properties and selection of effective materials for reinforcing heterogeneous membranes for the purpose of producing materials with the desired properties [1].

An urge towards achieving more uniform distribution of chargers and better electrochemical properties resulted in creation of cation-exchange membranes ‘Policon K’, in which fabrics based on novolac phenolformaldehyde (NPF) fibers are used as the reinforcing system. The material possesses the required and sufficient thermal stability (practical temperature limit of continuous maintenance up to 150°C in ambient air condition, and from 200 up to 250 °C in absence of oxygen), and stability to action of aggressive agents.

## Experimental

Studying the possibility and efficiency of the novolac phenolformaldehyde fabric fibers sulfiding by the method of energy dispersion analysis (Table 1) allowed to define high reactive ability of the vacant parapositions of the aromatic rings.

**Table 1: The elementary composition of NPF fibers**

Material type	Elements composition, % wt.			Total
	Carbon (C)	Oxygen (O)	Sulfur (S)	
Nonsulfided NPS fiber	75,2	24,8	0	100.00
Sulfided NPS fiber	65,4	30,0	4,6	100.00

Energy dispersion analysis proves, that sulfur content in sulfided fiber reaches about 5% of the mass. So, it is possible to speak about the high degree of substitution of the aromatic rings parapositions of the fiber-forming polymer, and achieving the sulfur content corresponding the strong acidulous cation-exchange resins of the resolious type.

As far as the concentrated sulfuric acid was used as the sulfiding agent, the correspondent tests of its influence on the physico-mechanical properties of the reinforcing fabrics were carried out. It was defined that the material retains in average 70% of strength (Table 2) in the simulated critical conditions (keeping in the concentrated sulfuric acid during 24 hours under 100°C).

**Table2: Change of the fabrics strength characteristics in a result of sulfiding**

Material	Liquid limit at elongation, MPa	Alongation at liquid limit, $\xi_{DT}$ , %	Tensile strength, $\sigma_{pp}$ , МПа	Alongation during rupture, $\xi_{pp}$ , %
Nonsulfided with a base	18,5	18,1	18,1	22,8
Nonsulfided by weft	9,6	16,0	9,4	16,1
Sulfided with a base	11,3	12,6	11,3	12,6
Sulfided by a weft	7,1	11,1	7,0	11,1

It is necessary to note, that the sulfiding completes after 120 minutes, driving to the high value of the exchange capacity (3,3 mg-eq./g) with minimal deterioration of physico-mechanical properties.

It is necessary to mention, that during manufacturing membranes of this type, it is possible to achieve the high grade of the phase interaction owing to the availability of the hydroxyl groups taking part both in chemical reaction of cross-linking with the material matrix hydroxyl groups and formation of a considerable number of Van de Waals bonds, that is proved by the results of scanning electron microscopy (Fig.1).

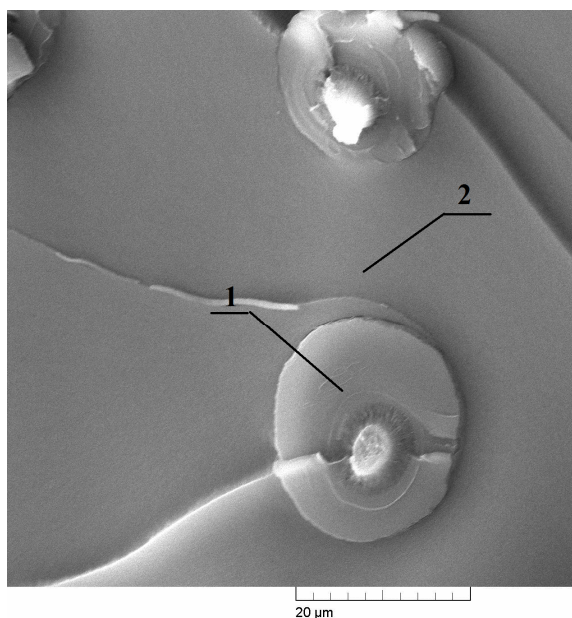


*Figure 1. Microphotography of the cross section structure of the material “Policon” based on nonsulfided NPF fiber: 1 – fiber, 2 – ion- exchange matrix*

The work has been carried out under the sponsorship of the Russian Foundation for Basic Research (project No.10-08-00074-a.)

#### **References**

1. *Kardash M.M., Aleksandrov G.V., Volkovich Yu.M. Directed adjustment of the ‘Polikon’ materials structure and properties // Chemical Fibers. 2010. No.5. P.38-41*

# IMPLEMENTATION OF FE NANOPOWDER INTO CHEMOSORPTION POLYMERIC MATERIALS - «POLYCON K»

Marina Kardash, Denis Terin, Ivan Tyurin, Margarita Batura

Engels Technological Institute, Saratov State Technical University, Engels, Russia

E-mail: kardash@techn.sstu.ru

## Introduction

The aim of this work is the production of high-performance, cationexchange chemisorption fibrous materials on basis of phenol, formaldehyde, sulfuric acid, polyacrylonitrile (PAN) fiber– «POLYCON K» [1].

## Experiments

We carried out research to state structure characteristics, morphology and electrodynamic properties of «POLYCON K» formed on basis of PAN fiber with addition of super dispersed admixture iron nanopowder [2].

It was defined, that introduction of additional heterophase medium into monomer-isomerization structure leads to changes in kinetics and thermodynamics of passing reactions.

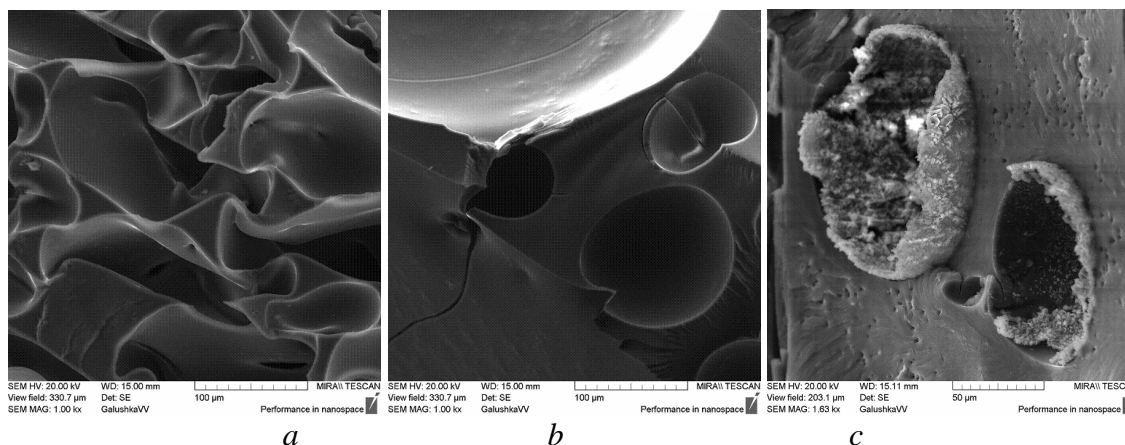


Figure 1. SEM images of «POLYCON K»: PAN (a), PAN + 1.5% Fe (b), PAN + 5% Fe (c)

## Results and Discussion

The increasing of thermal effect in curing reaction and displacement of thermal peak to lower temperature region was distinguished. Those facts confirm the influence of super dispersed admixtures on basic material.

The introduction of nanopowder abruptly changes the morphology of basic material. The surface becomes more dense, homogeneous with presence of open pores. Rising iron percentage the PAN folded character disappears. Areas with spherulitic inclusions could be observed (Fig.1).

We investigated electrodynamic properties of modified materials in a wide frequency range, notably frequency dependences of capacity and dielectric loss tangent to define complex dielectric permeability. We examined servicing characteristics of sorption modulus for water refining from petrochemicals. Introduction of Fe nanopowder permitted us to raise the sorption capacity of petrochemicals up to 25 %.

*This work supported by RFBR (Project Number 10-08-0074-a)*

## References

1. Kardash M., Tyurin I., Volkovich Y. Cation-exchange chemisorption fibrous materials «Polycon» based on oxidized PAN fiber // Conf. proc. Ion transport in organic and inorganic membranes, Krasnodar, Russia, 2011. P. 77-78.
2. Bilenko D.I., Galushka V.V., Dobren'kii E.A., Terin D.V., Elerman Y. Investigation of nanodisperse Fe and Ni properties // Conf. Proc. APED- 2010, Saratov, Russia, P.149-150.

# MODIFICATION AND IMPLEMENTATION OF NI NANOPOWDER INTO «POLYCON K». STRUCTURE CHARACTERISTICS, MORPHOLOGY AND ELECTRODYNAMIC PROPERTIES OF CHEMOSORPTION POLIMERIC MATERIALS

Marina Kardash, Denis Terin, Ivan Tyurin, Margarita Batura

Engels Technological Institute, Saratov State Technical University, Engels, Russia

E-mail: kardash@techn.sstu.ru

## Introduction

The aim of this work is the production of high-performance, cationexchange chemisorption fibrous materials on basis of phenol, formaldehyde, sulfuric acid, polyacrylonitrile (PAN) fiber–«POLYCON K» [1].

## Experiments

We carried out research to state structure characteristics, morphology and electrodynamic properties of «POLYCON K» formed on basis of PAN fiber with addition of super dispersed admixture nickel nanopowder [2]. It was defined, that introduction of additional heterophase medium into monomer-isomerization structure leads to changes in kinetics and thermodynamics of passing reactions. The increasing of thermal effect in curing reaction and displacement of thermal peak to lower temperature region was distinguished. Those facts confirm the influence of nickel super dispersed admixtures on basic material. The introduction of nanopowder abruptly changes the morphology of basic material. The surface becomes more dense, homogeneous with presence of open pores. Rising nickel percentage the PAN folded character disappears. Areas with spherulitic inclusions could be observed (Fig.1).

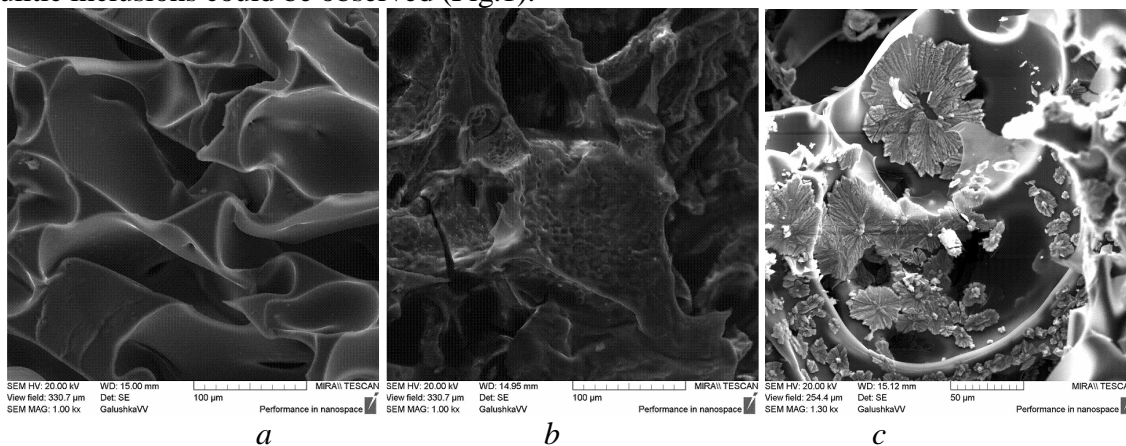


Figure 1. SEM images of «POLYCON K»: PAN (a), PAN + 1.5% Ni (b), PAN + 5% Ni (c)

## Results and Discussion

We investigated electrodynamic properties of modified materials in a wide frequency range, notably frequency dependences of capacity and dielectric loss tangent to define complex dielectric permeability. We examined servicing characteristics of sorption modulus for water refining from petrochemicals. Introduction of Ni nanopowder permitted us to raise the sorption capacity of petrochemicals up to 45 %. The received materials have a complex, multilevel system of pores, which allows their usage in high velocity water flow. In this study, carried out we also studied the effectiveness of water purification from ions of heavy metals.

This work supported by RFBR (Project Number 10-08-0074-a)

## References

1. Kardash M., Tyurin I., Volfkovich Y. Cation-exchange chemisorption fibrous materials «Polycon» based on oxidized PAN fiber //Conf. proc. Ion transport in organic and inorganic membranes, Krasnodar, Russia, 2011, P. 77-78.
2. Bilenko D.I., Galushka V.V., Dobren'kii E.A., Terin D.V., Elerman Y. Investigation of nanodisperse Fe and Ni properties //Conf. Proc. APED-2010, Saratov, Russia, P.149-150.

# STUDY OF SULFONIC ACID GROUP DISSOCIATION AND WATER CONNECTIVITY IN POLYSTYRENE AND PERFLUORINATED MEMBRANES

<sup>1</sup>Larisa Karpenko-Jereb, <sup>1</sup>Anne-Marie Kelterer

<sup>1</sup>Graz University of Technology, Graz, Austria,

E-mail: larisa.karpenko-jereb@tugraz.at; kelterer@tugraz.at

## Introduction

The ion-exchange membranes are applied widely in electro-membrane processes as well in the separation and purification of organic solvents by pervaporation [1]. The transport characteristic and membrane selectivity depends on the thermodynamic properties of the water and ion-exchange pairs. The goal of the work was to analyze the water binding energy and the dissociation of -SO<sub>3</sub>H groups in polystyrene membranes MK-40 and perfluorinated membranes Nafion-117 at various hydration levels (from 0 up to 11) using quantum chemical methods.

## Computational Methods

The chemical structures of the studied membranes are shown in Figure 1. The quantum chemical calculations were carried out for the membrane models are marked with squares. The calculations were performed by the Program ORCA [2]. The geometries had been optimized by the Restricted Hartree Fock (RHF) method with the 6-31G (d,p) basis set [3] and tight optimization criteria. The quality of minima has been checked via frequency analysis. The calculation of the binding energy of the membrane-water complexes were carried out using the local pair natural orbital - coupled-electron pair approximation (LPNO-CEPA/1). From the values of the electrons energy of dry ( $E_{dry}$ ) and hydrated membranes ( $E_{cluster}$ ) the specific binding energy ( $E_B$ ) of the water molecules was computed by the following expression:

$$E_B = \frac{E_{cluster} - E_{dry}}{X} - E_{H_2O} \quad (1),$$

where  $E_{H_2O}$  is the electrons energy of one water molecule, X is the number of water molecules in the membrane. The specific binding energy indicates the binding energy per water molecule.

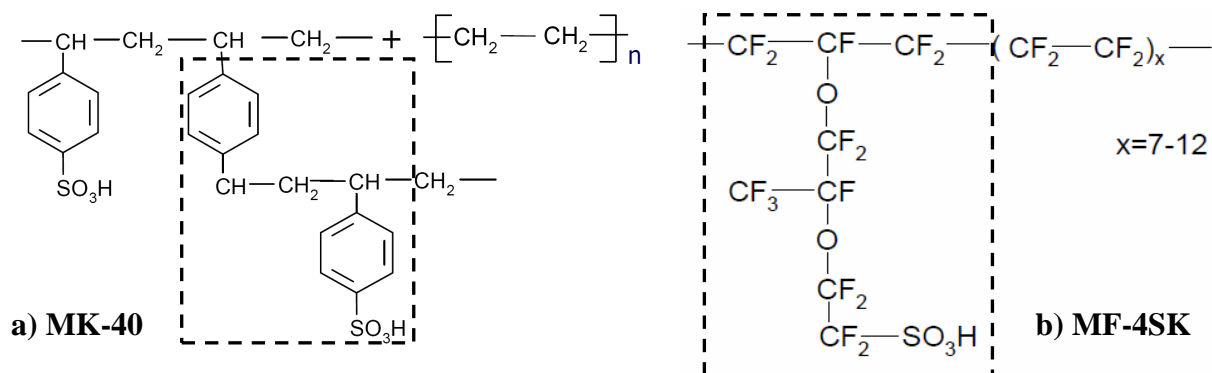


Figure 1. Chemical structure of the membranes: a) MK-40 and b) MF-4SK. The membrane models used in the quantum chemical calculations are marked with squares

## Results and Discussion

The optimized structures of the membranes with the hydration levels  $X=0; 1; 3; 6$  and  $8$  are shown in Figure 2. As seen from the figure in membrane MK-40 the sulfonic acid groups are in a non-dissociated state in the whole studied range of the hydration level, while in the perfluorinated membrane Nafion the dissociation of the ion-exchange group is observed for  $X \geq 3$ . Moreover, the water molecules in the polystyrene membrane MK-40 are dislocated around the

end-group, while the water molecules in the Nafion membrane locate under the end-group and form a cluster.

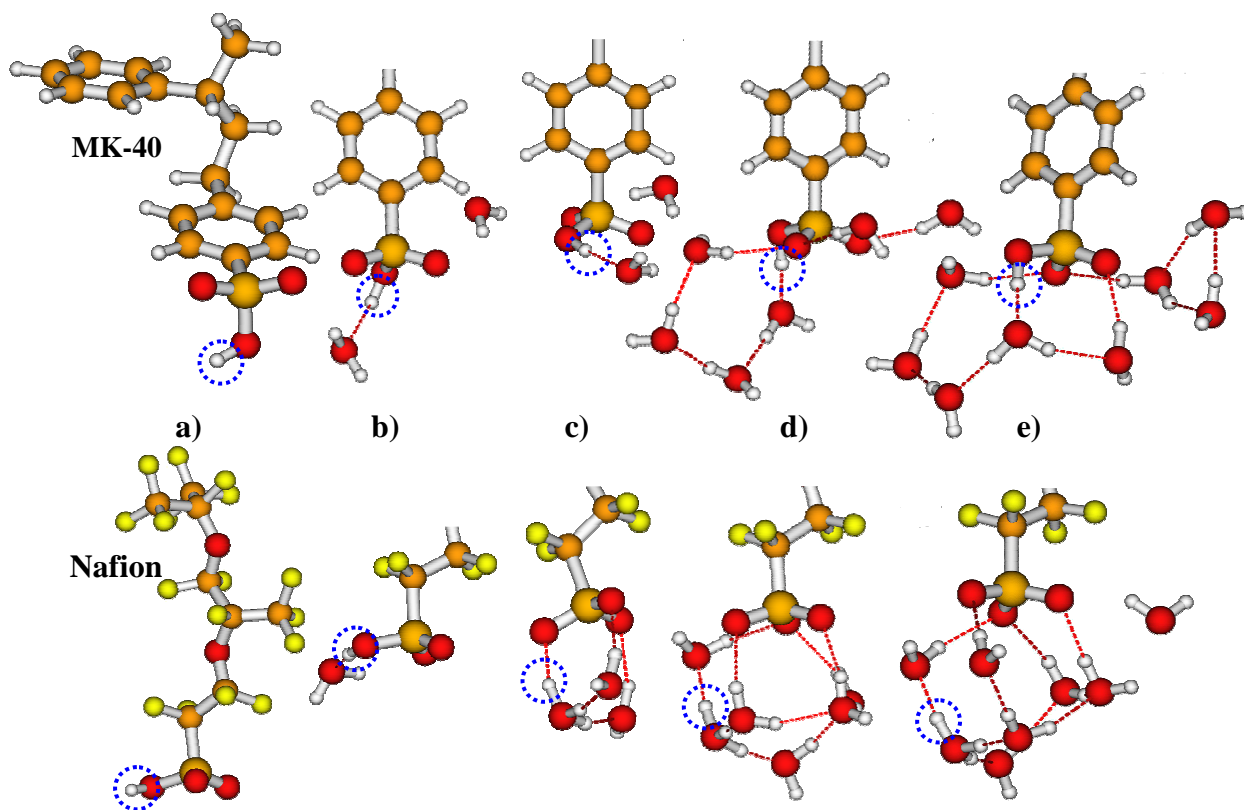


Figure 2. Calculated geometries of dry membranes (a) and membrane fragments (b-e) at various hydration levels:  $X=1$  (b);  $X=3$  (c);  $X=6$  (d);  $X=8$  (e). Protons are marked with a dotted circle

Figure 3 demonstrates the distance between proton and sulfonic groups as a function of the membrane hydration level. As can be seen the distance between  $-SO_3^- \dots H^+$  in MK-40 grows very insignificantly from  $0,949 \text{ \AA}$  (dry state,  $X=0$ ) to  $1,010 \text{ \AA}$  ( $X=8$ ). The distance in MF-4SK changes slightly from  $0,951 \text{ \AA}$  ( $X=0$ ) to  $0,990 \text{ \AA}$  ( $X=2$ ), then increases to  $1,568 \text{ \AA}$  (for  $X=3-4$ ) and at the transition to hydration level from four to five sharply rises to  $3,195 \text{ \AA}$ , then grows slightly again in the range of  $5 \leq X \leq 11$ .

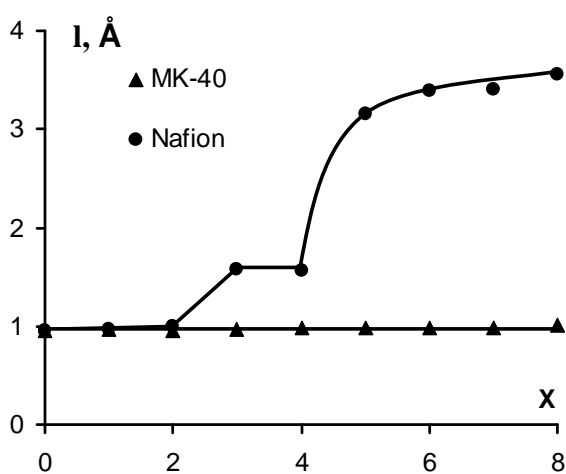


Figure 3. Distance between the proton and sulfonic group as a function of the membrane hydration level

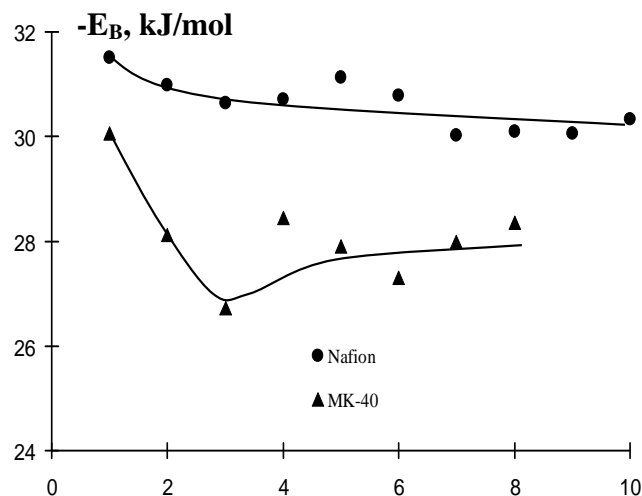


Figure 4. Specific binding energy of water vs. membrane hydration level

Figure 4 presents the specific binding energy as a function of the membrane hydration level. As seen from the figure the water molecules are bound stronger in the Nafion than in the MK-40 membrane.

The obtained results show that the chemical nature of the membrane polymer matrix has some influence on the dissociation of the sulfonic acid group as well as on the building of the water cluster in the ion-exchange membranes. The observed dissociation of  $-SO_3^- \dots H^+$  in Nafion membranes and well-networked water molecules promote the improved transport of the protons by the Grotthuss mechanism. The results explain some experimental investigations which indicate higher proton mobility in the perfluorinated membranes in comparison to polystyrene membranes [4-5].

*The investigation was carried out in the framework of the Austrian-Polish Cooperation Project No.PL 08/2012 supported by the Austrian Agency of International Cooperation.*

### References

1. *Kujawski W., Poźniak G.* Transport properties of ion-exchange membranes during pervaporation of water-alcohol mixtures // *Separation Science and Technology*. 2005. V. 40 (11). P. 2277-2295
2. *Neese F.* ORCA Version 2.8, An ab initio, density functional and semi-empirical program package, University Bonn, September 2010.
3. *Hehre W.J., Ditchfield R., Pople J.A.* Self-Consistent Molecular Orbital Methods. XII. Further Extensions of Gaussian-Type Basis Sets for Use in Molecular Orbital Studies of Organic Molecules // *J. Chem. Phys.* 1972. V. 56. P. 2257-2261.
4. *Knauth, P., Sgreccia, E., Donnadio, A., Casciola, M., Di Vona, M.L.* Water activity coefficient and proton mobility in hydrated acidic polymers // *Journal of the Electrochemical Society* 2011. V. 158 (2). P. B159-B165
5. *Karpenko-Jereb L., Kelterer A.-M.* Conductometric and computational study of cation-exchange membranes in  $H^+$  and  $Na^+$  forms with the various hydration level // *Book of abstracts, ICOM, Netherlands*. 2011. ICOM603. P.29

# TRANSPORT OF SALT MIXTURES THROUGH POLYLAYERED COMPOSITE ULTRAFILTRATION MEMBRANE

Victor Kasperchik, Alla Yaskevich, George Poleshko

Institute of Physical Organic Chemistry NASB, Minsk, Belarus, E-mail: *ufm@ifoch.bas-net.by*

## Introduction

In previous paper [1] we have observed transport filtration characteristics of polylayered composite ultrafiltration (UF) membranes for the different types of individual salt dilute solutions. For the system: aromatic polyamide (PA) as initial membrane matrix – poly-[N, (2-amino ethyl) acryl amide] (PAEAA) as modification agent composite structures with high rejection ability to electrolytes of 2-1 type and low rejection ability to electrolytes of 1-2 type were obtained. It can be supposed that this composite membrane will be perspective for the effective separation of the salt mixtures.

## Experiments

Stirred filtration cell was used for the investigation of salt mixtures separation. Individual ion concentrations in the bulk solutions and filtrates were determined on the ion chromatograph Dionex ISC-3000. The rejection abilities of the composite PA membrane to the different ions are presented in the table.

**Table: Rejection abilities of the composite PA membrane to mono- and bi-charged ions during ultrafiltration of the salt mixtures**

Salt mixture composition	Salt ratio in solution	R* (%)			
		Na <sup>+</sup>	Cl <sup>-</sup>	Mg <sup>2+</sup>	SO <sub>4</sub> <sup>2-</sup>
MgCl <sub>2</sub> - NaCl	100:0	-	88	88	-
	80:20	1	74	87	-
	50:50	24	66	92	-
	20:80	38	55	90	-
	0:100	44	44	-	-
MgCl <sub>2</sub> -MgSO <sub>4</sub>	80:20	-	42	51	67
	50:50	-	33	42	51
	20:80	-	25	33	38
	0:100	-	-	43	43
MgCl <sub>2</sub> - Na <sub>2</sub> SO <sub>4</sub>	80:20	7	48	64	73
	50:50	12	24	50	39
	20:80	11	12	41	19
	0:100	12	-	-	12

\* R (rejection coefficients) at 0,35 MPa, 293 K and  $\omega = 5 \text{ s}^{-1}$ . Total electrolyte concentration in all solutions –  $10^{-3} \text{ mol/l}$

## Results and Discussion

As can be seen from the experimental data adding of Na<sup>+</sup> ions to MgCl<sub>2</sub> solution is almost no effect on the membrane rejection ability to Mg<sup>2+</sup>. From the other hand free transfer of mono-charged cations through the membrane is observed at low partial concentration of Na<sup>+</sup> in the bulk solution (<20 %). Adding of Na<sup>+</sup> to bulk solution to high partial concentration level (up to 80 %) leads to Na<sup>+</sup> substantial increasing rejection ability (up to 38 %). After complete substitution of Mg<sup>2+</sup> on Na<sup>+</sup> in the bulk solution membrane rejection ability for mono-charged cations is still increasing but not so sharp (up to 44 %).

Another situation was observed when SO<sub>4</sub><sup>2-</sup> ions were added to MgCl<sub>2</sub> solution. In this case little adding of bi-charged anions to the bulk solution leads to sharp decreasing of membrane selectivity to Mg<sup>2+</sup> (from 88 to 51%). Then membrane rejection ability to Mg<sup>2+</sup> is decreasing slowly: to level of 43 % after complete substitution of Cl<sup>-</sup> to SO<sub>4</sub><sup>2-</sup> in the bulk solution.

As can be expected the highest changes in the membrane transport characteristics were observed when different mono- and bi-charged cations and anions were added to the bulk

solution. After adding of  $\text{Na}_2\text{SO}_4$  little quantity to  $\text{MgCl}_2$  bulk solution substantial decreasing of membrane rejection ability to  $\text{Mg}^{2+}$  (from 88 to 64 %) and to  $\text{Na}^+$  (from 44 to 7 %) was observed. Then increasing of  $\text{Na}^+$  and  $\text{SO}_4^{2-}$ -partial concentration to 80 % level in the  $\text{MgCl}_2$  bulk solution leads to gradual decreasing of membrane rejection ability to  $\text{Mg}^{2+}$  (from 64 to 41 %) and little increasing of rejection to  $\text{Na}^+$  (up to 12 %).

Thus it was established that presence in the bulk solution of different ions was expressed more complicated influence on the membrane transport characteristics as it can be supposed from experimental data for the membrane separation of individual salts. In this case theoretical interpretation of obtained results is difficult due to complicated interactions of bulk solution mono- and bi-charged cations and anions with uncompensated charges in the composite membrane matrix and its surface.

### References

1. *Kasperchik V.P., Yaskevich A.L.* // Ion transport in organic and inorganic membranes: Int. conf. proceedings. Krasnodar, 2011. P. 79-80.

# POLYETHYLENETEREPHTALATE TRACK ETCHED MEMBRANES WITH ASYMMETRICAL SHAPE PORES

Yury Kochnev, Alexandr Vilensky, Boris Mchedlishvili

Shubnikov Institute of Crystallography RAS, Moscow, Russia, E-mail: very-cool@rambler.ru

Commonwidened track etched (T-E) membranes have symmetrical cylindrical pores. The transition from a long cylindrical pores to different geometry, such as elliptical pores is a promising area of technology of T-E. Elliptical pores (pores with varying cross-sectional eccentricity) are appealing because the change of degree of asymmetry (ratio of the pore axes) can substantially change their characteristics such as efficiency and selectivity. The aim of our work was to investigate the influence of polymer film thermo-elongation in different stages of T-E production on T-E pore shape and characteristics of resulting membranes. The second claim was to investigate the electrokinetic characteristics of T-E membranes in different etching solutions. Obtained data were used to produce T-E membranes with assymetrical pore shape.

The objects of our study were amorphous PET film (50  $\mu$ ), subjected to irradiation and subsequent etching in alkali solutions. The film was subjected to thermo-elongation on different stages of T-E formation (i.e. before irradiation of film with high energy heavy ions beam, after the irradiation and elongation of formed membranes). The degree of stretching ( $\lambda$ ) controlled by birefringnase index and by changing in sample longness. Irradiation of films was carried out in the cyclotron of JINR (Dubna) at the cyclotron U-400 high-energy ions Kr (fluence of  $10^8 - 10^9$   $\text{cm}^{-2}$ , the energy of 1,2 - 3 MeV / amu.). Etching of films was carried in a solution of KOH concentration of 1 M under 70°C. Etching process was accompanied by mass loss ( $\Delta m$ ) of the polymer, which was evaluated on the mass of the initial sample (before etching).

Before the influence of orientation on the kinetics of etching and shape of pores was necessary to determine the influence of irradiation on the etching of non-oriented films.

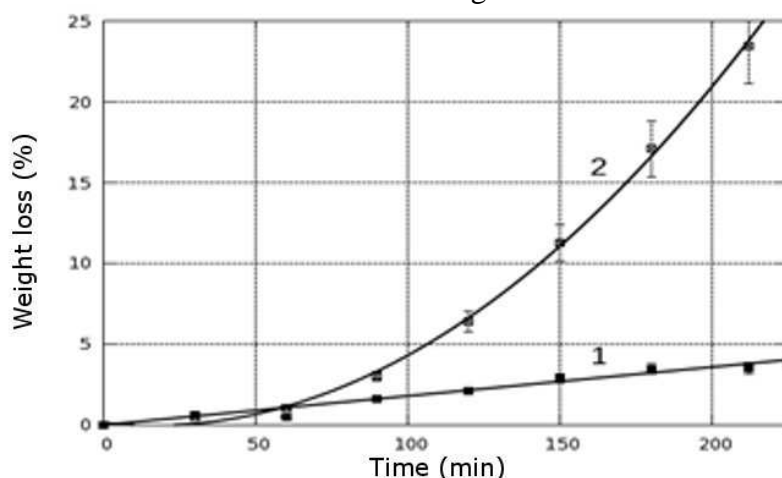


Figure 1. Relative mass loss ( $\Delta m$ ) from the time of etching ( $\tau$ ) unoriented PET film. 1 - unirradiated sample, 2 - irradiated sample

Etching of the unirradiated film (Fig. 1, curve 1) shows a linear dependence of  $\Delta m$   $\tau$ , while the sample irradiated film (Fig. 1, curve 2) is characterized by an exponential dependence. This is due to the fact that the process of irradiation leads to significant changes in the structure of the polymer, especially in education latent tracks (LT). In accordance with [2], the structure of LT has a significant change: the central part - it was destroyed with a graphitized polymer center with a diameter of 10 nm, then with increasing radius followed by the field with varying degrees of destruction and decreasing cross-linking areas. Thus, the irradiated sample has a significant number of local defects - active centers (surface and volume), which leads to the acceleration of etching in comparison with the unirradiated film. As the etching of the film quickly etched defect area than the rest of the films. This in turn leads to increased contact surface with KOH etched areas of LT, which accelerates the degradation in accordance with Fig. 1 (cur. 2).

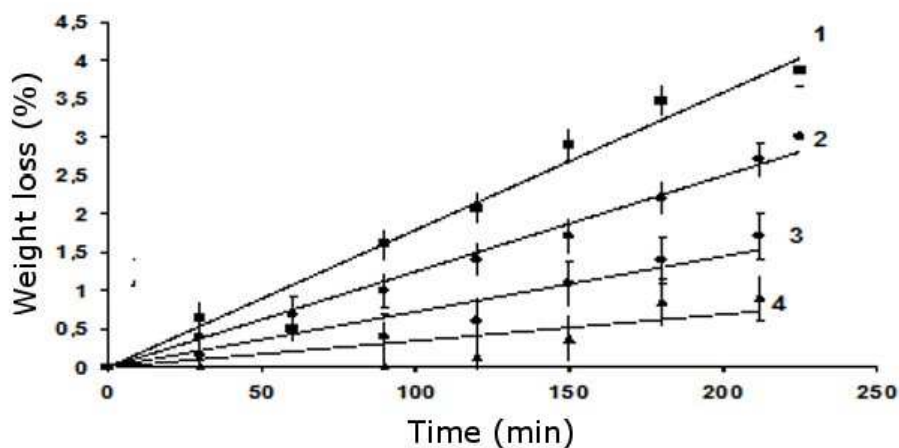


Figure 2. Dependence of mass loss ( $\Delta m$ ) from the time of etching ( $\tau$ ). Unirradiated PET. Multiplicity extract ( $\lambda$ ): 1 - 1; 2 - 3.2; 3 - 4.7; 4 - 5

The nature of relationships in Fig. 2, 3 is similar to the established in Fig. 1. As expected, the orientation of PET with increasing  $\lambda$  leads to a decrease in the etching rate of both irradiated and unirradiated films (Fig. 2 and 3).

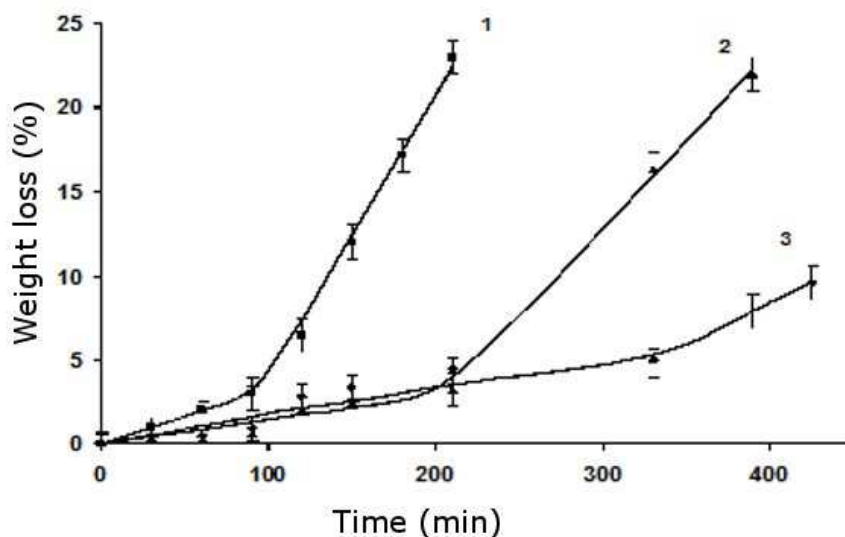


Figure 3. Dependence of mass loss from the time of etching. Irradiated PET ( $Kr$ , fluence  $3 \cdot 10^6 \text{ ion/sm}^2$ ). Multiplicity extract ( $\lambda$ ): 1-1; 2 - 1.8; 3 - 3.7

Photomicrograph of the surface film obtained after etching-based sample shown in Fig. 4, which shows that the orientation can receive T-E surface with elliptical pores.

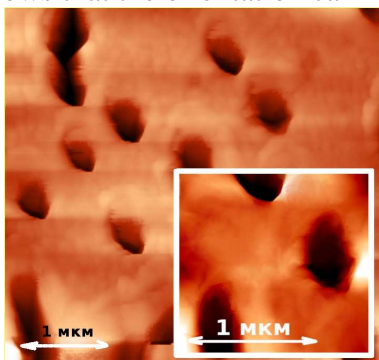


Figure 4. AFM image of PET film irradiated by  $Kr$  (fluence  $3 \cdot 10^6 \text{ ion/sm}^2$ ), focused on 300% and etched for 4 hours

Thus, we have shown that orientation elongation can be used to produce T-E membranes with elongated pores.

# PREPARATION OF COMPOSITES BASED ON MF-4SC MEMBRANE AND POLYANILINE IN EXTERNAL ELECTRICAL FIELD

Natalia Kononenko, Ninel Berezina, Sergey Dolgoplov, Irina Falina  
Kuban State University, Krasnodar, Russia, E-mail: kononenk@chem.kubsu.ru

## Introduction

Perfluorinated sulfocationic membranes of type Nafion (Du Pont, USA) and MF-4SC (Plastpolymer, Russia) are used as a template for the synthesis of conducting polymers, such as polyaniline that exhibits unique electrical, electrochemical and optical properties. Very often such materials are obtained in static conditions by chemical template synthesis, where various redox systems are electron acceptors during the oxidative polymerization of aniline [1, 2]. The aim of this work is to study the influence of external electrical field on the synthesis of polyaniline in MF-4SC membrane. One of the tasks of this work is to investigate the electrotransport properties of the obtained composites.

## Experimental

Template synthesis of polyaniline in MF-4SC as a basic matrix was carried out with the help of electro dialysis cell in two stages. The first stage was saturation of the membrane by monomer (ion  $C_6H_5NH_3^+$ ) in the electric field. The polymerization of aniline under the action of the initiator ( $FeCl_3$ ) under the same conditions was carried out in the second stage. Working solutions of monomer and polymerization initiator were moved to the desalting chamber, sulfuric acid solution circulates in other chambers of the cell. The current density ranged from 40 to 100  $A/m^2$ , the timing of each stage was from 15 min up to 3 hours. The concentration of sulfuric acid was 0.005 M  $H_2SO_4$ . It is 100 times lower than by the synthesis of polyaniline (PAn) in the static conditions. The concentration of the polymerization initiator solution was 0.01 M. Characterization of the composite samples MF-4SC/PAn was carried out by the membrane conductometry and voltammetry methods.

## Results

Table 1 presents characteristics of a series of samples obtained in different conditions in an external electric field. It presents also the properties of the initial MF-4SC membrane and composite membranes MF-4SC/PAn which were obtained under static conditions during 3 hours.

Table 1: Characteristics of MF-4SC and MF-4SC/PAn membranes

№	Membrane	The current density $i$ , $A/m^2$	Time of contact with solutions		$K_{iso}$ , S/m	$P \cdot 10^{12}$ , $m^2/s$	$i_{lim}$ , $A/m^2$
			Stage 1	Stage 2			
1	MF-4SC	–	–	–	4,1	3–4	170-190*
2	MF-4SC/PAn	0	3 h	3 h	3,5	3–4	150±4
3	MF-4SC/PAn	83	3 h	3 h	3,0	–	–
4	MF-4SC/PAn	54	2 h	1 h	3,5	4–5	180±5
5	MF-4SC/PAn	54	15 min	1 h	3,0	4–5	180±7
6	MF-4SC/PAn	40	30 min	1 h	3,2	2,6–3,0	200±7

Table 1 shows that all the composite membrane which were obtained in an external electric field (samples № 3-6) have a sufficiently high ionic conductivity (equal  $\approx 3$  S/m). Diffusion permeability ( $P$ ) and limiting current density ( $i_{lim}$ ) of these samples are comparable to those characteristics for the initial membrane and composite MF-4SC/PAn which was obtained in static conditions. It was found that a composite membrane MF-4SC/PAn can be prepared:

- with reduction of the current density up to 40  $A/m^2$  (sample № 6),
- with reduction of the concentration of aniline solution up to 0.001 M,

\* The  $i_{lim}$  value of initial membrane varied in dependent on technological conditions of synthesis.

- with reduction of the time of the  $C_6H_5NH_3^+$  ions saturation stage up to 15 min and the polymerization aniline stage up to 60 min (sample № 5).

Thus, the method of polymerization of aniline in the MF-4SC membrane matrix in an external electric field is faster and more resource-saving compared with static conditions.

The current-voltage characteristics of the initial and composite membranes are shown in Figure 1. As can be seen from the figure, the slope of the ohmic part of the curve, which characterizes the conductivity of electromembrane system, is practically the same for all samples. It is consistent with the independent determination of samples electrical conductivity by mercury-contact method. The length of the limiting current plateau increases by 30%. The same effect is always observed for the composites MF-4SC/PAn. The asymmetry of current-voltage curve is absent by the reversal of the current (curve 2, 3, Fig. 1). It confirms the bulk character of the modification of membrane MF-4SC by polyaniline in an external electric field.

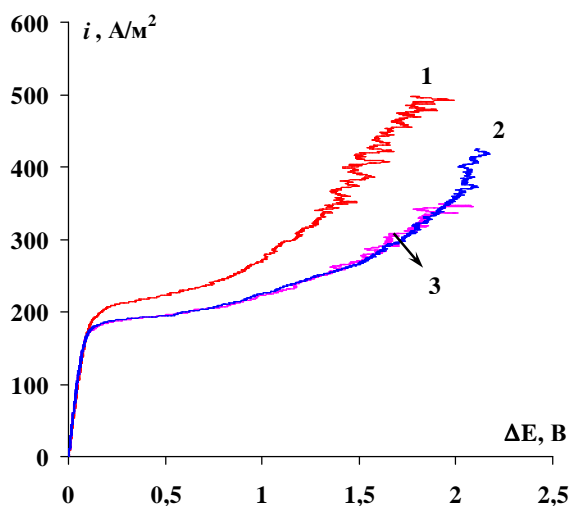


Figure 1. Current-voltage curves of MF-4SC (1) and MF-4SC/Pan (2, 3) in 0,05 M HCl solution

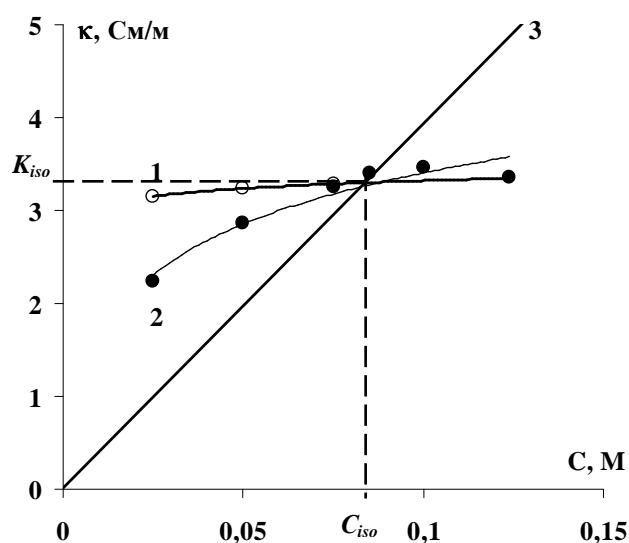


Figure 2. Concentration dependences of the conductivity of MF-4SC (1) and MF-4SC/Pan in HCl solutions (3)

Figure 2 shows the concentration dependences of the conductivity ( $\kappa$ ) of template and composite membranes in HCl solutions. Both initial membrane and composite sample have identical value of the  $\kappa$  near to the "isoconductivity" point ( $\kappa_{iso}-C_{iso}$ ). There is essential decrease of the  $\kappa$  value in area  $C < C_{iso}$  for a composite in comparison with a base membrane. It indicates on the same conductivity of gel phase and increase of a volume fraction of an internal solution in the MF-4SC membrane after polyaniline intercalation.

The parameters three-conducting and micro-heterogeneous model of ion-exchange membranes conductivity were calculated from the concentration dependences (Fig. 2):

$a$  is the current fraction through the mixed channel a gel-solution;

$b$  is the current fraction through a gel;

$c$  is the current fraction through a solution;

$d$  is the fraction of solution in mixed channel;

$e$  is the fraction of gel in mixed channel;

$f_1$  is the volume fraction of gel phase;

$f_2$  is the volume fraction of inner solution phase;

$\alpha$  is the parameter characterising the arrangement of phases in the material ( $\alpha = +1$  for parallel orientation of conducting phases,  $\alpha = -1$  for serial orientation of phases).

According to above-mentioned model:  $a + b + c = 1$ ,  $d + e = 1$ ,  $f_1 + f_2 = 1$ . The model parameters of initial and composite membranes which were obtained in different conditions are shown in Table 2.

**Table 2. The model parameters of initial and composite membranes**

Membrane	<i>a</i>	<i>b</i>	<i>c</i>	<i>d</i>	<i>e</i>	<i>f</i> <sub>1</sub>	<i>f</i> <sub>2</sub>	<i>α</i>
MF-4SC [3]	0,21	0,79	$5,34 \cdot 10^{-3}$	0,46	0,54	0,90	0,10	0,44
MF-4SC/Pan (5 h in static conditions) [3]	0,32	0,68	$8,35 \cdot 10^{-7}$	0,22	0,78	0,93	0,07	0,19
MF-4SC/Pan (30 days in static conditions) [3]	0,77	0,23	$3,23 \cdot 10^{-8}$	0,19	0,81	0,85	0,15	0,11
MF-4SC/Pan (in electric field)	0,93	0,07	$4 \cdot 10^{-7}$	0,25	0,75	0,77	0,23	0,10

As can be seen from the table, the essential reorganization of conducting ways takes place in the case of composite preparation in an electrical field. The increase of the contribution of the mixed channel of conductivity correlates with data of the standard porosimetry method. The formation of specific morphology of polyaniline in a membrane was confirmed also by methods of differential scanning calorimetry, thermogravimetry and IR-spectroscopy. Polyaniline is located on surface of the transport channels.

### Conclusions

The new method of polyaniline synthesis in MF-4SC membrane in conditions of an electrical field was developed. The obtained composite materials have high conductivity and stable hydrophilicity which is necessary for application in fuel cells.

### Acknowledgments

*The present work is supported by the Russian Foundation for Basic Research (project № 12-08-01092-a)*

### References

1. Berezina N.P., Kononenko N.A., Sytcheva A.A.-R., Loza N.V., Shkirskaya S.A., Hegman N., Pungor A. // *Electrochimica Acta* 2009. V.54. P. 2342-2352.
2. Berezina N.P., Kubaisy A.A., Timofeev S.V., Karpenko L.V. // *J. Solid State Electrochem.* 2007. Vol. 11. N 3. P. 378.
3. Berezina N.P., Gnusin N.P., Dymina O.A., Annikova L.A. // *Elektrokhimiya (Rus .J. Electrochemistry)*. 2009. V.45. N 11. P. 1325-1332.

# ANALYTICAL SOLUTIONS BOUNDARY PROBLEMS MODELS ELECTROCONVECTION IN MEMBRANE SYSTEMS (MS)

<sup>1</sup>Anna Kovalenko, <sup>1</sup>Mahamet Urtenov, <sup>2</sup>Aminat Uzdenova

<sup>1</sup> Kuban State University, Krasnodar, Russia, E-mail: urtenovmax@mail.ru

<sup>2</sup> Karachev-Cherkess State University, Karachaevsk, Russia

## Introduction

The study of electroconvection in membrane systems (MS) is important for understanding the mechanisms of current-limiting, the intensification of mass transfer, manipulation of liquid flow in microfluidic devices. At currents above the limit value appears the space charge, which is the source of electroconvection in the MS. The large number of papers devoted to mathematical modeling of electroconvection (SS Dukhin, Derjaguin BV, I. Rubinstein, B. Zaltzman, M. Bazant, etc.), but mathematical theory of electroconvection is still at an early stage of development. This is due primarily to the study of mathematical problems and solving the corresponding boundary-value problem for a coupled system of equations, the Nernst-Planck-Poisson and Navier-Stokes equations used to model the electroconvection. We offer a rather simple approximate analytic solutions based on the asymptotic analysis of this problem.

## Mathematical model

The mass transfer in view of electroconvection in the electro-systems described by equations of electrodiffusion Nernst-Planck-Poisson (1-4) and the Navier-Stokes equations (5,6), taking into account the spatial force. The vector recording of this system for binary electrolyte in the absence of chemical reactions in the dimensionless variables has the form [1]:

$$\vec{J}_i = z_i D_i C_i \vec{E} - D_i \nabla C_i + Pe C_i \vec{V}, \quad i = 1, 2 \quad (1)$$

$$Pe \frac{\partial C_i}{\partial t} = -\text{div} \vec{J}_i, \quad i = 1, 2 \quad (2)$$

$$\varepsilon \Delta \varphi = -(z_1 C_1 + z_2 C_2) \quad (3)$$

$$\vec{I} = z_1 \vec{J}_1 + z_2 \vec{J}_2 \quad (4)$$

$$\frac{\partial \vec{V}}{\partial t} + (\vec{V} \nabla) \vec{V} = -\nabla P + \frac{1}{\text{Re}} \Delta \vec{V} + \varepsilon K_{el} \vec{E} \text{div} \vec{E} \quad (5)$$

$$\text{div}(\vec{V}) = 0, \quad (6)$$

where  $\nabla$  - the gradient,  $\Delta$  - Laplace operator,  $\vec{V}$  - the rate of flow of the solution,  $P$  - the pressure,  $\vec{J}_1, \vec{J}_2, C_1, C_2$  - flow and concentration of cations and anions in solution,  $z_1, z_2$  - the charge of cations and anions,  $\vec{I}$  - current density,  $D_1, D_2$  - the diffusion coefficients of cations and anions,  $\varphi$  - electric potential,  $t$  - time. These equations to put natural boundary conditions [1], for example, no-slip condition at the membrane surface for speed.

The dimensionless parameters have the following specific range:  $x \in [0, 1], y \in [0, L]$ , and the number  $\varepsilon = \frac{RT_0 \varepsilon_0}{F^2 H^2 C_0}$  varies from  $10^{-4}$  to  $10^{-14}$ , the Peclet number  $Pe = \frac{V_0 H}{D}$ , depends linearly on the initial velocity  $V_0$  and when it changes varies widely. When the flow velocity  $V_0 > 1 \frac{MM}{c}$  and width of the channel  $H = 1MM$  Peclet number can be regarded as a large parameter, and accordingly,  $\lambda = 1/Pe$  a small parameter, which varies from  $10^{-2}$  to  $10^{-5}$ .

The parameter  $K_{el} = \frac{RTC_0}{\rho_0 V_0^2}$  estimate. The formula it follows that,  $K_{el} \sim \frac{1}{V_0^2}$  so with a

decrease  $V_0$  in value rapidly, with a decrease  $V_0$  from  $10^{-1} \frac{M}{c}$  to  $10^{-6} \frac{M}{c}$ ,  $K_{el}$  increases from

$K_{el} \approx 244$  to  $K_{el} \approx 2.44 \cdot 10^{13}$ . The Reynolds number  $Re = \frac{V_0 H}{\nu}$  is small and varies in the range 10-100. The above formulas  $F$  - Faraday constant,  $R$  - the gas constant,  $T$  - the absolute temperature,  $\epsilon_0$  - the dielectric constant of an electrolyte  $\rho_0$  - a characteristic density of the solution -  $\nu$  the coefficients of kinematic viscosity.

The system of equations, in some cases, be up to three small parameters  $\epsilon > 0$ ,  $\lambda = 1/Pe > 0$  and  $\sigma = 1/K_{el}$ .

The smallness of the parameters we use, and we have shown [1, 2] that with high accuracy  $\vec{f} = \epsilon \vec{E} \operatorname{div} \vec{E} = \frac{\sqrt{-2\tilde{S}}}{\|\vec{I}\|} \vec{I} \operatorname{div} \left( \frac{\sqrt{-2\tilde{S}}}{\|\vec{I}\|} \vec{I} \right)$ , where  $\tilde{S}(x, y) = C_1 + C_2 - \frac{\epsilon}{2} \|\vec{E}\|^2$  - the generalized concentration, which is near the cation-exchange membrane can be approximated by a linear function  $\tilde{S}(x, y) = -i_{av}x - \alpha_0 y + \gamma$ , where  $i_{av}$  - the dimensionless current density in the channel,  $\alpha_0 > 0$  a small number. Then from the above formula it follows that  $\vec{f} = (i_{av}, \alpha_0)^T$ . A small section take of the channel desalting and assume transcendental mode occurs in a small area near the exit channel desalination.

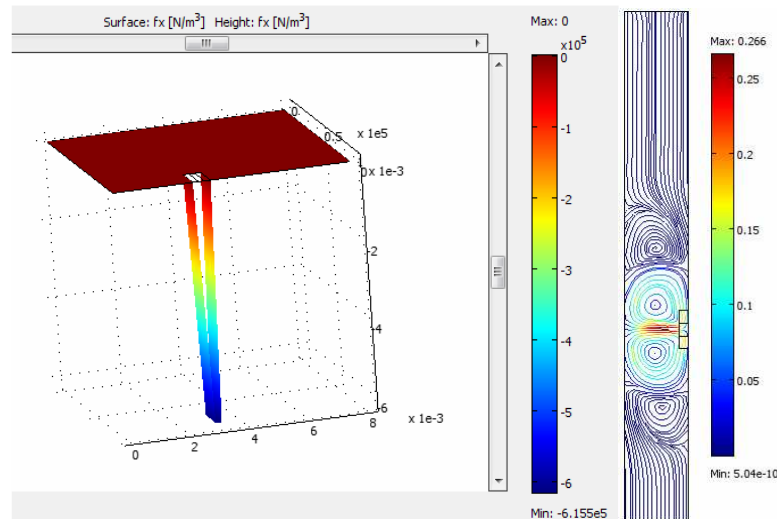


Figure 1. Piecewise-linear model "point" force and streamline the solution

The force of the electric field simulated with the use  $\delta$  - the function, namely, we assume  $\vec{f} = (i_{av}, \alpha_0)^T \delta(x - x_0, y - y_0)$ . The numerical calculations, the piecewise linear approximation of the "point" forces  $\delta$  - function (Figure 1) and fluid flow lines are calculated using equations (5) (6).

### Basic laws of electroconvection

It is known that fluid flow in a channel with no obstructions (in the smooth channel) at low Reynolds numbers and in the absence of external forces will be laminar Poiseuille parabola, and wonder. However, if the input has a different distribution of velocities, even at a distance equal to approximately three times the width of the channel is established from the beginning of a parabolic distribution. If an external force  $\vec{F}$  such that  $\operatorname{rot} \vec{F} = 0$ , by passing from the equations (5.6) in variables "velocity-pressure" to an equivalent system in the variables "stream function-vorticity" can be shown that such a force has no effect on the stream function and vorticity and, consequently, the rate of fluid flow, ie the movement of fluids in general. This force is compensated by the change in pressure. It can be shown that the strength of the electric field acting on the space charge in the space charge is constant with great accuracy. However, this force changes at the boundary of the space charge region from almost zero to a constant value of

the above. If this change in the first approximation, we assume a linear, then the rotor of such a force would be constant, both positive and necessarily negative. Thus, the rotor of the electric field force acting on the charge density, we can approximate the constant function with, for example, two non-zero value, and always one of them is positive and the other negative. Incidentally, this explains the observed in all the calculations and experiments, the phenomenon of the emergence of pair of vortices.

Figure 1 shows the distribution of electric field and the resulting vortex motion  $V_0 = 1 \text{ cm/c}$ ,  $i_{av} = 0.05 \text{ A/m}^2$ . It is evident that the primary vortex pair with a maximum speed of approximately equal  $26 \text{ cm/c}$ , causes a secondary pair of vortices. This is due to the fact that the velocity of vortex motion of the solution is much higher than the initial flow rate of the solution. The results are in qualitative agreement with theoretical results [3] and experimental data [4].

### References

1. *Uzdenova A., Urtenov M., Kovalenko A.* Mathematical model of electroconvection in the electro-systems. Monograph. - Karachaevsk: KCHGU, 2011. - 156.
2. *Uzdenova A.*, Mathematical modeling of electroconvection in membrane systems. thesis. Candidate. Sci. Mr. by special order. 05.13.18: Krasnodar - Kuban State University. - 144 p.
3. *Rubinstein I., Zaltzman B., Lerman I.* Electroconvective instability in concentration polarization and nonequilibrium electro-osmotic slip // Physical review E. 2005. V. 72, 011 505. P. 1-19.
4. *Rubinstein S., Manukyan G., Staicu A., Rubinstein I., Zaltzman B., Lammertink R. G. H., Mugele F., Wessling M.* Direct observation of a nonequilibrium electro-osmotic instability // Physical review letters. 2008. 101, 236 101. P. 1-4.
5. *Rubinstein I., Zaltzman B., I. precedent, and K. Linder.* Experimental verification of the electroosmotic mechanism of formation of "transcendental" in the current system with a cation exchange membrane electrodialysis. Electrochemistry.2002. Vol. 38. № 8. P. 956-967

# ESTIMATION OF INFLUENCE OF WATER TRANSFER THROUGH A MEMBRANE ON THE TRANSFER OF BINARY ELECTROLYTE IN ELECTRODIALYSIS

<sup>1</sup>Anna Kovalenko, <sup>2</sup>Andriy Yaroshchuk, <sup>1</sup>Victor Nikonenko, <sup>1</sup>Mahamet Urtenov

<sup>1</sup>Membrane Institute, Kuban State University, Krasnodar, Russia, *E-mail*: v\_nikonenko@mail.ru

<sup>2</sup>ICREA and Polytechnic University of Catalonia, Barcelona, Spain, *E-mail*: andriy.yaroshchuk@upc.edu

## Introduction

It is known that osmotic and electroosmotic water transport through ion exchange membranes affects the process of desalting and concentrating in electrodialysis. Mutual influence of ion and water transport also takes place in other electromembrane devices including microfluidic ones. In this paper we propose a two-dimensional transient mathematical model of binary electrolyte ion transfer through ion exchange membranes under conditions where simultaneous transport of water occurs; a similar 1D model is proposed earlier [1]. It is assumed that the cation-exchange membrane is porous, and together with the ions water molecules (convective transport) are transported through it, while the anion-exchange membrane is impermeable to convection. The rate of water transport through the cation exchange membrane is considered as a given parameter. The model allows to evaluate the impact of the transfer of water through the membrane on the transport of salt ions.

## Mathematical model

The motion of a single electrolyte solution is considered through a desalting compartment of an electrodialyzer. Let  $H$  and  $L$  be the height (=intermembrane distance) and the length of the desalting chamber, respectively;  $V_0$  is the initial (linear) velocity of solution flow between the membranes;  $x=0$  corresponds to the conditional cation exchange membrane/solution boundary,  $x=H$  relates to the anion exchange membrane/solution boundary,  $y=0$  corresponds to the compartment input, and  $y=L$ , to the output.

### 1. Equations

To simulate the ion and water transport, we use a coupled system of equations of convective diffusion and the Navier-Stokes equations, with the condition of electroneutrality  $z_1C_1 = -z_2C_2 = C$ :

$$\left\{ \begin{array}{l} \frac{\partial \vec{V}}{\partial t} + (\vec{V}\nabla)\vec{V} = -\frac{1}{\rho_0} \nabla P + \nu \Delta \vec{V} \end{array} \right. \quad (1)$$

$$\left\{ \begin{array}{l} \text{div}(\vec{V}) = 0 \end{array} \right. \quad (2)$$

$$\left\{ \begin{array}{l} \frac{\partial C}{\partial t} = D\Delta C - \text{div}(C\vec{V}), \quad D = \frac{D_1D_2(z_1 - z_2)}{z_1D_1 - z_2D_2} \end{array} \right. \quad (3)$$

$$(x, y) \in (0, H) \times (0, L), \quad t > 0,$$

where  $\nabla$  is the gradient,  $\Delta$  is the Laplace operator,  $\vec{V}$  is the electrolyte solution velocity,  $\rho_0$  is the characteristic density of the solution,  $P$  is the pressure,  $C$  is the electrolyte concentration,  $z_1, z_2$  are the charge numbers of cation and anion, respectively,  $D_1, D_2$  are the diffusion coefficients of cations and anions, respectively,  $t$  is the time,  $\nu$  is the viscosity coefficient. Here  $P, \vec{V}, C$  are unknown functions on  $t, x$  and  $y$ .

### 2. Boundary and initial conditions

Appropriate boundary conditions must be added to Eqs. (1)-(3).

1) We will consider a short fragment of desalting compartment where the variation of the electrolyte concentration at the membrane surface,  $C_s$ , is negligible:

$$C(H, y, t) = C_s$$

2) For the velocity at the surface of anion-exchange membrane, we will use the slip condition:

$$V_1(t, 0, y) = 0, \quad V_2(t, 0, y) = 0,$$

at the surface of cation exchange membrane  $x = H, y \in [0, L], t \geq 0$ , the condition of seepage is used:

$$V_2(t, H, y) = 0, \quad V_1 = - \left( \frac{\partial C}{\partial x} \right)_{x=H} \frac{t_w D z_1 M_w}{S(T_1 - t_1) s_p} \quad y \in [0, L], t \geq 0, \quad (4)$$

where  $t_w$  is the water transport number,  $M_w$  is the water molar,  $s_p$  is the membrane surface fraction available for water transfer ( $s_p = 0.5$ ),  $S$  is the membrane unit area ( $S = 1 \text{ cm}^2$ ),  $T_1$  and  $t_1$  are the counterion transport numbers in the membrane and in solution, respectively ( $T_1 = 1, t_1 = 0.5$ ).

3) At the entrance into the region under consideration ( $y = 0, x \in [0, H], t \geq 0$ ), we will assume a concentration distribution close to a steady state corresponding to the case where the boundary concentration is equal to  $C_s$ . We use the parabolic approximation:

$$C(t, x, 0) = C_s + 6(C_0 - C_s) \frac{x}{H} \left( 1 - \frac{x}{H} \right), \quad \text{where } C_0 = \frac{1}{H} \int_0^H C(t, x, 0) dx.$$

We will assume also that at  $y=0$  the fluid velocity is distributed according the Poiseuille's parabola:  $V_1 = 0, V_2 = 6V_0 \frac{x}{H} \left( 1 - \frac{x}{H} \right)$ , where  $V_0$  is the average velocity.

4) At the exit of the region ( $y = L, x \in [0, H], t \geq 0$ ), we will use "soft" conditions on the concentration and set the pressure drop between the entrance and the exit:

$$\frac{\partial C(t, x, L)}{\partial y} = 0, \quad P(t, x, 0) - P(t, x, L) = P_0 - P_1 = \frac{3\mu L}{(H/2)^2} V_0 \quad (5)$$

5) Initial conditions,  $t = 0$ , should match the boundary. When the initial conditions are as follows:

$$t = 0: V_1 = 0, \quad V_2 = 6V_0 \frac{x}{H} \left( 1 - \frac{x}{H} \right), \quad C(0, x, y) = C_s + 6(C_0 - C_s) \frac{x}{H} \left( 1 - \frac{x}{H} \right),$$

a steady state is established very rapidly.

To solve the problem, we have used the finite element method.

### Acknowledgments

Part of the work was carried out in accordance with the cooperation programme of International Associated French-Russian Laboratory "Ion-Exchange Membranes and Related Processes". The authors are grateful to the CNRS, RFBR (Grant Nos. 11-08-93107, 11-08-96511, 11-08-00599) and FP7 Marie Curie Actions "CoTraPhen" Project PIRSES-GA-2010-269135.

### References

1. *Nikonenko, V.V., Lebedev, K.A., Suleimanov, S.S.*, Influence of the convective term in the Nernst-Planck equation on properties of ion transport through a layer of solution or membrane // *Rus. J. Electrochem.* 2009. V. 45, No 2. P. 160-169.

# CHEMICAL AND ION-EXCHANGE REACTIONS IN METAL – ION EXCHANGER NANOCOMPOSITES

Tamara Kravchenko

Voronezh State University, Voronezh, Russia, E-mail: [krav280937@yandex.ru](mailto:krav280937@yandex.ru)

## Introduction

A metal nanoparticles can be introduced into ion-exchange matrixes by ion exchange and chemical deposition in required quantity for an end process [1]. A chemical reactions between the nanoparticles and the reagents or a catalytic reactions between the reagents on the nanoparticles can be the end processes. It is a fundamental importance that the fixed ions are the internal sources and sinks for ionic reagents. Consequently the macrokinetics of the processes take into account the bifunctionality of the metal - ion exchanger nanocomposites (NC). Our purpose is to develop a mathematical model of the oxygen redox sorption from water by NC so that sorption process included the chemical redox reaction and ion exchange.

## Experiments

The investigation objects are the copper- and silver-containing NC on the basis of cation and anion exchangers. It was determinated that the metal particles (sizes 5-100 nm) are combined in larger aggregates. The microphotography of NC is presented on figure 1.

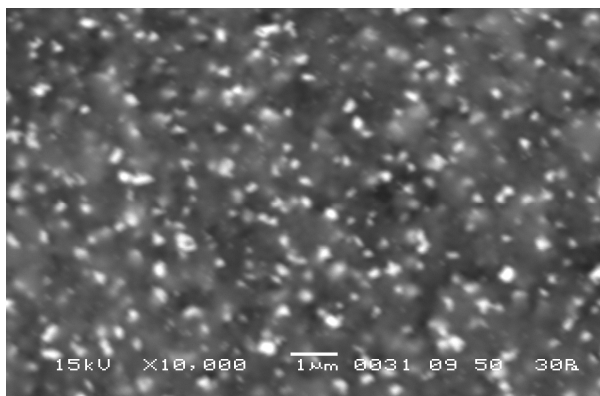


Figure 1. Microphotography of the nanocomposite  $Ag^0 \cdot KU-23$

The oxygen redox sorption is investigated by NC on basis of the different ion-exchanger matrixes. The obtained data allow to classify silver–ion exchanger NC by chemical or catalytic activity (table 1). Some of them could be used as oxygen redox sorbents, other–as catalysts.

**Table 1: Oxygen redox sorption rate versus nature of  $Ag^0 \cdot NC$**

Rise of chemical activity ←		Rise of catalytic activity →	
Strong acid cation exchangers in $H^+$ -form (KU-23)	Strong and week acid cation exchangers in $Na^+$ -form (KU-23, Granion D113)	- Week acid cation exchangers in $H^+$ -form (Granion D113); - week alkaline anion exchangers in free aminoform (Fuji CS-07, Duolite A365)	- Strong acid cation exchangers in $Ag^+$ -form (KU-23); - week alkaline anion exchangers in complex forms (Fuji CS-07, Duolite A365 in $NO_3^-$ -form); - strong alkaline anion exchangers (AV-17-8, AV-17-10P in $Cl^-$ , $F^-$ , $NO_3^-$ , $OH^-$ -forms)
<b>Redox sorbents of oxygen</b>		<b>Catalysts</b>	

Kinetic curves of the oxygen redox sorption rate is shown in figure 2.

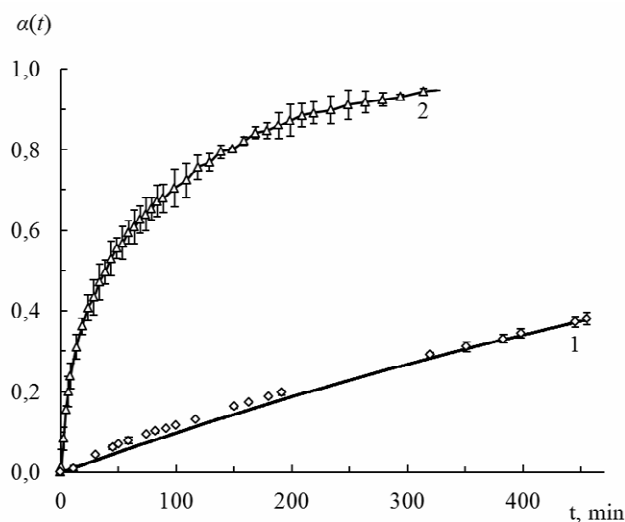


Figure 2. Kinetic curves of redox sorption  $\alpha(t)$  of molecular oxygen from water by  $\text{Ag}^0 \cdot \text{KU-23}(\text{H}^+)$  (1) and  $\text{Cu}^0 \cdot \text{KU-23}(\text{H}^+)$  (2). Points are an experimental values, Curves are a model calculations

### Results and Discussion

Redox sorption consists of the reagents diffusion and redox reaction between reagents and metal particles. Reaction between the NC on basis of sulphonic cation exchanger matrix  $[\text{RSO}_3\text{H}^+]_z \cdot \text{Me}^0$  and oxygen dissolved in water can be presented as:



Here  $z$  is the metal ion charge.

At initial time, the surface of a nanocomposite grain begins to react according to equation (1). A concentration gradient of  $\text{H}^+$  and  $\text{Me}^{z+}$  counter-ions between inside and outside grain regions appears which results in their interdiffusion (Fig. 3). The rate of interdiffusion determines medium pH in reaction zone and can therefore substantially influence the rate and mechanism of the process as a whole. Hydrogen counter-ions are one of reaction (1) participants, and their concentration explicitly enters into the formal kinetic equation for the rate of redox sorption.

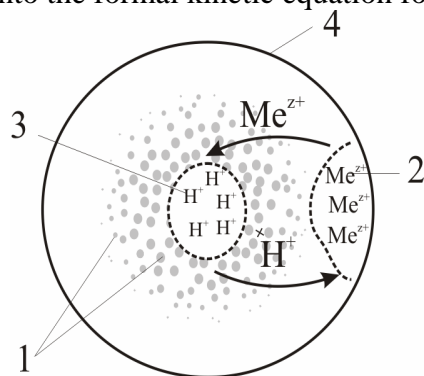


Figure3. Scheme of hydroxygen and metal counter-ions distribution in process of oxygen redox sorption: 1 – metal particles, 2 – metal counter-ions, 3 – hydrogen counter-ions, 4 – NC granule

In this work a mathematical formulation of the problem including the stage of the interdiffusion of metal ions (metal oxidation products) and hydrogen ions (matrix counter-ions) is given [2]. The numerical solution to this problem for the metal-containing NC and molecular oxygen in water systems is analyzed. Proposal model describes satisfactorily the experimental curves of oxygen redox sorption by copper- and silver-containing NC (Fig. 2).

The ions interdiffusion contribution in a total redox sorption rate versus metal component nature, concentration and particle size is estimated. The ions interdiffusion contribution is assessed by relative increasing of time  $\Delta\tau$  of the process completed for 85%. The most essential impact of the interdiffusion stage is determined for high capacity metal NC (Fig. 4).

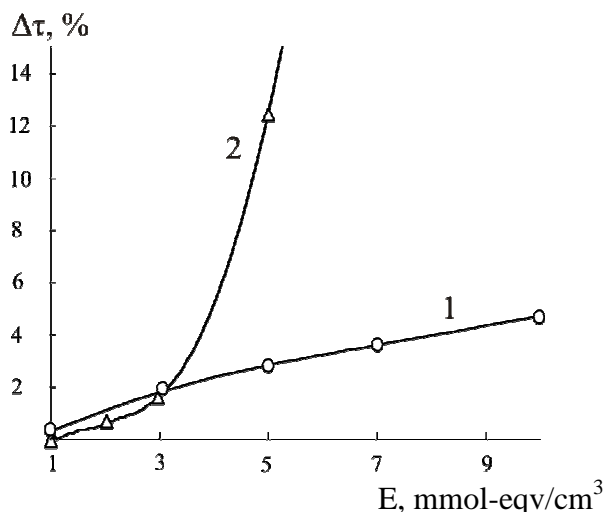
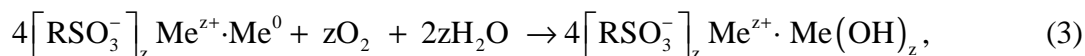


Figure 4. Dependence of  $\Delta\tau$  on the metal capacity  $E$ : 1 –  $\text{Ag}^0\cdot\text{KV-23}$ , 2 –  $\text{Cu}^0\cdot\text{KV-23}$

In addition, under the conditions of a sharp gradient of ionic participants, complete mechanism changing is possible with the formation of solid-state products according to the reactions



that causes oxidation deceleration.

Significant role of the reaction (2) is to increase the internal medium pH. The reaction (3) or (4) replaces the reaction (2). In result, the redox reaction mechanism and the total redox sorption rate are changed.

*This work is supported by the RFBR (Rus. Fund of Basic Research, grant № 11-08-00174\_a)*

### References

1. Kravchenko T.A., Polyanskii L.N., Kalinichev A.I., Konev D.V. Metal - Ion Exchanger Nanocomposites, Moskow, Science, 2009.
2. Kipriyanova E.S., Konev D.V., Kravchenko T.A., and Khorofskaya. Ion exchange and redox reactions in metal - ion exchanger nanocomposites // Russian J. Physical Chemistry. 2012. V. 86. № 7. P. 1128-1133.

# ATOMIC FORCE MICROSCOPY FOR THE STUDY OF ION-EXCHANGE MEMBRANE FBM SURFACE MORPHOLOGY

Elena Krisilova, Tatyana Eliseeva

Voronezh State University, Voronezh, Russia, E-mail: elena.vsu@mail.ru

## Introduction

Study of a relationship between the morphological characteristics of materials and their physicochemical properties plays a very important role. The performance of ion-exchange membranes in various processes depends on the state and structure of their surface. Atomic force microscopy (AFM) is a suitable method to characterize a membrane surface [1]. In particular, at present, transport and equilibrium properties of ion-exchange membranes are considered with due account for their structure heterogeneity [2].

Bipolar ion-exchange membranes are widely used in the technology of electrodialysis (EDBM). Thus, the present study focuses on the surface properties of bipolar ion-exchange membranes.

## Experiments

The object of this study is homogeneous bipolar membrane Fumasep<sup>®</sup> FBM (produced by 'Fuma-Tech', Germany). The membrane samples were prepared according to the technique described in [3].

The AFM images were obtained using a Solver P47 Pro scanning probe microscope (NT\_MDT, Russia, Zelenograd) in a tapping mode in air at a temperature of  $25 \pm 1^\circ\text{C}$ . The sensitivity of the probe and the accuracy of the scanner made it possible to obtain surface images with a lateral resolution of up to 20 nm and a vertical resolution up to 0.5 nm. The surface of ion-exchange membranes was studied in two modes, i.e., topography and phase contrast. We recorded the surface relief in topography mode. The phase contrast mode was used to identify regions that differ in chemical composition, adhesive behavior, and elastic properties [4]. The data were processed using the FemtoScan Online software [5].

## Results and Discussion

The three-dimensional images of the surface of Fumasep<sup>®</sup> FBM membranes (HCl-form), which were obtained using atomic force microscopy in the topography mode, are depicted in Fig. 1 (scanning area is  $2 \times 2 \mu\text{m}$ ).

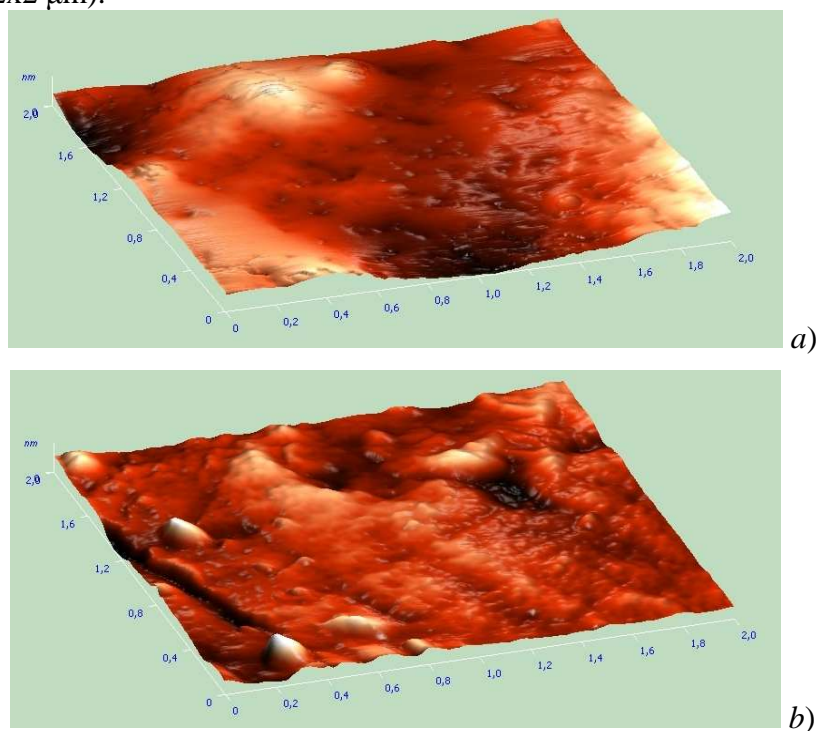


Figure 1. Three-dimensional topographic images of Fumasep<sup>®</sup> FBM membrane surface: a – anion-exchange layer, b – cation-exchange layer

The topographic images of the membranes show that their surface is relatively flat, comparing to the heterogeneous MK-40 membrane topographic images, obtained in our previous work [2]. Cation-exchange layer seems to be more rough than anion-exchange layer. The both layers of bipolar membrane (cation- and anion-exchange) have the same values of maximum level difference about 50-60 nm. For heterogeneous membrane the values of maximum level difference and roughness are much higher than for homogeneous bipolar membrane layers under study, and reach about thousand nanometers, indicating on a significant difference in the structural arrangement of the membranes.

The AFM images were obtained at the Center for the Collective Use of Scientific Equipment at Voronezh State University.

*The authors would like to thank Dr. Bernd Bauer for kindly providing the membrane sample.*

### References

1. *Khulbe K.C., Feng C.Y., T. Matsuura* Synthetic Polymeric Membranes: Characterization by Atomic Force Microscopy, Springer - Verlag, Berlin - Heidelberg, 2008.
2. *Krisilova E.V., Eliseeva T.V., Oros G.Yu.* Assessment of Effect of Sorption of Amino Acids on Surface State of Ion Exchange Membranes Using Atomic Force Microscopy Data // Protection of Metals and Physical Chemistry of Surfaces. 2011. V. 47, P. 39.
3. *Berezina N.P. et al.* The Physicochemical Properties of Ion-Exchange Materials: Practical Course), Krasnodar: Kuban. Gos. Univ., 1999.
4. *Rykov S.A.* Scanning Probe Microscopy of Semiconductor Materials and Nanostructures, St. Petersburg: Nauka, 2001.
5. FemtoScan Online Scanning Probe Microscopy Software, Moscow: Advanced Technologies Center; [www. Nanoscopy.net](http://www.Nanoscopy.net).

---

# HYBRID MATERIALS BASED ON MF-4SC MEMBRANE AND CERIA SYNTHESIZED BY THE CASTING METHOD

<sup>1,2</sup>Ekaterina Kuznetsova, <sup>2</sup>Ekaterina Safronova, <sup>2</sup>Andrei Yaroslavtsev

<sup>1</sup>Mendeleyev University of Chemical Technology of Russia, Moscow, Russia, E-mail: svkati@mail.ru

<sup>2</sup>Kurnakov Institute of General and Inorganic Chemistry RAS, Moscow, Russia

## Introduction

Today Nafion type membranes are of great interest and are demanded for industrial purposes as well as for research ones. MF-4SC is a Russian analogue of the American Nafion membrane. To maintain the profitability of such membranes in the future, they must be modified to address the following shortcomings: poor mechanical properties of the polymer, small operating temperatures range, and low conductivity at low humidity. Implementing various types of nanoparticles in the membrane matrix can improve their properties.

In this paper we report transport properties of hybrid membrane materials based on MF-4SC and ceria obtained by casting method.

## Experiments

The samples were synthesized by the casting method as follows. An appropriate amount of MF-4SC polymer solution in dimethyl formamide (10 wt/%) was mixed with the calculated quantity of cerium (III) nitrate ( $\text{Ce}(\text{NO}_3)_3$ ), that is a precursor for the following ceria synthesis. Then solution was cast in a Petri dish and heated to remove the solvent at 130°C for 15 h. The recast membranes were detached from the Petri dish by addition of bidistilled water. Then excess of water was removed by filter paper and membranes were hot-pressed at 130°C and 60 bar for 3 min to improve mechanical strength. Then all samples with the exception of initial MF-4SC membrane were immersed into 10 wt.% ammonia solution and stirred during 30 min at room temperature to obtain ceria nanoparticles from precursors. All membranes were treated one after another by 5% solution of  $\text{HNO}_3$  and twice by bidistilled water at 80°C. As a result samples with 0, 1.3, 2.5, 4.2 and 5.5 wt.% of  $\text{CeO}_2$  were obtained. All obtained samples were visually homogeneous, mechanically stable. Water uptake of membranes was determined by thermogravimetric analysis with the use of Netzsch-TG 209 F1 in the temperature range 20-150°C in aluminum crucibles. The heating rate was 10 °C/min.

The sorption exchange capacity (SEC) of membranes was determined as follows. Weighed air-dry membrane was immersed into 0.5 M NaCl solution ( $V_{\text{NaCl}}$ , l) and obtained heterogeneous solution was stirred for 24 hours. Then solution was decanted and titrated by 0.1 M NaOH solution. Titration was carried out by pH-meter Expert-001 (produces by 'Econics-expert'). SEC was calculated using Eq. (1):

$$SEC = \frac{c_{H^+} \cdot V_{NaCl}}{m} \cdot 10^{-3}, \quad (1)$$

where  $c_{H^+}$  - concentration of protons in NaCl solution after membrane (mol/l), m - membrane mass (g).

The proton conductivity was measured as a function on temperature in the range from 25°C to 100°C at 100% humidity and as a function on relative humidity (RH) at 25°C with the use of '2B- $\Gamma$ ' impedance analyzer (frequency was ranged from 10 Hz to 1 MHz) in carbon/membrane/carbon symmetrical cells, with the active surface area varied from 0.2 to 0.5 cm<sup>2</sup>. Conductivity values were obtained by semicircle extrapolation to the resistance axis.

The diffusion permeability was analyzed in the two-chamber cell. The electrolyte (NaCl or HCl solution) was transferred through the membrane into a bidistilled water filled compartment. The electrolyte transfer rate was controlled by the conductivity measurement or pH technique using a conduct meter Expert-002 (Ekoniks-expert) or Mettler Delta 340 pH-millivoltmeter, respectively.

## Results and Discussion

SEC of the membranes has been studied. For the initial membrane it is equal to 0.98 mg-eq/g. Membrane modification with ceria leads to the SEC increase up to 1.03 mg-eq/g for the

MF-4SC + 5.5 wt.% CeO<sub>2</sub> membrane. According to TGA data incorporation of ceria nanoparticles into membrane matrix results in the water uptake growth (Table 1). It increases from 12.4 % to 19.2% with the ceria content increase.

**Table 1: Water uptake of investigated membranes**

The sample	MF-4SC	MF-4SC + 1.3% CeO <sub>2</sub>	MF-4SC + 4.3%CeO <sub>2</sub>	MF-4SC+5.5% CeO <sub>2</sub>
W (H <sub>2</sub> O), %	12.4%	18%	18.2%	19.2%

MF-4SC membrane modification with ceria leads to a significant conductivity increase (Fig. 1). It should be noted that dependence of conductivity as a function on ceria content passes through a maximum at 4.2 wt.% of CeO<sub>2</sub>. The following increase of ceria content leads to the decrease of proton conductivity.

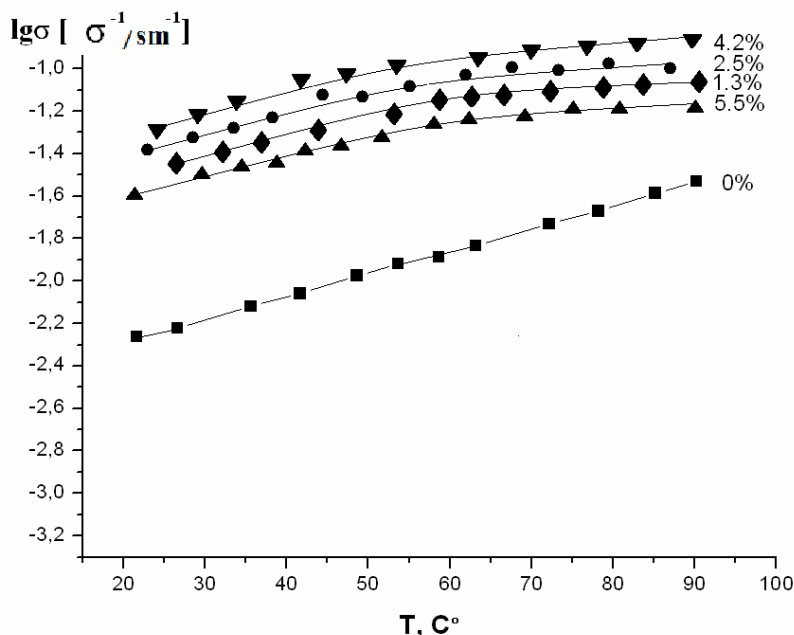


*Figure 1. Temperature dependences of conductivity for MF-4SC+X wt.% CeO<sub>2</sub> membranes*

Proton conductivity as a function on relative humidity was investigated also (Fig. 2). The decrease of RH results in the considerable conductivity reduction for all samples due to the water uptake decrease that is followed by membrane channels lengthening and narrowing. MF-4SC membranes doped with ceria show appreciably high conductivity than the initial MF-4SC membrane under the same conditions.

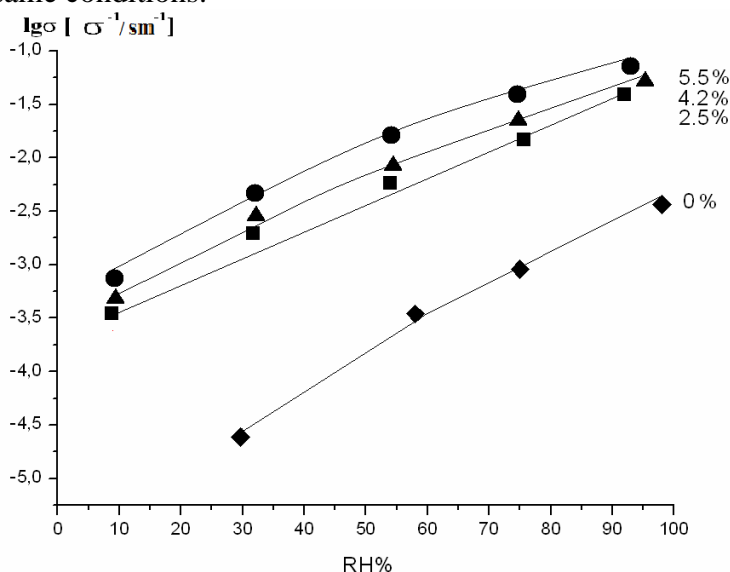


*Figure 2. Dependences of conductivity as a function on the relative humidity for MF-4SC+X wt.% CeO<sub>2</sub> membranes*

Diffusion permeability coefficients of 0.1M HCl and NaCl solutions and interdiffusion  $H^+/Na^+$  coefficients of investigated membranes were determined (Table 2). Diffusion permeability coefficients decrease with the ceria content increase. Since MF-4SC is cation-exchange membrane diffusion permeability is determined by the anion diffusion rate. Thus, the incorporation of ceria into MF-4SC membrane leads to the cation selectivity improvement.

**Table 2: The diffusion permeability coefficients and  $H^+/Na^+$  interdiffusion coefficients ( $cm^2/s$ ) of investigated membranes**

D, ( $cm^2/s$ )	MF-4SC	MF-4SC+ 1.3%CeO <sub>2</sub>	MF-4SC + 2.5%CeO <sub>2</sub>	MF-4SC + 4.2%CeO <sub>2</sub>	MF-4SC + 5.5%CeO <sub>2</sub>
0.1M HCl	$1.37 \cdot 10^{-6}$	$1.21 \cdot 10^{-6}$	$1.16 \cdot 10^{-6}$	$1.15 \cdot 10^{-6}$	$1.01 \cdot 10^{-6}$
0.1M NaCl	$2.63 \cdot 10^{-7}$	$2.56 \cdot 10^{-7}$	$2.53 \cdot 10^{-7}$	$2.32 \cdot 10^{-7}$	$1.96 \cdot 10^{-7}$
0.1M HCl/ 0.1M NaCl	$3.12 \cdot 10^{-5}$	$2.88 \cdot 10^{-5}$	$2.87 \cdot 10^{-5}$	$2.66 \cdot 10^{-5}$	$1.97 \cdot 10^{-5}$

Obtained data are agreed with the model of the semielasticity of membrane pores and channels [1]. MF-4SC membranes modification with ceria oxide results in the increase of water uptake, increase ion conductivity, increases cation transport selectivity.

*This work was financially supported by the federal target program “Educational and scientific-educational staff on innovative Russia” for 2009-2013 years (project GK 02.740.11.0847).*

#### References

1. Novikova S.A., Safronova E.Yu., Lysova A.A., Yaroslavtsev A.B. Influence of incorporated nanoparticles on MF-4SC membrane ion conductivity // Mend. Comm. 2010. V. 20. P. 156-157.

# ELECTROCHEMICAL SYNTHESIS OF NiO/C COMPOSITION MATERIAL

<sup>1</sup>Darya Leontieva, <sup>2</sup>Alexey Rychagov, <sup>1</sup>Nina Smirnova, <sup>2</sup>Yury Volkovich

<sup>1</sup>South-Russian State Technical University, Novocherkassk, Russia

<sup>2</sup>Frumkin Institute of Physical Chemistry and Electrochemistry RAS, Moscow, Russia

E-mail: da.leontyva@mail.ru

## Introduction

Electrochemical capacitors (ECs) (also known as supercapacitors, pseudocapacitors or ultracapacitors), combining the advantages of the high power of dielectric capacitors and the high energy of rechargeable batteries, have played an increasingly important role in power source applications particularly for digital communications, hybrid electric vehicles and short-term power sources for mobile electronic devices, etc.

Currently, the anode material in asymmetric supercapacitors are such materials as conductive fine carbon black, polymers, and transition metals oxides [1, 2]. Among the various transition metal oxide materials RuO<sub>2</sub> and IrO<sub>2</sub> exhibit prominent properties as pseudocapacitor materials, but the high cost of these noble metal materials and poisoning nature of ruthenium oxide limits it from commercialization. NiO is prominent candidates for supercapacitors because NiO inexpensive and exhibit pseudocapacitance behavior similar to that of ruthenium oxide.

## Experiments and Discussion

There are many different various chemical techniques for the synthesis of nanostructured NiO/C composite. Most of them are based on the deposition of nickel oxide from solutions of nickel salts in the presence of different stabilizers, followed by calcining the material at high temperatures [3]. This synthesis leads to accumulation of impurities in the product, which affects its properties negative, also results in significant energy consumption.

Our method is based on the oxidation and further dispergation of nickel foil under asymmetric alternating current with simultaneous deposition nickel oxides/hydroxides on a carbon support (Vulcan XC-72) [4]. Such technique allows to obtain nanoparticles NiO and prevents trace-element contamination as well.

Scanning electron microscope images which demonstrated the morphology of nickel oxide deposited on Vulcan XC-72 was presented in Fig.1.

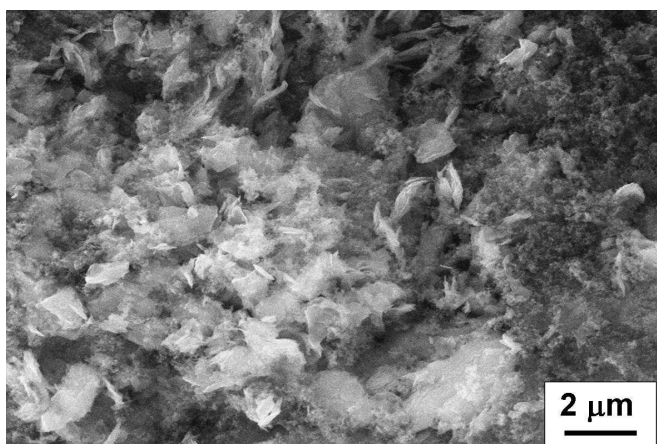


Figure 1. SEM image of NiO/C composite

XRD pattern shows the five broadened characteristic peaks of the face-centered cubic structure of  $\beta$ -NiO. The average grain size of synthesized materials estimated using Scherrer equation was 3 nm. However as indicates SEM image (Fig.1) NiO crystallites agglomerated into thin plates, with an average size of 500-800 nm, so there is an increase active surface area of the material.

Low temperature N<sub>2</sub> adsorption and desorption measurements were performed using a Micromeritics ASAP 2020 Analyzer at 77 K. The specific surface area (SSA) was determined in the relative pressure range  $0.05 \leq p/p_0 \leq 0.20$  according to the Brunauer-Emmett-Teller (BET)

method. The total pore volume was calculated from the nitrogen adsorption isotherm at relative pressure  $p/p_0 \rightarrow 1$ . Analysis of the pore size distribution was performed with nonlocal density functional theory (NLDFT).

Composite material NiO/C has properties of its components: mesoporosity, characteristic of carbon black Vulcan-XC ( $D = 12-35$  nm), macroporosity of pure NiO ( $D = 40-100$  nm). The composite has a relatively high specific surface area ( $152,4 \text{ m}^2 \text{ g}^{-1}$ ) and the hierarchical structure of the porosity, which is extremely important for ion transport in the presence of electrolyte.

Specific capacity is one of the important characteristics of NiO/C composites. CV curves of NiO/C and carbon support Vulcan are present in Fig.2. Capacitance measurements were carried out in galvanostatic condition using (i) standard threeelectrode cell and (ii) two electrode cell with the activated carbon as counter electrode, which has capacity higher than capacity of the investigated electrode (Fig.3). In the first case capacitance, calculated as integral characteristic, are  $650 \text{ F g}^{-1}$ , but in the second case capacitance are  $180 \text{ F g}^{-1}$ .

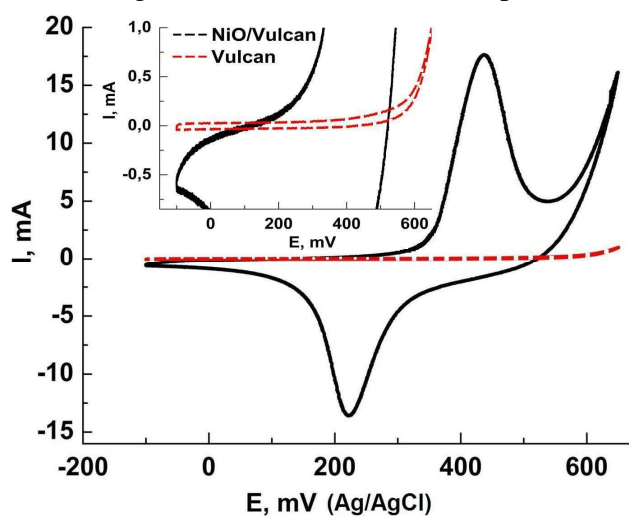


Figure 2. Cyclic voltammogram of the NiO/C (1M NaOH), scan rate 5 mV/s

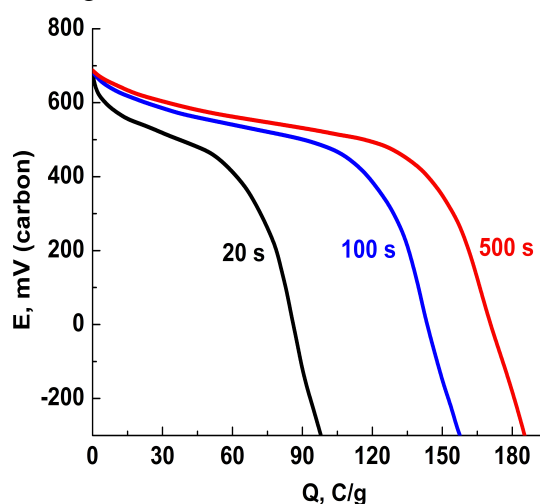


Figure 3. Discharge curves of NiO/C (40%) at different time of the electrode charges

Thus, we have provided a simple electrochemical route toward preparation the NiO/C nanocomposite with high specific capacity. More over it is low cost and high degree of purity method. We suppose that synthesized NiO/C composites could be promising for use in supercapacitors.

### Acknowledgment

This work was supported by the Ministry of Education and Science of Russian Federation (No 14.740.11.0371) and the Foundation for Assistance to Small Innovative Enterprises in Science and Technology (No 8962p/14125/5 on 19.04.2011).

### References

1. Hosogai S., Tsutsumi H. // Journal of Power Sources, 2009, V.194, P.1213-1217.
2. Volkovich Yu.M., Sedyuk T.M. Electrochemical capacitors // Russian journal of Electrochemistry, 2002, V.38, P.1043-1068.
3. Ji Yeong Lee, Kui Liang, Kay Hyeok An, Young Hee Lee Nickel oxide/carbon nanotubes nanocomposite for electrochemical capacitance // Synthetic Metals, 2005, V.150, P.153-157.
4. Smirnova N.V., Leontieva D.V., Kuriganova A.B. // RU. Appl. No. 2010140535/02(058106), filed Oct. 10, 2010.

# EFFECTS OF pH CHANGE IN ELECTROMEMBRANE SYSTEM WITH MF-4SC SURFACE MODIFIED BY POLYANILINE

<sup>1</sup>Natalia Loza, <sup>1</sup>Sergey Dolgoplov, <sup>1</sup>Natalia Kononenko, <sup>1</sup>Ninel Berezina, <sup>2</sup>Sergey Lakeev

<sup>1</sup>Kuban State University, Krasnodar, Russia. E-mail: nata\_loza@mail.ru

<sup>2</sup>Karpov Institute of Physical Chemistry, Moscow, Russia

## Introduction

The various phenomena were found during research of physical and chemical behavior of the anisotropic composites based on MF-4SC membrane and polyaniline (PANI). It is asymmetry of the diffusion permeability and the current-voltage characteristic [1, 2], barrier effect of a PANI layer for electroosmotic flow [3], and also blocking effect for the transport of protons in an electrical field [4]. The aim of this work is to study the pH change effects in sulfocationic MF-4SC membranes, surface modified by PANI.

## Experimental

A Nafion type perfluorinated sulfocationic membrane MF-4SC produced by ‘Plastpolymer’ (St.-Petersburg, Russia) was used as a template matrix for composites preparation. Composite membrane was obtained by the chemical synthesis of polyaniline in surface layer of membrane. 1 M aniline solution in 1 M HCl and 0.1 M  $(\text{NH}_4)_2\text{S}_2\text{O}_8$  solution as initiator of aniline polymerization were used for preparation of composites MF-4SC/PANI.

The current-voltage curves were measured in the 0.05 M NaCl solution with help of a cell with platinum polarizing and silver chloride measuring electrodes. The change of pH solution was recorded in the chambers of the cell in the polarization condition in special experiments. The membrane was kept in the fixed value of membrane potential ( $\Delta E$ ) consisting of 0.05 V (up to limiting regime) and 1 V (limiting regime) in the 0.05 M NaCl solution. The pH of solution was checked every 30 minutes.

## Results

The current-voltage curve of composite membranes measured in 0.05 M NaCl is shown on the Figure 1. If  $\Delta E$  is order 2 V the system transits to the overlimiting state due to the water splitting on the membrane/solution boundary. ‘Pseudo-limiting’ state of the system at low potentials region ( $\Delta E \approx 30$  mV) is observed. It indirectly indicates on the occurrence of fast ions at the inner boundary MF-4SC/PANI (Fig.1b).

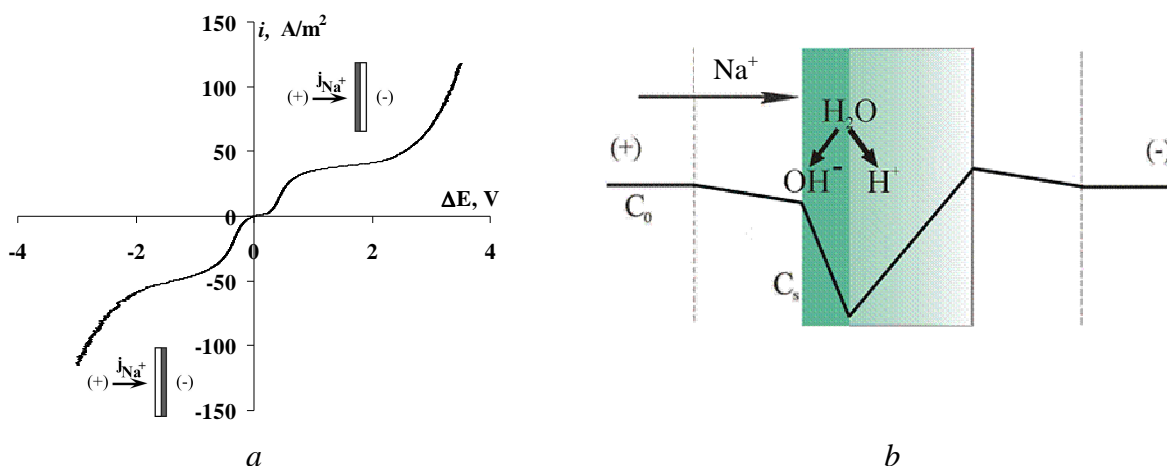


Figure 1. The current-voltage curve of the MF-4SC/PANI composite membrane in the 0,05 M solution (a) and the concentration profile of the composite membrane in the polarization conditions (b)

The analysis of the pH solution in the chambers shows that the water splitting takes place on the membrane/solution boundary only if the unmodified membrane layer looks to the anode. The behavior of electromembrane system in this case is similar to the system with the unmodified membrane. If the modified membrane surface looks to the anode the behavior of electromembrane system is the same as the system with the typical bipolar MB-3 membrane (Fig. 2)

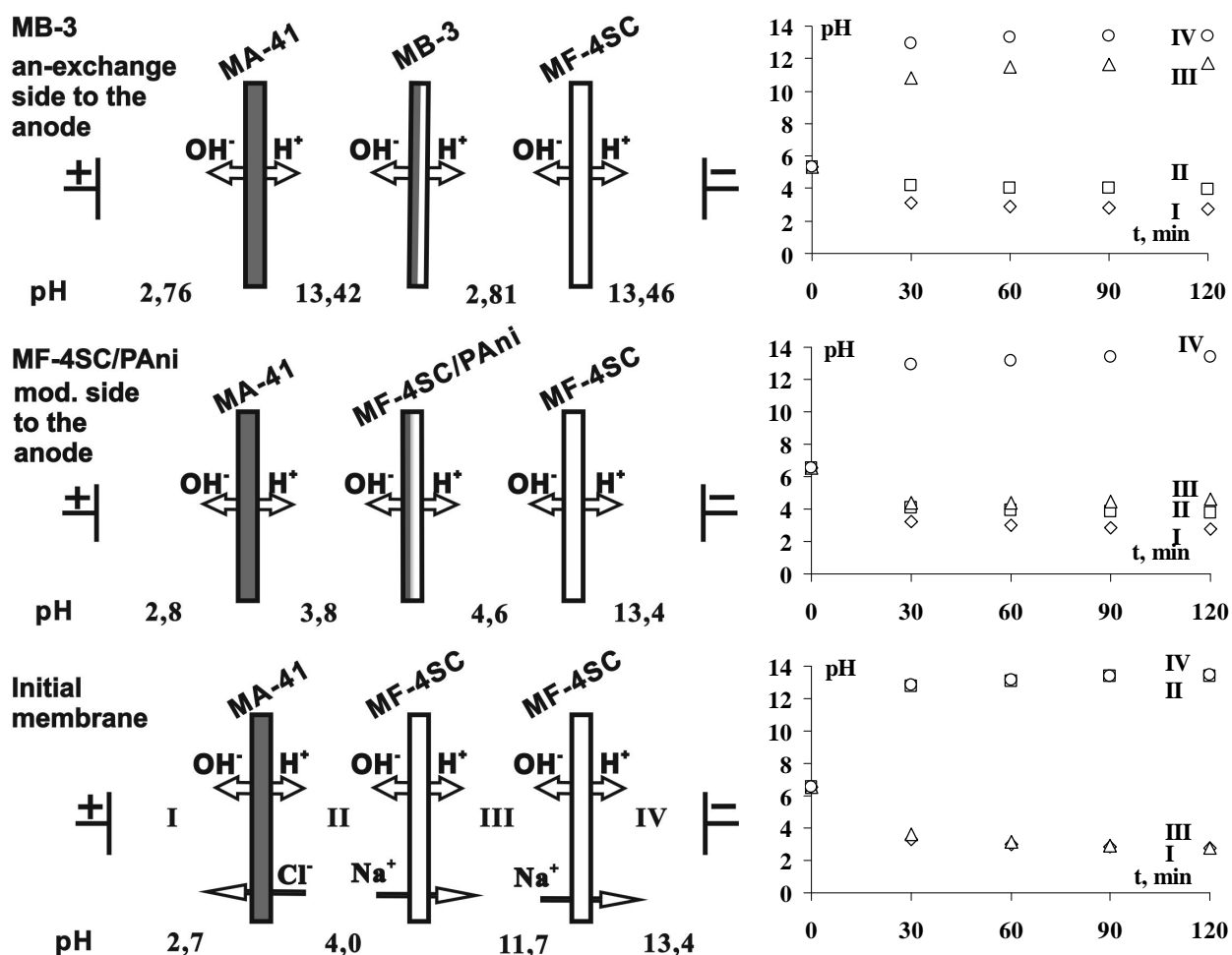


Figure 2. The flow ions scheme and plots pH value of the time in the cells on the 0.05 M NaCl solution ( $\Delta E = 1$  V) for the membranes MB-3, MF-4SC and MF-4SC/PANI

However, the water splitting on the internal contacts between membrane sulfo groups and the positively charged nitrogen atoms of polyaniline is not the only process in the composite membrane. The chemical reactions and transformations of polyaniline occur simultaneously with the appearance of  $H^+$  and  $OH^-$ -ions. So the electrochemical behavior of the composite membrane system is distinguishes from the behavior of a typical bipolar membrane MB-3.

### Conclusions

New information about the electrochemical behavior of the anisotropic composite membrane MF-4SC/PANI in polarization conditions was gained. It was found that the source of hydrogen and hydroxyl ions generation occurs on the internal interface at the certain orientation of modified membranes. It looks like functions of the inner boundaries in bipolar membranes.

The present work is supported by the Russian Foundation for Basic Research (project № 12-08-01092).

### References

1. Berezina N.P., Kononenko N.A., Sytcheva A.A.-R., Loza N.V., Shkirskaya S.A., Hegman N., Pungor A. // *Electrochimica Acta*. 2009. V.54. P. 2342-2352.
2. N.P. Berezina, N.A. Kononenko, Filippov A.N., Shkirskaya S.A., Falina I.V., Sytcheva A.A.-R. // *Elektrokhimiya*. 2010. V. 46. P. 515-524.
3. Berezina N.P., Shkirskaya S.A., Sytcheva A.A.-R., Krishtopa M.V. // *Kolloidnyi J.* 2008. T. 70. P. 437-446.
4. N.A. Kononenko, N.P. Berezina S. Dolgopolov, N. Loza, S. Lakeev // *Elektrokhimiya*. 2012. V. 48. №8. (in press).

# DEVELOPMENT AND RESEARCH OF ELECTRODIALYZER FOR DEMINERALIZATION OF ELECTROLYTE SOLUTIONS BASED ON PROFILED MEMBRANES

Sergey Loza, Victor Zabolotsky

Kuban State University, Krasnodar, Russia

The disadvantage of the known electro dialyzers with profiled membranes is the presence of bipolar contacts between shaped protrusions of the profiled membrane and the smooth side of the other membrane. The presence of such contacts has led to dissociation of water on it and the appearance of spurious current "leakage" [1, 2].

The aim of this work is to increase the current efficiency and to lower energy costs for carrying out the process of electro dialysis. This goal is achieved by the proposed construction of electro dialyzers with electrical contacts between the membranes are broken by applying a thin layer of insulating material on the top of the profiled membranes (Fig. 1, item 7), which eliminates the bipolar contacts in desalination cell and reduces thus the intensity of the dissociation of water in the membrane system [3].

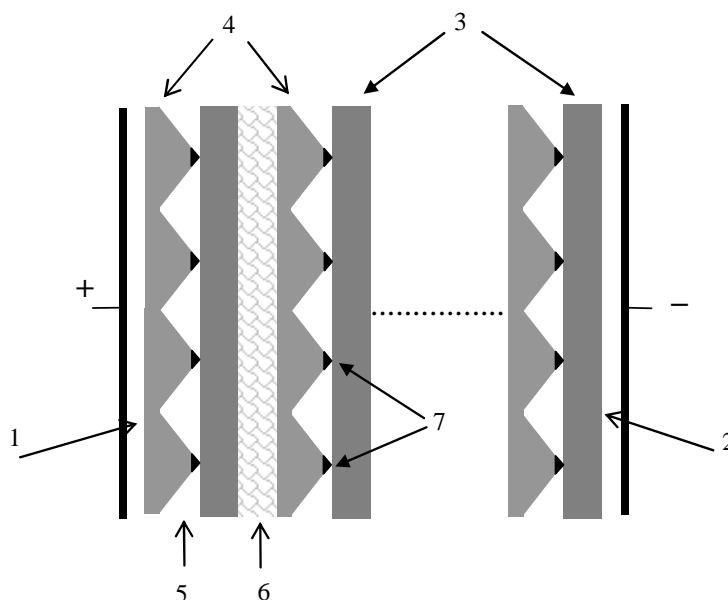


Figure 1. A Schematic representation of electro dialysis apparatus: 1 – Anode-chamber, 2 – Cathode chamber, 3 – Smooth membrane, 4 – Profiled (shaped) membrane, 5 – Desalting cell, 6 – Concentration cell, 7 – Electrical insulation

Studies were investigated on laboratory-size electro dialyzers with a working area of the membranes 45x45 mm, number of paired cells in the work package 10. Desalting chamber (Fig. 1, item 5) is formed by elements of the profile of the membranes and in the concentration chamber (Fig. 1, item 6) membrane separated by the lining of binded net." Tests carried out on electro dialyzers with NaCl solution ( $C = 5 \text{ mmol/l}$ ) circulating in the quasi-stationary regime [4]. The voltage on electro dialyzers was from 1 to 10 Volts by pair of cells.

Laboratory electro dialyzers with membrane pairs MC-40/MA-40P and MC-40/MA-40PI were tested (index "P" means profiled (shaped) membrane, and the shaped membrane with the insulating material deposited on the top of the profile is marked by the subscript "PI"). From the data obtained by measuring the electrical conductivity and pH of the investigated solutions the current efficiency and specific energy consumption for desalination was calculated, which are represented in Table 1.

**Table 1: Some characteristics of the desalination process of NaCl solution from the concentration of 4 mmol/l to 0.4 mmol/l**

	The current efficiency, $\eta$				Energy consumption for desalination (kW•h/m <sup>3</sup> )			
	1V	2V	5V	10V	1V	2V	5V	10V
<b>Prototype MC-40/MA-40P</b>	0.53	0.29	0.16	0.11	0.26	0.78	3.48	10.00
<b>The proposed electro dialyzer MC-40/MA-40PI</b>	0.61	0.49	0.28	0.23	0.23	0.48	1.61	5.02

As can be seen from Table 1 electro dialyzer with proposed design provides an increase of the current efficiency and lower specific energy consumption for all values of voltage. Moreover, with increasing voltage, this difference increases. For example, when a voltage is 10V per a pair of cells specific energy consumption for desalination reduces two times after the insulation of bipolar contacts.

Thus, in electro dialyzers of proposed design we can avoid the leakage of current through the bipolar membrane contacts. The density of current flowing through electro dialyzers decreases, and the output current increases. Total energy consumption for desalination can be reduced by 1.5 - 2 times.

### References

1. Electro dialysis / *Grebenyuk V.D.*—Kiev: Engineering, 1976—160p.
2. *Belobaba A.G., Pevnitskaya M.V., Kozina A.A., Nefedova G.Z., Freidlin Yu.G* Electro dialysis of dilute solutions in the apparatus with profiled ion-exchange membranes // Sib. acad. of sci. USSR. Chem. Sciences. 1980. V.4, issue 12, 9. P.161-165.
3. Loza S.A. Candidate Dissertation, Krasnodar, 2008, 175p.
4. Pat. 2033850 Russian Federation MKI5 01 D 13/02. Electro dialyzers / *Zabolotsky V.I., Nikonenko V.V., Pismenskaya N.D., Pismenskiy V.F., Laktionov E.V.*, "Membrane Technology" (Krasnodar, Russia).- № 93006226, appl. 04.02.93, publ.27.04.95, Bull. Number 12. - P.124.

---

# DETERMINATION OF THE DIFFUSION LAYER THICKNESS OF THE WARBURG IMPEDANCE SPECTRA, TAKING INTO ACCOUNT THE CONCENTRATION DEPENDENCE OF THE DIFFUSION COEFFICIENT

Semyon Mareev, Victor Nikonenko, Natalia Pismenskaya

Kuban State University, Krasnodar, Russia, E-mail: mareev-semyon@bk.ru

## Introduction

The thickness of the diffusion boundary layer (DBL),  $\delta$ , is one of the important parameters of the membrane system, hence the development of the Nernst conception of diffusion layer and the determination of its parameters is important for understanding the transport processes in heterogeneous systems and for engineering calculations. The electrochemical impedance spectroscopy (EIS) is the multipurpose method for studying the properties of the membrane system and evaluating the thickness of DBL.

Usually the EIS is associated with the vector representation of variables in phasor form [1, 2]. This representation, with the assumption of small amplitude oscillations of the AC allows solving differential equations, eliminating the dependence on time. However, this approach is not flexible enough: there are no analytical solutions for any complication of the problem with changing the basic equations and boundary conditions.

## Theory

In this paper we propose a new approach for the mathematical description of the impedance based on the numerical solution of unsteady transport equations. The equations are solved for the case when the current density is defined as the sum of steady-state current and the AC signal of small amplitude. Further the resulting response of potential drop is processed in the same way as during the experimental measurements of impedance. The proposed approach allows the use the non-stationary model of ion-transport of any complexity, including taking into account the dependence of the diffusion coefficients of the local concentration of the solution.

We consider time-dependent model of ion transport through the membrane, which consists of the membrane with two adjacent diffusion boundary layers (DBL) and the two mixed solutions with a constant concentration [2]. Ion transport in the DBL described by the Nernst-Planck and the material balance equations:

$$J_i = -D_i \left( \frac{\partial c_i}{\partial x} + z_i c_i \frac{F}{RT} \frac{\partial \varphi}{\partial x} \right)$$

$$\frac{\partial c_i}{\partial t} = -\frac{\partial J_i}{\partial x}$$

where  $J_i$  is flux,  $D_i$  is diffusion coefficient,  $c_i$  is concentration,  $z_i$  is the charge number of the  $i$ -th ion,  $\varphi$  is electrical potential, the notation  $R$ ,  $T$  and  $F$  have their usual meaning; the index "1" refers to the counterion (in this case - anions) the index "2" - to the co-ion.

In the membrane ion flux densities  $J_{im}$  are constant and equal to:

$$J_{im} = \frac{iT_i}{z_i F}$$

where  $i$  is the current density,  $T_i$  is the effective transport number.

The total potential difference between capillary is calculated by using the equation:

$$U = -j \frac{L_b}{\kappa} + \int_{-\delta}^0 \frac{\partial \varphi}{\partial x} dx + \int_0^d \frac{\partial \varphi}{\partial x} dx + \int_d^{d+\delta} \frac{\partial \varphi}{\partial x} dx$$

When we are using the concentration dependence of the diffusion coefficient given in [3], the shape of the impedance spectrum is the same as in the approximation  $D = \text{const}$ : the spectrum corresponds to the spectrum for the Warburg of finite length segment. However, accounting dependence  $D = D(c)$  brings to the expansion of "arch" of the spectrum with the other

parameters constant. For a narrow of arches of the spectrum and ensuring of appropriate of calculated and experimental spectra is necessary to use a smaller value  $\delta$  compared with the case  $D = \text{const}$  (Fig. 1): in the case of anion exchange membranes AMX and the stationary current density  $i = 1.25 \text{ mA cm}^{-2}$  fitted value of  $\delta = 185 \text{ }\mu\text{m}$  at  $D = \text{const}$ , while  $\delta = 175$  at  $D = D(c)$ . At the same time, the theoretical value calculated from the Leveque's equation increases, when given the relationship  $D = D(c)$ : when  $D = D_0$ ,  $\delta_{Lev} = 230 \text{ }\mu\text{m}$ ; when  $D = D(c)$ ,  $\delta_{Lev} = 240 \text{ }\mu\text{m}$ .

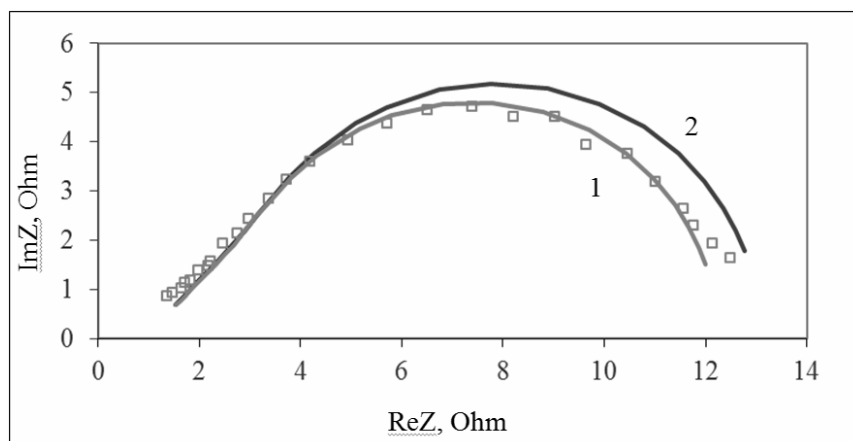


Figure 1. Experimental (points) and calculated (curves) spectra of low-frequency impedance of the membrane AMX in 0.02 M NaCl solution at a density of DC  $i = 1.25 \text{ mA cm}^{-2}$ . Curve 1 is the result of the calculation for two cases:  $D = D_0$ ,  $\delta = 185$  microns and  $D = D(c)$ ,  $\delta = 175$  microns, curve 2 is calculated when  $D = D(c)$  and  $\delta = 185$  microns

### Conclusion

Taking into account the concentration dependence of the diffusion coefficient leads to a better appreciation of the differences between the theoretical value  $\delta$  calculated without accounting current-induced convection, and the value  $\delta$  obtained in terms of concentration polarization caused by the flow of direct electric current. Therefore, a more accurate mathematical description of ion transport in the membrane system leads to the conclusion that the contribution of the current-induced convection to mass transfer should be more important than it was previously thought.

### Acknowledgements

Part of the work was carried out within the framework of joint French-Russian laboratory "Ion-Exchange Membranes and Related Processes". The authors are grateful to the CNRS, RFBR (grants 11-08-93107, 11-08-96511, and 11-08-00599), and FP7 "CoTraPhen" Project PIRSES-GA-2010-269135.

### References

1. Barsoukov E., Macdonald J.R. Impedance Spectroscopy: Theory, Experiment, and Applications, John Wiley & Sons, New York, 2005, 595 pp.
2. Sistat P., Kozmai A., Pismenskaya N., Larchet C., Pourcelly G., Nikonenko V. Low-frequency impedance of an ion-exchange membrane system // Electrochim. Acta. 2008. V. 53. P. 6380-6390.
3. Larchet C., Nouri S., Auclair B., Dammak L., Nikonenko V. Application of chronopotentiometry to determine the thickness of diffusion layer adjacent to an ion-exchange membrane under natural convection // Adv. Colloid Interface Sci. 2008. V. 139. P. 45-61.

---

# INFLUENCE OF CRAZING ON PERVAPORATION PROPERTIES OF PA-6

Natalia Matushkina, Alla Dolgova, Evgeny Ageev

Department of Chemistry, Lomonosov Moscow State University, Moscow, Russia,

E-mail: ageev@phys.chem.msu.ru

## Introduction

The polymer used in this work was polyamide-6 (PA-6) with different degrees of uniaxial stretching in dioxane, which wets the polymer, but swelling (i. e. absorption with the volume change of the sorbent) does not take place. In the process of stretching in such so-called adsorption-active media, there form zones of plastic deformation of the material, such zones consist of highly-ordered fibril-pore structure. Such structures are called crazes, and the process of their forming is called crazing. Crazes form in a direction perpendicular to the direction of stretching, and crazing itself is caused by the destabilizing action of mechanical stress and instability of the polymer structure [1].

It is impossible to predict the change of transport properties of crazed materials *a priori*. The ‘opening’ of the polymer structure and the increase of the free volume upon swelling must result in the increase of efficiency, but apparently can have a negative effect on selectivity. The goal of this work is to ascertain the influence of crazing on pervaporation properties of polymers using PA-6 as an example.

## Experiments

The objects of the study were commercial PA-6 films of the brand PK-4 with the thickness of 100  $\mu\text{m}$ ,  $\text{MM} = 2.3 \times 10^4$  Da, and crystallinity degree of 35 %. The films were subjected to stretching by 50 %, 90 %, 130 %, and 180 % in dioxane, a typical adsorption-active medium for crazing. Pervaporation experiments were conducted at 20 °C in the pervaporation into vacuum mode. The selectivity of separation was characterized by the difference in the compositions of the permeate and the initial solution. Aqueous solutions of isopropanol with various concentrations were used as model mixtures.

## Results and Discussion

Figure 1 shows the concentration dependencies of flux density of crazed PA-6 with different stretching degrees in the pervaporation process. The obtained data show that crazing results in the increase of the membrane permeability. It should be noted that the most pronounced increase of the permeability is observed for stretching degrees  $\lambda = 50$  % and 90 %, while for  $\lambda = 130$  % and  $\lambda = 180$  % the permeability decreases. In the first stages of the polymer stretching in liquid media, a certain number of crazes with fibril-pore structure is generated on the surface. Upon further stretching the crazes grow in a direction perpendicular to the axis of stretching of the polymer until they cross the cross-section of the sample. In this process the main transformation of the polymer into oriented (fibrillized) porous state occurs. But when a considerable part of the polymer turns into oriented fibrillized state, there begins the collapse of the porous structure, accompanied by a decrease of the cross-section of the deformed sample, which leads to the decrease of its porosity, the average pore size, and the specific surface.

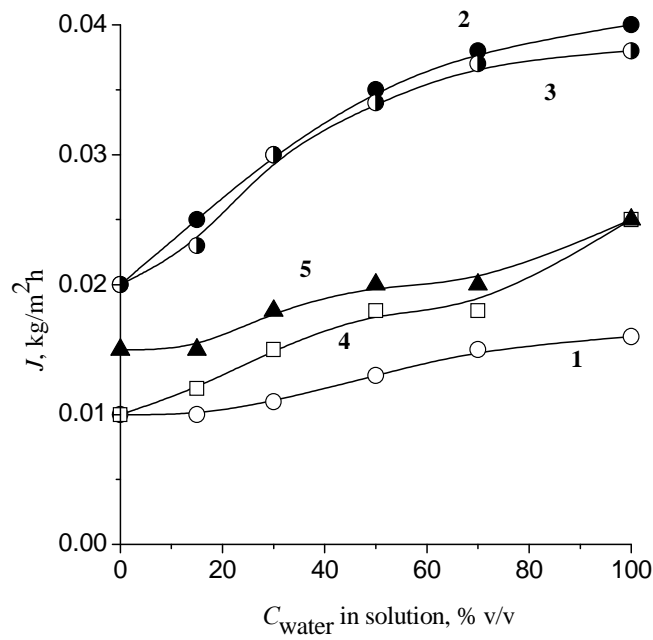


Figure 1. Concentration dependencies of flux density  $J$  in the system: crazed PA-6 – water – isopropanol in the pervaporation process at  $20\text{ }^{\circ}\text{C}$ ,  $S = 2\text{ cm}^2$ . 1 –  $\lambda = 0\%$ ; 2 –  $\lambda = 50\%$ ; 3 –  $\lambda = 90\%$ ; 4 –  $\lambda = 130\%$ ; 5 –  $\lambda = 180\%$

As seen in Figure 2, crazing does not exercise a significant influence on the separation selectivity. This result apparently means that at the used stretching degrees and the film thickness the through porosity does not form, i. e. capillary flow is not added to the diffusion mass transfer mechanism.

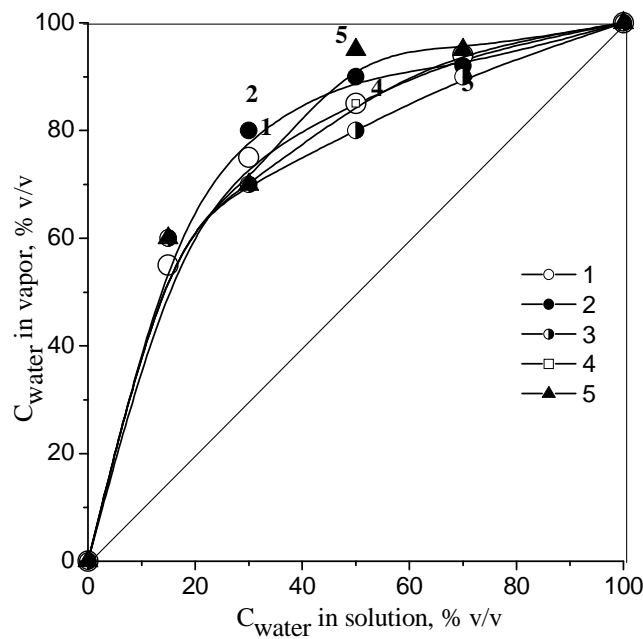


Figure 2. Separation diagrams for the system: crazed PA-6 – water – isopropanol in the pervaporation process at  $20\text{ }^{\circ}\text{C}$ ,  $S = 2\text{ cm}^2$ . 1 –  $\lambda = 0\%$ ; 2 –  $\lambda = 50\%$ ; 3 –  $\lambda = 90\%$ ; 4 –  $\lambda = 130\%$ ; 5 –  $\lambda = 180\%$

A more informative quality characterizing the separation efficiency is the excess partial flux density of the target component,  $J^*$ . The excess partial flux density of pure target component (in this case water) combines two main qualities of the separation process: the permeability (productivity) and the selectivity (the change of the target component concentration in the permeate). It is equal to the flux density of pure target component above its initial content in the solution. For example, if 80% solution passed through unit membrane area in unit time from the initial 50% solution, then the excess partial flux density of the target component in relative units is equal to 30.

Figure 3 shows the concentration dependencies of the excess flux density of water for crazed PA-6 with different stretching degrees. The data show that at stretching degrees  $\lambda = 50\%$  and  $90\%$ , the excess flux density of water is approximately 3 times higher than through the initial PA-6.

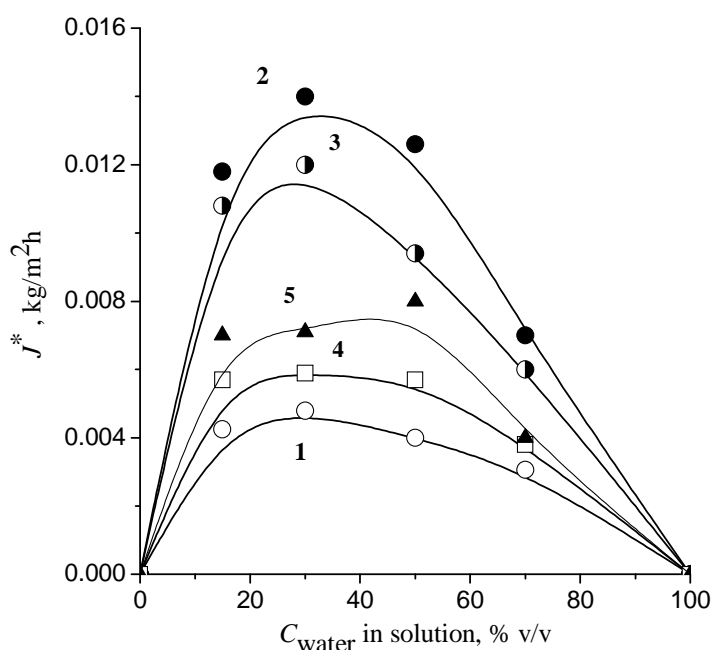


Figure 3. Concentration dependencies of the excess flux density of water  $J^*$  in the system: crazed PA-6 – water – isopropanol in the pervaporation process at  $20\text{ }^\circ\text{C}$ ,  $S = 2\text{ cm}^2$ .  
 1 –  $\lambda = 0\%$ ; 2 –  $\lambda = 50\%$ ; 3 –  $\lambda = 90\%$ ; 4 –  $\lambda = 130\%$ ; 5 –  $\lambda = 180\%$

The data obtained also show that the maximum efficiency of pervaporation separation of water-alcohol mixtures on PA-6 is achieved at stretching degrees  $\lambda = 50\%$  and  $90\%$ . For stretching degrees  $\lambda = 130\%$  and  $180\%$  the separation efficiency decreases and remains approximately constant for all concentrations.

Thus, the presented results show that crazing of PA-6 increases the efficiency of pervaporation separation of water-organic systems without the change of selectivity.

## References

1. Volynskii A. L., Bakeev N. F. Structural self-organization of amorphous polymers. Moscow, Fizmatlit, 2005. 232 p.

# THE KINETICS OF ARGININE AND HISTIDINE SORPTION BY CATION-EXCHANGE MEMBRANES

Nina Maygurova, Elena Krisilova, Tatiana Eliseeva, Anastasiya Sholokhova  
Voronezh State University, Voronezh, Russia, E-mail: nina.vsu@gmail.com

## Introduction

Studies of amino acids' sorption are very important for the description of their mass transfer processes in membranes. They are essential for the development of techniques for the separation and demineralization of amino acids by membrane methods and allow one to improve theoretical concepts of the nature and mechanism of amino acids transport in synthetic and biological membranes. Knowledge of sorption peculiarities is necessary for a mathematical description of transport processes in ion-exchange membranes [1-2]. At the same time, data on the sorption of amino acids by ion-exchange membranes are limited [3-4].

## Experiments

The objects of this study are amino acids – arginine (2-amino-5-guanidinopentanoic acid) and histidine (2-amino-3-imidazolylpropanoic acid) as well as heterogeneous sulfocation-exchange membranes MK-40 (produced by 'Shchekinoazot', Russia) and Fumasep® FTCM (produced by 'Fuma-Tech', Germany), homogeneous perfluorinated sulfocation-exchange membrane MF-4SK (produced by 'Plastpolymer', Russia).

The solutions of arginine are analyzed by the method of photometry based on cooper complexes formation [5] and histidine - by spectrophotometric method [6]. The membranes are prepared according to GOST State Standard 17553-72 and converted into H<sup>+</sup>-form according to the technique described in [7].

Amino acid sorption by membranes was studied in the static conditions. The initial concentration was 0.02 mol/dm<sup>3</sup>. The initial pH value corresponded to the isoelectric point of the amino acid used. The membrane peaces immersed in amino acid solution were shaken, and the samples were taken and analysed periodically. The amount of absorbed amino acid was calculated from the change in its concentration in solution. The kinetic curves were presented in the coordinates of the process completion degree (F) as a function of time (t).

## Results and Discussion

The kinetic curves of basic amino acids' sorption obtained are shown in the Fig. 1.

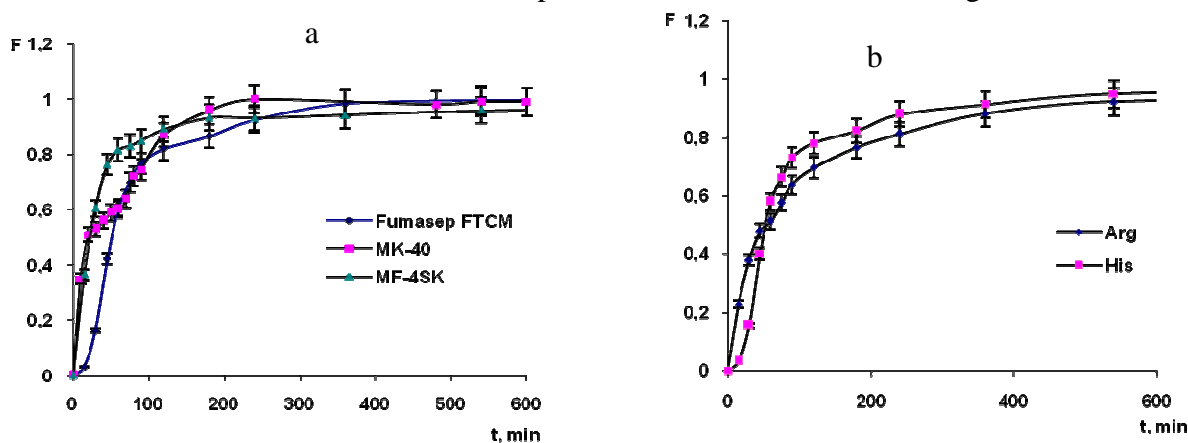


Figure 1. Kinetic sorption curves: a – histidine sorption by the different membranes, b – histidine and arginine sorption by Fumasep FTCM membrane

The dependencies are of saturation curves type. The equilibrium in the system histidine solution–the Fumasep FTCM membrane is reached in circa 360 minutes, in the system including MK-40 membrane - in 240 minutes. In the system including MF-4SK membrane process is completed by 90 % in 180 minutes, and the equilibrium is reached in 540 minutes (Fig. 1a). The equilibrium in

the system arginine solution–Fumasep FTCM membrane is reached in circa 360 minutes as in the case of histidine solution with the same concentration (Fig. 1b).

The experiment with phase contact interrupt is conducted in order to reveal the limiting stage of basic amino acids sorption by the cation-exchange membrane Fumasep® FTCM in H<sup>+</sup>-form. Fig.2 shows the initial section of histidine sorption kinetic curve with interrupt for the membrane Fumasep® FTCM ( $C_0 = 0.02 \text{ mol/dm}^3$ ).

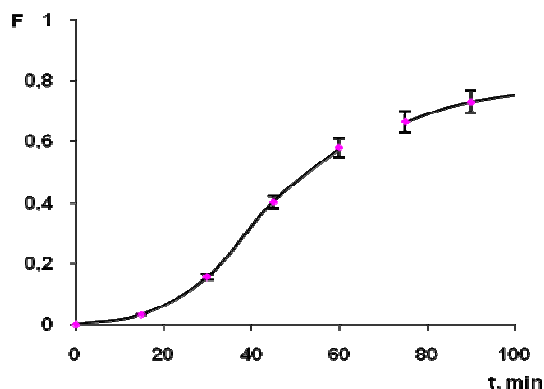


Figure 2. The initial section of the kinetic sorption curve with interrupt for histidine (membrane Fumasep FTCM)

The shape of the curve does not change after the interrupt of phases contact. The similar situation one can observe for arginine solution. This enables to suppose that the external diffusion is the limiting stage in basic amino acids' sorption process for the studied membrane.

#### References

1. *Timashev S.F.* Physicochemistry of Membrane Processes. Moscow: Khimiya, 1988. 240 p.
2. *Zabolotskii V.I., Nikonenko V.V.* Ion Transfer in Membranes. Moscow: Nauka, 1996. 392 p.
3. *Kikuchi K. et al.* // J. Chem. Eng. Jap. 1994, V. 21, P. 391-398.
4. *Gotoh T., Kikuchi K.* // Bioseparation. 2000, V. 9, P. 37-41.
5. *Roshal E.R. et al.* // Russian Chem.-Pharm. J. 1988, V. 6, P. 30.
6. *Kotova D.L. et al.* Spectrophotometric detection of amino acids in water solutions. Treatise. Voronezh: VSU, 2004.–55 p.
7. *Berezina N.P. et al.* Physicochemical Properties of Ion-Exchange Materials: Practical Course, Krasnodar: Kuban. Gos. Univ., 1999.

---

# STUDY OF MASS TRANSFER CHARACTERISTICS OF THE MODIFIED MEMBRANES IN ELECTRODIALYSERS SIMULATING LARGE-SCALE APPARATUS

Nadezhda Melnik, Natalia Pismenskaya, Victor Nikonenko

Membrane Institute, Kuban State University, Krasnodar, Russia, E-mail: melnik\_nadezhda@inbox.ru

## Introduction

Desalination/deionization of dilute solutions is one of the largest ED applications [1, 2]. However, the process rate in this case is limited by the delivery of electrolyte from bulk solution to the membrane interface. Under conventional current densities, this delivery occurs mainly as electrolyte diffusion while the contribution of forced convection is vanishing when approaching the interface [3-5]. The usage of intensive current modes might be of practical interest, since it can significantly raise the ED process rate [1, 5]. This work is aimed at study the behavior of modified ion exchange membranes in conditions close to those applied in large-scale electrolysers.

## Experiment

Two membrane pairs were studied: MK-40//MA-40 and MK-40/Nf//MA-40M. MK-40 and MA-40 are Russian commercial membrane manufacturing by JSC ‘Shchekinoazot’. The MK-40/Nf membrane was obtained from a cation exchange MK-40 membrane by casting a thin film of a Nafion-type material on the surface. To produce the MA-40M membrane, the surface of MA-40 was processed with a strong polyelectrolyte containing quaternary ammonium bases.

The principal scheme of experimental setup for mass transfer characteristics study is shown in Fig. 1. The membranes forming desalination (DC), concentration (CC), and electrode (EC) compartments are separated from one another by an inert net spacer (S) of extrusion type with rhombic cells, situated at 45° to ingoing stream. The step of the spacer cell is 5 mm, the thickness is 1.0 mm, and the porosity is 0.91.

The membranes under study are designated with an asterisk (MK-40\*, MA-40\*). They can be commercial membranes or modified ones. Auxiliary commercial MK-40 and MA-40 membranes serve to separate the products of electrode reactions from the central compartment under study.

Two plastic Luggin’s capillaries (0.5 mm in external diameter) are built in the spacer. Both capillary tips are situated at the center of polarized area in CC at about 0.5 mm from the surface of the membrane forming the central DC. Another end of each capillary is connected to a reservoir with a (0.02 M) NaCl solution where a measuring Ag/AgCl electrode is inserted.

The membrane stack imitates an industrial electrolysers with internal collectors. At the stack entrance, each compartment has a non-polarized section of 5 cm length for hydrodynamic stabilization of the solution flow. The polarized membrane area is 3 cm in width ( $a$ ) and 10 cm in length ( $L$ ), the total membrane length is 22 cm. Our previous investigations [6, 7] showed that the mass transfer characteristics obtained in a stack of  $L = 10$  cm in length can be quantitatively scaled to predict the behavior of industrial electrolysers.

An intermediate tank, inserted into the desalting stream (Fig. 1), contains a stirrer and sensors to control temperature, pH and specific electrical conductivity ( $\kappa$ ). In the concentrating streams (CS), a 0.02 M NaCl solution is supplied from a separate tank (not shown in Fig. 1), it continuously passes through auxiliary CC and DC, then through EC and is discharged. The average linear flow velocity in all compartments is equal to  $2.5 \text{ cm s}^{-1}$ .

Before the experiment, the tank, the central desalination compartment and the hoses were filled with 1200 mL of a 0.03 M NaCl solution. Then a constant voltage controlled with the Luggin’s capillaries (Fig. 1) was applied and electro dialysis process was realized at  $25 \pm 0.5$  °C maintained in the tank. The solution circulated through the intermediate tank and the central DC with volume flow rate  $W$ . The salt concentration in the tank decreased with time because of the electro dialysis desalination: the outlet concentration,  $C_d$ , was lower than the inlet one,  $C$ . Besides, there were changes in pH of the solution passed through the DC due to different rates of

water splitting at the cation exchange (MK-40 or MK-40/Nf) and the anion exchange (MA-40 or MA-40M) membranes. In order to maintain pH=7 in the solution in the tank, alkaline (NaOH) or acid (HCl) solution were added into the tank, depending on the sign of the pH changes in the outlet solution. The desalination process was realized in quasi-steady-state conditions, the amount of the solution put in the system was so that allowed us to keep a slow (less than 1 % per minute) [6] decrease in the electrolyte concentration of the solution in the intermediate tank. The total duration of every run was 8-10 hours. The electric current, as well as the specific conductivity of the solution (converted then into the NaCl concentration) in the tank, were measured as functions of time.

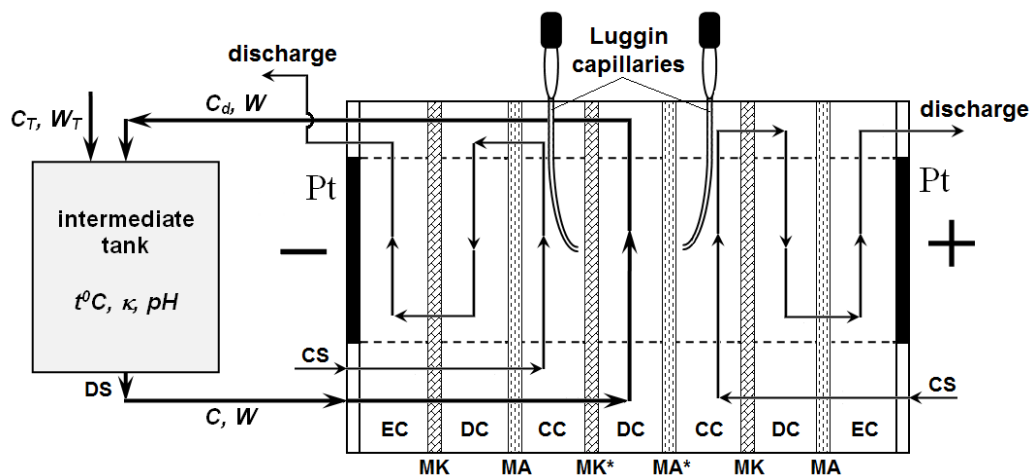


Figure 1. Principal scheme of the experimental setup used for measuring mass transfer characteristics. A desalting (DS) and two concentrating (CS) streams, desalination (DC), concentration (CC) and electrode (EC) channels, polarizing platinum electrodes (Pt) are shown. Dashed straight lines mark out the active section of membrane stack polarized by electric current

## Results and Discussion

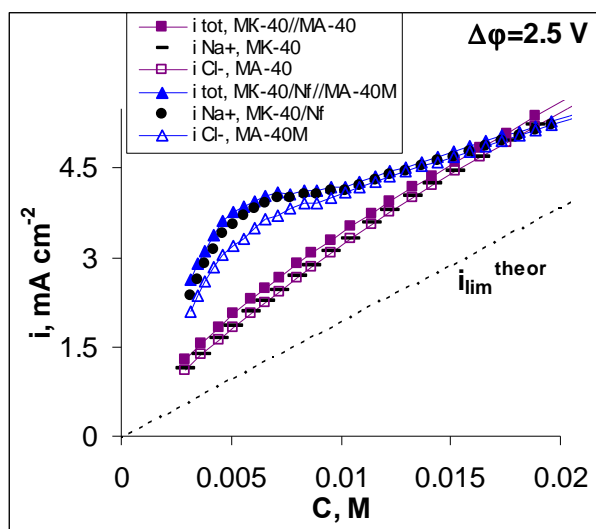
Total ( $i_{tot}$ ) and partial ( $\text{Na}^+$  and  $\text{H}^+$  ions through cation exchange membranes and  $\text{Cl}^-$  and  $\text{OH}^-$  ions through anion exchange ones, respectively) current densities are shown in Fig. 2 as functions of the feed NaCl concentration. The data were obtained at a potential difference (registered with Luggin's capillaries as shown in Fig. 1) equal to 2.5, 4.0 or 6.0 V per cell pair. A potential difference was fixed while the feed concentration decreased with time since a fixed volume of solution circulated through a central desalination compartment and a tank.

The data presented in Fig. 2 show that in all studied systems the current transport is carried out mainly by ions of salt. Current efficiency increased correspondingly, when the commercial membranes were replaced with the modified ones. The effect is maximum at 4 V per cell pair. With increasing voltage to 6 V the difference decreases between the behavior of the modified and commercial membranes. Apparently, the reason is in high water splitting rate, in spite of the modification of both membranes.

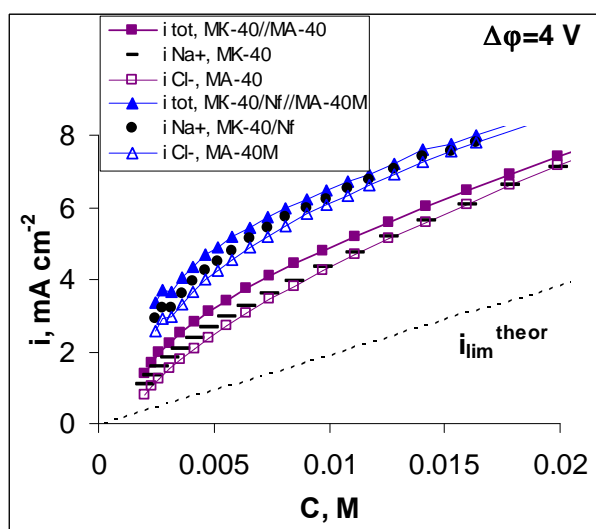
Our investigations show that overlimiting electro dialysis can be essentially improved by applying specially modified ion exchange membranes. Note that the ways and materials of modification are commercially available. In practical terms, this means that there are new opportunities to produce inexpensive ion-exchange membranes effective in electro dialysis of dilute solutions.

## Acknowledgments

Part of the work was carried out in accordance with the cooperation programme of International Associated French-Russian Laboratory "Ion-Exchange Membranes and Related Processes" The authors are grateful to the CNRS, RFBR (Grant Nos. 11-08-00599, 12-08-00188) and FP7 Marie Curie Actions "CoTraPhen" Project PIRSES-GA-2010-269135.

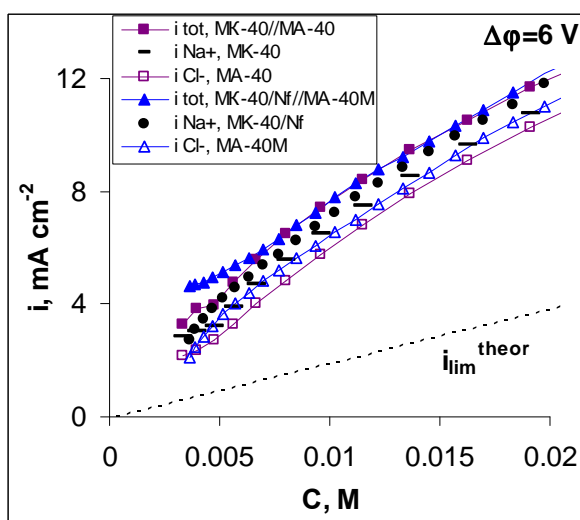


a



b

Figure 2. Total ( $i_{tot}$ ) and partial ( $Na^+$ ,  $i_{Na^+}$ , and  $H^+$ ,  $i_{H^+}$ , ions through cation exchange membranes and  $Cl^-$ ,  $i_{Cl^-}$ , and  $OH^-$ ,  $i_{OH^-}$ , ions through anion exchange ones, respectively) current densities in the electro dialysis cell shown in Fig. 1 as functions of the feed NaCl concentration. The potential drop across a cell pair is 2.5 V (a), 4 V (b) and 6 V (c)



c

## References

1. *Strathmann H.* Electrodialysis, a mature technology with a multitude of new application // *Desalination*. 2010. V. 264. P. 268-288.
2. *Tanaka Y.* Ion Exchange Membranes: Fundamentals and Applications. Membrane Science and Technology Series, 12, Elsevier, Netherlands. 2007. 531 p.
3. *Spiegler K.S.* Polarization at ion exchange membrane-solution interfaces // *Desalination*. 1971. V. 9. P. 367-385.
4. *Długolecki P., Anet B., Metz S.J., Nijmeijer K., Wessling M.* Transport limitations in ion exchange membranes at low salt concentrations // *J. Membr. Sci.* 2010. V. 346. P. 163-171.
5. *Nikonenko V.V., Pismenskaya N.D., Belova E.I., Sizat Ph., Huguet P., Pourcelly G., Larchet Ch.* Intensive current transfer in membrane systems: Modelling, mechanisms and application in electro dialysis // *Adv. Colloid and Interface Sci.* 2010. V. 160. P. 101-123.
6. *Lactionov E.V., Pismenskaya N.D., Nikonenko V.V., Zabolotsky V.I.* Method of electro dialysis stack testing with the concentration regulation feed solution // *Desalination*. 2002. V. 152. P. 101-116.
7. *V.V. Nikonenko, N.D. Pismenskaya, A.G. Istoshin, V.I. Zabolotsky, A.A. Shudrenko,* Description of mass transfer characteristics of ED and EDI apparatuses by using the similarity theory and compartmentation method, *Chem. Eng. Process.* 2008. V. 47. P. 1118-1127.

# TRANSPORT PROPERTIES OF HYBRID MF-4SC MEMBRANES DOPED BY SILICA AND SILICA WITH SURFACE MODIFIED BY AMINO-GROUPS

Alexandr Mikheev, Ekaterina Safronova

Kurnakov Institute of General and Inorganic Chemistry, Moscow, Russia,

E-mail: miheevalge@gmail.com

## Introduction

An interest to ion-exchange membranes that occupy important place in modern technologies has grown last decade. Perfluorinated sulfocation exchange membranes such as Nafion and MF-4SC membranes are ones of the most used materials. However, commercially available membranes do not meet the requirements of modern industry. It was shown that incorporation of various nanoparticles, including silica with high sorption ability, into the membrane matrix leads to the considerable properties improvement. As properties of composite materials are determined in general by the surface of the components, namely by sorption capacity and specific area, it was proposed that silica surface fictionalization can influence on the properties of hybrid MF-4SC membranes. Silica surface was functionalized by proton-acceptor amino groups.

In this paper we report the properties of hybrid materials based on MF-4SC membrane and hydrated SiO<sub>2</sub> with unmodified surface and with the surface modified by hydrocarbon fragments containing amino group (3-aminopropyl-(**R**<sub>1</sub>), 3-(2-imidazoline-1-yl)-propyl-(**R**<sub>2</sub>)).

## Experiments

The hybrid materials were prepared by casting from a polymer solution containing a calculated amount of precursors for further synthesis of SiO<sub>2</sub> and SiO<sub>2</sub> with modified surface followed by precursor's hydrolysis to obtain oxides. Tetraetoxysilane (Si(OC<sub>2</sub>H<sub>5</sub>)<sub>4</sub>, Fluka, >98%) 3\_aminopropyltrimethoxysilane (97%, Alfa Aesar) and 3\_(2\_imidazolin\_1\_yl)-propyltriethoxysilane (≥98.0%, Fluka) were used.. All membranes were treated one after another by 5% solution of HCl and twice by bidistilled water at 80°C.

## Results and Discussion

MF-4SC membranes doped by SiO<sub>2</sub> have higher water uptake and sorption exchange capacity (SEC) than the initial membrane (table 1). It was shown that dependence of ion conductivity on silica content pass through the maximum at 3 wt.% SiO<sub>2</sub>. Thus ass the following experiments with silica with modified surface were carried out with MF-4SC membranes doped with 3 wt.% SiO<sub>2</sub>. Concentration of modified groups on silica surface was varied: 5 and 10 mol.% of **R**<sub>1</sub> and **R**<sub>2</sub> from silica content.

Table 1: SEC and water uptake of MF-4SC membranes doped by SiO<sub>2</sub>

Sample	SEC, mg-eq/g	SEC <sub>cat</sub> <sup>*</sup> , mg-eq/g	w(H <sub>2</sub> O), %
MF-4SC	0.93	0.93	14.2
MF-4SC+1.5 wt.% SiO <sub>2</sub>	1.07	1.09	15.2
MF-4SC+3 wt.% SiO <sub>2</sub>	0.95	0.97	19.5
MF-4SC+5 wt.% SiO <sub>2</sub>	0.89	0.94	6.5
MF-4SC+7 wt.% SiO <sub>2</sub>	0.92	0.99	-
MF-4SC+10 wt.% SiO <sub>2</sub>	0.89	0.99	-
MF-4SC+3 wt.% SiO <sub>2</sub> +5 mol.% <b>R</b> <sub>1</sub>	0.74	0.76	18.5
MF-4SC+3 wt.% SiO <sub>2</sub> +10 mol.% <b>R</b> <sub>1</sub>	0.65	0.67	13.7
MF-4SC+3 wt.% SiO <sub>2</sub> +5 mol.% <b>R</b> <sub>2</sub>	0.88	0.91	12.6
MF-4SC+3 wt.% SiO <sub>2</sub> +10 mol.% <b>R</b> <sub>2</sub>	0.73	0.75	-

\* SEC<sub>cat</sub> is a SEC divided to the cation exchanger weight  $SEC_{cat} = SEC/W_{MF-4SC}$ ,  $W_{MF-4SC}$  is a mass concentration of the membrane.

Incorporation of silica with modified surface leads to the water uptake decrease in comparison with MF-4SC+3 wt.% SiO<sub>2</sub> (table 1). This phenomenon can be explained by the fact that the surface modification by bulk groups leads to the decrease of free space inside of the membrane pore according to the model of the limited elasticity of the membrane pores<sup>1</sup> that is followed by the displacement of a part of water molecules from the system of pores and channels.

The conductivity data of hybrid membranes doped with silica with modified surface are presented on the Figure 2. Incorporation of silica with modified surface into membrane matrix leads to the conductivity increase on comparison with the conductivity of MF-4SC + 3 wt.% SiO<sub>2</sub> despite of the less water uptake. At the same time the increase of modifying group content on SiO<sub>2</sub> surface is accompanied by conductivity reduction. The increase of the molecular weight of modifying group results in the conductivity reduction. The obtained data can be explained by the fact that the incorporation of silica with amino-groups into membrane leads to an increase in the number of transfer centers, namely the protonated amino-groups, which are involved in the ion transport processes in the membrane also.

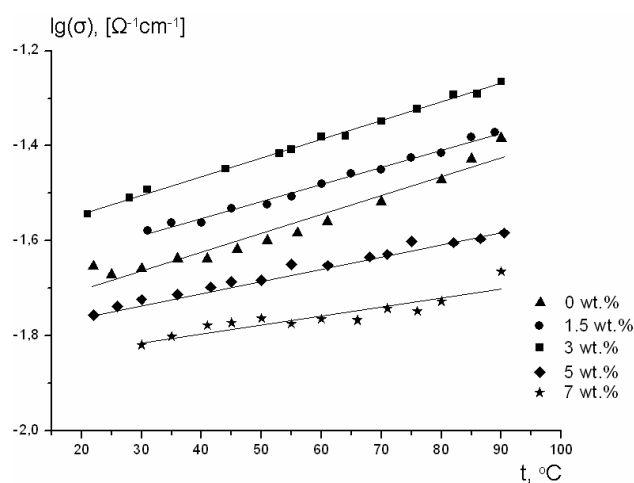


Figure 1. Ion conductivity as a function on temperature for MF-4SC+X wt.% SiO<sub>2</sub> membranes

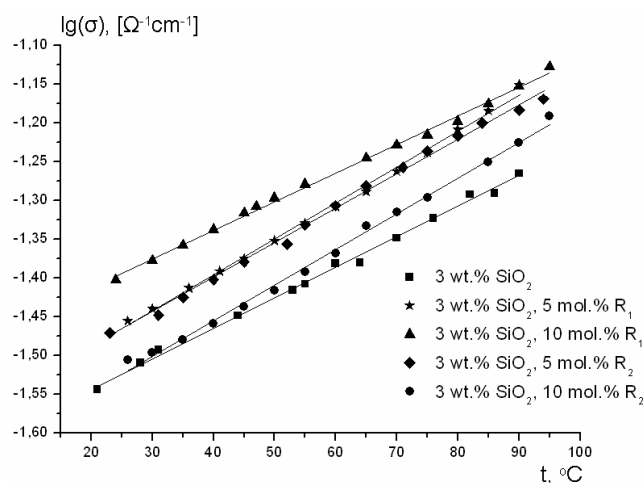


Figure 2. Ion conductivity as a function on temperature for MF-4SC+3 wt.% SiO<sub>2</sub> with modified surface

Diffusion permeability coefficients of NaCl and HCl solution and H<sup>+</sup>/Na<sup>+</sup> interdiffusion coefficients of the hybrid membranes have been investigated. Silica nanoparticles incorporation into membrane results in the diffusion permeability increase. As MF-4SC is cationexchange membrane the limited stage of permeability process it anion transfer through the membrane. The highest anions diffusion rate is observed for membranes contained 3-5 wt.% SiO<sub>2</sub>. That agrees with the model of limited elasticity of the membranes pores and channels. Thus, the hybrid membranes with small amounts of SiO<sub>2</sub> are less selective that initial membrane, while further increase of dopant concentration cause the increase in selectivity of cation transport. For membranes contained 3 wt.% SiO<sub>2</sub> + 5 mol.% **R**<sub>1</sub> and **R**<sub>2</sub>, the diffusion permeability coefficients decrease in comparison with MF-4SC+3 wt.% SiO<sub>2</sub>. At the same time increase of modified groups content to 10 mol.% results in the sharp increase of the anion diffusion rate (from 0.5 to 1 order of magnitude).

Obtained data can be explained as follows. The determinant factor of ions diffusion rate in the membranes doped with 3 wt.% of SiO<sub>2</sub> and 5 mol.% of modified groups is the increase of the particles size that is followed by the reduce of free space in the pore. When the concentration of the modified groups increases up to 10 mol.% diffusion permeability increases sharply. This can be explained by the interaction between proton acceptor groups of the dopant and sulfo-groups of the membrane leading to the formation of the fixed-NR<sub>3</sub> ions. This assumption is proved by the SEC decrease. At the same the areas with the reduced cations and increased anions

concentration may occur in the membrane. This leads to the anions transfer acceleration and as a consequence - to decrease the selectivity.

**Table 2: Diffusion permeability and  $H^+/Na^+$  interdiffusion coefficients ( $cm^2/s$ ) of hybrid membranes**

Diffusing solution Membrane	0.1 M NaCl / H <sub>2</sub> O	0.1M HCl / H <sub>2</sub> O	0.1 M HCl / 0.1 M NaCl
MF-4SC	$5.21 \cdot 10^{-8}$	$4.20 \cdot 10^{-7}$	$6.34 \cdot 10^{-6}$
MF-4SC+1.5 wt.% SiO <sub>2</sub>	$6.98 \cdot 10^{-8}$	$6.27 \cdot 10^{-7}$	$1.09 \cdot 10^{-5}$
MF-4SC+3 wt.% SiO <sub>2</sub>	$2.33 \cdot 10^{-7}$	$1.21 \cdot 10^{-6}$	$1.02 \cdot 10^{-5}$
MF-4SC+5 wt.% SiO <sub>2</sub>	$2.77 \cdot 10^{-7}$	$7.98 \cdot 10^{-7}$	$5.76 \cdot 10^{-5}$
MF-4SC+7 wt.% SiO <sub>2</sub>	$1.56 \cdot 10^{-7}$	$6.29 \cdot 10^{-7}$	$4.60 \cdot 10^{-5}$
MF-4SC+10 wt.% SiO <sub>2</sub>	$1.10 \cdot 10^{-7}$	$6.39 \cdot 10^{-7}$	$1.08 \cdot 10^{-5}$
MF-4SC+3 wt.% SiO <sub>2</sub> + 5 mol.%R <sub>1</sub>	$8.80 \cdot 10^{-8}$	$4.68 \cdot 10^{-7}$	$8.97 \cdot 10^{-6}$
MF-4SC+3 wt.% SiO <sub>2</sub> + 10 mol.%R <sub>1</sub>	$4.54 \cdot 10^{-7}$	$2.79 \cdot 10^{-6}$	$5.15 \cdot 10^{-5}$
MF-4SC+3 wt.% SiO <sub>2</sub> + 5 mol.%R <sub>2</sub>	$4.61 \cdot 10^{-8}$	$2.13 \cdot 10^{-7}$	$6.62 \cdot 10^{-6}$
MF-4SC+3 wt.% SiO <sub>2</sub> + 10 mol.%R <sub>2</sub>	$2.99 \cdot 10^{-7}$	$1.28 \cdot 10^{-6}$	$5.15 \cdot 10^{-5}$

In this work the properties of hybrid materials based on MF-4SC membrane and SiO<sub>2</sub> nanoparticles with unmodified and with modified surface were investigated. It was shown that modification of MF-4SC membrane leads to the improvement of its transport properties.

*This work was financially supported by the RFBR (project 11-08-93105).*

#### References

1. Novikova S.A., Safronova E.Yu., Lysova A.A., Yaroslavtsev A.B. Influence of incorporated nanoparticles on MF-4SC membrane ion conductivity // Mend. Comm. 2010. V.20. P. 156-157.

# HYDROGEN PERMEABILITY OF METAL FILMS OF CU,PD-ALLOYS BY THE DATA OF POENTIOSATIC DOUBLE-STEP MEASUREMENTS

Natalya Morozova, Alexandr Vvedenskii, Alexandr Maximenko, Irina Beredina

Voronezh State University, Voronezh, Russia, E-mail: [mnb@chem.vsu.ru](mailto:mnb@chem.vsu.ru)

## Introduction

The permeation of hydrogen into metal materials noticeably changes their corrosive-electrochemical characteristics and causes serious problems with a selection of constructional materials for nuclear power, aircraft, shipbuilding and other industries [1]. On the other hand, hydrogen accumulation in metal causes considerable interest for the solution of problems of its safe transportation and storage; here the palladium and its alloys are especially perspective. Available methods of investigation of hydrogenation are rather laborious, not express and hardly sensitive to the estimation of a role of a structural state of metal that is especially important in case of thin metal films. The electrochemical method of the estimation of hydrogenation level [2] is alternative. This in situ method combines processes of a cathodic hydrogenation of metal, usually at constant controllable potential, with anode dissolution of atomic hydrogen H from the surface layer representing a diffusive zone on the introduced H. The aim of this paper was the determination of parameters of introduction and issue of atomic hydrogen on film electrodes with a composition of 53 at. % of Cu and 47 at. % of Pd used for precision purification of gaseous hydrogen from impurity.

## Experimental

The investigation were carried out on the film Cu,Pd-electrodes consisted of 53 at.% Cu and 47 at.% Pd. This alloy is prone to the ordering with the formation of  $\beta$ -phase solid solution Cu-Pd with the increased hydrogen permeability [1]. Studied film electrodes with a thickness of  $L = 2-8$  microns were obtained by magnetron dispersion by condensation in vacuum [3] on substrates from Si (111), SiO<sub>2</sub>, glass and fluorine-phlogopite (FP) at temperatures of substrates of  $T_s$  from 300 to 800 K (Table 1).

**Table 1: Parameters of Film Electrodes**

Number of a Sample	1	2	3	4	5	6	7
$T_s, K$	423	573	300	800	300	623	623
Substrate	Si (111)	Si (111)	Si (111)	SiO <sub>2</sub>	стекло	SiO <sub>2</sub>	FP
$L, \mu m$	4	8	2	4	5	4	4

Unlike compact electrodes, membrane electrodes have two sides – gloss (the side turned to a substrate) and matte (outer side). These surfaces differ in a roughness, a substructure and phase composition; therefore the electrochemical investigations were carried out on two surfaces. The hydrogenation of samples was carried out at potential of hydrogen evaluation of  $E_c = -0.08$  V changing time of a hydrogenation  $\tau_H$  largely. Studying of ionization of H introduced in metal was carried out by voltammetry and chronoammetry with using the IPC-Compact with computer management. Researches are executed in aqua solution of 0.1M H<sub>2</sub>SO<sub>4</sub> deaerated by argon at 298 K. Potentials are given relatively SHE.

## Results and Discussion

It was established that the hydrogenation (at cathodic polarization) and a hydrogen release (at anodic polarization) is limited by solid-phase diffusion of atomic hydrogen in a metal phase. Thus the stage of charge/ionization of  $H^+ + e^- \rightarrow H$  is not equilibrium, and proceeds with a final rate. The theoretical analysis foretells that in the conditions of solid-phase diffusion the cathodic and anodic current transients after integration will look like follows:

$$\frac{Q_H^n(\tau)}{\tau^{1/2}} = i_{H^+}^n(0)\tau^{1/2} - 2FK_D \quad \text{and} \quad \frac{Q_H^a(\tau)}{\tau^{1/2}} = -i_{H^+}^a(0)\tau^{1/2} + 2FK_D. \quad (1)$$

Here  $i_{H^+}^n(0)$  and  $i_{H^+}^a(0)$  are the rates of charge and ionization of atomic hydrogen at the initial time,  $K_D = c_H^s \cdot D_H^{1/2}$  is a parameter of diffusion permeability;  $c_H^s$  and  $D_H$  are the surface concentration and the diffusion coefficient of atomic hydrogen.

The cathodic  $Q_c$  and anodic  $Q_a$  charges were calculated from the current transients obtained on membrane electrodes at different times of hydrogen accumulation. The anodic charge was counted for 100 s, when the ionization current reached a constant value. The  $Q/\tau^{1/2} - \tau^{1/2}$  dependences plotted on the calculated values appeared linear (Fig. 1), as it was expected.

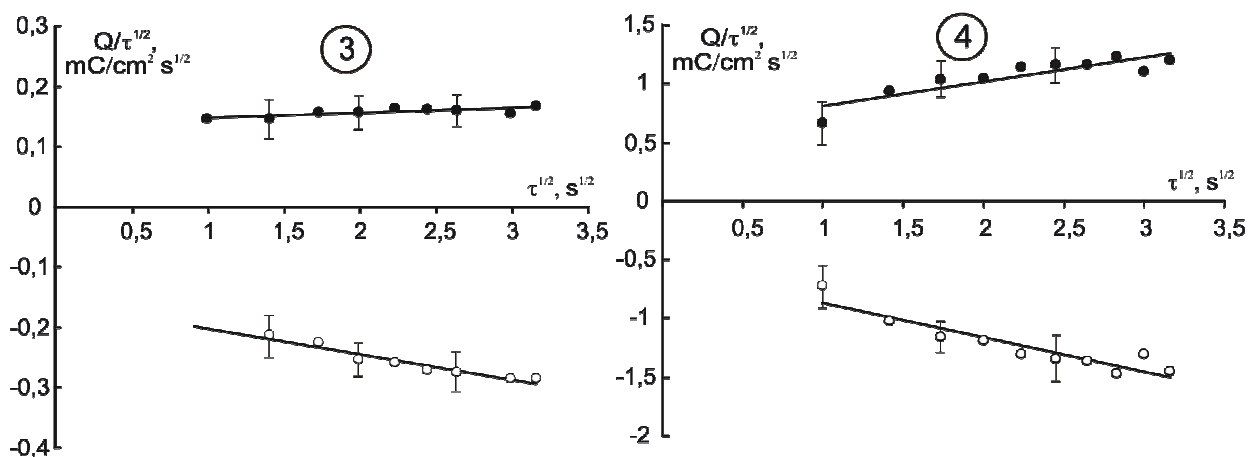


Figure 1. Dependences of Cathodic and Anodic Charges on the Hydrogenation Time for the Film Electrodes 3 and 4

With use of expression (1) the parameters of anode and cathodic processes  $K_D$ ,  $i_{H^+}^k(0)$  and  $i_{H^+}^a(0)$  were calculated. As criterion of selection of the most typical results, we chose the constant of diffusive permeability  $K_D$ , which usually coincided for cathodic and anode processes within each experiment. Therefore  $K_D$  values for cathodic and anode processes for each of the parties of a film were average (Fig. 2).

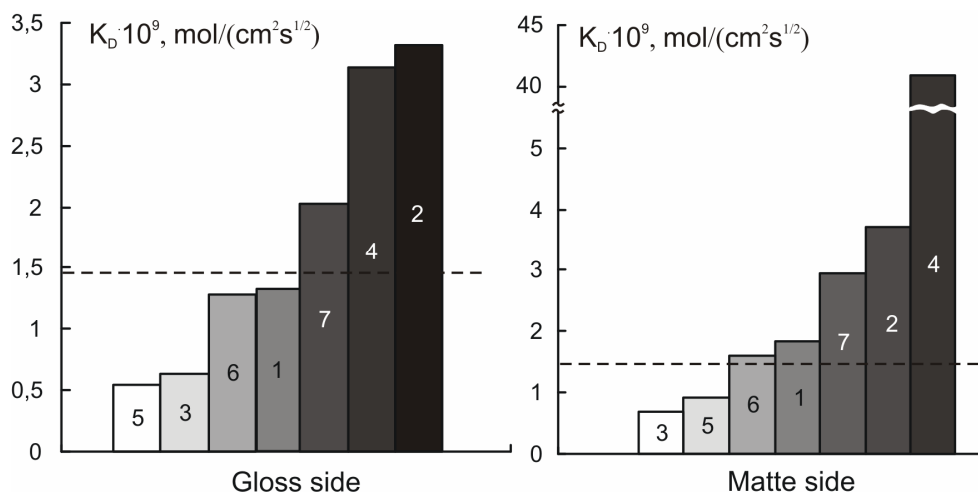


Figure 2. Parameter of Hydrogen Permeability for the Film Electrodes. Value of  $K_D$  for Compact Electrode is a Dotted Line

Values of a constant of diffusive permeability  $K_D$  for the majority of samples of membrane electrodes on the matte party for 20-30 % are higher, than on the gloss side. The exception makes a sample No. 4. Such difference is connected with various structure of Cu,Pd-film on external and internal surfaces. This sample belongs to high-temperature films for which the formation of mainly ordered  $\beta$ -phase of Cu-Pd solid solution on an external surface is typical.

Existence of this phase promotes the better permeability of atomic hydrogen that is shown in considerable increase of  $K_D$ . At the same time, upon transition from an internal to outer side of film the growth of crystalline particles of solid solution is observed that also promotes increase of hydrogen permeability.

An increase of temperature of film membranes preparation to 623 K leads to the increase of  $K_D$  value regardless of surface type (outer or internal). Such distinction of  $K_D$  values can be connected only with the increase in the sizes of crystalline particles. At the same time, at increase in  $T_s$  over 623 K along with increase in the sizes of crystalline particles from inside to external side, there is a change of phase composition of films. On the outer side of a film contains the ordered phase generally. Such gradient of phase composition remains to  $T_s = 850$  K when the disordering  $\beta \rightarrow \alpha$  in Cu-Pd solid solution begins.

By consideration of the membrane electrodes No. 1-3 prepared on Si (111) substrate it is possible to note that with growth of a film thickness the value of  $K_D$  grows, both for gloss, and for the matte side and regardless of preparation temperature. For the film No. 3 with thickness of 2 microns,  $K_D$  for different sides are approximately identical. As a whole there is a tendency of  $K_D$  growth with temperature of a substrate and thickness of a film since both factors lead to increase in the sizes of crystalline particles.

The film grown on fluorine-phlogopite shows higher hydrogen permeability, in comparison with the films received on  $\text{SiO}_2$  at 623 K. For gloss and matte sides the values of hydrogen permeability for films with a thickness of 4 microns, with identical preparation temperature are the following:  $K_D(\text{FP}) > K_D(\text{Si}) > K_D(\text{SiO}_2)$ .

For the membranes prepared on Si (111) substrate the cathodic reduction of hydrogen proceeds with greater speed, than its ionization. An objective growth of ionization rate is observed only for the matte side of the film that can be connected both with increase in thickness, and with increase in temperature of a film preparation.

### References

1. Hydrogen in Metals II / Ed. G. Alefeld and J. Völkl, Springer-Verlag, Berlin Heidelberg New York, 1978, p. 430.
2. Pound B.G. A potentiostatic double-step method for measuring hydrogen atom diffusion and trapping in metal electrodes. II. Experimental // Acta metall. 1987. V.35. P. 263-270.
3. Ievlev V.M., Darinskii B.M., Bugakov A.V. Orientatsionnye sootnosheniya pri epitaksial'nom roste metallicheskikh plenok na muscovite i ftorflogopite // PMM. 1976. 42. P.1236–1240.

# EFFECT OF THERMAL TREATMENT ON HYDROPHOBICITY OF NAFION SURFACE

Kseniya Nebavskaya, Andrey Nebavsky, Victor Nikonenko, Natalia Pismenskaya  
Kuban State University, Krasnodar, Russia, E-mail: [neanhim@gmail.com](mailto:neanhim@gmail.com)

## Introduction

The acquisition of new knowledge about the properties of perfluorinated sulfocationic Nafion materials is an important task because of great number of these materials' applications. However, it is known that their behavior is greatly dependent on material pretreatment. In our previous works [1,2] we tried to create a better understanding of influence of material oxidizing-thermal pretreatment on its hydrophobicity. This work was conducted to further study of hydrophobicity of Nafion as a function of external conditions.

## Theory

Nafion is an ionomer, containing hydrophobic perfluorinated matrix and side chains carrying hydrophilic sulfonic groups. The balance of hydrophilic and hydrophobic components on the surface of material determines its contact angle. Normally, the surface of Nafion is mostly covered with crystalline hydrophobic domains, formed by fluorocarbon chains structured by hydrophobic interactions [3]. However, this surface structure of Nafion can possibly be an object to change: it is known that the organization of Nafion polymer chains in volume can possibly be changed through the action of external conditions, for example, by drying at elevated temperatures [4] or by oxidizing-thermal treatment [2,5].

## Experiments

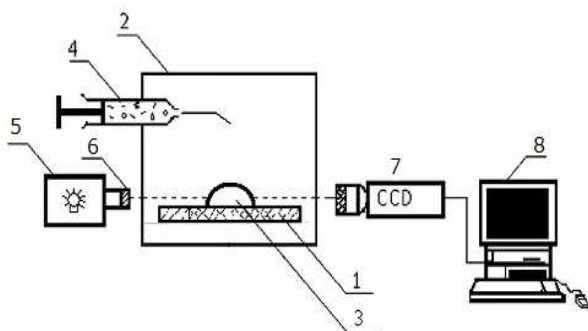


Figure 1. Experimental setup

- 1–sample
- 2–chamber with opening lid
- 3–drop of liquid
- 4–liquid dozer
- 5–source of light
- 6–diaphragm diffusing a light
- 7–video detector
- 8–computer

A commercial Nafion® 117 (DuPont, USA) membrane (further: Nafion membrane) and a laboratory produced film of Nafion casted on polymethylmethacrylate (PMMA) were chosen as the subjects of study. The film was produced by casting a 5% solution of Nafion in isopropanol (manufactured by Aldrich) onto the polished and degreased surface of a PMMA flat plate and drying until the full evaporation of the solvent at ambient temperature. Consisting of the same polymer material, membrane and film differed in thickness—the membrane is almost 10 times thicker than the film (170  $\mu\text{m}$  and 20  $\mu\text{m}$ , correspondingly).

Contact angle measurements were conducted using a sealed experimental setup pictured in Figure 1. After the start of video recording, a dry sample was placed in the chamber and a

drop of water of 7  $\mu\text{L}$  in volume was applied onto its surface.

For investigation of effect of thermal treatment the membrane and the film were each exposed to temperatures of 50, 60, 70 and 80°C with cumulative treatment time of 2 hours between each two steps. Contact angle measurements were repeated for at least 3 times for initial untreated samples and after each temperature treatment.

## Results and Discussion

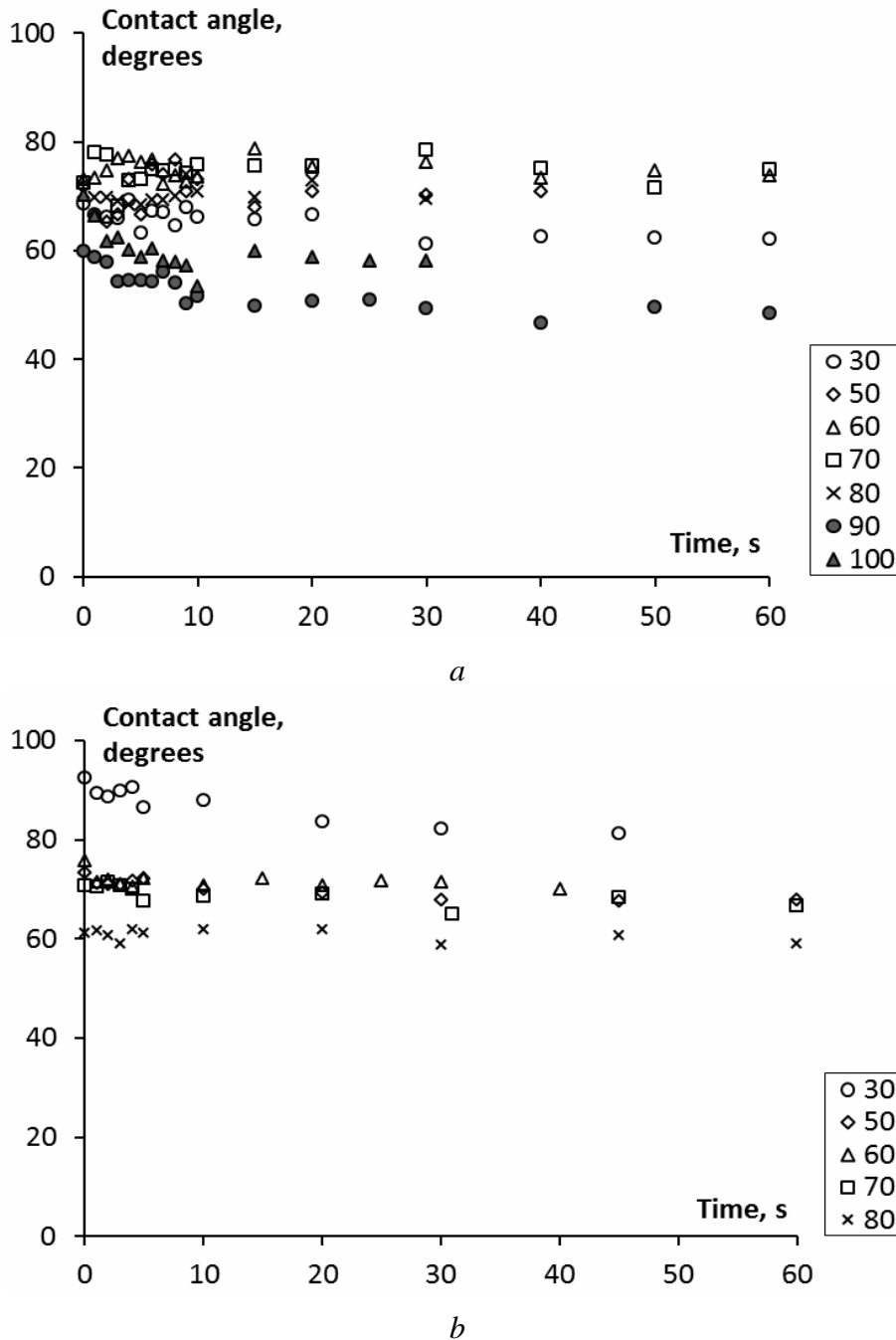


Figure 2. Kinetic dependences of contact angle for Nafion membrane (a) Nafion film (b) dried at different temperatures (shown in Celsius degrees in the legend)

Figure 2 shows the kinetic dependence of the contact angles on the surface of dry thermally treated membranes and films. As can be seen, the contact angle of both the membrane and the film decrease with the temperature of treatment. However, in case of film the dependence of the contact angle on the temperature is stronger and a noticeable decrease in hydrophobicity occurs at lower temperatures. For the film, a temperature as high as 50°C causes a significant decrease in contact angle, but the contact angle values for the membrane do not show any noticeable dependence on temperature until 90°C, which was observed when extra experiments were conducted to investigate the initial difference between the effect of thermal treatment on Nafion membrane and film. We assume that the reason for observed decrease of contact angle values lays in instability at elevated temperatures of hydrophobic crystalloid structures presented on the surface of Nafion. Really, the structuring forces of such formations are relatively weak Van der

Waals interactions. With increasing temperature, these domains are readily destroyed by chaotic temperature movement of molecules. As a result, hydrophobic domains on the surface are partially replaced with more or less homogeneous mixture of hydrophobic chains and hydrophilic groups. After steep decline of temperature, the hydrophobic domains have not time to reorganize themselves, so the contact angle for such materials corresponds to their state at elevated temperature. Furthermore, flatter (or even 2D) crystals are less stable than 3D ones. Flat crystals or films tend to be destroyed or transformed into 3D structures [6]. As a consequence, the structural changes in the Nafion film occur at lower temperature than in the case of membrane.

### Conclusions

Nafion material in form of membrane or film shows similar behavior in terms of contact angle dependence on temperature. For both of them a decrease of contact angle with temperature of treatment was observed. This is caused by the partial destruction of hydrophobic domains presented on the Nafion surface at low temperatures. However, this effect was more pronounced for the Nafion film than for the membrane as a result of different stability of conformation of their polymer chains in 3D and 2D geometry.

### Acknowledgments

*Part of the work was carried out within International Associated French-Russian Laboratory "Ion-Exchange Membranes and Related Processes" The authors are grateful to the CNRS, RFBR (Grant Nos. 11-08-93107, 11-08-96511 and 12-08-00188) and FP7 Marie Curie Actions "CoTraPhen" Project PIRSES-GA-2010-269135*

### References

1. *Belashova E.D., Melnik N.A., Pismenskaya N.D., Shevtsova K.A., Nebavsky A.V., Lebedev K.A., Nikonenko V.V.* Overlimiting mass transfer through cation-exchange membranes modified by Nafion film and carbon nanotubes // *Electrochimica Acta*. 2012. V. 59. P. 412-423.
2. *Shevtsova K. Nebavskiy A. Nikonenko V. Pismenskaya N.* Contact angle of water on Nafion materials // *Proceedings of the international conference "Ion transport in organic and inorganic membranes"* June 6-11, Krasnodar. 2011. P. 132-135.
3. *Bass M., Berman A., Singh A., Konovalov O., Freger V.* Surface structure of Nafion in vapor and liquid // *J. Phys. Chem.* 2010. V. 114. P. 37843790.
4. *Alberti G., Narducci R., Sganappa M.* Effects of hydrothermal / thermal treatments on the water uptake of Nafion membranes and relations with changes of conformation, counterelastic force and tensile modulus of the matrix // *J. Power Sources*. 2008. V. 178. P. 575-584.
5. *Berezina N.P., Timofeev S.V., Kononenko N.A.* Effect of conditioning techniques of perfluorinated sulphocationic membranes on their hydrophylic and electrotransport properties // *J. Membr. Sci.* 2002. V. 209. P. 509-518.
6. *Evans J.W., Thiel P.A., Bartlett M.C.* Morphological evolution during epitaxial thin film growth: Formation of 2D islands and 3D mounds // *Surf. Sci. Rep.* 2006. V. 61. P. 1-128.

# DETERMINATION OF HYDROTARTRATE DIFFUSION COEFFICIENT IN INFINITELY DILUTE SOLUTION

Andrey Nebavsky, Veronica Sarapulova

Membrane Institute, Kuban State University, Krasnodar, Russia, E-mail: neanhim@gmail.com

## Introduction

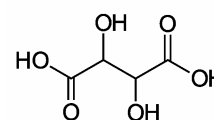
For evaluation of transport parameters of ion exchange membranes in tartrate containing solutions diffusion coefficients of hydrotartrate ( $HT^-$ ) and tartrate ( $T^{2-}$ ) ions should be known. In scientific publications and handbooks we have found only data considering double charged ion. For example, the article [1] contains temperature and concentration dependences of equivalent electrical conductivity of ammonium tartrate and alkali metals tartrates. These dependences were used for determination of temperature dependence of equivalent electrical conductivity of  $T^{2-}$  at infinite dilution ( $\lambda_0$ ). As a result, at solution temperature equal to 298,15 K  $\lambda_0(1/2 T^{2-}) = 60,49 \text{ S cm}^2/\text{eq}$ ,  $\lambda_{H^+} = 349,85 \text{ S cm}^2/\text{eq}$ . This data agree well with another literature sources, e.g. [2,3]. The aim of this work is to determine the value of equivalent electrical conductivity at infinite dilution and to calculate another transport characteristics of this ion in diluted tartrate containing solution with use of the obtained value.

## Experiments

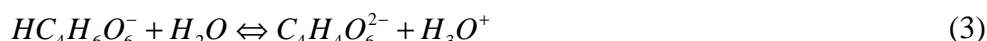
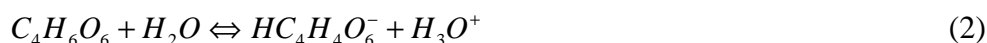
Tartaric acid solution with concentration of 0.01 M was prepared from the deionized water (1M $\Omega$  cm) and dry tartaric acid (analytical grade, manufactured by Vekton Ltd.). Another tartaric acid solutions were prepared through dilution. Specific electrical conductivity and pH of these solutions were determined using conductivity meter Econics Expert 002 and pH meter Econics Expert 001 at 298 K.

## Experimental Data Analysis

D-tartaric acid, or (R) 2,3-dihydroxybutanedioic acid, present in natural objects such as wine, has the following structure:



Chemical reactions taking place at aqueous solutions of tartaric acid can be schematically represented as following reactions:



Tartaric acid, its anions and oxonium are denoted for simplicity as:  $C_4H_6O_6 \Rightarrow H_2T$ ;  $C_4H_5O_6^- \Rightarrow HT^-$ ;  $C_4H_4O_6^{2-} \Rightarrow T^{2-}$ ;  $H_3O^+ \Rightarrow H^+$ .

In tartaric acid solutions charge can be carried by protons, hydroxyl ions, tartrate ions and hydrotartrate ions. These solutions have acidic reaction (pH = 2 - 4), hence the impact of hydroxyl ions is negligible. Specific electrical conductivity of tartaric acid solution is described by equation:

$$\kappa = \lambda_{H^+} C_{H^+} + \lambda_{HT^-} C_{HT^-} + 2\lambda_{T^{2-}} C_{T^{2-}} \quad (4)$$

from which it is relatively easy to find the equivalent conductivity of hydrotartrate anion. Here  $\lambda_i$  is equivalent electrical conductivity of ion  $i$ ,  $C_i$  is molar concentration of ion  $i$ .

For calculations using the equation (1) ionic content of solution at different concentrations of tartaric acids should be known. This content was numerically calculated from following system of equations:

$$K_1 = \frac{C_{HT^-} C_{H^+}}{C_{H_2T}} \quad (5)$$

$$K_2 = \frac{C_{T^{2-}} C_{H^+}}{C_{HT^-}} \quad (6)$$

$$C_{T^{2-}} + C_{HT^-} + C_{H_2T} = C_0 \quad (7)$$

$$2C_{T^{2-}} + C_{HT^-} = C_{H^+} \quad (8)$$

Constant values  $K_1=1.047 \times 10^{-3} \text{ mol L}^{-1}$  and  $K_2=4.57 \times 10^{-5} \text{ mol L}^{-1}$  are adopted from [4]

### Results and Discussion

Concentration dependences of specific electrical conductivity and pH of tartaric acid solutions are presented in Fig. 1. Dependence of species content, calculated using Eq. (5)–(8), upon concentration of tartaric acid solution is shown in Fig. 2.

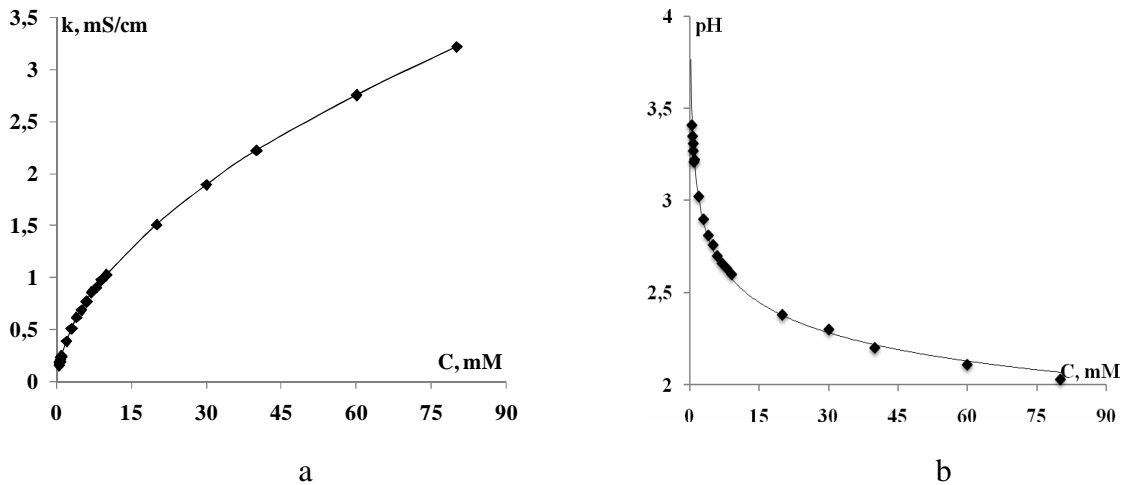


Figure 1. Concentration dependences of specific electric conductivity (a) and pH (b) of tartaric acid aqueous solutions

Values of limiting equivalent conductivity calculated with Eq. (1) using experimental values of specific electrical conductivity of tartaric acid aqueous solutions and known equivalent conductivity of tartrate anions at  $T = 298 \text{ K}$  [1] are shown in Fig. 3.

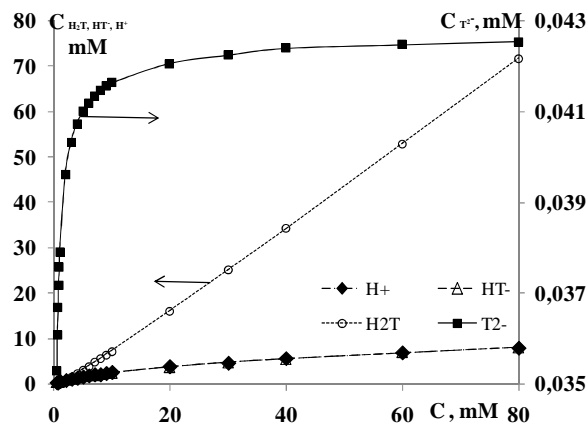


Figure 2. Component content vs concentration of tartaric acid solutions

It follows from obtained data that value of equivalent electrical conductivity of hydotartrate anion weakly depends on tartaric acid concentration in studied concentration range. Processing of experimental dependence with regression analysis method gives the value of limiting equivalent electrical conductivity  $\lambda_{HT^-} = 38,2 \text{ S cm}^2/\text{eq}$ .

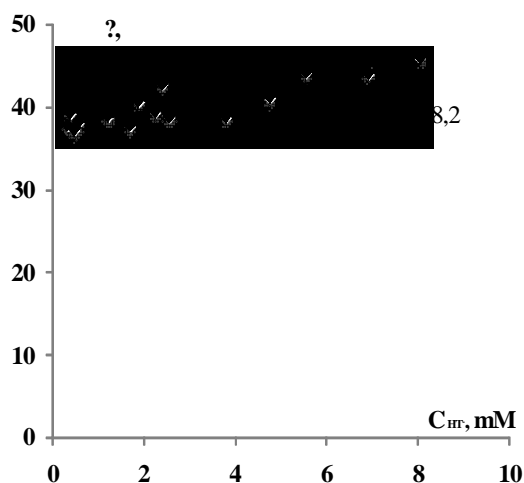


Figure 3. Dependence of equivalent electrical conductivity of hydrotartrate anion upon its concentration in 0,5 mM – 80 mM tartaric acid solutions ( $T=298\text{ K}$ )

For diffusion coefficient calculations of hydrotartrate ion at infinite dilution known equation was used:

$$D_i = \frac{RT}{|z_i| F^2} \lambda_i \quad (9)$$

where  $R$  is universal gas constant,  $F$  is Faraday number,  $T$  is temperature and  $\lambda_i$  is equivalent electrical conductivity of ion  $i$ ,  $z_i$  is its charge. Obtained value  $D_{HT^-} = 1.02 \times 10^{-5} \text{ cm}^2/\text{s}$ .

Calculation of analogous coefficient for tartrate ion using of Eq. (9) and limiting equivalent electrical conductivity of this ion, found in paper [1], gives the value:  $D_{T^{2-}} = 0.8 \times 10^{-5} \text{ cm}^2/\text{s}$ .

Obtained values seem reasonable if keeping in mind values for other single and double charged bulk ions of another ampholytes, for example, with phosphoric acid anions, diffusion coefficients for which are equal to, correspondingly:  $D_{H_2PO_4^-} = 0.96 \times 10^{-5} \text{ cm}^2/\text{c}$  and  $D_{HPO_4^{2-}} = 0.76 \times 10^{-5} \text{ cm}^2/\text{c}$  [5].

### Acknowledgement

The study was realized within French-Russian laboratory “Ion-exchange membranes and related processes”. We are grateful to CNRS, France, and to RFBR (grant 12-08-93106), RFTP (contract 02.740.11.0861), Russia, for financial support.

### References

1. Bester-Rogae M., Neueder R., Barthel J., Apelblat A. *Conductivity Studies on Aqueous Solutions of Stereoisomers of Tartaric Acids and Tartrates. Part I. Alkali Metal and Ammonium Tartrates* // *J. Solution. Chem.*, 1997. V. 26, P. 127-134.
2. D.R. Lide (Ed.), *Handbook of Chemistry and Physics*, N.Y.: CRC Press, 1997.
3. Vásquez-Garzón M., Bonotto G., Marder L., Ferreira J., Bernardes A. Transport properties of tartrate ions through an anion-exchange membrane // *Desalination*. 2010. V. 263. P. 117-121.
4. Boulton R.B., Singleton V.L., Bisson L.F. *Principles and practices of winemaking* // N.Y.: Chapman & Hall, 1996. 604 p.
5. Robinson R., Stokes R. *Electrolyte Solutions, The measurement and interpretation of conductance, chemical potential and diffusion in solutions of simple electrolytes*. London: Butterworths, 1959. 571 p.

# ELECTRICAL CONDUCTIVITY OF GEL PHASE OF SOME COMMERCIAL MEMBRANES IN AMPHOLYTE SOLUTIONS

Ekaterina Nevakshenova, Victor Nikonenko, Natalia Pismenskaya

Kuban State University, Krasnodar, Russia, E-mail: nevakshenova-ekaterina@yandex.ru

## Introduction

The application of electromembrane technologies to the food industry contributes to the increase of quality of food products. In particular, the important tasks are receiving of high quality drinking water, conditioning of wine, juices, dairy products and the separation of products of biochemical synthesis. Many of these products contain hydrocarbonates, hydrotartrates and hydrophosphates.

This work is aimed at studying the conductivity of the gel phase of a variety of commercial anion exchange membrane in solutions containing these anions, as well as at ampholytes transfer mechanisms analysis: its similarities and differences in comparison with chloride ions transfer.

## Experiments

Commercial anion exchange membranes MA-40 and MA-41 (Shchekinoazot, Russia); FTAM-E and FTAM-EDI (Fumatech, Germany); Ralex-AMH PES (MEGA, Czech Republic); AMX (Astom, Japan) and AX were chosen as the object of this study. Using the differential method and "clip" cell [1], concentration dependences of conductivity were obtained for each of the membranes in the NaCl (pH = 6,5), KHC<sub>4</sub>H<sub>4</sub>O<sub>6</sub> (pH = 4,1), NaH<sub>2</sub>PO<sub>4</sub> (pH = 4,4) and NaHCO<sub>3</sub> (pH = 8,4) solutions. Conductivity at the isoelectrical point was found as an intersection of these curves with the concentration dependences of the electrical conductivity of the solutions. According to the microheterogeneous model [2] this point characterizes the conductivity of the gel phase of the membrane  $k_{iso} = \bar{k}$  and gives insight on the transport properties of ion conducting polymer used for fabrication of membrane. The total exchange capacity of membranes was determined using back acid-base titration method [3].

## Results and Discussion

The results are summarized in Table 1.

**Table 1: Some characteristics of the studied membranes in NaCl and ampholytes solutions**

Membrane	Density g/cm <sup>3</sup>	*Exchange capacity, mmole/cm <sup>3</sup> <sub>sw</sub>	$k_{iso}^{NaCl}$ mSm/cm	$k_{iso}^{KHT}$ mSm/cm	$k_{iso}^{NaH_2PO_4}$ mSm/cm	$k_{iso}^{NaHCO_3}$ mSm/cm
FTAM-EDI	1,006	3,02	8,2	3,2	3.47	6
FTAM-E	1,075	1,85	3,2	1,2	1.51	2,3
MA-40	1,09	3,5	5,2	0,4	0.26	0,1
MA-41	1,16	1,25	3,4	0,7	1.08	1,8
Ralex AMH-PES	1,052	1,92	5,5	1,9	2.27	4
AMX	1,14	1,74	4,4	0,9	1.57	2,3
AX	1,06	3,05	6,3	1,7	2.53	4

\*for the swollen membrane in the Cl<sup>-</sup> form

Obtained data analysis shows that electrical conductivity of membranes' gel phase decreases with replacing NaCl with ampholytes solution. In membranes mostly containing quaternary ammonium groups (all investigated membranes except MA-40) electrical conductivity decreases in row NaCl > NaHCO<sub>3</sub> > NaH<sub>2</sub>PO<sub>4</sub> > KHT. For MA-40 membrane, which mainly contains secondary and tertiary amines, electrical conductivity decreases in row: NaCl >> KHT > NaH<sub>2</sub>PO<sub>4</sub> > NaHCO<sub>3</sub>. The ratio of electrical conductivities of membrane's gel phase in the form of ampholyte ions (i) and Cl<sup>-</sup> form can be represented as:

$$\frac{\bar{k}_i}{\bar{k}_{Cl^-}} \approx \frac{\sum z_i^2 \bar{D}_i \bar{c}_i}{z_{Cl^-}^2 \bar{D}_{Cl^-} \bar{c}_{Cl^-}} \approx \frac{\sum z_i^2 \bar{D}_i \bar{c}_i}{\bar{D}_{Cl^-} \bar{Q}_{Cl^-}} \quad (1)$$

Here,  $z_i$  - counterion charge;  $\bar{D}_i$  - counterion diffusion coefficient in the gel phase; the product of multiplication of the molar concentration of mobile counterions by their charge gives the exchange capacity of gel phase:  $z_i \bar{c}_i = \bar{Q}$  (eq L<sup>-1</sup>). In case of ampholytes it should be kept in mind that the gel phase can contain not only the singly charged anions present in solution, but also double charged anions produced by hydrolysis reaction in the membrane because the pH of the pore solution is higher than the pH of the equilibrium external solution. The latter is due to Donnan exclusion of H<sup>+</sup> ions as co-ions from the pore solution [4]. In order to evaluate the degree of differences between membrane transport of the ampholyte's counterion and the Cl<sup>-</sup> ion, the value of  $\bar{k}_i / \bar{k}_{Cl^-}$  is normalized to the ratio of the diffusion coefficients of the corresponding counterions in the solution ( $D_i / D_{Cl^-}$ ). The results of this data processing is presented in Table 2. We used the following values of ratios of the chloride and ampholytes ion diffusion coefficients in solution:

$$\frac{D_{Cl^-}}{D_{HT^-}} = 2,01; \quad \frac{D_{Cl^-}}{D_{H_2PO_4^-}} = 2,11; \quad \frac{D_{Cl^-}}{D_{HCO_3^-}} = 1,71.$$

**Table 2: The value  $\frac{\bar{k}_i}{\bar{k}_{Cl^-}} \frac{D_{Cl^-}}{D_i}$  for some singly charged ions of ampholytes**

Membrane	$\frac{\bar{k}_{HT^-}}{\bar{k}_{Cl^-}} \frac{D_{Cl^-}}{D_{HT^-}}$	$\frac{\bar{k}_{H_2PO_4^-}}{\bar{k}_{Cl^-}} \frac{D_{Cl^-}}{D_{H_2PO_4^-}}$	$\frac{\bar{k}_{HCO_3^-}}{\bar{k}_{Cl^-}} \frac{D_{Cl^-}}{D_{HCO_3^-}}$
FTAM-EDI	0,77	0,89	1,26
FTAM-E	0,74	1,00	124
MA-40	0,15	0,11	0,03
MA-41	0,41	0,67	0,91
Ralex AMH-PES	0,69	0,87	1,25
AMX	0,41	0,75	0,90
AX	0,54	0,85	1,09

Analysis of the data shows that the transport ability of MA-40 membrane is markedly reduced in the transition from acidic solutions ampholytes KHC<sub>4</sub>H<sub>4</sub>O<sub>6</sub> (pH = 4,1), NaH<sub>2</sub>PO<sub>4</sub> (pH = 4,4) to an alkaline solution of NaHCO<sub>3</sub> (pH = 8,4). This effect may be related to the interaction of secondary and tertiary groups of the membrane with hydroxyl ions, which leads to blockage of the fixed ionic groups. The result of this interaction should be a reduction in the effective exchange capacity of the membrane.

In the case of membranes, which mainly contain quaternary amine groups, "deceleration" of the ampholyte counterion compared with Cl<sup>-</sup> ion is reduced in the transition to a more alkaline equilibrated solution. The reason for this reduction is an increasingly strong enrichment of the pore solution with the corresponding doubly charged ampholyte counterions. This phenomenon can be taken into account using the microheterogeneous model, augmented by the equation of ion-exchange equilibrium as well as equations of ampholyte hydrolysis reactions equilibrium in the pore solution.

*The study was realized within French-Russian laboratory "Ion-exchange membranes and related processes". We are grateful to CNRS, France, and to RFBR (grants 11-08-96511, 11-08-93107, 12-08-93106), RFTP (contract 02.740.11.0861), Russia for financial support.*

### References

1. Lteif R., Dammak L., Larchet C., Auclair B. // Europ. Polymer J. 1999. V.35, No 7. P. 1187-1195.
2. Zabolotsky V.I., Nikonenko V.V. // J. Membr. Sci. 1993. V. 79. P 181-198.
3. GOST 17552-72. Ion-exchange membrane. Methods for determination of total and equilibrium exchange capacity. M.: Standards publishing, 1972.
4. Helfferich F. Ion Exchange. New York : McGraw Hill, 1962

---

# THEORETICAL AND EXPERIMENTAL STUDY OF OVERLIMITING MASS TRANSFER IN ELECTRODIALYSIS

<sup>1</sup>Victor Nikonenko, <sup>1</sup>Mahamet Urtenov, <sup>1</sup>Aminat Uzdenova, <sup>1</sup>Natalia Pismenskaya, <sup>2</sup>Vera Vasil'eva

<sup>1</sup>Kuban State University, Krasnodar, Russia, *E-mail: nikon@chem.kubsu.ru*

<sup>2</sup>Voronezh State University, Voronezh, Russia, *E-mail: viv155@mail.ru*

## Introduction

The interest to ion transfer and concentration polarisation in ion-exchange membrane systems, especially at intensive currents, is now increasing. It is due, firstly, to attempts to optimise electrodialysis (ED) of dilute solutions where its rate is low, and, secondly, to expanding research of nano- and microfluidic systems. In both cases there is a strong coupling between charge and volume transfer [1, 2], and the details of mechanism of this phenomenon is of great interest.

To attain a better understanding of these interfacial phenomena, both accurate experiment and advanced mathematical modelling are needed. In this paper we present the results of experimental and theoretical study of overlimiting ion transfer in an ED membrane system.

## Theory

For modeling ion transfer under conditions of forced convection and electroconvection, a coupled system of electrodiffusion equations with a convective term and the Navier-Stokes equations are used, taking into account the body electric force (per unit volume). A desalination channel formed by a cation exchange and an anion exchange membranes is considered. Potentiostatic mode is considered. This mode is described by the condition:

$$\Delta\varphi_{tot} = \Delta\varphi_{DC} - \frac{RT}{F} \ln \frac{c''}{c_{cm}} - \frac{RT}{F} \ln \frac{c''}{c_{am}} - iR_{m+s} = \text{const} \quad (1)$$

meaning that the potential drop (PD) across a desalination compartment is constant (or a slow function of time).  $\Delta\varphi_{tot}$  consists of the PD within the desalination compartment ( $\Delta\varphi_{DC}$ ), the Donnan PD over both membranes (determined by the counterion concentrations at the membrane surface,  $c_{cm}$  and  $c_{am}$ , as well as by the electrolyte concentration in the concentration compartment,  $c''$  (assumed a known constant), and the ohmic resistance beyond the desalination compartment.

At the conventional boundary of ion exchange membrane with the solution,  $x=0, y \in [0, L], t \geq 0$  (anion exchange membrane), and  $x=h, y \in [0, L], t \geq 0$  (cation exchange membrane), we will use two type of conditions. The first one is the Dirichlet condition firstly used by Rubinstein and Shtilman [3] where the counterion concentration is set:

$$c_2(0, y, t) = c_{am}, \quad c_1(h, y, t) = c_{cm}, \quad \text{‘1’: cation, ‘2’: anion} \quad (2)$$

The second type of boundary condition is that of Neumann:

$$\frac{\partial c_2}{\partial x}(0, y, t) = 0, \quad \frac{\partial c_1}{\partial x}(h, y, t) = 0 \quad (2a)$$

Condition (14a) follows from the assumption of quasi-uniform distribution of the space charge density (QCD) [4].

Besides, the co-ion flux through the membranes is assumed to be zero.

The velocity at the solution/membrane boundary is set zero (the no-slip condition):

$$V_x(0, y, t) = 0, \quad V_y(0, y, t) = 0, \quad V_x(H, y, t) = 0, \quad V_y(H, y, t) = 0 \quad (3)$$

At the entrance of the channel,  $y=0, x \in [0, h], t \geq 0$ , the electrolyte concentration is given; the velocity distribution here is parabolic according to Poiseuille's law:

$$c_1(x, 0, t) = c_2(x, 0, t) = c_0 \quad (4)$$

$$V_x(x,0,t) = 0, \quad V_y(x,0,t) = 6V_0 \frac{x}{h} \left(1 - \frac{x}{h}\right) \quad (5)$$

At the exit of the channel,  $y=L$ ,  $x \in [0, h]$ ,  $t \geq 0$ , we use ‘soft’ conditions on the concentration and potential; the velocity distribution is again assumed parabolic:

$$\frac{\partial c_i}{\partial y}(x, L, t) = 0, \quad i = 1, 2, \quad \frac{\partial \varphi}{\partial y}(x, L, t) = 0, \quad (6)$$

$$V_x(x, L, t) = 0, \quad V_y(x, L, t) = 6V_0 \frac{x}{h} \left(1 - \frac{x}{h}\right)$$

Conditions (6) correspond to the solution of problem (1)-(5) under the local electroneutrality assumption, where no current-induced convection occurs.

The initial conditions at  $t = 0$  are consistent with the other boundary conditions

### Discussion

At underlimiting current densities, the novel model based on the Nernst-Planck-Poisson-Navier-Stokes equations (NPP-NS model) gives the same results as the convective diffusion (NP-NS) model developed earlier [5]. When considering a section normal to the fluid flow, it is possible to compare the NPP-NS model with a 1D model, which uses the Nernst conception of diffusion boundary layer (NPP model).

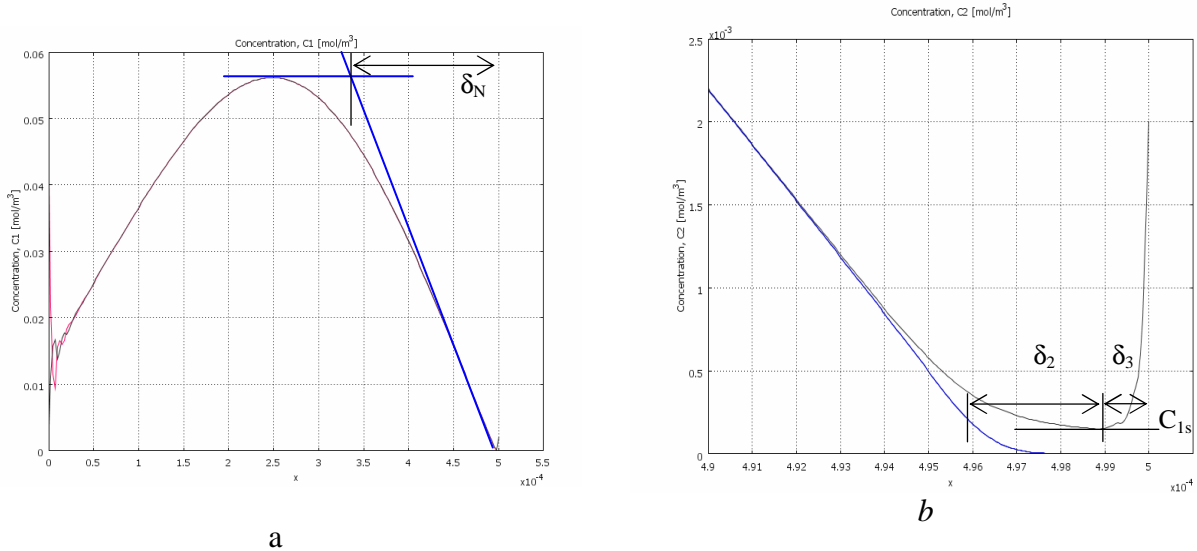


**Figure 1.** Concentration profile calculated according to NPP-NS model at a current density close to  $i_{lim}^{theor}$ . An anion-exchange membrane is on the left, and a cation-exchange membrane, on the right

To compare the NPP-NS model with the NPP model, the concentration profile of cations was calculated at the distance equal to 1.7 mm from the entrance (Fig. 1) at  $\Delta\varphi_{tot} = 0.6$  V. The local current density, according to the NPP-NS model, is slightly higher than the theoretical limiting one and equal to  $i_{1.7mm} = 0.0969$  A m<sup>-2</sup>. The thickness of the Nernst DBL,  $\delta_N$ , found by the intersection of tangents as shown in Fig. 1a is 153.3  $\mu$ m. By applying the values of current density and  $\delta_N$  for the bulk concentration  $0.056$  mol m<sup>-3</sup>, we can find, by using the NPP model, the minimum counterion concentration  $C_{1s} = 1.51 \times 10^{-4}$  mol m<sup>-3</sup>, the thickness of the quasiequilibrium zone of the space charge region (SCR),  $\delta_3 = 1.15$   $\mu$ m, and the thickness of the electromigration zone of SCR,  $\delta_2 = 3.1$   $\mu$ m. As Fig. 1b shows, the found values match very well the results of the numerical solution of the NPP-NS model. The PD in the depleted DBL of the thickness 153  $\mu$ m, according to the NPP model, is 513 mV.

Fig. 2 shows experimental and calculated current-voltage curves. The ratio  $i / i_{lim}^{theor}$  is presented as a function of the ‘corrected’ PD equal to the measured pd reduced by the ohmic pd. If the LEN

assumption is used (NP-NS model), the current density is limited by the  $i_{\text{lim}}^{\text{theor}}$  value. The  $I$ - $V$  curve calculated according to the NPP-NS model qualitatively matches well experimental curves. The limiting current density,  $i_{\text{lim}}^{\text{exp}}$ , determined by the point of tangents intersection does not coincide with  $i_{\text{lim}}^{\text{theor}}$  and depends on the membrane surface properties.

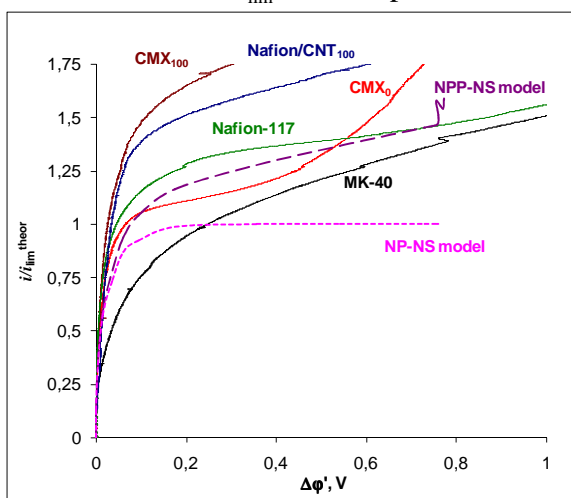


Figure 2. Ratio  $i/i_{\text{lim}}^{\text{theor}}$  as a function of the “corrected” pd. Experimental data for different cation-exchange membranes (heterogeneous MK-40, homogeneous Nafion-117 and CMX, Nafion-117 covered with carbon nanotubes (CNT), and calculations according to NP-NS model and to a model based on the Nernst-Planck-Poisson and Navier-Stokes equations (NPP-NS model). The subscript shows the number of hours of membrane treatment at an overlimiting current. A part of experimental data is taken from [3, 4]

Fluid and electric current streamlines in a desalination channel formed by an anion- and a cation-exchange membranes calculated according to NPP-NS model are shown in Figs. 2 and 3. In all cases a  $0.01 \text{ mol m}^{-3}$  NaCl solution is considered as a feed solution. The channel length and height are 2 and 0.5 mm, respectively. The forced flow average velocity is  $0.1 \text{ mm s}^{-1}$ .

Time=232 Surface: Velocity magnitude (m/s) Streamline: Velocity field Streamline:

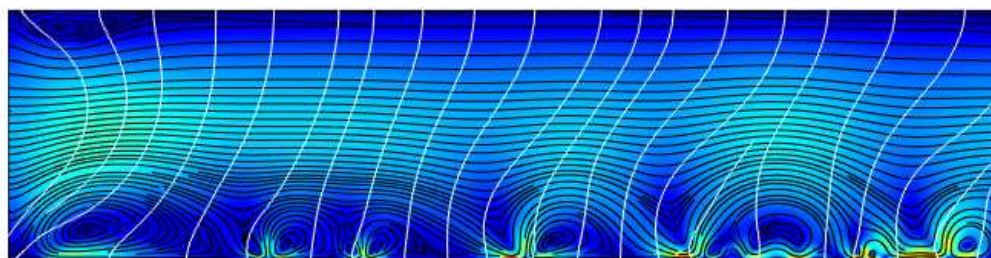


Figure 3. Velocity and electric current streamlines calculated according to NPP-NS model at  $i > i_{\text{lim}}^{\text{theor}}$ . Vortices arise at the cation-exchange membrane situated at the bottom

### Acknowledgments

The study was realized within French-Russian laboratory “Ion-exchange membranes and related processes”. We are grateful to CNRS, France, and to RFBR (grants 11-08-00599, 11-01-96505, 11-08-93107 and 12-08-00188), Russia, and to FP7 Marie Curie Action “CoTraPhen” project PIRSES-GA-2010-269135 for financial support.

### References

1. Zaltzman B., Rubinstein I., // J. Fluid Mech. 2007. V. 579. P. 173–226.
2. Nikonenko V., Pismenskaya N., Belova E., Sistat Ph., Larchet Ch., Pourcelly G. Intensive current transfer in membrane systems: Modelling, mechanisms and application in electro dialysis // Adv. Colloid Interface Sci. 2010. V. 160. P. 101-123.
3. Rubinstein I.; Shtilman L. Voltage against current curves of cation exchange membranes // J. Chem. Soc., Faraday Trans. 1979. V. 75. P. 231-246.
4. Urtenov M.A.-Kh., Kirillova E.V., Seidova N.M., Nikonenko V.V. Decoupling of the Nernst-Planck and Poisson equations. Application to a membrane system at overlimiting currents // J. Phys. Chem. B. 2007. V. 111, № 51. P.14208-14222.

# SILVER-ION-EXCHANGE NANOCOMPOSITE ELECTRODE MATERIAL BASED ON HOMOGENEOUS PERFLUORINATED MEMBRANE AND CARBON SUPPORT

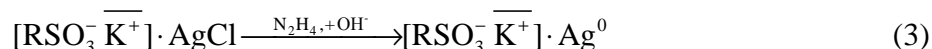
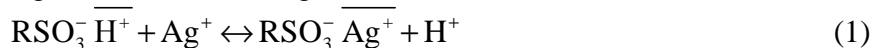
Viktoriya Novikova, Mikhail Chayka, Tamara Kravchenko  
Voronezh State University, Voronezh, Russia, E-mail: krav@chem.vsu.ru

## Introduction

In recent years substantial progress towards the creation of advanced electrochemical devices has been achieved thanks to the use of perfluorinated membranes and based on them composites increasing the aggregative stability of metal nanoparticles. The membranes act as templates for the formation of nanoparticles. They have a developed system of pores, where the metal particles are formed, whose size corresponds to the initial pore size membrane, that is a few nanometers. Ionogenic centers in the matrix are the source of the ions required for reaction and a place to drain products.

## Experiments

The object of study of this paper was the silver-ion-exchange nanocomposite based on perfluorinated cation exchange membranes–carbon black Ag<sup>0</sup>/MF-4SK/C. Prior to the synthesis a homogeneous membrane (in isopropyl alcohol 7.0% solution) was mixed with carbon black UM-76 and subjected to ultrasonic dispersion. The suspension in an amount of 0.02 ml was applied to a graphite electrode and dried to the solvent dull removal. Chemical deposition of silver in the membrane MF-4SK and composite MF-4SK/C consisted of ion-exchange saturation followed by reduction, including an intermediate stage of silver chloride formation:



Analysis of the microstructure of nanocomposite Ag<sup>0</sup>/MF-4SK/C was performed using transmission electron microscopy unit JEM-101 Jeol company at an accelerating voltage of 100 kV. Qualitative and quantitative analysis of the samples in the reduced form Ag<sup>0</sup>/MF-4SK/C and ion Ag<sup>+</sup>/MF-4SK/C with different mass fraction of polymer (20% - 40%) was performed by energy dispersive analysis unit JSM 6380LV (Japan) with the attachment INCA Energy - 250.

## Results and Discussion

Transmission electron microscopy detected silver particles of chemically deposited in the nanocomposite Ag<sup>0</sup>/MF-4SK/C size of 3 nm (Fig. 1). It was established that the silver particles are formed in the pores of the membrane that limit their size [1].

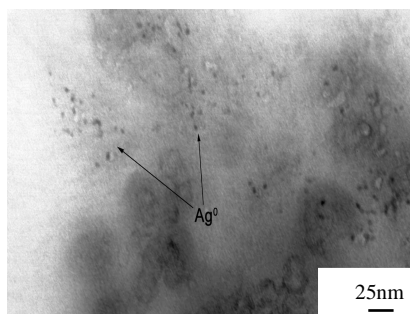


Figure 1. Electron micrographs of the surface of the nanocomposite Ag<sup>0</sup>/MF-4SK/C

As a result of energy dispersive analysis of samples in the reduced Ag<sup>0</sup>/MF-4SK/C and ion Ag<sup>+</sup>/MF-4SK/C form of silver (Fig. 2), we can conclude that with increasing of the mass fraction MF-4SK, and hence the ionic groups, the silver content increases linearly.

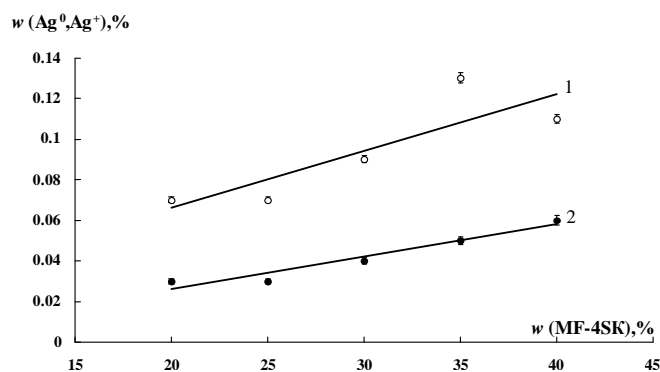


Figure 2. The dependence of the atomic fraction of silver embedded in the composite of the mass fraction of MF-4SK in the nanocomposite  $\text{Ag}^0/\text{MF-4SK}/\text{C}$ : 1 -  $\text{Ag}^+$  - form; 2 -  $\text{Ag}^0$ -form

The electrochemical activity of the nanocomposite  $\text{Ag}^0/\text{MF-4SK}/\text{C}$  was studied in the reaction of molecular oxygen electroreduction. For membrane MF-4SK deposited on a graphite electrode (Fig. 3a) decrease of the limiting current  $i_{\text{lim}}$  compared with the C-electrode was found. This is due to diffusion limitations in the film, and as a consequence, difficult course of the reaction of oxygen on a carbon substrate. Some increase  $i_{\text{lim}}$  in the nanocomposite  $\text{Ag}^0/\text{MF-4SK}$  compared with MF-4SK may be due to the increasing contribution of the four-electron reaction mechanism to electroreduction of molecular oxygen, as a result of oxygen reaction on the dispersed particles of silver (Fig. 3b). The introduction of carbon black into the membrane MF-4SK makes composite MF-4SK/C electroconductive. The increase in current on the polarization curve in the MF-4SK/C in comparison with the membrane MF-4SK is associated with an increase in the electronic conductivity of the composite, and the occurrence of oxygen reduction reaction on carbon black particles (Fig. 3c). Some increase  $i_{\text{lim}}$  in the composite MF-4SK/C in comparison with bulk graphite electrode may be due to the occurrence of reactions to the carbon black particles dispersion (Fig. 3d). While the current growth in the nanocomposite  $\text{Ag}^0/\text{MF-4SK}/\text{C}$  compared with the composite MF-4SK/C (Fig. 3d) can be explained by the presence of silver nanoparticles, which leads to an acceleration of the reaction of electroreduction of molecular oxygen by the catalytic action of the particles, and well as the contribution of four-electron mechanism.

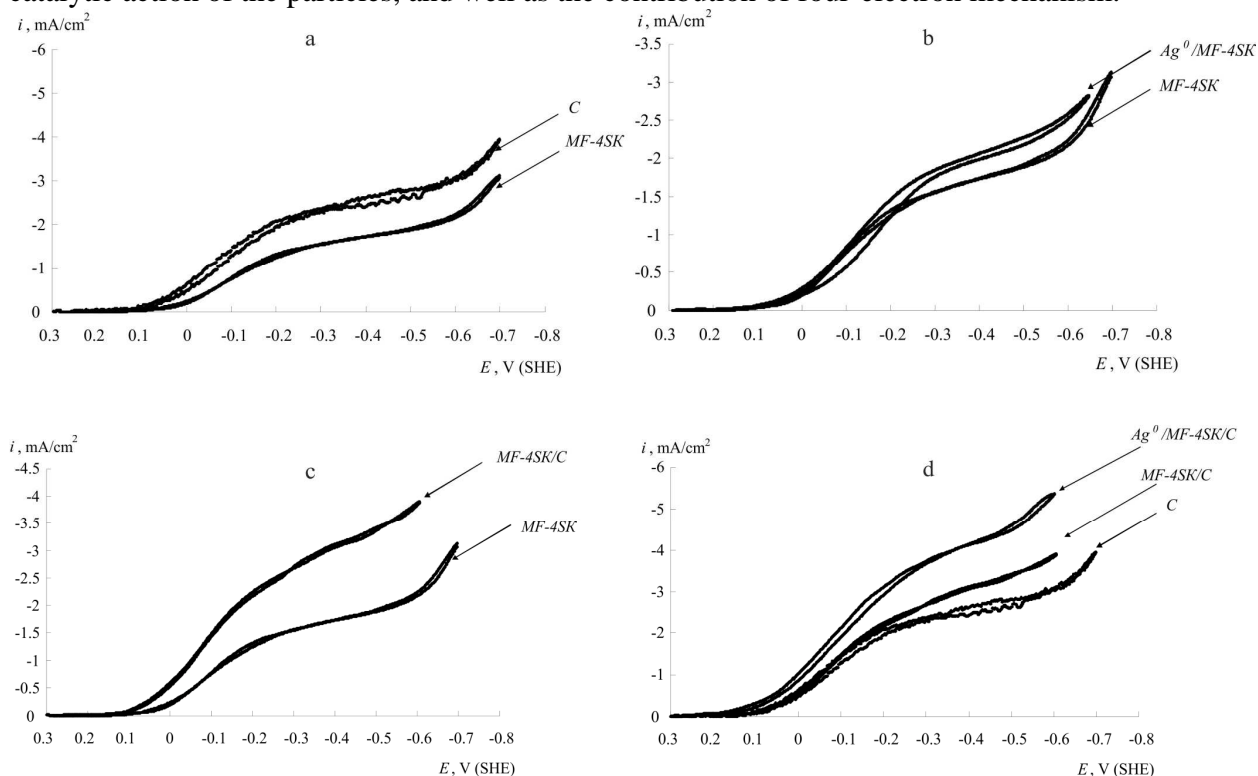


Figure 3. Polarization curves of electroreduction of molecular oxygen in 0.1 M  $\text{H}_2\text{SO}_4$  solution at the electrodes studied. The speed of rotation of the electrode  $\omega = 600 \text{ rev/min}$

The value of Tafel slope of 0.112-0.121V in high overpotential on composite electrodes (Table 1) corresponds to delayed stage of the first electron addition to the oxygen molecule:



Reducing of the slope in the low overpotential (Table 1) is not associated with a the rate change of the determining step, possibly due to adsorption  $\text{OH}_{\text{ads}}$ , as well as the formation of surface oxides, which prevent oxygen adsorption [2-3].

**Table 1: Tafel slope for studied at the electrode in 0.1 M  $\text{H}_2\text{SO}_4$**

Lg[(i-j <sub>lim</sub> )/(i <sub>lim</sub> -j)]-E, V					
Ag	C	MF-4SK	Ag <sup>0</sup> /MF-4SK	MF-4SK/C	Ag <sup>0</sup> /MF-4SK/C
0.112	0.135	I 0.056	I 0.059	I 0.056	I 0.057
		II 0.112	II 0.113	II 0.117	II 0.121

The linear dependence of the limiting current of oxygen electroreduction  $i_{\text{lim}}$  vs the square root of electrode rotation speed  $\omega$  indicates that the process is limited by external diffusion (Fig. 4).

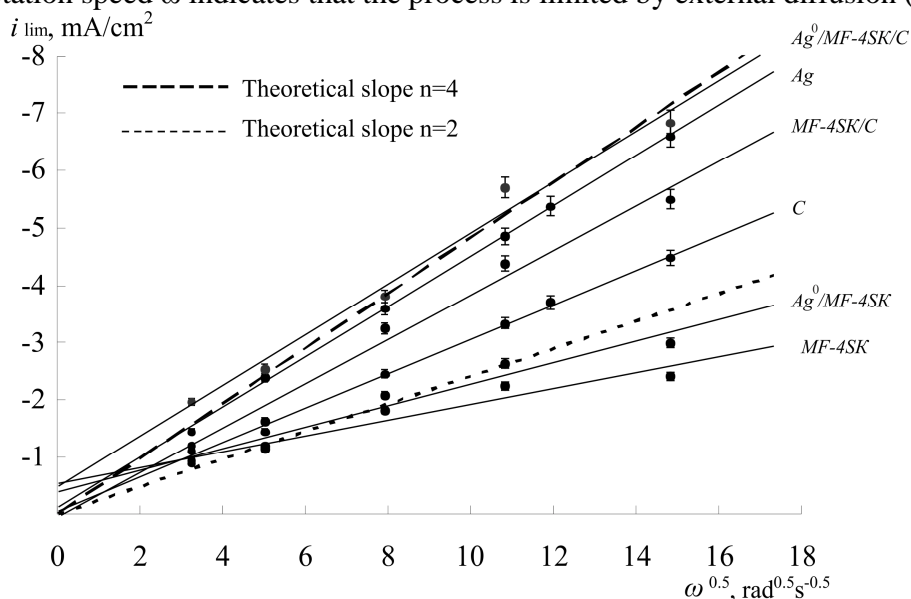


*Figure 4. Dependence of limiting diffusion current  $i_{\text{lim}}$  of molecular oxygen electroreduction vs the square root of disk electrode rotation speed  $\omega$  in 0.1 M  $\text{H}_2\text{SO}_4$  solution for studied at the electrode*

### Conclusion

Chemical deposition of silver in ion-exchange matrix created a nanocomposite  $\text{Ag}^0/\text{MF-4SK/C}$  that allows to change the amount of deposited silver varying the concentration of ionic groups in the membrane MF-4SK. The increase in current electroreduction of molecular oxygen on  $\text{Ag}^0/\text{MF-4SK/C}$  nanocomposite compared to the composite MF-4SK/C is due to the presence of silver particles, leading to an acceleration of the reaction. The process of oxygen reduction is limited by external diffusion of the oxidant.

*The work is supported by the Russian Foundation for Basic Research (№ 10-08-00847, № 11-08-00174\_a).*

### References

1. Novikova S.A., Yurkov G.Y., Yaroslavtsev A.B. Synthesis and transport properties of materials based on perfluorinated membrane MF-4SK and sulfonated polyetheretherketone with particles of copper and silver // *Inorganic materials*. 2010. V.46. № 7. P. 885-891.
2. Sarapuu A., Kasikov A., Laaksonen T. et al. Electrochemical reduction of oxygen on thin-film Pt electrodes in acid solutions // *J. Electrochimica Acta*. 2008. V. 53. P. 5873-5880.
3. Markovic N.M., Gasteiger H.A., Grgur B.N. et al. Oxygen reduction reaction on Pt (111): effects of bromide // *J. Electroanal. Chemistry*. 1999. V. 467. P. 157-163.

## MEMBRANE SCALING ISSUES IN ELECTRODIALYSIS OF BRACKISH WATER REVERSE OSMOSIS BRINES

Yoram Oren, Evgenia Gulaev, Meital Assraf-Snir, Nofar Asa-Wolfson, Jack Gilron

Zuckerberg Institute for Water Research, Ben-Gurion University of the Negev, Beer-Sheva, Israel,

E-mail: yoramo@bgu.ac.il

Today, electrodialysis (ED) is considered as optional stage in the treatment chain of brackish water reverse osmosis (BWRO) brines towards near-zero liquid discharge (ZLD), and, in general, is used for increasing the recovery ratio of inland desalination processes to values over 95% [1, 2]. However, in the ED-ZLD approach, the concentrations involved in the concentrate compartments of the ED stack are high (up to 12-15 wt% TDS) and may be saturated or supersaturated with respect to some sparingly soluble salts such as calcium and barium sulfates and silica. This may pose precipitation problems within the ED stack on the membranes, spacers, inlets and outlets. Scales of sparingly soluble minerals have deleterious effects on the ED performance, resulting in a significant, often irreversible increase of electrical and hydraulic resistance of the stack and, consequently in a larger energy demand.

In this study we investigate the effect of different physico-chemical parameters on silica transport across ion exchange membranes as well as the nucleation and crystal growth of calcium sulfate on and inside ion-exchange membranes, as the two key scaling factors in the above system.

Silica is present in significantly high concentrations (> 10 ppm) in many brackish water sources. It may reach its solubility limits (80-100 ppm depending on the TDS) in the RO brines. Depending on the ED electrochemical operational conditions, silica may either largely remain in the ED diluate or transported through the ion exchange membranes to the ED concentrate. In the former case some limitations may be imposed on the further use of the ED diluate while in the latter, silica may precipitate within the ED stack or foul the ion exchange membranes, thus impairing its efficacy.

Silica transport through anion exchange membranes was studied with respect to current-voltage characteristics, type of membranes (homogeneous and heterogeneous), its concentration and type of the electrolyte. It was concluded that the extent of water splitting at the interface is a major factor dictating silica flux through anion exchange membranes. It was also found that silica can diffuse through ion exchange membranes in its non-charged form. The effect of current density and membrane type on silica flux is depicted in Figures 1.

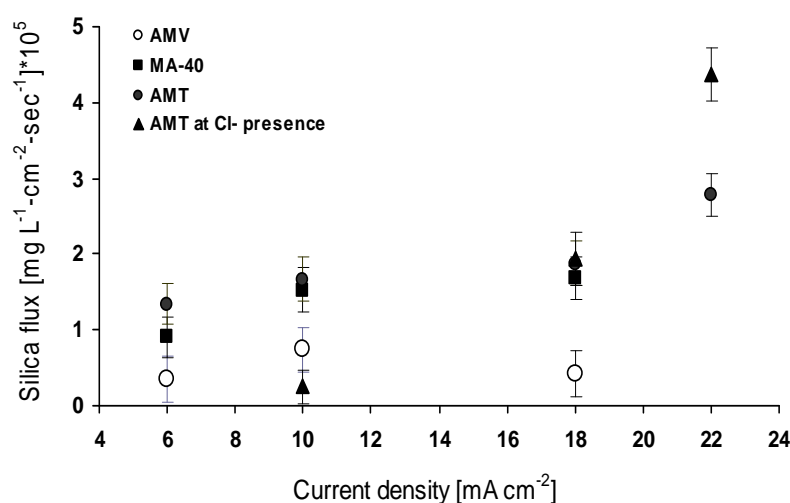


Figure 1.  $\text{SiO}_2$  fluxes through AMT, MA-40 and AMV membranes in the presence of sulfate and AMT in the presence of chloride at ionic strength  $0.015 \pm 0.002\text{N}$ , with initial silica concentration of 100 ppm

Calcium sulfate precipitation was studied in a Donnan exchange experimental setup as a first step towards characterizing the conditions under which scaling occurs on or within ion exchange membranes. In this setup an anion exchange membrane separates  $\text{CaCl}_2$  and  $\text{Na}_2\text{SO}_4$  solutions

while scaling occurs as  $2\text{Cl}^-$  ions are exchanged with  $\text{SO}_4^{2-}$ . Figure 2 shows SEM photographs of scaled homogeneous (AMV) and heterogeneous (MA-40) membranes. It is clearly seen that  $\text{CaSO}_4$  scaling mostly occurs on the AMV outer surface (2A) while it is typically located within the MA-40 membrane (2B), indicating a clear dependence of the precipitation sites and its nature on the membrane structure.

Figure 3 shows the concentration change of scaled calcium as a function of time within the MA-40 membrane. The amount of calcium found inside the membrane after 15 minutes ( $\sim 0.2 \text{ mg/cm}^2$ ) is similar to that found in a pristine membrane after equilibration in  $0.5\text{M CaCl}_2$ . This indicates an insignificant  $\text{CaSO}_4$  precipitation in this time range. A significant increase in calcium concentration is, however, observed after 30 minutes. This correlates well with a sulfate flux decline observed after this time of operation. After one hour, calcium concentration reaches practically a constant value ( $\sim 0.5 \text{ mg/cm}^2$ ). This is probably due to the lack of availability of additional sites for crystal growth inside the membrane and from this point, on any precipitation will occur on, rather than inside the membrane.

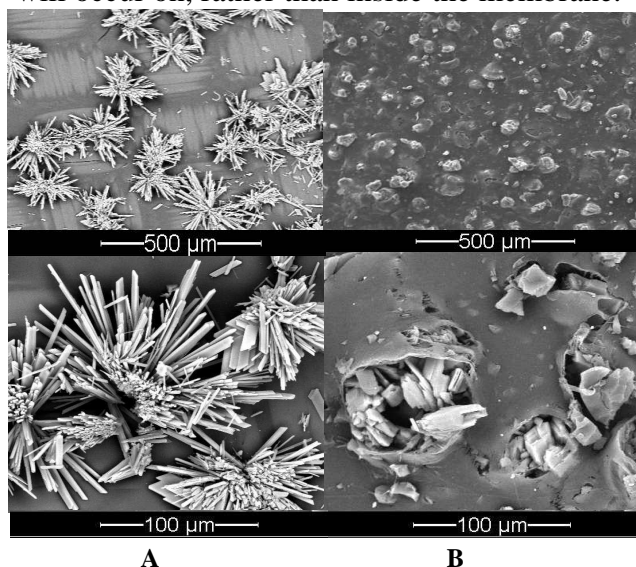


Figure 2. SEM images of  $\text{CaSO}_4$  scale on: A) homogeneous AMV. Showing crystals on the surface; B) heterogeneous MA-40 membranes. Showing crystals protruding from a defect in the membrane

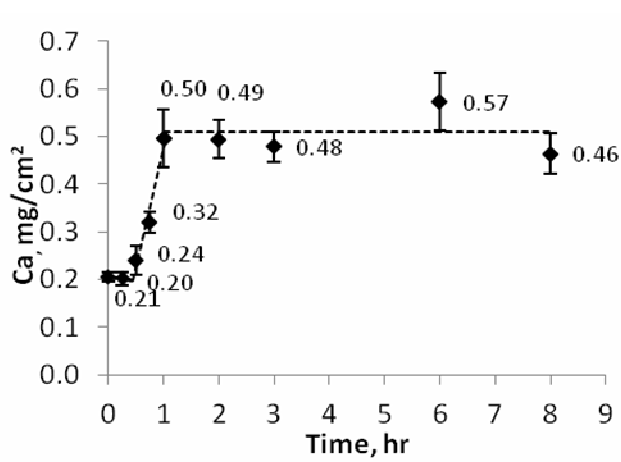


Figure 3. Calcium concentration in scaled MA-40 as a function of time operation; feed solutions are  $0.5\text{M Na}_2\text{SO}_4$  and  $0.5\text{M CaCl}_2$  in each scaling experiment

## References

1. Oren Y., Korngold E., Daltrophe N., Messalem R., Volkman Y., Aronov L., et al., Pilot studies on high recovery BWRO-EDR for near zero liquid discharge approach // Desalination. 2010. Vol. 261. P. 321.
2. Rautenbach R., Habbe R. Seeding technique for ‘Zero-Discharge’ processes, adaption to electrodialysis // Desalination. 1991. Vol. 84. P. 153.

---

# MICROSTRUCTURAL CHARACTERISTICS OF CARBON SUPPORTED $Ag_x@Pt$ ELECTROCATALYSTS FOR LOW TEMPERATURE FUEL CELLS

Helena Pakhomova, Aleksey Mar'janov, Aleksey Mikheykin, Vasily Pryadchenko, Aleksey Kozakov, Maria Evstegneeva, Vladimir Guterman

Southern Federal University, Rostov-on-Don., Russia, E-mail: [pahomova-elena@yandex.ru](mailto:pahomova-elena@yandex.ru)

## Introduction

Hydrogen-air fuel cells (FC) are an important component of hydrogen power engineering. However, cost of the energy produced by low temperature fuel cells still remains rather high for their commercialization. It's due to the using of an expensive material - the platinum electrocatalyst, which composes of platinum nanoparticles supported to highly dispersed carbon. Platinum shows high catalytic activity and chemical stability. It is possible to obtain stable nanoparticles of small size which possesses big surface area. Unfortunately an effective non-platinum catalyst hasn't been created yet. One of the ways to improve the electrocatalyst efficiency and to reduce the cost of electrode material is preparation metallic nanoparticles with special structure such as the "Pt-shell M-core" type. M-core could show positive effect on the Pt-shell catalytic activity. Additional advantage of "Pt-shell M-core" nanoparticles in comparison with Pt-alloy nanoparticles consist in core, protected by the shell from aggressive environment. Usage of nanoparticles with "Pt-shell M-core" structure allows to avoid membrane pollution by  $M^+$  cations and its following destruction. The choice of silver as a core metal is dealt with a higher thermodynamic stability in comparing with copper or nickel. It has a crystal lattice similar to platinum (face-centered cubic) with close parameter of an elementary cell that is more suitable for platinum monolayer growth on Ag-core surface. The aims of this investigation were preparing  $Ag_x@Pt/C$  by "wet" synthesis, and studying microstructural characteristics and morphological stability of  $Ag_x@Pt/C$  electrocatalysts in as-prepared and post-treated states.

## Experiments

The primary and the secondary  $Ag_x@Pt/C$  materials were prepared, respectively, by successive and simultaneous reduction of  $Ag^+$  and Pt (IV) in water-ethylene-glycol solutions of their precursors at room temperature. Carbon black (Vulcan XC-72) was used as support for nanoparticles. Then both types of materials were treated by perchloric acid at  $90^\circ C$  aiming to remove uncovered Ag-core from the primary  $Ag_x@Pt/C$  and to form secondary  $Ag_x@Pt$  nanoparticles. Microstructure and electrochemical active surface area (ECSA) of the electrocatalysts were investigated. XRD, TEM, XPS, gravimetry, cyclic voltammetry and some other methods were used for the characterization of prepared Ag-Pt/C materials.

## Results and Discussion

Using described above technique we have prepared  $Ag_x@Pt/C$  ( $1 \leq x \leq 3$ ) and Pt-Ag/C nanoscale materials with metal loading from 15 to 53 % wt/wt. The average diameter of crystallites was from 3 to 9 nm. ECSA was from 15 to  $100 \text{ m}^2/\text{g(Pt)}$ . XRD patterns of prepared catalysts show the presence of mixture of silver and Pt-Ag alloy nanoparticles (Fig. 1). After materials treatment in the boiling  $HClO_4$ , silver was partly washed out of the materials, the surface of nanoparticles was enriched with platinum. It was observed that silver dissolution was less characterized for the primary  $Ag_x@Pt/C$  materials in comparing with  $Ag_xPt/C$  alloy catalysts. Besides, after the treatment the average grain size of Pt-Ag/C increased. Fig. 2 shows a decrease in the amount of silver after the treatment of materials in boiling acid. This suggests that the silver nanoparticles and partly silver from core was dissolved and washed out. Note, these changes were observed at the initial stage of the aggressive environment impact.

Peaks of Ag dissolution ( $\sim 430 \text{ mV}$ ) and  $Ag^+$  reduction ( $\sim 350 \text{ mV}$ ) were observed on cyclic voltammogram for as-prepared PtAg/C catalysts (Fig.3). Cyclic voltammograms for  $Ag@Pt/C$  and  $Ag_3@Pt/C$  materials hadn't such peaks and were similar to Pt/C curves.

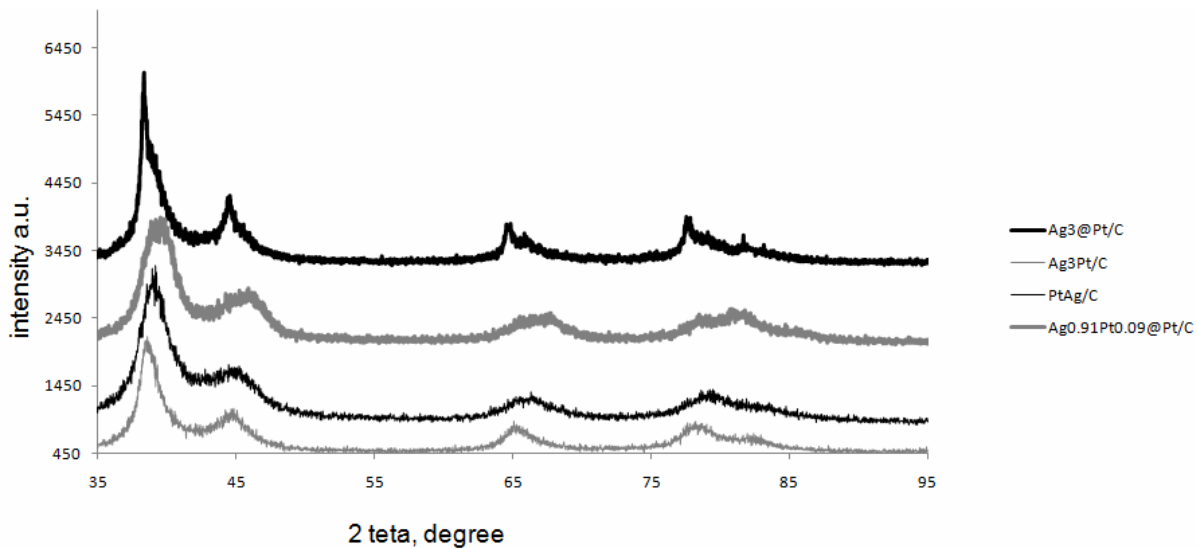


Figure 1. XRD patterns of Pt-Ag/C electrocatalysts

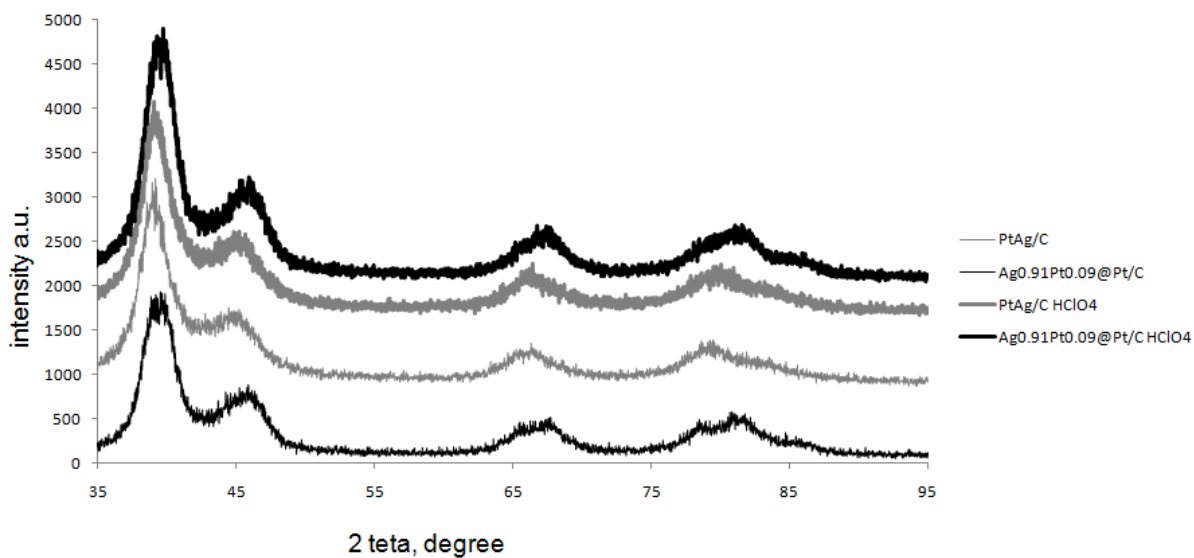


Figure 2. XRD patterns of Pt-Ag/C electrocatalysts before and after (HClO<sub>4</sub>) acid treatment

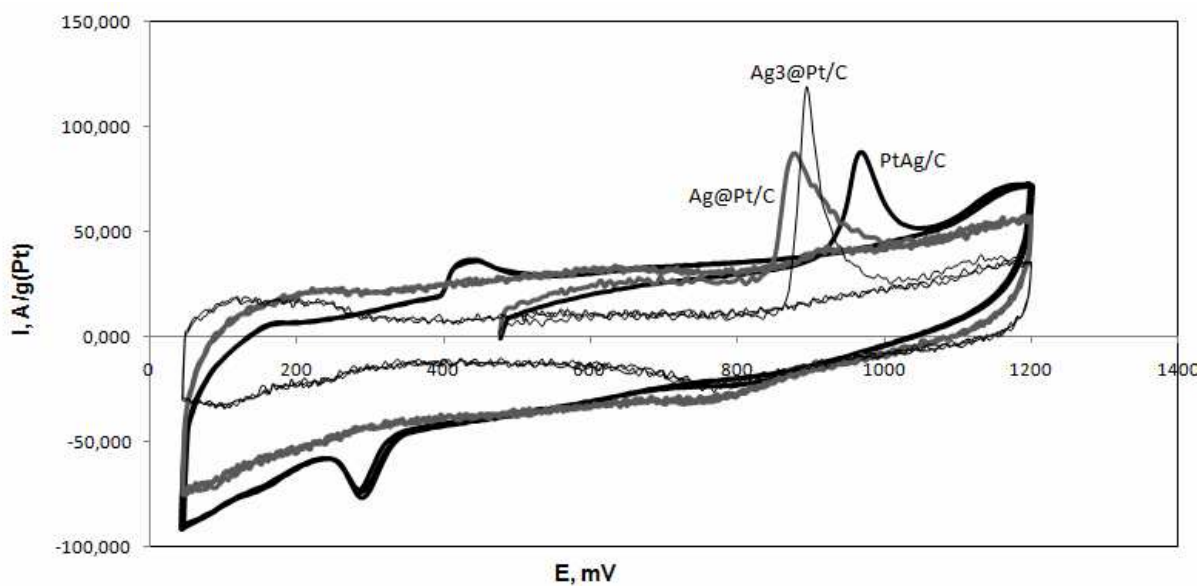


Figure 3. Cyclic voltammograms of Pt-Ag/C electrocatalysts in 1M H<sub>2</sub>SO<sub>4</sub>. Potential rate 40 mV/s. Ar atmosphere

Formation of nanoparticles with “core-shell” structure was indirectly confirmed by XPS and XANES data.

We have concluded the acid treatment was a necessary stage of Pt-Ag/C catalysts preparation because it allowed to form “core-shell” structure and prevented membrane pollution.

*This work was supported by Russian Foundation for Basic Research, projects nos. 10-03-00474a and 11-08-00499a.*

### References

1. *Chen Y., Yang F., Dai Y., Wang W., Chen S.* Ni@Pt Core–Shell Nanoparticles: Synthesis, Structural and Electrochemical Properties // *J. of Phys. Chem. C.* 2008. V.112. I. 5. P.1645-1649.
2. *Liu Ru-Shi., Chen H.-M., Hu S.-F.* Synthesis and characterization of nano metals with core-shell structure // *CHINA PARTICUOLOGY.* 2004. V. 2. No. 4. P. 160-163.

---

## BEHAVIOUR FEATURES OF ION-EXCHANGE MEMBRANES IN THE AMMONIUM SALT SOLUTIONS

<sup>1</sup>Ivan Pantyukhin, <sup>2</sup>Darya Medyantseva, <sup>1</sup>Svetlana Shishkina

<sup>1</sup>Vyatka State University, Kirov, Russia, *E-mail: vgu\_tep@mail.ru.*

<sup>2</sup>KCKK Mineral Fertilizer Plant, CJSC, Kirovo-Chepetsk, Russia. *E-mail: Darya.Medyantseva@kckk.ru*

### Introduction

At the present time polymer ion-exchange membranes are used in separation processes of the mineral fertilizers production (in particular, the ammonium nitrate production) and in alternative technologies when putting galvanic coatings (ammine electrolytes). This makes it necessary to study properties of ion-exchange membranes in the solutions containing ammonium salts. It is known [1] that the ammonium ion is formed by the interaction between a pair of electrons of the nitrogen atom and fourth proton in the ammonia molecule generating coordination bond. It is also known that this ion has a number of behavior features in water solutions, such as: negative values of hydration [2] and peculiar hydrolysis mechanism having an ammonium hydrate as a result [1].

The purpose of this paper is to investigate the influence of ammonium salts on a number of properties of polymer ion-exchange membrane, such as: water contents, electro conductivity and limiting current of the current voltage curve. Heterogeneous membranes domestically produced were investigated: the cation exchange MC-40 membrane and the anion exchange MA-40 and MA-41 ones. MC-40 contains the  $\text{SO}_3^-$  fixed groups, MA-40 has generally secondary and tertiary amino groups and MA-41 holds basically quaternary ammonia hydroxides.

### Experiments

Maximum of the water content was estimated by means of gravimetric analysis, contents of free and bound water were determined with the differential scanning calorimetry (DSC-60, Shimadzu corporation). The resistant values were measured by means of the Z-2000 Impedancemeter. The current and voltage ones to draw current-voltage curves were taken in the four-chamber cell having platinum electrodes. The voltage drop values on the membrane after investigation were measured by means of two chlorine-silver electrodes those were contacting with the membrane through the Luggin's capillaries closely brought.

### Results and Discussion

The MC-40 membrane that has been equilibrated with the sodium chloride and sodium and ammonium nitrate solutions has practically equal common water content. The count of water molecules on one fixed group is almost equal for all of the solutions and it is in the 6.5–7 interval. If we accept that the hydration number of sulfonate group is 2 [3], then the count of the water molecules connected with a simple alkali counterion is in the 4–5.5 interval that is coordinated with the data [4] for singly-charged cation in the water solutions.

The MA-40 membrane has its common water content decreased in the ammonium nitrate solutions. It should be noted that the share of free water even a bit increased, but the bound water content and the count of molecules on one fixed group decreased sharply. It could be explained by existing of the ammonium ion at low concentrations in the form of neutral-charged particles of ammonia hydrate [1], those when getting in the membrane deprotonate its secondary and tertiary fixed amino groups [5].

Deprotonated groups having no charge do not interact with counterions and lose hydration water. The ammonium cations those are formed by the deprotonating of fixed groups leave the gel phase by the Donnan effect, but they could exist in the inter-gel one and also in meso- and macropores. This cations have the negative values of hydration and could randomize water structure, that increases the count of free molecules. The decreasing in the hydration of ion pairs in the MA-41 membrane that have been equilibrated with the sodium chloride solution can be associated with existing of secondary and tertiary amino groups in the membrane phase (until 20% [6]) and with their deprotonation.

**Table 1: Hydration properties of the membranes**

Membrane type	Solution type, concentration 0,2 M	Water content, %	Free water mass, g/g. dry membrane	Free water percentage, %	Bound water mass, g/g. dry membrane	Bound water percentage, %
MC-40	NaCl	53,59	1,84	28,78	1,59	24,81
	NH <sub>4</sub> NO <sub>3</sub>	57,12	1,89	32,11	1,48	25,01
MA-40	NaCl	64,18	1,94	28,89	2,36	35,29
	NH <sub>4</sub> NO <sub>3</sub>	61,04	2,32	30,17	2,38	30,87
MA-41	NaCl	41,86	1,11	18,81	1,36	23,05
	NH <sub>4</sub> NO <sub>3</sub>	31,77	0,92	14,88	1,05	16,89

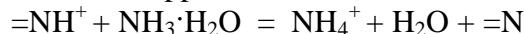
The electro conductivity values of the MC-40 membrane are much larger in the ammonium salt solutions than the ones in the sodium chloride solutions due to the presence of protons those are formed by hydrolysis (ph of the NH<sub>4</sub>NO<sub>3</sub> solutions is ca. 4.8–5.5) and due to large mobility of the ammonium ions ( $\lambda_{Na^+} = 52$ ,  $\lambda_{NH_4^+} = 76 \text{ S} \cdot \text{cm}^2 \cdot \text{g}^{-1} \text{equiv}^{-1}$ ).

The MC-40 and MA-41 membranes have the same styrenedivinilbenzene matrix and the similar ion-exchange capacity values: 1.54 and 1.44 respectively. In addition, the functional groups of these membranes are strong acid (MC-40) and strong-basic (MA-41), so they are completely dissociated in any conditions. Therefore, the electro conductivity values of the MC-40 and MA-41 membranes are larger than those of the MA-40 one.

In the sodium chloride and ammonium nitrate solutions the electro conductivity values of the membranes under investigation decreases as follows:

$$\alpha_{MC-40} > \alpha_{MA-41} > \alpha_{MA-40}.$$

In the ammonium nitrate solutions, however, the MA-40 membrane electro conductivity value decreases by near 10 times. It could be supposed that due to the following deprotonation reaction:



the ammonium ion has formed leaves the anion exchange membrane, consequently the counts of active fixed groups and mobile counterions decreases.

An infrared spectroscopy method was used to confirm the interaction between the MA-40 membrane fixed groups and particles containing in the solution. The MC-40 membrane IR spectra those were obtained by means of Infracum FT-801 have only four peaks in the sodium chloride solutions. According to [7], the  $=NH^+Cl$  и  $\equiv N \cdot Cl$  bonds do not appear in the 4000–400  $\text{cm}^{-1}$  interval. A new peak in the oscillation area of secondary amino groups (1660–1610  $\text{cm}^{-1}$ ) was appeared in the ammonium nitrate solution in the MA-40 membrane IR spectrum. Also there was a peak in 1034.63  $\text{cm}^{-1}$ , that can be applied to the deformation oscillation of the  $OH^-$  ions, those are linked to the carbon atoms and amino groups of the resin. This indicates the change in the conditions of secondary and tertiary amino groups in the membrane.

The courses of the current-voltage curves of the membrane under investigation correlate to their electro conductivity values.

### References

1. Remy G. Lehrbuch der anorganischer chemie. Band 1. M, 1972. 591 p.
2. Robinson R., Stoks R. Rastvory electrolytov. M.1963. 646 p.
3. Berezina N., Gnusin N., Dyomina O., Timofeev S. // J. Membr. Sci.1994. V.86. P.207.
4. Damaskin B.B., Petry O.A., Tzirlina G.A. // Electrochimija. M., 2001.624 p.
5. Saldadze K.M., Kopylova-Valova V.D. Complexoobrazujuchie ionity. M., 1980. 336 p.
6. Lopatkova G.Yu., Volodina E.I., Pismenskaja N.D., Fedotov Yu.A., Cot D., Nikonenko V.V. // Russian J. of Electrochemisry. 2006.V.42. P.942.
7. Semushin A.M. Yakovlev V.A., Ivanova E.V. IR absorption spectra of ion-exchange materials. Chemistry, 1980. 96 p.

---

# INFLUENCE OF ION-MOLECULAR COMPOSITION OF THE MF-4SC MEMBRANE ON THE CHARACTERISTICS OF PD-SENSORS IN MULTIIONIC AQUEOUS SOLUTIONS

<sup>1</sup>Anna Parshina, <sup>1</sup>Olga Bobreshova, <sup>2</sup>Sergey Timofeev

<sup>1</sup>Voronezh State University, Voronezh, Russia, *E-mail: parshina\_ann@mail.ru*

<sup>2</sup>Plastpolimer, St. Petersburg, Russia

## Introduction

Recently, we described the development of a novel potentiometric sensor (PD-sensor), which measures the Donnan potential at an ion-exchange membrane/ electrolyte test solution interface [1-4]. The Donnan potential is the Galvani potential between two points outside the external interfaces of double electrical layers at the membrane/ test solution interface. Consequently, it is impossible to directly measure the Donnan potential; however, it is possible to estimate its value. Similarly, we determine the Donnan potential by measuring the EMF of the electrochemical circuit, but it is measured from the potential jump at the individual membrane/ test solution interface. The use of the membrane potential equilibrium constant as an analytical signal, which is the Donnan potential at the membrane/ test solution interface, allows us to eliminate issues related to migration and diffusion in ionophore-based potentiometric sensors. This process ultimately increases the accuracy, stability and sensitivity of organic and inorganic ion measurements.

## Experiments

The aqueous solutions of glycine (Gly),  $\alpha$ -,  $\beta$ -alanine ( $\alpha$ -,  $\beta$ -Ala), leucine (Leu), nicotinic acid (Niacin), pyridoxine hydrochloride (PyridoxinHCl), thiamine chloride (ThiaminCl) with pH ranged from 1.0-7.0 were investigated. The aqueous solutions of Gly, cysteine (Cys) with pH ranged from 7.0-14 were investigated.

The MF-4SC membranes in mixed type were used to increase the selectivity of PD-sensor to cations and zwitterions of amino acids and vitamins in the presence of  $H_3O^+$  ions in acid aqueous solutions. The samples of membranes in mixed type were obtained by two procedures. In the first procedure the membranes were treated in solutions of amino acids and vitamins at boiling temperature of solution. In the second procedure the membranes were treated by keeping in ethylene glycol (EG) at glass transition temperature of membrane (110°C) and than in solutions of amino acids and vitamins respectively at boiling temperature of solution.

The MF-4SC membranes with gradient  $ZrO_2$  distribution were used to find of sensitivity of PD-sensor to organic anions in alkali solutions. The samples of membranes with 3.5, 4, 4.5, 5 wt.% of  $ZrO_2$  were investigated. The samples of modified membranes were given by cand.ch.sc. Ekaterina Yu. Safronova and corresponding member RAS, dr.ch.sc., prof. Andrey B. Yaroslavtsev (Kurnakov Institute of general and inorganic chemistry of RAS, Moscow, Russia).

The sensor array included PD-sensor, pH-selective electrode (pH-SE) and a silver chloride/silver reference electrode. Moreover, a set of ion-selective electrodes (ISEs) can be included in the sensor array as it was presented in [3, 4]. The potentials of PD-sensor and pH-SE were measured by the reference electrode using a high resistance electronic voltmeter. The responses from the PD-sensor were registered after 5-7 min, which was the time it took to reach a quasi-equilibrium state [1, 2].

The PD-sensor [1, 2] included two plastic encasements. There was Ag/AgCl electrode in upper encasement (volume is 5 cm<sup>3</sup>). There was MF-4SC membrane in lower encasement (volume is 0.5 cm<sup>3</sup>). The tip of MF-4SC membrane was in upper encasement. Another tip of MF-4SC membrane projected from upper encasement and was immersed in the test solution. The upper encasement was filled by the reference solution. Depending on the ionic type of the membrane, 1 M solutions of HCl or KCl were used as reference solutions. The lower encasement in work was empty and prevented the MF-4SC membrane from drying.

The multivariate regression methods were used for calibration of sensors in multiionic solutions. The coefficients of multivariate calibration equations were determined by the method

of least squares with nonorthogonal experimental design. The calibration coefficients were compared with determination errors for checking the significance. The spread of the calculated and experimental values of sensor responses was compared with the spread of the results of duplicated experiments for checking the adequacy of calibration equations [5].

### Results and Discussion

In aqueous solutions of vitamins and pharmaceuticals the concentrations of the organic ionic forms of electrolyte and aqueous dissociation products are correlated. The protolytic and ion-exchange reactions at the interfaces of ion-exchange membranes and test solutions are potential determining for the PD-sensors. Multiionic composition of the test solutions determines response from the cross-sensitive PD-sensor. Quantitative determination of vitamins and pharmaceuticals in aqueous solutions is difficult due to correlation of components concentrations.

The influence of ion-molecular composition of the MF-4CK membrane on the characteristics of PD-sensors in acid aqueous solutions of Gly,  $\alpha$ -,  $\beta$ -Ala, Leu, Niacin, PyridoxinHCl, ThiaminCl were investigated. It was shown that several factors influence on the value of Donnan potential on the interface membrane MF-4SK/ aqueous solution of amino acid and vitamins. Firstly, it is the differences in the hydration ability, differences of solubility and differences of size of the ions of amino acids and vitamins. Secondly, it is differences in the potential determining reactions on the interface membrane MF-4SK/ test solution.

The influence of ion-molecular composition of the MF-4CK membrane on the characteristics of PD-sensors in alkali solutions of Gly, Cys were investigated. The use of membrane with gradient ZrO<sub>2</sub> distribution for PD-sensor organization leads to significant contribution of anions into analytical signal of sensor in contrast to unmodified samples. Sensitivity of PD-sensor to counter-ions varies nonmonotonically with increasing concentrations of ZrO<sub>2</sub>. Sensitivity of PD-sensor to co-ions increases with increasing concentrations of ZrO<sub>2</sub>. The difference in electrochemical behaviour of unmodified and modified with ZrO<sub>2</sub> MF-4SC, samples depends on next factors. Firstly, concentration of dissociated cation-exchange fixed groups of membrane (-SO<sub>3</sub>H) decreases after ZrO<sub>2</sub> incorporation due to reduce of free volume of pores and channels. Secondly, ZrO<sub>2</sub> particles in modified membranes give evidence of both cation- and anion-exchange properties [6]. So co-ions concentration near modified MF-4SC/ test solution of electrolyte interface increases in comparison with initial membranes. This allows to increase sensitivity of gradient modified MF-4SC -based PD-sensors to co-ions in aqueous solutions.

### Acknowledgements

This work was financially supported by the RFBR (projects 12-08-00743-a), «P.Y.S.I.C.»: Fund of assistance to development of small forms of the enterprises in scientific and technical sphere (research projects 9591p/14212, 01.08.2011).

### References

1. Bobreshova O.V., Parshina A.V., Agupova M.V., Timofeev S.V. RF Patent 2376591, 2009, Byull. izobret., 2009, no. 35, 6 p.
2. Bobreshova O.V., Agupova M.V., Parshina A.V., Polumestnaya K.A. // Russian J. of Electrochem. 2010. V.46. P.1252-1262.
3. Bobreshova O.V., Parshina A.V., Ryzhkova E.A. // Russian J. of Anal. Chem. 2010. V.65. P. 866-872.
4. Bobreshova O.V., Parshina A.V., Polumestnaya K.A., Timofeev S.V. // Petroleum Chemistry. 2011. V. 51. P. 496-505.
5. Vershinin V.I., Pertsev N.V. Experimental Design and Mathematical Data Processing in Chemistry: A Tutorial (Omsk. Gos. Univ., Omsk, 2005) [in Russian].
6. Voropaeva E.Yu., Stenina I.A., Yaroslavl'tsev A.B. // Zhurnal neorganicheskoi khimii. 2008. V. 53. P. 1677. (Russ. J. Inorg. Chem., 2008, 53, 1797).



overlapping electric double layers of the particle and the membrane pore surface; (b) van-der-Waals molecular attraction. Using Deryaguin's approach under supposition of low electric potentials,  $e\psi/kT < 1$ , the interaction energy and force between curved and charged surfaces of the particle and the membrane pore were calculated as the function of minimal distance  $h_0$  between them. Corresponding formulas consist of electrostatic and molecular components:

$$U^\sigma(h_0) \equiv U_e(h_0) + U_m(h_0) = -\frac{4\pi^2}{g\varepsilon_0\varepsilon_r\kappa^2} \left( (\sigma_p + \sigma_m)^2 \ln(1 - \exp(-\kappa h_0)) + (\sigma_p - \sigma_m)^2 \ln(1 + \exp(-\kappa h_0)) \right) - \frac{A}{6gh_0} \quad (1)$$

$$F^\sigma(h_0) \equiv -\frac{dU(h_0)}{dh_0} = \frac{8\pi^2}{g} \frac{1}{\kappa\varepsilon_r\varepsilon_0} \left( \frac{2\sigma_p\sigma_m \exp(\kappa h_0) + (\sigma_p^2 + \sigma_m^2)}{\exp(2\kappa h_0) - 1} \right) - \frac{A}{6gh_0^2} \quad (2)$$

where  $\sigma_p, \sigma_m$  - surfacial densities of charges of the particle and the membrane;  $\kappa$  - reverse Debye length;  $\varepsilon_0$  - permittivity of vacuum and  $\varepsilon_r$  - relative dielectric constant of the liquid medium;  $A$  - Hamaker constant (if  $A > 0$ , then we have molecular attraction, otherwise ( $A < 0$ ) - molecular repulsion);  $g$  - steric factor, which depends fully on the interacting surfaces geometry, and was calculated earlier inside the main regions [1] (fig.1):  $g_1 = 1/a$  (spherical particle interacts with the plane  $z = 0$ ),  $g_2 = \sqrt{\left(\frac{1}{a} + \frac{1}{b}\right)\left(\frac{1}{a} - \frac{1}{r_0 + b}\right)}$  (spherical particle interacts with closed toroidal surface at the pore entrance),  $g_3 = \sqrt{\frac{1}{a}\left(\frac{1}{a} - \frac{1}{r_0}\right)}$  (spherical particle interacts with the inner surface of the cylindrical cavity).

We should note that under location of the particle in the Region I, the minimal distance between interacting surfaces is equal to  $h_0 = z - a$ , where  $z$  is the axial coordinate of the particle center, which has an origin at the pore center on the plane  $z = 0$  (Fig.1). If the particle is located inside Regions II or III, then, in order to account for the closure of the surfaces, we need to take into consideration the second minimal distance  $h'_0$ , which is symmetrical to the main minimal distance  $h_0$  [1], that is,

$$U_i = U_i(h_0) + U_i(h'_0), \quad (i = 2, 3). \quad (3)$$

So we can calculate for the Region II, that  $h_0 = \sqrt{(a + r_0 - r)^2 + (b + z)^2} - b - a$ ,  $h'_0 = \sqrt{(a + r_0 + r)^2 + (b + z)^2} - b - a$ , and for Region III, that  $h_0 = r_0 - a - r$ ,  $h'_0 = r_0 - a - r$ , where  $r$  is the radial coordinate of the particle center in cylindrical coordinate system.

Under the same signs of the charge densities it follows from the formula (2) for the interaction force that there is such a value of intersurficial distance  $h_0$ , at which the force is equal to zero (in the case of molecular attraction, of course). It means the existence of potential barrier under approaching the particle to the membrane surface. It is necessary to mention that analogous barrier is initiated in the case of given zeta-potentials [1, 2]. Fig.2 schematically illustrates the profile of the interaction energy (1) for the more probable position of the particle center at the axis of symmetry of the pore,  $r = 0$ . Our analysis shows that the potential barrier can be shifted into the bulk solution (the shift is larger when radius  $b$  of rounding at the pore

entrance is smaller). It allows removing the particles from the vicinity of the membrane pore surface by applied tangential liquid flow and therefore increasing the system productivity.

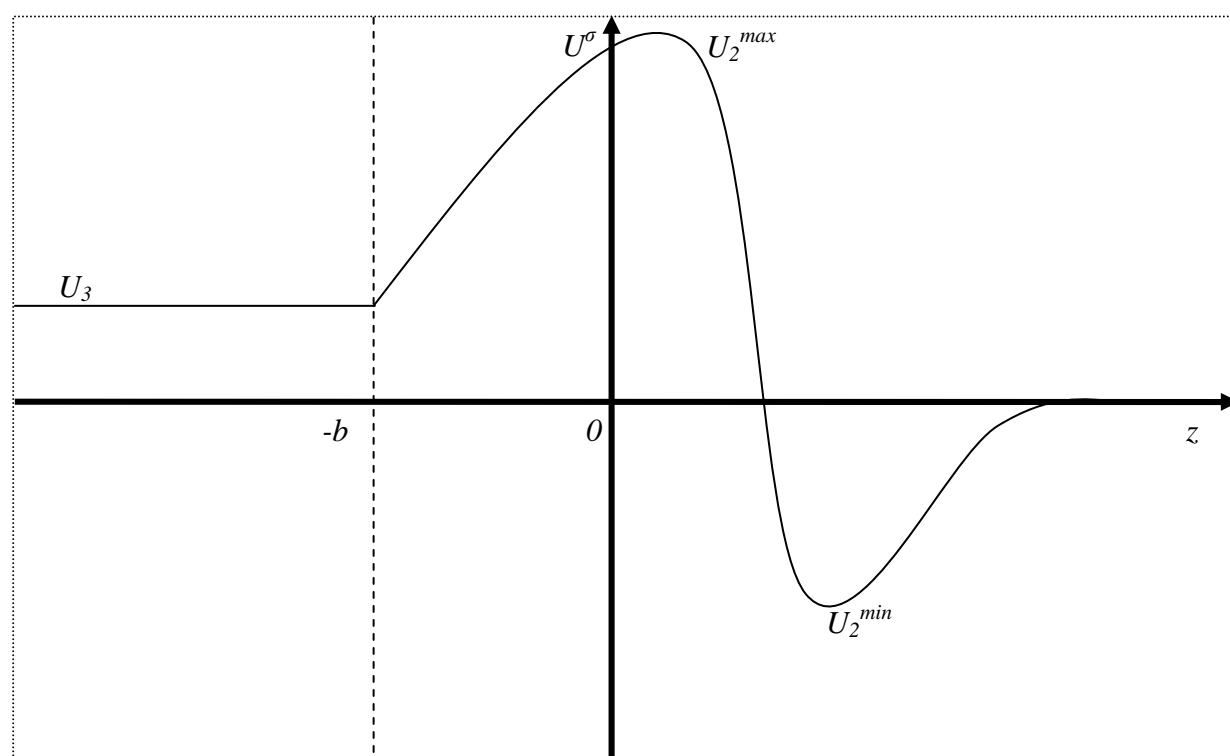


Figure 2. Characteristic profile of the interaction energy between a charged particle which is centerline located and a charged pore with equal charge densities

### Conclusion

Hence the model suggested here allows us qualitatively imagine and quantitatively evaluate the picture of interaction between a charged particle and a cylindrical membrane pore taking into account the influence of intermolecular forces. We derived the boundaries for physicochemical parameters under which the potential barrier exists. The model can be further expanded taking into consideration fluid hydrodynamics near hydrophilic or hydrophobic surfaces and inequality of the surface charge densities.

*This work is supported by the Russian Foundation for Basic Research (project № 11-08-01043\_a).*

### References

1. Bowen W.R., Filippov A.N., Sharif A.O., Starov V.M. A Model of the Interaction between a Charged Particle and a Pore in a Charged Membrane Surface // *Adv. Colloid Interface Sci.* 1999. V.81. No. 1. P. 35-72.
2. Filippov A.N., Iksanov R.Kh., Volkov A.V. Interaction of a Charged Spherical Particle with a Pore of a Charged Hydrophobic Membrane in an Electrolyte Solution // *Membrane and Membrane Technologies.* 2011. V. 1. No. 2. P.92-97. (English translation in: *Petroleum Chemistry.* 2011. V. 51. No. 7. P. 536-541.

---

## WHAT MEMBRANE PROPERTIES HAVE IMPACT ON THE ELECTROCONVECTION IN ELECTRODIALYSIS OF DILUTE SOLUTIONS?

<sup>1</sup>Natalia Pismenskaya, <sup>1</sup>Nadezhda Melnik, <sup>1</sup>Victor Nikonenko, <sup>2</sup>Gerald Pourcelly

<sup>1</sup>Membrane Institute, Kuban State University, Krasnodar, Russia, *E-mail: n\_pismen@mail.ru*

<sup>2</sup>Institut Européen des Membranes, CNRS-Université Montpellier 2, Montpellier, France, *E-mail: gerald.pourcellyt@iemm.univ-montp2.fr*

### Introduction

This work is aimed at better understanding of the relationship between the ion-exchange membrane properties and current-induced convection occurring as electroosmosis of the first or second kind [1-3] (electroconvection) in conditions where this phenomenon controls the enhancement of the salt ion transfer in electrodialysis of dilute solutions.

### Experiment

Several ion-exchange membranes with different morphologies and different degrees of the surface hydrophobicity are studied. The idea is to modify the surface of a homogeneous (Nafion-117, CMX) and a heterogeneous (MK-40) cation-exchange membrane with sulfonic fixed groups in several ways, in order to decrease its hydrophobicity (by mechanical removal of surface hydrophobic layer) or to increase it (by coating the surface with a Nafion film containing or not carbon materials of a high hydrophobicity as well as treating of CMX membrane under intensive current modes), and to see how these modifications affect the overlimiting transfer. In the case of anion-exchange membranes MA-40 water splitting rate was reduced by replacement of secondary and tertiary amine fixed groups into quaternary amines. Commercial Nafion-117, CMX, MK-40, MA-40 membranes were used for comparison.

Electrochemical and mass transfer characteristics of the studied membranes were obtained in a flow-through electrochemical cell. Specially selected geometric parameters of the cell and the laminar hydrodynamic regime of solutions pumping allow the use of convection-diffusion model to determine the theoretical value of the limiting current, which can be achieved in the absence of coupled effects of concentration polarization. Using the modified Kharkats equation makes it possible to determine contributions to overlimiting mass transfer of water splitting products and the exaltation effect as well as that of the salt counterion flux, enhanced by electroconvection. Visualizations of membrane surface and cross-sections were performed using scanning electron microscopy. The contact angles on the surface of membrane in swollen state (pre-equilibrated with a NaCl solution) were measured by the sessile drop method [4,5]. Concentration dependences of specific electrical conductivity as well as diffusion permeability of the membranes were determined correspondingly by differential method using clip-cell [6] and partial method using flow pass cell [4].

### Results and Discussion

Specific electrical conductivity and diffusion permeability of the membranes do not play a key role in development of electroconvection which enhance overlimiting transport of salt counterions in overlimiting electrodialysis of dilute solutions.

There is a significant correlation between the degree of the surface hydrophobicity and the limiting as well as the overlimiting transfer of salt counterions for membranes with a similar surface morphology (Fig. 1a). The higher the surface hydrophobicity, the more intense the transfer caused by electroconvection (Fig.2a). The reason is in facilitation of the slip of electroconvective vortexes along the interface [3,4].

The appearance of micrometer-scale cavities (characteristic size is of 1 micron) on the sufficiently highly hydrophobic ion-exchange surface (CMX membrane) enhances electroconvection and overlimiting mass transfer (Fig.2b,c). The effect increases with increasing fraction of the surface occupied by the cavities (Fig. 1b). The reason is the generation of the tangential electric force applied to the extended space charge region at cavity's wall (Fig. 3).

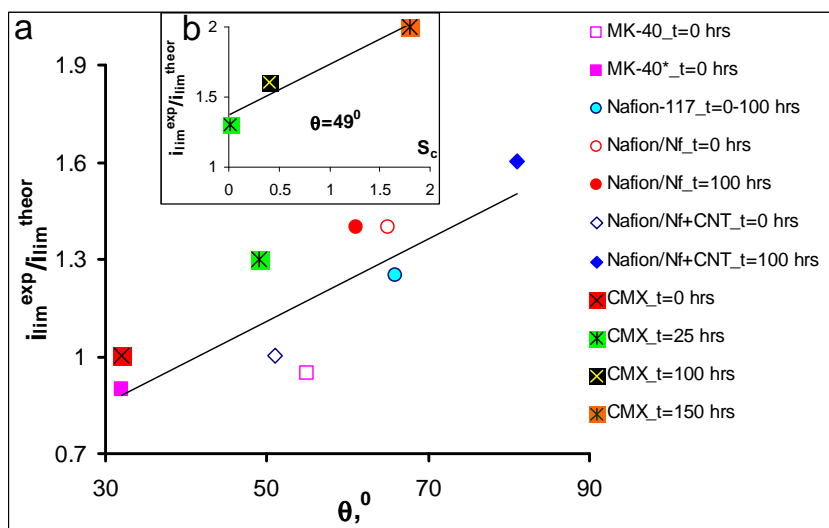


Figure 1. Experimental limiting current density divided by the theoretical limiting current density vs the membrane surface contact angle,  $\Theta$  (a) and the fraction of surface occupied by the micrometer-scale cavities,  $S_c$ , at a fixed contact angle (b);  $t$  is the time of membrane operation under current

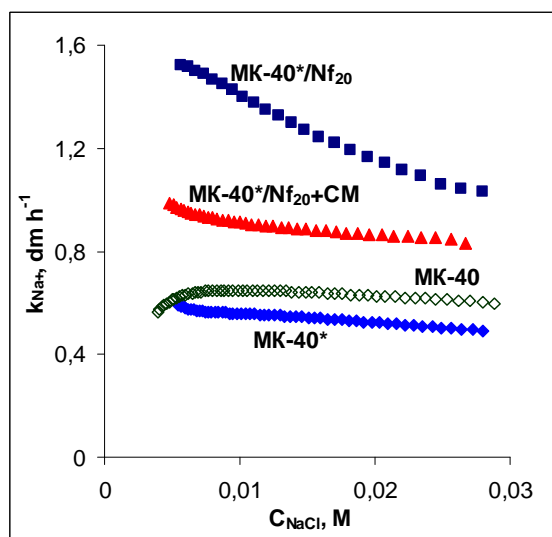
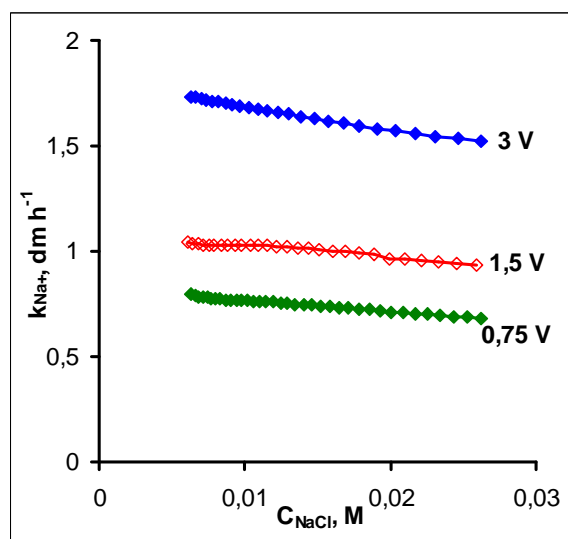
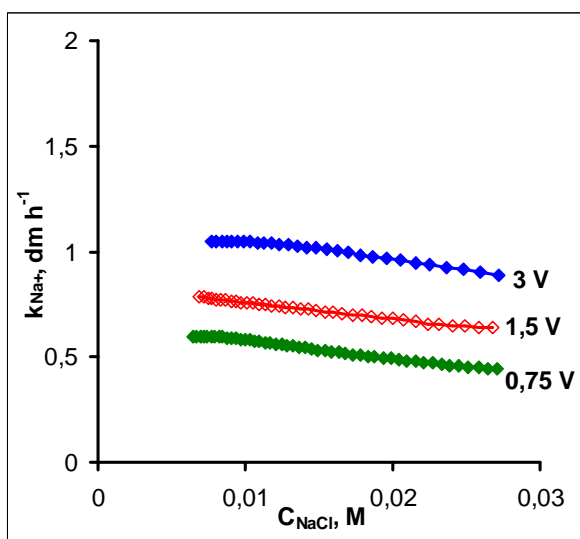


Figure 2. Concentration dependence of  $Na^+$  mass transfer coefficient of a MK-40 membrane and its modifications (a) and of a CMX membrane treatment under overlimiting current during 10 h (b) and 100 h (c). The potential drops applied over the membrane were 2 V (a) and 0.75, 1.5, and 3 V (b,c). The subscript number (a) shows the thickness of Nafion surface layer in micrometers.



This force contributes to the generation of electroconvective paired vortices that drive the fluid inside the cavity and over the adjacent smooth surface [4]. Suppression of water splitting at the membrane/solution interface promotes the development of electroconvection; enhancement of water splitting reduces this effect and its influence on overlimiting salt ion transfer (Fig.4). The reason is in reducing concentration polarization (resulting in a decrease of the space charge density) by water splitting products, and the tunneling (Grotthuss) mechanism of  $H^+$  and  $OH^-$  ion transfer, which does not involve fluid into the movement [1,3].

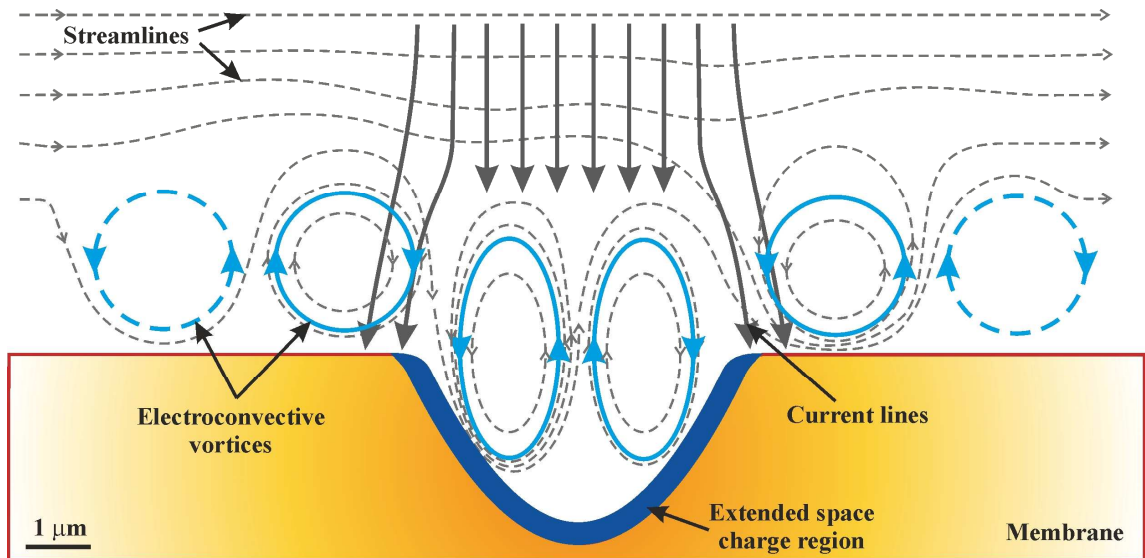


Figure 3. Possible mechanism of occurring paired electroconvective vortices on the surface of ion-exchange membrane under an electric current directed normally to the membrane surface. Streamlines and electric current lines are shown schematically

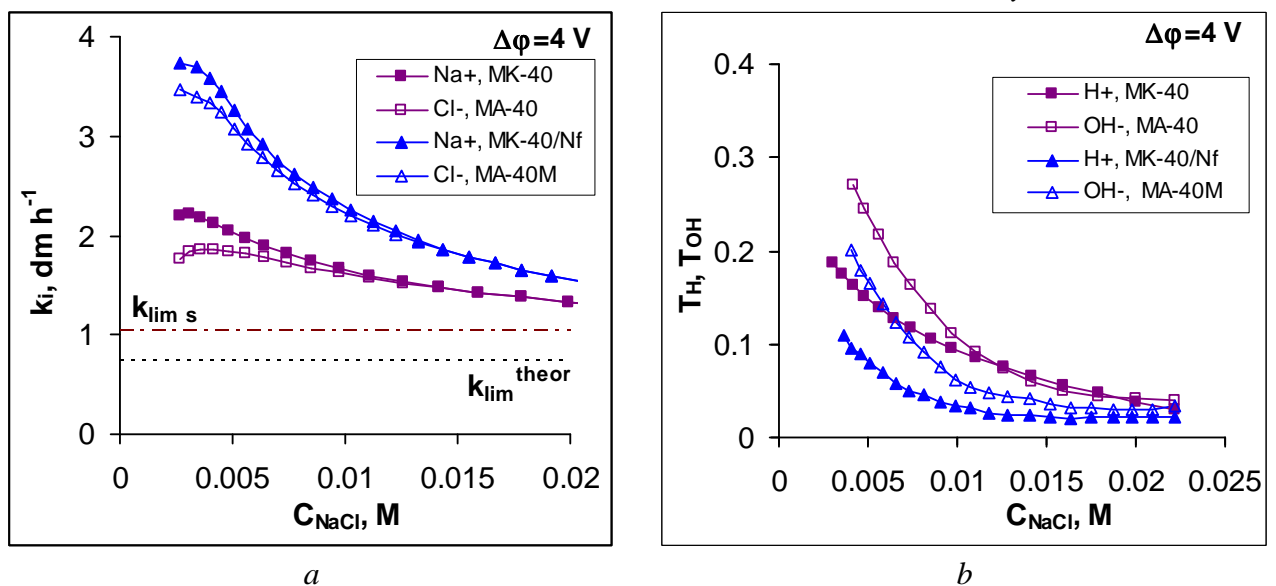


Figure 4. Concentration dependence of  $Na^+$  mass transfer coefficients (a) and effective transport number of protons (b) across MK-40 and MK-40/Nf cation-exchange membranes as well as Cl<sup>-</sup> mass transfer coefficients (a) and effective transport number of hydroxyl ions (b) across MA-40 and MA-40M anion-exchange membranes forming desalination channels, DC (desalination length  $L=10$  cm), under potential drops per cell pair 4.0 V (b). The limiting mass transfer coefficient for the DC without spacer,  $k_{lim}^{theor}$ , is calculated using convective-diffusion model; the limiting mass transfer coefficient for DC with spacer,  $k_{lim,s}$ , is evaluated from experimental current voltage curves and pH of desalinated solution

## Acknowledgments

Part of the work was carried out in accordance with the cooperation programme of International Associated French-Russian Laboratory "Ion-Exchange Membranes and Related Processes" The authors are grateful to the CNRS, RFBR (Grant Nos. 11-08-93107, 11-08-96511, 11-08-00599 and 12-08-00188) and FP7 Marie Curie Actions "CoTraPhen" Project PIRSES-GA-2010-269135

## References

1. *Mishchuk N.A., Dukhin S.S.* In: Delgado A, editor. Interfacial electrokinetics and electrophoresis, 10. Marcel Dekker, New York. 2002. p. 241.
2. *Rubinstein I., Zaltzman B.* Electro-osmotically induced convection at a permselective membrane // *Phys. Rev. E.* 2000. Part A, V. 62, No 2. P. 2238-2251.
3. *Nikonenko V., Pismenskaya N., Belova E., Sistas Ph., Larchet Ch., Pourcelly G.* Intensive current transfer in membrane systems: Modelling, mechanisms and application in electrodialysis // *Adv. Colloid Interface Sci.* 2010. V. 160. P. 101-123.
4. *Pismenskaya N.D., Nikonenko V.V., Melnik N.A., Shevtsova K.A., Belova E.I., Pourcelly G., Cot D., Dammak L., Larchet C.* Evolution with Time of Hydrophobicity and Microrelief of a Cation-Exchange Membrane Surface and Its Impact on Overlimiting Mass Transfer // *J. Phys. Chem. B.* 2012. V. 116. P. 2145-2161.
5. *Belashova E.D., Melnik N.A., Pismenskaya N.D., Shevtsova K.A., Nebavsky A.V., Lebedev K.A., Nikonenko V.V.* Overlimiting mass transfer through cation-exchange membranes modified by Nafion film and carbon nanotubes // *Electrochimica Acta.* 2012. V. 59. P.412–423.
6. *Berezina N.P., Kononenko N.A., Dyomina O.A., Gnusin N.P.* Characterization of ion-exchange membrane materials: Properties vs structure // *Adv. Colloid Interface Sci.* 2008. V. 139. P. 3-28.

# CURRENT-VOLTAGE CHARACTERISTICS AND ELECTRIC BREAKDOWN OF THE METAL-COATED TRACK-ETCHED MEMBRANES

<sup>2</sup>Sergey Podojnitsyn, <sup>1</sup>Tatyana Tsyganova, <sup>1</sup>Sergey Shatov, <sup>1</sup>Boris Mchedlishvili

<sup>1</sup>Institute of Crystallography of RAS, Moscow, Russia, E-mail: tvts@mail.ru

<sup>2</sup>Institute of Biochemical Physics of RAS, Moscow, Russia

## Introduction

Contemporary intensive development of vacuum nanoelectronics is defined by progress in technologies of field emission nanostructures, such as traditional lithographic methods, nanowires on the anodized oxide of aluminum, and matrixes of vertical carbon nanotubes [1]. Field emission nanostructures obtained by a metallization method of track-etched membranes is a one of these essentially various technologies. Existence of sealing contact of metal with a polymeric matrix is a distinctive feature of such nanostructures, i.e. processes of internal field emission of electrons into dielectric in similar objects can be observed.

## Experiments

Current-voltage characteristics and electrical breakdown of the metal-coated track membranes with part-through conic pores were investigated.

The 10 microns thickness polyethyleneterephthalate film was irradiated by high energy ions of Ar and was etched by the water-alcohol alkali solutions for obtaining of part-through conical pores. One of surfaces of such film with part-through conic pores was covered a silver layer by method of a vacuum thermal deposition and then a copper layer by method of electrochemical deposition for strengthening of metal contact [2, 3]. The sample of a polymeric film with part-through conical pores and the metal structure replicating a form of conical pores are represented on Figure 1a. Figure 1,b demonstrates the micrograph of metal replica after a full etching of a polymeric matrix.

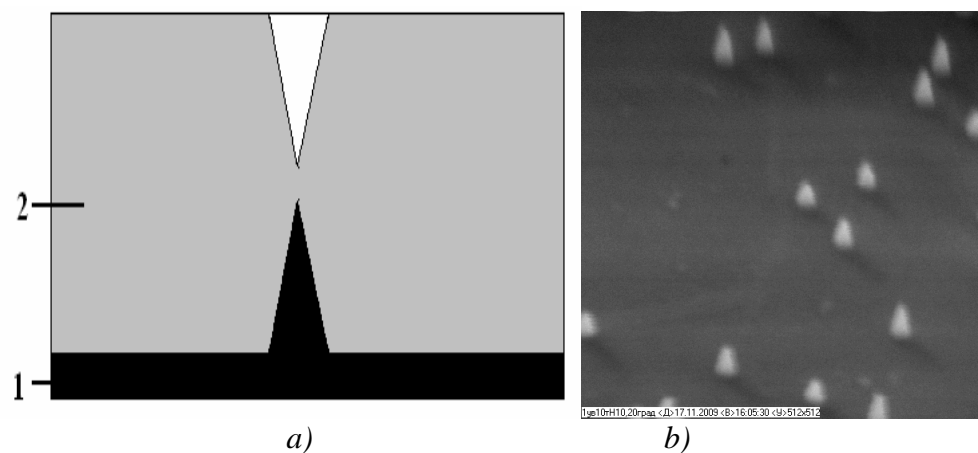


Figure 1. The Schematic Sketch of a Sample of Studied Structure (1 - metal covering; 2 - polymeric film) and the Micrograph of Structure of the Metal Replica, TESLA-BS 340. Magnification 10000

The flexible sample holder (6 mm diameter) for measurement of voltage-current characteristic was made. This sample holder provides the uniform clip between flat contacts of the specified structures.

The current-voltage characteristic of a polymeric film with the metallized part-through conical pores has two characteristic parts (Figure 2): an initial straight line corresponding to the law of Ohm and approximately exponential increase of a current to the point of electric breakdown in the region of the last measured point. As a result of breakdown the current value increased to 10-100 times more, and at the same time the voltage value keeps 1-2 volts that there corresponds to the resistance reduction to 1000 and more times.

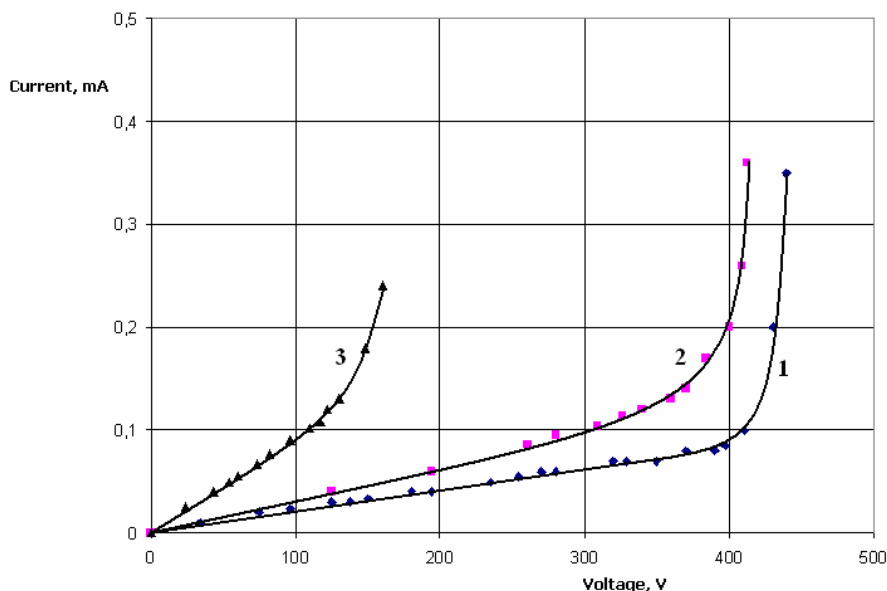


Figure 2. Current-voltage characteristic of a polymeric film with the metallized part-through conical pores. Curves 1, 2, 3 - three subsequently measurements

It should be noted that rather often electric breakdown wasn't irreversible, i.e. after switching-off of the power supply and repeated giving of voltage on a sample the characteristic type of current-voltage dependence was restored. Figure 2 shows three subsequently measurements (curves 1, 2, 3). In this case, irreversible change of a film resistance took place only after the third breakdown. It is obvious that film resistance and voltage value of the subsequent breakdown decreases after each breakdown.

Slow increase of a current at constant voltage (Figure 3) was other effect in nonlinear area of the current-voltage characteristic. Characteristic times of access to the plateau of a current varied from ten to hundred seconds for various samples.

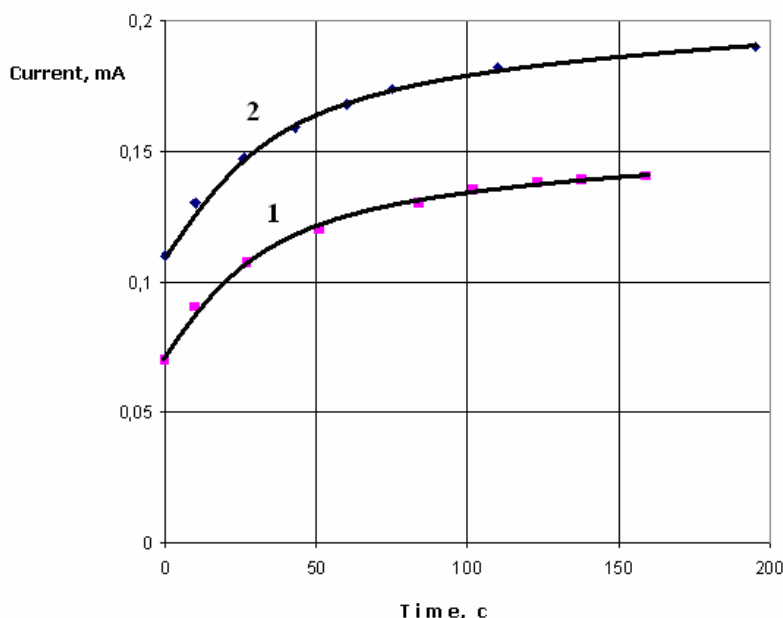


Figure 3. Dependence of the Current Sample from Time in the Metallized Polymeric Film with the Conic Pores (at the Constant Voltage). Curves 1, 2 - Corresponding to 73 and 92 Volt

### Results and Discussion

Processes of passing of electric current through the metallized track membranes corresponds to ohmic linear and power dependence of a current on voltage. But at this point current-voltage characteristic is lacking in S-shaped plot of the features to process for traditional dielectrics.

Before main breakdown, there are observed many partial breakdowns on the mechanism of ionization by collision in the destructed polymer in separate nanochannels over the metal conic.

For the studied samples it is possible to note large quantity of "reversible" breakdowns unlike traditional irreversible breakdown of dielectric.

Probably value of breakdown voltage and intensive growth of the current-voltage characteristic are defined by curvature radius of emitting elements, so the less of a curvature radius, the lower voltage of breakdown. In this connection, the measurement of electric properties is possible to consider as a simple and quick way of obtaining quality information for solution of technological problems of manufacturing of field emission nanostructures on the basis of the metallized track membrane.

#### References

1. *Tatarenko N.I., Kravchenko V.F.* Field emission nanostructures and devices on their basis. M. Fizmatlit. 2006.
2. *Flerov G.N.* Vestnik's crapes of Academy of Sciences of the USSR. 1984. No. 4. P. 35.
3. *Martin C.R.* Nanomaterials: A membrane-based synthetic approach. Science. 1994. V. 226. P. 1961-1966.

# DYNAMICS OF OXYGEN REDOX SORPTION BY METAL (AG, CU, BI) – ION EXCHANGER NANOCOMPOSITES

Lev Polyanskiy, Svetlana Khorolskaya, Dmitriy Konev, Tamara Kravchenko  
Voronezh State University, Voronezh, Russia, E-mail: krav280937@yandex.ru

## Introduction

Redox sorption (sorption accompanied by oxidation-reduction reaction) is the basis for dissolved oxygen removal from water by sorption-chemical method. The mathematical description of the macrokinetics of the process is given previously [1]. In this paper the dynamics of the process for deep removal of dissolved oxygen is studied.

## Experiments

The metal-containing nanocomposites based on sulfonic cation-exchange matrix KU-23 are investigated. Figure 1 shows obtained experimentally dynamic elution curves of oxygen redox sorption by metal (Ag, Cu, Bi)–ion exchanger KU-23 nanocomposites. As can be seen oxygen is sorbed by copper-containing nanocomposite more completely. The obtained results provide a basis for a theoretical analysis of the parameters of the water deoxygenation dynamics by copper-ion exchanger nanocomposite.

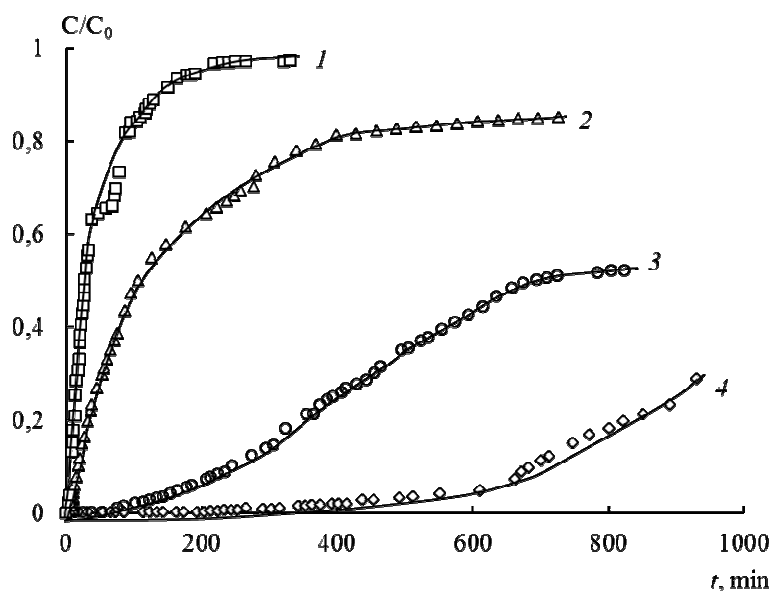


Figure 1. Dynamic elution curves of the dissolved oxygen redox sorption by the granular layer of the nanocomposites: silver- (1 – synthesis  $(\text{NH}_2)_2\text{CSO}_2$ , 2 – synthesis  $\text{N}_2\text{H}_4$ ), bismuth- (3 – synthesis  $\text{Na}_2\text{S}_2\text{O}_4$ ) and copper-containing nanocomposites (4 – synthesis  $\text{Na}_2\text{S}_2\text{O}_4$ ) in the  $\text{H}^+$ -ionic form.  $c_0$  and  $c$  – inlet/outlet oxygen concentration to/out of the granular layer, respectively, metal capacity  $\varepsilon_{\text{Me}^0} = 0.9\text{-}1.0 \text{ mmol-eqv/cm}^3$ , height of the granular layer  $l=0.12 \text{ m}$ , section  $S=1 \text{ cm}^2$ , water flow rate  $u=4.8 \text{ m/h}$ ,  $c_0 = 0.26 \text{ mmol/l}$  (8.3 mg/l)

## Results and Discussion

The problem formulation of the oxygen redox sorption dynamics is made. Here is a scheme of the process proceeding between copper nanoparticles and oxygen in the ion-exchange matrix in the H-form:



We consider that oxygen transfer along the nanocomposite granular layer  $y$  with height  $l$  is described by equation:

$$(1-\chi) \frac{\partial c}{\partial t} + u \frac{\partial c}{\partial y} = \frac{3}{R_0} \chi j(t, y) \Big|_{R=R_0} \quad (3)$$

Here,  $j(t, y) \Big|_{R=R_0} = -D \frac{\partial c}{\partial R} \Big|_{R=R_0}$ ,  $j(t, y)$  is the oxygen flow, which is estimated on the basis of kinetic model [1], in the grain with radius  $R_0$ ,  $D$  is oxygen internal diffusion coefficient through the nanocomposite pores,  $\chi$  is the volume part of the column occupied by the nanocomposite granulars,  $u$  is the flow rate of the water containing dissolved oxygen with the concentration  $c(t, y)$ .

We introduce the dimensionless coordinates defined by the relations:

$$c = c_0 \cdot \bar{c}; \quad t = T \cdot \bar{t}; \quad R = R_0 \cdot \bar{R}; \quad y = l \cdot \bar{y}, \quad (4)$$

where  $c_0$ ,  $T$ ,  $R_0$  and  $l$  are the typical scales of the relevant variables;  $T = \frac{l}{u}$ .

By substituting (4) in (3) and introducing the notations

$$A = \frac{1}{1-\chi}, \quad B = -\frac{\chi}{1-\chi} \cdot \frac{3lD}{uR_0^2}, \quad (5)$$

we obtain the following dimensionless equation

$$\frac{\partial \bar{c}}{\partial \bar{t}} + A \frac{\partial \bar{c}}{\partial \bar{y}} = B \frac{\partial \bar{c}}{\partial \bar{R}} \Big|_{\bar{R}=1} \quad (6)$$

and unambiguity conditions

$$\bar{t} \geq 0; \quad \bar{y} = 0; \quad \bar{c} = 1. \quad (7)$$

The values of the derivative can be found by solving a problem of the kinetics [1] after matching the time scales:

$$\begin{aligned} \bar{t}_{\text{dyn}} \cdot \frac{l}{u} &= \bar{t}_{\text{kin}} \cdot \frac{R_0^2}{D}, \\ \bar{t}_{\text{dyn}} &= \bar{t}_{\text{kin}} \cdot \frac{uR_0^2}{Dl}. \end{aligned} \quad (8)$$

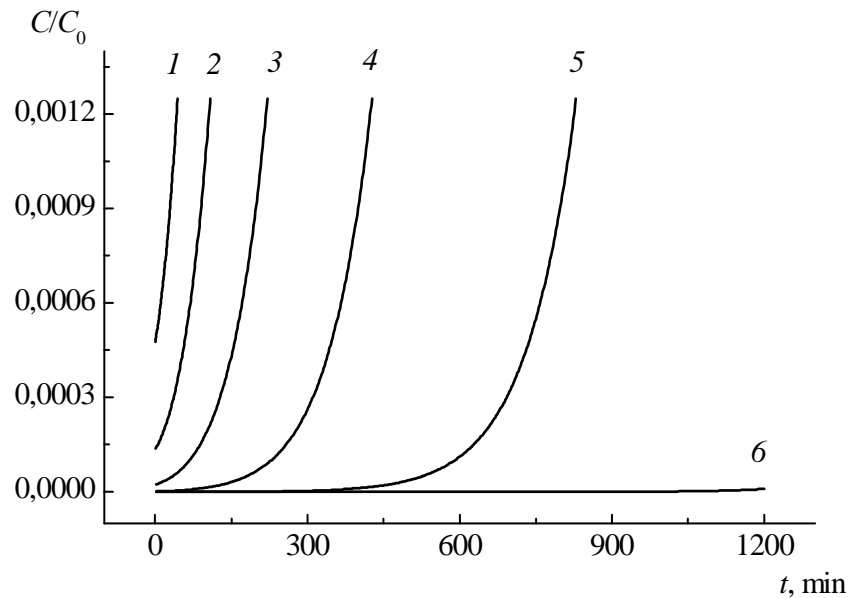


Figure 2. Before breakthrough segment of the elution curves of water deoxygenated by granular layer of nanocomposite  $\text{Cu}^0 \cdot \text{KV-23}$  in  $\text{H}^+$  - ionic form at different water flow rates  $u$ ,  $\text{m/h}$ : 1 - 35, 2 - 30, 3 - 25, 4 - 20, 5 - 15, 6 - 10. The calculation is done before reaching oxygen threshold level outlet of granular layer (10 ppb, curves 1-5) or before 1200 min of water passing (curve 6)

The calculation results of water deoxygenation dynamics in a flow system are illustrated in figure 2. The calculation is done for nanocomposite  $\text{Cu}^0\text{-KY-23 (H}^+)$  with single metal settling, i.e. with an equivalent content of copper particles and hydrogen counter-ions. The dynamic elution curves of oxygen for different water flow rates are given. As can be seen from figure 2 time of oxygen breakthrough into filtrate and volume of water deoxygenate to 10 ppb are related naturally with the water flow rate.

The theoretical description above is useful for the calculations at any parameters of the process without having to long and labor-intensive experiments.

*This work is supported by the RFBR (Rus. Fund of Basic Research, grant № 11-08-00174\_a)*

### References

1. *Peshkov S.V., Konev D.V., Kiprijanova E.S., Kravchenko T.A.* Regard for particle size distribution in a model of the macrokinetics of the reduction of oxygen dissolved in water by a metal - ion exchanger nanocomposite // *Zhurnal Fizicheskoi Khimii*. 2011. V. 85. №9. P. 1735-1741.

# SYNTHESIS AND PROPERTIES OF THE PROTON EXCHANGING POLYVINYLIDENE FLUORIDE-SULFONATED POLYSTYRENE MEMBRANES AND TESTING THEM IN THE HYDROGEN AND METHANOL FUEL CELLS

<sup>1</sup>Ardalion Ponomarev, <sup>1</sup>Emil Abdrashitov, <sup>1</sup>Veslav Bokun, <sup>1</sup>Dina Kritskaya,

<sup>2</sup>Evgeny Sanginov, <sup>2</sup>Yury Dobrovolskiy

<sup>1</sup>Branch of Institute of Energy Problems for Chemical Physics of RAS, Chernogolovka, Russia;

*E-mail: ponom@binep.ac.ru*

<sup>2</sup>Institute of Problems of Chemical Physics of RAS, Chernogolovka, Russia, *E-mail: sun\_e@mail.ru*

## Introduction

Previously we have developed the method of polystyrene (PSt) implantation into polyvinylidene fluoride (PVDF) films by thermal polymerization of styrene without radiation treatment and without using of any special chemical initiators [1]. The subsequent sulfonation of implanted PSt by the conventional methods gives the opportunity to produce the ion exchanging membranes with good transport and physic-chemical properties. AFM and ESM investigations of the produced membranes allowed studying the distribution of PVDF and PSt phases on the membrane surface [2]. It was estimated that the dimensions of the surface areas with the reduced hardness are in the range of 10–500 nm. It was also shown that these areas have increased through conductivity.

The purpose of this work is to investigate the kinetics of the PSt-implantation in PVDF films from styrene-toluene-divinylbenzol solution, to measure the base transport properties of the produced membranes, and to perform comparative testing of these membranes and Nafion-115 in hydrogen-air and methanol-air fuel cells.

## Experiments

The amount of PSt implanted into PVDF films as a function of the immersed time in the styrene-toluene-divinylbenzol solution (1:1:0.05) at 90–93°C is shown in fig. 1. The average implantation rate was about 3% (weight)/hour. The PVDF films containing from 5 to 50% (weight) of PSt were obtained.

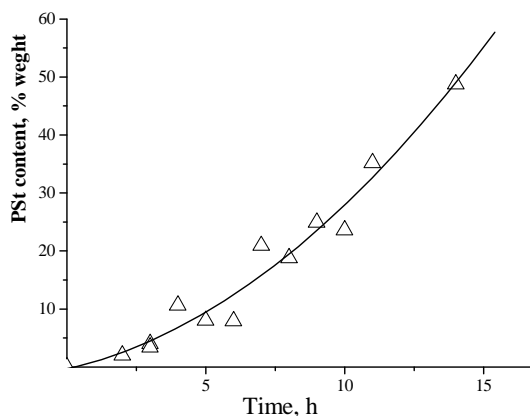


Figure 1. The amount of PSt implanted into PVDF films as a function of immersed time in the monomer solution

The ion exchange capacity of the films reached 2–2.4 mmol/g. Proton conductivity  $\sigma$  of the membranes as a function of the exchange capacity (EC) was investigated at RH = 75%. The  $\sigma$ -value was significant when EC reached a threshold of  $EC_{th} \geq 0.5$  mmol/g (Fig. 2). The obtained percolation dependence  $\sigma = \sigma_0(EC - EC_{th})^n$  ( $n = 1.5 \div 1.7$ ) shows the nanoheterogeneous distribution of the implanted sulfonated PSt in the membrane. This result is in a good agreement with the data of AFM analysis [2].

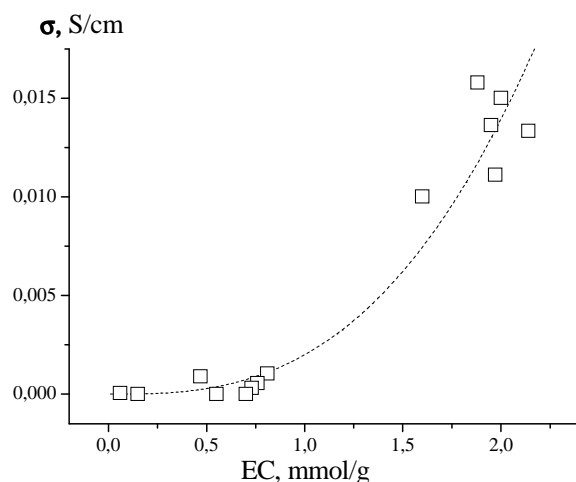


Figure 2. Proton conductivity of the synthesized membranes as a function of the exchange capacity,  $RH = 75\%$ ,  $T = 30C$

Water, methanol and water-methanol solution sorption capacity of the synthesized membranes with the exchange capacity of 2 mmol/g was measured. It was shown that the amount of absorbed liquid in the membranes decreases with the increase of methanol concentration in the surrounding solution. The sorption capacity of the synthesized membrane with  $EC = 2\text{mmol/g}$  was equal to 45% (weight) for pure water and 30% (weight) for pure methanol. It should be noted that the other picture was observed in the case of Nafion and MF-4SC membranes. Their sorption capacity of pure methanol was more than that of pure water.

The synthesized membranes (M1 and M2) were tested as components inside the hydrogen-air (HAFC) and methanol-air (MAFC) fuel cells and compared with the performance of Nafion-115 membranes. The all membranes under study had similar proton conductivity (8 - 12 mS/cm) and thickness (100–120  $\mu\text{m}$ ). Carbon Paper with applied catalyst (for anode: ETEK Pt-Ru/C, Pt/Ru = 1:1, Pt-content = 20% mass; for cathode: ETEK C1-40Pt/C, Pt-content = 40% mass) was used as the electrodes of the fuel cells. The Pt concentration was 0.35  $\text{mg}/\text{cm}^2$  on the anode and 1  $\text{mg}/\text{cm}^2$  on the cathode. The active electrode surface of the cells was 1  $\text{cm}^2$ . All the membranes were tested in the similar conditions. The fuel cells under test were operated at room temperature.

The volt-ampere and power characteristics of HAFC on the base of two synthesized membranes (M1, M2) and nafion-115 membranes with similar values of thickness and conductivity are shown in fig. 3. It can be seen (fig. 3a) that electromotive forces (EMF) of HAFC on the base of M1, M2 and Nafion-115 are practically similar and equal to 0.95–1.0 V. These values are in a good accordance with well-known literature data. The current-voltage curves at low load are similar for all of the studied membranes. It points to the similarity of the electrocatalytic and transport characteristics of the fabricated fuel cells. It should be noted

(fig. 3a) that the voltage drop of HAFC on the base of M1 and M2 membranes at high current density is appreciably less than that in the case of Nafion-115. The maximum power of HAFC containing the synthesized membranes (95–100  $\text{mW}/\text{cm}^2$ ) is noticeably large than in the case of Nafion-115 membrane (72  $\text{mW}/\text{cm}^2$ , fig. 3b).

Fig. 4 shows the comparative current-voltage and power characteristics of the methanol-air fuel cells with synthesized M1 membrane and Nafion-115. It can be seen that these functions are practically identical for both membranes. The electromotive force is about 0.6 V. This value is lower than the theoretical one (1.18 V) but it practically coincides with known literature data. The observed relatively low electric power of MAFC in our experimental conditions can be explained by low catalyst concentration on the electrodes and low temperature. It should be noted that these data indicate that catalytic and transport characteristics of MAFC on the base of synthesized membrane M1 are not worse than these characteristics in the case of Nafion-115.

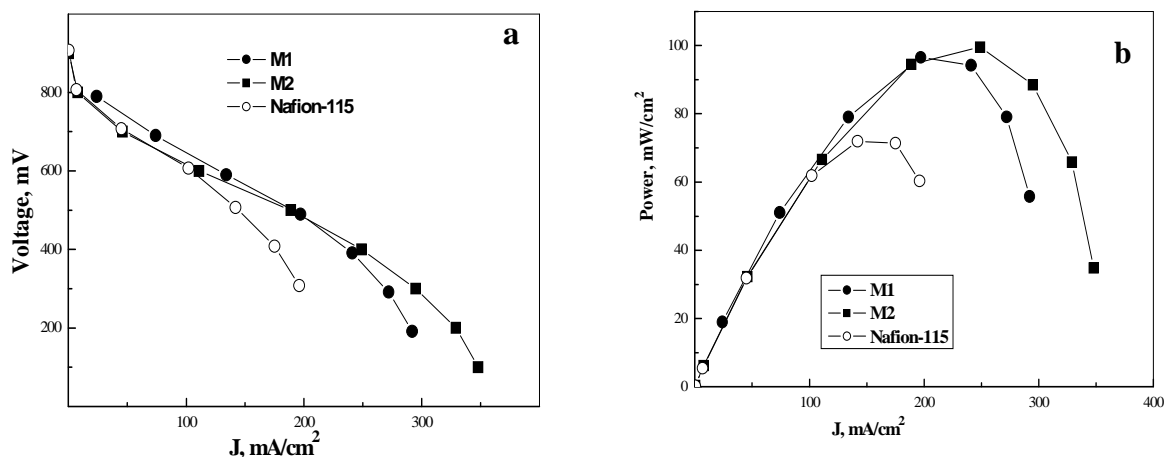


Figure 3. Volt-ampere (a) and power (b) characteristics of the HAFC on the base of synthesized membranes (M1, M2) and Nafion-115

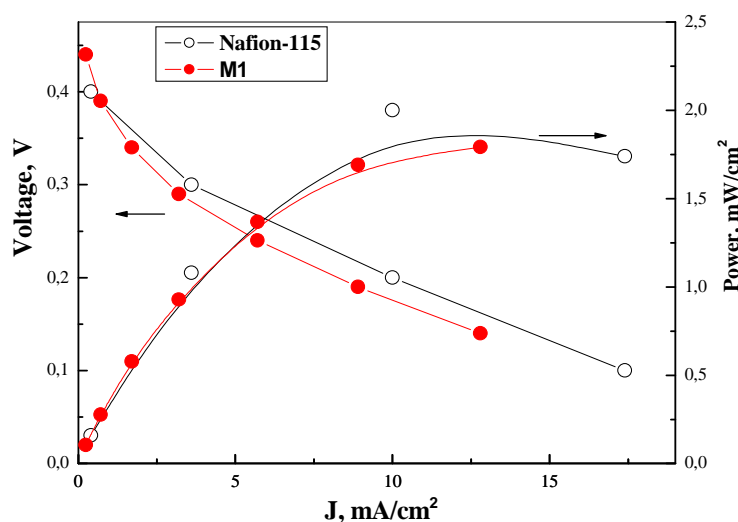


Figure 4. Volt-ampere and power characteristics of the MAFC on the base of synthesized membrane M1 and Nafion-115

This research has been supported by RFBR, grant № 08-09-00161-a, and by RAS Program № 24 “Base investigation for nanotechnology and nano-materials”

### References

1. Abdrashitov E.F., Bokun V.Ch., Kritskaya D.A., Sanginov E.A., Ponomarev A.N., Dobrovol'ski Yu.A. Synthesis and Transport properties of Proton conducting Membranes based on polyvinilidene films with introduced and sulfonated polystyrene. // Russian Journal of Electrochemistry, 2011, Vol. 47, № 4, P.387–394.
2. Abdrashitov E.F., Kritskaya D.A., Voilov D.N., Dremova N.N., Sanginov E.A., Ponomarev A.N., Dobrovol'ski Yu.A. Structure investigation of the composite PVDF – sulfonated polystyrene membranes by AFM and electron scanning microscopy. // Membranes and membrane technology, 2011, Vol.1, № 4, P. 1–8.

---

# COMPARATIVE STUDY OF ELECTRODIALYSIS DESALINATION OF A WINE MODEL SOLUTION WITH COMMERCIAL AND EXPERIMENTAL ION EXCHANGE MEMBRANES

Mikhail Porozhnyi, Semen Mareev, Natalia Pismenskaya, Victor Nikonenko,  
Veronica Sarapulova

Kuban State University, Krasnodar, Russia

## Introduction

Electrodialysis (ED) is one of the most effective methods of wine stabilization from the tartrate sedimentation. This sediment is the potassium salt of tartaric acid, hence the main goal of the electrodialysis process is to reduce the content of potassium and hydrotartrates to certain concentrations. The efficiency of this process and its production validity are determined by using a pilot ED stack. To improve characteristics of the electrodialysis stabilization of wine, commercial and experimental anion exchange membranes were used.

## Experiments

The process of ED desalination of a wine model solution was studied by using commercial Japanese (Astom) anion-exchange membranes AMX and experimental anion exchange membranes MA-41PM produced by OAO ShchekinoAzote and modified by Membrane Technology IE. In both cases Japanese (Astom) cation-exchange membranes CMX were used. The membrane stack consisted of 10 anion-exchange membranes and 12 cation-exchange membranes forming 10 cell pairs.

Experiment was conducted in two stages, first, with the AMX membranes, and then with MA-41PM membranes. Both of the stages were managed under the same operation conditions:

- a constant current density was maintained at a value of  $8 \text{ mA/cm}^2$ ;
- the flow rate in the concentration loop, CL, and the desalination loop, DL, was  $18 \text{ L/(h dm)}$ ;
- the flow rate in the electrode loop, EL, was  $200 \text{ L/(h dm)}$ ;
- 10 L of a 5 g/L NaCl solution circulated in the concentration loop, 10 L of a 30 g/L  $\text{KNO}_3$  solution circulated in the electrode loop.

10 L of a wine model solution circulated in the desalination loop at each stage of the experiment. The initial chemical composition of the model solution was as follows:

- tartaric acid      2 g/L;
- KCl                0,4 g/L;
- $\text{CaCl}_2$             0,36 g/L;
- acetic acid        0,48 g/L;
- lactic acid        1 g/L;
- pH = 3,25.

The desalting process was stopped, when the electrical conductivity  $k_i$  decreased by 30 % in comparison with its initial quantity  $k_0$ .

Kinetic dependences of the electrical conductivity, pH and temperature of the desalting solution, as well as the voltage across the membrane stack were registered during the experiment. Sampling for the following analysis of the component composition of the desalted solution was carried out at three different values of its electrical conductivity  $k_1 = 0,9 k_0$ ;  $k_2 = 0,8 k_0$  and  $k_3 = 0,7 k_0$ .

The experiments with each set of membranes were repeated several times. After each run, all loops of the ED module were rinsed with distilled water. Before each subsequent run, each loop was rinsed with an appropriate solution: NaCl (CL),  $\text{KNO}_3$  (EL), the model solution (DL), in order to achieve a constant electrical conductivity of the circulating solution in each loop.

## Results and Discussion

Figure 1 presents the potential drop across the ED stack as a function of the feed solution electrical conductivity, the latter varies with time during electro dialysis. Fig. 2 shows the kinetic dependences of the ratio of the feed solution electrical conductivity to its initial value.

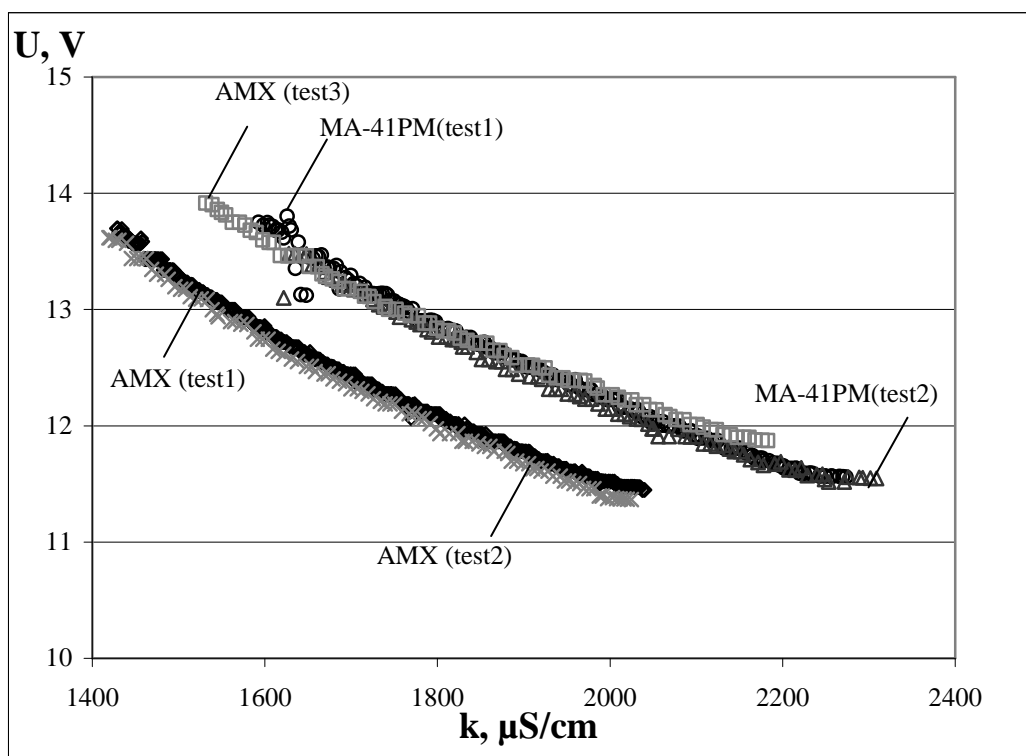


Figure 1. The rise of the potential drop across the ED stack as a function of the conductivity of the desalting model solution. (Numerals in parentheses indicate the sequence number of the experiment run)

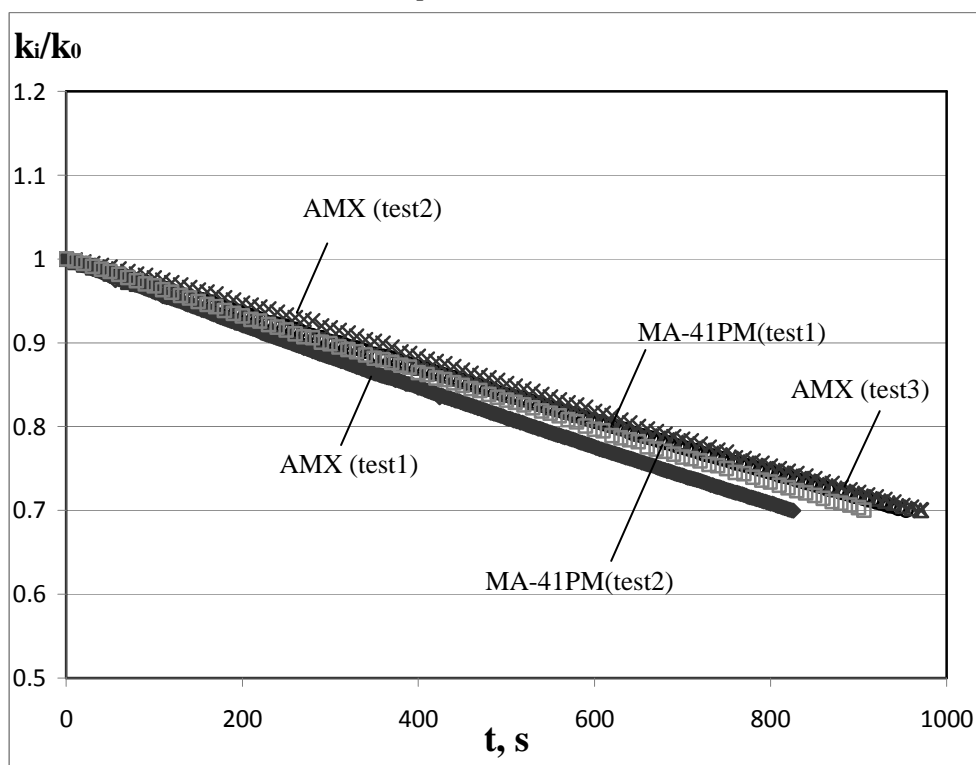


Figure 2. Kinetic dependences of the ratio of the feed wine model solution electrical conductivity to its initial value

The analysis of the obtained data shows that the power consumptions of the desalting process of the wine model solution are close when using commercial AMX or experimental MA-41PM membranes. This result is consistent with the measurements of the surface resistance,  $R$ , of these membranes. In 0.02 M solution of potassium hydrogen tartrate  $R$  is equal to 29 ohm/cm<sup>2</sup> in the case of MA-41PM membrane and to 20 ohm/cm<sup>2</sup> in the case of AMX membrane, while the surface resistance of the commercial MA-41 membrane is equal to 56 ohm/cm<sup>2</sup>.

In all experiments (in the range of the measurement error), the kinetics of the wine model solution ED desalination is also close in the case of AMX and MA-41PM membranes.

### **Acknowledgement**

*The study was realized within French-Russian laboratory “Ion-exchange membranes and related processes”. We are grateful to CNRS, France, and to RFBR (grant 12-08-93106); RFTP (contract 02.740.11.0861), Russia for financial support and EURODIA INDUSTRIE S.A., France, as equipment supplier and for financial support*

## MODIFYING OF POLYMERIC RAW MATERIALS FOR THE PURPOSE OF REGULATION OF STRUCTURE AND PROPERTIES OF SELECTIVELY NONTIGHT MEMBRANES

Larisa Potehina, Valentiny Sedelkin, Antonina Surkova, Olga Chirkova

Engels Technological Institute (Branch), Gagarin Saratov State Technical University, Saratov, Russia  
E-mail: larisa\_potehina@mail.ru

For realization of processes micro, ultra - nanofiltrations are necessary membranes with adjustable properties. One of ways of the solution of this problem is modifying of initial polymeric raw materials. In the real work polymer modifying – powdery air and dry cellulose diacetate (CDA) was carried out, data on kinetics of swelling of CDA in pairs of water and organic mix, and also experimental data about structure and properties of membranes are obtained. As water and organic mixes binary mixes of the distilled water and solvents [a dimethyl sulfoxide (DMSO) and dimethyl acetamide (DMAA)] are used. For carrying out experiences the ratio water was chosen: solvent in a binary mix = 90:10 (on liquid volume). Updating of CDA carried out at temperature  $25 \pm 2^\circ\text{C}$  in the hermetically sealed vessel which has been partially filled with a mix of water and solvent. Quantity absorbed vapors determined by a weight method by a difference of mass of a hinge plate after and before steam processing. In drawing kinetic curve swellings of a powder CDA are given in pairs of water and organic mixes.

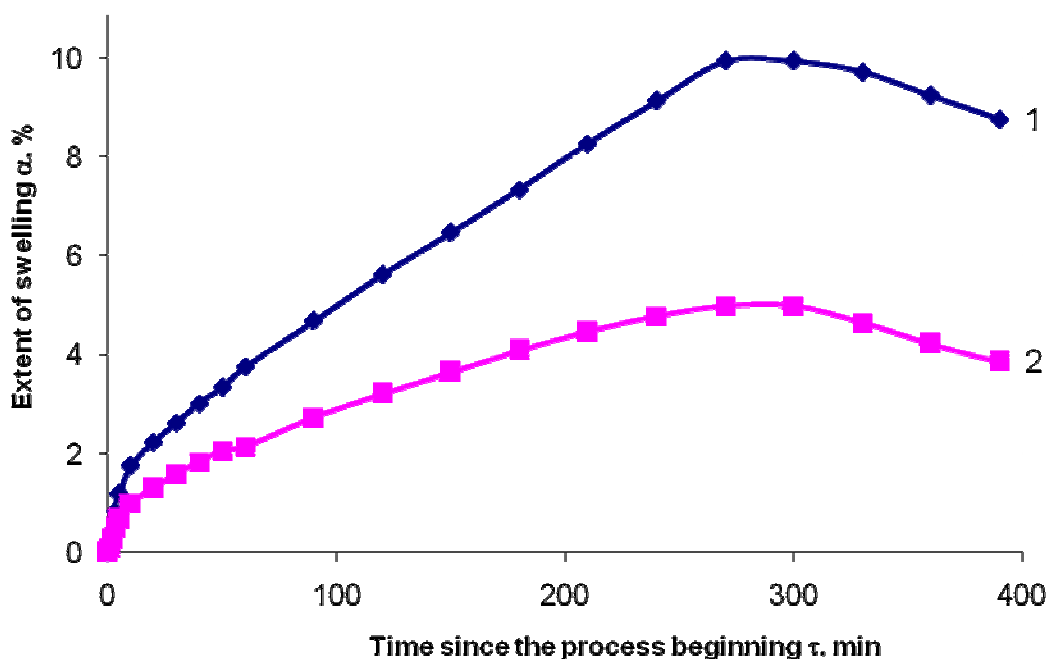


Figure 1. Kinetic curve swellings of a powder CDA in pairs of mixes of water with DMSO (1) and DMAA (2)

During researches defined sizes of speeds and swelling constants on various sites of the kinetic curves which values are given in the table. The analysis of the results given in the table, showed that pairs of mix of water with DMSO are absorbed by CDA much quicker and in bigger volume, than with DMAA. It testifies to higher penetration vapors with DMSO in structure of acetates of cellulose in comparison with pairs with DMAA. Besides, rheological and optical properties of solutions cellulose diacetate, prepared on the basis of the modified polymer are investigated. Polymeric filtrational membranes were made of these solutions.

During experiments data on structure of membranes are obtained, in particular, it concerns research of porometric characteristics. It is established that use of modified CDA allows to increase porosity of membranes to 35 %.

**Table 1: Average values of speeds and swelling constants on various sites of kinetic curves**

Parameters	Numbers of sites				
	1 ( $\Delta T=0-3\text{min}$ )	2 ( $\Delta T=3-10\text{min}$ )	3 ( $\Delta T=10-60\text{min}$ )	4 ( $\Delta T=60-300\text{min}$ )	5 ( $\Delta T=300-390\text{min}$ )
Speed of swelling $\varphi$ , g/min $\left(\frac{DMMS}{DMMA}\right)$	$\frac{0,17}{0,084}$	$\frac{0,16}{0,07}$	$\frac{0,06}{0,03}$	$\frac{0,03}{0,01}$	$\frac{0,005}{0,003}$
Swelling constant $\bar{K}$ $\left(\frac{DMMS}{DMMA}\right)$	$\frac{0,336}{0,291}$	$\frac{0,221}{0,220}$	$\frac{0,046}{0,054}$	$\frac{0,008}{0,009}$	$\frac{0,007}{0,005}$

Research of operational characteristics of membranes (selectivity and permeability) showed that modifying of initial polymer also leads to improvement of these characteristics. So selectivity of the modified membranes on syvorotochny protein made 78÷85 %.

The received results showed that at the expense of physical and chemical updating of polymeric raw materials, in particular, cellulose diacetates, various mezofazogenny substances possible to regulate structure and properties of selectively nontight membranes.

*Work is executed with support of Fund of assistance to development of small forms of the enterprise in the scientific and technical sphere.*

---

# A REVIEW OF ELECTRODIALYTIC PHENOMENA AND APPLICATIONS IN THE FOOD, BEVERAGE AND NUTRACEUTICAL INDUSTRIES

<sup>1</sup>Gérald Pourcelly, <sup>2</sup>Laurent Bazinet

<sup>1</sup>“European Membrane Institute”, University Montpellier 2, Montpellier, France,  
E-mail: *Gerald.Pourcelly@univ-montp2.fr*

<sup>2</sup>“Institute of Nutraceuticals and Functional Foods” Laval University, Québec, Canada,  
E-mail: *Laurent.Bazinet@fsaa.ulaval.ca*

The use of membranes in the food industry has increased steadily for the past 25 years. Membrane technologies used in the processing industry include reverse osmosis, ultrafiltration, microfiltration and electrodialysis (ED). ED systems annual sales account for about 15 % of the total systems sold.

ED is providing new membrane separation processes with numerous applications in the food, nutraceutical and beverage industries. ED with ion membranes or bipolar membranes or filtration membranes allowed, amongst others, the coagulation of proteins, the electro-reduction of the medium and/or the fractionation of several food proteins. Moreover, ED with filtration membranes allowed the recovery of molecules with bioactive properties such as antioxidant, anticancer and antihypertensive peptides [1-6].

Pertinent characteristics of ED systems adopted by the food industry are:

- Improvement of process performance and food quality in preparation of traditional food products;
- Innovation of processes and products aimed at satisfying evolving food requirements related to nutrition and health;
- ED gives the food industry three advantages as compared to competing technologies: increased food safety, economic competitiveness, and environmental friendliness.

ED gives the food industry three advantages as compared to competing technologies: increased food safety, economic competitiveness and environmental friendliness. Current applications of ED in the juice, wine and dairy industries highlight the innovation and diversity of ED in food processing.

A special stress will be put on emerging electromembrane technologies and applications for added-values dairy ingredients, fruit juices, biotechnologies, nutraceutical and biopharmaceutical industries.

## References

1. *Hesketin J, Ho Thang and Patts T.* ED in the food industry, in: *Membranes for Food Applications*, Eds: Peineman K.V, Periera Nunes S., Giorno L., Wiley-VCH, vol.3 2010.
2. *Fidaelo M, Moresi M.*, ED applications in the food industry // *Adv. Food., Nutrition Research*, Vol.51, 266-360, 2006.
3. *Pourcelly G, Bazinet L.* Development of bipolar membrane technology in food and bio-industries, in ‘*Handbook of membrane Separation, Chemical, Pharmaceutical and Biotechnological Applications*’, Marcel Dekker Publishers, 2008.
4. *Bazinet L, Doyen A, Roblet C.* Electrodialytic phenomena, associated electromembrane technologies and applications in the food, beverage and nutraceutical industries, in ‘*Separation, Extraction and Separation Processes in the Food, Beverage and Nutraceutical Industries*’, Ed. S Rivzi, Woodhead Publishing Ltd, pp. 202-218, 2010.
5. *Bazinet L, Firdaous L.* Applications of electromembrane processes to the production of nutraceuticals or functional foods, in ‘*Handbook of Membrane Research: Properties, Performances and Applications*’ Ed. S. V. Gorley, Nova Science Pub., pp: 291-312, 2010.
6. *Vera E, Sandeaux J, Persin F, Ruales J, Dornier M, Pourcelly G.* Deacidification of clarified juice by ED // *J. Food. Eng.* 78, 1427-1438, 2007.

---

## ADSORPTION CHARACTERISTICS OF CELLULOSE ACETATE SEMIPERMEABLE MEMBRANES

Marina Pozdeeva, Valentine Sedelkin, Olga Chirkova

Engels Technological Institute (branch) SSTU Gagarin, Saratov, Russia, E-mail: Pozdeevamg@mail.ru

In this paper we investigate the adsorption of amino acids in the process of filtration of aqueous solutions through a porous polymeric membrane. The authors have developed cellulose acetate ultrafiltration membrane modified with activated charcoal fine and coarse fractions, the composition of which is protected by the Patent. The membranes are used for filtration separation of the secondary dairy whey protein consisting of amino acids. This process is based on the detention of solute particles by membrane, when particle size exceeds the size of the pores in the surface layer of the membrane. The detention of dissolved particles in the ultrafiltration may also be due to adsorption of the particle by the surface and the pores of membrane. Thus, the process of ultrafiltration is accompanied by adsorption of the protein components in membranes. To study the adsorption process and model it is necessary to know the nature, structure and other properties and characteristics of the adsorbent. The nature of the adsorbent surface, the size and shape of its pores affects the adsorption and changes its characteristics (the adsorption model).

In this paper, a model of adsorptives solutions  $\beta$ -alanine, albumin, and NaCl was used. All investigated adsorptives had significant difference in refractive index. This is important for interfering method of determining the concentration of solutions, which we have chosen. As an adsorbent in the study of adsorption of binary solutions of amino acids polymer film ultrafiltration membrane from cellulose secondary acetate with various modifiers (UF PF CSA-membranes) was used. The settling time of the adsorption equilibrium in the system was determined by readings of the kinetic curves of adsorption. Equilibrium solutions were analyzed for the interferometer ITR - 2. The composition of the equilibrium solution was determined. The magnitude of the excess adsorption was calculated from the calibration curve. Analysis of the adsorption systems was carried out on the basis of the Gibbs excess quantities and method of the full content. The model treats the adsorption as a process of mutual displacement of the components in the surface layer under the condition of additivity of molecular areas of components. This model is taken as a model of the adsorption solution. The limiting value of adsorption on the example of  $\beta$ -alanine were calculated based on the assumption of incompressibility of the solution and the dense packing of the components in the surface layer. The values of limiting values of adsorption  $m_s$  were equal to 0.0189 mmol / g - for membranes with a small fraction of coal, 0.0167 mmol / g - for membranes with a large fraction of coal. The model of the adsorption solution, consisting of a single layer was considered in this paper. The values of free energy were calculated to assess the validity of the model solution of the adsorption and characteristics of the adsorption solution. The were calculated by the method of excess quantities of Gibbs and method full content for systems of  $\beta$ -alanine-water-CSA-membrane and albumin-water-CSA-membrane. Comparison of  $\Delta G_{\text{mod}}$  and  $\Delta G_{\text{gib}}$  showed good agreement between the data obtained. This is the criterion for selecting the correct model of the adsorption layer. The change of thermodynamic functions of adsorption and the bulk solutions were calculated for a system of  $\beta$ -alanine-water-CSA-membrane: activity coefficient of the solution components ( $\gamma_i, \gamma_i^s$ ) and the excess free energy of mixing  $g^E$  and  $g^{ES}$ . Comparison of the properties of the bulk solutions and adsorption solutions showed that in the studied systems, negative deviations from ideality are observed for the adsorption solutions. Similar results were obtained for a system of albumin - water-CSA-membrane.

### Conclusion

The experimental data have been obtained by thermodynamic analysis. Monomolecular adsorption model of the solution is justified and the main thermodynamic functions of adsorption and the bulk solutions were identified. It was established that the significant role played by adsorption processes for separation of protein-carbohydrate raw materials by the CSA-membrane, i.e. ultrafiltration membrane doesn't work only by the molecular-sieve mechanism.

---

# NON-EQUILIBRIUM THERMODYNAMICS OF COLLOIDAL SYSTEMS

Vjacheslav Roldugin

Frumkin Institute of Physical Chemistry and Electrochemistry of RAS, Moscow, Russia,

E-mail: roldugin@phych.e.ac.ru

## Introduction

At the present time, there is much increased interest in the non-equilibrium thermodynamics of colloidal systems: for the last ten years, have been published many papers on this topic. This interest is due to both the discovery of new effects, and the unexpectedly strong manifestation of a number of classical effects. Some effects have not yet received a definitive explanation, and there are inconsistencies in the treatment of well-known phenomena.

## Basic principles of non-equilibrium thermodynamics

The essence of non-equilibrium thermodynamics is the following. Any physical quantity due to uncontrolled interaction of subsystem with the rest of the system changes over time: there are random fluctuations around the mean. These fluctuations are referred to as the fluctuations of the corresponding physical quantities. To determine the magnitude of fluctuations, as well as to describe patterns of change over time is required at the microscopic level to describe the behavior of a non-equilibrium system. This problem is still unsolved, so the pattern of fluctuations of thermodynamic quantities, as well as their evolution over time are determined using the approach developed by Gibbs. For this purpose, the entropy of the system  $S$  is represented as a function of physicochemical characteristics of the subsystem  $\mathbf{W} = (W_1, W_2, \dots, W_n)$  and the probability of finding the subsystem in a given state is expressed as

$$P_r(\mathbf{W}) \propto \exp[S(\mathbf{W})]. \quad (1)$$

This formula, in particular, shows that the most probable is the system state with the maximal entropy  $S_0$ . This condition is usually associated with the state of thermodynamic equilibrium, in which the physical characteristics  $\mathbf{W}_0$  take values that provide the maximum value of  $S_0$  for given initial conditions. Equation (1) is also a reflection of the second law of thermodynamics, according to which a non-equilibrium system evolves in the direction corresponding to an increase in entropy.

Onsager basing on the relation (1) and using the assumption that the relaxation of fluctuations proceeds according to the laws established for the relaxation of macroscopic quantities, on the basis of the principle of microscopic reversibility showed the following. If we introduce through the relationship ( $a_i = W_i - W_{i0}$ )

$$\hat{X}_i = -\frac{\partial S}{\partial a_i} = \sum_j g_{ij} a_j, \quad (2)$$

quantities called thermodynamic forces, and derivatives  $\frac{da_i}{dt}$ , which are thermodynamic fluxes, in the relaxation equations

$$\frac{da_i}{dt} = \sum_j L_{ij} \hat{X}_j \quad (3)$$

kinetic coefficients  $L_{ij}$  obey the symmetry relations

$$L_{ij} = L_{ji}. \quad (4)$$

Equations (1) - (4) are the essence of non-equilibrium thermodynamics

## Generalized transport equations

First of all, note that for a correct description of non-equilibrium processes involving boundary layers the generalized non-equilibrium thermodynamics of transport processes in the bulk phase should be used. In the generalized non-equilibrium thermodynamics there are

additional fluxes and forces. Without going into details, we note that in this case the phenomenological equation for the vector fluxes, say, for the one-component gas are as follows

$$\begin{aligned}\mathbf{q} &= -\Lambda_{11}\nabla\ln T - \Lambda_{12}\Delta\mathbf{u}, \\ \mathbf{J}^v &= -\Lambda_{21}\nabla\ln T - \Lambda_{22}\Delta\mathbf{u},\end{aligned}\quad (5)$$

where  $\mathbf{q}$  is the heat flux density,  $T$  is the temperature,  $\mathbf{u}$  is the velocity of the fluid. Since  $\Delta\mathbf{u}$  up to a factor equal to the pressure gradient, we see that the heat flux can be caused by the pressure gradient. This issue disputed in the classical books with reference to the second law of thermodynamics. One can show that there is no contradiction with the second law of thermodynamics, since additional flux  $\mathbf{J}^v$  is involved in the consideration. This flux is difficult to give a physical meaning because it is in a rather complicated way expressed through the velocity of the molecules. However, its existence can not be doubted, as the heat flux caused by the pressure gradient was measured in real experiments

In the approximation corresponding to the system (5), as well should be modified tensor equations, which are now as follows

$$\begin{aligned}\mathbf{\Pi} &= -\lambda_{11}\overline{\nabla\mathbf{u}} - \lambda_{12}\frac{\overline{\nabla\nabla T}}{T}, \\ \mathbf{J}^T &= -\lambda_{21}\overline{\nabla\mathbf{u}} - \lambda_{22}\frac{\overline{\nabla\nabla T}}{T},\end{aligned}\quad (6)$$

where  $\mathbf{\Pi}$  is the stress tensor,  $\mathbf{J}^T$  is a generalized tensor, and the bar over the two vectors means the symmetrical combination of their components. Equations (6) describe not only viscous but also the thermal stresses.

### The non-equilibrium thermodynamics of boundary conditions

The methods of non-equilibrium thermodynamics can be used for constructing the boundary conditions. Without going into details of the calculation we can represent a set of boundary conditions for one-component system in the form

$$\begin{aligned}\frac{T(0)-T_0}{T_0} &= L_{00}\frac{q_n}{T_0}, \\ \mathbf{u}_\tau(0) + \frac{2}{5}\frac{\mathbf{q}_\tau}{p} &= L_{11}\mathbf{\Pi}_{n\tau} + L_{12}\frac{1}{T^2}\frac{\partial T}{\partial\tau} + L_{13}\frac{1}{T}\frac{\partial p}{\partial\tau}, \\ \hat{\mathbf{j}}_{b\tau}^q &= L_{21}\mathbf{\Pi}_{n\tau} + L_{22}\frac{1}{T^2}\frac{\partial T}{\partial\tau} + L_{23}\frac{1}{T}\frac{\partial p}{\partial\tau}, \\ \hat{\mathbf{j}}_{b\tau} &= L_{31}\mathbf{\Pi}_{n\tau} + L_{32}\frac{1}{T^2}\frac{\partial T}{\partial\tau} + L_{33}\frac{1}{T}\frac{\partial p}{\partial\tau},\end{aligned}\quad (8)$$

where  $p$  is the pressure,  $\hat{\mathbf{j}}_{b\tau}^q$ ,  $\hat{\mathbf{j}}_{b\tau}$  are the heat and mass fluxes in the boundary layer. The first (scalar) equation describes the temperature jump. The system of equations (8) describes the effects of slip and heat and mass transfer in the boundary layers. In particular, the first term on the right side determines the slip of the fluid under the action of tangential stresses

$$\mathbf{\Pi}_{x\tau} = -\eta_f\frac{d\mathbf{u}_\tau}{dx}:$$

$$\mathbf{u}_\tau(0) = -L_{11}\eta_f\frac{d\mathbf{u}_\tau(x)}{dx} = b_h\frac{d\mathbf{u}_\tau(x)}{dx},\quad (9)$$

where  $b_h$  is the length of slip, which is now called the hydrophobic slip. The other two terms describe the thermal slip and pressure slip. The boundary conditions obtained within the framework of non-equilibrium thermodynamics predict a number of new effects.

### Non-equilibrium thermodynamics of particle motion in non-uniform media

Now we present an approach to the construction of non-equilibrium thermodynamics of particle motion in a liquid or a gas in a non-uniform temperature field. We note at once that we

could consider more general situation, when the dispersion medium is a mixture, an electrolyte, there are non-uniform concentration field, an external electric field, etc. But this would lead to very cumbersome relations, which made the essence of the approach difficult. The general case can easily be reproduced on the basis of the partial equations, one pair of which proposed below. One can obtain the following phenomenological equations

$$\begin{aligned} \mathbf{U} &= \lambda_{00} \mathbf{F} + \lambda_{0T} \nabla T, \\ \frac{4\pi \mathbf{A}}{T_0} &= \lambda_{T0} \mathbf{F} + \lambda_{TT} \nabla T, \end{aligned} \quad (10)$$

where  $\mathbf{U}$  - the velocity of the particle,  $\mathbf{F}$  - the force acting on it,  $\mathbf{A}$  - the temperature dipole moment of the particle. Note that if a particle is nonspherical, then the equations retain their form, but the kinetic coefficients in this case become tensors.

The coefficient  $\lambda_{00}$  determines the velocity of the particle motion in a fluid under the action of external forces. This coefficient for a spherical particle of radius  $R$  is determined from the Stokes law and equal  $\lambda_{00} = 1/6\pi\eta R$ .

The coefficient  $\lambda_{0T}$  relates the velocity of the particles with a temperature gradient. The view of  $\lambda_{0T}$  fairly substantially depends on the nature of the dispersion medium, particle size and their physical and chemical characteristics. The motion of particles caused by the temperature gradient is called thermophoresis. Although the history of this effect is already more than century-long period, it still remains the object of attention of researchers.

Coefficient  $\lambda_{TT}$  determining the magnitude of the temperature dipole moment that arises in the particle, placed in a non-uniform with respect to temperature medium, is well known for the large particles whose size is substantially greater than the thickness of the boundary layers. It is easy to install, based on the continuity of temperature field and heat flux on the surface of a spherical particle that

$$\lambda_{TT} = 4\pi \frac{\lambda_e - \lambda_i}{\lambda_i + 2\lambda_e} \frac{R^3}{T_0}, \quad (5.17)$$

where  $\lambda_i, \lambda_e$  are the heat conductivity coefficients of the particle and the dispersion medium.

Less well known is the effect determined by coefficient  $\lambda_{T0}$ . This coefficient sets the value of the temperature dipole moment that arises in the particle moving under the action of an external force in a uniform medium. This effect was first predicted theoretically and later observed experimentally for the case of particle motion in gases. Its appearance is due to the presence of isothermal heat fluxes in the boundary layers. In the case of gases, isothermal heat flux takes place also in the bulk and is proportional to the pressure gradient. Since there is non-uniform pressure field in the gas flow over the particles, the isothermal heat flux arises. Similar to (10) equations can be obtained for the motion of particles in non-uniform mixtures and electrolytes.

### Conclusion

From the above it is clear that non-equilibrium thermodynamics becomes a relevant tool in the study of colloidal systems. It allows you to predict new phenomena and to find original solutions to traditional problems of physics and chemistry of colloids. Modern development of scientific research has revived interest in surface phenomena which are part of colloid chemistry. The colloid chemistry is a basis of modern microfluidics that makes it possible to create new miniature devices, becomes a base for the original experiments and discoveries unexpected effects.

---

# EFFECT OF SURFACE DIFFUSION ON THE BINARY GAS MIXTURE SEPARATION

<sup>1</sup>Vjacheslav Roldugin, <sup>1</sup>Elena Sherysheva, <sup>2</sup>Vladimir Zhdanov

<sup>1</sup>Frumkin Institute of Physical Chemistry and Electrochemistry of RAS, Moscow, Russia,

*E-mail:* roldugin@phyc.che.ac.ru

<sup>2</sup>National Research Nuclear University "MEPhI", Moscow, Russia, *E-mail:* VMZhdanov@mail.ru

## Introduction

In recent years, greatly increased the interest in the study of transport processes in membranes with a complex structure [1, 2]. For gas flow in composite membranes some interesting effects were observed. The most attractive of them is related to the asymmetry of transport characteristics. In [3] it was shown that the asymmetry of the permeability of bilayer membranes may be related to surface diffusion. The asymmetry is due to the strong dependence of the surface diffusion coefficient on the degree of surface coverage. In this report we examine the effect of surface diffusion coefficient on the separation of a binary gas mixtures. We consider the flow of a binary mixture in a single-layer nanosize membrane and a bilayer membrane, which one layers is finely porous, while another is coarse. The flow of the mixture in finely porous layer is described in the free-molecular regime, and the flow in coarse layer is considered in the hydrodynamic approximation.

## Effect of surface diffusion

We begin our consideration with analysis of the binary gas mixture transport in the nanosize channels, where surface diffusion significantly contributes to the overall flux. We assume that the adsorption of components is described by the Langmuir isotherms

$$\begin{aligned}\Gamma_1 &= \Gamma_{\max} \frac{p_1 / \alpha_1}{1 + p_1 / \alpha_1 + p_2 / \alpha_2}, \\ \Gamma_2 &= \Gamma_{\max} \frac{p_2 / \alpha_2}{1 + p_1 / \alpha_1 + p_2 / \alpha_2},\end{aligned}\tag{1}$$

where  $\Gamma_{\max}$  is the maximum value of adsorption  $\Gamma_i$  is adsorption of component  $i$ ,  $p_i$  is its partial pressure,  $\alpha_i$  is the parameters of the adsorption isotherms.

Unfortunately, no data on surface diffusion dependence on surface coverage in the case of multicomponent systems. However, we can get the proper dependence using the following considerations. The diffusion flux is usually written in the form

$$J = -\frac{Dn}{kT} \nabla \mu,\tag{2}$$

where  $\mu$  is the chemical potential of diffusing component,  $n$  is its concentration,  $k$  is the Boltzmann constant,  $T$  is the temperature,  $D$  is the diffusion coefficient. This form allows us to take into account the steric interaction between molecules in the adsorption layer at high surface coverage. In fact, equation (2) is classical Fick's law, written using the Einstein relation between mobility of the particles and their diffusion coefficient. Chemical potential gradient in this case, obviously, is the average force acting on the particle. Since the gas in the bulk phase at pressures can be considered as an ideal, the chemical potentials of components can be written in the form

$$\mu_i = kT \ln(p_i / p_0),\tag{3}$$

where  $p_0$  is the normalization constant. Using the equality of chemical potentials of components in the bulk phase and in the adsorption layer and the Langmuir isotherm we can be obtained the following relation between the equilibrium partial pressures and degrees of surface filling  $\theta_i = \Gamma_i / \Gamma_{\max}$ :

$$p_i = \frac{\alpha_i \theta_i}{1 - \theta_1 - \theta_2}.\tag{4}$$

Taking into account equation (4) the flux of  $i$ -th component in the cylindrical channel with radius  $R$  can be represented as

$$J_i = \pi R^2 \frac{D_{vi}}{kT} \frac{dp_i}{dz} + 2\pi R D_{si} \Gamma_{\max} \theta_i \frac{d}{dz} \ln \left( \frac{\alpha_i \theta_i}{1 - \theta_1 - \theta_2} \right), \quad (5)$$

where  $D_{vi}$  is the coefficient of the diffusion in channel bulk,  $D_{si}$  is the coefficient of surface diffusion of component  $i$ . It is easy to see that expression (5) accounts for a significant increase in the diffusion flux when the surface coverage tends to unity, and this increase corresponds to the dependence of the effective diffusion coefficient used in [3] in the case of one-component gas.

Equation (5) takes into account the mutual influence of components on their transfer in the adsorption layer. In particular, the non-uniformity of the surface concentration of the second component causes the transfer of the first in the direction of lower concentrations. This is due to steric interactions of adsorbed molecules, where one component is trying to display the second component from the surface. As a second component also diffuses to lower concentration, the above effect can be considered as a mutual drag of the components.

Expressing the degree of surface coverage through the pressure, we can obtain the following pair of transfer equations

$$\begin{aligned} J_1 &= \pi R^2 \frac{D_{v1}}{kT} \frac{dp_1}{dz} + 2\pi R D_{s1} \Gamma_{\max} \frac{1/\alpha_1}{1 + p_1/\alpha_1 + p_2/\alpha_2} \frac{dp_1}{dz}, \\ J_2 &= \pi R^2 \frac{D_{v2}}{kT} \frac{dp_2}{dz} + 2\pi R D_{s2} \Gamma_{\max} \frac{1/\alpha_2}{1 + p_2/\alpha_2 + p_1/\alpha_1} \frac{dp_2}{dz}. \end{aligned} \quad (8)$$

Equations (8) were used as the basis for calculating the coefficient of separation of binary mixtures in the nanosize channel and the bilayer membrane. An approximate analytical solution of equations (8) was obtained and the component fluxes were calculated, basing on which the separation factor was determined. It is found that surface diffusion can strongly influence the magnitude of the separation factor of the gas mixture in the nanosize channel.

A comparison of the separation factors for bilayer membrane shows that the efficiency of the mixture enrichment is nearly tenfold higher when the separating layer is located at the input than that when it is at the output. Note that, as a matter of fact, the concentration drop at the separating layer is higher in the second case; however, this advantage is eliminated by the presence of a supporting layer before the separating layer.

## References

1. Volkov V.V., Mchedlishvili B.V., Roldughin V.I., Ivanchev S.S., Yaroslavtsev A.B. Membranes and nanotechnology // Nanotechnol Russia 2008 V. 3. P. 656-687.
2. Roldughin V.I., Zhdanov V.M. Asymmetric gas mixture transport in composite membranes // Adv. Colloid Interface Sci. 2011. V. 168. P. 223-246.
3. Roldughin V.I., Zhdanov V.M., Sherysheva E.E. Effect of surface diffusion on asymmetry of bilayer porous membrane permeability // Kolloid. Zhurn. 2012. V. 74.

---

# POTENTIOMETRIC MULTISENSORY SYSTEMS WITH PD-SENSORS FOR QUANTITATIVE DETERMINATION OF LYSINE AND THIAMINE IN AQUEOUS ORGANICS MEDIUM

Elena Ryzhkova, Anna Parshina, Olga Bobreshova

Voronezh State University, Voronezh, Russia, E-mail: ryzhkova-helen@mail.ru

## Introduction

The falsification of milk and dairy products (due to the use of dry milk) this is an actual problem of modern dairy industry. When you add a reconstituted milk in drinking reduced the nutritional value of the product at the expense of loss of amino acids (lysine, cysteine), vitamins (B1, B6, C) and ion-molecular calcium as a result of multiple thermal processing [1]. Gostirovannye methods of identification of dairy products on the basis of reconstituted milk are not available. The aim of this work was the develop of the potentiometric multisensory systems, including PD-sensors [2-4] for express quantitative determination of lysine monohydrochloride and thiamine chloride in aqueous-organic medium.

## Experimental

In the capacity of a model system investigated aqueous solutions lysine monohydrochloride LysHCl and thiamine chloride ThiaminCl (vitamin B<sub>1</sub>), of containing inorganic electrolytes (NaCl, KCl and MgSO<sub>4</sub>). Real objects of analysis were samples of milk drink with a mass interrelation of milk powder from 5 to 40%.

For organization PD-sensors perfluorinated sulphocation-exchange membranes MF-4SC in the K<sup>+</sup>-type, H<sup>+</sup>-type, LysH<sub>2</sub><sup>2+</sup>-type were used. A pH-selective electrode, Ca-selective electrode, NH<sub>4</sub>-selective electrode, Na-selective electrode and silver chloride/silver reference electrode (EVS-1M3.1) were used.

## Results and Discussion

The potentiometric multisensory systems were developed for a multicomponent quantitative analysis of solutions LysHCl+KCl+NaCl, ThiaminCl+KCl+NaCl and LysHCl+KCl+NaCl+MgSO<sub>4</sub> [2, 3]. The potentiometric multisensory system used to analyse LysHCl+KCl+NaCl+MgSO<sub>4</sub> solutions was used for the analysis of therapeutic «Mineral salt with low content of sodium chloride» samples [4]. This product contained NaCl, KCl, MgSO<sub>4</sub> and LysHCl in the following mass rations (%): 0.35-0.58; 0.31-0.40; 0.05-0.10 and 0.02-0.10. These values matched to the mass relationship in the dry sample: 0.02±0.008% NaCl, 0.38±0.02% KCl, 0.53±0.04% MgSO<sub>4</sub> and 0.054±0.004% LysHCl. Thus, the measured composition of the therapeutic salt samples was in agreement with the stated product composition.

The potentiometric sensors for control of reconstituted milk in drinking milk were chosen. The influence of the concentration of milk powder the value of response of the PD-sensors with membranes MF-4SC in K<sup>+</sup>-type, H<sup>+</sup>-type, LysH<sub>2</sub><sup>2+</sup>-type were found.

## Acknowledgements

Authors thank cand.ch.sc., the chief of laboratory of membran processes OSS "Plastpolymer" (St.-Petersburg, Russia) Sergey V. Timofeev for giving samples of membranes. This work was financially supported by the RFBR (projects 12-08-00743-a) and «P.Y.S.I.C.» (research projects 9591p/14212, 01.08.2011).

## References

1. Prosenkov A.Y., Kopotkaya E.V., Mudrikova O.V. Dairy industry. February, 2010
2. Bobreshova O.V, Parshina A.V., Ryzhkova E.A. // Russian J. of Anal. Chem. 2010. V. 65. P. 885-891.
3. Bobreshova O.V, Parshina A.V., Ryzhkova E.A. // J. Zav. lab. Diagnostics of materials. 2011. V. 77. P. 22-25.
4. Bobreshova O.V, Parshina A.V., Timofeev S.V., Ryzhkova E.A. RF Patent 107590, 2011. Byull. izobret. no. 23. 2p.

# ELECTROSURFACE AND STRUCTURAL PROPERTIES OF POLYMER MATRIX BASED ON PET

<sup>1</sup>Konstantin Sabbatovsky, <sup>2</sup>Aleksandr Vilensky, <sup>1</sup>Vladimir Sobolev,

<sup>2</sup>Boris Mchedlishvili

<sup>1</sup>Frumkin Institute of Physical Chemistry and Electrochemistry of RAS, Moscow, Russia, E-mail: vsobolev@phyche.ac.ru

<sup>2</sup>Shubnikov Institute of Crystallography of RAS, Moscow, Russia, E-mail: track@eimb.ru

## Introduction

We used PET film of 10 microns thickness, which were irradiated with accelerated ions of Kr with a flux density of  $1,5 \cdot 10^8$  and  $2 \cdot 10^9$  ions/cm<sup>2</sup> at the energy of 2 MeV/a.m.u., and then etched in a weak alkaline solution to obtain the array of membrane pores of a certain radius. Structural and electrosurface characteristics of the membranes were studied in continuous electrolyte filtration on the installation diagram as shown on [1]. The design allows simultaneous installation in continuous filtration membranes to measure the resistance (R), hydrodynamic permeability and streaming potential ( $\Delta E/\Delta P$ ) of membrane in the electrolyte solution  $10^{-4}$ – $5 \cdot 10^{-1}$  M KCl. The average hydrodynamic diameter of the pores was calculated from the equation of Poiseuille by the following formula  $K_f = \pi r^4 N / 8 \eta h$ , where  $K_f$  - filtration coefficient,  $r$  - hydrodynamic radius of the membrane;  $N$  - pore density;  $\eta$  - viscosity of the solution;  $h$  - thickness.

$K_f$  was calculated on the hydrodynamic porosity (Ph) of track membrane (TM). The R measure was performed at a frequency of 100 kHz. The surface charge ( $\sigma$ ) was calculated using the Schmid and Schwarz model for fixed charges in the fine pores. The calculation of the zeta potential ( $\zeta$ ) was performed using the Helmholtz-Smoluchowski equation corrected for the contribution of double layers.

## Results and Discussion

Figure 1 shows the dependence of the surface charge density ( $\sigma$ ) of the concentration of KCl for membranes of different sizes. For wide-porous TM (Fig. 1, curve 4)  $\sigma$  does not depend on the electrolyte concentration and is equal to  $3$ – $4 \cdot 10^{-4}$  C/m<sup>2</sup>. The membrane surface charge increases in magnitude by more than an order with decreasing pore size and reaches  $10^{-2}$  C/m<sup>2</sup> (Fig. 1, curves 1-3). In our opinion, increase of the values of  $\sigma$  can also be associated with increasing oxidative and destructive processes in the polymer, as a result of which is an increase in the content of functional groups at the approach to the trajectory of the track. Lowering of the  $\zeta$ -potential as a source and heat-treated membranes to 0.25 M solution of KCl, in the range of 6,5–25 nm pore radius is almost linear (Fig. 2). Note, that for close values of the radii of heat-treated samples have been lower  $\zeta$ -potential compared with baseline. The radius 25 nm corresponds to the size of the local area of swelling of the Kr latent track.

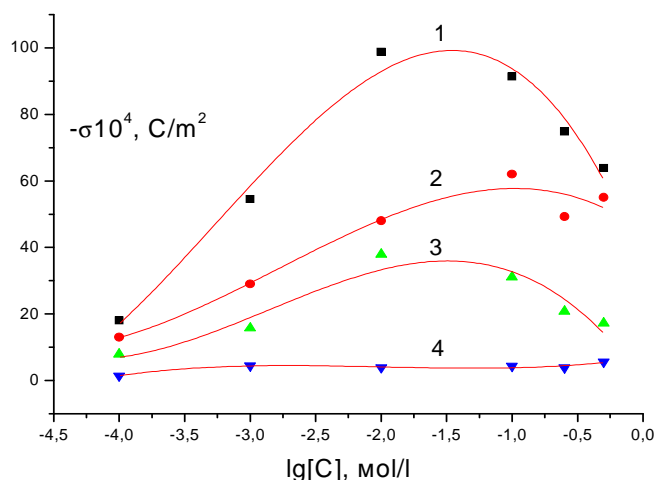


Figure 1. Dependence of surface charge density ( $\sigma$ ) of membranes on the concentration of KCl at pH 6.5. Membrane pore radius:  $r = 6.5$  (1), 12.5 (2), 17 (3), 40 nm (4).  $N = 2 \cdot 10^9$  pore/sm<sup>2</sup>

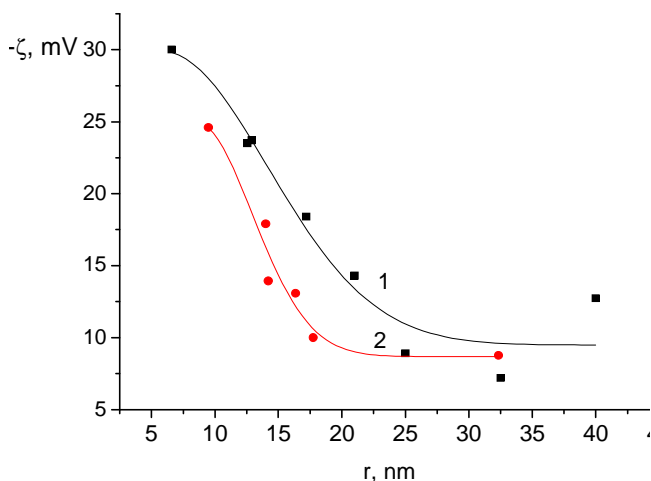


Figure 2. Dependence of the  $\zeta$ -potential on the pore radius of TM: 1 - original samples, 2 - sample after heat treatment. The measurements were performed for 0.25 M KCl solution.  $N = 2 \cdot 10^9$  pore/cm<sup>2</sup>

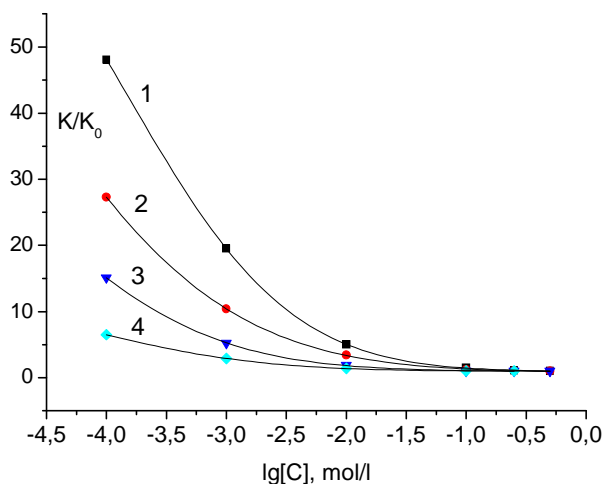


Figure 3. Dependence of the ratio  $K/K_0$  on the KCl concentration. Membrane pore radius  $r = 6.5$  (1),  $12.5$  (2),  $21$  (3),  $40$  nm (4).  $N = 2 \cdot 10^9$  sm<sup>-2</sup>

Figure 3 displays the change in the relations of the electrolyte conductivity in the pores of the membrane to the bulk electrical conductivity at the same concentration of electrolyte in the membranes with different pore radius. In general, a fairly predictable downward trend in the relationship of  $K/K_0$  is decrease in the degree of contribution of double layers in the pores of the membrane.

For membranes with pore radius 6.5 and 25 nm found little difference between 1  $K/K_0$  already for 0.25 M solutions of KCl (1.12 and 1.06, respectively). For the 0.1 M KCl solution indicated a significant excess of the electrical conductivity of the electrolyte in the pores of the membrane over the bulk values (33 and 17%, respectively). At the concentration of  $10^{-4}$  mol/l, this ratio reached 48 units for the most thin-porous membrane (curve 1), which is associated with excess counterions in the pores. Attention is drawn to the fact that at wide-porous membranes in the absence of overlapping DEL (for example, has a radius of 40 nm), the ratio  $K/K_0$  high enough (about 6.5).

Many authors attribute this to the existence of the annular zone of the polymer around the loosened channel pore, which is distributed in the COOH group. In the neutral pH region loosened polymer occurs and the space charge region with an additional conductivity.

The appearance of the gel layer due to the fact irradiation of the polymer by heavy ions in the track is not only the degradation of macromolecules, but also their cross-linking. As a result, there is a spatial grid. In alkaline solution the hydrolysis affect only linear macromolecule polymer, and cross-linked remain unchanged. As a result the selective etching loosened structure filled to electrolyte is formed (gel layer on the surface of the pores).

### References

1. Sabbatovsky K.G., Sobolev V.D, Churaev N.V. // Colloid Journal. 1991. V. 53. №1.P. 74.

---

# MF-4SC BASED HYBRID MEMBRANES WITH INCORPORATED NANOPARTICLES OF SILICA AND ZIRCONIA WITH FUNCTIONALIZED SURFACE

<sup>1</sup>Ekaterina Safronova, <sup>2</sup>Philippe Sizat, <sup>1</sup>Andrey Yaroslavtsev

<sup>1</sup>Kurnakov Institute of General and Inorganic Chemistry RAS, Moscow, Russia,

E-mail: safronova@igic.ras.ru

<sup>2</sup>University of Montpellier 2, Montpellier, France

## Introduction

It is well known that the reason of ion transport acceleration in composite materials, including hybrid membranes, is sorption processes on the interface that are determined by the surface properties (sorption ability, hydrophobicity) of material components. Earlier it was shown that perfluorosulfonic cation-exchange membranes such as Nafion (Du Pont, USA) and MF-4SC (Plastpolymer, Russia) that are widely used for proton exchange membrane fuel cells design, electrochemical synthesis and water cleaning processes modification by means of silica and zirconia incorporation results in the considerable properties changing, particularly, ion transport rate (conductivity, diffusion permeability) and ion selectivity. Thus it can be supposed that variation of sorption-exchange properties of incorporated nanoparticles surface will result in considerable properties improving of hybrid membranes.

This work summarizes results on the MF-4SC membrane modification with silica and zirconia with functionalized surface.

## Experiments

Hybrid membranes were synthesized by casting method from MF-4SC polymer solution in isopropyl alcohol. Tetraetoxysilane ( $\text{Si}(\text{OC}_2\text{H}_5)_4$ , Fluka, >98%) and zirconium oxychloride ( $\text{ZrOCl}_2$ , Merck) were used as precursors for dopant nanoparticles synthesis. Surface of silica and zirconia was functionalized by variation of the acidity by means of precipitation at different pH (in acid: MF-4SC+ $\text{SiO}_2(\text{H}^+)$  and in basic: MF-4SC+ $\text{SiO}_2(\text{OH}^-)$  solutions) and by chemical modification by hydrophilic groups with different acidity (sulfo-:  $\text{SO}_3\text{H}^-$ , amino-: *aminopropyl R<sub>1</sub>*, *3-(2-imidazolin-1-yl)-propyl R<sub>2</sub>*) and hydrophobic groups (*1H,1H,2H,2H-perfluordodecyl, PFD*). All samples with the exception of membranes doped by oxides with sulfonated surface were obtained by membrane casting from polymer solution contained calculated quantities of precursors and modified fragments followed by precursor's hydrolysis to obtain oxides. Materials with oxides with sulfonated surface was obtained by casting from polymer solution contained beforehand prepared oxides due to the impossibility of surface sulfonation in side of membrane matrix. All membranes were treated one after another by 10% solution of  $\text{H}_2\text{O}_2$ , 5% solution of HCl and twice by bidistilled water at 80°C.

The water uptake of membranes was determined as a difference between the starting membrane weight and the weight of the membrane dried at 110°C. Thermal analysis was performed on a Netzsch-TG 209 F1 instrument in aluminum crucibles, heating rate 5°/min in argon atmosphere. Proton conductivity was measured in water in the temperature range 20-100°C with the use of "2B-F" impedance analyzer (frequency was ranged from 10 Hz to 1 MHz) in carbon/membrane/carbon symmetrical cells, with the active surface area varied from 0.2 to 0.5 cm<sup>2</sup>. Conductivity values were obtained by semicircle extrapolation to the resistance axis.

The diffusion permeability was analyzed in the two-chamber cell. The electrolyte (NaCl or HCl solution) was transferred through the membrane into a bidistilled water filled compartment. The electrolyte transfer rate was controlled by the conductivity measurement or pH technique using a conduct meter Expert-002 (Ekoniks-expert) or Mettler Delta 340 pH-millivoltmeter, respectively.

## Results and Discussion

Earlier it was shown that dependence of proton conductivity on dopant content pass through the maximum at 2.5 wt.% of  $\text{ZrO}_2$  and 3 wt.% of  $\text{SiO}_2$ . Thus all membranes doped by oxides with functionalized surface were carried with these concentrations.

Incorporation of oxides with functionalized surface into membrane matrix leads both to conductivity increase and decrease in comparison with MF-4SC membrane doped with pure oxides depending on the nature of terminal groups and the route of the hybrid membrane synthesis. The conductivity of membranes doped with silica precipitated at different pH (in acid ( $\text{SiO}_2(\text{H}^+)$ ) and alkaline ( $\text{SiO}_2(\text{OH}^-)$ ) solutions) and silica with surface contained PFD-groups is high than that for initial membrane and membrane doped with pure silica. Conductivity increase can be explained by the model of the semielasticity of membranes pores<sup>1</sup>. Incorporation of oxides functionalized with amino- and sulfo-groups, on the contrary, leads to the decrease of ion conductivity. The decrease of conductivity in the case of modification with amino-groups is a result of the mobile protons concentration reducing due to absorption of the part of them by  $-\text{NH}_2$  - groups. The conductivity decrease of materials doped by oxides with sulfonated surface is caused by the great particles size: it is about 150 nm, while the initial membrane pore size of about 5 nm.

Diffusion permeability and interdiffusion coefficients are also important characteristics of ion-exchange membrane that can give useful information about ion transport processes in material. Silica and zirconia surface functionalization by means of acid protons concentration increase ( $\text{SO}_3\text{H}$ -groups,  $\text{SiO}_2(\text{H}^+)$ ) leads to the diffusion permeability decrease and to the slowdown of anion diffusion rate. This indicates the improvement of membrane selectivity in comparison with both initial membrane and membrane doped with pure oxides. These results can be explained as follows. Incorporation of nanoparticles with high  $\text{H}^+$ -concentration leads to the formation of the thin Debye layer inside of membrane pores where the cations concentration is much higher than anions one. Thus, the anions concentration in the pores decreases and such distribution of ions reduces the anions transfer rates and increases selectivity. Hybrid membranes doped with silica contained PFD groups also have higher ion selectivity than initial membrane and membrane doped with pure  $\text{SiO}_2$ .

Silica surface functionalization by proton-acceptor amino-groups ( $\text{R}_1$  and  $\text{R}_2$ ) significantly affects on the diffusion permeability of membranes. Thus, incorporation of particles containing 5 mol.% of  $\text{R}_1$  or  $\text{R}_2$  leads to the some reduce of diffusion permeability coefficient in comparison with the initial membrane, while increase of modified groups concentration on silica surface to 10 mol.% results in the significant rise of the diffusion permeability coefficient, and to the increase of anion transfer rate and reduction in anion selectivity. This effect can be explained by the interaction between proton-acceptor amino-groups and functional sulfo-groups of membrane that leads to the formation of the fixed  $\text{NR}_3^+$ -ions. This assumption is proved by the decrease of conductivity and sorption exchange capacity of membranes doped with silica with modified surface decrease. Areas with the low cations and high anions concentration may occur as a result of these interactions. This leads to the anion transfer rate increase. Also, the molecular weight of hydrocarbon fragment influences on the diffusion permeability coefficients. Incorporation of silica with surface contained branchier modified group ( $\text{R}_2$  in comparison with  $\text{R}_1$ ) leads to the diffusion permeability coefficient decrease. It can be suggested that decrease of free volume within the membrane pores due to incorporation nanoparticle with more volumetric modified group on the surface that leads to the selectivity improvement.

Thus it was shown the influence of the nanoparticles surface functionalization incorporated into ion-exchange membranes on the transport properties and selectivity.

*This work was financially supported by the federal target program "Educational and scientific-educational staff on innovative Russia" for 2009-2013 years (project GK P872) and RFBR (project 11-08-93105).*

## References

1. Novikova S.A., Safronova E.Yu., Lysova A.A., Yaroslavtsev A.B. Influence of incorporated nanoparticles on MF-4SC membrane ion conductivity // Mend. Comm. 2010. V. 20. P. 156-157.

---

# APPLICATIONS OF ION EXCHANGERS WITH SILVER NANOPARTICLES FOR OXIDATION OF METHANAL IN WATER AND ETHANAL IN ETHANOL: EFFECT OF MOLECULAR OXYGEN

<sup>1</sup>Ekaterina Sakardina, <sup>1,2</sup>Ekaterina Zolotukhina, <sup>1</sup>Tamara Kravchenko, <sup>3</sup>Svetlana Nikitina

<sup>1</sup>Voronezh State University, Voronezh, Russia, *E-mail: krav@chem.vsu.ru*

<sup>2</sup>Institute for Problems of Chemical Physics, RAS, Chernogolovka, Russia, *E-mail: ks-chem@mail.ru*

<sup>3</sup>Voronezh State Architectural University, Voronezh, Russia, *E-mail: sunik@mail.ru*

## Introduction

Composites based on polymeric ion exchangers in the form of globules or membranes with chemically deposited metal nanoparticles can be applied practically as chemical/biochemical or catalytically active materials. Reaction activity of such composites depends not only on the metal nature and oxidation state but also on its distribution inside the polymer matrix, in its volume or its periphery, and also on the nature of the matrix, i.e. cation- or anion-exchange groups, porosity, etc. Some metal-ion exchanger composites which are not so active in chemical reactions can function as catalysts. In this case an important example is given by the oxidation reaction of aldehyde impurities in water or alcohols. It is currently a crucial problem to find a catalyst for this reaction which is both active under mild conditions (low temperature) and efficient (maximal degree of the process completeness). Metal-ion exchanger composites are bifunctional materials which combine ion-exchange and metal properties. It means that even in the case of incomplete oxidation of aldehydes (to corresponding acid instead of CO<sub>2</sub> and H<sub>2</sub>O) the formed acid can be adsorbed by ionogenic centers of the matrix. That is why metal-ion exchanger composites can be considered as prospective catalysts for aldehydes' removal.

## Experiments

Strongly basic anion-exchange polymers types of AV-17-8 or AV-17-2P with chemically deposited silver were chosen in the case of methanal removing from water medium. Matrices with different nature (cation-exchange, anion-exchange, complexing, natural tuff as a zeolite) with chemically deposited silver were used for removing of ethanal from ethyl alcohol. NaBH<sub>4</sub> or N<sub>2</sub>H<sub>4</sub> alkaline solutions were reducers.

1 or 5 mM concentration of methanal in water and 4 mM of ethanal in ethanol were used. The concentration of methanal was determined via redox-titration analysis with hydrogen peroxide and sodium hydroxide. The concentration of ethanal in ethanol was studied via gas chromatography (GC) method.

## Results and Discussion

Silver containing polymers were prepared via special procedure described earlier [1]. For removing of above-mentioned aldehydes one should create a layer of silver oxide on the surface of particles. As it is well-known, silver is stable to molecular oxygen oxidation because of forming of thin (and X-ray amorphous) but very dense oxide layer on the particles surface in oxygen atmosphere which block subsequent oxidation. To create of such oxide layer on the surface of silver particles inside the ion-exchange matrices all samples of composites were preliminary oxidized in water by uninterrupted oxygen flow through the layer of composite and water.

After this procedure all composites were tested in gasometric cell and it was found that subsequent oxidation with molecular oxygen did not take place.

Methanal and ethanal did not oxidize with molecular oxygen in normal conditions. They can be removed from liquids via sorption/chemi-sorption or catalytic oxidation. Therefore, we tested firstly the sorption ability of ion exchange matrices to aldehydes. Silver oxide can be used also as a reagent to aldehydes oxidation (reaction of "silver mirror"). That is why we checked primary the possibility of this reaction in inert (argon) atmosphere.

In Fig. 1 one can see the degree of the methanal oxidation completeness,  $\alpha$ , in water with argon atmosphere and with oxygen atmosphere. One should be mentioned, that activity of

composite catalyst in inert argon atmosphere is diminished progressively in time whereas in oxygen atmosphere the activity of composite increased in time up to the maximal degree of process completeness. The activity of composite in the last case remains at the same level even by multiple repetitions of this process with the same sample of composite.

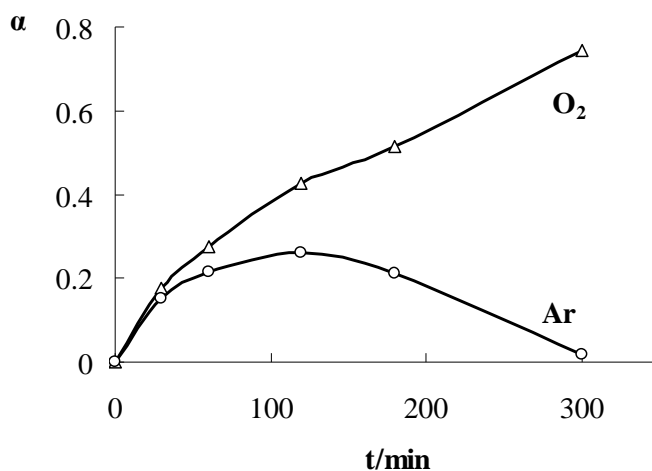


Figure 1. The degree of the methanal oxidation completeness,  $\alpha$ , in water by inert or oxygen atmosphere in the presence of composite  $\text{Ag}_2\text{O}(\text{Ag})\cdot\text{AH-17-8}$  (reduced with  $\text{NaBH}_4$ )

Ethanal oxidation in ethanol medium was realized by means of composites based on various matrices (Table 1) because of specific in both swelling ability and sorption ability of cross-linked ion-exchange matrix in alcohol (instead of water).

**Table 1: The degree of the process completeness,  $\alpha$ , in ethanol medium in the case of ethanal sorption by matrix and its oxidation in the molecular oxygen atmosphere.**

**Reducer  $\text{NaBH}_4$**

Matrix of composite (ionic form)	$\alpha$ , % Sorption in 5 h	$\alpha$ , % Oxidation in 5 h
CU-23-15/100 ( $\text{Na}^+$ )	21.4	52.6
CU-2-8 ( $\text{Na}^+$ )	15.9	10.4
AH-17-8 ( $\text{OH}^-$ )	49.4	68.0
AL-830 ( $\text{OH}^-$ )	78.2	82.3
AH-17-2P ( $\text{OH}^-$ )	58.7	97.9

All these data showed that metal-ion exchanger composites played the role of renewable catalysts in the presence of molecular oxygen which are active and efficient even in mild reaction conditions (room temperature). In this respect such composites, especially based on strongly-basic anion-exchange matrix, are much better than known analogues in literature.

*This work is supported by RFBR (project 10-08-00847)*

### References

1. Zolotukhina E. V., Kravchenko T. A. Synthesis and kinetics of growth of metal nanoparticles inside ion-exchange polymers // *Electrochimica Acta*. 2011. V. 56. P. 3597-3604.

## D-METALS BASED MATERIALS FOR HYDROGEN ENERGETICS

Mykola Sakhnenko, Marina Ved, Marina Mayba, Marina Glushkova, Svetlana Zjubanova

National Technical University "Kharkov Politechnic Institute", Kharkov, Ukraine,

E-mail: samara@kpi.kharkov.ua

### Introduction

The materials based on platinum group metals are the most effective for the majority of electrocatalytic reactions, but their use is limited by high cost [1]. Therefore, the creation of electrocatalysts with a high specific surface area and low noble metals content is of great interest. Electrochemical methods allow synthesizing d-metals based the alloys and oxide systems, which are catalytically active materials and can be used in hydrogen energetic.

### Experiments

Coatings based on transition metals oxides  $TiO_2 \cdot M_xO_y$  ( $M = Mn, Co, Ni$ ) were formed on titanium alloy by the microplasma oxidation method, the Ag-Co alloy was deposited on the copper substrate by the pulse mode. Electrocatalytic activity of both types of coatings was investigated in the electrode reactions of hydrogen and oxygen evolution by the polarization technique. The measurements were carried out in sulfuric acid and sodium hydroxide solutions in the 1M  $H_2SO_4$  by the potentiostatic mode. Catalytic activity of the materials was tested in the CO oxidation process in a tubular flow reactor. Initial mixture of CO and air was fed to the reactor inlet at the rate of 0,025 l/min and at the concentration of 1 % vol. Quartz glass tube with a coaxially wound heating coil was used as a catalytic reactor. Reactor temperature was increased from 20 to 420 °C at the rate of 1 °C/s. CO content in the outer mixture after passing it through the reactor were analyzed using the indicator-analyzer.

### Results and Discussion

Kinetic parameters of the electrolytic oxygen evolution reaction – Tafel constants  $a$ ,  $b$  and the exchange current density  $j_0$  (table 1) for the mixed oxide coatings are similar to those of the platinum electrode [2]. The calculated constants  $a$ ,  $b$  and  $j_0$  values for the hydrogen evolution on the Ag-Co alloy indicates that the optimal in terms of catalytic activity content is a silver 15–20 % wt.

The research of mixed oxide coatings catalytic properties showed that the 100 % conversion degree ( $X$ ) of CO to  $CO_2$  is achieved on  $Mn_xO_y \cdot TiO_2$  at the ignition temperature ( $T_i$ ) of 250 °C. Conversion degree of 100 % on the Ag-Co alloys was observed independently of the noble component content in the alloy, although  $T_i$  reduces from 250 to 240 °C with increasing of silver in the coatings.

**Table 1: The mixed oxide and silver-cobalt alloy coatings characteristics**

Electrode materials, metal content $\omega$ , % wt.		Tafel constants		Exchange current density $-\lg j_0$ , [A/cm <sup>2</sup> ]	Conversion degree CO/ $CO_2$ $X$ , %	Ignition temperature $T_i$ , °C
		$a$ , V	$b$ , V			
Oxygen evolution reactions	Pt <sub>theor.</sub> [2]	1,08	0,118	-9,1	100	200
	Pt <sub>exp.</sub>	1,10	0,138	-8,1		
	Mn <sub>x</sub> O <sub>y</sub> ·TiO <sub>2</sub>	1,12	0,124	-9,1		250
	Co <sub>x</sub> O <sub>y</sub> ·TiO <sub>2</sub>	1,00	0,167	-5,9	65	260
	Ni <sub>x</sub> O <sub>y</sub> ·TiO <sub>2</sub>	0,96	0,180	-5,4	58	270
Hydrogen evolution reactions	Pt <sub>theor.</sub> [2]	0,31	0,10	3,1	100	200
	Pt <sub>exp.</sub>	0,30	0,10	6,0		
	Ag-Co; $\omega(Ag) = 8$	0,72	0,14	5,1		250
	Ag-Co; $\omega(Ag) = 15$	0,18	0,10	1,8		245
	Ag-Co; $\omega(Ag) = 20$	0,20	0,10	2,0		240

### References

1. Popova N.M. Catalysts for gas emissions purification from industrial plants, Chemistry, Moscow, 1991.
2. Antropov L.I. Theoretical Electrochemistry, Lybid, Kyiv, 1993.

# ELECTRICAL CONDUCTIVITY OF ANION EXCHANGE MATERIALS IN SODIUM CHLORIDE AND POTASSIUM HYDROTARTRATE SOLUTIONS

<sup>1</sup>Veronica Sarapulova, <sup>1</sup>Natalia Pismenskaya, <sup>1</sup>Victor Nikonenko,

<sup>2</sup>Tatyana Garshina, <sup>2</sup>Piotr Kulintsov

<sup>1</sup>Kuban State University, Krasnodar, Russia, E-mail: [Abbadon.Sarapulova@yandex.ru](mailto:Abbadon.Sarapulova@yandex.ru)

<sup>2</sup>JSC Shchekino-Azot, Shchekino, Russia

## Introduction

At present time tartrate containing solutions (wines, juices, etc.) are processed using electro dialysis with IE membranes manufactured by Astom, Japan. These membranes allow conducting electro dialysis at relatively low power consumption. Nevertheless, they are expensive and their initial characteristics has deteriorated relatively fast [1]. Anion exchange membranes are especially inclined to change of characteristics. The goal of this work was the comparative study of different anion exchange resins aiming to choice of optimal material to producing of new anion exchange membrane. After the selection of resin JSC ShchekinoAzot produced the experimental samples which were studied and whose properties were compared with common commercial membranes.

Concentration dependences of surface resistance analysis of serial heterogeneous membranes manufactured by Fumatech, Germany; MEGA, Czech Republic and ShchekinoAzot, Russia, showed [2] that membranes containing mainly secondary and tertiary amines and produced with strongly crosslinked ion exchange resins have remarkably high resistance in hydrotartaric form. Basing on this hypothesis it was suggested that membrane for treatment of tartaric containing solution must (a) contain mainly quaternary ammonium groups; (b) be produced from weakly crosslinked ion exchange resin. In this case (a) fixed groups of membrane will not react with OH<sup>-</sup> ions which may be produced in membrane pore solution as a product of tartrates hydrolysis reactions and Donnan exclusion of the protons out of this solution; (b) Young module of weakly crosslinked membranes should decrease, resulting in increase of pore radius and amount of water in pore solution, leading to increase mobility of tartrates in it.

## Experiments

To validate the assumptions listed above, 8 anion exchange resins produced by Russian and foreign manufacturers (Table 1), which are already used or can be used for heterogeneous membranes production, were studied. Resins chosen for investigation mainly consisted of (according to manufacturers), polystyrene - divinylbenzene matrix and contained quaternary ammonium groups. Crosslinking degree varied by different (from 2 to 20 %) amount of crosslinking agent, divinylbenzene (DVB), introduced into reaction mass during ion exchange resin synthesis. Anion resin electrical conductivity was determined through value in isoelectrical conductivity point  $k_{iso}$  (Fig. 1) using U-shaped cell [3]. Concentration dependences of electrical conductivity of membranes produced from these resins were found by difference method with clip-cell [4]. Measurements were conducted using immitance meter MOTTECH MT4080 at 1 kHz frequency and temperature of 25±0,2 °C.

**Table 1: Some characteristics of studied anion exchange resins and values of their electrical conductivity in NaCl and KHT solutions**

Anion exchange resin	DVB content, %	Ion exchange capacity, mole/L	$k_{iso}$ , mS cm <sup>-1</sup>	
			NaCl	KHTr
AV-17 2	2	-	0,35	<0,06
AV-17 6	6	1.30	0,2	0,032
AV-17 10	10	-	0,15	0,021
AX 1	-	-	0,42	<<0,065
AX 2	-	-	0,073	0,012
A-400	8	1,30	0,32	<<0,07
A-500PS	2	0,8	0,16	0,032
A-860S	2	0,8	0,35	<0,06

## Results and Discussion

Some characteristics of studied anion exchange resins and obtained values of their electrical conductivity in NaCl and potassium hydrotartrate, KHT, solutions are presented in Table 1. Fig. 1 illustrates the procedure of isoelectrical conductivity points determination for resins, manufactured from identical monomers but containing different amount of DVB in reaction mass.

Experimental data confirmed the correctness of suggested assumptions. Decrease of crosslinking degree of resins is accompanied by growth of their electrical conductivity. Moreover in the case of KHT solutions, as supposed, this effect was more noticeable (Fig. 1b) than in the case of NaCl one (Fig. 1a). Macroporous AX, as well as A-400 anion exchange resin, demonstrates the highest electrical conductivity values in KHT solutions. The preference was given to Russian resin, so basing on it ShchekinoAzot manufactured 2 experimental set of heterogeneous membranes: MA-41P<sub>I</sub> and MA-41P<sub>II</sub>.

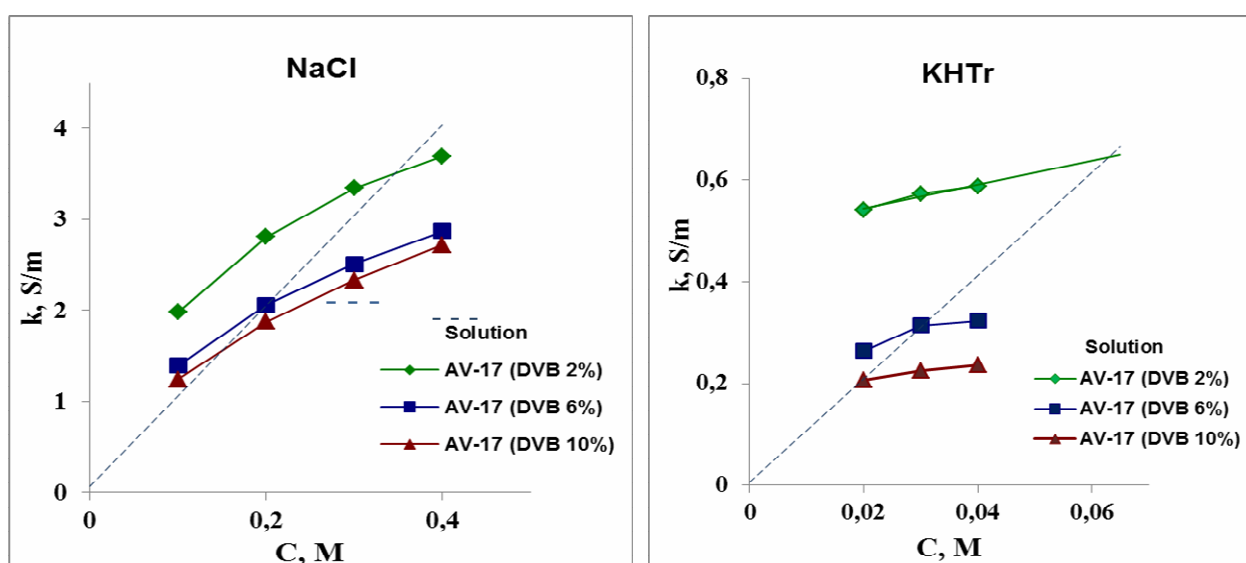


Figure 1. Concentration dependences of AV-17 ion exchange resin electrical conductivity in NaCl and KHT solutions. Dashed line shows the electrical conductivity of solution in absence of resin

Some characteristics of these membranes, as well as their  $k_{iso}$  values in NaCl and KHT solutions are given in Table 2. Concentration dependences of surface resistance of these membranes in sodium chloride and potassium hydrotartrate solutions are shown in Fig. 2. Data for commercial MA-41 (ShchekinoAzot, Russia) and AMX (Astom, Japan) membranes are given for comparison.

The obtained data show that:

- 1) usage of macroporous resin leads to  $k_{iso}$  increase of heterogeneous MA-41 membrane in 1,7–2,1 times (NaCl) or in 2.4–3,5 times (KHT), making electrical conductivity of MA-41P<sub>I</sub> and MA-41P<sub>II</sub> ion exchange material higher than such of AMX membrane;
- 2) decrease in thickness of membrane produced from AX 2P ion exchange resin helps to reduce the surface resistance; in case of MA-41P<sub>II</sub> membrane in KHT solution this resistance becomes comparable to such of AMX membrane.

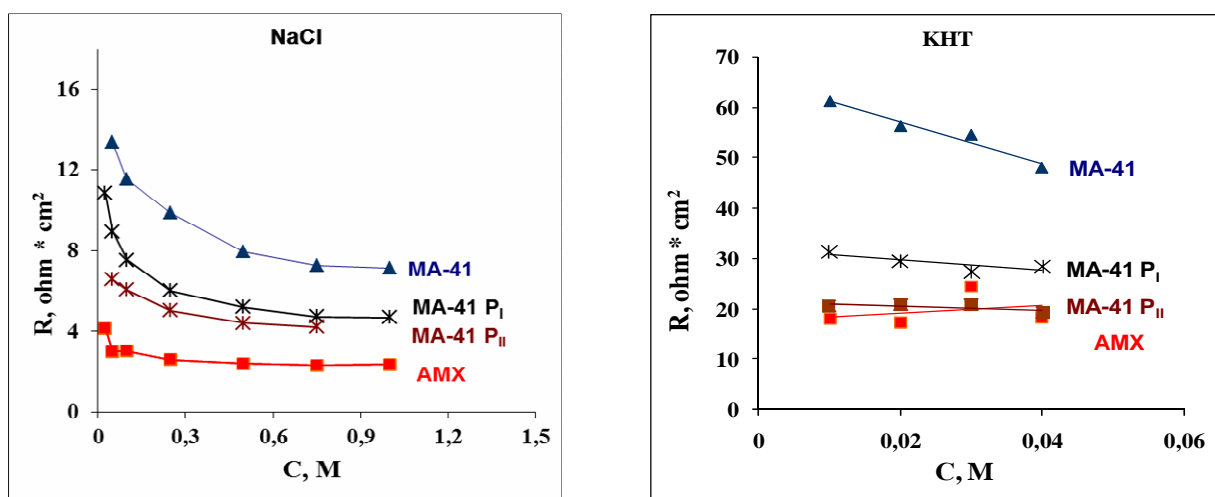


Figure 2. Concentration dependences of membrane surface resistance in NaCl and KHT solutions

Table 2: Some properties of studied membranes and electrical conductivity of their gel phase in NaCl and KHT solutions

	AMX	MA-41	MA-41P <sub>I</sub>	MA-41P <sub>II</sub>
Membrane composition	aminated styrene-divinylbenzene randomly cross-linked copolymer and 45 - 55% of polyvinylchloride	AV-17, polyethylene	AX 1, polyethylene	AX 2, polyethylene
<b>NaCl</b>				
IE Capacity*, mM / mL	1,56	1,25±0,05	0,65±0,05	0,65±0,05
Thickness, μm **	140±10	480±10	500±15	470±10
$k_{iso}$ , mS cm <sup>-1</sup>	4,4	3,4	5,8	7,3
<b>KHT</b>				
Thickness, μm **	150±10	500±10	535±10	510±10
$k_{iso}$ , mS cm <sup>-1</sup>	0,9	0,7	1,7	2,5

\* for the swollen membrane in the Cl<sup>-</sup> form

\*\* for the swollen membrane

### Acknowledgement

The study was realized within French-Russian laboratory "Ion-exchange membranes and related processes". We are grateful to CNRS, France, and to RFBR (grants 11-08-96511, 11-08-93107, 12-08-93106), Russia, and EURODIA INDUSTRIE S.A., France, as equipment supplier and for financial support.

### References

- Ghalloussi R., Garcia-Vasquez W., Bellakhal N., Larchet C., Dammak L., Huguet P., Grande D. Ageing of ion-exchange membranes used in electro dialysis: Investigation of static parameters, electrolyte permeability and tensile strength // Sep. Pur. Tech. 2011. V. 80. P. 270-275.
- Gaynulina A., Vedernikova E., Pismenskaya N., Nikonenko V. // Conference "Ion transport in organic and inorganic membranes" Book of Abstracts. Krasnodar 2010. P.57-58.
- Gnusin N., Grebenyuk V., Pevnitskaya M. Electrochemistry of ion exchangers // Nauka. Novosibirsk. 1972, P. 19.
- Karpenko L., Demina O., Dvorkina G., Parshikov S., Larcher C., Berezina N. Comparative study of methods used for the determination of electroconductivity of ion-exchange membranes // Elektrokimiya (Rus). 2001. V. 37. № 3. P. 328-335.

# STUDY OF ELECTROCHEMICAL CHARACTERISTICS OF MODIFIED BIPOLAR MEMBRANES

Olga Shapovalova, Nicolai Sheldeshov, Victor Zabolotsky

Kuban State University, Krasnodar, Russia, E-mail: sheld\_nv@mail.ru

## Introduction

Bipolar membranes are bilayer composites, in which one of the layers is the cation-exchange, and another is anion-exchange. These membranes allow to obtain hydrogen and hydroxyl ions from water molecules under the influence of an electric current. The dissociation of water molecules in such systems is "working" process and the effectiveness of electromembrane process as a whole depends on overvoltage and current efficiency of generation of  $H^+$  and  $OH^-$  ions. It is known that catalytic additives introduced in the bipolar region affect at the rate of reaction of water dissociation in bipolar membranes. Introduction of additives can be carried out in various ways: during manufacturing of the membrane by hot pressing, chemical, electrochemical methods. Such additives may be both organic and inorganic substances.

## Experiments

The objects of study were heterogeneous bipolar ion-exchange membranes, obtained by means of: a) rolling, containing a catalyst ionpolymer with phosphonic groups and without a catalyst, b) pressing without catalyst and with catalyst - chromium hydroxide, which was obtained in the membrane after formation by a chemical method.

Frequency spectra of the membrane impedance were measured in four-chamber flow cell (Fig. 1) at four-electrode circuit by virtual impedance meter-analyzer in 1 Hz–1 MHz frequency range ( $S_{cell} = 2,27 \text{ cm}^2$ ). Dependence of the resistance of the bipolar region on the current density was determined from the frequency spectra of membrane had been measured at different electrical currents. Then the partial current-voltage characteristic of the bipolar region was calculated using the formula:

$$\eta_b = \int_0^{I^*} R_b dI, \quad (1)$$

where  $\eta_b$ —overvoltage of a bipolar region.

Coion transport numbers of sodium and chloride through the bipolar membrane was measured using a modified Hittorf method. The essence of the method consists in determining the total flux of sodium cations from 0.5 M sodium hydroxide solution to 0.5 M hydrochloric acid solution and the total flow of chloride anions in the opposite direction through the membrane. The concentration of chloride ions in sodium hydroxide solution at the inlet and outlet of the alkaline cell was determined by potentiometric titration with silver nitrate solution, after neutralizing the excess of alkali with nitric acid with bromothymol blue indicator. The concentration of sodium ions in hydrochloric acid solution at the inlet and outlet of the acid chamber was determined by direct potentiometric method with standard additions with the known slope of the electrode function, taking into account dilution and pre-neutralizing excess of acid by ethylenediamine, as follows:

$$C_x = C_s \left( \frac{V_s}{V_p + V_s} \right) \left[ 10^{\Delta E/S} - \left( \frac{V_p}{V_p + V_s} \right) \right]^{-1} \quad (2)$$

where  $S$  – slope of electrode function;  $V_s$  – volume of added standard solution;  $V_p$  – volume of studied solution;  $C_s$  – concentration of added standard solution;  $C_x$  – concentration of studied solution;  $\Delta E$ —potential drop between  $Na^+$ -selective electrode immersed into studied solution with small addition of sodium chloride of known concentration and electrode immersed into studied solution. In both cases, the potential of the  $Na^+$ -selective electrode was measured against standard silver chloride electrode.

In addition, the concentration of chloride ions and the sodium ions were determined in the initial solutions, which are fed into the cell.

Effective transport numbers of sodium ions and chloride ions through the bipolar membrane is calculated by the formula (3), and hydrogen ions and hydroxyl—according to the formula (4).

$$T_{\pm} = \frac{(C_{\pm} - C_{\pm}^0)v_{\pm}F}{I} \quad (3)$$

$$T_{H^+, OH^-} = 1 - T_{Na^+} - T_{Cl^-} \quad (4)$$

where  $T_{Na^+}$  and  $T_{Cl^-}$ —transport numbers of sodium ions and chloride ions;  $C_{\pm}$  and  $C_{\pm}^0$ —the concentration of these ions in solution at outlet and inlet of electrochemical cell, mol/L;  $v_{\pm}$ —volume rate of solution through the cell, L/s;  $F$ —the Faraday constant, C/mol;  $I$ —current supplied to the cell, A.

### Results and Discussion

From the dependence of the resistance of bipolar regions of studied membranes (fig. 1a, fig. 2a) one can see that the resistance of the membranes, which included a catalytic additive, essentially, a 3–100 times lower than that of the original membranes, which indicates the efficiency of used catalytic additives. The resistance of the bipolar membranes containing phosphonic groups with high catalytic activity in the water dissociation reaction does not depend practically on the current (fig.1a). If the membrane does not contain a catalytic additive, and it contains ionic groups with low catalytic activity, the resistance of the bipolar region is highly dependent on the current density (fig. 1a, curve 2; fig. 2a).

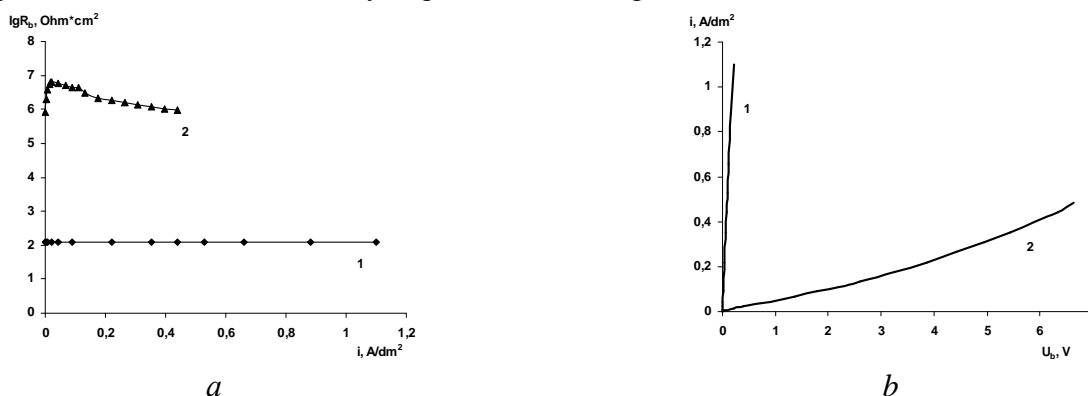


Figure 1. The dependence of the logarithm of the surface resistance of a bipolar region on the current density (a), and partial overvoltage current-voltage characteristics of bipolar region (b) of bipolar membranes: 1 – with ionpolymer containing phosphonic group; 2 – without a catalyst in the system of 0,01 M HCl / 0,01 M NaOH. The bipolar membranes were prepared by rolling the CM-PES and the AMH-PES membranes

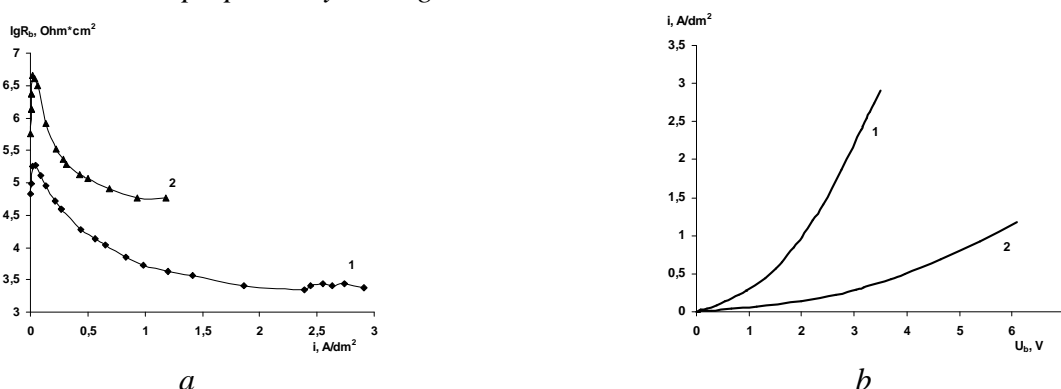


Figure 2. The dependence of the logarithm of the surface resistance of a bipolar region on the current density (a), and partial overvoltage current-voltage characteristics of bipolar region (b) of bipolar membranes. 1 – chromium hydroxide(III), which was obtained in the membrane after formation by chemical method, 2 – without a catalyst in the system of 0,1 M HCl / 0,1 M NaOH. The bipolar membranes were prepared by rolling the CM-PES and the AMH-PES membranes

The introduction of catalytic additives in the bipolar membrane significantly reduces the overvoltage of the bipolar region (fig. 1b, 2b). Thus introduction of phosphonic groups containing ionpolymer in bipolar region, reduces the overvoltage on it from 10 V up to 0.2 V at 1 A/dm<sup>2</sup> current density (Fig. 1b), and the introduction of chromium hydroxide(III) reduces the overvoltage from 6 V to 2 V at the same current density.

Despite the fact that the sodium and chloride coion fluxes through the bipolar membrane increases with increasing current density (fig. 3) due to increased electromigration contribution to the transfer, the effective transport numbers of these ions decrease with increasing current density (fig. 4), and the current efficiency of hydrogen and hydroxyl ions in these membranes increase from 0.89 at 0.5 A/dm<sup>2</sup> current density to 0.96 at 3 A/dm<sup>2</sup> current density.

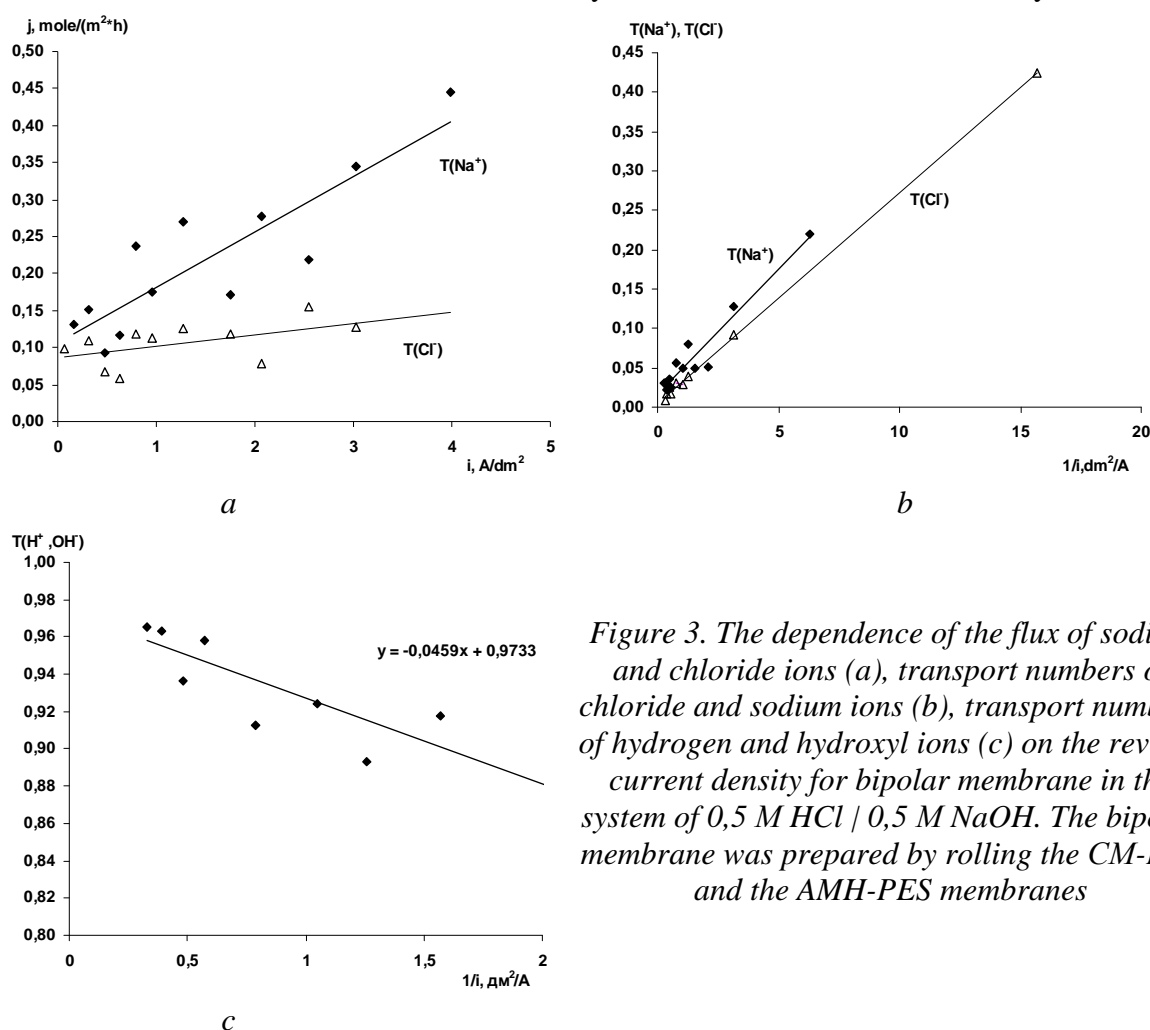


Figure 3. The dependence of the flux of sodium and chloride ions (a), transport numbers of chloride and sodium ions (b), transport numbers of hydrogen and hydroxyl ions (c) on the reverse current density for bipolar membrane in the system of 0,5 M HCl | 0,5 M NaOH. The bipolar membrane was prepared by rolling the CM-PES and the AMH-PES membranes

The current efficiency of hydrogen ions and hydroxyl on these membranes is not lower than 0.88 in the range of operating current densities (up to 3 A/dm<sup>2</sup>).

*This work was supported by Foundation for Assistance to Small Innovative Enterprises in Science and Technology, State Contract № 9836p/14244.*

# ELECTROKINETIC PROPERTIES OF COMPOSITE MEMBRANES MF-4SC/POLYANILINE IN DEPENDENCE ON THE COUNTER-IONS TYPE

Svetlana Shkirskaya, Ninel Berezina, Mariya Kolechko  
Kuban State University, Krasnodar, Russia

## Introduction

Electroosmotic permeability is the key factor in the solution concentrating processes by electro dialysis and membrane electrolysis. Recently the many different modifications of the ion-exchange membranes are prepared due to including of additions to the nanosize structure of the perfluorinated sulphocationic membranes. The aim of this research is the revealing of electroosmotic permeability and conductance dependences on the concentration and electrolyte types in the set of metallic and proton counterions in the MF-4SC membranes before and after modifications by polyaniline.

## Results and Discussion

The composites MF-4SC/polyaniline were obtained by ‘short’ synthesis method by one-side diffusion with help of concentrated solutions of aniline, acid and  $(\text{NH}_4)_2\text{S}_2\text{O}_8$  during only 25 min. As a result we prepared the surface-modified films with the thin polyaniline layer (25-30 mcm) [1].

Figure 1 demonstrates the concentration dependences of the water transport numbers ( $t_w$ ) in the wide interval of salt and acid solutions. The  $t_w$  values are measured by volume method, which was described in [2]. The comparison of the data for composite and initial membranes has shown the effect of essential decrease of the water electrotransport across the polyaniline layer which is equal 50% for all counterions, including proton water transport. These data confirmed the identical effect observed earlier in [3, 4] (for other morphology of polyaniline layer).

The other interesting result is the set of water transport numbers in the concentrate electrolyte solution (0,75 – 1M) for composite samples (Fig. 1) which have  $t_w$  values from 7 → 4 → 3 → 3 → 1 mol  $\text{H}_2\text{O}/\text{F}$  in the number  $\text{Li}^+ \rightarrow \text{Na}^+ \rightarrow \text{K}^+ \rightarrow \text{Cs}^+ \rightarrow \text{H}_3\text{O}^+$  accordingly. Practically these values are close to the hydration numbers of the same ions in the electrolyte solutions, which dependence on the ion radii [5]. It is interesting to note that the surface polyaniline layer hinder the water electrotransport practically in the all concentration region (Fig. 1 b). So, blocking properties of surface polyaniline layers can be used for the determination of close hydration numbers of transported ions in the electric field.

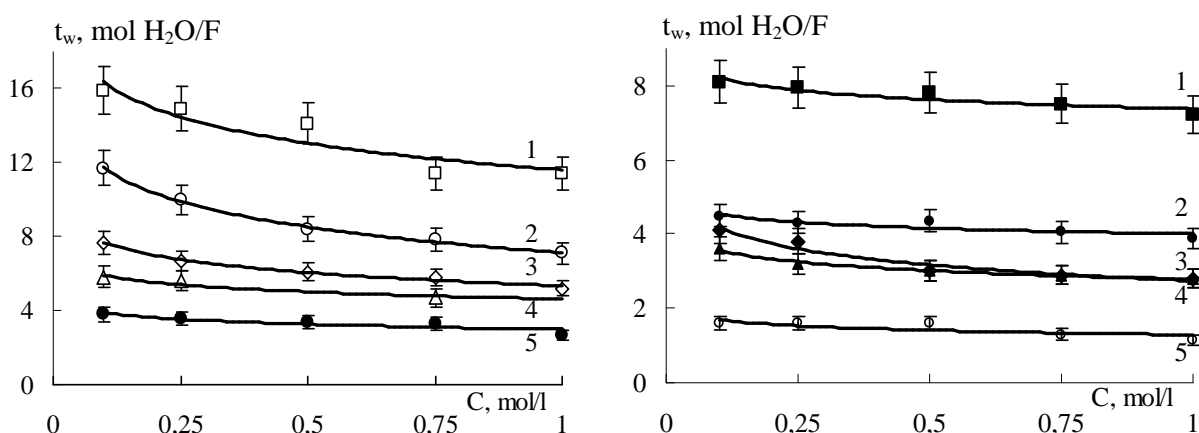


Figure 1. Concentration dependences of the water transport numbers for membranes MF-4SC (a) and MF-4SK/PAn (b) in dependence on the counter-ions type:

1 –  $\text{Li}^+$ , 2 –  $\text{Na}^+$ , 3 –  $\text{Cs}^+$ , 4 –  $\text{K}^+$ , 5 –  $\text{H}^+$

The investigations of conductance in the same interval of electrolyte solutions permits to reveal the change of the mechanism of proton transfer across the polyaniline layer. It was shown, that due to blocking property of polyaniline layer the relay mechanism is retarded because proton does not find water molecules with favorable orientations [2].

### Acknowledgments

*The authors are thankful to the Russian Foundation for Basic Research for financial support (project No 11-08-96514) and the Federal Program "Scientific and scientific-pedagogical personnel of innovative Russia" (2009-2013) № P1359.*

### References

1. *Berezina N.P., Shkirskaya S.A., Kolechko M.V., Popova O.V., Sentchichin I.N., Roldugin V.I.* Barrier effects of polyaniline layer in surface-modified membranes MF-4SC/polyaniline // *Electrochimiya*, 2011, V.47, № 9. P. 1066-1077.
2. *Berezina N.P., Shkirskaya S.A., Sytcheva A.A.-R., Krishtopa M.V.* Water electrotransport with proton in nanocomposite membranes MF-4SC/PAn // *Kolloidny jurnal*. 2008. V.70. №4. P.437-446
3. *Protasov K.V., Shkirskaya S.A., Berezina N.P., Zabolotskii V.I.* Application of composite sulphocationic membranes, modified by polyaniline, for electro dialysis concentrating of salt solutions // *Russian Journal of Electrochemistry*. 2010. Vol. 46. No. 10. P. 1131-1140.
4. *Berezina N.P., Kononenko N.A., Filippov A.N., Shkirskaya S.A., Falina I.V., Sytcheva A.A.-R.* Electrotransport properties and morphology of MF-4SC membranes surface modified by polyaniline // *Electrochimiya*. 2010. V. 46, №5. P. 515-524
5. *Robinson, R. and Stokes, R.* *Electrolyte Solutions*, London, 1959.

# SINGLE-WALLED CARBON NANOTUBE-PMMA COMPOSITES FOR POLYMER GEL ELECTROLYTES: INFLUENCE ON PROTON CONDUCTIVITY

<sup>1</sup>Liudmila Shmukler, <sup>2</sup>Nguyen Van Thuc, <sup>1,2</sup>Liubov Safonova

<sup>1</sup>Institute of Solution Chemistry of RAS, Ivanovo, Russia, E-mail: [les@isc-ras.ru](mailto:les@isc-ras.ru)

<sup>2</sup>Ivanovo State University of Chemistry and Technology, Ivanovo, Russia

## Introduction

Single-walled carbon nanotubes (SWNTs) exhibit unique mechanical, electrical properties and are of great interest in using them in the form of nanocomposites in various electronic devices, ultra-high strengths materials. However, the dispersion of SWNTs in organic solvents and polymer matrices is hindered because of their strong agglomeration, which occurs due to van der Waals interactions. The new strategy that efficiently graft poly(methyl methacrylate) (PMMA) on SWNTs by *in-situ* free radical polymerization in a poor solvent of PMMA has been introduced in [1]. This process is analogous to a ‘fishing’ process; that is, during polymerization the ‘living’ polymeric radicals (‘fish’) are expelled from the poor solvent and enthalpically favored to absorb to the surface of SWNTs (‘fishhook’). This approach is promising for production of polymer nanocomposites. In the present work, the method of production of proton conducting gel electrolytes and membranes has been introduced on the base of this approach. The aim of the work was to study the influence of additions of functionalized single-walled carbon nanotubes on the electrical conductivity of polymer gel electrolytes based on PMMA, doped with solutions of phosphoric acid in *N,N*-dimethylformamide (DMF).

## Experiments

SWNTs were synthesized in the Institute of Problems of Chemical Physics of the RAS (Chernogolovka). The proton-conducting gel electrolytes prepared by the method described in [2]. Benzoyl peroxide was applied as the polymerization initiator. The resulting functionalized SWNTs was dispersed in the gel electrolyte composition of 5 wt% PMMA-[0.1M H<sub>3</sub>PO<sub>4</sub>-DMF] in an ultrasonic bath at a frequency of 35 kHz for 1 hour. The result was an opaque gel with gray colour. Next, the gel was processed by repeated centrifugation at 15 000 rev/min of the gel until a stable transparent suspension appearance.

The conductivity of gels was determined by electrochemical impedance method with Solartron 1260A over frequency range of 0.1 Hz-1 MHz with signal amplitude of 10 mV.

The fluorescence spectra were recorded on a spectrophotometer Avantes 2048 in the range of 0 to 1000 nm.

## Results and Discussion

The resulting composite was studied by fluorescence spectroscopy in order to prove that process of functionalization of nanotubes, conducted by the method of [1] was successful. Figure 1 shows the fluorescence spectra of functionalized and non functionalized nanotubes are dispersed in ethyl acetate.

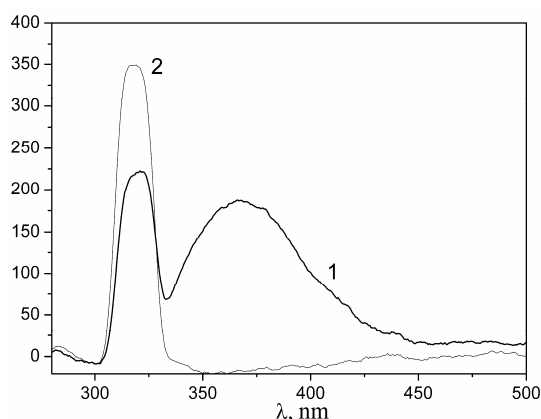


Figure 1. The fluorescence spectra of non functionalized SWNTs, and PMMA nanocomposite at a wavelength of 320 nm exciting light

The peak fluorescence observed in the spectrum of SWNTs at  $\sim 370$  nm, in the case of a solution with the addition of functionalized nanotubes is not appear. This may be evidence of functionalization of SWNTs. The spectra of impedance for gel electrolytes with compositions of 5 wt % PMMA-[0.1M  $H_3PO_4$ -DMF] and for the same gel with nanocomposite addition are presented in Fig. 2.

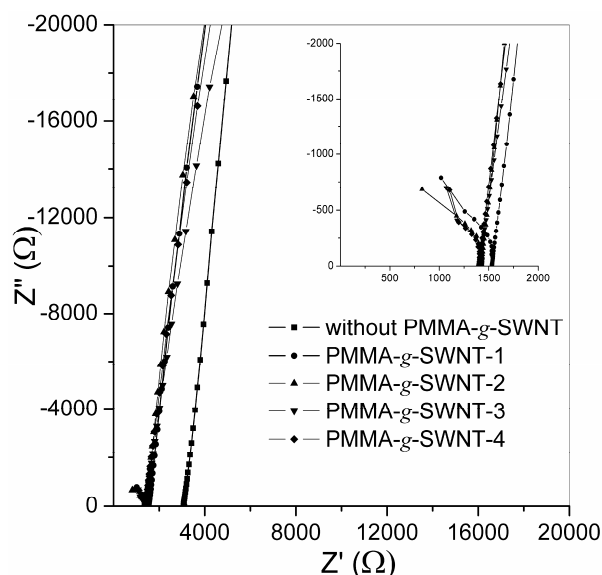


Figure 2. Impedance spectra of systems containing of 5wt % PMMA (350 000)-[0.1M  $H_3PO_4$ -DMF] and nanocomposites dispersed in gel electrolyte

As result of composite effect, the conductivity reduces as twice for gel electrolyte containing of functionalized carbon nanotubes as compared with conventional gel electrolyte. Nanoparticles dispersed in the gel increases the transport of protons due to the fact that they create local regions in which charge transfer is facilitated. It should be noted that repeated centrifugation system does not change significantly the conductivity of gel electrolyte (Tabl.).

**Table: Conductivity of gel electrolyte 5 wt% PMMA-SWNT-[0.1M  $H_3PO_4$ -DMF] at various PMMA-g-SWNTs contents**

	$\kappa \cdot 10^4, \text{ohm}^{-1}\text{cm}^{-1}$
<b>without SWNTs</b>	1.49
<b>with PMMA-g-SWNTs</b>	3.12
<b>after centrifugation</b>	3.26

This fact may be evidence of the stability of the resulting proton-conducting gel electrolyte.

*This work was financially supported by Russian Foundation for Basic Researches (grants 11-03-00311-a and 12-03-97534).*

### References

1. Guo G., Yang D., Wang C., Yang S. "Fishing" polymer brushes on single-walled carbon nanotubes by in-situ free radical polymerization in a poor solvent // *Macromolecules*. 2006. V. 39. P. 9035-9040.
2. Shmukler L. E., Safonova L. P., Nguen Van Thuk, Gruzdev M. S. Proton-conducting gel electrolytes based on poly(methyl methacrylate) doped with phosphoric acid in *N,N*-dimethylformamide // *Polym. Sci. Ser. A*. 2011. V. 53. P. 44-51.

---

# TRANSIENT ELECTROCHEMICAL METHODS FOR THE TRANSPORT STUDY THROUGH ION-EXCHANGE MEMBRANES – REVIEW AND NEW TRENDS

<sup>1</sup>Philippe Sizat, <sup>1</sup>Stella Lacour, <sup>1</sup>Gérald Pourcelly, <sup>1,2</sup>Ekaterina Belashova

<sup>1</sup>Institut Européen des Membranes”, Université Montpellier 2, UMR5635 ENSCM/UM2/CNRS, CC047, Place Eugène Bataillon, Montpellier cedex 5, FRANCE, *E-mail: philippe.sizat@iemm.univ-montp2.fr*

<sup>2</sup>Membrane Institute, Kuban State University, Krasnodar, Russia

## Introduction

Since a long time, ion transport through ion exchange membranes is studied by a large variety of techniques. Most of them rely on electrochemical measurements. In the palette of available tools, steady-state techniques are the first choice in conventional investigations. However, transient electrochemical techniques are more powerful because they are able to separate different contribution to the transport in the time domain or its dual equivalent the frequency domain.

We are now facing new challenges, if the global behavior of membranes is now relatively known; some phenomena occurring at the micro-scale are still open problems for *membranologists*. This is the case for the well known concentration polarization that opened the topic of coupled transport phenomena and the debate around gravitational/ non gravitational induced convection, electroconvection, hydrodynamic instabilities, water dissociation gives rise to lively discussions.

Henceforth, in labs around the world the increasing level of equipments allow a new access to very smart approaches. It's the aim of the present paper to discuss about the new trends in transient electrochemical methods.

## The classical transient electrochemical methods

Three main class of transient electrochemical methods working in the time-domain are very classical:

1. voltammetry, linear sweep voltammetry, cyclic voltammetry, carried out in galvanostatic or potentiostatic mode
2. chronopotentiometry, time-domain record of the potential as the response to a galvanostatic step.
3. chronoamperometry, time-domain record of the intensity as the response to potentiostatic step.

Depending on the goal of the studies, the fitting of the experimental data is done with an theoretical model, diffusion coefficient, transport coefficient and geometrical descriptors (thickness, etc.) are the parameters for the fit.

Another kind of standard transient electrochemical method is the impedance spectroscopy (EIS) that is working in the frequency domain for small amplitude sinusoidal signals. Fitting is usually done through electrical equivalent circuit.

## The next steps

We definitively think that we can go beyond the usual framework of transient techniques. Some studies have shown for instance that some information is contained in the electrical noise inherent to chronopotentiometric or chronoamperometric experiments. Not all kind of transport can be the source of all sort of noise and depending on the experimental conditions some instructive information can be obtained. By the way, noise analysis (generally power spectra) also gives the limits of the reliability of electrochemical data (chronopotentiometry or EIS).

Multivariate analysis [1] can bring now a very interesting contribution to transient techniques. The usual confrontation between a theoretical model can be to some extent avoided because the multivariate analysis like factorial analysis can easily extract latent factor contributing to the response of membrane systems. The only condition is to smartly varies some experimental

parameter and to process as a whole the global data set hence obtained. These techniques can take advantage of the additive property of the voltage distribution in membrane systems.

Other fashionable contributions come from the use of network element simulation with software like SPICE normally devoted to electronic circuit analysis. They can help the user for the modeling and parameter estimation of electrochemical and membrane cells [2].

Impedance spectroscopy is also an evolving domain for membrane system. For a long time, EIS was considered as an experimental and theoretical way to linearize the system response for small stimuli thus allowing the decomposition of all contributions with analytical expressions. The power of new computer can allow now the numerical simulation of impedance to be confronted to real life experiment and to directly extract parameters from experimental data. There is no longer need for analytical expression of impedance functions. More complex systems can be then addressed with EIS technique. The numerical model can be directly realized with network component (SPICE) or finite difference equations of transport or finite element analysis. On the other hand, simulation can be done in the time domain by considering the response in potential to a small current step followed by a fast Fourier transform [3].

At last we can consider the contribution of the micro-electrochemistry with the high resolution of ultra micro-electrodes than can carry out a real imaging of membrane surface at work and the revolution of microfluidic system that can help the experimenter to isolate some very small part of ionic membrane systems.

### **Conclusion**

A new class of experimental techniques and theoretical approaches need now to be incorporated in the toolbox of *membranologist* and the networking operations like the LIA MEIPA or the FP7 Cotraphen project are unique chances to build a very solid assembly.

### **Acknowledgments**

The authors wish to thanks the CNRS LIA MEIPA, RFBR (*Grant Nos. 11-08-93107, 12-08-00188*) and FP7 Marie Curie Actions “CoTraPhen” Project PIRSES-GA-2010-269135 for the funding of the networking activities of this study.

### **References**

1. *Malinowski E.R.*, Factor Analysis in chemistry, 2002, Wiley-Interscience, New York.
2. *Moya A.A.*, Electric circuits modelling the low-frequency impedance of ideal ion-exchange membrane systems // *Electrochimica Acta*. 2012 V.62. P.296-304.
3. *Brumleve TR; Buck RP*, Numerical-Solution Of Nernst-Planck And Poisson Equation System With Applications To Membrane Electrochemistry And Solid-State Physics // *J. Electroanal. Chem.* 1978. V. 90. P. 1-31.

---

## ALTERNATING CURRENT SYNTHESIS OF NANOMATERIALS THE BASED ON METALS AND METAL OXIDES

Nina Smirnova, Alexandra Kuriganova, Daria Leontyeva

South-Russian State Technical University, Novochercassk, Russia, E-mail: smirnova\_nv@mail.ru

At present composition materials containing nanoparticles of metals or metal oxides are widely used in many different areas of modern industry. Catalysts on the based on nanoparticles of Pt or Pd and active carbon with high surface area are used as electrocatalysts for anode and cathode for low temperature fuel cells, for electrolyze of water. The oxidation catalysts Pt and Pd on support of nanostructured  $\text{Al}_2\text{O}_3$  or other oxide materials are effective for the control of carbon monoxide and volatile organic compounds emissions from a variety of exhaust gas streams from industrial processes. Nickel oxide with high surface area is used for batteries and hybrid supercapacitors. Nanostructured tin and tin oxides are well known as effective catalysts and elements of gas sensors.

Today as long-known methods of "soft chemistry" as many new physical methods are widely used for preparation of different composition materials containing nanoparticles of metals or metal oxides. In the first case particle formation proceeds via chemical reduction of the relevant precursors by different reducing agents. In the second case nanoparticles are formed under strong physical action.

Our proposed method of composition nanomaterials synthesis is based on the phenomenon of electrochemical destruction of metals under alternating current.

It seems under alternating current mass of electrodes didn't must change because metal which moved from surface of electrode to solution during positive period must reduce during negative period. But if products of anodic reaction didn't reduce completely the process of metals destruction is possible under symmetric alternating current. In alkaline solutions many metals destruct with the nanopowder oxide formation, for example Ni, Al, Cu, but in aced solutions they dissolved. Under alternating current electrolysis the electrode potential changes are far from equilibrium conditions. Consequently for transit metals it supposed many electrode stages of the formation of oxide products with different degrees of oxidation of the metal which has a defective structure. For noble metals as Pt or Pd we proposed mechanism of intercalation of alkaline metals under crystal structure of metal and its following dispergation [1].

Important stage of metals electrochemical destruction under alternating current with powder metal or oxides metals formation are the stage of water chemisorptions, evaluation of oxygen and hydrogen during positive and negative pulls respectively.

We prepared several composition materials containing nanoparticles of metals or metal oxides:

- Pt/C, Pd/C;
- $\text{Al}_2\text{O}_3$  and Pt/ $\text{Al}_2\text{O}_3$ ;
- Sn,  $\text{SnO}_2$  and Pt/ $\text{SnO}_2$ /C;
- NiO, NiO/C, Pt/NiO/C.

We study its structure using XRD, SEM, TEM, BET, TG-DSK, EDAX and chemical and electrochemical properties for different applications. Composition, structure and functional properties of products of alternating current electrolysis depend on the properties of metals, the nature of electrolyte; temperature; current densities.

*The work was supported by the Ministry of education and science of Russian Federation (contract № 14.740.11.0371).*

### References

1. Kyrikanova A.B., Gerasimova E.V., Leont'ev I.N., Smirnova N.V., Dobrovolsky Yu.A. // Alternative Energy and Ecology. 2011. №5. P. 58-63

# RHEOLOGICAL, OPTICAL AND STRUCTURAL PROPERTIES SOLUTIONS OF CELLULOSE DIACETATE TO MOLD SEMIPERMEABLE MEMBRANES

Antonina Surkova, Valentine Sedelkin, Olga Chirkova, Olga Pachina, Larisa Potekhina, Sergey Apostolov

Engels Technological Institute (Branch) Saratov State Technical University of YA Gagarin  
E-mail: pochta-mpp@mail.ru

## Introduction

Effect of cellulose diacetate solution in acetone was investigated on their rheological and optical properties. Methods of viscometry and turbidity spectrum used for the study of viscosity and optical properties of the solutions. Dependence of the effective viscosity, the number and size of the globules from the composition of the solutions has obtained.

## Experiments

Structural changes in polymer solutions are shown by the conformational state of macromolecules - their shape, construction, location. The most informative methods for studying the conformation of macromolecules in solution are a measurement of their rheological and optical properties [1].

This paper discusses the results of research solutions. The solutions prepared from powdered air-dry cellulose diacetate (CDA) cotton's origin has modified vapor of binary mixtures with distilled water and solvents - dimethylsulfoxide (DMSO) and dimethylacetamide (DMAA). Acetone (analytical grade) was used to dissolve the polymer.

Flow curves for polymer solutions of varying concentrations of CDA are shown in Figure 1. The values of effective viscosity of the solvents and pore-formation agents are shown for comparison. All results for concentrated solutions were obtained on a rotational viscometer, which increases their relative reliability.

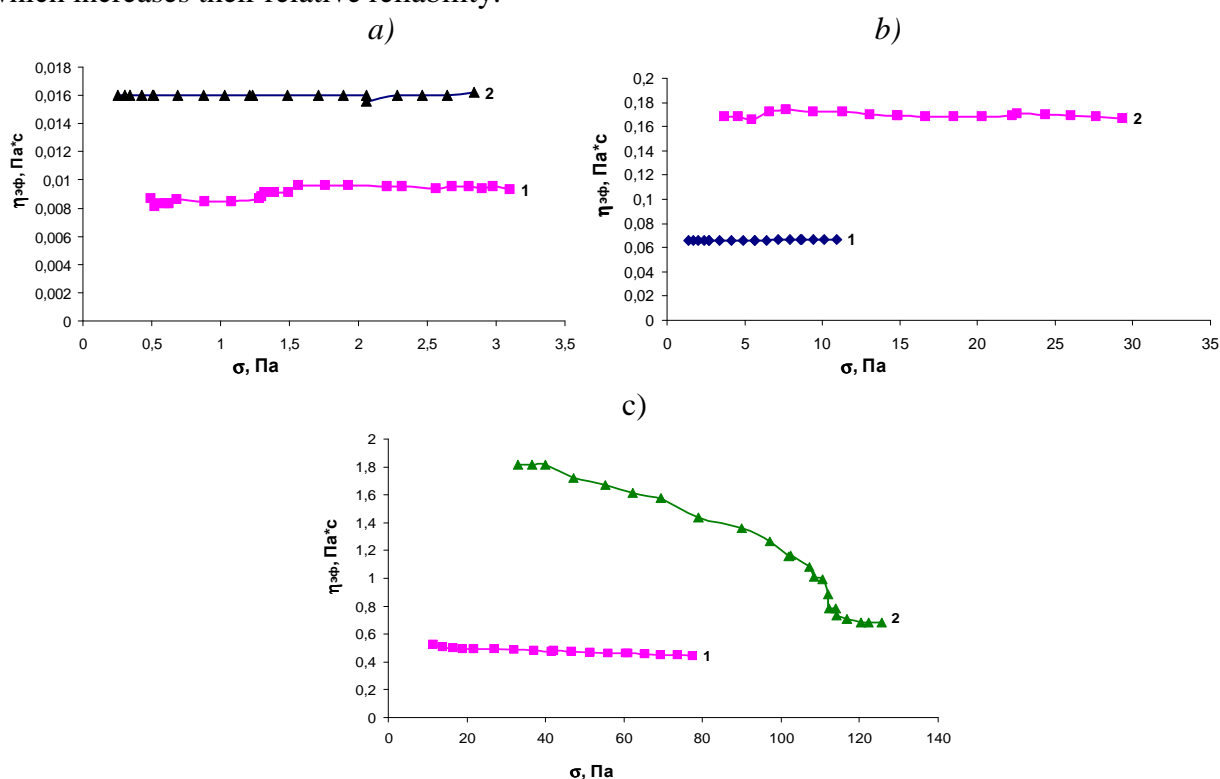


Figure 1. Flow curves of polymer solutions in acetone of various CDA concentration: a) 1 – 3% CDA; 2 – 5% CDA; б) 1 – 7% CDA; 2 – 10% CDA c) 1 – 15% CDA; 2 – 20% CDA

As can be seen from Figure 1, the viscosity of polymer solutions is highly dependent on the concentration and increases with increasing polymer content in solution, and this dependence is nonlinear. The presence of macromolecules and their relaxation processes are strongly

dependent on molecular weight and polymer concentration, lead to major differences in the structure, including the viscosity of polymer solutions.

Structural changes in polymer solutions and solvents made involving supramolecular and intermolecular spatial relationships are usually retained after removal of the solvent during the phase inversion process of obtaining the filtration material [2].

Flow curves of polymer solutions are shown in Figure 2. The solutions prepared from cellulose acetate powder, modified vapor of water-organic mixtures and the solution prepared from the unmodified CDA.

The results show that the viscosity of solutions made from modified CDA, more than comparative viscosity of the base (no steam treatment). Particularly strong  $\sim$ (70%) the viscosity increases for solutions containing 0.1% mixture of water with DMSO, then its value begins to decrease, not reaching, however, the values of  $\eta_{ef}$  solution for the base of the unmodified polymer.

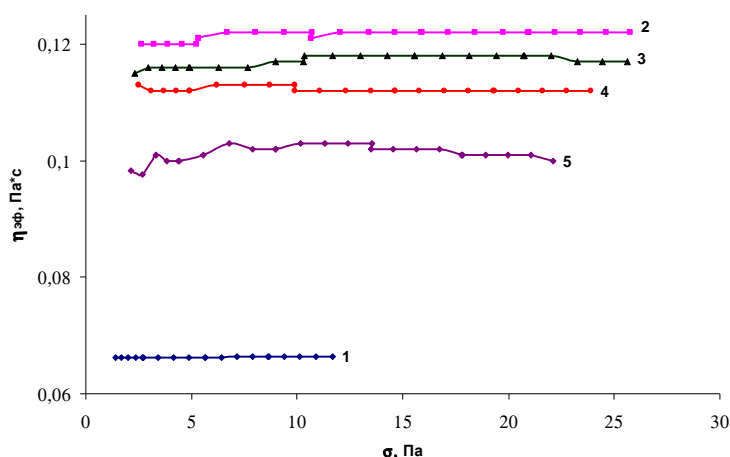


Figure 2. Flow curves of acetone solutions based on 7% of CDA, a modified of water-organic mixture vapor (water-DMSO): 1 - untreated, 2 - 0,1%; 3 - 0,5%; 4 - 1,0%; 5 - 5,0%

The dependence of viscosity on the degree of swelling recorded in the experiments clearly demonstrated in Figure 3. The nature of the influence of powder processing CDA water-organic vapor mixtures on the viscosity of the solutions can be explained as follows. The initial low-dose vapor adsorbed on the surface of the open pores of powder (average pore radius of powdered CDA is 1.65 nm, specific surface adsorption of  $S_{sp} = 11.5 \text{ m}^2 / \text{g}$ ), which is associated with the processes of adsorption of vapor mixtures on the surface of the pores. Therefore, in the first stage of swelling observed the highest rate of swelling.

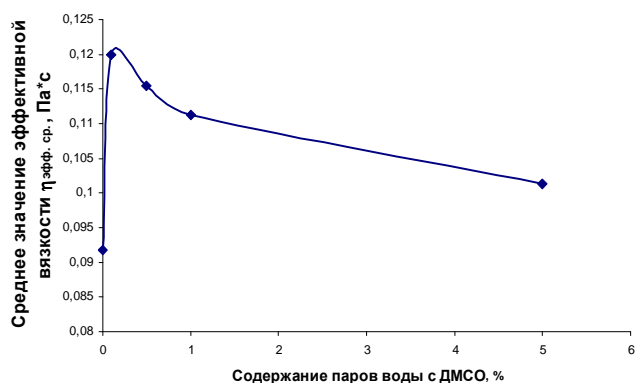


Figure 3. The dependence of the mean effective viscosity of the content in the polymer vapor mixture of water DMSO

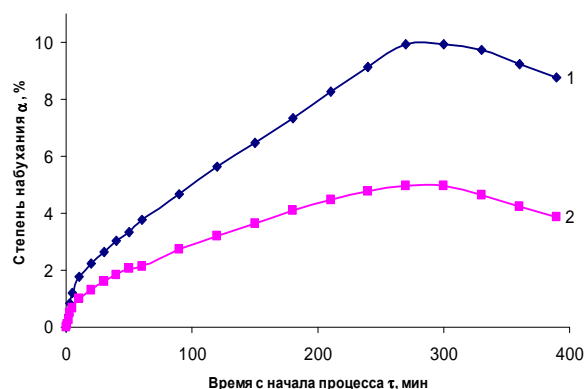


Figure 4. The kinetic curves CDA swelling powder in vapor mixtures of water with DMSO (1) and DMAA (2)

Sorbate condenses on the surface of the pores filled by the diffusion of all the leaks supramolecular packing of the polymer ("free volume" between the crystalline and amorphous

regions, packing leaks packs of macro- and microfibers, consisting of a set of parallel arranged macromolecules with a diameter about 1-2 Å), which leads to increase the adhesion forces between the sorbate and the bundles of macromolecules and is manifested in the increase of friction in the viscous flow of a solution of the modified polymer.

To the extent that large doses of sorbate (0.5, 1.0, 5.0%) and the limiting saturation of macromolecules, it is increasingly penetrating into the space between macromolecules, pushing them, reducing the intermolecular hydrogen bonds, which leads then to a decrease in the proportion of intermolecular forces cohesion in general, viscous friction and a decrease in the viscosity of the polymer solution with increasing concentration of vapor modifies the mixture.

Since DMSO has a higher dielectric constant, it has a significant influence on the conformational transformations of macromolecules.

The results of the investigation of the solutions by the method of turbidity spectrum also show this. The change of optical parameters that characterize the structure of the polymer solutions, the degree of swelling powder CDA is shown in Figure 5. Increasing the degree of swelling from zero to maximum, the equilibrium value is accompanied by a continuous monotonic increase in the number of microgel particles and decreases their size i.e. fragmentation of macromolecular associates is going and increases the degree of isotropy of the solution. The nature of relationships  $N = f_1(\alpha)$  and  $r_{MГЧ} = f_2(\alpha)$  shows that the most intense disaggregation MGP observed in solutions prepared from powder with small doses of CDA absorption of sorbate.

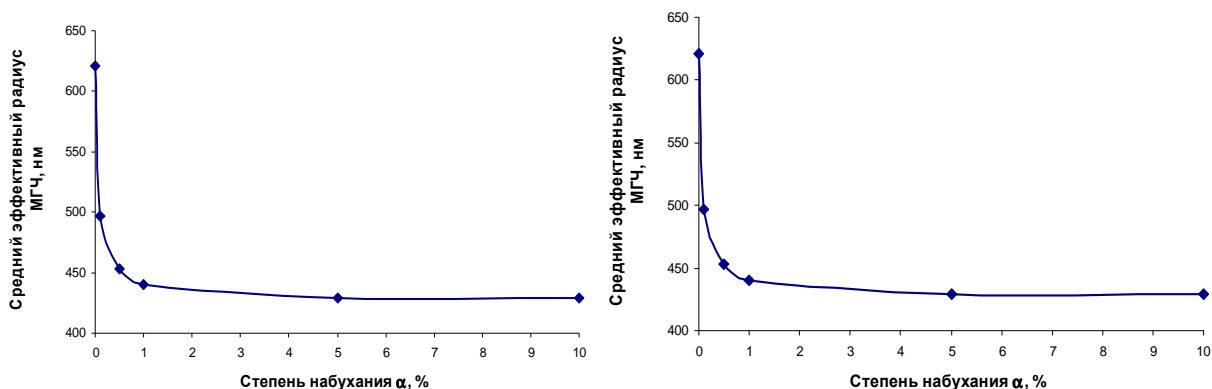


Figure 5. Depending on the number of MGP (a) and mean effective radius MGP (b) the degree of swelling

The solutions prepared from the polymer with the degree of swelling > 2-3%, differ little in their structure. This indicates that the polymer undergoes a major conformational change in its modification of vapor water-organic mixtures containing small doses of specific solvents, actively interacting with the functional groups of cellulose esters.

Thus, modification of polymer materials - cellulose diacetate pairs of water-organic mixtures allows for a comprehensive approach to the management structure and properties of solutions and filtration membrane materials based on cellulose acetate. Features of the kinetics of modification identified in the research process, it was found that the degree of swelling depends on the composition of the modifying compounds. The relationship of the individual stages of swelling of the polymer occurring in its adsorption, diffusion, and conformational changes.

## References

1. Klenin V., Fedusenko I. Macromolecular compounds: A textbook for students of Chemistry Department. Saratov: Publisher: University of Saratov. 2008. 440 p.
2. Sedelkin V., Surkova A., Potekhina L. Technology and properties of ultrafiltration membranes based on modified cellulose acetates // Bulletin of Saratov State Technical University. 2011. № 1 V. 52. P. 109-115.

# POLYMER GEL ELECTROLYTES: INFLUENCE OF COMPOSITION ON PROTON CONDUCTIVITY

<sup>1</sup>Nguyen Van Thuc, <sup>2</sup>Liudmila Shmukler, <sup>2</sup>Yulia Fadeeva, <sup>1,2</sup>Liubov Safonova

<sup>1</sup>Ivanovo State University of Chemistry and Technology, Ivanovo, Russia, E-mail: les@isc-ras.ru

<sup>2</sup>Institute of Solution Chemistry of RAS, Ivanovo, Russia, E-mail: les@isc-ras.ru

## Introduction

The expediency of application of polymer gel electrolytes in electrochemical devices is connected with their high electrical conductivity ( $\sim 1 \text{ mS cm}^{-1}$  at room temperature) in the wide region of temperature and humidity, availability, ease of preparation and also chemical, thermal, time stability, and elasticity. All abovementioned demands might be reached at optimal combination of consisting gel compounds, namely polymer matrix, plasticizer and proton donor.

Properties of gel electrolytes based on PMMA, doped by acids solutions in aprotic solvents (N,N-dimethylformamide (DMF), propylene carbonate (PC) and N,N-dimethylacetamide (DMAC)), depending on the concentration of the acid and the polymer in the system, as well as polymer molecular weight have been investigated in this work.

## Experiments

For synthesis of gel electrolytes both commercial polymer ( $M_w = 120\,000$ ;  $350\,000$  and  $996\,000$ ) and one obtained by method of MMA radical polymerization were used. The average molecular weight of new-synthesized PMMA was estimated by viscometric method ( $M_w = 325\,000$  and  $413\,000$ ).

The conductivity of gels was determined by electrochemical impedance method with Solartron 1260A over frequency range of  $0.1 \text{ Hz}$ - $150 \text{ kHz}$  with signal amplitude of  $10 \text{ mV}$ . Gels viscosity was measured with rotational viscometer BROOKFIELD DV-II with accuracy  $\pm 1\%$ . The TGA of gels was performed on a Netzch TG 209 F1 analyzer in a flow of argon ( $20 \text{ ml/min}$ ) at a heating rate of  $10 \text{ K/min}$ . Proton-conducting gel electrolytes were prepared as described in ref. [1]. Optically transparent and time-stable gels were obtained. Properties of all gels were invariable even after 6 months since they had been synthesized.

## Results and Discussion

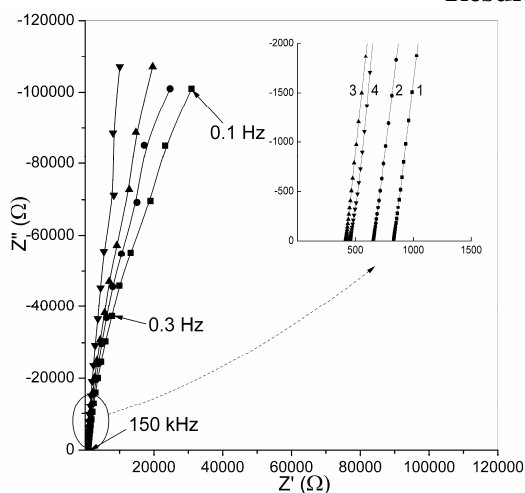


Figure 1. Impedance spectra of systems  $\sim 9 \text{ wt} \% \text{ PMMA (413 000)-[yH}_3\text{PO}_4\text{-DMF]}$  at various acid concentrations:  $y = 0.3$  (1),  $0.4$  (2),  $0.6$  (3), and  $0.7$  (4),  $\text{mol l}^{-1}$ ; at  $T = 25^\circ\text{C}$

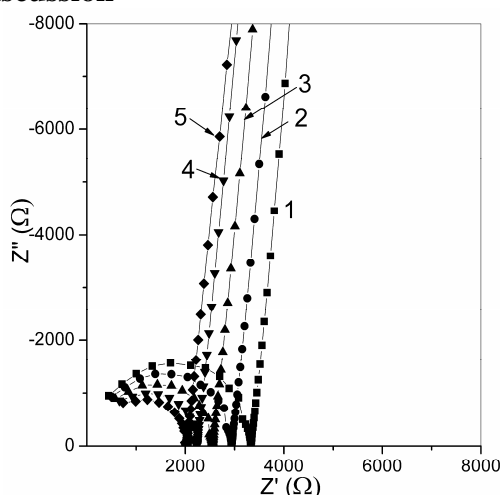


Figure 2. Impedance spectra of systems  $\sim 8.93 \text{ wt} \% \text{ PMMA (350 000)-[0.1M H}_2\text{SO}_4\text{-PC]}$  at various temperatures:  $T = 25$  (1),  $35$  (2),  $45$  (3),  $55$  (4) and  $65^\circ\text{C}$  (5)

The spectra of impedance for gel electrolytes with compositions of  $\sim 9 \text{ wt} \% \text{ PMMA-[y H}_3\text{PO}_4\text{-DMF]}$  are presented in Fig. 1. Hodographs are similar in appearance for all the studied gel-electrolytes with DMF, regardless of polymer molecular weight and nature of the acid. The hodograph of impedance for the system with DMAC is similar to the one obtained for the gel electrolytes with DMF while with PC has a different form (Fig. 2). The conductivity of gels,

prepared with different solvents, decreases in the following series: DMF > DMAC > PC, that is mainly determined by the influence of viscosity. The gel conductivity decreases in the series of acids as following: sulfuric > salicylic > phosphoric > benzoic. This sequence correlates with the values of the dissociation constants of acids in DMF, which have following values: (pKa = 4.3, 8.23, 8.41, 11.70) for sulfuric, salicylic, phosphoric, benzoic acids, respectively. It should be noted that the conductivity of the obtained gels higher than the electrical conductivity of acid solutions in DMF, which are used in the gels synthesis. The increase of the conductivity in the gel compared to conductivity in solution, possibly due to the fact that the polymer matrix may be involved in the Grotthuss-type charge transfer mechanism and lead to increase of acid dissociation as well.

The effect of acid concentration on the conductivity of gel electrolytes has been studied on the example of systems with sulfuric and phosphoric acids.

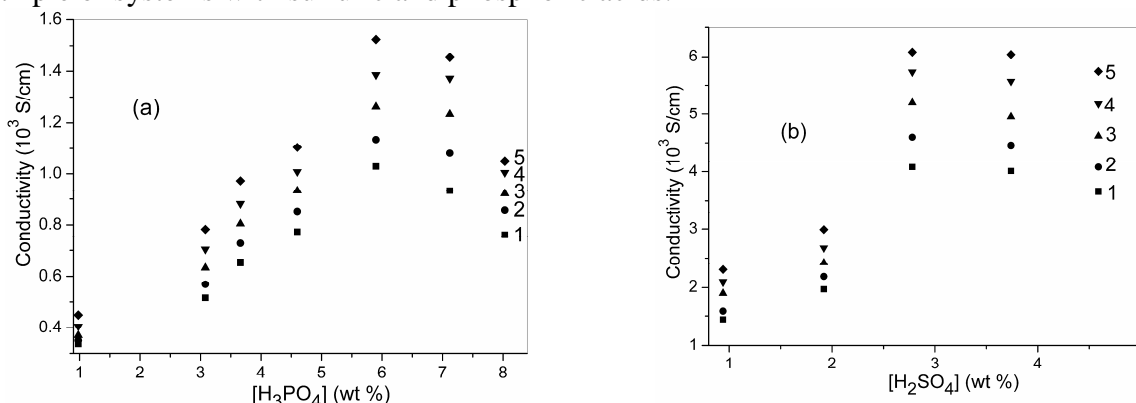


Figure 3. Conductivity of gel electrolytes ~ 9 wt % PMMA ( $M_w = 413\,000$ )–[y acid–DMF] as a function of  $H_3PO_4$  (a) and  $H_2SO_4$  (b) concentrations at various temperatures:

$$T = 25\ (1),\ 35\ (2),\ 45\ (3),\ 55\ (4)\ \text{and}\ 65\ ^\circ\text{C}\ (5)$$

The conductivity of gel electrolytes on the concentration of acids has an extreme character. The position of extremum depends on the nature of the electrolyte. Appearance of a maximum is explained by two opposing factors. On the one hand, with an increase in the acid concentration, the number of charge carriers increases and, consequently, the electrical conductivity should increase. On the other hand, there is an increase in viscosity of the system, leading to a decrease of ion mobility.

The dependence of the gel conductivity on the concentration of PMMA may be the confirmation that the polymer matrix is not an inert component in the gel electrolyte (Fig. 4). The figure demonstrates that when the content of PMMA up to 5 wt%, the gel is not formed. There is a decrease of electrical conductivity due to, first of all, influence of viscosity over this concentration range. Extreme dependence of the conductivity is found to be for the gel (at a concentration of PMMA from 5 to 15 wt%). The increase of electrical conductivity in the concentration range from 5 to 10 wt% of PMMA with an increase in viscosity of the system can also indicate an involvement of the polymer matrix in increasing the degree of the acids dissociation.

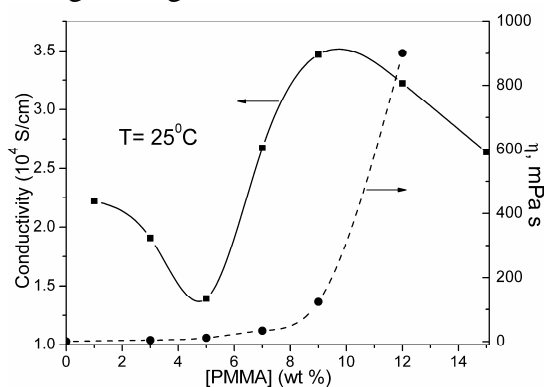


Figure 4. Conductivity and dynamic viscosity of gel electrolytes x PMMA (350 000)–[0.1 M  $H_3PO_4$ –DMF] depending on PMMA concentrations at  $T = 25^\circ\text{C}$

With increasing molecular weight of polymer the gel conductivity increases (Fig. 5). The observed increase the conductivity of gels with increasing of viscosity systems by increasing the molecular weight of the original polymer might be an argument confirming the participation of the polymer matrix in the process of acids dissociation.

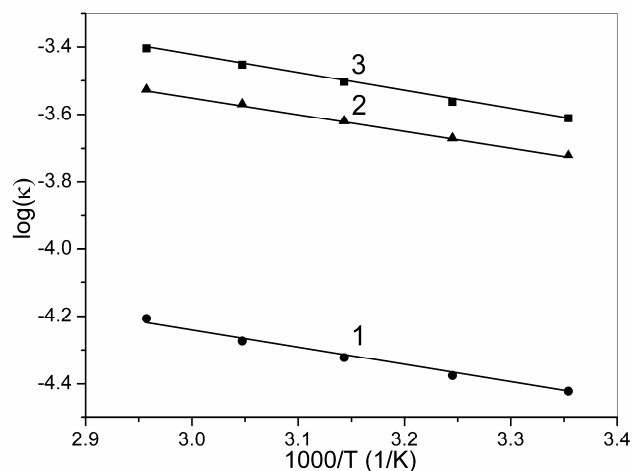


Figure 5. Temperature dependences of conductivity of gel electrolytes ~ 18-20 wt % PMMA–[0.1 M  $H_3PO_4$ –DMF] for PMMA of  $M_w = 120\ 000$  (1), 325 000 (2) and 413 000 (3).

The thermal behavior of gel electrolytes are similar and independent on the nature of the acid, so we presented to only one example of the differential gravimetric curve (DTG) for the gel with sulfuric acid.

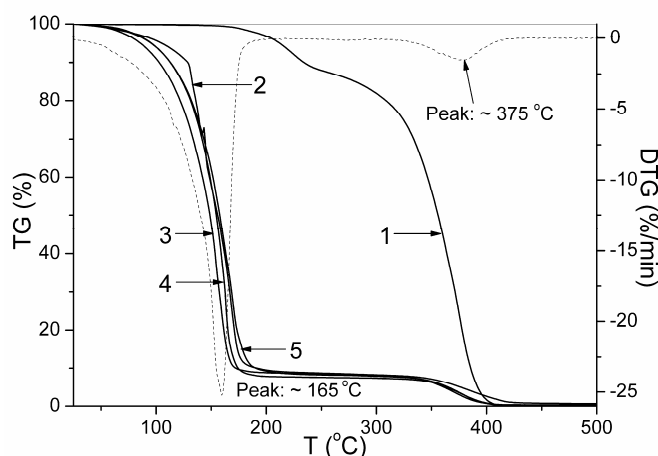


Figure 6. TGA curves for PMMA (413 000) (1) and the gel electrolytes ~ 9 wt % PMMA (413 000)–[0.1 M acid–DMF], acid: benzoic (2); sulfuric (3); phosphoric (4) salicylic (5) and DTG curve for the gel electrolyte 8.99 wt % PMMA–[0.1 M  $H_2SO_4$ –DMF]

The first and main weight loss occurs for  $T \sim 165\ ^\circ\text{C}$ . The weight loss may be associated with the removal of unbound solvent from the sample. The second peak at  $T \sim 375\ ^\circ\text{C}$  in the differential curve corresponds to a complete degradation of the polymer.

This work was financially supported by Russian Foundation for Basic Researches (grants 11-03-00311-a and 12-03-97534).

## References

1. Shmukler L.E., Safonova L.P., Nguen Van Thuk, Gruzdev M.S. Proton-conducting gel electrolytes based on poly(methyl methacrylate) doped with phosphoric acid in *N,N*-dimethylformamide // Polymer Science. Ser. A. 2011. Vol. 53, No. 1. P. 44-51.

# NOVEL MF-4SK MEMBRANES FOR HYDROGEN-AIR FUEL CELLS

<sup>1</sup>Sergey Timofeev, <sup>1</sup>Lyubov' Bobrova, <sup>2</sup>Elena Lyutikova, <sup>3</sup> Lyubov' Fedotova,  
<sup>3</sup>Valery Dyakov, <sup>2</sup> Sergey Grigoryev

<sup>1</sup>Plastpolymer, Sankt Petersburg, Russia, *E-mail: stimof@yandex.ru*

<sup>2</sup>National Research Centre "Kurchatov institute", Moscow, Russia

<sup>3</sup>ZAO Ecoflon, Sankt Petersburg, Russia

## Introduction

One of the most important aspects in the modern development of hydrogen-air fuel cell (FC) with a solid polymer electrolyte is the development of ion-exchange membranes (IEM) which provide the most favorable water management up to temperatures of about 100 °C when high chemical as well as physical and mechanical stability and low resistivity are constant [1]. In Russia, OAO Plastpolymer in St. Petersburg develops this type of membranes (MF-4SK) over the past thirty years [1, 2]. The main disadvantage of IEM is the dehydration at high current densities and high temperatures, resulting in a significant decrease in the ionic conductivity of membranes. This drawback can be overcome by reducing of IEM thickness, which allows to increase the water flow associated with back diffusion in working FC or by generating of nanosized centers in the membrane structure, capable to hold water (usually hydrophilic centers) even at elevated temperatures or centers that generate water in the fuel cell while in operation. In addition, the membrane must have high mechanical strength and low gas permeability. This effect can be achieved with the use as a reinforcing material of thin porous polytetrafluoroethylene films (TPPF) [3]. In the membrane polymer embedded Pt nanoparticles can serve as water generating centers [4].

## Experimental

In the present paper IEM on the basis of biaxially-oriented TPPF (thickness 8-40 microns, porosity > 70%) and perfluorinated sulfo-containing polymer solutions in isopropanol (EM = 980, concentration 10%) were obtained and analyzed. Nanoparticle catalysts were introduced directly into the IEM through the chemical reduction of Pt precursors. The current-voltage characteristics were obtained using a hydrogen-air fuel cell without gas pressure (collector - Carbon paper Pantex, temperature 40 ° C, catalyst Pt40 on carbon). Experiments were performed both with and without humidification of gases. Once the parameters of the cell with gas humidification reached their steady-state values, moisture gas was eliminated, and the measurements were taken at regular intervals.

## Results and Discussion

Technological characteristics of reinforced membranes compared to the preliminary one are presented in Table 1.

**Table 1: Properties of IEM reinforces with biaxially oriented TPPF of various thickness** ( $\delta_{\text{TPPF}}$  -film thickness,  $\Delta_m$  -IEM thickness,  $\rho$  -density,  $W$ - water absorption,  $\sigma_p$  -tensile strength,  $\varepsilon$ -relative elongation,  $\rho_v$  -specific volume resistivity in the H<sup>+</sup>-form at 20 ± 2 ° C).

$\delta_{\text{TPPF}}, \mu\text{m}$	$\Delta_m, \mu\text{m}$	$\rho, \text{g/cm}^3$	$W, \%$	$\sigma_p, \text{MPa}$	$\varepsilon, \%$	$\rho_v, \Omega^*\text{cm}$
non	30	2,13	32	5,2	118	9,2
8	30	1,75	38	11,0	117	9,9
10	40	1,79	40	11,3	112	9,3
12	40	1,78	37	11,4	101	9,5
20	73	1,82	45	12,1	108	10,5

Reinforced IEM samples, in contrast to the preliminary membrane exhibit excellent strength characteristics, including a slight change in linear dimensions during swelling in water, as well as low electrical resistance. All IEM have no micropuncture.

Fig. 1 shows the results of IEM tests in the fuel cell. We investigated the reinforced IEM, reinforced IEM with water generating catalytic centers and Nafion-212 membrane (for comparison). It is evident from the figure that with wetted gases all the membranes show similar and high performance. Current-voltage characteristics are particularly limited when dry gases are fitted into the cell, and most dramatically for the unreinforced Nafion-212 membrane (characteristics of reinforced IEM are somewhat higher, do to the possibility of presence therein of additional free water at interfacial surface of hydrophobic TPPF and hydrophilic polymer membrane, which is confirmed by data in Table 1). Current-voltage characteristics of reinforced IEM with water generating catalytic centers are also reduced depending on the time of the cell function, but remain significantly higher in comparison with other membranes. Performance of fuel cells with these membranes reached stable values after 1,5 to 2,0 hours.

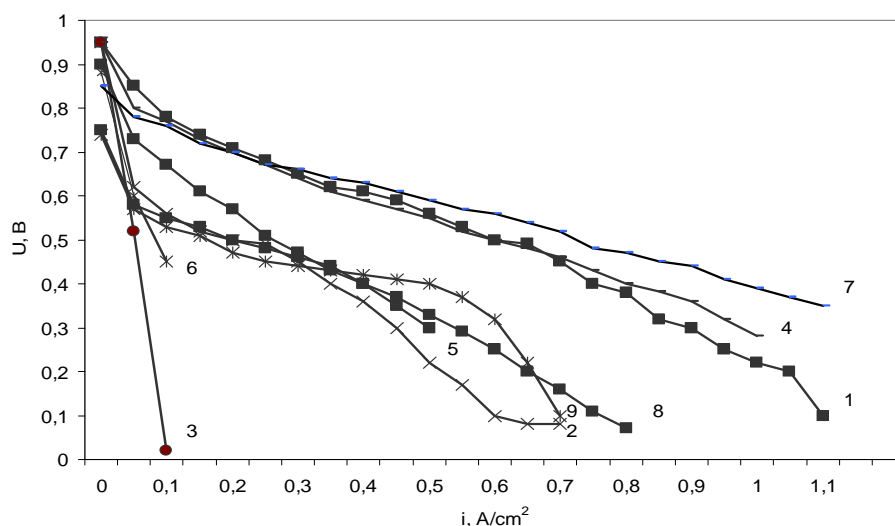


Figure 1. Current-voltage characteristics of various membranes. (Nafion 112 membrane: humidified gases – 1; dry gases (10 min) - 2; dry gases (20 min) – 3; Reinforced MF-4SK (35  $\mu\text{m}$ ): humidified gases – 4; dry gases (10 min) – 5; dry gases (20 min) – 6; Reinforced MF-4SK with catalyst (30  $\mu\text{m}$ ): humidified gases – 7; dry gases (10 min) – 8; dry gases (20 min) – 9)

Accordingly it is shown that the new composite membranes based on porous polytetrafluoroethylene films and perfluorinated sulfopolymers with water generating catalytic centers shows high strength, small shrinkage when moisture content varies, sufficiently high ionic conductivity at temperatures up to 100 °C and significantly exceeds samples of preliminary membranes when tested in fuel cells.

## References

1. Panshin Y.A, Dreyman N.A., Andreeva A.I, Manechkina O.N. Properties of perfluorinated sulfocationite membranes MF-4SK // *Plasticheskie Massy*, 1977, V. 8. P. 7-8.
2. Bobrova L.P., Ostrizko F.N., Timofeev S.V., Deruzov Ju.M. TFE random terpolymer with functionalized perfluorinated comonomers and its production method // RF Patent 2006, No. 2267498.
3. Bahar R., Hobson A.R., Kolde J.A., Zuckerbrod D. Ultra-thin integral composite membrane // Patent USA 1996, № 5547551.
4. Xiao-Bing Zhu, Hua-Min Zhang, Yong-Min Liang, Yu Zhang, Bao-Lian Yia. A Novel PTFE-Reinforced Multilayer Self-Humidifying Composite Membrane for PEM Fuel Cells // *Electrochemical and Solid-State Letters*, 2006. V. 9. №2. P. 49-52.

# INFLUENCE OF MAGNETIC FIELD ON HYDRODYNAMIC PERMEABILITY OF A MEMBRANE

<sup>1</sup>Ashish Tiwari, <sup>2</sup>Satya Deo, <sup>3</sup>Anatoly Filippov

<sup>1</sup>Birla Institute of Technology and Science, Pilani-333031, India

<sup>2</sup>University of Allahabad, Allahabad-211002, India

<sup>3</sup>Gubkin Russian State University of Oil and Gas, Moscow, Russia, *E-mail: a.filippov@mtu-net.ru*

## Introduction

The present work concerns the influence of the magnetic field on the permeability of a membrane of solid cylindrical particles covered with porous layer. Here, we have considered the flow along the axis of cylinder and the alignment of uniform magnetic field is assumed to be perpendicular to the axis. The Brinkman equation is used for flow through porous region and Stokes equation is used for flow through clear fluid region. To model flow through assemblage of particles, cell model technique has been used i.e. the porous cylindrical shell is assumed to be confined within a hypothetical cell of same geometry. The stress jump condition has been employed at the fluid-porous interface and all four alternative conditions Happel, Kuwabara, Kvashnin and Mehta-Morse/Cunningham are used at the hypothetical cell. Effect of the Hartmann number on the hydrodynamic permeability of the membrane is discussed.

## Theory

Here, we have considered an axi-symmetric Stokes flow of an electrically conducting viscous incompressible fluid through a swarm of porous cylindrical particles of radii  $\tilde{b}$ , each enclosing an impermeable core of radius  $\tilde{a}$ . The above model is equivalent to a co-axial porous cylindrical shell enclosing an impermeable core (Fig. 1). We assume also that axes of all cylinders are parallel. By virtue of cell model, each porous shell is assumed to be enveloped by a concentric cylinder of radius  $\tilde{c}$  ( $\tilde{c} > \tilde{b}$ ), named as cell surface. The Stokes flow of a Newtonian fluid with absolute fluid viscosity is assumed to be steady and axi-symmetric. We assume that the fluid is approaching towards the cell surface as well as partially passing through the composite cylinder along the axis of cylinders (z-axis) with velocity  $\tilde{U}$  from left to right. The radius  $\tilde{c}$  of hypothetical cell is chosen in such a way that the particle volume fraction of the porous cylinder is equal to the particle volume fraction of the cell, i.e. relative to this composite cylinder (i.e. a core with porous shell) in the hypothetical cell, i.e.  $\gamma = \pi \tilde{b}^2 / \pi \tilde{c}^2$ .

A transverse magnetic field of uniform intensity is applied. The Magnetic Reynolds number is assumed to be very small and there is no external electric field so that the induced current is very small and hence it can be neglected. The governing equations for the creeping flow of an incompressible Newtonian fluid, which lies in the region outside the porous cylindrical shell under the above assumptions, can be expressed by

$$\tilde{\mu}^{(1)} \tilde{\nabla}^2 \tilde{\mathbf{v}}^{(1)} + \tilde{\mathbf{J}}^{(1)} \times \tilde{\mathbf{B}} = \tilde{\nabla} \tilde{p}^{(1)}. \quad (1)$$

Also, the flow inside the porous cylindrical shell is governed by the Brinkman equation

$$\tilde{\mu}^{(2)} \tilde{\nabla}^2 \tilde{\mathbf{v}}^{(2)} - (\tilde{\mu}^{(1)} / \tilde{k}) \tilde{\mathbf{v}}^{(2)} + \tilde{\mathbf{J}}^{(2)} \times \tilde{\mathbf{B}} = \tilde{\nabla} \tilde{p}^{(2)}, \quad (2)$$

where the tilde denotes dimensional magnitudes; indices (1) and (2) refer to the external zone and porous layer, respectively;  $\tilde{\mu}^{(1)}$  is the viscosity of the fluid,  $\tilde{\mu}^{(2)}$  denotes the effective viscosity of porous medium;  $\tilde{k}$  being the permeability of porous medium. Here,  $\tilde{\mathbf{v}}^{(i)}$ ,  $\tilde{p}^{(i)}$ ,  $i = 1, 2$  be the velocity vector and pressure outside and inside the porous cylindrical shell respectively.  $\tilde{\mathbf{J}}^{(1)}$ ,  $\tilde{\mathbf{J}}^{(2)}$  are the electric current density vectors in appropriate regions and  $\tilde{\mathbf{B}}$  is the magnetic induction vector of applied uniform magnetic field. As we assume that external electric field is absent and internal causes such as separation of charges or polarization do not originate induced electric field, so  $\tilde{\mathbf{J}}^{(i)} = \tilde{\sigma}^{(i)} (\tilde{\mathbf{v}}^{(i)} \times \tilde{\mathbf{B}})$ , where  $\tilde{\sigma}^{(i)}$ ,  $i = 1, 2$ , are the electrical

conductivities of fluid refer to the external zone (1) and porous layer(2), respectively. Therefore, we conclude that Lorentz forces  $\tilde{\mathbf{F}}_L^{(i)} = \tilde{\mathbf{J}}^{(i)} \times \tilde{\mathbf{B}}$  and velocity  $\tilde{\mathbf{v}}^{(i)}$  are collinear and opposite directed:  $\tilde{\mathbf{F}}_L^{(i)} = -\tilde{B}_0^2 \tilde{\mathbf{v}}^{(i)}$ , where  $\tilde{B}_0 = |\tilde{\mathbf{B}}|$ . Further, we also assume that electrical conductivities of fluid in the external zone (1) and porous layer (2) are equaled, i.e.  $\tilde{\sigma}^{(1)} = \tilde{\sigma}^{(2)} = \tilde{\sigma}$ . In addition, the equations of continuity for incompressible fluids must be satisfied in both regions:

$$\tilde{\nabla} \cdot \tilde{\mathbf{v}}^{(i)} = 0, \quad i = 1, 2. \quad (3)$$

We set as usually the sticking condition on the surface of a rigid cylinder:

$$\tilde{u}^{(2)} = 0, \quad \tilde{r} = \tilde{a}. \quad (4)$$

For the convenience of analysis, let us introduce the following dimensionless magnitudes:

$$\ell = \frac{\tilde{a}}{\tilde{b}}, \quad \tilde{c} = \frac{1}{\sqrt{\gamma}}, \quad \lambda = \sqrt{\frac{\tilde{\mu}^{(2)}}{\tilde{\mu}^{(1)}}}, \quad \eta = \frac{\tilde{b}}{\sqrt{k}}, \quad \alpha = \frac{\eta}{\lambda}$$

At the porous-fluid interface ( $\tilde{r} = \tilde{b}$ ), we use the continuity condition for velocity and the jump condition for tangential stresses:

$$\tilde{u}^{(1)} = \tilde{u}^{(2)}, \quad \tilde{T}_{rz}^{(2)} - \tilde{T}_{rz}^{(1)} = \frac{\beta \tilde{\mu}^{(1)}}{\sqrt{k}} \tilde{u}^{(2)}. \quad (5)$$

where  $\beta$  is dimensionless parameter of order 1 [2].

In the case under consideration, the Happel, Kuwabara, Kvashnin, and Cunningham boundary conditions on the cell surface lead to the following single result:

$$\frac{d\tilde{u}^{(1)}}{d\tilde{r}} = 0 \text{ at } \tilde{r} = \tilde{c}. \quad (6)$$

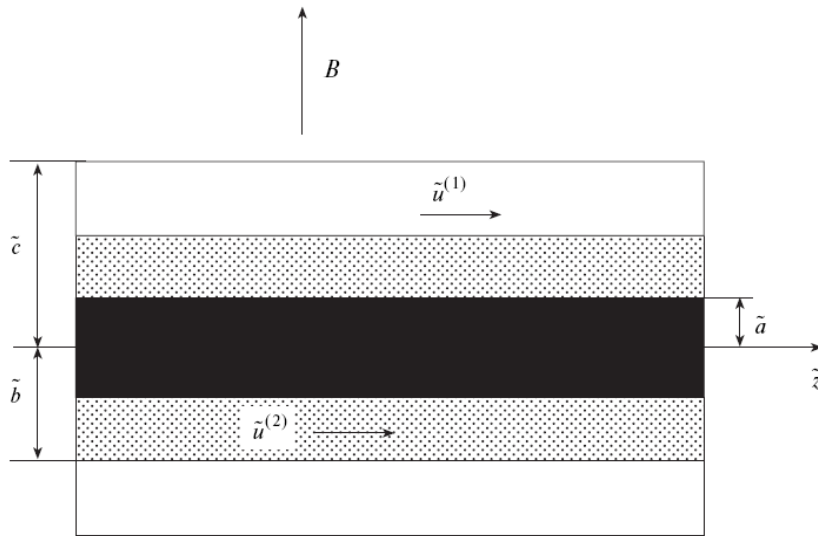


Figure 1. Scheme of the flow along the  $z$ -axis of cylinder

The boundary value problem (1)-(7) was solved analytically [1] in the cylindrical system of coordinates  $(\tilde{r}, \theta, \tilde{z})$ , in which the axis is directed along the flow (Fig 1). Equations (1)-(2) that describe the flow outside and inside the porous layer have, respectively, the following forms [1]:

$$\tilde{\mu}^{(1)} \frac{1}{\tilde{r}} \frac{d}{d\tilde{r}} \left( \tilde{r} \frac{d\tilde{u}^{(1)}}{d\tilde{r}} \right) - \tilde{\sigma} \tilde{B}_0^2 \tilde{u}^{(1)} = \frac{d\tilde{p}}{d\tilde{z}}, \quad (\tilde{b} < \tilde{r} < \tilde{c}) \quad (1')$$

$$\tilde{\mu}^{(2)} \frac{1}{\tilde{r}} \frac{d}{d\tilde{r}} \left( \tilde{r} \frac{d\tilde{u}^{(2)}}{d\tilde{r}} \right) - \frac{\tilde{\mu}^{(1)}}{\tilde{k}} \tilde{u}^{(2)} - \tilde{\sigma} \tilde{B}_0^2 \tilde{u}^{(2)} = \frac{d\tilde{p}}{d\tilde{z}}, \quad (\tilde{a} < \tilde{r} < \tilde{b}) \quad (2')$$

where  $\tilde{u}^{(1)}$ ,  $\tilde{u}^{(2)}$  – are flow velocities of clear fluid and Brinkman medium along the cylinder and  $\frac{d\tilde{p}}{d\tilde{z}}$  – is the pressure drop, which is considered to be constant and preset. We introduce also two

important dimensionless quantities:  $M = \sqrt{\frac{\tilde{\sigma} \tilde{B}_o^2 \tilde{b}^2}{\tilde{\mu}^{(1)}}}$  being the Hartmann number and

$$s^2 = \frac{(\eta^2 + M^2)}{\lambda^2}.$$

## Results and Discussion

Using obtained analytical solution [1], the dependence of hydrodynamic permeability on magnetic field is depicted in Fig. 2.

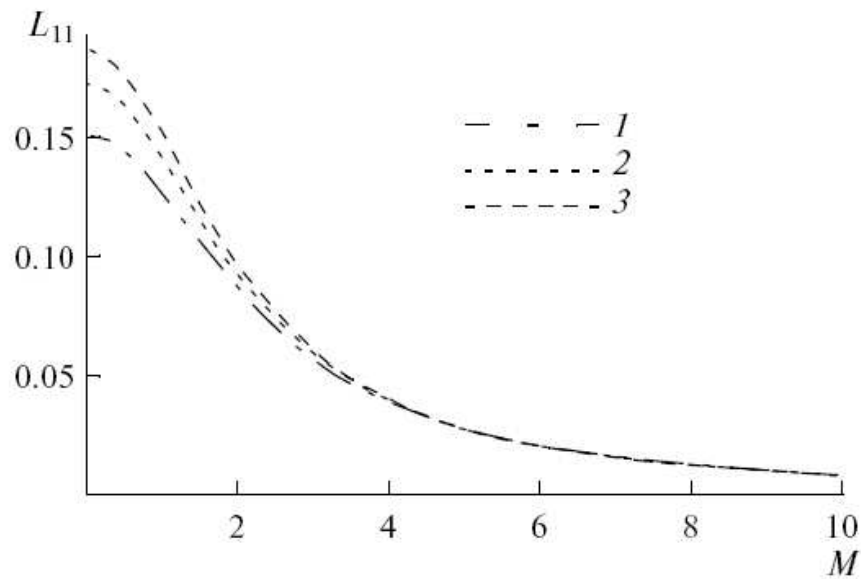


Figure 2. Dependence of dimensionless hydrodynamic permeability  $L_{11}$  of a membrane of cylindrical particles under longitudinal flow on Hartmann number  $M$ : 1 –  $\beta = -0.6$ , 2 –  $0.2$ , 3 –  $0.6$ ;  $\eta = 1$ ,  $l = 0.4$ ,  $\lambda = 2$ ,  $\gamma = 0.5$ .

The hydrodynamic permeability  $L_{11}$  decreases with Hartman number  $M$  and increases with jump coefficient  $\beta$  signifying lesser resistance offered against flow for a relatively higher shear stress in porous region compared to the clear fluid region. At Hartman number  $M > 4$ , there is no difference between curves for various values of parameter  $\beta$ . We believe that taking into consideration external magnetic field allows us to describe more accurately the influence of magnetic stirrers on flows of conducting liquid through porous membranes.

*The present work is supported by the Russian Foundation for Basic Research (projects nos 10-08-92652\_IND and 12-08-92690\_IND).*

## References

1. Tiwari A., Deo S., Filippov A. Effect of the Magnetic Field on the Hydrodynamic Permeability of a Membrane // Colloid J. 2012. V.74. No 4 (in press).
2. Ochoa-Tapia J.A., Whitaker S. Momentum transfer at the boundary between a porous medium and a heterogeneous fluid-I. Theoretical development // Int. J. Heat Mass Transfer. 1995. V. 38. P. 2635.

# MECHANISM OF ASYMMETRIC TRANSMEMBRANE TRANSFER THROUGH THE MODIFIED MEMBRANE

<sup>1</sup>Valery Ugrozov, <sup>2</sup>Anatoly Filippov

<sup>1</sup>The All-Russian Institute of Finance and Economic, Moscow, Russia, *E-mail: vugr@rambler.ru*

<sup>2</sup>Gubkin Russian State University of Oil and Gas, Moscow, Russia, *E-mail: a.filippov@mtu-net.ru*

## Introduction

Dependence of diffusion permeability of composite or asymmetric membrane on the direction of substance transfer through it (asymmetric transport) is discussed widely in the literature. Up to now a number of the possible mechanisms which are capable to source the given effect have been suggested. The effect of asymmetry in the case of gaseous transport can be caused by conic-shaped pores [1, 2] in a porous asymmetric membrane. In the case of ionic transport the asymmetry effect can be originated by spatially non-uniform distribution of a fixed charges in a membrane and geometrical features of its porous structure in a porous bi-layer membrane [3-5] or heterogeneity of exchange capacity of a membrane on its thickness [6, 7]. Various mechanisms for the asymmetric transfer of gases and liquids through composite or asymmetric membranes are discussed elsewhere [1, 8].

This work presents the new mechanism for explanation of asymmetry transfer through a modified membrane [9].

## Theory

We assume that: 1) transfer rate of the dissolved component through the membrane is determined by bulk diffusion and the rates of establishing of the adsorption equilibrium on the surfaces of the membrane ; 2) modification one of the surfaces of the membrane can result in noticeable change in its sorption-kinetic characteristics (such as coefficients of adsorption and desorption rate, etc.).

Let us consider the case when the dissolved substance in liquid diffuses through the membrane from the modified membrane surface 1 to the unmodified surface 2 (Fig. 1a). Pure solvent (water) is located near the surface 2.

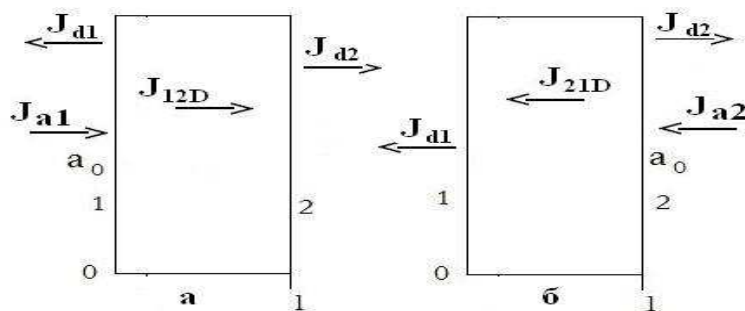


Figure 1. The scheme of transfer of dissolved substance through the modified membrane depending on the transport direction: a) transfer from surface 1 to surface 2; b) transfer from surface 2 to surface 1

Mass balance in the case (a) can be written as

$$J_{a1} = J_{d1} + J_{d2} \quad (1)$$

where  $J_{a1} = k_{1a}a_0(c_{\infty} - c_1)$ ;  $J_{d1} = k_{d1}c_1$ ,  $J_{d2} = k_{d2}c_2$ ;  $k_{a1}$ ,  $k_{a2}$  and  $k_{d1}$ ,  $k_{d2}$  - adsorption and desorption rate coefficients of the dissolved substance on the modified and unmodified surfaces of the membrane, respectively;  $c_{\infty}$  - the maximum accessible concentration of the adsorbed substance on the surface,  $c_1$  and  $c_2$  - the concentrations of the substance on the surfaces 1 and 2, respectively;  $a_0$  - the concentration of the dissolved substance.

The diffusion flux through the membrane can be written in the steady state in the following form:

$$J_{12D} = D \frac{c_1 - c_2}{l} \quad (2)$$

where  $l$  - the membrane thickness,  $D$  - the diffusion coefficient.

The expression of diffusion permeability coefficient  $P_1$  for the case (a) can be obtained by taking into account relations (3) - (4) and the condition of diffusive flux absence (in the case of equal concentrations on both surfaces of the membrane)

$$P_1 = \frac{KD}{[1 + \frac{Ka_0}{c_\infty} + \frac{D}{l} (\frac{1}{k_{d2}} + \frac{1}{k_{d1}} + \frac{Ka_0}{k_{d2}c_\infty})]} \quad (3)$$

where  $K$  is the Henry coefficient.

The permeability coefficient  $P_2$  for the opposite direction i.e. (b), can be obtained similarly

$$P_2 = \frac{KD}{[1 + \frac{Ka_0}{c_\infty} + \frac{D}{l} (\frac{1}{k_{d1}} + \frac{1}{k_{d2}} + \frac{Ka_0}{k_{d1}c_\infty})]} \quad (4)$$

Expression for the asymmetry coefficient was obtained using (3) - (4)

$$\eta = \frac{P_1}{P_2} = \frac{[1 + \frac{Ka_0}{c_\infty} + \frac{D}{l} (\frac{1}{k_{d1}} + \frac{1}{k_{d2}} + \frac{Ka_0}{k_{d1}c_\infty})]}{[1 + \frac{Ka_0}{c_\infty} + \frac{D}{l} (\frac{1}{k_{d2}} + \frac{1}{k_{d1}} + \frac{Ka_0}{k_{d2}c_\infty})]} \quad (5)$$

## Results and Discussion

According to (5) the asymmetry effect of diffusion permeability of the membrane can occur if there is a noticeable difference between the coefficients of the desorption rate on the modified and unmodified surfaces of the membrane.

Analysis of a number of limiting transport cases revealed that

1) The limiting stage of transport is the kinetics of desorption rate on the surfaces of the membrane  $\frac{l}{D} \ll \frac{1}{k_{di}}$ , ( $i = 1, 2$ ). Then from (5) we easily obtain the expression for the asymmetry coefficient of diffusion permeability:

$$\eta = \frac{P_1}{P_2} = \frac{[\frac{1}{k_{d1}} + \frac{1}{k_{d2}} + \frac{Ka_0}{k_{d1}c_\infty}]}{[\frac{1}{k_{d2}} + \frac{1}{k_{d1}} + \frac{Ka_0}{k_{d2}c_\infty}]} \quad (6)$$

From (6) it follows that the effect of AEDPM (asymmetry effect of diffusion permeability of the membrane) may occur due to changes in the coefficient of desorption rate on the surface 1 due to modification of this surface.

If the modification of surface does not change the coefficient of desorption rate on the surface of a 1, the effect of AEDPM does not arise.

2) The limiting stage of transport is diffusion in the membrane ( $\frac{l}{D} \gg \frac{1}{k_{di}}$ ). In this case, the effect of AEDPM does not occur and so,  $\eta = 1$ .

3) Equation (7) for the proposed mechanism of the asymmetry of diffusion permeability is followed from (3) - (4)

$$\frac{1}{P_2} - \frac{1}{P_1} = \frac{a_0}{c_\infty l} \left[ \frac{1}{k_{d1}} - \frac{1}{k_{d2}} \right] \quad (7)$$

This ratio can be used to determine the presence of the considered mechanism of the asymmetry of the diffusion permeability using experimental data.

### Conclusion

Thus, the effect of AEDPM may occur when significant influence of the surface rates of sorption kinetics on the transport through the modified membrane under the condition of significant divergence between these rates on different surfaces.

### References

1. Volkov V.V., Mchedlishvili B.V., Roldughin V.I., Ivanchev S.S., Yaroslavtsev A.B. // Nanotechnol Russia. 2008. Vol. 3. P. 67-99.
2. Awasthy K., Kulshreshtha V., Tripathi D., Acharya N.K, Singh M., Vijay Y.K. Bull. Mater. Sci. 2006. Vol. 29. P. 261.
3. Filippov A.N., Starov V.M., Kononenko N.A., Berezina N.P. Asymmetry of diffusion permeability of bi-layer membranes // Advances Colloid Interface Sci. 2008. V.139. P.29-44.
4. Filippov A.N., Iksanov R.Kh., Kononenko N.A., Berezina N.P., Falina I.V. Theoretical and Experimental Study of Asymmetry of Diffusion Permeability of Composite Membranes // Colloid Journal. 2010. Vol. 72. No. 2. P. 243-254.
5. Berezina N.P., Kononenko N.A., Filippov A.N., Shkirskaia S.A., Falina I.V., Sycheva A. A.-R. Electrotransport Properties and Morphology of MF-4SK Membranes after Surface Modification with Polyaniline // Russ. J. of Electrochemistry. 2010. V. 46. N. 5. P. 485-493.
6. Filippov A., Iksanov R. Modeling of asymmetry of diffusion permeability of nanocomposites ionexchange membranes having linear density of fixed charges // Book of abstracts. Int. Conf. "Ion transport in organic and inorganic membranes". Krasnodar: 2009. P. 52-53.
7. Filippov A.N., Iksanov R.Kh. Study of Asymmetry of Diffusion Permeability of Nanocomposites Ionexchange Membranes: Model of Linear on Membrane Thickness Density of Fixed Charges // Russ. J. of Electrochemistry. 2011. V. 47 .
8. Roldughin V.I., Zhdanov V.M. Asymmetrical gas mixture transport in composite membranes // Advances in Colloid and Interface Science. 2011. V.168. P.223.
9. Ugrozov V.V., Filippov A.N. // Colloid Journal. 2012 (in press).

---

# DIFFUSION OF ANTI-CANCER DRUG MOLECULES IN MEMBRANE-MODIFIED HYDROGEL

**Raushan Usenkyzy, Kuanyshbek Musabekov, Nurlan Musabekov**  
Kazakh National University Al-Farabi, Almaty, Republic of Kazakhstan,  
E-mail: *ussenkizi.rausha@mail.ru*

## Introduction

Treatment of malignant neoplasm is one of the most important issues of the day. Therefore, in recent years, particular attention is paid to the development of high-effected anti-cancer products and new dosage forms of cytostatics[1]. New approach to the solution of this problem is to use polymeric carriers of drugs. Especially use of hydrogels on the basis of natural polymeric materials - gelatin, agar-agar, alginate metals, pektovy acid were successful. [1-3]. Varying the physicist-chemical properties of hydrogels on a basis of alginate calcium in presence of gelatin and agar-agar, it was possible to create new highly effective medicine carriers and prolonged its effect of medicinal action[4].

Further development of these works is the creation on a surface of hydrogels of a thin layer of the membrane consisting also of natural polymers, in a particular from chitosan and a sulfate dextran[5].

This work results showed that the influence of thickness of the polymeric membrane coated hydrogel alginate of calcium depends on the speed of liberation of a anti-cancer preparation from hydrogel [2].

## Experiments

Membrane layers on a surface of hydrogels calcium alginate formed as follow. Solution of chitosane  $\text{CaCl}_2$  was dropped slowly to sodium alginate. It is known that ions of calcium have small molecular weight and interact with polymeric chain of alginate quicker than chitosane. Formation of hydrogel of calcium alginate occurs quicker than formation of a polyelectrolyte of alginate complex with chitosan. As a result, microparticles formed on the surface of calcium alginate form the membrane layer chitosan. Thickness of this layer defined by a light microscope of brand of "Leica Eclipse TE 300" ( Table 1).

**Table 1: Influence of concentration of chitosan in solution on thickness of the membrane formed on a surface of hydrogel of calcium alginate**

Concentration of chitosan solution, %	Thickness of a membrane, mcm
0,25	25±3
0,50	40±5
1,00	65±5
2,00	125±10

The release anticancer drug-cyclophosphamide from calcium alginate modified with adsorbed layer of chitosane have been studied.

## Results and Discussion

It is established that at increases in thickness of chitosane membranes from 25  $\mu\text{m}$  to 125  $\mu\text{m}$  results to decrease of diffusion coefficient of cyclophosphamide in 2 times.

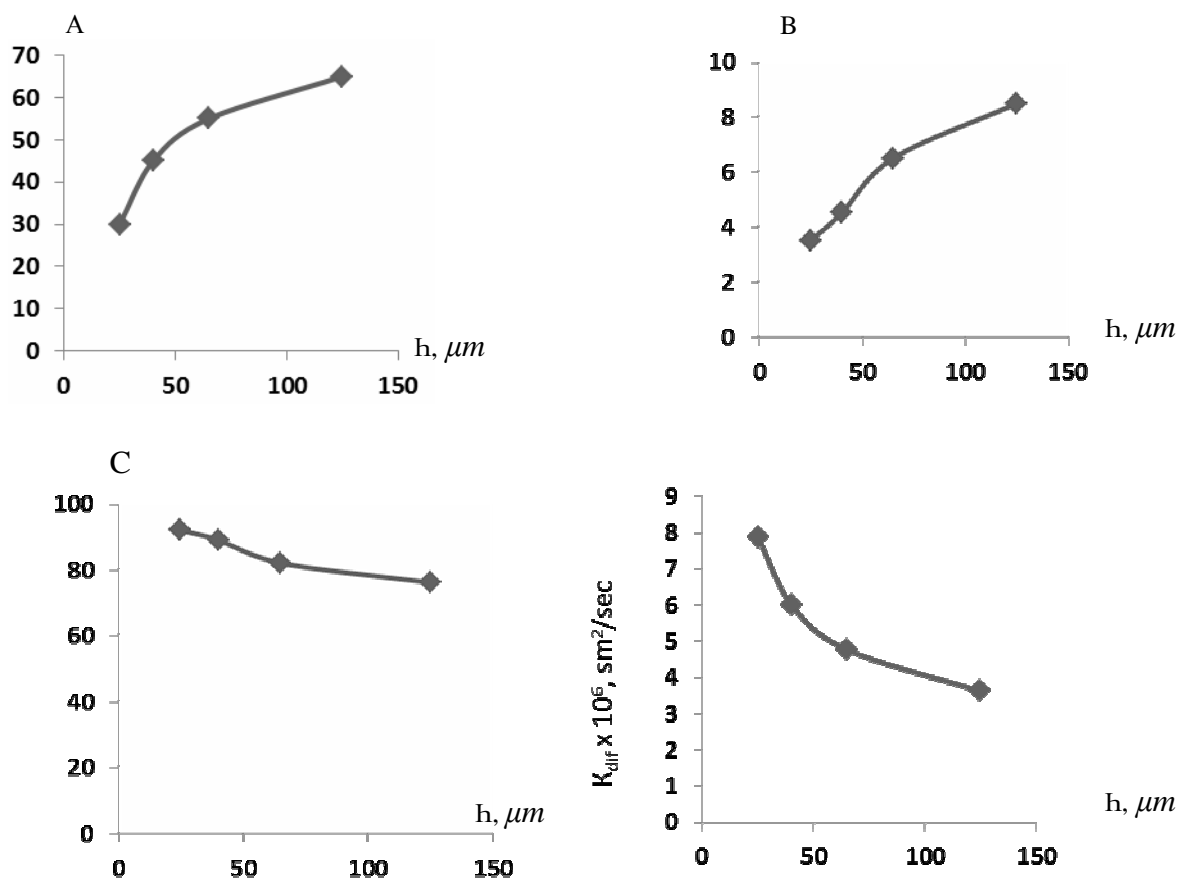


Figure 1. The parameters of cyclophosphamide release from microparticles of calcium alginate, covered with adsorbed layer of chitosane  $h$  - thickness of chitosane layer,  $\mu\text{m}$ ; A- time of an exit of 50 % of a preparation, min; B- time of the maximum exit of a preparation, hour; C- maximum exit, %

Thus, change of thickness of a chitosane membrane on hydrogel surfaces permit to operate by speed of release of medicine (cyclophosphamide) from hydrogel. It is perspective way of development of medicines of the prolonged action.

### References

1. Martinsen A., Storo I., Skjak-Braek G. Alginate as immobilized material: III. Diffusional properties // *Biotechnol. Bioeng.* 1992. Vol.36. P. 186-194.
2. Kulkarni A.R., Soppimath K.S., Aminabhavi T.M. Controlled release of diclofenac sodium from sodium alginate beads crosslinked with glutaraldehyde // *Pharmaceutica Acta Helvetiae.* 1999. Vol.74. P. 29-36.
3. Tonnesen H.H., Karlsen J. Alginate in Drug Delivery System // *Drug Dev. And Ind. Pharm.* 2002. Vol.28, №6. P. 621-630.
4. Batyrbekov Y., Rakhimbaeva D., Musabekov K., Zhubanov B. Alginate Nano- and Microparticles as Carriers of Anticancer Drug Cyclophosphane // *Abst.of 2010 MRS Springl Meeting.*—San Francisco, CA, USA, 2010.—Abst. PP 9.5.
5. Batyrbekov E., Rakhimbaeva D., Musabekov K., Zhubanov B., Luckham P. Modified Microcapsules of Calcium Alginate for Controlled release of Antitumor drug Cyclophosphamide // *Journal of Materials Science and Engineering.* 2010. Vol.4. №29. P. 47-53.

---

## REGULARITIES OF ELECTROLYTE DILUTE SOLUTIONS pH CORRECTION BY ELECTRODIALYSIS WITH BIPOLAR MEMBRANES

Stanislav Utin, Victor Zabolotsky, Konstantin Lebedev, Nikolay Sheldeshov,  
Polina Vasilenko

Kuban State University, Krasnodar, Russia, *E-mail: vizab@chem.kubsu.ru*

### Introduction

Among a wide spectrum of electrodialysis with bipolar membranes applications dilute solutions pH correction process takes considerable part in water treatment [1, 2], chemical [3, 4] and food industry [5-8]. pH correction process of dilute solutions is fundamentally differs from conversion of salt solutions to corresponding acids and bases. Low concentration of analyzed solutions and necessity's absence to get concentrated or pure acids and bases allow to simplify the technological schemes and reduce the demands for bipolar membranes selectivity. On the other side in dilute solutions of salts, the limiting current is attained on monopolar membranes, which leads to water dissociation starts, as it does on bipolar membranes. The current efficiency in the electrodialyzer depends not only on the electrochemical characteristics of bipolar membrane, but also on the properties of monopolar membranes in the electrodialyzer stack. Further real solutions contain considerable number of components taking part in chemical reactions with  $H^+$  and  $OH^-$  ions and experimental investigations and theoretical description of dilute solutions pH correction process is complicated.

### Experiments

The objects of investigation are alkali and acid electrodialysis chambers [9] formed by bipolar membranes MB-3 or asymmetric bipolar membranes<sup>1</sup> and anion-exchange membranes MA-40 or MA-41. Electrodialysis pH correction process was studied in different dilute solutions: sodium chloride solution, solution contained sodium bicarbonate and carbonic natural water after ion-exchange softening.

### Results and Discussion

In work [9] pH correction process of sodium chloride dilute solution ( $C=0,01$  mol/l) was studied. The regularity concerned with influence of anion-exchange membrane, forming investigated chambers together with bipolar membranes, on proton and hydroxyl ions current efficiencies was revealed. This influence is concluded in proton and hydroxyl ions current efficiencies decrease. The reason of such decrease was water dissociation on medium-basic anion-exchange membrane MA-40. On the basis of measurement of real hydroxyl transport number through anion-exchange membrane MA-40 and MA-41 by the method, described in [10] in different pH values it was established that in the area of a limiting current on membrane MA-40 the hydroxyl ions transport numbers equals approximately 0,1. Further growth of current and solution pH near membrane leads to hydroxyl ions transport numbers decreased. This indicates that water dissociation reaction on medium-basic anion-exchange membrane MA-40 is suppressed under high pH values. Such decrease of water dissociation rate is concerned with deprotonation of MA-40 tertiary amino groups at high pH values.

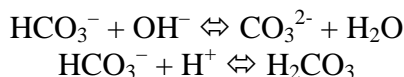
In contrast to electrodialysis of sodium chloride solution, where decrease of the ions concentration in alkali chamber is exactly equal to its increase in acid chamber, when flow rates through these chambers are identical, in case of bicarbonate solutions such equality is observed only for chloride ions which don't takes part in chemical reactions with products of water dissociation and for overall amount of ionic forms of carbonic acid in alkaline and acid chambers.

Chemical reactions between carbonate ions and water dissociation products provoke transformation from one form of carbonate to another and don't lead to change of carbon total amount ( $\Sigma C$ ), change of carbon sum in acid and alkali chambers is defined only by electromigration of carbonate and bicarbonate ions through anion-exchange membrane.

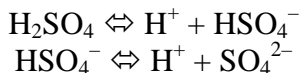
---

<sup>1</sup> The asymmetric bipolar membrane (MA-40+MF-4SC) was kindly supplied by S. Melnikov

Unbalance between diminution of bicarbonate ions concentration in alkali chamber and its increment in acid chamber (fig.1) is concerned with chemical reactions of bicarbonate ions with water dissociation products generated in bipolar membranes:



Mathematical model of natural waters pH correction process is complicated because it contains bicarbonate and sulfate ions. Presence of different sulfate forms depends on pH. In softened tap water with sulfate ions ( $\text{SO}_4^{2-}$ ) there can be hydrosulfate ions ( $\text{HSO}_4^-$ ) at  $\text{pH} < 4$ . In this case calculation of concentrations is carried out on basis of sulfuric acid dissociation reaction (on two steps):



Finally mathematical model describing process of softened tap water pH correction represents system of nonlinear equations which contains 15 equations with 15 variables relative to concentrations and ionic fluxes. The system is solved by means of Newton's modified method. Analysis of dependences of different carbonic acid ionic forms concentrations in outlets from alkali and acid chambers on current density (fig. 1) shows that experimental data of softened tap water pH correction are well described by models one of which takes account of water dissociation on anion-exchange membrane (continuous lines) and simplified model doesn't take account of water dissociation (dotted lines). Possibility this simplification is caused by presence of amino group deprotonation effect and water dissociation suppression at high pH values and also by buffer properties of bicarbonate solutions.

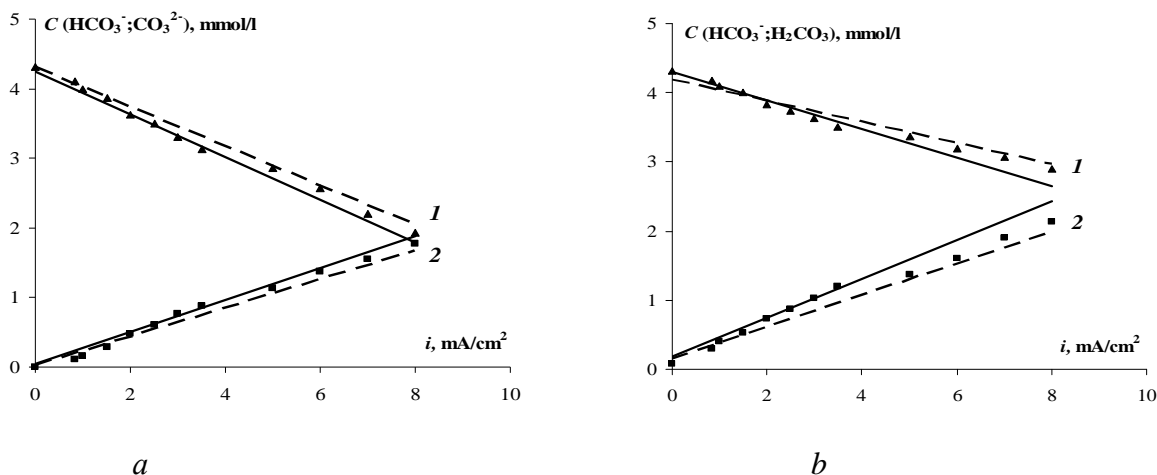


Figure 1. Dependence of ion concentrations in softening water on current density: a – bicarbonate ions (1) and carbonate ions (2) in alkaline chamber; b – bicarbonate ions (1) and carbonic acid (2) in acid chamber; Dots – experimental values, continuous lines – calculated values by the model with account of hydroxyl transport numbers through anion-exchange membrane, dotted lines – calculated values without account of hydroxyl transport numbers through anion-exchange membrane

It was established the general regularity during pH correction of dilute solutions confirming outdiffusion kinetic of ions transfer through monopolar membrane. In this case theoretical calculation of effective anion transport numbers can be carried out on the basis of ionic concentrations, charge numbers and diffusion coefficients in solution without of additional membrane characteristics and empirical coefficients.

This work was supported by RFBR grant № 11-01-96512-r\_yug\_c and № 11-03-96504-r\_yug\_c.

### References

1. Grabowski A., Zhang G., Strathmann H. and Eigenberger G. // Separation and Purification Technology. 2008. V. 60. P. 86

2. *Badruzzamana M., Oppenheimer J., Adhamb S., Kumarc M.* Innovative beneficial reuse of reverse osmosis concentrate using bipolar membrane electrodialysis and electrochlorination processes // *Journal of Membrane Science*. 2009. V. 326 P. 392
3. *Greben', V.P., Kozlova\_Markova, K.N., and Kornienko, I.I.* in *Elektrokhimiya ionitov*. Nauch. tr. Kuban. gos. univ. (Ionite Electrochemistry: Transactions of Kuban State University), Krasnodar, 1979, P. 45
4. *Yu LX, Guo QF, Hao JH, et al.* //Recovery of acetic acid from dilute wastewater by means of bipolar membrane electrodialysis. *Desalination* 2000. V. 129. P. 238
5. *Balster J., Pünt J. I., Stamatialis D.F., Lammers H., Verver A.B., Wessling M.* Electrochemical acidification of milk by whey desalination // *Journal of Membrane Science*. 2007. V. 303. P. 213
6. *Pourcelly G., Bazinet L.* Developments of bipolar membrane technology in food and bio-industry, in: *Handbook of Membrane Separation; Chemical, Pharmaceutical, Food, and Biotechnological Applicat N.-Y.:* CRC Press, Taylor & Francis Group. 2009. P. 581-633
7. *Bazinet L., Lamarche F., Ippersiel D.* Bipolar-membrane electrodialysis: applications of electrodialysis in the food industry // *Trends Food Sci. Technol.* 1998. V. 9. P. 107
8. *Bazinet L, Lamarche F, Labrecque R, Toupin R, Boulet M, Ippersiel D.* Electroacidification of soybean proteins for production of isolate // *Food Technology*. 1997. V. 51. P. 52
9. *Zabolotsky, V.I., Utin S.V., Sheldeshov N.V., Lebedev K.A., Vasilenko P.A.* *Elektrokhimiya*. 2011. V.47. №3. P. 343
10. *Zabolotsky, V.I., El'nikova, L.F., Shel'deshov, N.V., and Alekseev, A.V.,* *Elektrokhimiya*, 1987. V. 23, P.1626
11. *Lebedev K.A., Nikonenko V.V., Zabolotsky V.I., Gnusin N.P.* // *Electrohimiya*. 1986. V.22. №5. P. 638

---

# DEVELOPMENT AND EXPERIMENTAL TESTING OF SOFTWARE PACKAGE FOR DETERMINING THE SHARE OF ION-CONDUCTIVE SURFACE OF HETEROGENEOUS MEMBRANES BY DATA OF SCANNING ELECTRON MICROSCOPY

Vera Vasil'eva, Ekaterina Sirota, Elmara Akberova, Mikhail Malykhin, Natalya Kranina, Larisa Krasnorutskaya

Voronezh State University, Voronezh, Russia, *E-mail: viv155@mail.ru, atoris@list.ru*

Software package that realizes the methods of digital processing of electron microscope images of the surface of heterogeneous ion-exchange membranes was developed. For automated analysis of surface morphology with aim of numerical estimation of the area of active ion-conductive plots (phase of the ion exchanger) the possibility of using noise reduction techniques, methods of threshold image processing, gradient methods, methods of growing regions were considered. It was established that the highest accuracy of numerical estimation of the area of ion exchanger phase is reached when applying the method of growing areas, which allows to highlight steadily structural components of the membrane surface. The software package was tested on real samples of heterogeneous ion-exchange membranes of different nature and structure.

## Experiments

The software package is an application developed on Delphi programming language. The application provides automated analysis of surface morphology of ion-exchange membranes by means of a digital photo processing. The method of growing regions was used to estimate the relative share of ion exchanger on the membrane surface. Besides this, the software package includes an additional module of construction the histogram of surface conductive areas distribution over the effective radii.

The selected objects of research are heterogeneous cation-exchange membrane MK-40, which is based on strongly acidic exchanger KU-2, and cation-exchange membrane MK-41, containing a weakly acidic phosphate cation-exchanger KF-1 produced by OJSC "Shchekinoazot" (Shchekino city) in an industrial scale.

Microscopic investigations were carried out using scanning electron microscopy (SEM), microscope model JSM-6380 LV (Japan), with golden evaporation on dry samples.

Samples of membranes for the study were square plates sized  $(4 \times 5) \cdot 10^{-3}$  m. Microscopic analysis of the surface morphology was carried out for commercial, conditioned and membrane samples after the current-temperature influences.

## Results and Discussion

When processing the electron microscope images of the membrane surface, analysis and research methods of noise reduction, image processing and threshold gradient methods, method of growing regions there were carried out step by step.

At the stage of preliminary processing of SEM images with the purpose of noise reduction a median filter was applied. The main function of median filter is to replace pixel value different from the background with another one, closer to its neighbors. Isolated dark or light (compared to the surrounding background) clusters with an area of not bigger than  $n^2/2$  were removed (replaced by median values of the surroundings) by a median filter with mask size  $n \times n$  [1]. In the developed complex a median filter on a surrounding  $3 \times 3$ ,  $5 \times 5$ ,  $7 \times 7$  has been realized.

Detection of active surface areas (phase of ion exchanger) was made by analyzing the histogram of brightness. The threshold transformations are central to the practical problems of image segmentation by intuitively understood features and simplicity of realization [1, 2]. The simplest method of threshold processing is to separate the image histogram (a histogram of brightness) into two parts using a single global threshold. The result of global threshold processing and histogram are shown in Fig. 1. The success of this method depends entirely on how well the histogram succumbs to separation. Share of bright objects corresponding to the

phase of ion exchanger, for investigated image of the membrane surface of the MK-41 made up 6.2%.

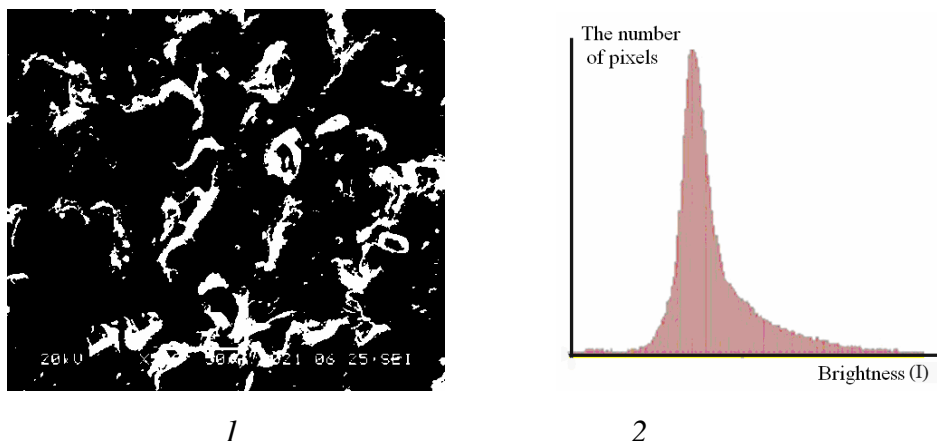


Figure 1. The result of global threshold processing (1) and a brightness histogram (2) of the image of MK-41 membrane surface

The distribution of outlet areas of ion-exchange grains on the surfaces has a complicated character, so for a more accurate estimation of the relative share of ion exchanger on the surface of the membrane, method of regions growing was realized. Growing of regions is a procedure that groups pixels or subregions into larger areas of predetermined criteria. The main approach is that at first, a set of points, playing the role of "crystallization centers", is taken and then areas are built up on them by accession to each center those pixels from number of neighbors, whose properties are close to the center of crystallization (for example, have the brightness or color in a certain range).

The primary task of using this method is to determine starting points for growing. In the problem under consideration the choice of starting points is carried out by the expert manually that almost eliminates the possibility of growing "false" areas in the case of automatic selection of "crystallization centers".

The result of applying the method of areas growing in the processing of SEM images of membrane surface is the image on which the phase of ion exchanger is painted in white, and the rest of the surface - in black background color. The approach implemented in the proposed program has a number of advantages compared with traditional methods because it allows to obtain on the image clear-cut contours and minimize the number of breaks at the phase boundaries. Table 1 shows the results on determining the proportion of ion-conductive membrane surface using the developed software package and professional program for working with photos Adobe Photoshop.

**Table 1. The share of the conductive surface of dry and swollen samples of ion-exchange membranes based on the results of processing of SEM images by different programs**

Image processing program	Membrane type			
	MK-40		MK-41	
	Dry	Swollen	Dry	Swollen
<b>Commercial</b>				
Adobe Photoshop	0,05±0,01		0,070±0,008	
Author program	0,039±0,005		0,048±0,008	
<b>After the conditioning</b>				
Adobe Photoshop	0,107±0,009	0,234±0,008	0,09±0,01	0,21±0,01
Author program	0,081±0,005	0,215±0,004	0,086±0,008	0,202±0,006
<b>After the current-temperature influences</b>				
Adobe Photoshop	0,14±0,02	0,27±0,02	0,19±0,02	0,29±0,02
Author program	0,112±0,006	0,237±0,008	0,151±0,005	0,259±0,006

The results on determining the share of conductive surface of the commercial samples in dry state showed that it is just 5-7%. The authors [3, 4] explained this effect by the extrusion of plastic polyethylene over the volume of heterogeneous membranes in the process of pressing and subsequent rolling (the effect of capsulation).

A divergence in estimating of the share quantity of ion-conductive surface, obtained by different methods of processing images was found. In this case coordination of results depends on the degree of development of the studied surface topography. Electron microphotos show that the heterogeneous membranes are characterized by clearly defined geometrically inhomogeneous surface with considerable roughness, in some cases, with defects and layering of structure, the presence of cracks and cavities. When receiving SEM images of the surface relief, additional mechanisms of formation of secondary slow electrons exist, contributing to the formation of a signal, which manifests itself in varying brightness of images depending on the angle of inclination of its various areas relative to the horizontal. As a result of "boundary effect", protruding on the surface phase not only of the ion exchanger, but also of polyethylene as a result its delamination and separation from the surface in places where the ion exchanger grain surface are characterized by high brightness. Therefore, in the case of a surface with a strongly developed relief, image contrasting and post-treatment using traditional methods gives higher value of share of ion-conductive surface.

### References

1. *Gonzalez R., Woods R.* Image Digital Processing. M.: Technosphaera, 2005. 1072 p. (in Russian)
2. *Furman Ya. I., Yuryev A.N., Yanshin V.V.* Digital processing techniques and identification of binary images. Krasnoyarsk: Krasnoyarsk Univ., 1992. P. 122-181. (in Russian)
3. *Greben V.P., Kovarsky N.Ya.* The influence of internal heat generation on the current-voltage characteristic of a bipolar membrane // *ZhFKh*. 1978. Vol.52, №92. P. 2304-2307. (in Russian)
4. *Zabolotsky V.I., Loza S.A., Sharafan M.V.* Physico-chemical properties of profiled heterogeneous ion-exchange // *Electrokhimia*. 2005. Vol. 41, № 10. P. 1185-1192. (in Russian)

---

# DIRECT OBSERVATION OF CONVECTIVE INSTABILITY IN ELECTROMEMBRANE SYSTEMS BY LASER INTERFEROMETRY

<sup>1</sup>Vera Vasil'eva, <sup>1</sup>Anna Zhiltsova, <sup>1</sup>Vladimir Shaposhnik, <sup>2</sup>Victor Zabolotsky,  
<sup>2</sup>Konstantin Lebedev, <sup>1</sup>Mikhail Malykhin

<sup>1</sup>Voronezh State University, Voronezh, Russia, *E-mail: viv155@mail.ru*

<sup>2</sup>Kuban State University, Krasnodar, Russia, *E-mail: lebedev@chem.kubsu.ru*

## Introduction

Solution of the problem of mass transfer intensification in the electromembrane systems is impossible without the investigations of the regularities of the ions transfer through membranes at the high and super-high values of the current density and searching for the new mechanisms of their supply to the interphase boundary of membrane-surface. Therefore, much attention is drawn towards making of the theoretical and experimental investigations of the over-limited state of a membrane. It should be noted that the elaboration of the general theory of over-limited state in the electromembrane system is restrained by the gap in the experimental investigations at the currents exceeding the limiting value. One of the reasons for these difficulties is a complex measuring technique for the thickness of diffusion layer and concentration field near the surface of membrane. Application of laser interferometry allowed visualization the process of formation and development of the diffusion layers in a solution near the surface of a ion-exchange membrane in a wide range of current densities.

## Experiments

In the present work we used a Zender-Mach interferometer which has certain advantages over other types of interferometers. Providing high contrast, it enables to study large objects and to localize the bands of equal thickness in an arbitrary plane. In order to calibrate an interferometer several standard solutions of the investigated substance were interferograms represent the concentration profiles of solutions and their scale should be determined by the calibration procedure. The experiments were made in the seven-compartment electro dialysis cell where compartments were separated by cation-exchange and anion-exchange membranes. Sodium chloride solution was supplied to the flow passage with the linear velocity thus corresponding to the laminar flow mode ( $Re < 5$ ). The experiment was performed at constant current intensities and the continuous feed of solutions.

Visualization of hydrodynamic pattern of the flow in this work was made as follows. Solutions of the investigated substances containing the particles of the aluminium powder or colophony in the suspension state were supplied into the cell compartment. The flow pattern was recorded using video camera with comparison beam of interferometer being shut. The flow rate in a certain local point was determined by the measurement the pass time of the particle for a certain pathway taking into account the preliminarily determined scale measure. Visualization of a hydrodynamic picture of interphase boundaries allows to define the characteristic size of the convective instability region arising at high-intensity regimes of an electro dialysis. The size of convective instability region  $d$  is defined as distance from a membrane surface on which a concentration profile has unstable, oscillatory character.

## Results and Discussion

Application of laser interferometry allowed visualization the membrane-solution interface allowed to reveal two stages in the development of convective instability. 1 stage: if the current exceeds the limiting diffusion current density within the range from one up to 3 times then the following facts are observed: stable vortices, oscillation stability of the concentrations profiles; the main transfer mechanism is migration and diffusion. 2 stage: for 3-4 fold exceeding of the limiting current value the following is characteristic: unstable vortices, turbulent pulsations of hydrodynamic flow rate towards the surface of membrane; concentration profiles loose their oscillation stability; transfer mechanism is convective one (i.e. transfer of a substance towards

membrane is performed due to pulsations of hydrodynamic flow rate that are normal to the surface of membrane).

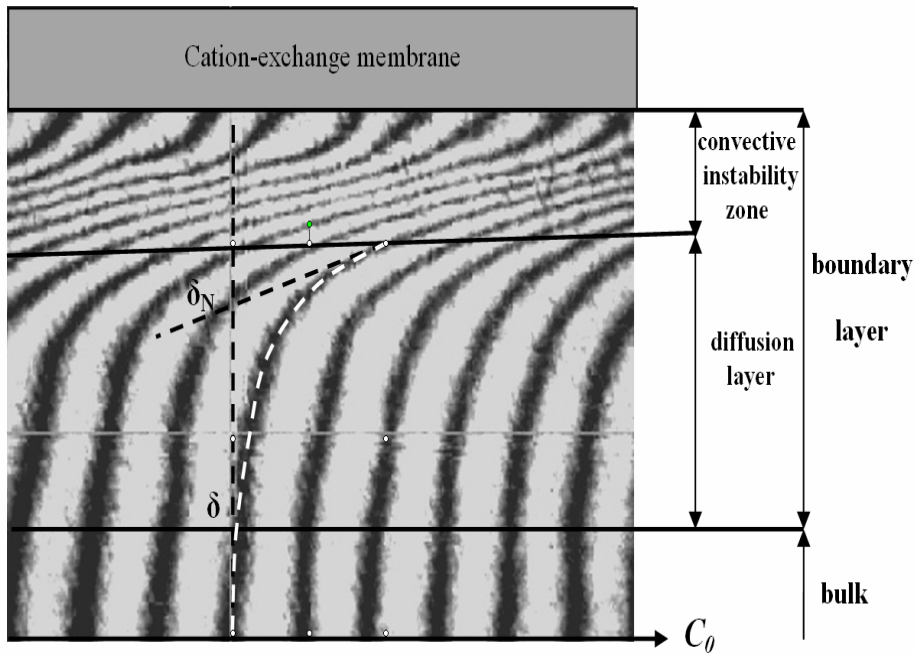


Figure 1. Structure of boundary layer near cation-exchange membrane in intensive current regime

The convection intermixing which appears spontaneously at the membrane-solution interphase destroys the diffusion boundary layer near ion-exchange membrane. The dimensions of the total diffusion layers  $\delta$  obtained by laser interferometry and linear Nernst approximations  $\delta_N$  obtained as the intersection of a tangent to the concentration profile drawn from interphase convective instability zone and stable diffusion layer to the straight line corresponding to the initial concentration are presented (fig. 1).

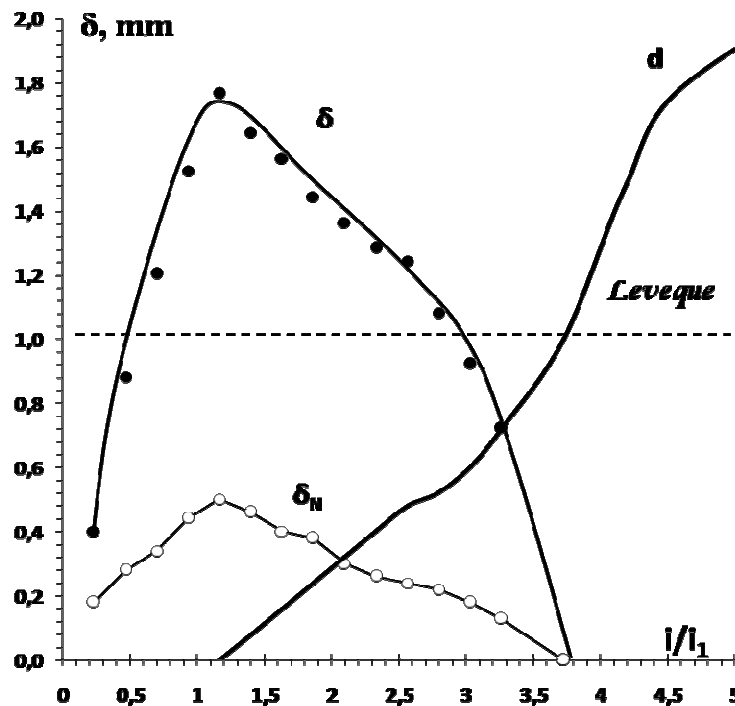


Figure 2. Total ( $\delta$ ), the Nernst ( $\delta_N$ ) thickness of the diffusion layer and the size of convective instability zone ( $d$ ) near cation-exchange membranes MK-40:  $C_0(\text{NaCl})=0.02\text{M}$ ,  $V=0.02\text{ cm/s}$ ,  $h=0.5\text{ cm}$ ; ---- the results of calculation by the Leveque equation [1]

Figure 2 presents experimentally obtained dependence of the total ( $\delta$ ), effective ( $\delta_N$ ) thickness of the diffusion boundary layer and the size of convective instability zone ( $d$ ) on the non-dimensional current density under stable stratification of electromembrane systems. At the current densities lower than the limiting current density  $i_l$  the value of the total diffusion layer  $\delta_{tot}$  increases significantly with  $i$ , while that of  $\delta_N$  increases more slightly. The increase in  $\delta_{tot}$  is explained by the fact that the expansion of concentration changes near the membrane is caused by the current flow through the membrane-solution interface. At  $i > i_{lim}$  the increase of the convection instability region of the solution in the vicinity of the membrane surface and the decrease of thicknesses of the diffusion layer with the uprising of the current density in an overlimiting region has been revealed experimentally. The obtained dependence proved to be unusual and makes the interpretation of the experimental results in accordance with common classical ideas when the thickness of diffusion layer is considered to be constant [1].

It is established that with reduction of solution flow supply rate and its concentration degree of concentration polarization at which there is a destruction of a diffusive boundary layer, decreases. Thus features of generation and development of convective instability in membranes of various type of ionogenic groups are caused by different speed of heterolytic reaction of water dissociation on each of membranes.

The study of hydrodynamic state in solution at the interphase boundary demonstrated that in the high-intensive current modes the values of the normal components of the flow rate for hydrodynamic pulsations supplying substance from the bulk of solution to the surface of membrane and intensifying mass transfer were comparable with supply flow rate of solution into membrane passage flow.

*The research was financially supported by Russian Foundation of Basic Researchers under the project №10-08-01060-a.*

#### References

1. Newman Y.S. eds., Electrochemical Systems, Prentice Hall, New York, 1973.

## COMPOSITE MICROCAPSULE IN A VISCOUS LIQUID

<sup>1</sup>Sergey Vasin, <sup>1</sup>Anatoly Filippov, <sup>2</sup>Tatiana Kharitonova

<sup>1</sup>Gubkin Russian State University of Oil and Gas, Moscow, Russia, *E-mails: s.vasin@rambler.ru,*

<sup>2</sup>Frumkin Institute of Physical Chemistry and Electrochemistry RAS, Moscow, Russia

The motion of capsules in the liquid flow is of great applied and theoretical interest. Capsules are used for the delivery of drugs and reagents; there are developments that involve the encapsulation of anticorrosive additives for paint and lacquer coatings. In all of these cases, the motion of the drop-shell system relative to the external flow takes place either at the stage of material production or in the course of the practical use of capsules.

Particles of different natures with a porous layer turned out to be a convenient element in the construction of the cell model of membrane systems and the rheological properties of concentrated colloidal dispersions. The problem of the flow around particles with porous shell and the filtration of viscous liquid in the porous medium with complex internal structure are closely interconnected.

In this work, we solved the problem of the flow around the capsule that contains the liquid, which cannot flow out of porous shell but is subjected to the action of viscous forces from the side of flowing liquid, i.e., the liquid carrier can penetrate into the porous medium of the capsule.

Let us consider the flow of liquid 3 (region 3), which is characterized by the preset velocity  $\tilde{U}$  at the infinity, around the spherical capsule with radius  $\tilde{a}$  that presents the drop of liquid 1 with radius  $\tilde{R}$  (region 1) coated by the porous layer with thickness  $\tilde{\delta}$  (region 2) (Fig. 1). It is assumed that liquid 3 penetrates into the porous layer and is not mixed with liquid 1.

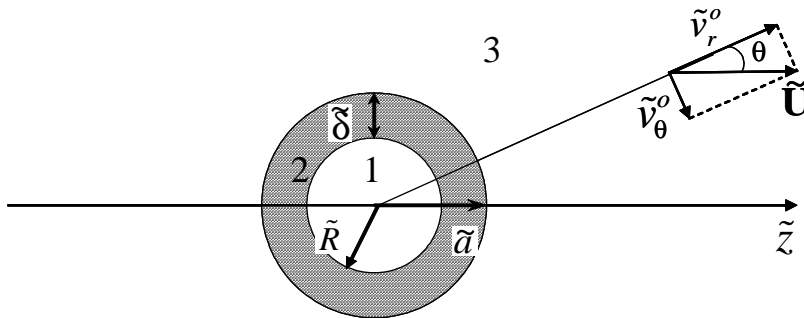


Figure 1. Schematic representation of spherical droplet coated with porous layer

At small Reynolds numbers, the motion of the liquid inside ( $0 < \tilde{r} < \tilde{R}$  - region 1) and outside ( $\tilde{a} < \tilde{r} < \infty$  - region 3) the capsule will be described by the Stokes and continuity equations as follows:

$$\left. \begin{aligned} \tilde{\nabla} \tilde{p}^{(i)} &= \tilde{\mu} \tilde{\Delta} \tilde{\mathbf{v}}^{(i)}, \\ \tilde{\nabla} \cdot \tilde{\mathbf{v}}^{(i)} &= 0. \end{aligned} \right\} (i=1,3) \quad (1)$$

The motion in the porous layer ( $\tilde{R} < \tilde{r} < \tilde{a}$  - region 2) will be determined by the Brinkman and continuity equations presented below:

$$\left. \begin{aligned} \tilde{\nabla} \tilde{p}^{(2)} &= \tilde{\mu}^{(2)} \tilde{\Delta} \tilde{\mathbf{v}}^{(2)} - \tilde{k} \tilde{\mathbf{v}}^{(2)}, \\ \tilde{\nabla} \cdot \tilde{\mathbf{v}}^{(2)} &= 0, \end{aligned} \right\} \quad (2)$$

where the tilde refers to dimensional values; superscript ( $i$ ) denotes the number of a region to which a value is relevant;  $\tilde{\mu}^{(i)}$  are the viscosity coefficients of the liquids and the Brinkman medium;  $\tilde{p}^{(i)}$  refers to pressures;  $\tilde{\mathbf{v}}^{(i)}$  refers to velocity vectors; and  $\tilde{k}$  is the Brinkman constant, which is inversely proportional to the specific permeability of the porous layer.

In order to formulate the boundary problem for Eqs. (1) and (2), we have to specify the boundary conditions.

Far from the capsule, we set the uniform flow as follows:

$$\tilde{\mathbf{v}}^{(3)} \rightarrow \tilde{\mathbf{U}}, \tilde{r} \rightarrow \infty. \quad (3)$$

At the liquid-porous layer external boundary ( $\tilde{r} = \tilde{a}$ ), the continuity conditions of velocity and normal stresses  $\tilde{\sigma}_{rr}$ , as well as of the jump of tangential stresses  $\tilde{\sigma}_{r\theta}$ , are set as follows [1, 2]:

$$\begin{aligned} \tilde{\mathbf{v}}^{(3)} &= \tilde{\mathbf{v}}^{(2)}, \\ \tilde{\sigma}_{rr}^{(3)} &= \tilde{\sigma}_{rr}^{(2)}, \\ \tilde{\sigma}_{r\theta}^{(3)} - \tilde{\sigma}_{r\theta}^{(2)} &= \beta \tilde{v}_\theta^{(3)} \sqrt{\tilde{k}_0 \tilde{\mu}^{(3)}}, \end{aligned} \quad (4)$$

where  $\beta$  is the parameter that characterizes the jump of tangential stresses and varies from 0 to 1 [2].

At the liquid-porous layer internal boundary ( $\tilde{r} = \tilde{R}$ ), the conditions of non-mixing of liquids are set; i.e., the equality of radial components of velocity to zero, the continuity of velocity tangential components, and the jump of tangential stresses  $\tilde{\sigma}_{r\theta}$  as follows:

$$\begin{aligned} v_r^{(1)} &= v_r^{(2)} = 0, \\ v_\theta^{(1)} &= v_\theta^{(2)}, \\ \tilde{\sigma}_{r\theta}^{(1)} - \tilde{\sigma}_{r\theta}^{(2)} &= -\beta v_\theta^{(1)} \sqrt{\tilde{k}_0 \tilde{\mu}^{(3)}}. \end{aligned} \quad (5)$$

The system of equations (1, 2) with boundary conditions (3)–(5) was solved analytically. Velocity and pressure distributions were determined.

An important characteristic of the problem under consideration is force  $\tilde{F}$  applied to the capsule by the external liquid:

$$\tilde{F} = \iint_S (\tilde{\sigma}_{rr} \cos \theta - \tilde{\sigma}_{r\theta} \sin \theta) ds, \quad (6)$$

where the integration is carried out over the surface of the porous layer.

Dimensionless force  $\Omega$  is determined by the ratio of force  $\tilde{F}$  to the Stokes force  $\tilde{F}_{st} = 6\pi \tilde{a} \tilde{\mu} \tilde{U}$ . Force  $\Omega(\delta, m, s_0, \beta)$  is a function of five arguments. Parameter  $\delta = \tilde{\delta} / \tilde{a}$  is the dimensionless porous layer thickness,  $m_1 = \tilde{\mu}^{(1)} / \tilde{\mu}^{(3)}$ ,  $m_2 = \tilde{\mu}^{(2)} / \tilde{\mu}^{(3)}$  are the viscosity ratios,  $s_0 = \tilde{a} / \sqrt{\tilde{\mu}^{(3)} / \tilde{k}}$  is the dimensionless Brinkman coefficient characterizing the drag of the porous medium, and parameter  $\beta$  characterizes the tangential stress jump at the porous medium-liquid interface.

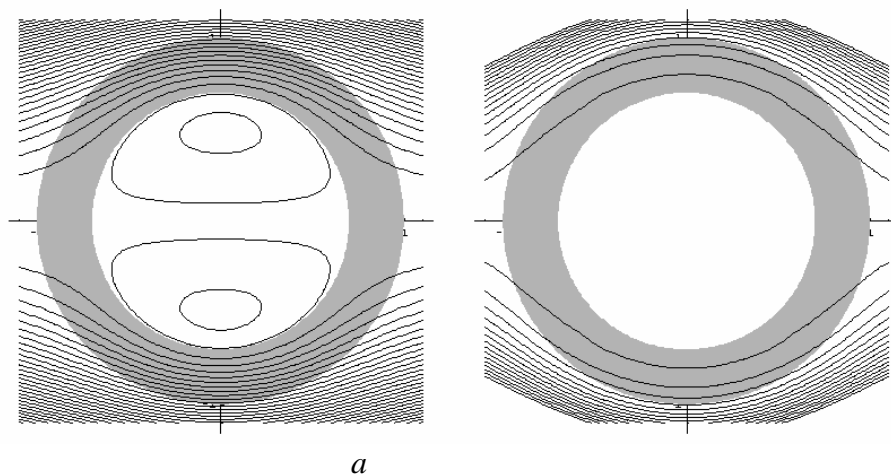


Figure 2. Flow lines at values of flow parameters  $\delta=0.3$ ,  $m_1=1.2$ ,  $m_2=0.9$ ,  $\beta=0.2$ ,  $s_0=0.5$  (2a), 10(2b)

Figure 2 shows the stream lines at different values of the flow parameters. At small dimensionless Brinkman parameter  $s_0 = 0.5$  (Fig. 2a), the porous medium weakly resists to the flow, liquid 3 penetrates throughout the porous medium and flows around the drop (region I).

Inside the drop, liquid 1 executes a circulatory motion by virtue of tangential stresses that arise on the surface (Fig. 2a). The resistance of porous medium rises with an increase in parameter  $s_0$  (Fig. 2b) and liquid 3 flows in the porous medium only in the layer whose thickness is approximately equal to the Brinkman radius  $\tilde{R}_b = \sqrt{\tilde{\mu}^{(3)} / \tilde{k}} < \tilde{\delta}$ . Outside the Brinkman layer, the flow in the porous medium nearly vanishes, tangential stresses at the boundary with drop are close to zero, and, as a result, liquid 1 rests inside the drop (Fig. 2b).

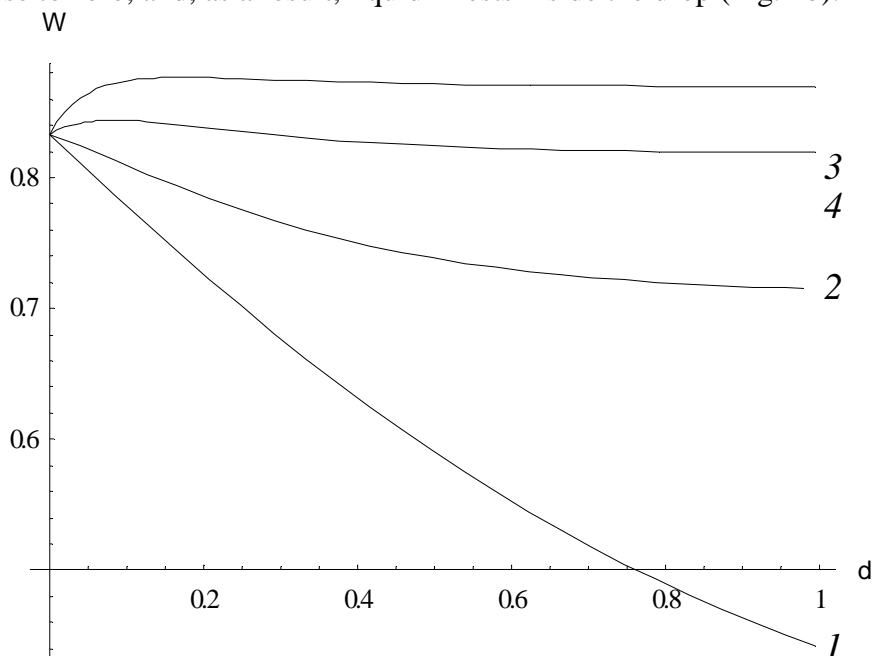


Figure 3. Dimensionless forces  $\Omega$  applied to (1–3) a capsule and (1'–3') a rigid particle coated with a porous layer as functions of parameter  $\delta$  at  $m = 1$ ,  $\beta = 0$ , and  $s_0 = (1, 1') 1, (2, 2') 3$ , and  $(3, 3') 5$

Dependences of the force ratio  $\Omega$  on the dimensionless thickness  $\delta$  of the porous layer at the various values of parameter  $s_0$  are shown in Fig. 3. All curves proceed outward from one point, since, at  $\delta = 0$ , we deal with a liquid drop and force  $\Omega$  can be calculated by Adamar-Rybchinski's formula. In our case,  $\Omega = 5/6$  at  $\delta = 0$  (see Fig. 3). With the enlargement of the porous layer, the force acting on the capsule behaves in differently depending on the value of parameter  $s_0$ , which characterizes the permeability of porous medium. The resistance of the porous layer and the pressure on the drop with radius  $R = 1 - \delta$  are the components of force  $\Omega$  acting on the capsule. The contribution of each component changes with the variations in parameter  $\delta$ . At small values of dimensionless Brinkman parameter  $s_0$  (curves 1 and 2), force  $\Omega$  decreases with an increase in the thickness of porous layer  $\delta$  due to the effect of filtration of liquid 3 through the porous medium. At larger values of parameter  $s_0$  (curves 3 and 4), a decrease in the drop radius due to increasing thickness of the porous layer at the initial stage leads to an increase in force  $\Omega$  to its maximal value. Further increase in thickness  $\delta$  results in a slight drop in force  $\Omega$ . At  $\delta \rightarrow 1$ , composite particle becomes absolutely porous and the force tends to its limiting value calculated by the formula derived in [3]. In our case of completely porous particle ( $\delta = 1$ ),  $\Omega = 0.441$ , 0.715, 0.819, and 0.87 at  $s_0 = 2, 4, 6$ , and 8, respectively (Fig. 3).

This work was supported by the Russian Foundation for Basic Research, project nos. 11-08-00807\_a and 12-08-92690-IND\_a.

### References

1. Ochoa-Tapia J.A., Whitaker S. // Int. J. Heat Mass Transfer. 1995. V. 38. P. 2635.
2. Ochoa-Tapia J.A., Whitaker S. // Int. J. Heat Mass Transfer. 1995. V. 38. P. 2647.
3. Vasin S.I., Filippov A.N. // Kolloidn. Zh. 2004. V. 66. P. 305.

# CAPACITIVE DEIONISATION OF WATER SOLUTIONS

<sup>1</sup>Yurii Volkovich, <sup>1</sup>Daniil Bograchev, <sup>1</sup>Alexey Mikhalin, <sup>1</sup>Alexey Rychagov,

<sup>2</sup>Daewook Park

<sup>1</sup>Frumkin Institute of Physical Chemistry and Electrochemistry of RAS, Moscow, Russia,

*E-mail: yuvolf40@mail.ru*

<sup>2</sup>Samsung Electronics Co., Ltd., Gyeonggi-do, Korea, *E-mail: daewook.park@samsung.com*

## Introduction

Capacitive deionization technology (CDT) is an effective new method of desalinating of brackish water [1, 2]. In CDT, a brackish water stream flows between pairs of high surface area carbon electrodes that are held at a potential difference  $\geq 1.2$  V. The ions and other charged particles are attracted to and held on the electrode of opposite charge. The negative electrode adsorbs cations, while the positive electrode adsorbs anions. Eventually the electrodes become saturated with ions and must be regenerated. The applied voltage is removed, and since takes place desorption of ions from electrodes and from the system, producing a more concentrated brine stream. In practice, for a gallon of water fed to the a CDT process, more than 80% emerges as fresh, deionized potable water, and the remainder is discharged as a concentrated brine solution containing virtually all of the salts in the feed. The main advantage of CDT is its low operating cost, which is about one third that of the main competitor, reverse osmosis. This is important because operating costs dominate the cost of desalination. Mechanism of the CDT operation is founded on charge - a discharge of electric double layer (EDL), as well as in electric double layer supercapacitor.

The purpose of this work was scientific research, development and verification of mathematic model of water capacitive deionization (CDI) process and also CDI regime optimization. Up present it is absent the adequate mathematical model of the process of CDI. On the other hand, they exist the models of electrochemical supercapacitors, in porous carbon electrodes which also take place the processes of ion electrosorption and electrodesorption ion. Processes of the ion transport along thickness of porous electrodes and separator are taken into account in these model as well as a process of charge-discharge of a EDL. However in these models also is not taken into account a hydrodynamic flow of water along external electrode surface. In CDI method the water flow is directed along of external of the surfaces of the electrodes, and so it is necessary to solve the two-dimensional problem: distribution of the processes both along, and across external of the surfaces of the electrodes and a porous spacer.

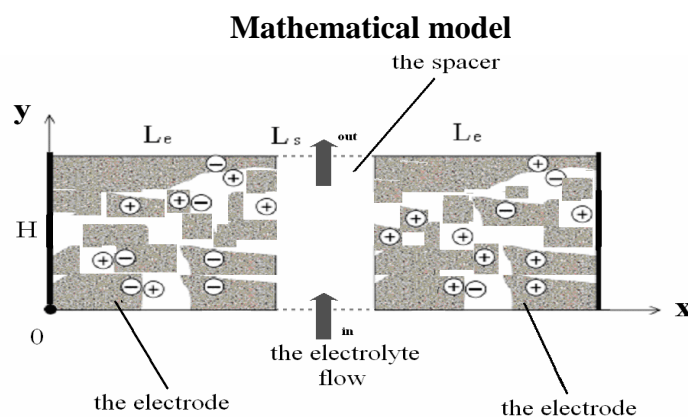


*Figure 1. Scheme of the functioning the dynamic cell*

As a result of our studies we have made a conclusion that process deionization of solution is very complex. In models we have taken into account following processes: charge- discharge of electric double layer (EDL); transport ion processes along of electrode and spacer thickness (x-direction) are diffusion and migration; transport ion process along of electrode external surface (y-direction): hydrodynamic flux; specific adsorption; characteristics of porous structures; characteristics of hydrophilic – hydrophobic properties; convective flux of electrolyte; surface

conductivity. The ion surface conductivity in EDL of carbon electrodes is longitudinal conductivity of EDL in high dispersed material. Our model has been based on the following assumptions: 1) The convective diffusion of electrolyte can be described by the average equations of mass-transfer based on dilute-solution theory in porous media. 2) The hydrodynamic velocity is precalculated, i.e. it can be treated as a given value. 3) The effective diffusion coefficients and effective electrolyte conductivities are calculated by the Arch's law. 4) The electrolyte can be presented as binary one with effective concentration in gram/mol dimension. 5) The full conductivity is sum of electrolyte conductivity as linear function of concentration and surface conductivity. 6) The diffusion can be neglected in all directions except x-direction along of electrode thickness. 7) The capacity of electrode is accepted as constant, i.e. it does not depend on potential. 8) In the equation of the potential, the derivative of potential in y directions can be neglected. 9) The porous electrode can be treated as having uniform potential; it means that the Ohm losses of the electrons can be neglected.

The equations for potential and concentration can be presented in the electrode region as follows:

$$C_s \frac{\partial \Phi - \Phi_c}{\partial t} = \frac{\partial}{\partial x} \left( k_E \frac{\partial \Phi}{\partial x} \right) + \frac{\partial}{\partial x} \left( k_E (t_+ - t_-) \frac{RT}{F} \frac{\partial \log c}{\partial x} \right) \quad (1)$$

$$\varepsilon_E \frac{\partial c}{\partial t} + v_y \frac{\partial c}{\partial y} = D_E \frac{\partial^2 c}{\partial x^2} - \frac{C_s}{F} A_E \frac{\partial \Phi - \Phi_c}{\partial t} - k_A c \quad (2)$$

where  $C_s$  - specific capacity,  $\Phi_c$  - potential of electrode,  $\Phi$  - potential of electrolyte,  $t_+$  and  $t_-$  are the cation and anion transfer numbers,  $\varepsilon_E$  - porosity in the electrodes,  $k_E = k_{E\lambda} c + k_{surf}$  - electrolyte conductivity in the electrodes,  $k_{E\lambda}$  - equivalent electrolyte conductivity in pores,  $k_{surf}$  - surface conductivity of electrode,  $D_E = D \varepsilon_E^n$  - effective diffusion coefficient in electrodes, (the exponent  $n$  is defined by property of porous media)  $k_A$  - specific adsorption coefficient,  $A_E = (t_+ \frac{dq_+}{dq} + t_- \frac{dq_-}{dq}) \approx \pm \frac{1}{2}$  - electric adsorption coefficient,  $v$  - vector of hydrodynamic velocity.

And the equations in the spacer region can be written:

$$\frac{\partial}{\partial x} \left( k_s \frac{\partial \Phi}{\partial x} \right) + \frac{\partial}{\partial x} \left( k_s \left( \frac{t_+ - t_-}{f} \right) \frac{\partial \log c}{\partial x} \right) = 0 \quad (3)$$

$$\varepsilon_s \frac{\partial c}{\partial t} + (v_x \frac{\partial c}{\partial x} + v_y \frac{\partial c}{\partial y}) = D_s \frac{\partial^2 c}{\partial x^2} \quad (4)$$

where  $\varepsilon_s$  - spacer porosity,  $k_s = k_{s\lambda} c$  - electrolyte conductivity in the spacer,  $k_{E\lambda}$  - reference electrolyte conductivity in spacer,  $D_s = D \varepsilon_s^n$  - effective diffusion coefficient in spacer. Porosimetric characteristics of electrodes and spacer were measured by the method of standard contact porosimetry [3].

### Surface conductivity

We at first have developed the method for measurement of surface conductivity for porous electrodes at controlled potentials. We have developed the two chamber five electrode electrochemical cell for this method (Fig. 2). Fig. 3 shows dependence conductivity on KCl concentration for carbon cloth electrode CH900 (made in Japan). This figures illustrates extrapolation obtaining of surface conductivity value. Extrapolation value of surface conductivity for solution concentration equal zero ( $C=0$ ) is defined by value of exchange capacity of its surface groups for a porous carbon electrode (Fig. 3).

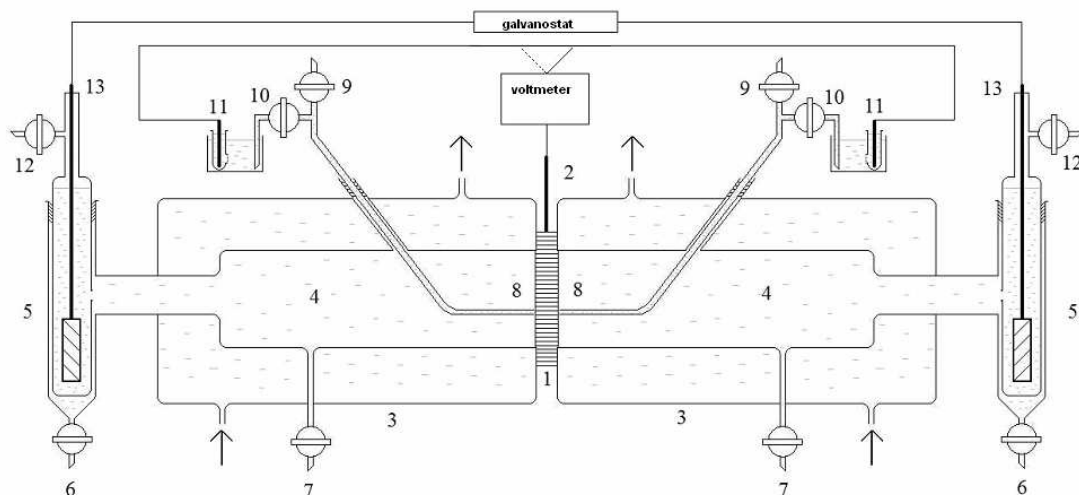


Figure 2. Electrochemical cell for measurement of surface conductivity: 1 – test electrode (carbon cloth), 2 – platinum current collector, 3- the chambers for a thermostating, 5 –two counter electrodes, 8 – two Luggin capillaries of reference electrodes 11 – two reference electrodes

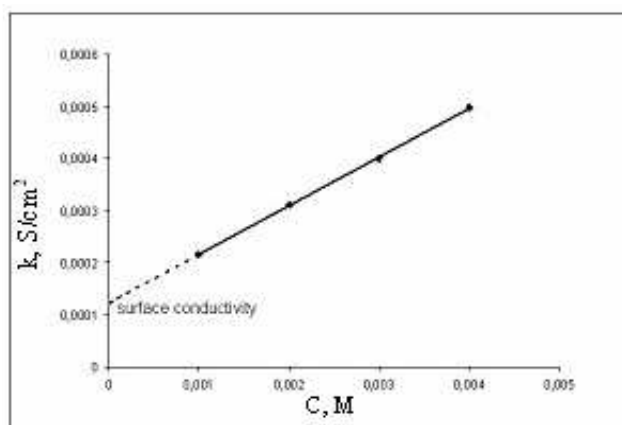


Figure 3. Dependence conductivity on KCl concentration for carbon cloth CH-900

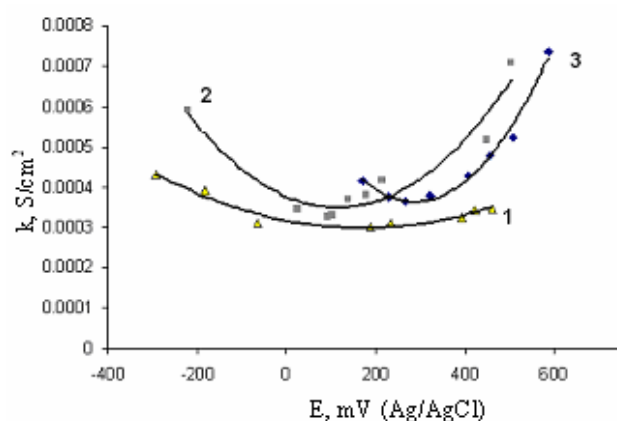


Figure 4. Dependences of surface conductivity of carbon cloth electrode conductivity on potential for different KCl concentrations: 1- 0.002 M, 2- 0.003 M, 3- 0.004 M

According to measurements the values of exchange capacity for carbon electrodes CH900 and SAIT (Korea) equals 1.14 and 0.37 mg-equiv/g accordingly. The values of surface conductivities are  $1.25 \times 10^{-4}$  and  $0.4 \times 10^{-4}$  S/cm<sup>2</sup> accordingly. Thus surface conductivity at  $C = 0$  is proportional to exchange capacity. This is surface conductivity caused by surface groups ( $k_{\text{surf group}}$ ). Fig 4 shows the measured dependences of surface conductivity of carbon cloth on potential for different KCl concentrations. In our opinion minima on these curves correspond to potentials of a zero charge. Total surface conductivity  $k_{\text{surf}}$  is sum of  $k_{\text{surf group}}$  and longitudinal conductivity of usual electrostatic EDL ( $k_{\text{electrostatic}}$ ). Thus method of measurement of surface conductivity is a new method for studying of a electrode double electric layer for porous electrodes.

The measured values of surface conductivity were used for calculations with the above described model. Fig. 5 demonstrates calculated dimensionless fluxes concentration in the outlet of the cell vs. time for adsorption and desorption stages, and Fig. 6 demonstrates corresponding concentration field.

### Verification of the model

We have carried out the capacitive deionization measurements by using the Samsung Electronics Co. (Korea) installation (Fig. 7). This installation contains: an electrochemical cell,

the pump for water pumping, conductometer, pH-meter, and the computer with the display. As electrodes in the cell were used activated carbon clothes CH900 with sizes 100x100x0.5 mm and with specific surface area 1500 m<sup>2</sup>/g.

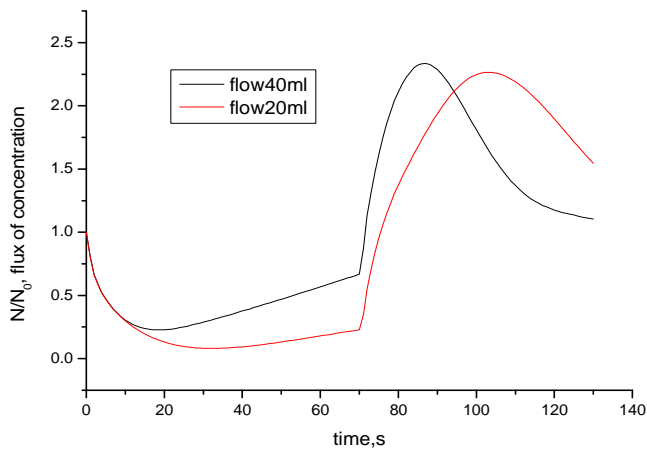


Figure 5. The dimensionless flux concentration in the outlet of the cell vs. time (20ml/min and 40ml/min) for adsorption and desorption stages

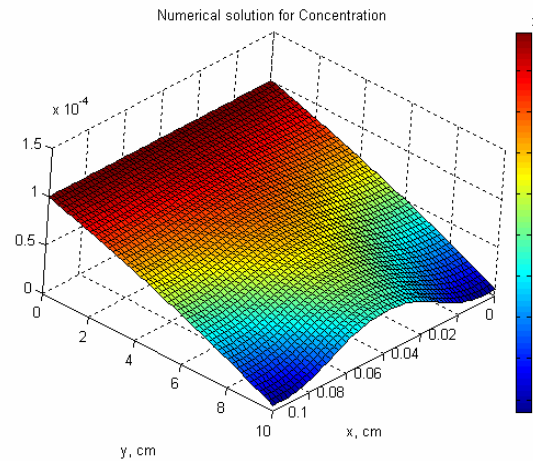


Figure 6. Concentration field;  $v=0.1$  cm/s,  $t=99$ s



Figure 7. Installation for capacitive deionization made by Samsung Electronics Co

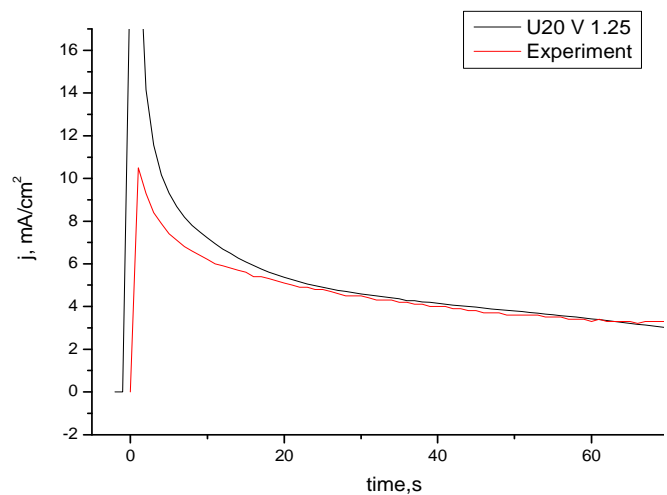


Figure 8. Experimental and modeling time-current dependences at flow rate 20ml/min and voltage 1.25V

The Fig.8 shows the satisfactory consent between calculated and experimental curves. Some differences model curve from experimental one for very small times are explained that we could not take into account the contact resistance between electrodes and current collectors. The satisfactory consent between calculated and experimental curves confirms a correctness of the developed mathematical model. Using model, we have calculated optimal regimes of adsorption and desorption stages for the minimization of energy consumption demanded for receiving of pure water.

### References

1. Anderson M.A., Cudero A.L., Palma. J. // *Electrochimica Acta*. 2010. V. 55. P. 3845.
2. Oren Y. // *Desalination*, 2008. V. 228. P. 10.
3. Volfkovich Yu.M., Bagotzky V.S. // *J. Power Sources*. 1994. V.48. P. 327-339.

# A NEW FAMILY OF ELECTROACTIVE POLYMER MATERIALS ON THE BASIS OF PORPHYRIN UNITS, WITH UNUSUAL ELECTRONIC AND OPTICAL PROPERTIES

<sup>1,2,3</sup>Mikhail Vorotyntsev, <sup>2,3</sup>Dmitriy Konev, <sup>2,3</sup>Ekaterina Zolotukhina, <sup>3</sup>Charles Devillers, <sup>4</sup>Igor Bezverkhyy, <sup>4</sup>Olivier Heintz

<sup>1</sup>Lomonosov Moscow State University, Moscow, Russia, *E-mail: mv@u-bourgogne.fr*

<sup>2</sup>Institute for Problems of Chemical Physics RAS, Chernogolovka, Russia, *E-mail: ks-chem@mail.ru*

<sup>3</sup>ICMUB-UMR 5260 CNRS, l'Université de Bourgogne, Dijon, France

<sup>4</sup>ICB-UMR 5209 CNRS, l'Université de Bourgogne, Dijon, France

## Introduction

Porphyrin molecules contain a conjugated macrocycle of 4 pyrrole rings linked via CH bridges, to which various substituent groups can be attached. Such substituted porphyrins demonstrated interesting properties in the areas of catalysis and electrocatalysis, sensors, non-linear optics, luminescence etc.

Numerous studies were devoted to incorporation of substituted porphyrins into a conducting-polymer matrix as counter-ions (porphyrins with attached negatively or positively charged groups) or owing to the polymer chain formation by a substituent (e.g. aniline). More recently the first examples of conducting *copolymers* with porphyrins and aromatic rings inside the principal chain were reported.

## Experiments

In our study we have synthesized for the first time representatives of a new family: conducting polymers based on an *unsubstituted* porphyrin ("*porphine*") as monomer unit. The deposition can be realized electrochemically with a stable growth of the conducting film. The properties of the resulting polymer depend crucially on the deposition potential, as demonstrated with the use of a set of experimental techniques (CV and chronoamperometry, in situ conductivity, optical microscopy, XPS, XRD, UV-visible spectroelectrochemistry, FTIR spectroscopy, MALDI-TOF).

## Results and Discussion

If the porphine oxidation is realized at a low potential the deposited polymer ("film of type I") consists of chains, with neighboring monomer units linked by a single bond in *meso*-positions. Its redox properties are conventional for conducting polymers (like polythiophene), with potential intervals for p- and n-doping (in which the polymer is electronically and ionically conducting) separated by an electro-inactivity range (in which the polymer is an insulator).

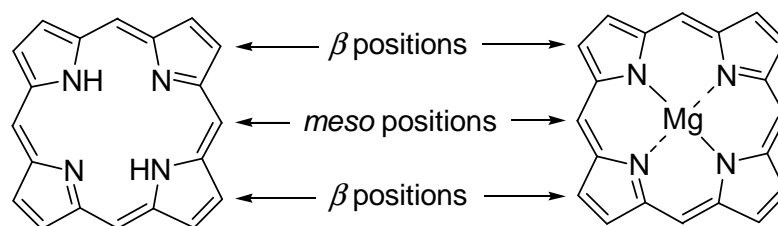


Figure 1. Structures of free-base porphine, magnesium (II) porphine, MgP

Electrochemical treatment of this polymer (or the oxidation of solute monomer) under a higher positive potential results in formation of quite a different material with very unusual properties ("film of type II"). In particular, it demonstrates an electroactivity *uniformly* distributed within an extremely broad potential interval (above 3 V), and the material retains its electronic conductivity within this whole potential range. It implies that the electronic delocalization occurs for a broad range of the polymer oxidation levels *including its neutral state* (for which conventional conducting polymers become insulating).

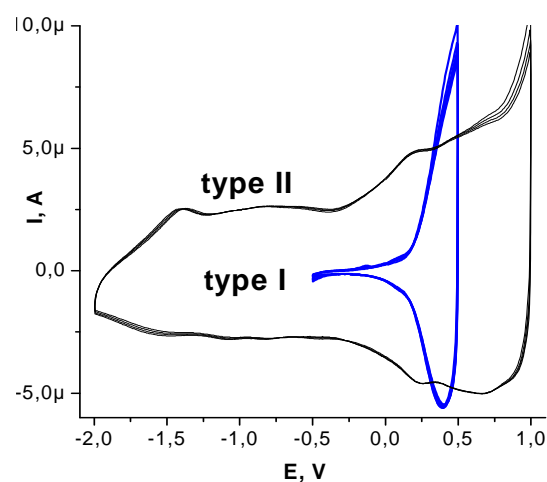


Figure 2. Cyclic voltammety response of film-coated electrodes in monomer-free solution: films of type I and of type II

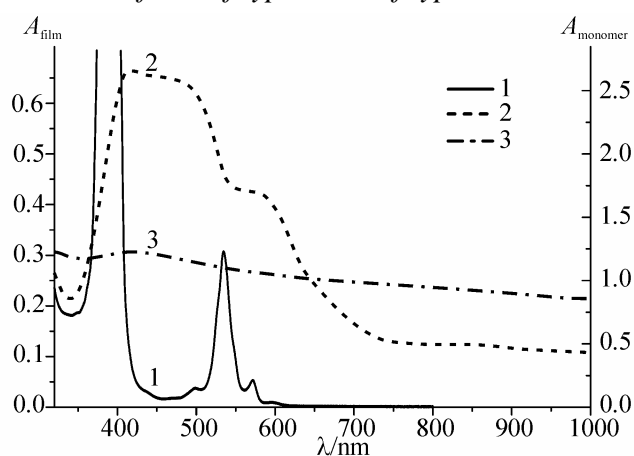


Figure 3. UV-visible spectra of (1) MgP monomer in solution; (2) film of type I; (3) film of type II (both films deposited at ITO electrode surface)

The spectral properties of the polymer in the UV, visible and IR ranges also change radically. This material with a zero width of the electrochemical band gap and particular optical properties is promising for various applications.

*Financial support of CNRS, Conseil Régional de Bourgogne, Université de Bourgogne and the Russian Foundation for Basic Research (project 12-03-01119-a) is acknowledged.*

---

# ONE-STEP CHEMICAL SYNTHESIS OF PD-POLYPYRROLE NANOCOMPOSITES AND THEIR APPLICATIONS IN ORGANIC CATALYSIS

<sup>1,2,3</sup>Mikhail Vorotyntsev, <sup>3</sup>Veronika Zinovyeva, <sup>2</sup>Ekaterina Zolotukhina, <sup>3</sup>Jean-Cyrille Hierso, <sup>4</sup>Igor Bezverkhy, <sup>4</sup>Olivier Heintz, <sup>1</sup>Tatiana Magdesieva, <sup>1</sup>Oleg Nikitin, <sup>1</sup>Oleg Levitsky

<sup>1</sup>Lomonosov Moscow State University, Moscow, Russia, *E-mail: mv@u-bourgogne.fr*

<sup>2</sup>Institute for Problems of Chemical Physics RAS, Chernogolovka, Russia, *E-mail: ks-chem@mail.ru*

<sup>3</sup>ICMUB-UMR 5260, Université de Bourgogne, Dijon, France

<sup>4</sup>ICB-UMR 5209, Université de Bourgogne, Dijon, France

## Introduction

Development of new nanocomposite materials with a dispersed transition metal component inside an electron-conducting polymer matrix attracts considerable attention in view of their advantageous properties which open prospects of their applications in various domains including catalysis and electrocatalysis. These polymers possess a developed porous system which allows reagents and products to exchange easily between pores and the solution in contact. Such systems are usually synthesized with the use of (micro)emulsions or/and surface-active components to stabilize pre-synthesized metal nanoparticles. As a result, the surface of the incorporated metal component inside the polymer remains covered by their layers which affect properties of these particles.

## Experiments, Results and Discussion

*Synthesis of metal-polymer composites.* The goal of our study was to elaborate a synthesis route which leads to the system where the aggregation of these metal particles is prevented solely by the polymer matrix. It was achieved via a one-step and one-pot non-template method based on a redox reaction between a conjugated monomer and a metal precursor, giving at once a conjugated polymer and metal particles [1].

This procedure has been successfully applied to prepare Pd/polypyrrole (Pd-PPy) composites via the reaction of palladium inorganic salts (acetate, Pd(OAc)<sub>2</sub>, or Pd(NH<sub>3</sub>)<sub>4</sub>Cl<sub>2</sub>) and the pyrrole monomer in acetonitrile (AN) or aqueous media [1, 2].

To ensure both an easy control of the reaction progress and the best quality of the resulting composite the process was performed in relatively dilute mixed monomer-precursor solutions (from the centimolar to millimolar range). In these conditions the colloidal solution generated owing to the redox reaction remains stable at the scale of many hours or even days, before sedimentation of particles. As a result, it was possible to trace properties of the mixed solution in situ by means of the UV-visible spectroscopy and the dynamic light scattering (DLS). Besides, the temporal evolution of this system was also studied by using portions of this solution to get SEM-EDX and TEM-EDS-SAED images of colloidal particles.

For all studied compositions of the mixed solution this DLS spectrum reveals a progressive diminution of the spectral band related to the Pd(II) component and the growth of absorption in the whole interval of wave lengths typical for colloid formation. According to well-matching data of DLS, SEM and TEM, the size of colloid particles changes with time from 20-30 nm in diameter to 100-250 nm (interrupted by sedimentation) depending on the initial solution composition, while at each moment the system is uniform, with a low dispersion of particle sizes (Fig. 1a). TEM images (Fig. 2) attribute these sizes to polymer globules which are semi-transparent for electrons, while each globule contains a great number of small non-transparent particles. Formation of PPy was confirmed by the IR spectroscopy. A low dispersion was also observed for sizes of dense inorganic nanoparticles. However, this parameter does not change in time or changes not strongly, in contrast to the growing size of PPy globules, while the number of such particles inside a globule increases proportionally to its volume. It implies that the redox reaction takes place near the external surface of each globule and that its products do not penetrate into the depth of the previously formed volume. The chemical composition of the composite determined by the XPS, HCNS and ICP-AES techniques shows the presence of the polymer (PPy) and palladium. XRD (Fig. 1b) reveals a very broad peak corresponding to

metallic palladium, its width matching well to the nanoparticle size for this composite given by TEM (about 2 nm). At the same time, XPS spectrum for Pd-PPy composites shows systematically a splitting of the palladium band, which corresponds to combination of Pd(0) and Pd(II), the ratio of their integral intensities correlating with the ratio of the numbers of surface and volume Pd atoms for this particle size (about 50% : 50%).

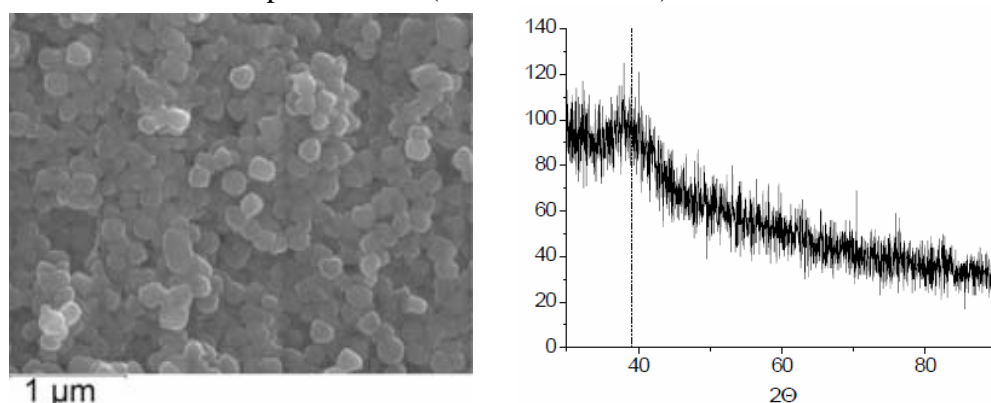


Figure 1. Pd-PPy composites: SEM (a, left), XRD (b, right)

Besides these common features of all studied systems, they demonstrate certain specific properties, in particular depending on the choice of the palladium precursor and the solvent.

The use of Pd(OAc)<sub>2</sub> in aqueous solution<sup>2</sup> results in formation of the composite as strongly aggregated spherical PPy globules (20-30 nm in diameter, Fig. 2a). Incorporated inorganic component consists of 2-3 nm particles giving large XRD peaks for both Pd(0) and PdO, the overall content of Pd being moderate (20-25 wt. %). If the synthesis is carried out in the presence of acetic acid (pH = 2-2.5) the content of Pd diminishes significantly to 7-14 wt. %, PdO is absent, the average size of metal particles increases to 6 nm.

Both Pd(OAc)<sub>2</sub> in AN [1] and Pd(NH<sub>3</sub>)<sub>4</sub>Cl<sub>2</sub> in water [2] results in well-dispersed spherical globules of the polymer. The size of inorganic nanoparticles for the former system is 2-3 nm while it may be diminished up to 1.2-1.4 nm for the ammonia complex of Pd (Fig. 2b). The total content of palladium is 30-35 and 32-45 wt. %, respectively.

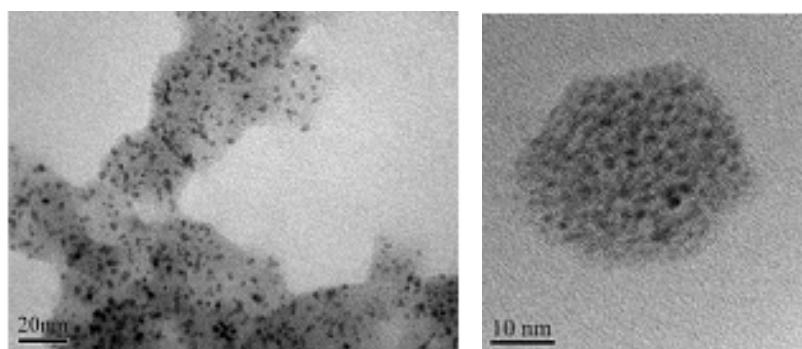
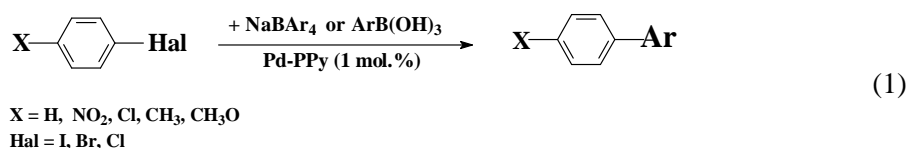


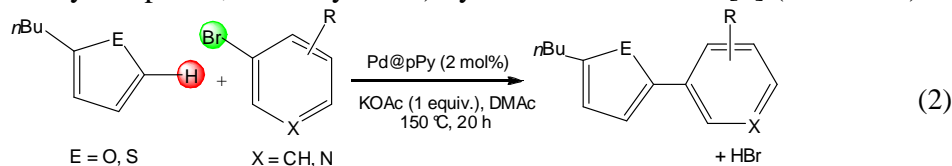
Figure 2. TEM images of Pd-PPy composites: Pd(OAc)<sub>2</sub> (a, left) or Pd(NH<sub>3</sub>)<sub>4</sub>Cl<sub>2</sub> (b, right) precursor in aqueous solution

*Catalytic tests.* Preliminary tests for application of Pd-PPy nanocomposite materials (obtained from Pd(NH<sub>3</sub>)<sub>4</sub>Cl<sub>2</sub> in water) have been carried out:

1) in catalysis of the cross-coupling Suzuki [3] (Scheme 1), Sonogashira and cyanation reactions:



2) as a ligand-free catalyst for the reaction of direct arylation of non-functionalized heteroaromatics (2-n-butylthiophene, 2-n-butylfuran) by various bromarenes [2] (Scheme 2).



For all these reactions our composite materials demonstrated advantageous catalytic properties. Especially interesting results have been found for formation of C-C bonds between two (hetero)aromatic molecules without their preliminary activation (Scheme 2) where the yield of the desirable product was very high (90-100% of the theoretical value) for a series of reactants with various functional groups.

### Acknowledgements

Support provided by the ‘Région Bourgogne’ (PARI SMT 8), CNRS, University of Burgundy and the Russian Foundation for Basic Research (project 12-03-00797-a) is gratefully acknowledged.

### References

1. Vasilyeva S. V., Vorotyntsev M. A., Bezverkhyy I., Lesniewska E., Heintz O., Chassagnon R. // *J. Phys. Chem. C*. 2008. V. 112. P. 19878.
2. Zinovyeva V. A., Vorotyntsev M. A., Bezverkhyy I., Chaumont D., Hierso J-C. // *Adv. Funct. Mater.* 2011. V. 21. P. 1064.
3. Magdesieva T. V., Nikitin O. M., Levitsky O. A., Zinovyeva V. A., Bezverkhyy I., Zolotukhina E. V., Vorotyntsev M. A. // *J. Mol. Catal. A: Chem.* 2011. V. 353-354. P. 50-57.

# POTENTIOMETRIC DETERMINATION OF ANIONS BY USING OF THE PERFLUORINATED SULFOCATION-EXCHANGE MEMBRANES MODIFIED WITH ZIRCONIA

<sup>1</sup>Kristina Yankina, <sup>1</sup>Olga Bobreshova, <sup>1</sup>Anna Parshina, <sup>2</sup>Ekaterina Safronova,

<sup>2</sup>Andrey Yaroslavtsev

<sup>1</sup>Voronezh State University, Voronezh, Russia, *E-mail: olga1@box.vsi.ru*

<sup>2</sup>Kurnakov Institute of General and Inorganic Chemistry of RAS, Moscow, Russia

## Introduction

In [1] we have suggested to use potentiometric sensors, analytical signal of which is the Donnan potential (PD-sensors) at the ion-exchange membrane/electrolyte solution interface, for the determination of some bioactive substances in polyionic solutions. But using of them to analysis of organic and sulfur anions is ineffective. The aim of this paper was to investigate the possibility of use perfluorinated sulfocation-exchange membranes MF-4SC, doped with zirconia, as electrodoactive material of potentiometric sensors, analytical signal of which is the Donnan potential, which are sensitive to anions of amino acid glycine, cysteine in polyionic aqueous solutions.

## Experiments

The aqueous solutions of amino acid glycine (Gly), cysteine (Cys) and potassium hydroxide (KOH) were investigated for estimation of the possibility of organic and sulfurous anions determination in polyionic aqueous solutions by MF-4SC-based PD-sensors. The ionic composition of solutions Gly+KOH is presented by anions Gly<sup>-</sup>, OH<sup>-</sup>, cations K<sup>+</sup> and zwitter-ions Gly<sup>±</sup> (pH ranged from 10.70±0.05 to 14.30±0.05). The ionic composition of solutions Cys+KOH is presented by anions CH<sub>3</sub>COCOO<sup>-</sup>, HS<sup>-</sup>, OH<sup>-</sup> and cations K<sup>+</sup>, NH<sub>4</sub><sup>+</sup> (pH ranged from 8.22±0.05 to 10.50±0.05). Analytical concentrations of the various components in individual and polyionic solutions ranged from 1.0·10<sup>-4</sup> to 5.0·10<sup>-2</sup> M.

Initial and doped with zirconia membranes MF-4SC were used as an active materials in PD-sensors. Modified membranes MF-4SC were obtained via two methods described in [2].

## Results and discussion

The calibration models (1) that did take into account the interference of three factors were utilised. These three factors are 1) pH; 2) negative decimal logarithm of analytical concentrations of cations (pC<sub>+</sub>); 3) negative decimal logarithm of analytical concentrations of anions Gly<sup>-</sup> and zwitter-ions Gly<sup>±</sup> in solutions Gly+KOH; negative decimal logarithm of analytical concentrations of anions CH<sub>3</sub>COCOO<sup>-</sup> and HS<sup>-</sup> in solutions Cys+KOH (pC<sub>-</sub>):

$$\Delta\varphi_D = b_0 + b_1 \cdot pC_- + b_2 \cdot pC_+ + b_3 \cdot pH, \quad (1)$$

where  $\Delta\varphi_D$  is analytical signal of PD-sensor (mV); C<sub>-</sub> is total concentration of anions (M); C<sub>+</sub> is total concentration of cations (M); b<sub>0</sub> is free term of calibration equations (mV); b<sub>1</sub>, b<sub>2</sub>, b<sub>3</sub> are coefficients of calibration equations (mV/pC), which are characteristics of sensitivity of PD-sensor to corresponding ions.

Analysis of characteristics of unmodified and of uniform distribution modified MF-4SC-based PD-sensors showed that insignificant influence of counter-ions nature on the value and sensitivity of sensors response is observed for all MF-4SC samples.

The use of membrane MF-4SC with gradient ZrO<sub>2</sub> distribution for PD-sensor organization leads to significant contribution of anions into analytical signal of sensor is observed for two party samples. Figure 1 demonstrates coefficients of calibration equations of gradient modified MF-4SC-based PD sensors in aqueous solutions Gly+KOH, Cys+KOH.

The difference in electrochemical behavior of unmodified and modified with ZrO<sub>2</sub> MF-4SC samples depends on next factors. Firstly, ZrO<sub>2</sub> incorporation into membrane matrix leads to the decrease of available cation-exchange groups due to their partial blocking in the membrane pores. Secondly, ZrO<sub>2</sub> particles in modified membranes demonstrate both cation- and anion-exchange properties [3].

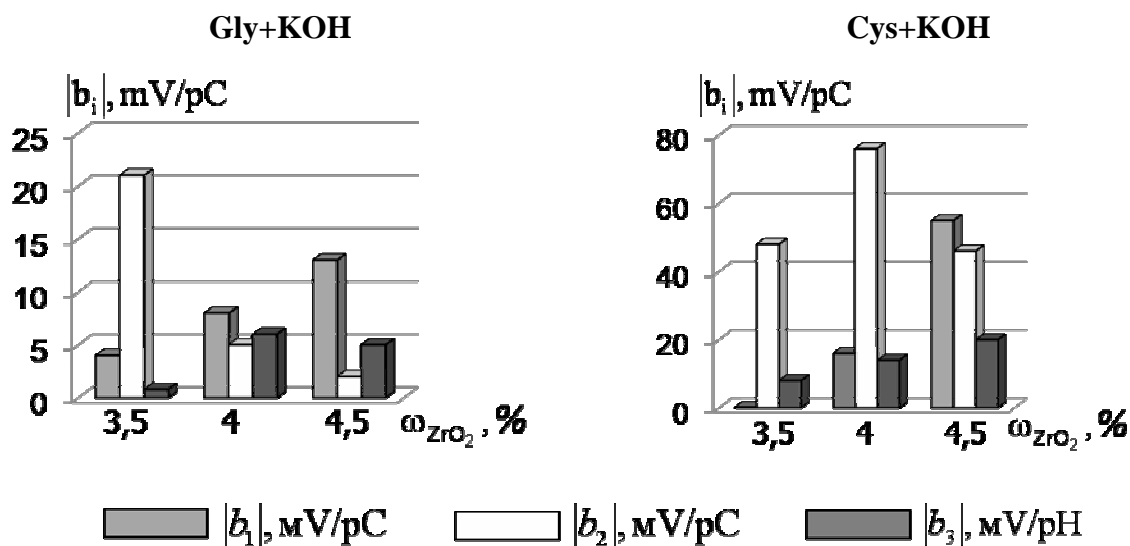


Figure 1. Coefficients of calibration equations of gradient modified MF-4SC-based PD sensors in aqueous solutions Gly+KOH, Cys+KOH

So co-ions concentration near interface modified MF-4SC/ electrolyte solution increases in comparison with initial MF-4SC. This allows to increase sensitivity of gradient modified MF-4SC-based PD-sensors to co-ions in aqueous solutions. The influence of co-ions nature on the response of uniform distribution modified MF-4SC-based PD-sensors is insignificant. The reason of this is that co-ions concentration gradients on the interfaces MF-4SC/ solution and MF-4SC/reference solution are oppositely directed and compensate each other.

Obtained results evidences of the possibility of use modified  $K^+$ -type MF-4SC samples with gradient on the length  $ZrO_2$  distribution as electrodoactive material in PD-sensors, which are sensitive to organic anions in aqueous solutions.

#### Acknowledgements

This work was financially supported by the RFBR (projects 12-08-00743-a and 11-08-93105), «P.Y.S.I.C.»: Fund of assistance to development of small forms of the enterprises in scientific and technical sphere (research projects 9591p/14212, 01.08.2011, № 8080p/14016 or 30.04.2011).

#### References

1. Bobreshova O.V., Parshina A.V., Agupova M.V., Timofeev S.V. RF Patent 2376591, 2009, Byull. izobret., 2009, no. 35, 6 p.
2. Voropaeva E.Yu., Stenina I.A., Yaroslavtsev A.B. // Zhurnal neorganicheskoi khimii. 2008. V.53. P.1677. (Russ. J. Inorg. Chem., 2008, 53, 1797).
3. Amphlett C.B. Inorganic Ion Exchangers. Elsevier Publ. Comp. Amsterdam-London-New York. 1964.

---

# HIBRID MEMBRANE MATERIALS: PROPERTIES AND PERSPECTIVES OF APPLICATION

<sup>1,2</sup>Andrei Yaroslavtsev

<sup>1</sup>Kurnakov Institute of General and Inorganic Chemistry RAS, Moscow, Russia;

*E-mail: yaroslav@igic.ras.ru*

<sup>2</sup>Topchiev Institute of Petrochemical Synthesis. RAS, Moscow, Russia

Hybrid ion-exchange membranes have become one of the most popular objects of research in recent decades, primarily due to the prospects of their use in fuel cells. Membrane modification can lead to a substantial change in their proton conductivity, permeability, strength, thermal stability and some other parameters. Recently, we have proposed a model according to which the dopant introduction into membrane pores leads to pores and channels expansion and conductivity increase [1]. In this report the dependences of some transport and mechanical properties of ion-exchange membrane on the dopant particles size, its concentration and on the dopant nature are considered. Particular attention is given to the possibility of varying the membrane properties due to changes in the surface of the dopant particles.

## 1. Selectivity of the transport processes

One of the most important properties of the membranes is their selectivity. The selectivity of ion-exchange membranes is determined by the transfer number or by the ratio of the conductivity and permeability of some neutral molecules of gases or liquids. The last one is especially important for hydrogen energetics applications [2]. The decrease in the permeability to gases or methanol is considered as an important advantage of the hybrid perfluorinated membranes containing silica first of all. Low methanol permeability, and the possibility of operating temperature increase makes these membranes extremely effective for the use in direct methanol fuel cells.

The distribution of ions concentration in ion-exchange membranes is nonuniform. This is determined by the negative charge on the pore walls due to the fixed ions presence. Because of this, a typical electric double layer is formed in the pores and the majority of the counterions are arranged in the thin Debye layer with a width of about 1 nm. In contrast, anions and molecules, destroying the strong hydrogen bonds system are excluded from it. Electrically neutral solution is localized in the pore center. Hydrophilic dopant nanoparticles displace "free" solution out of the membrane pores, without affecting the thin Debye layer, localized near the walls. Therefore, the counterions transfer rate remains the same or even increases, while the rate of anions and neutral molecules transport (hydrogen and alcohols) is significantly reduced.

## 2. The influence of the dopant nature

Previously described model of the limited elasticity of the membrane pores walls takes into consideration only the geometric factors. At the same time the dopant nature can change the membranes water uptake (hydrophilic, hydrophobic) and carrier concentration (different protonaccepting ability). Both of these factors significantly affect the value of conductivity.

Silica is a classic example of nanoparticles with a hydrophilic surface. The influence of the first factor is in the center of the most authors' attention, using SiO<sub>2</sub> nanoparticles as dopant for the cation-exchange membranes. Nafion perfluorinated membranes or polyether(ether)ketone modification by other oxide systems or acidic zirconium phosphate additives gives the similar result. This can increase the water uptake and allows to use membranes at elevated temperatures. In contrast, membrane doping by hydrophobic particles (carbon, silicon carbide, metals) decrease membrane water uptake.

Effect of carrier concentration is more significant. Proton transfer occurs in the membranes by means of interstitial mechanism (due to proton hopping from one water molecule to another).

Incorporation of silica nanoparticles obtained in an acidic solution, allows to get a higher conductivity in comparison with the similar particles obtained in an alkaline medium. It is possible to increase the dopant acidity by means of strong acids addition. This is achieved, for

example, by sulfonation of the particle surface or by heteropolyacids addition. Such membranes have shown good results in fuel cells due to their high proton conductivity and low methanol permeability [2]. This modification provides a double effect. On the one hand, it leads to an increase in the current carriers' number, whose concentration is proportional to the current. On the other hand, the moisture content of the membranes is primarily determined by the osmotic pressure, which is determined by the amount of dissociated acid groups in its matrix. Therefore, this modification will be accompanied by an increase of water uptake. The increase in the dopant surface acidity can increase the effect of the modification, even for hydrophobic particles, such as single-wall carbon nanotubes.

The opposite example is a particles containing fragments capable of functional groups binding (amines, polyaniline). In this case, the dopants are not hydrophobic, but the basic nitrogen-containing groups strongly bind protons and form strong hydrogen bonds with  $-\text{SO}_3\text{H}$  groups. This leads to a sharp decrease in the carriers concentration, simultaneously reducing the membranes hydrophilicity and its water uptake.

### **3. Ion conductivity at low humidity**

High proton conductivity at low humidity can be mentioned as one of the main advantages of hybrid membranes [2]. This ensures successful fuel cells operation at low humidity. Part of the pore volume in the hybrid membranes is occupied by dopant particles. This prevents a sharp pore contraction. As a consequence, a higher channel size is also typical for hybrid membranes. On the other hand, the narrow sites are formed inside the pores, which limit proton transfer by Grothguss mechanism.

At high humidity proton transfer occurs between closely spaced water molecules, having the same protonaccepting affinity. Functional groups are localized on the membrane pore walls and are characterized by low affinity. They are almost excluded from the proton transfer. At the same time, a direct proton transfer between  $\text{H}_5\text{O}_2^+$  ions is virtually impossible because of the high enthalpy of the proton transfer reaction. The high distance between these groups at low humidity is of great importance. This increases the role of the pore walls surface in the transfer process. As soon as  $-\text{SO}_3^-$  groups have smaller protonaccepting ability, the transfer between them and the water molecules is difficult and has large activation energy. So hybrid membranes have a great advantage, because their pores contain a number of additional oxygen-containing groups, which are also able to participate in the proton transfer process. Their presence results in a significant decrease in the length of the proton jump. This factor is most likely a major contributor to the increase in the conductivity of hybrid membranes at low humidity. The use of nanoparticles whose surface has a pronounced acid function gave the great advantage. An excellent example of such systems is membrane doped with  $\text{SiO}_2$  nanoparticles and heteropolyacids. Proton conductivity of such membranes at low humidity is of several orders higher in comparison with the original membrane conductivity [3].

### **4. Mechanical properties of hybrid membranes**

Improved mechanical properties of hybrid membranes are often postulated as one of their main advantages. However, in the most cases membranes modification leads to a completely opposite effect. The strength of the overwhelming number of solids is by several orders lower than theoretically calculated one. This is determined by the presence of extended defects (nanoscale cracks) in their structure. The larger the crack, the smaller the load, at which its growth takes place and the lower is the mechanical strength of the material as a whole. Pores in membranes play the role of the cracks. The higher concentration of dopant, the larger the pore size and the more significant became the decrease in the membrane strength. The pore walls are deformed by the osmotic pressure. The osmotic pressure is not enough to compensate the forces of the elastic strain for a large size of nanoparticles and the membranes water uptake markedly reduced. This increases the concentration of protons in the pore solution and, consequently, the osmotic pressure which tends to break the membrane. The combination of these factors leads to a decrease in the membrane strength with the increase of the dopant particle size.

Hardening of the membranes occurs in the case of the extended one-dimensional nanoparticles introduction with a high strength (carbon nanotubes). The most likely place for the hydrophobic particles localization is membrane matrix. Therefore, carbon nanotubes are analogous to a reinforcing material for the membrane matrix. The introduction of a small number of single-walled carbon nanotubes in the membrane led to an increase in their elastic modulus and strain at break [4].

All this determines the possibility of wide area of practical application of the hybrid membranes. At present time, these membranes are widely used for the construction of fuel cells. In addition, increasing the selectivity of the transport processes determine the possibility of their effective use in water treatment processes [5] and for sensor electrodes construction [6].

### References

1. *Novikova S.A., Safronova E.Yu., Lysova A.A., Yaroslavtsev A.B.* Influence of incorporated nanoparticles on ion conductivity of MF-4SC membrane // *Mendeleev Commun.*, 2010, V.20, N3 P.156-157.
2. *Yaroslavtsev A.B., Dobrowolski Yu.A., Shaglaeva N.S., Frolova L.A., Gerasimova E., Sanginov E.A.* Nanomaterials for low temperature fuel cells. // *Rus.Chem.Rev.* 2012. V.81. № 3. P.191-220.
3. *Safronova E.Yu., Stenina I.A., Yaroslavtsev A.B.* Synthesis and study of hybrid membranes MF-4SK-SiO<sub>2</sub>, modified by phosphotungstic heteropolyacid. // *Rus.J.Inorgan.chem.* 2010, V.55. №1. P.6-20.
4. *Perepelkina A.I., Safronova E.Yu., Shalimov A.S., Yaroslavtsev A.B.* Hybrid materials based on membranes MF-4SC modified by silicon carbide and carbon nanotubes. // *Membranes and Membrane Technology* 2012, V.2 , №1. P. 27-32.
5. *Zabolotsky V.I., Protacov K.V., Sharafan M.V., Yaroslavtsev A.B.* A method of modified ion-exchange membrane production. *Rus.patent № 2010150228/05 (072502)* from 07.12.2010.
6. *Bobreshova O.V., Parshina A.V., Polumestnaya K.A., Safronova E.Yu., Yankina K.Yu., Yaroslavtsev A.B.* Perfluorinated sulfocation-exchange membranes modified with zirconia for sensors susceptible to organic anions in multiionic aqueous solutions // *Mendeleev Commun.* 2012. V.22. №2, P.83-84.

# SYNTHESIS AND DIFFUSION PROPERTIES OF CATION-EXCHANGE MEMBRANE BASED ON MC-40, MF-4SC AND POLYANILINE

Polina Yurova, Yuliya Karavanova, Andrei Yaroslavtsev

Kurnakov Institute of General and Inorganic Chemistry RAS, Moscow, Russia,

E-mail: yuka@igic.ras.ru

In the modern world membranes are widely used in industrial processes such as electro dialysis water treatment method. An interesting and important task is to search for new materials with better selectivity or transfer asymmetry.

## Results and Discussion

In this work asymmetric cation-exchange materials based on industrial membranes MC-40 with surface modified with a thin layer of MF-4SC with the 0, 1, 2, 3, 5 and 15% polyaniline content were obtained. Due to applying a thin layer of more expensive, but more permeable membrane MF-4SC we can significantly improve the diffusion parameters of MC-40 and only slightly increase the cost. The introduction of polyaniline, actively sorbing cations, can increase amount of structural defects and the rate of cation transport.

Investigation of diffusion parameters included study of membrane diffusion permeability and interdiffusion in HCl and NaCl solutions, the ionic conductivity of membranes in various mixed-alkali  $H^+/Na^+$  forms and at various temperatures by impedance spectroscopy. Based on these data we calculated the ionic conductivity activation energy and  $H^+$  and  $Na^+$  diffusion coefficients.

**Table 1: The diffusion coefficients of membranes,  $cm^2/s$**

	MC-40	MC-40 + MF-4SC		MC-40 + MF-4SC + PANI 5%		MC-40 + MF-4SC + PANI 15%	
		modified side	unmodified side	modified side	unmodified side	modified side	unmodified side
0,1M HCl	$1,3 \cdot 10^{-6}$	$2,4 \cdot 10^{-6}$	$1,3 \cdot 10^{-6}$	$5,9 \cdot 10^{-6}$	$5,0 \cdot 10^{-6}$	$4,7 \cdot 10^{-7}$	$7,4 \cdot 10^{-7}$
0,1M NaCl	$1,3 \cdot 10^{-7}$	$1,1 \cdot 10^{-6}$	$1,0 \cdot 10^{-6}$	$1,2 \cdot 10^{-7}$	$4,3 \cdot 10^{-7}$	$1,2 \cdot 10^{-7}$	$9,0 \cdot 10^{-7}$
0,1M HCl/ 0,1M NaCl	$9,7 \cdot 10^{-6}$	$1,2 \cdot 10^{-5}$	$9,9 \cdot 10^{-6}$	$1,3 \cdot 10^{-5}$	$1,6 \cdot 10^{-5}$	$1,5 \cdot 10^{-5}$	$1,6 \cdot 10^{-5}$

In a pure MC-40 anion transport is slowly than the cation, with a rate of HCl is higher than in NaCl (it was shown experimentally that in an acidic medium moisture content, and, consequently, the pore size is much larger). In a membrane with a MF-4SC layer cation transport rate is almost unchanged, while the rate of anion transport is growing. This is due to the fact that in the modified membrane pores enlarged. The introduction of 5% polyaniline into the MF-4SC matrix leads to 10-20% increase in the cations diffusion coefficients. For all modifications the observed asymmetry of diffusion permeability is up to 50%. Inversion of the diffusion constant at 5 and 15% of polyaniline was observed (diffusion coefficients more with unmodified side). Polyaniline occupies the central part of the channel in which the anions were localized, and which they carry mostly flowed. This leads to a decrease in the concentration of anions with a modified side. It explains how a general decrease in the diffusion of membrane permeability, as well as the most significant decrease in the rate of anion transport with modified side. Same way the inversion asymmetry of the cation transport occurs. However, since cationic transport occurs near charged walls, where their concentration varies less, and this gradient is much smaller. The increase in the rate of cation transport observed with unmodified part only due to the broadening of the pores and the fact that the transport of cations takes place in this case, artificially created by their concentration gradient.

Also, with the method of impedance spectroscopy the ionic conductivity of described membranes has been studied.

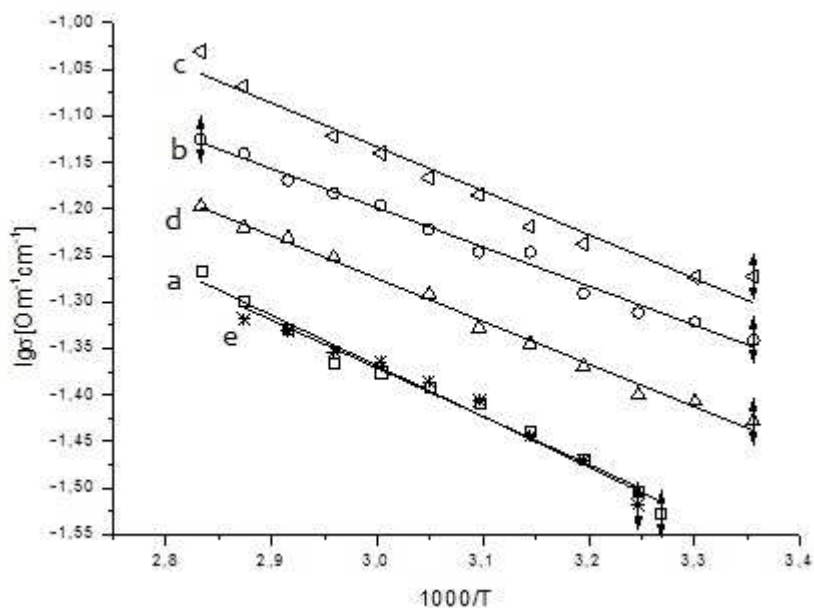


Figure 1. Dependence of membranes conductivity on the temperature.  
 a – MC-40; b – MC-40+MF-4SC; c – MC-40+MF-4SC+PANI 2%; d – MC-40+MF-4SC+PANI 5%; e – MC-40+MF-4SC+PANI 15%

The application MF-4SC layer increases the proton mobility, membranes with 2% of polyaniline show maximum ionic conductivity and with increasing concentration of polyaniline membranes results in decline of conductivity.

In order to determine the diffusion coefficients of individual cations the ionic conductivity of membranes in mixed-alkali form was investigated. The experimental points are well described by the theoretical curve and allow us to determine diffusion coefficients.

**Table 2: The diffusion coefficients of individual cations, cm<sup>2</sup>/s.**

	D(H <sup>+</sup> )	D(Na <sup>+</sup> )
<b>MC-40</b>	1.3·10 <sup>-6</sup>	5.9·10 <sup>-7</sup>
<b>MC-40 + MF-4SC</b>	2.2·10 <sup>-6</sup>	6.3·10 <sup>-7</sup>
<b>MC-40 + MF-4SC + PANI 5%</b>	2.6·10 <sup>-6</sup>	6.9·10 <sup>-7</sup>
<b>MC-40 + MF-4SC + PANI 15%</b>	1.9·10 <sup>-6</sup>	5.7·10 <sup>-7</sup>

It should be noted that the introduction of small amounts of polyaniline leads to an increase in the proton transport rate, and further increases - on the contrary to decrease because of the "binding" of protons.

Obtained samples of membrane are selective to cations and have asymmetric of diffusion permeability. This results show the prospects of developing such materials for electro dialysis water treatment.

*This work was financially supported by the RFBR (project 10-08-00715-a).*

# STUDY OF DIARY WHEY MODEL SOLUTION ELECTRODIALYSIS DEMINERALIZATION

Victor Zabolotsky, Aslan Achoh, Stanislav Melnikov  
Kuban State University, Krasnodar, Russia

## Introduction

Dairy whey processing is an important issue the of electromembrane technology nowadays. On one side whey is a secondary raw (90% of enterprises engaged in processing and manufacturing of dairy products in Russia do not use whey), on the other hand dairy whey is rich in biological components, it contains more than 50% of dry matter, including 30% proteins of milk. The second important factor is the environmental aspect: 1 T of whey drained into the sewers, pollute waterways as well as 100 m<sup>3</sup> of domestic wastewater. The third aspect - the resource as well as the cost of raw materials for dairy products reached 80% of the cost.

Therefore, the demand for dairy whey has been steadily increasing, which leads to the need for high-performance industrial processes of its pretreatment. One such process is electrodialysis. The main objective of whey electrodialysis processing is the removal of mineral salts to the demineralization level varied from 70 to 90%. The main mineral components of whey are sodium cations and chloride, dihydrogen phosphate, sulfate anions. At the same time intensified human impact on the environment leads to the appearance of nitrate ions in dairy products. Since nitrates are carcinogens, their content in foods is highly regulated by various standards.

The purpose of this work is studying of the nitrate ions removal from dairy whey model solution. And selection of the best anion exchange membrane for this process.

## Experiments

Table 1 shows the mineral composition of whey model solution supplied to the processing by electrodialysis. The main feature and the complexity of this object is 60-fold excess of chloride ions to nitrate ions.

Table 1: Composition of model solution

$\kappa$ , mS/cm	pH	Cl <sup>-</sup> , mol/L	SO <sub>4</sub> <sup>2-</sup> , mol/L	H <sub>2</sub> PO <sub>4</sub> <sup>-</sup> , mol/L	NO <sub>3</sub> <sup>-</sup> , mol/L	Na <sup>+</sup> , mol/L
39	6.5	0.313	0.022	0.105	0.005	0.445

Whey demineralization process has been studied in the laboratory electrodialysis cell under the following conditions: the voltage applied to the cell remained constant during the experiment and was 1 V/cell pair, model solution was circulating in the desalination chamber, and sodium sulfate solution with a concentration of 20 g/L was circulating in the concentration and electrode chambers. Volume flow rate of solutions was 50 L/h. Taking into account high concentrations of feed solutions, low current applied to the membrane stack and turbulent hydrodynamic regime in desalination chambers we can tell that cell was functioning in the underlimiting current mode during the entire experiment.

To study the electrodialysis process three heterogeneous anion-exchange membranes were selected: Ralex AMH (produced by Mega a.s., Czech Republic), russian industrial membrane MA-40 and the experimental membrane MA-41-2PM<sup>2</sup>. The main characteristics of membranes are presented in table 2.

Table 2: Studied anion-exchange membranes properties

Membrane	Functional groups	Ionite volume fraction, %	Ion-exchange capacity, mmol/g dry	Transport number
Ralex AMH	—N <sup>+</sup> (CH <sub>3</sub> ) <sub>3</sub>	70	1,8	0,95
MA-40	—NR <sub>3</sub> <sup>+</sup> , =NH, ≡N	55	3,8±0,4	0,94
MA-41-2PM*	—N <sup>+</sup> (CH <sub>3</sub> ) <sub>3</sub> in thin surface layer, ≡N in the bulk of membrane	65	2,0±0,3	0,96

<sup>2</sup> Membrane was created from porous anionite AB-17-2 and modified by Chermit Ruslan

The concentrations of anions in the model solution during the experiment were measured by ion chromatography. In one sample concentrations of all the anions were determined.

### Results and Discussion

Typical curves of the ions concentration in the model solution during the experiment (fig. 1 a, b) shows that chloride, sulfate and nitrate ions are removed monotonically at the beginning of the process. At the same time, the concentration of dihydrogen phosphate ions are not significantly altered. Only when concentration of chloride and ions are leveled begins removal of the later. This is probably due to the low mobility of dihydrogen phosphate ions. This phenomenon leads to a change of the model solution macrocomponents ( $\text{Cl}^-$  and  $\text{H}_2\text{PO}_4^-$ ) relation. The initial molar ratio of chloride and dihydrogen phosphate ions is 0.7 and 0.28, respectively. By the end of the experiment, this ratio changed to 0.3 for chloride ions and 0.7 for dihydrogen phosphate ions.

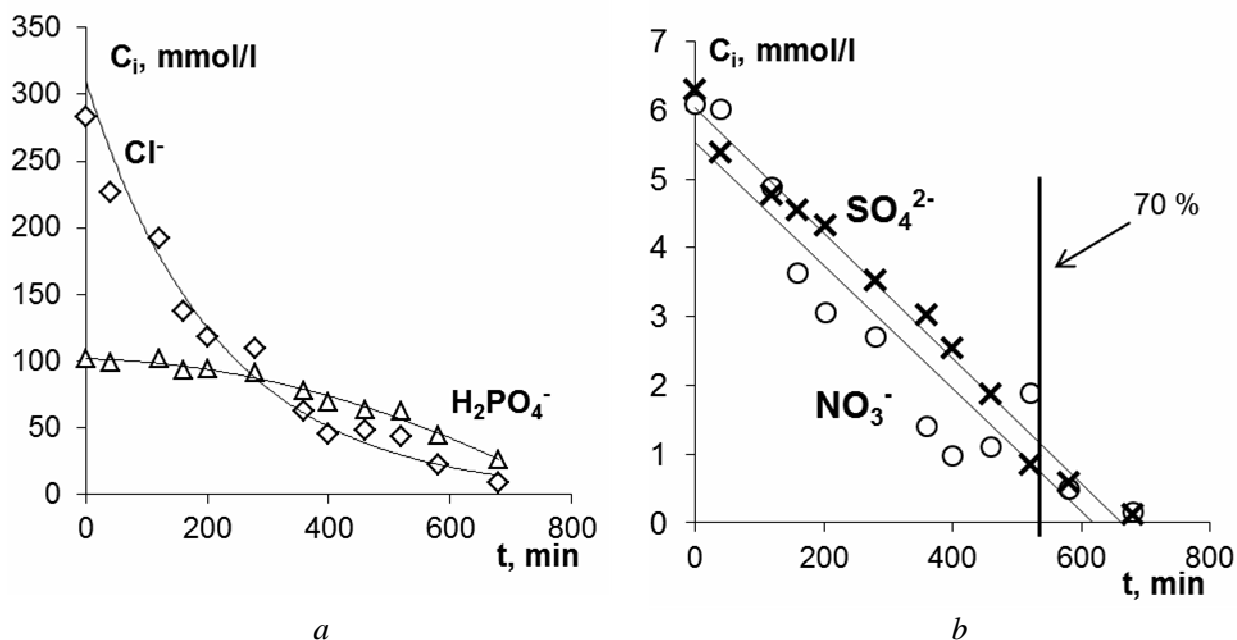


Figure 1. Concentration of different anions in model solution vs time. a – Chloride and dihydrogen phosphate ions, b – sulfate and nitrate ions

The main interest was to study nitrate ions concentration changes during electro dialysis, depending on which anion-exchange membrane was used. Since the initial concentration of nitrate ions in the different experiments vary slightly – the presented data was submitted to the initial nitrate concentration (fig. 2 a). The data presented show that achievement of the nitrate ions desired concentration (0.3 mmol/L) at 70% demineralization rate of model solution is not possible. Membranes containing quaternary ionic groups in the selective surface layer show slightly better results compared with the membrane MA-40, which contains low and medium based aminogroups.

However, the calculated data on the current efficiency of nitrate ions removal shows no significant differences in selectivity between the studied membranes, and the current efficiency for all the membranes is less than 3% regardless of solution ionic composition (fig. 2 b).

Also interesting feature is visible in the current efficiency of dihydrogen phosphate ions removal. As long as molar ratio of dihydrogen phosphate ions in the solution is lower than 0.4 membranes MA-40 and MA-41 2PM are not involved in the transport of dihydrogen phosphate ion (fig. 3). After this point membrane MA-40 shows the best selectivity.

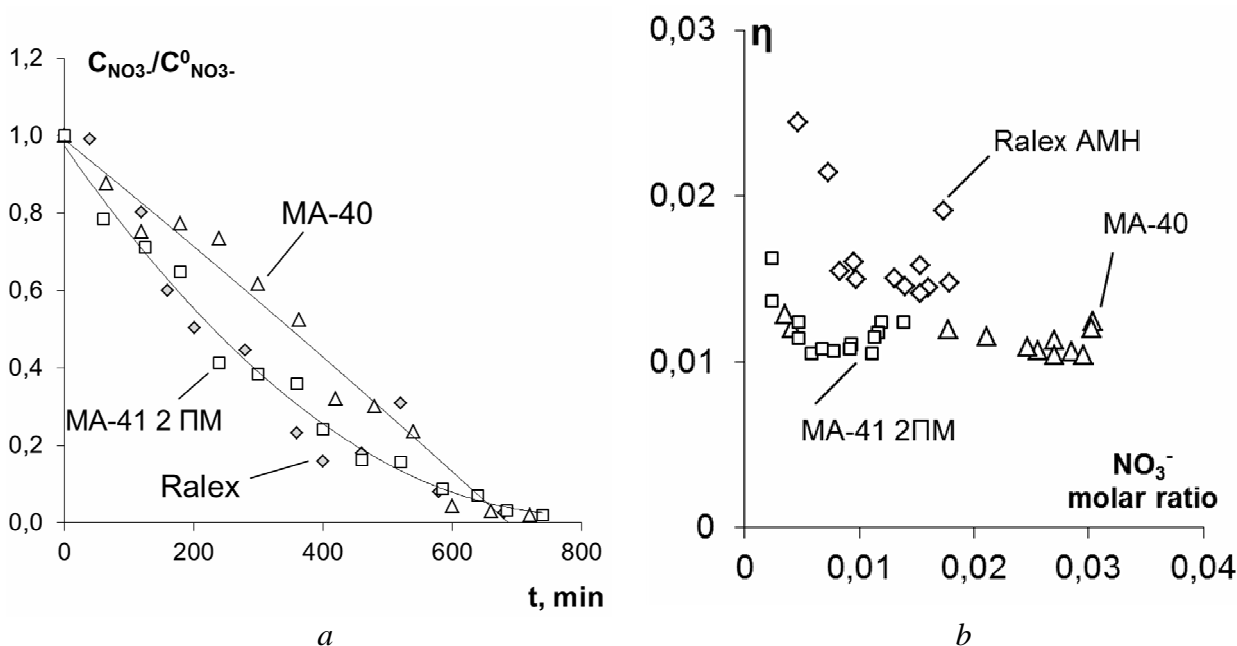


Figure 2. Dimensionless concentration of nitrate ions vs time (a), current efficiency vs nitrate ions molar ratio in model solution

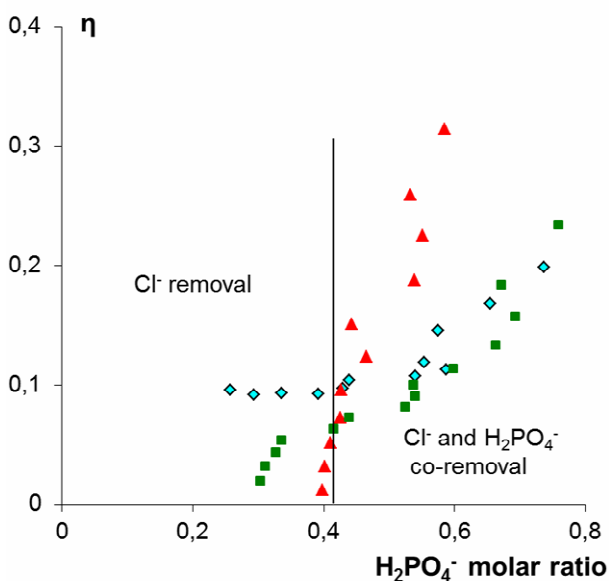


Figure 3. Current efficiency vs dihydrophosphate ions molar ratio in model solution

The use of studied anion-exchange membranes does not allow to bring the concentration of nitrate ions to the level of 0.3 mmol/L at 70% demineralization rate of model solution. Low, not exceeding 3%, current efficiencies of the nitrate ions for all investigated membranes is due to a large excess of chloride ions, which is maintained throughout the experiment. Further studies will be directed to the selection or creation of a selective membrane to nitrate ions by chemically modifying the surface or volume of the membranes.

*This work was supported by RFBR grant № 11-08-00718-a.*

---

# TRANSPORT CHARACTERISTICS OF HYBRID CATION-EXCHANGE MEMBRANES IN ELECTRODIALYSIS CONCENTRATION PROCESS OF ELECTROLYTES FROM NONAQUEOUS SOLVENTS

Victor Zabolotsky, Olga Dyomina, Svetlana Eterevska, Kirill Protasov  
Kuban State University, Krasnodar, Russia

## Introduction

In recent years, attempts have been made to use electromembrane methods for electro dialysis concentration of electrolytes from mixed and nonaqueous solvents, for regeneration of mixed process solutions and purification of organic products from inorganic electrolytes [1- 4]. Organic solvents are known [5 - 7] to effect on the structure and physicochemical and transport characteristics perfluorinated membranes. A treatment of the MF-4SK perfluorinated membranes with the aqueous-organic solutions containing N,N-dimethylacetamide (DMAA) leads to growth of their water content, diffusion and electroosmotic permeability [6]. It is known [4] that the brine concentration is mainly determined by the electroosmotic permeability of membranes which decreases with decreasing water content in the ion-exchange material. Modification of ion-exchange membranes is one of the methods that reduce the water content in the membrane and thus increase the efficiency of the electro dialysis concentration. Method of making hybrid membranes with a low value of the electroosmotic permeability was proposed in work [8].

The goal of this study was to examine the transport characteristics of the hybrid membranes in process of the electro dialysis concentration of LiCl from its solutions in DMAA.

## Experiments

The experiments on the electro dialysis concentration of LiCl were performed in a laboratory electro dialysis cell with the hydraulically closed concentration chambers filled with a solution due to the transfer of salt and organic solvent across anionite and cationite membranes as result of electromigration, electroosmosis and osmosis. The membrane package of the electro dialysis cell was assembled from industrial MA-40 heterogeneous anion-exchange membranes and hybrid MF-4SK+TEOS cation-exchange membranes with a low value electroosmotic permeability. The hybrid membranes were made on the basis of the MF-4SK perfluorinated membranes and tetraethoxysilane (TEOS) [8]. In order to obtain samples with a low value of the electroosmotic permeability the modified membranes were subjected additional heat treatment. The heat treatment of the hybrid samples was carried out at 100°C.

The membrane pair in which the hybrid MF-4SK+TEOS membrane was replaced by MF-4SK was also used in the work. The dependences of concentration of the LiCl solutions in the concentration chambers on current density were obtained for the investigated membrane pairs. Initial concentration of the LiCl in DMAA was equal to 0.14 mol/dm<sup>3</sup>. The concentration of LiCl and DMAA in the concentration chamber of the electro dialysis cell and the concentrate volume were determined at different current densities. The current density was changed from 1 to 4 A/dm<sup>2</sup>.

The experimental data were processed using the extended model of the limiting electro dialysis concentration [4]. The model allows one to calculate not only the brine concentration, but also the current efficiency ( $\eta$ ) and the transport characteristics of the membrane pair: its diffusion ( $P_s^*$ ) and osmotic ( $P_{DMAA}^*$ ) permeabilities and transport number of DMAA ( $t_{DMAA}^*$ ).

## Results and Discussion

The dependences of the salt concentration in the concentration chamber on current density are showed in Fig. 1. It can be seen, that in the case of hybrid MF-4SK+TEOS membrane the concentration of LiCl is 13-17 % higher that in the case of MF-4SK membrane.

The transport characteristics of membrane pairs obtained by model calculations based on the dependences of the LiCl and DMAA flows on current density are shown in Table.

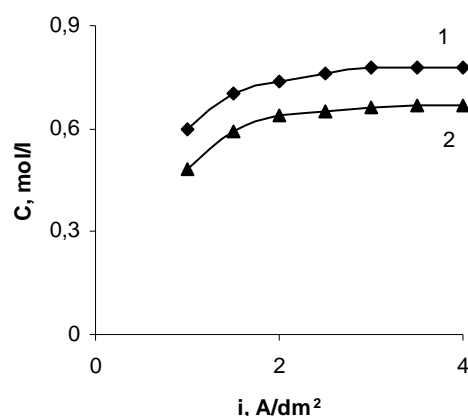


Figure 1. Dependences of the LiCl solution concentration in the concentration chambers on current density. Membrane pair: 1- MF-4SK+TEOS/MA-40; 2 - MF-4SK/MA-40

As can be seen from Table, the current efficiency are practically independent of the cation-exchange membranes type. At the same time, the DMAA transport number of the MF-4SK+TEOS/MA-40 membrane pair is 20% lower that of the MF-4SK/MA-40 membrane pair.

**Table 1: Transport characteristics of membrane pairs**

Membrane pair	$\eta$ , %	$t_{DMAA}^*$ , mol DMAA/F	$P_{DMAA}^* \times 10^5$ , m/s	$P_s^* \times 10^7$ , m/s
<b>MF-4SK/MA-40</b>	79	11.7	0.42	1.75
<b>MF-4SK+TEOS/MA-40</b>	73	9.6	1.11	5.33

This is the result of lower DMAA content in the hybrid membranes as compared with the original MF-4SK samples. The diffusion and osmotic permeabilities of the investigated membrane pairs on DMAA are small and not practically influence on process of the limiting electro dialysis concentration of LiCl from its solutions in DMAA.

The life tests of the electro dialysis cell showed that the hybrid MF-4SK+TEOS membrane with a low value electroosmotic permeability retain their transport characteristics for a long time and can be used to concentrate the electrolytes solutions from nonaqueous solvents.

#### Acknowledgments

This research was supported by the RFBR, grant № 11-03-96505.

#### References

1. Sridhar S., Feldmann C. // J. Membr. Sci. 1997. V. 124. P. 175.
2. Xu F., Innocent Ch., Pourcelly G. // Sep. Purif. Technol. 2005. V. 43. P. 17.
3. Kameche M., Xu F., Innocent Ch., Pourcelly G. // Desalination. 2003. V. 153. P.9.
4. Zabolotsky V.I., Dyomin A.V., Dyomina O.A. // Elektrokhimiya. 2011. V. 47. P. 349. [Zabolotskii V.I., Demin A.V., Demina O.A. Russian J. Electrochemistry. 2011. V. 47. No. 3. P. 327.].
5. Doyle M., Lewtts M.E., Roelofs M.G., et al. // J. Membr. Sci. 2001. V. 184. P. 257.
6. Dyomina O.A., Dyomin A.V., Gnusin N.P., Zabolotsky V.I. // Visokomolekulyarnye Soed. Ser. A. 2010. V. 52. P. 2078. [Demina O.A., Demin A.V., Gnusin N.P., Zabolotskii V.I. Polymer Sci. Ser. A. 2010. V. 52. No. 12. P. 1270].
7. Chaabane L., Dammak L., Nikonenko V.V., et al. // J. Membr. Sci. 2007. V. 298. P. 126.
8. Zabolotsky V.I., Protasov K.V., Sharafan M.V. // Elektrokhimiya. 2010. V. 46. P. 1044. [Zabolotskii V.I., Protasov K.V., Sharafan M.V. // Russian J. Electrochemistry. 2010. V. 46. No. 9. P. 979.].

# MATHEMATICAL MODEL OF ELECTROCONVECTION IN SYSTEMS WITH IONEXCHANGE MEMBRANES

Victor Zabolotsky, Konstantin Lebedev, Polina Vasilenko

Kuban State University, Krasnodar, Russia, E-mail: klebedev@fpm.kubsu.ru

## Introduction

In work the results of mathematical modelling of influence of a surface morphology of heterogeneous cationo-(MK-40) and aniono exchange (MA-40) membranes on electroconvection, and also calculations of structure the electroconvective whirlwinds generated by electric volumetric force are reported. The estimation of volumetric force and its distribution are made in view of parameters of morphology of a surface of membranes. Calculations of whirlwinds is lead by the decision of equations Navie-Stocks and the equations the Nernst-Planck-Poisson with boundary conditions of nonslip and a constancy of concentration on borders and difference of potential on the electro dialysis cell.

## Results and Discussion

For an estimation of influence electroconvection on processes in the desalinate cell of ЭДА the two-dimensional hydrodynamic carry ions model considering the electric heterogeneity of a membrane surface is considered. In [1, 2] the model electroconvection based on equations Navie-Stocks is presented and force electroconvection, was set as constant on the spatial area modelling heterogeneity. In this model, together with equation Navie-Stocks are presented the equations the Nernst-Planck-Poisson. Operating electroconvection force is proportional to an arising charge on areas of heterogeneity. The chemical dissociation reactions of water on the border of cell are not considered in the given model. Vector equations of all system for binary electrolyte looks like:

$$\vec{j}_i = \frac{F}{RT} z_i D_i C_i \vec{E} - D_i \nabla C_i + C_i \vec{V}, \quad i = 1, 2, \quad (1)$$

$$\frac{\partial C_i}{\partial t} = -\text{div} \vec{j}_i, \quad i = 1, 2, \quad (2)$$

$$\varepsilon \Delta \varphi = -F(z_1 C_1 + z_2 C_2), \quad (3)$$

$$\vec{I} = F(z_1 \vec{j}_1 + z_2 \vec{j}_2), \quad (4)$$

$$\frac{\partial \vec{V}}{\partial t} + (\vec{V} \nabla) \vec{V} = -\frac{1}{\rho_0} \nabla P + \nu \Delta \vec{V} + \frac{1}{\rho_0} \vec{f}, \quad (5)$$

$$\text{div}(\vec{V}) = 0, \quad (6)$$

where  $\nabla$  – gradient,  $\Delta$  – operator Laplasa,  $\vec{V}$  – solution current speed,  $\rho_0$  – density of a solution,  $P$  – pressure,  $C_1, C_2$  – cation and anion concentration in a solution,  $z_1, z_2$  – charging numbers cation and anion,  $D_1, D_2$  – diffusion coefficients of cation and anion,  $\varphi$  – electric field potential,  $\varepsilon$  – dielectric permeability of electrolit,  $F$  – Faraday constant,  $R$  – Gas constant,  $T$  – absolute temperature,  $t$  – time,  $\nu$  – coefficient of kinematic viscosity,  $\vec{f}$  – force density of an electric field

The Nernst-Planck equations (1) describe the stream of ions caused by migration in an electric field, diffusion and convection; (2) – equation material balance; (3) – Poisson equation; (4) – current density in a solution of electrolyte; (5) – Navie-Stocks equations; (6) – the equation incompressibility. The problem was solved in a dimensionless kind. On an input the parabolic profile of speed is used. Force  $f = k(C_1 - C_2)$  proportional to a spatial charge acts on 6 sites which model heterogeneity of a structure ionexchange material and are shown on figure 1.

It is shown, that the volumetric force induced by course of a current is capable to generate pair electroconvective vortexes (the second sort electro osmosis), and the sizes of the induced

vortexes are comparable with membrane distance in electro dialysis cell. Electroconvection and cross-section speed arise due the action of two volumetric electric forces equal caused by a spatial charge which is sufficient for occurrence electroconvection. Significant vortex arise in the beginning and in the end of the channel. Internal vortexes are mutually repaid. Despite of the significant compelled current vortical movement leads to increase in delivery of a solution from a kernel of a stream to border of a membrane. This provides an intensification of mass transfer.

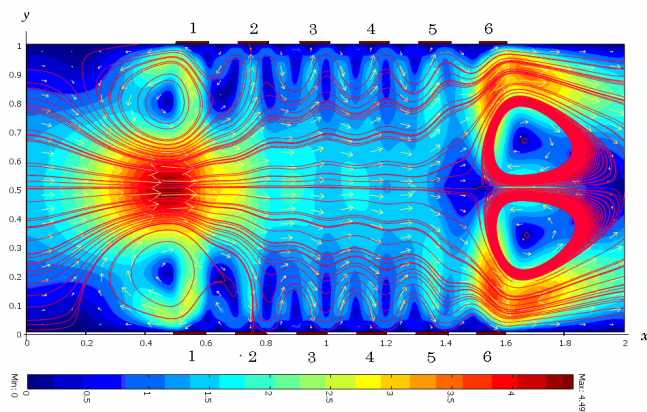


Figure 1. A field of speeds, lines of a current and vectors of speeds in system with scopes electroconvective forces:  $0.5 < x < 0.6$ ,  $0.7 < x < 0.8$ ,  $0.9 < x < 1.0$ ,  $1.1 < x < 1.2$ ,  $1.3 < x < 1.4$ ,  $1.5 < x < 1.6$

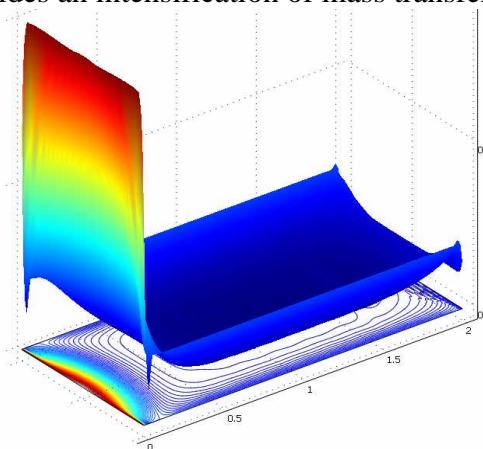


Figure 2. Distribution of concentration counterions in the channel of electro dialysis

Taking into account of presence coulomb forces on interphase border leads to occurrence of whirlwinds. It is shown, that with increase in linear speed of solution in cell the contribution electroconvection in overlimiting mass transfer is decreased. With reduction of entrance concentration or with increase the current density the contribution electroconvection in mass transfer is increased. The space charge is formed both at cation- and anion membranes and their sizes can be various because for arising dissociation on border, but in the given model it is not considered.

Distribution of concentration counterions is shown on figur2. Presence of significant mixing lead to fast falling of concentration counterions in the beginning of the channel already. The model allows to calculate distribution of intensity, potential, concentrations in the channel, to investigate the differential and integrated characteristics of concentration and speed fields.

*Work is executed at financial support of the RFFI (the grant 10-08-01060-a)*

### References

1. Zabolotsky V.I., Nikonenko V.V., Yrtenov M.X., Lebedev K.A., Bygakov V.V., Electroconvection in systems with heterogeneous ionexchange //Russian Electrochemical. 2012 (in press).
2. Zabolotsky V.I., Lebedev K.A., Yrtenov M.X., Nikonenko V.V., Vasilenko P.A., Shaposhnik V.A., Vasil'eva V.I. Mathematical model for the description voltamper curves and numbers transfer ions at intensive regime of an electro dialysis // Russian Electrochemical. 2012 (in press).

# MATHEMATICAL MODEL OF NATURAL WATER PH CORRECTION BY ELECTRODIALYSIS WITH BIPOLAR MEMBRANE IN LONG MEMBRANE CHANNELS

Victor Zabolotsky, Konstantin Lebedev, Polina Vasilenko, Stanislav Utin

Kuban State University, Krasnodar, Russia, E-mail: klebedev@fpm.kubsu.ru

## Introduction

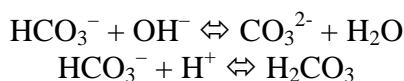
The problem of determining the concentrations at the outlets of the electro dialyzer chambers during pH correction of dilute solutions containing a large number of components that can enter into chemical reactions is multiparametric and requires a considerable array of experimental data. Creation of mathematical models describing this process in long electro dialyzer channels allows fastening the calculation process and predicting mass transfer characteristics of the real industrial modules.

## Experiments

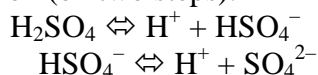
The study is carried out in electro dialyzer which acid and alkaline chambers were formed by bipolar membranes MB-3 and anion-exchange membranes MA-40. The studies were conducted at three different flow rates of solution through the elementary cell under study: 3, 5 and 7,5 L/h. Electro dialyzers contained 10 paired chambers; the working area of the membrane was 4 dm<sup>2</sup>, intermembrane distance–0.8 mm.

## Results and Discussion

Electrodialysis of softened water is complicated by chemical reaction with single- and double-charge ionic forms of carbonic acid at pH change in acid and alkaline chambers. In presence of bicarbonate ions in softening water their interaction with hydroxyl and hydrogen ions generated in bipolar membrane is described:



In addition softened water contains considerable amount of sulfate-ions. Presence of different sulfate forms depends on pH. In softening water with sulfate ions (SO<sub>4</sub><sup>2-</sup>) there can be hydrosulfate ions (HSO<sub>4</sub><sup>-</sup>) at pH<4. In this case calculation of concentrations is carried out on basis of sulfuric acid dissociation reaction (on two steps):



Calculation of transport numbers through anion-exchange membrane is carried out on basis of teoretical approach, describing in [1]. According to this approach and with assumption about ideal selectivity of ion-exchange membrane at current equal or above limiting, it is possible to calculate transport numbers through anion-exchange membrane only from ions concentration and their diffusion coefficients in solution:

$$T_{j,np} = \frac{j_{j,np}}{\sum_{j=1}^4 j_{j,np}} = \frac{(1 - \frac{z_j}{z_A}) D_j c_j}{\sum_{j=1}^4 (1 - \frac{z_j}{z_A}) D_j c_j},$$

where  $J_{j,lim}$ –flux of sort  $j$  ions through ion-exchange membrane at  $i=i_{lim}$ , mol/cm<sup>2</sup>\*s,  $\delta$ –thickness of diffusion layer, cm,  $z_i$  – charge of sort  $j$  ion,  $z_A$  –charge of coion,  $D_j$ –diffusion coefficient of sort  $j$  ion in solution, cm<sup>2</sup>/s,  $c_j$ – concentration of sort  $j$  ion in solution. The sum of transport numbers through anion-exchange membrane is 1:

$$T_{Cl^-}^A + T_{HCO_3^-}^A + T_{OH^-}^A + T_{SO_4^{2-}}^A = 1.$$

Finally mathematical model represents system of nonlinear equations which contains 15 equations with 15 variables relative to concentrations and ionic fluxes. The system is solved by means of Newton's modified method.

More complex and important from a practical point of view is to build the mathematical model describing pH correction process of the softened water in a long electrolysers channel.

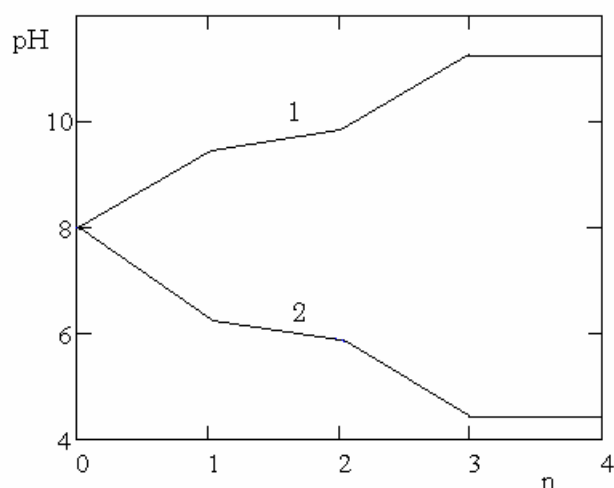


Figure 1. Distribution of pH along the length of the module, 1 – alkali chamber, 2 – acid chamber

It is shown that two-dimensional model of multicomponent solutions electro dialysis, based on kinetic equations for calculation of the transport numbers and ionic equilibrium thermodynamic equations can be obtained by upgrading compartmentation method [2], which consists in partitioning of membrane channel at a sufficiently large number of layers perpendicular to the direction of flow of the solution. Channel length was 40 cm and electrolysers model was applied to a distance of 10 cm (n) so that the output estimated in the previous section were input to the subsequent section. The developed program allows the calculation of the stratified structure of the solution as it passes through the channel and find the way the local value of the ion concentration, pH, current density and the effective transport numbers of ions through the membrane.

For example, the distribution of pH along the length of the module at a current density of  $8 \cdot 10^{-4} \text{ A/cm}^2$  and solution flow rate through one chamber of 5 L/h was calculated (fig. 1). Near the entrance to the channel pH change rate with increasing of the channel length, which is associated with the presence of bicarbonate ion chemical reactions with water molecules dissociation products and buffer properties of the solution. It is shown that the greatest change in pH of the solution occurs in the early parts of the apparatus and in the middle of the apparatus.

*This work was supported by RFBR grant № 11-01-96512-r\_yug\_c.*

#### References

1. Lebedev K.A., Nikonenko V.V., Zabolotsky V.I., Gnusin N.P. // *Electrokhimiya*. 1986. V.22. №5. P. 638
2. Nikonenko V.V., Pis'menskaya N.D., Istoshin A.G., Zabolotsky V.I., Shudrenko A.A. // *Elektrokhimiya* 2007. V. 43. № 9. P.1125

# FORECASTING OF MASS EXCHANGE CHARACTERISTICS OF CONCENTRATOR ELECTRODIALYZERS BY COMPARTMENTATION METHOD

<sup>1,2</sup>Victor Zabolotsky, <sup>1</sup>Stanislav Melnikov, <sup>1</sup>Olga Dyomina, <sup>1</sup>Svetlana Eterevska, <sup>3</sup>Lubosh Novak, <sup>3</sup>Filipp Auinger, <sup>4</sup>Lubomir Machuca

<sup>1</sup>Kuban State University, Krasnodar, Russia

<sup>2</sup>LLC «Innovative Enterprise «Membrane Technology», Krasnodar, Russia

<sup>3</sup>«Mega a.s.», Straz-pod-Ralskem, Czech Republic

<sup>4</sup>«MemBrain s.r.o.», Straz-pod-Ralskem, Czech Republic

## Introduction

Semi-empirical approach making possible to generalize, forecast and scale the mass exchange characteristics of the electrodialyzers intended for desalination of the dilute solutions of electrolytes was suggested in work [1]. The compartmentation method serves as the basis of the approach used for scaling of the electrodialyzers of pointed type. Main point of the method, adapted for the electrodialysis, is that the long desalting channel ( $L$ ) of the electrodialyzer is considered as a sequence of the elementary channels ( $L_0$ ). Application of the method allows to find the solution concentration at the outlet of the desalting channel with length  $L > L_0$  if the concentration of the initial solution and a desalting factor ( $F = c^{out}/c^0$ ) are known and linear velocity of the solution at the desalting channel of the original and scaled electrodialyzers are approximately equal.

The aim of this study was to investigate the possibility of using of the compartmentation method for prediction of the mass exchange characteristics of the industrial concentrator electrodialyzers on the basis of the experimental data obtained in a laboratory cell.

## Experiments

The objects of study were two types of the concentrator electrodialyzers: laboratory EDC-Y module and pilot EDC-II module, based at the commercial unit ED-II. Both devices have non-flowing concentration chambers, made in accordance with the technical solution of LLC «Innovative Enterprise «Membrane Technology» [2, 3]. The membrane packages of the concentrator electrodialyzers were assembled from the Ralex CM-PES cation-exchange and Ralex AMH-PES anion-exchange membranes. The Ralex membranes and the modules ED-II are produced by «Mega a.s.». Characteristics of the studied objects in conjunction with the flow rates of solution at the desalting channel are listed in the Table.

**Table: Characteristics of membrane packages of the investigated concentrator electrodialyzers and solution linear velocity at desalination channel**

EDC	Type of electrodialyzer	Channel length, $m$	Number of elementary chambers	Linear velocity, $m/s$
EDC-II	pilot	$3L_0$	125	0.0482
EDC-Y	laboratory	$L_0$	12	0.0351

Feed solution was 5 g/L ammonium nitrate. In the steady state the solution conductivity at the inlet and outlet of the desalting channels, the rate of the concentrate drip from the concentration chambers and its electrical conductivity, voltage and current were recorded. The experiments were carried out at the currents densities less than the limit current density.

## Results and Discussion

The experimentally determined mass exchange characteristics of the EDC-II pilot module and laboratory EDC-Y cell are shown in Fig. 1 as the dependences of the  $\text{NH}_4\text{NO}_3$  concentrations at the outlet from the concentration chambers on the current density.

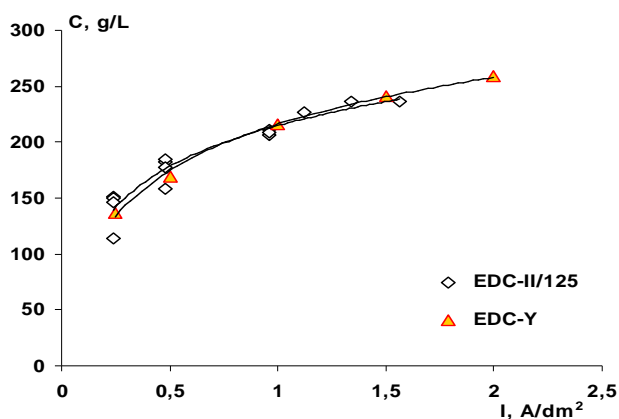


Figure 1. Dependences of the  $\text{NH}_4\text{NO}_3$  concentrations at the outlet from the concentration chambers on the current density

Calculation of the solution concentration at the outlet of the desalting channel of the pilot EDC-II module, for which  $L=3L_0$  (see Table), was performed according to the equation:

$$c_3^{out} = c^0 \Gamma(c^0) \Gamma(c_1^{out}) \Gamma(c_2^{out}) \quad (1)$$

The equation (1) was obtained using the recurrence formulas of the type:

$$c_N^{out} = c_{N-1}^{out} \Gamma(c_{N-1}^{out}) \quad (2)$$

where  $N$  is number of sections to which the channel can be broken and  $c_{N-1}^{out}$  is concentration at the outlet of the  $(N-1)$  section. The desalting factor ( $\Gamma(c^0)$ ) was calculated on the basis of the experimental data obtained in laboratory EDC-Y cell.

The experimentally obtained during the test of the EDC-II module and theoretically calculated values of the  $\text{NH}_4\text{NO}_3$  concentrations at the outlet of the desalting channel and the demineralization degree at various current densities are shown in Fig. 2 a, b.

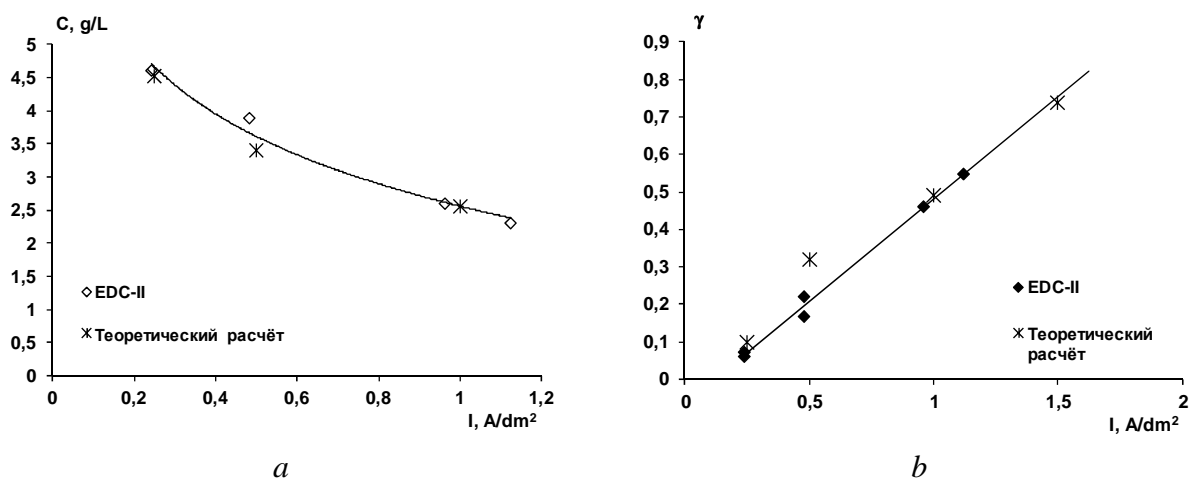


Figure 2. The dependence of the  $\text{NH}_4\text{NO}_3$  concentration at the outlet of the desalting channels (a) and the demineralization degree (b) on the current density

It is seen that the theoretical values are in good agreement with the experimental data. Thus, the data obtained in laboratory cell can be successfully used to process of scaling and predicting of the properties of the industrial the concentrator electrodesalters such as EDC-II.

#### Acknowledgments

The present work was supported by the Russian Foundation for Basic Research, project № 11-08-96528. This problematic was solved within FR-TI3/729 project and was supported by the state budget of The Czech Republic by the Czech Ministry of Industry and Trade.

#### References

1. Nikonenko V.V., Pis'menskaya N.D., Istoshin A.G., Zabolotskii V.I., et al. // Russian J. Electrochemistry. 2007. V. 43. No. 9. P. 1069.]
2. Pis'mensky V.F., Gnusin N.P., Zabolotsky V.I., Istoshin G.N. Patent RF № 949890. 1993.
3. Zabolotsky V.I., Doymin A.V., Okulich O.M., Lakunin V.U., Slugin I.V. Patent RF № 2398618.

---

# TRANSPORT PROPERTIES OF ANION EXCHANGE MEMBRANES IN CHROME-CONTAINING SOLUTIONS

Evgenija Zhelonkina, Tatyana Kononova, Vladimir Mamaev, Svetlana Shishkina

<sup>1</sup>Vyatka State University, Kirov, Russia; E-mail: vgu\_tep@mail.ru.

## Introduction

Membrane methods of processing waste waters have a number of advantages in comparison with traditional ones, such as: universality of the process, absence of any reagents introduced in waste waters, essential decrease in waste amount, relative simplicity and compact size of the plants [1].

At the same time, there are multiple charged ions of metals in waste waters and technological mixes from many manufactures, effect of which on the attributes of ion exchange membranes has not been studied sufficiently until now [2]. One of the actual problems in electroplating is purification and regeneration of the electrolytes containing tri- and hexavalent chrome compounds.

Electric conductivity is one of the main attributes determining practical feasibility of ion exchange membranes. At the same time, current carrier mobility in the membrane phase is determined by hydration of the "fixed group-counterion" associates i.e. by water content.

## Experiments

Water content of the membranes was estimated by gravimetric method.

A mercury contact cell including the membrane under investigation having a mercury electrode astride was used for estimating resistance of the membranes, which made it possible to carry out the measurements without mechanical breakage and changes in the chemical state of the samples. The resistance was measured with Elins Impedancemeter Z-2000.

The experimental data was processed with the EIS Spectrum Analyzer program which is able to analyze impedance spectra with the method of equivalent circuit design. The electric conductivity was calculated and its concentration diagrams were drawn using the membrane resistance values obtained. The electric conductivity of the MA-40 and MA-41 anion exchange membranes and of the MC-40, MF-4SC cation exchange membranes equilibrated with the chrome chloride, chrome (VI) oxide and sodium chloride (for the purpose of comparison) solutions in the 0.02–0.3 N concentration interval was studied.

## Results and Discussion

The electric conductivity values of the MC-40 membrane in the sodium chloride solutions is 2 times larger than the ones in the chrome chloride solutions, which could be explained by less mobility of the triple-charge counterion associated with several functional groups and so having its potential well deepened. It is also necessary to take into account that there are several chrome (III) chloride hexahydrate compounds, such as the  $[\text{CrCl}_2(\text{OH}_2)_4]\text{Cl}\cdot 2\text{H}_2\text{O}$  dark green hexahydrate, the  $[\text{CrCl}(\text{OH}_2)_5]\text{Cl}_2\cdot \text{H}_2\text{O}$  light green hexahydrate and the  $\text{Cr}(\text{OH}_2)_6\text{Cl}_3$  blue-gray hexahydrate [3]. The calculations have shown that concentration of the  $[\text{CrCl}(\text{OH}_2)_5]^{2+}$  complexes is maximum in the chrome (III) chloride solutions. Mobility of such complex is expected to be very low in the membrane phase. In addition, the transition from the sodium chloride solutions to the chrome chloride ones is accompanied by 20 % decrease in the water content.

The electric conductivity of the MC-40 membrane in the chrome chloride solutions is much larger than the one in the NaCl solutions. Equilibrium between the chromic  $\text{H}_2\text{CrO}_4$  and dichromic  $\text{H}_2\text{Cr}_2\text{O}_7$  acids is set in the  $\text{CrO}_3$  solutions. Both acids are dissociated in the first stage almost completely, but there are practically no molecules dissociated in the second stage [Remy].

The hydrogen ions released at dissociation and having abnormal mobility replace the sodium ions, so the MC-40 membrane turns into its  $\text{H}^+$  - form and has its electric conductivity increased. In addition, the water content of the MC-40 membrane seems to increase by 39% on average because of strong linkage between the proton and the water molecules (the  $\text{H}_5\text{O}_2^+$  particles have

been found even in the air-dry sulfonic cation exchange membrane samples [4]), which also promotes the increased mobility of the counterions.

The electric conductivity values of the MA-40 membrane are a bit larger in the chrome chloride solutions than the ones in the sodium chloride solutions. This could be attributed to complexation [2] which occurs between the functional groups of the EDE-10P resin (which is an active component of the MA-40 membrane) and the  $\text{Cr}^{3+}$  cations which percolate through the anion exchange membrane via the Donnan sorption effect. This is indicated by a new peak in the oscillation area of secondary amino groups ( $1650 - 1610 \text{ cm}^{-1}$ ) in the MA-40 membrane IR spectrum. This results in growth of the matrix general positive charge. Such membrane is able to involve more chlorine ions in the exchange with subsequent increase in the electric conductivity. The MA-41 membrane active component is the AH-17 highly basic resin, the quaternary amino groups of which are not inclined to the complexation with polycharged cations, so the electric conductivity values of this membrane are similar to each other both in the chrome chloride and the sodium chloride solutions. Thus, both anion exchange membranes are in the  $\text{Cr}^-$  - form and do not decrease their transport attributes in the  $\text{CrCl}_3$  solutions.

In the chrome (III) oxide solutions, however, both of them decrease the water content sharply (by 50% on average), which is attributed to their transition to the  $\text{CrO}_4^{2-}$  ( $\text{Cr}_2\text{O}_7^{2-}$ ) - form. In addition, they change their color from pale brown to dark brown (MA-40) and black (MA-41). The electric conductivity values of both membranes decrease by the factor of hundred in comparison with the chloride solutions.

Stripes typical for oscillation of the  $\text{C}=\text{O}$  ( $1720 - 1660 \text{ cm}^{-1}$ ) and  $\text{OH}$  ( $1390 - 1350 \text{ cm}^{-1}$ ) groups were obtained for the MA-41 membrane samples in their IR spectra, which indicates to oxidation of the ionite matrix into the  $-\text{COOH}$  group [5].

Thus, the MA-40 and MA-41 membranes retain their transport properties in the chrome (III) chloride solutions. This makes it possible to use them in purification and regeneration of the solutions. In the  $\text{CrO}_3$  solutions, however, these membranes are subject to full or half-way destruction. The MA-40 membrane can be used for purification of the chromate solutions from the trivalent iron and trivalent chrome admixtures by means of the membrane electrolysis method.

### References

1. *Dubyaga V.P., Besfamilyny I.B.* // Membranes. 2005. V. 27. №3 (27). P.11.
2. *Shishkina S.V., Pechenkina E.S., Dyukov A.V.* // Electrochemistry. 2006. V.42. №12. P.1457
3. *Remy G.* Lehrbuch der anorganischer chemie. Band 1. M, 1972. 591 p.
4. *Timashev S.F.* Physical chemistry of membrane processes. M. Chemistry, 1988. 258 p.
5. *Semushin A.M., Yakovlev V.A., Ivanova E.V.* IR absorption spectra of ion-exchange materials. Chemistry, 1980. 96 p.

---

# THE NATURE INFLUENCE MEMBRANES ON THE FORMATION AND DEVELOPMENT OF CONVECTIVE INSTABILITY IN ELECTROMEMBRANE SYSTEMS

<sup>1</sup>Anna Zhiltsova, <sup>1</sup>Vera Vasil'eva, <sup>1</sup>Mikhail Malykhin, <sup>2</sup>Natalia Pismenskaya,

<sup>2</sup>Mahamet Urtenov, <sup>2</sup>Aminat Uzdenova, <sup>2</sup>Victor Nikonenko

<sup>1</sup>Voronezh State University, Voronezh, Russia, *E-mail: viv155@mail.ru*

<sup>2</sup>Kuban State University, Krasnodar, Russia, *E-mail: nikon@chem.kubsu.ru*

## Introduction

Convective instability in electromembrane systems has been visualized by means of different optical methods [1-5]. The method of laser interferometry allows obtaining valuable information about the state of near-membrane solution layer. One of the main factors determining behavior of ion-exchange membranes at a current density exceeding its limiting value is the properties of membrane surface. In particular, electrical heterogeneity of the surface facilitates the onset of formation of electroconvective vortices [6]; surface hydrophobicity gives rise to slip of the fluid at the surface, which enhances electroconvection and the delivery of fresh solution to the membrane surface from the core flow [7, 8].

The aim of the present work consists in investigation of dynamics of a development of the convective instability region in solution by the method of laser interferometry. In particular, the thickness of diffusion boundary layer (DBL) in intensive current regimes was measured.

## Experiments

Concentration fields are studied in an electro dialysis desalination cell formed with a cation exchange and an anion exchange membranes. We have studied two cation exchange membranes: a commercial MK-40 and a MK-40+Nf membranes. To obtain the MK-40+Nf membrane, the surface of MK-40 was coated with a thin layer of liquid Nafion (of about 20 microns thickness). A commercial MA-40 membrane and a modified MA-40M membrane were used. The MA-40M was obtained from the MA-40 by surface modification using a strong polyelectrolyte [9].

The length of membrane channel  $L$  is  $4,4 \cdot 10^{-2}$  m, the width is  $1,5 \cdot 10^{-2}$  m, the intermembrane distance  $h$  is  $5,0 \cdot 10^{-3}$  m. The distance from the entrance to the section in which the concentration profiles are measured is  $2,7 \cdot 10^{-2}$  m.

The method of laser interferometry of Mach-Zender type was applied. The interference pattern was registered by a video camera with a digitization frequency of 15 Hz. The convective instability region is defined as a near-membrane zone of solution where concentration profile has unstable, oscillatory character. It is possible to find the Nernst ( $\delta_N$ ) and the total ( $\delta$ ) thicknesses of DBL.  $\delta_N$  is determined by the point of intersection of the tangents drawn to the concentration profile near the surface and in the middle part of the channel;  $\delta$  is defined as the thickness of layer where 99% of the concentration variation occurs.

In order to avoid the effect of gravitational convection, the membrane under study was set horizontally in a position of stable stratification. The current has been directed in such a way that counterions moved upwards and the depleted DBL was under the membrane.

## Results and Discussion

The effect of membrane surface properties on the current-voltage (I-V) curves and concentration profiles is detected.

Coating of MK-40 by a Nafion film leads to an increase in the limiting current density and to a reduction of the «plateau» length of I-V curves.

We visualize in situ salt concentration profiles in solution at the boundary with membranes. Fluctuations of concentration profile in the depleted solution at the MK-40+Nf membrane (fig. 1a) arise when the limiting current density ( $i_{lim}$ ) is achieved. In the case of MK-40, an excess of limiting diffusive current density is needed to produce the fluctuations:  $i$  should be 1,2 to 1,5 times higher than  $i_{lim}$ . Effective current-induced convection arisen at the depleted membrane surface mixes the near-surface solution. As a result, the concentration profile at the depleted

surface becomes flat showing that the diffusion does not contribute in this region. However, the diffusion layer does not disappear. It is shifted from the membrane boundary towards the flow core. There the convection (mainly the forced convection) becomes important again, and the profile is smoother. Thus, under the action of current-induced convection, the diffusion boundary layer ceases to be “boundary”.

Qualitatively similar concentration profiles are obtained by numerical solution of a boundary-value problem based on the Nernst-Planck equations coupled with the Poisson and Navier-Stokes equations (Fig. 1b).

It is to note that up to as high current density applied as  $3i_{lim}$ , there are no electroconvection near the anion exchange membrane forming a desalination channel together with the cation exchange one.

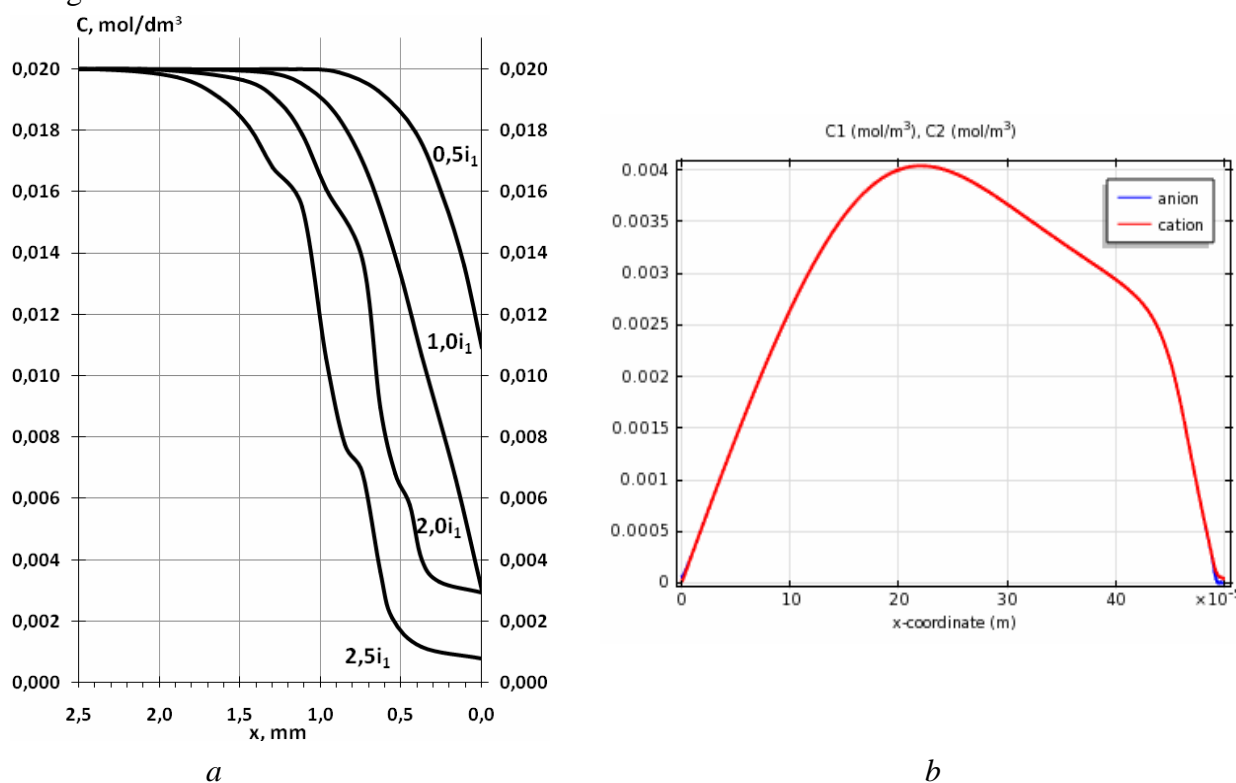


Figure 1. Concentration profiles of sodium chloride solution near the cation-exchange membrane MK-40+Nf under different current densities;  $C_0$  (NaCl)=0.02 M,  $V=0.02$  cm/s (a); result of numerical calculation of Nernst-Planck - Poisson-Navier-Stokes equations at  $i=2i_1$ (b);  $i_1$  is the limiting current density found by the intersection point of tangents to I-V curves

The values of  $\delta_N$  and  $\delta$  are presented in Figs 2a and 2b as functions of the ratio of current density  $i$  to  $i_1$ . It is found that the decrease of effective thickness  $\delta_N$  near the MK-40+Nf membrane occurs at the currents corresponding to beginning of the convection instability. As  $i_1$  is higher for the MK-40+Nf membrane in comparison with the MK-40 one, at the same ratio  $i / i_1$  the current density  $i$  in the case of MK-40+Nf is higher. That explains the lower values of  $\delta_N$  and  $\delta$  for MK-40+Nf presented as functions of  $i / i_1$ . Under the same potential drop the current density and electroconvection are higher for the MK-40+Nf membrane.

Apparently, the main effect of surface modification on the membrane behaviour is due to the variation of the surface hydrophobic/hydrophilic balance. It is known [8, 9] that an increase in the membrane surface hydrophobicity facilitates electroconvection owing to replacing the boundary condition of adhesion with the slip condition. Such replacing makes easier the formation of paired electroconvective vortexes.

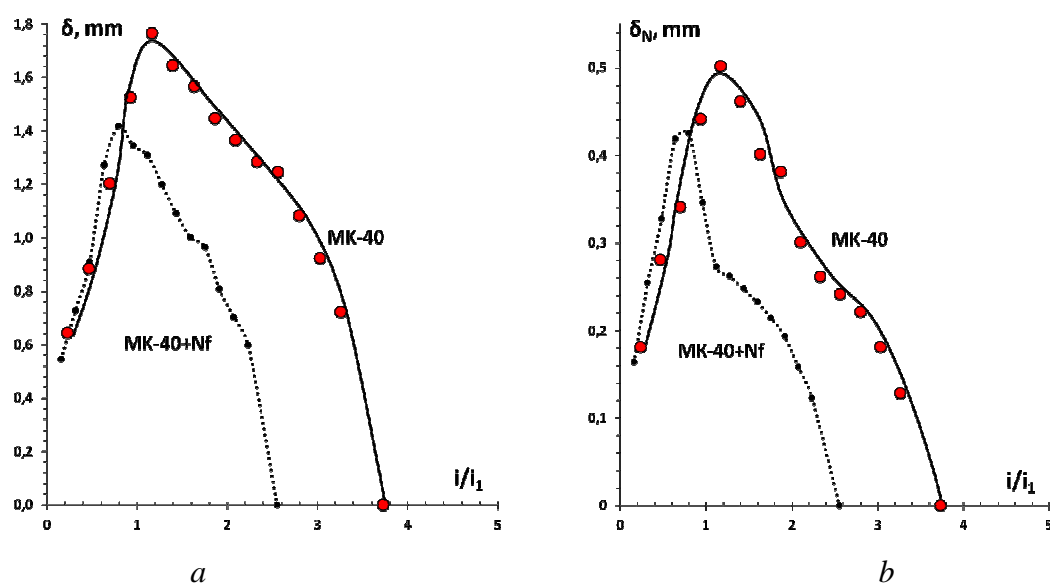


Figure 2. The thickness of the total (a) and the Nernst (b) diffusion layers near MK-40 and MK-40+Nf cation exchange membranes as a function of the current density:  $C_0(\text{NaCl})=0.02\text{M}$ ,  $V=0.02\text{ cm/s}$

### Acknowledgments

The research was financially supported by Russian Foundation of Basic Research (projects №11-01-96512- r\_south\_ts, 12-08-00188 and 11-08-93107) and by FP7 “CoTraPhen” project PIRSES-GA-2010-269135.

### References

1. Block M., Kitchener A. Polarisation phenomena in commercial ion-exchange membranes // J. Amer. Chem. Soc. 1966. V.113. №9. P. 947-953.
2. Lifson S., Gavish B., Reich S. Flicker-noise of ion selective membranes and turbulent convection in the depleted layer // Biophys. Struct. Mech. 1978. V.4, № 1. P.53-65.
3. Pevnitskaya M.V. Intensification mass transfer at an electro dialysis of the diluted solutions // Elektrokhimiya. 1992. V.28. №1. P. 1708-1715 (in Russian).
4. Varentsov V.P, Pevnitskaya M.V. Transfer of ions through ion-exchange membranes at an electro dialysis // News of the Siberian Branch of the USSR Academy of Sciences. Series of Chemical Sciences. 1973. Issue 4. No 9. P. 134-137 (in Russian).
5. Rubinstein S.M., Manukyan G., Staicu A., Rubinstein I., Zaltzman B., Lammertink R.G.H., Mugele F., Wessling M. Direct Observation of a Nonequilibrium Electro-Osmotic Instability // Phys. Review Letters. 2008. Vol. 101. P. 236101.
6. Rubinstein I., Zaltzman B. Electro-osmotically induced convection at a permselective membrane // Phys. Rev. E. 2000. Part A, Vol. 62, No 2. P. 2238-2251.
7. Nikonenko V., Pismenskaya N., Belova E., Sistat Ph., Larchet C., Pourcelly G. Intensive current transfer in membrane systems: Modelling, mechanisms and application in electro dialysis // Adv. Colloid Interface Sci. 2010. V. 160. P. 101-123.
8. Belashova E.D., Melnik N.A., Pismenskaya N.D., Shevtsova K.A., Nebavsky A.V., Nikonenko V.V. Overlimiting mass transfer through cation-exchange membranes modified by NAFION film and carbon nanotubes // Electrochimica Acta. 2011. V. 56. P. 10853-10865.
9. Lopatkova G.Yu., Volodina E.I., Pismenskaya N.D., Fedotov Yu.A., Cot D., Nikonenko V.V. Effect of chemical modification of ion-exchange membrane MA-40 on its electrochemical characteristics // Rus. J. Electrochem. 2006. V. 42. P. 847-854.

# WHEY SEPARATION BY MEANS OF ELECTRODIALYSER WITH NON CIRCULATING CONCENTRATION CELLS

<sup>1</sup>Yuriy Zmievskiy, <sup>1</sup>Valeriy Myronchuk, <sup>2</sup>Dmitriy Kucheruk, <sup>1</sup>Inna Gudzovska

<sup>1</sup>National University of Food Technologies, Kyiv, Ukraine, *E-mail: yrazm@meta.ua*

<sup>2</sup>Dumansky Institute for Colloid and Water Chemistry, Academy of Sciences of Ukraine, Kyiv, Ukraine

## Introduction

Recently the process of electrodialysis for demineralization of whey in dairy industry has been implemented intensively. Electrolyzers with circulating cells of concentration are used in most of the cases. The concentration of the obtained electrolyte exceeds the allowable emission rate to sewage system though it is much lower than needed for other technological usage. Thus, each  $\text{dm}^3$  of the desalted whey forms about  $0,3-1 \text{ dm}^3$  of electrolyte [1] which should be additionally cleared. This paper presents the results of researches on demineralization of whey by means of electro dialyzers with non circulating concentration cells in order to increase electrolyte concentration and to decrease its volume.

## Experiments

The electro dialyser consisted of two electrodes and three working chambers between which Cationites (MK-40) and Anionites (MA-40) membranes were placed in turn. The installation had two circulation flows: one was with electrode solution and the other one with whey. There was one non circulating cell of concentration in the electro dialyzer. Electrolyte excess which was formed by ions transfer and ions hydrated shells were removed from the concentration cells by free-run flow through a special capillary. The effective area of each membrane was  $0.01 \text{ m}^2$ , the thickness of diluate cells was 1mm and the thickness of the concentration cells was 6mm. Speed of solutions pumping was  $60 \text{ dm}^3/\text{h}$ . Constant current density was maintained at  $150 \text{ A/m}^2$ . The whey which was used in the experiments was obtained in the manufacture producing lactic cheese. The content of minerals was determined by conductometer with temperature compensation HANNA Instruments.

## Results and Discussion

It has been determined that upon electric current density of  $150 \text{ A/m}^2$  the electrolyte of  $80-120 \text{ g/dm}^3$  concentration is formed by means of electric ions and their hydrated membranes flow in the concentration cells. The average volume of the formed electrolyte is  $4.42 \text{ dm}^3$  per kilogram of salt transferred through membranes. Table 1 presents the volume of the concentrate formed during processing of  $1 \text{ m}^3$  of natural whey at different levels of demineralization.

During calculation it was assumed that the content of mineral substances in whey is 0.5 %.

**Table 1: Volume of the formed concentrate**

Level of demineralization, %	Volume of the concentrate of per $1 \text{ m}^3$ of whey, $\text{dm}^3$
50	11,05
60	13,26
70	15,47
80	17,68
90	19,89

Table 1 shows that in the case of non circulating concentration cells the volume of the electrolyte concentration is 27-50 times less than the case of the same condition with circulating concentration cells.

However, it should be noted that with this setting the current efficiency which is an important indicator of the technological process is more than 20 % lower compared to the one in the circulating concentration cells. This is explained by diffusive ion transfer of the reverse direction

and by accumulation of sparingly dissoluble particles on the membrane surface that can be confirmed by visual inspection after the experiment. Obviously, the current efficiency can be increased if the whey is cleared of hardness salts ( $\text{Ca}^{2+}$ ,  $\text{Mg}^{2+}$ ) by ion exchange [3].

### Summary

Electrodializer with non circulating concentration cells reduces the volume of concentrate to 27-50 times comparing to the one with circulating concentration cells. At the same time its concentration is 80-120 g/dm<sup>3</sup> that can be used in other technological processes. However, this construction stimulates intensive accumulation of sediments on the membrane surface which requires prior cleaning from hardness salts.

### Acknowledgements

*The presented paper was supported by the State Fund for Fundamental Research of Ukraine, state registration № 0108U011256.*

### References

1. *Hoppe, G.K., and Higgins, J.J.* 1992. In: Zadow, J.G. (ed.) *Whey and lactose processing*, pp.91-133. Elsevier Science Publishers Ltd, Essex.
2. *Laktionov, E.V., Pismenskaya, N.D., Nikonenko V.V.* Method of electro dialysis stack testing with the feed solution concentration regulation. // *Desalination*. 2002. V. 151. P. 101-116.
3. *Polyanskiy K.K., Shaposhnyk V.A. and Ponomaryev A.N.* Demineralization of whey by means of electro dialysis // *Molochnaya promyshlennost*. 2004. №10. P. 48-49. In Russian.